

THE GEOCHEMISTRY OF COALS: A CHARACTERISTIC FUNDAMENTAL IN DETERMINING LIQUEFACTION BEHAVIOR. P. H. Given, A. Davis and R. G. Jenkins. College of Earth and Mineral Sciences, Pennsylvania State University, University Park, PA 16802, U.S.A.

The characteristics of coals have been determined by a variety of factors, such as the character of the environment of deposition and temperature/time/pressure history. The varying relative importance of these factors has produced an extraordinary level of diversity in the world's coal reserves. The coals of the geographical area of the U.S. exhibit a wide variety of liquefaction characteristics. Data comprising conversion in coal/tetralin interactions and 14 other properties for a set of 104 coals had to be partitioned by cluster analysis into 3 more homogeneous populations before valid regression analyses could be performed, and the multiple regression analyses predicting conversion called out a different selection of properties for each group. The coal properties mostly responsible for the partitioning into groups were contents of sulfur and of carbon, and the groups consisted largely, but not entirely, of coals from different geological provinces. The inorganic matter in coals is of various types and its nature is determined by the geology and geochemistry of the basin in which a coal is formed. It importantly influences such diverse phenomena as the catalytic effect of coal minerals and the extent of abrasion or erosion of valves and pipework in commercial reactors. Experience in pilot plants has shown a widely varying incidence of problems due to deposition of largely inorganic or largely organic solids in the reactor, both phenomena being dependent on the degree of metamorphism of the coal, the geochemistry of the inorganic matter and the petrography of the coal, the latter property being a function of the geochemistry of the original peat swamp.

RELATIONSHIPS BETWEEN COAL LIQUEFACTION BEHAVIOUR
AND THE COMPOSITION OF SOUTH AFRICAN COALS

D. GRAY, G. BARRASS AND J. JEZKO

FUEL RESEARCH INSTITUTE
P.O. BOX 217
PRETORIA 0001 R.S.A.

GEOLOGICAL ORIGIN OF SOUTH AFRICAN COALS

The coal deposits of South Africa were formed during the Permian age just after a retreat of glaciation. This makes it almost certain that the climate was temperate rather than subtropical and may explain the differences between the plant life in South Africa at that time and the flora of the North American carboniferous era. The predominance of the inertinite maceral group in South African coals is indicative of drier swamp conditions in which rotting processes as well as peatification played a more dominant role than in the formation of the humic coals of Europe (1). South African coals were thought to be deposited in deltaic or fluvial environments where fluctuations in water level may have caused deposition of large quantities of mineral matter. South African coals generally have not reached a very high rank although in Natal anthracites are found. This rank increase seems to be due to metamorphism brought about by dolerite intrusions rather than by stratigraphic depth.

GEOGRAPHICAL LOCATION AND COAL RESERVES OF SOUTH AFRICA

The main coal fields lie in the Highveld area of the Orange Free State, South-eastern Transvaal and Natal. Other coal fields are located in the Northern part of the country, the Waterberg field on the Botswana border and the Limpopo and Pafuri fields on the borders of Rhodesia and Mocambique.

Table 1 shows the raw bituminous coal reserve figures at various ash contents (2). The total figure of 81,274 million tonnes is for total mineable coal in situ down to 300 meters. About half of the coal reserves contain between 30 to 35% mineral matter, thus by world standards South African coal is of poor quality.

TABLE 1: SUMMARY OF COAL RESERVES : MILLIONS OF TONNES

| ASH % | 5-10 | 10-15 | 15-20 | 20-25 | 25-30 | 30-35 | TOTAL |
|-----------|------|-------|-------|--------|--------|--------|--------|
| PROVEN | 18 | 794 | 3,720 | 6,197 | 7,912 | 13,582 | 32,223 |
| INDICATED | - | 645 | 2,866 | 5,507 | 5,224 | 11,785 | 26,027 |
| INFERRED | 2 | 60 | 2,034 | 3,516 | 5,429 | 11,983 | 23,024 |
| TOTAL | 20 | 1,499 | 8,620 | 15,220 | 18,565 | 37,350 | 81,274 |

LIQUEFACTION BEHAVIOUR OF A VARIETY OF SOUTH AFRICAN COALS

Experimental:

Two experimental procedures were used in this preliminary study of the liquefaction behaviour of South African coals. These were:

- (i) dry hydrogenation using the hot-rod reactor (3).
- (ii) slurried hydrogenation using a rotating autoclave.

(i) Hot-Rod Method:

This system was very similar to the one used by Hiteshue at the U.S.B.M. except that larger quantities of coal were used. In this method sand (0.42 - 0.15 mm) was mixed with the coal in a 2:1 mass ratio. It was found that the addition of sand to the coal helped to prevent agglomeration (4) thus enhancing the diffusion of hydrogen through the coal and the removal of the liquefaction products from the coal. In experiments using a catalyst an aqueous solution of stannous chloride was added to the coal, evaporated to dryness, and then mixed with the sand. The amount of catalyst added on a tin basis was 1% of the mass of the coal. These mixtures were placed in a hot-rod reactor, pressurized with hydrogen to 25 MPa and heated to 500°C at a heating rate of 200°C per minute. Reaction time at temperature was 15 minutes.

(ii) Rotating Autoclave Method:

The reactor was a 1 liter stainless steel rotating autoclave. In the experiments using anthracene oil, the ratio of oil to coal was 2:1, and the final reaction temperature was 430°C. The autoclave was pressurized with hydrogen to 10 MPa at room temperature. Final pressure at reaction temperature was approximately 25 MPa. The products after liquefaction were filtered while hot, and the residue was Soxhlet extracted with toluene for 24 hours.

The overall conversion of coal to liquid and gaseous products was obtained from the formula:

$$\text{Percentage conversion} = 100 \left\{ 1 - \frac{\text{Organic material in the residue}}{\text{Organic material in the coal}} \right\}$$

The oil is the n-hexane soluble portion of the product, and the asphaltene is the toluene soluble n-hexane insoluble portion.

Analyses of Coals Studied:

The coals used in these experiments were from Landau, Sigma, Spitzkop, Kriel, Matla, New Wakefield and Waterberg collieries. Table 2 shows their proximate and ultimate analyses.

The petrographic analyses of the coals are shown in Table 3. One-third of the semi-fusinite, the largest component of the inertinite in Sigma coal, is considered reactive and is included in the total reactive maceral content.

TABLE 2: PROXIMATE AND ULTIMATE ANALYSES OF COALS USED IN THE LIQUEFACTION EXPERIMENTS

| COAL | PROXIMATE ANALYSES (AIR DRIED BASIS) | | | | ULTIMATE ANALYSES (D.A.F. BASIS) | | | | | % VOL. MAT. (DAF) | H/C RATIO |
|---------------|---|------|-----------|------------|-------------------------------------|------|------|------|-------|-------------------|-----------|
| | % | % | % | % | % | % | % | % | % | | |
| | H ₂ O | ASH | VOL. MAT. | FIX. CARB. | C | H | N | S | O | | |
| MATLA | 6.0 | 10.9 | 35.3 | 47.8 | 78.84 | 5.48 | 2.03 | 0.53 | 13.12 | 42.5 | 0.83 |
| WATERBERG | 3.4 | 12.7 | 34.8 | 49.1 | 80.68 | 5.47 | 1.47 | 1.04 | 11.34 | 41.5 | 0.81 |
| NEW WAKEFIELD | 4.9 | 14.9 | 32.8 | 47.4 | 79.15 | 5.41 | 2.11 | 2.28 | 11.05 | 40.9 | 0.82 |
| KRIEL | 3.8 | 20.2 | 30.3 | 45.7 | 79.13 | 5.28 | 2.04 | 2.88 | 10.67 | 39.9 | 0.80 |
| SPITZKOP | 3.2 | 12.7 | 32.7 | 51.4 | 81.68 | 5.33 | 2.07 | 1.31 | 9.61 | 38.9 | 0.78 |
| SIGMA | 6.6 | 29.6 | 21.9 | 41.9 | 76.71 | 4.42 | 1.55 | 1.08 | 16.24 | 34.3 | 0.69 |
| LANDAU | 2.5 | 14.3 | 23.3 | 59.9 | 84.10 | 4.41 | 1.91 | 0.64 | 8.94 | 28.0 | 0.63 |

TABLE 3: PETROGRAPHIC ANALYSES OF COALS USED IN THE LIQUEFACTION EXPERIMENTS

| COAL | MACERAL ANALYSES | | | |
|---------------|------------------|---------|------------|------------------|
| | % | % | % | % |
| | VITRINITE | EXINITE | INERTINITE | VISIBLE MINERALS |
| MATLA | 75.9 | 6.2 | 15.6 | 1.0 |
| WATERBERG | 83.2 | 4.2 | 5.7 | 6.9 |
| NEW WAKEFIELD | 72.2 | 5.0 | 13.2 | 9.6 |
| KRIEL | 50.8 | 12.1 | 21.5 | 15.6 |
| SPITZKOP | 55.0 | 6.3 | 35.9 | 2.8 |
| SIGMA | 27.9 | 3.1 | 58.9 | 10.1 |
| LANDAU | 57.2 | 6.0 | 28.4 | 8.4 |

Results of the Preliminary Investigation:

The effect of the following parameters was studied in relation to liquid yields and conversions during coal liquefaction:

- 1) volatile matter content
- 2) H/C atomic ratio
- 3) reactive maceral content
- 4) mineral matter constituents
- 5) process parameters

Emphasis in this paper is placed on the coal parameters 1 - 4, and only brief mention is made concerning the process parameters.

Figures 1 and 2 show the percentage conversion (d.a.f. basis) of the coals plotted against the H/C ratio, the volatile matter and the reactive maceral content for the anthracene oil runs. Figures 3 and 4 show the percentage conversion and the oil yield plotted against the H/C ratio, volatile matter and reactive macerals. These results were obtained from dry hydrogenation runs using the hot-rod reactor. Figures 5 and 6 show the total liquid product obtained (oil plus asphaltene) plotted against the H/C ratio, volatile matter and reactive maceral content of the coals.

The effect of the inorganic constituents in the coal was studied in two ways. Firstly, a sample of coal from Kriel colliery was subjected to a float and sink separation. The analyses of the float and sink fractions is shown in Table 4.

TABLE 4: ANALYSES OF FLOAT/SINK FRACTIONS

| Relative Density | Vitrinite | Exinite | Inertinite | Visible Minerals | Ash |
|------------------|-----------|---------|------------|------------------|------|
| 1.4 float | 80.6 | 7.5 | 6.5 | 5.4 | 6.7 |
| 1.4 - 1.5 | 78.3 | 8.3 | 9.1 | 4.3 | 7.0 |
| 1.5 - 1.65 | 65.5 | 9.1 | 15.9 | 9.7 | 16.0 |
| 1.65 sink | 66.6 | | | 33.4 | 45.3 |

Figure 7 shows the product distribution obtained from dry hydrogenation of these float/sink fractions.

The second procedure studied the particular effects of the pyrite content of the coals during hydrogenation. Unwashed coals were selected so that the only parameter to show significant variation was the total sulfur content. Of this total sulfur, approximately 1% was organic, and the rest was pyritic. Since total mineral matter was also known to affect conversion, it was kept as constant as possible.

Table 5 shows the analyses of the coals used to study the effect of pyrite.

TABLE 5: ANALYSES OF UNWASHED COALS USED TO DETERMINE THE EFFECT OF PYRITES

| NUMBER | V+E | TOTAL ASH % | MOISTURE % | SULFUR % | VM |
|---------------------------|------|----------------------|------------|----------|------|
| 555 O | 83.0 | 24 | 2.4 | 6.5 | 31.9 |
| 524 K | 83.8 | 22 | 3.0 | 5.7 | 29.1 |
| 651 J | 83.7 | 26 | 2.3 | 5.0 | 32.2 |
| 553 H | 82.0 | 22 | 2.8 | 4.1 | 32.5 |
| 524 B | 82.0 | 22 | 2.7 | 2.2 | 32.1 |
| 554 C | 83.2 | 24 | 2.5 | 1.9 | 30.2 |
| 555 A | 80.0 | 22 | 2.4 | 1.3 | 32.5 |
| V+E = Vitrinite + Exinite | | VM = Volatile Matter | | | |

Reaction conditions used in the hot-rod reactor for the pyrite experiments were 25 MPa, 450°C and a 2:1 sand:coal ratio.

A process temperature study was conducted using Waterberg, New Wakefield, Sigma and Landau coals, and at 650°C the conversions for these coals were 89, 87, 90 and 88% respectively. Within experimental error the conversions had all converged to the same value regardless of the characteristics of the individual coals. The product distribution of oil and gas, however, was different, the higher temperature resulting in higher gas make and lower oil yield. If, however, the vapor residence times are shortened it may be possible to quench the vapors before extensive cracking to gas occurs.

Relationships Between Liquefaction Behaviour and the Coal Composition

Organic coal properties

The results of liquefaction using anthracene oil shown in figures 1 and 2 indicate a good correlation between conversion and the H/C atomic ratio, volatile matter and reactive maceral content of the coals. Comparison of these anthracene oil results with results from dry hydrogenation in the absence of anthracene oil (figures 3 and 4) shows that the slopes of the linear correlations are very similar. In the case of conversion against volatile matter, the slopes are identical. The significance of this is not clear as a different mechanism is probably operative in the two techniques. The anthracene oil most certainly acts as a hydrogen donor solvent, and the molecular hydrogen rehydrogenates the solvent. In the case of dry hydrogenation radical stabilization occurs directly by reaction with molecular hydrogen.

No oil yield data are available from the anthracene oil experiments because of the complications in separating product oil, which results from coal liquefaction, and anthracene oil. In the case of dry hydrogenation this complication does not exist, and very reliable oil and oil plus asphaltene yield data are available. Excellent correlations are obtained by plotting oil plus asphaltene yield against H/C ratio and volatile matter content of the coals with correlation coefficients of 0.96 and 0.95, respectively (Figure 5).

It must be stressed that there is an intercorrelation between the coal properties themselves. The correlation between the volatile matter and the H/C ratio for the South African coals studied is extremely high, the correlation coefficient being 0.99. Thus a good correlation of yield with one of these properties obviously implies a similarly good correlation with the other. However, the correlations between the volatile matter and the reactive maceral content and between the reactive maceral content and the H/C ratio were not statistically significant for the coals studied.

The correlation against the concentration of reactive macerals present (Figure 6) is not as good as for the H/C ratio and the volatile matter. A partial explanation of this may be that for South African coals, portions of the inertinite content seem to be definitely reactive to liquefaction. The semi-fusinite, often very high in these coals, is particularly reactive to hydrogenation, and also other maceral constituents of the inertinite group show some reactivity in this regard.

The correlation of conversion against the coal parameters is consistently not as good as with the oil and oil plus asphaltene data. This may be explained by the very high mineral matter contents of South African coals. At conversion conditions, the chemical composition of this mineral matter may undergo considerable change. For example, decarboxylation of carbonates and dehydroxylation of clay minerals

could occur, resulting in a higher measured weight loss of the coal. When calculating conversions, the mineral matter is considered to be unchanged after the hydrogenation reaction, but this is not necessarily the case.

Conversion data from South African coals were compared to data from a selection of Australian coals, also of Gondwanaland origin. These coals were hydrogenated in the presence of a tar derived solvent at 400°C, 11 - 20 MPa and in a ratio 5:1 oil : coal (5). This selection of coals used by the A.C.I.R.L. included three non-Australian coals, and these were omitted in the correlations reported here. An excellent correlation was found between the conversion and the reactive maceral content of the coals. In addition a correlation existed between the conversion and the H/C atomic ratio.

Table 6 shows the linear regression analyses and the correlation coefficients for the conversion data from South African and Australian coals.

TABLE 6 : REGRESSION EQUATIONS FOR SOUTH AFRICAN AND AUSTRALIAN COALS

| COUNTRY | REGRESSION EQUATION | CORRELATION COEF. | CONDITIONS |
|--------------|--|-------------------|----------------|
| SOUTH AFRICA | $C = 0.56 R + 39.0$ | 0.63 | DRY (Sn) |
| | $C = 1.4 (VM) + 25.0$ | 0.63 | DRY (Sn) |
| | $C = 91.8 \left\{ \frac{H}{C} \right\} + 7.2$ | 0.61 | DRY (Sn) |
| | $C = 0.47 R + 48.0$ | 0.92 | ANTHRACENE OIL |
| | $C = 1.4 (VM) + 40.0$ | 0.89 | ANTHRACENE OIL |
| | $C = 106.6 \left\{ \frac{H}{C} \right\} + 1.0$ | 0.96 | ANTHRACENE OIL |
| AUSTRALIA | $C = 0.65 R + 26.0$ | 0.92 | TAR OIL |
| | $C = 83.5 \left\{ \frac{H}{C} \right\} + 1.6$ | 0.70 | TAR OIL |

C = CONVERSION, R = REACTIVE MACERALS, VM = (D.A.F.) VOLATILE MATTER

Inorganic Coal Properties:

There is positive evidence that mineral matter behaves beneficially during coal conversion. It has been demonstrated that certain coal minerals, particularly iron compounds, catalyze the hydrogenation of coal-derived solvents (6). Mukherjee et al (7) hydrogenated float/sink fractions of an Indian coal and found that the conversion increased continuously with the amount of mineral matter present in the fraction. It is difficult to assess the effect of the mineral matter in the coal on liquefaction. When using float/sink fractions of the same coal, the petrographic constitution of the coal fractions usually changes significantly with more inertinite being found in the higher density fractions. Also the mineral matter distribution changes from fraction to fraction, and the physical distribution of the mineral phases causes considerable variation in the surface areas available for possible catalysis. In addition, the combination of the effects of increased mineral matter and decreased reactive maceral content in increasing density fractions decreases the tendency of the coal to agglomerate. This allows more effective diffusion in the system (4).

To try to overcome these difficulties, a series of unwashed coals was chosen so that the only parameter to change significantly was the total sulfur content. Table 5 shows the analysis of the coals, and Figure 8 clearly shows the effect

of pyrite content of the coal on conversions and liquid product yields during liquefaction. Conversions increased from about 50 to 70% using the hot-rod reactor with no added catalyst. Thus it would appear that pyrite can act catalytically in the dry hydrogenation reaction as well as in slurried reactions.

The results from the float/sink fractions (Figure 7) are more difficult to interpret because of the simultaneous variation of mineral matter and petrography (see Table 4). It could be that the increase in oil yield obtained with the higher mineral matter fractions is due to the increase in sulfur that varies from 0.5% in the 1.4 float to 9% in the 1.65 sink fraction. The significance as far as South African coals are concerned is that mineral matter does not necessarily mean poor performance during coal liquefaction. Evidence so far suggests that the mineral matter can be beneficial in increasing conversion and liquid product yields. From a processing viewpoint, high mineral matter can create other problems, and a trade off between possible catalytic benefits and engineering process difficulties must be arrived at.

SUMMARY:

For the South African bituminous coals studied so far the following conclusions can be made:

- (i) Conversion data obtained from coal liquefaction under dry hydrogenation conditions, and in the presence of anthracene oil show good correlations with the H/C ratio, the volatile matter and the reactive maceral content of the coals.
- (ii) For dry hydrogenation, excellent correlations are obtained between total liquid product and oil yield with the H/C ratio and the volatile matter of the coals. The correlation of liquid product yield with reactive maceral content is not as good, but liquid product increases with an increase in reactive maceral content.
- (iii) The pyrite in the coal, as estimated from the total sulfur, appears to act catalytically in the dry hydrogenation reaction and enhances the overall liquid yield.
- (iv) It appears that as the severity of processing is increased, the importance of the coal characteristics themselves become less significant when considering overall conversion.

REFERENCES:

- (1) M-Th. Mackowsky. Coal and Coal Bearing Strata. Editors O.G. Murchison and T.S. Westroll. Oliver and Boyd (1968).
- (2) Department of Mines. Report of the Commission of Inquiry into the Coal Resources of South Africa (Petrick Report). (1975).
- (3) R.W. Hiteshue, S. Friedman and R. Madden. U.S.B.M. R.I 6125 (1962).
- (4) D. Gray. Fuel, 57, 213 (1978).
- (5) R.E. Guyot and J.F. Cudmore. Australian Coal Industry Research Laboratories Ltd. Report P.R. 75-6, PART 1 (1975).
- (6) J.A. Guin, A.R. Tarrer, J.W. Prather, D.R. Johnson and J.M. Lee. Ind. Eng. Chem. Process Des. Dev. 17, 2, 118 (1978).
- (7) D.K. Mukherjee and P.B. Chowdhury. Fuel, 55, 4 (1976).

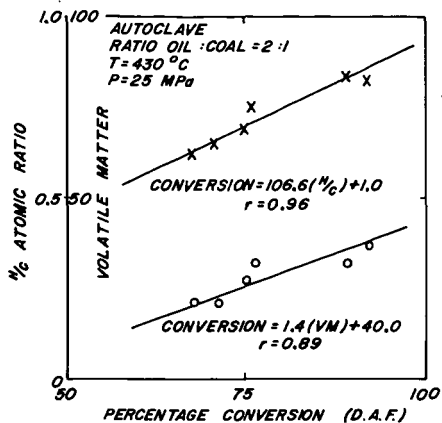


FIGURE 1 VARIATION OF THE PERCENTAGE CONVERSION (D.A.F.) WITH THE % RATIO AND VOLATILE MATTER OF THE COAL.

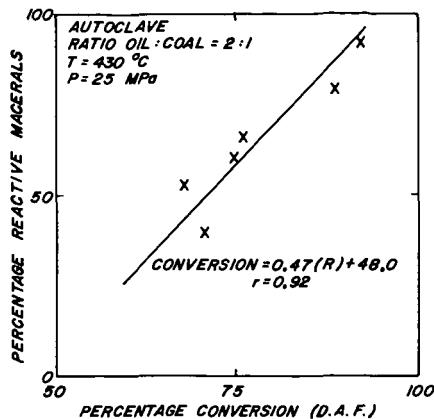


FIGURE 2 VARIATION OF THE PERCENTAGE CONVERSION (D.A.F.) WITH THE REACTIVE MACERAL CONTENT OF THE COAL.

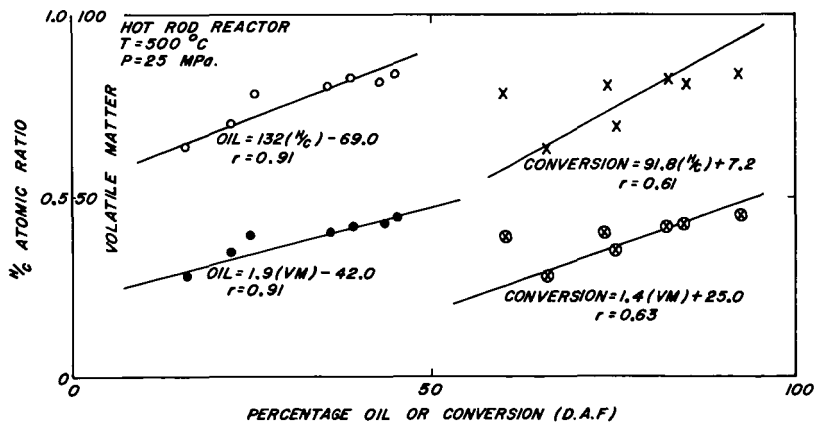


FIGURE 3 VARIATION OF THE PERCENTAGE CONVERSION AND OIL YIELD WITH THE VOLATILE MATTER AND THE % ATOMIC RATIO OF THE COAL.

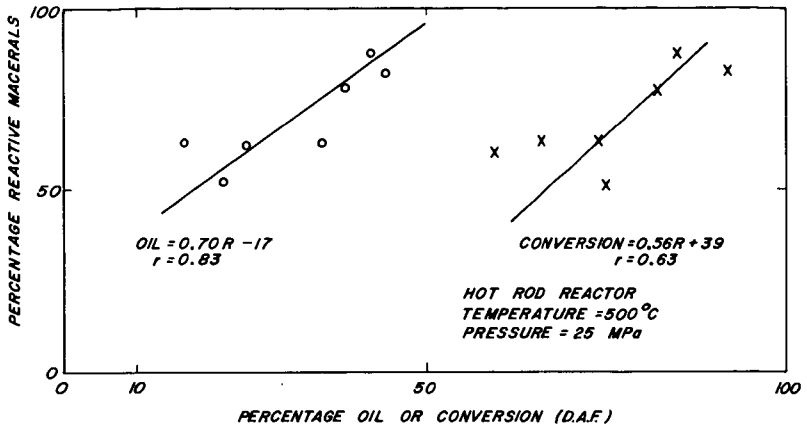


FIGURE 4. VARIATION OF THE PERCENTAGE CONVERSION AND OIL YIELD WITH THE REACTIVE MACERAL CONTENT.

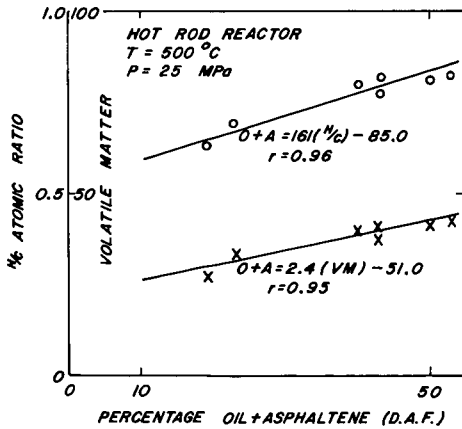


FIGURE 5. VARIATION IN THE OIL + ASPHALTENE YIELD WITH THE % RATIO AND VOLATILE MATTER OF THE COAL.

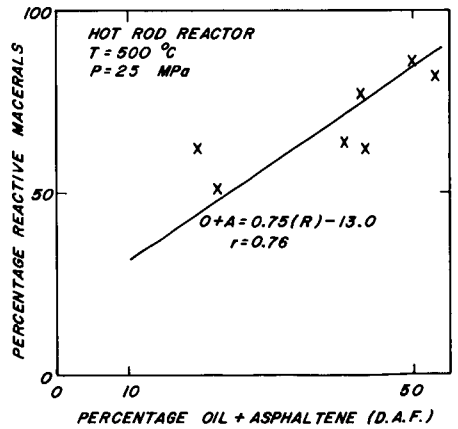


FIGURE 6. VARIATION IN OIL + ASPHALTENE YIELD WITH THE REACTIVE MACERAL CONTENT OF THE COAL.

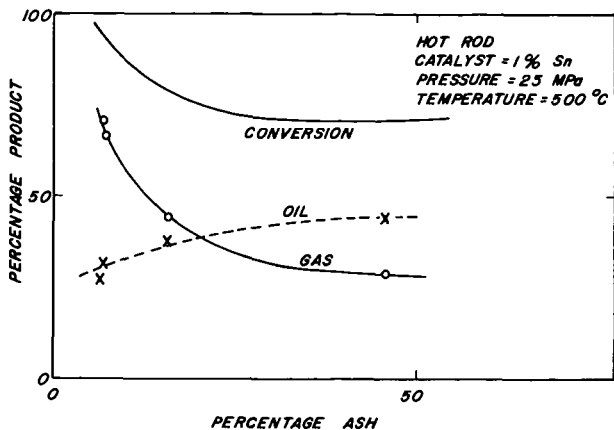


FIGURE 7 VARIATION IN PRODUCT DISTRIBUTION WITH ASH CONTENT FOR KRIEL COAL (0.149 mm / 0.074 mm)

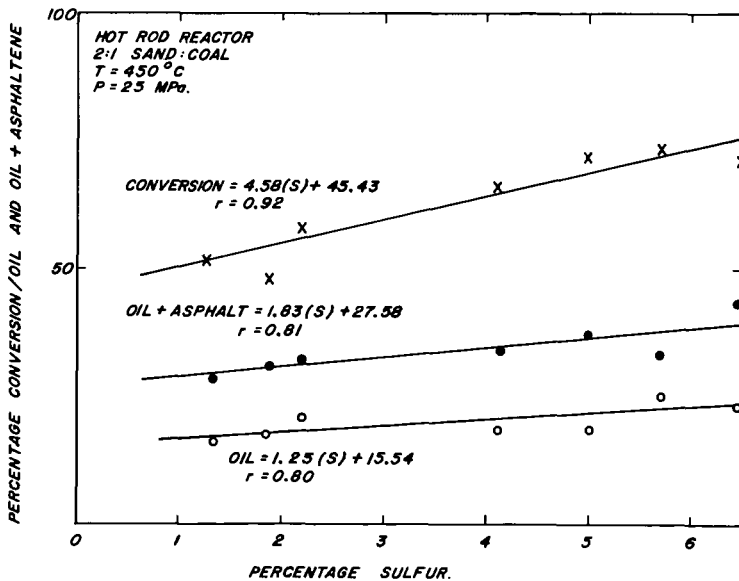


FIGURE 8 VARIATION IN CONVERSION, OIL AND OIL PLUS ASPHALTENE YIELD WITH SULFUR CONTENT.

THE CHARACTERISTICS OF AUSTRALIAN COALS AND THEIR IMPLICATIONS IN COAL LIQUEFACTION

R. A. Durie

R.W. Miller & Co. Pty. Ltd.
213 Miller Street, North Sydney, N.S.W., 2060

INTRODUCTION

In Australia, coal represents, in energy terms, over 97% of the country's non-renewable fossil fuel based energy resources, yet indigenous oil which barely represents 1% of these resources, together with imported oil, supply over 50% of the energy demand with much of this from the transport sector. This situation, catalyzed by the OPEC oil embargo in 1973, has led to strong and sustained interest in the prospects for producing liquid fuels from the abundant coal resources. The reserves of recoverable fossil fuels (1) and the present pattern of energy demand in Australia (2) are shown in more detail in Tables 1 and 2, respectively.

LOCATION, GEOLOGY AND GENERAL CHARACTERISTICS OF AUSTRALIAN COALS

The geographical distribution of Australia's coal resources is shown in Fig. 1. New South Wales and Queensland possess large reserves of black coals in the Sydney and Bowen Basins, respectively, adjacent to the eastern seaboard. Significant deposits of bituminous coals are also known to occur in remote areas in South Australia at Lake Phillipson in the Arckaringa Basin and at currently inaccessible depths (2000-3000 m) in the Cooper Basin (3,4). [An estimated 3.6×10^6 million tonnes in the latter].

Large reserves of brown coals occur in Victoria with smaller deposits in New South Wales and South Australia.

Whereas the majority of the black coals in the northern hemisphere, including the USA and Europe, were formed during the Carboniferous age, the black coals of Australia are, in the main, Permian. The latter include the coals from the two major basins - the Sydney and the Bowen - and also large deposits in the Galilee Basin (Queensland), at Oaklands (N.S.W.), Lake Phillipson (South Australia) and Collie (West Australia) as well as the deep coal in the Cooper Basin (South Australia). These Permian coals, together with counterparts in India, South Africa, Antarctica and South America, are referred to as Gondwana coals after the hypothetical super-continent which subsequently broke up into the continents and sub-continents mentioned above (5).

The climatic conditions prevailing in the Permian during the formation of these Gondwana coals were different from those for the Carboniferous coals of North America and Europe. As a result of a cooler climate with alternating dry and wet periods, and of the consequent difference in the original plant materials, the conditions of accumulation, and the slower rate, and prolonged duration of sinking, the Australian (and other Gondwana) Permian coals differ in many respects from the Carboniferous coals of the northern hemisphere. Thus for the former coals, seam thickness tends to be greater, vitrinite content lower, semi-fusinite content higher, mineral matter content high and sulphur content generally low; the ash derived from the mineral matter is usually refractory with high fusion temperatures. These coals occur in seams near the surface, and at depth.

The Australian Permian coals vary widely in rank (maturity) and type (vitrinite content) from the Oaklands (N.S.W.) coal at 72% (dry ash-free basis) carbon, a hard brown coal (6), at one extreme - though high volatile bituminous coals such as Galilee (Queensland) coal at 77% carbon, 16% vitrinite; Blair Athol (Queensland) coal at 82% C, 28% vitrinite; Liddell (N.S.W.) coal at 82% C, and >70% vitrinite, - to low volatile bituminous such as Peak Downs (Queensland) at 89% C, 71% vitrinite,

and Bulli seam (N.S.W.) 89% C, 45% vitrinite.

In addition to the Permian coals there are occurrences of Mesozoic and Tertiary coals in Australia. Mesozoic coals occur in small basins in South Australia, Tasmania, New South Wales and Queensland and vary in rank from brown to bituminous. Perhaps the most notable occurrences in the present context are the Wallon coals in the Clarence-Morton basin in Queensland, e.g. Millmerran sub-bituminous coal (78% carbon, vitrinite plus exinite ~90%).

The most significant Tertiary coals are represented by the vast brown coal deposits in Victoria, particularly in the Latrobe Valley. These brown coals with 68-70% carbon, occur in very thick seams (up to 200 meters) under shallow cover (<30 meters). These coals differ from the Tertiary brown coals of North America in that they have a much lower ash yield and significant amounts of the ash-forming inorganic constituents are present as cations on the carboxylic acid groups which are a characteristic of low rank coals.

COAL CHARACTERISTICS AND THEIR EFFECTS IN LIQUEFACTION PROCESS

The wide variation in Australian coals in rank, type and inorganic impurities and the significant differences between these coals and those from the USA and elsewhere, emphasize the need for detailed understanding of how specific coal characteristics influence liquefaction reactions and the properties of the liquid product. The heterogeneity and variability of coals make them a complex feedstock on the one hand and presents major challenges to efforts to identify and quantify those parameters of most significance. However, until this is achieved the application of a process developed and optimized on a coal, or similar coals, from one region to coals in another region is fraught with danger. In recognition of this, research is in progress in a number of laboratories in Australia to elucidate the chemistry of Australian coals in relation to their liquefaction. This encompasses both black and brown coals and liquefaction via pyrolysis, non-catalytic hydrogenation (solvent refining) and catalytic hydrogenation. The results obtained in these studies are informative but some give rise to more questions than answers. In the remainder of this paper selected highlights from these Australian studies will be presented and discussed.

EFFECTS OF PETROGRAPHIC COMPOSITION AND RANK

It is possible to produce some liquid hydrocarbons from most coals during conversion (pyrolysis and hydrogenation, catalytic and via solvent refining) the yield and hydrogen consumption required to achieve this yield can vary widely from coal to coal. The weight of data in the literature indicate that the liquid hydrocarbons are derived from the so-called 'reactive' macerals, i.e. the vitrinites and exinites present (7,8,19). Thus, for coals of the same rank the yield of liquids during conversion would be expected to vary with the vitrinite plus exinite contents. This leads to the general question of effect of rank on the response of a vitrinite and on the yield of liquid products; and, in the context of Australian bituminous coals, where semi-fusinite is usually abundant, of the role of this maceral in conversion.

A number of research projects in Australia are being addressed to these questions. The Australian Coal Industry Research Laboratories (ACIRL) have been approaching the question through a study of the conversion behaviour of a selected range of Australian bituminous coals under non-catalytic solvent refining conditions (9,10). The Commonwealth Scientific and Industrial Research Organization (CSIRO) is considering the question with regard to pyrolysis (11) and catalytic hydrogenation (12) of bituminous and brown coals, with support from studies of the behaviour of individual maceral types during conversion with the aid of petrographic techniques (12).

Experimental data published recently by Cudmore (10) for eight Australian bituminous coals, reproduced in Fig. 2, show a good direct linear correlation between conversion (to gas + liquids), under non-catalytic hydrogenation conditions

using tetralin as vehicle, and the vitrinite plus exinite contents over the range 40 to 80% for coals in the rank range where the mean maximum reflectance (R_0 max.) of the vitrinite varies from 0.43% to 0.68%, i.e. for carbon content over the range of about 75% (dry ash-free) to about 82%. This encompasses the sub-bituminous coals and high volatile bituminous coals. However, for coals where R_0 max. is greater than 1.47% the yield was markedly lower than might otherwise have been expected from the vitrinite plus exinite contents (refer Fig. 2). The information in Fig. 2 would further suggest that the rank effect in decreasing conversion yield increases rapidly with increase in rank from R_0 max. 1.47% to 2.64%, i.e. carbon (dry ash-free basis) 88% to >90%. This, of course, leaves open the question of where the decrease in the conversion of the vitrinite (+ exinite) starts in the rank range 83 to 88% carbon.

An implication of Cudmore's data (10) for the sub-bituminous and high volatile bituminous coals is that the semi-fusinite appears to contribute little to the conversion products, otherwise the apparent dependence of yield on the vitrinite (+ exinite) content would not be so linear.

The whole question relating to the possible role of semi-fusinite is receiving the attention of Shibaoka and his associates in the CSIRO (12). Although the project is still at an early stage, direct observations on the changes occurring in semifusinite-rich coal grains during conversion under a wide variety of conditions suggest that the possible contributions of this maceral in conversion cannot be ignored although further work is required to define the nature and magnitude of such contributions.

Studies initiated by the author while still with CSIRO (13) seek to throw light on the role of the various macerals by studying the conversion, under catalytic hydrogenation conditions, in tetralin as vehicle, of maceral concentrates from a high volatile bituminous coal. Some preliminary results, given in Fig. 3, show conversions as almost complete for the hand picked vitrain (>90% vitrinite) from a high volatile bituminous coal (Liddell seam N.S.W., 83.6% carbon and 43% volatile matter both on a dry ash-free basis). However, it is evident that the conversion of the 'whole' coal increases rapidly with increase in hydrogen pressure (under otherwise similar conditions - batch autoclave, 4h. @ 400°C). This could suggest either that conversion of the vitrinite is suppressed by other components in the coal, particularly at the lower pressures, or more likely, that other macerals are participating to an increasing extent as the hydrogen pressure increases.

Consideration of the latter results in relation to those of Cudmore (10), discussed above, emphasise the need for caution when generalising on the influence of coal characteristics on conversion. Indeed, it would appear that the absolute and relative contribution of the various petrographic components is dependent on the process conditions which include, inter alia, the hydrogen potential.

The petrography of brown coals differs from that of black coals and is less well developed. However, evidence is mounting that brown coals can vary significantly, even within the same seam, and that these variations may effect their conversion behaviour. The Victorian Brown Coal Development Commission has initiated studies in this area (with advice from the German Democratic Republic). No results are available as yet.

THE EFFECT OF ELEMENTAL COMPOSITION

It is well established that for any coal the so-called reactive macerals, vitrinite and exinite, are richer in hydrogen than the inert macerals. Therefore, since the conversion of coals to liquid fuels involves the production of lower molecular weight products having atomic hydrogen to carbon ratios in the range 1.7 to 2 compared with <1 for most coals, it is of interest to consider the effect of the hydrogen content, or alternatively the hydrogen/carbon ratio on the conversion of coals to liquid and gaseous fuels under a wide range of conditions.

Pyrolysis

In this context it is relevant to consider initially the effect of hydrogen contents on tar yields during pyrolysis (carbonization). This is particularly so, since, in all coal conversion processes little happens until the coal is at a temperature above that where active thermal decomposition normally sets in. In other words, all coal conversion processes may be regarded as pyrolysis under a variety of conditions which determine the nature of the primary decomposition and the reactions which follow.

Fig. 4 represents a plot of the atomic H/C ratio versus tar yields obtained by the former CSIRO Division of Coal Research for a wide variety of Australian coals during low temperature (600°C) Gray-King carbonization assays (14) over several years. This figure shows that, despite a wide variation in rank and inorganic impurities, there is a significant linear correlation between the tar yield and the atomic H/C ratio. A variety of factors may account for the scatter - the empirical nature of the assay, wide variations in the ash yield and nature of the ash (see below), weathering of the coal, the multitude of analyses involved and the long time span over which the results were accumulated.

The steep dependence on hydrogen content of the tar yields obtained during the low temperature (500°C) fluidized bed carbonization of 14 Australian coals, ranging in rank from 72% to -89% (dry ash-free basis) carbon content, is clearly demonstrated in Fig. 5 (15,16).

In current CSIRO investigations into the production of liquid fuels via the flash pyrolysis of selected Australian coals (11) the importance of the hydrogen content, or more precisely the atomic H/C ratio of the coal with regard to the total yield of volatile matter and tar, has been demonstrated also. This is shown in Fig. 6 (20) together with the reproduction of the correlation line for the low temperature Gray-King Carbonization assay transferred from Fig. 4. Also included are data obtained for one USA bituminous coal (Pittsburgh No. 8) and one lignite (Montana). The former coal plots consistently with the Australian bituminous coals for both the volatile matter and tar yield; but whereas the raw Montana lignite, together with the raw Australian brown coal, are consistent with the bituminous coals for total volatile matter yield, the tar yields from the lignite and brown coal fall significantly below those to be expected from Fig. 4 for bituminous coal with similar atomic H/C ratios with one exception - a low ash sample of Loy Yang brown coal. The reason for the 'deviation' is considered in the next section of the paper.

Hydrogenation

Cudmore (13) in his studies of the non-catalytic hydrogenation (solvent refining) of six Australian coals has indicated that the conversion systematically increases as the atomic H/C ratio of the coal increases over the range 0.60 to 0.85. This is shown in Fig. 7 (10) which also includes data for the catalytic hydrogenation of six Canadian coals (17). These results, together, indicate the importance of the hydrogen contents of coal in general for both non-catalytic and catalytic hydrogenation.

With regard to the implications of the elemental composition (ultimate analysis) of Australian coals, brown coals (lignites) call for special attention by virtue of their high oxygen contents (as high as 30%). During hydrogenation of brown coals it is usually considered that significant amounts of hydrogen are consumed in the elimination of oxygen as water and that this places these coals at a disadvantage because the cost of hydrogen is a significant factor in the economics of conversion. White has recently considered oxygen balances in the catalytic hydrogenation of some Australian brown coals (18). This study indicates that, whereas the overall conversion, under comparable conditions, is higher for brown coals than for bituminous coals studied, the yield of hydrocarbon liquids is higher for the latter; but, surprisingly, the hydrogen consumption in the primary conversion is actually lower for the brown coals than for any of the bituminous

coals studied (H/C in range 0.57 to 0.72). Further, the results show that the present hydrocarbon liquid yield (dry ash-free basis) per cent of hydrogen consumed is actually as high, or higher, for a low ash yield (0.5%) brown coal (H/C = 0.81) by comparison to the bituminous coals studied. Indeed, the evidence suggests that much of the oxygen (~30%) is eliminated as carbon monoxide and carbon dioxide.

EFFECT OF INORGANIC CONSTITUENTS

Despite much speculation on the possible effects of the inorganic ash-forming constituents in a coal on its behaviour during conversion, there is still no clear understanding on the subject. It is generally suspected that where pyrite is present in a coal this is converted to pyrrhotite under the conditions of coal hydrogenation and can act as a catalyst (19). The effectiveness will, of course, be dependent on how the pyrite is disseminated through the coal including the maceral association; this may be the cause where no significant effect has been noted (8). In the majority of Australian coals the sulphur, and hence pyrite, content is very low and hence the possibility of a catalytic effect from pyrite is negligible. As mentioned earlier, Australian bituminous coals tend to be high in mineral matter. This consists primarily of aluminosilicate minerals (20). To prepare most coals for use as a feedstock in conversion these will need to be processed in a coal preparation plant to reduce the ash yield. Otherwise reactor throughput in terms of effective coal feed rates, are adversely affected and excessive ash can 'blind' added catalysts and cause other operational problems. Since aluminosilicates are the basis of cracking catalysts, the mineral matter in the coal might well act in this way and be either to the advantage or disadvantage of the conversion process.

A project initiated by the author when with CSIRO has, as one of the objectives, the study of effect of the mineral matter in selected Australian coals during catalytic hydrogenation (13). The initial approach has been to compare, under otherwise identical conditions, the conversion behaviour of a coal sample before and after demineralization. Some very preliminary results are shown in Fig. 8 for a sample of Liddell seam coal (ash yield 7.35% air dried basis; volatile matter 43.2% and total sulphur 0.48% dry ash-free basis) before and after demineralization to reduce the ash yield to 0.5%. Fig. 8 shows the effect of temperature on the total conversion and yield of bitumen, (i.e. residue from atmospheric and vacuum distillation to 210°C of the hydrogenation product) during batch catalytic (a commercial Co-Mo on alumina catalyst) hydrogenation using tetralin as solvent. The main effect of the mineral matter appears to be to give an increased scatter in the experimental data with regard to total conversion. This is also evident, but to a lesser degree, in Fig. 3 where the effect of pressure on total conversion for the same coal is indicated.

Since the scatter of experimental points for total conversion is both above and below the curve for the demineralized sample, it is not possible to assign the behaviour to either catalyst blinding or enhanced catalytic effects. With regard to the yield of 'bitumen' (Fig. 8), the bias on the high side in yield could be interpreted to suggest that some catalytic effect was exhibited by the mineral matter. Obviously further studies of this type are required to determine the nature of the effects, if any, of the aluminosilicates in Australian bituminous coals on the response of these coals during conversion.

Australian brown coals are of special interest with regard to the possible influence of the inorganic constituents during pyrolysis and hydrogenation. In the low ash yield Australian brown coals, a considerable proportion of the inorganic ash-forming constituents are present as cations associated with the carboxylic acid groups in the coal (21,22,23). Studies in CSIRO have shown that the nature and amount of the cations can exert marked effects on the behaviour of the coal during thermal decomposition (pyrolysis). In particular, Schafer (24) has shown that the presence of cations facilitate the elimination of the oxygen during pyrolysis in a manner that is still not understood. This could have interesting and practical implications for hydrogenation which remain to be investigated.

In the USA, observations with North Dakota lignites have suggested that sodium associated with the carboxyl groups have a beneficial catalytic effect with regard to the quality of the liquid product (8). Further, the superiority of CO-steam over hydrogen in the 'non-catalytic' hydrogenation of lignite has been attributed again to the catalytic effects of alkali and alkaline earth metals present on the coal (25) which are known to be effective catalysts in the carbon-steam and carbon monoxide-steam reactions. It has been suggested that the hydrogen generated accordingly in-situ is more effective since it probably passes transiently through the reactive 'nascent' hydrogen-form and avoids the need to dissociate the strong bond in molecular hydrogen.

The ability to exchange cations on the carboxylic acid groups in brown coal (26) has led to interest into the effectiveness of transition metals exchanged onto the carboxyl groups as catalysts. This aspect was first looked at by Severson and his colleagues in North Dakota with negative results (27). However, the matter is now being re-examined in Australia in the context of Victorian brown coals. Careful studies in this area could well help contribute to the better understanding of the role of the catalyst in coal hydrogenation, e.g. does it facilitate the direct transfer of hydrogen from molecular hydrogen in the gas phase, or in solution, to the fragments derived from the thermally decomposing coal? or does it simply facilitate in the regeneration of the hydrogen donor capacity of the 'solvent'?

It is appropriate to conclude this section by reference to one aspect of the CSIRO flash pyrolysis project involving, again, brown coals. Here, it has been shown (28) that the presence of cations on the carboxyl groups strongly suppresses the tar yield obtained during rapid pyrolysis, although the total conversion to volatile products appears to be unaffected. For example, a sample of raw Gelliondale (Victoria) brown coal having a 7.2% (dry basis) ash yield, yielded 12% (dry ash-free basis) of tar during flash pyrolysis but, when this coal was acid washed 0.7% (dry basis) ash yield, the tar yield increased to 20% (dry ash-free basis). Further reference to Fig. 6 shows that the latter tar yield now plots with the bituminous coals with reference to the effect of the atomic H/C ratio. Similarly a second brown coal sample (Loy Yang) which, as recovered from the seam, has a very low ash yield (0.4% dry ash-free basis), and most of the carboxyl groups in the acid form, plots with the bituminous coals in Fig. 3; however, when the sodium-salt is produced from this coal before flash pyrolysis the tar yield is almost completely suppressed.

It is interesting to speculate on the significance these observed effects of the presence of cations on the carboxylic acid groups in brown coals. It would appear that the cations either inhibit the tar forming reactions in some way or else cause the tars, once formed, to break down to more volatile components with no solid residue since the total volatile matter yield is independent of whether the carboxyl groups are in the salt- or acid-form. The former possibility appears to be more plausible which, in turn, implies that the tars are formed from lower molecular weight precursors by reactions which are blocked by the presence of a cation, or cations, on the carboxyl groups. The clue to the detailed explanation perhaps resides with the observations, already mentioned, of Schafer (24) on the effects of cations associated with carboxyl groups on the oxygen elimination reactions during the thermal decomposition of brown coals.

Further detailed studies in this area are obviously needed to resolve the chemistry involved. Such pyrolysis studies supplemented by hydrogenation experiments with acid-form and salt-form brown coals offer promise of resolving the precise role of pyrolysis in the hydrogenation of these coals and of how the ash-forming cations participate in the hydrogenation reactions. For example, how does the presence of the cations effect the hydrogen consumption? A question that needs also to be considered in the context of the observations of White (18).

CONCLUDING REMARKS

The first part of this paper has shown that Australian black and brown coals differ significantly in a number of respects from coals of similar ranks from North

America and elsewhere in the northern hemisphere. The rest of the paper then proceeded to indicate the progress being made to determine how the characteristics of Australian coals influence their conversion to volatile and liquid products during pyrolysis and hydrogenation.

The results presented and discussed here for on-going investigations on Australian black coals indicate strongly that, over a rank range up to about 83% (dry ash-free) carbon, the vitrinite and exinite contents and overall, the atomic hydrogen-to-carbon ratio are the important parameters with regard to total volatile and liquid yields during pyrolysis and hydrogenation of such coals. In these respects there appears to be no major differences relative to northern hemisphere coals. The strong dependence of conversion on atomic H/C ratio suggest that the subtleties of variation in chemical composition or structure with change in rank are of secondary importance. Also the near linear dependence of conversion yields on the atomic H/C ratio further suggest that the effects of the mineral matter in the Australian black coals may be secondary.

The results mentioned for Australian brown coals raise many interesting questions concerning the effect of coal characteristics on conversion during pyrolysis and hydrogenation. These relate to the similarity of the behaviour of the acid-form brown coals with the black coals in terms of the effect of the atomic H/C ratio on conversion during pyrolysis; the suppression of the tar yield when the carboxyl groups are in the salt-form; and the elimination of oxygen during the primary hydrogenation without the involvement of hydrogen. Again, within the limitations of the investigations mentioned, there is no reason to believe that the effects observed should be unique to Australian brown coals.

To conclude, it is emphasised that many of the results discussed relate to on-going investigations and need confirmation on other coals. Also, many of the effects mentioned relate to the overall conversion. In coming to grips with the effects of coal characteristics, attention must be given to the quality as well as the quantity of liquid products obtained during conversion; as well as to the rate at which the conversion occurs under various conditions. These aspects, which have not been considered in this presentation, call for careful experimentation where the emphasis is not on maximising conversion but on careful control of experimental conditions with termination of experiments at only partial conversion.

ACKNOWLEDGEMENTS

The author gratefully acknowledges the co-operation and help he has received from the Australian Coal Industry Laboratories (ACIRL), the Melbourne Research Laboratories of the Broken Hill Pty. Ltd., MRL/BHP, the Commonwealth Scientific & Industrial Research Organization (CSIRO), in providing information and data, often unpublished, to assist in the preparation of this paper. In particular, he wishes to thank Dr. N. White (MRL/BHP), Mr. J. Cudmore (ACIRL), and the following former colleagues in CSIRO - Prof. A.V. Bradshaw, Dr. D. Jones, Mr. H. Rottendorf, Mr. H.W. Schafer, Dr. M. Shibaoka, Mr. I.W. Smith, Dr. G.H. Taylor and Mr. R.J. Tyler.

REFERENCES

1. National Energy Advisory Committee (Commonwealth of Australia), "Australia's Energy Resources : An Assessment", Report No. 2, (published by Dept. of National Development), December 1977.
2. R.A. Durie, "Coal Conversion Research in Australia", Paper B1, Third Int. Conf. on Coal Res., Sydney Aust., October 1976.
3. G.H. Taylor and M. Shibaoka, "The Rational Use of Australia's Coal Resources", Paper 8, Institute of Fuel (Australian Membership) Conference on "Energy Management", Sydney, Aust., November 1976.
4. Australian Petroleum Institute, Petroleum Gazette, March 1978, p. 12.

5. E. Stach, M.Th. Mackowsky, M. Teichmüller, G.H. Taylor, D. Chandra, R. Teichmüller, "Coal Petrology", Borntraeger, Berlin 1975.
6. International Committee for Coal Petrology, 2nd Edition, Paris, Centre National de la Recherche Scientifique, 1963.
7. C.H. Fisher, et al., "Hydrogenation and Liquefaction of Coal, Part 2 - Effect of Petrographic Composition and Rank of Coal", Tech. Paper 642, US Bureau of Mines, 1942.
8. P.H. Given, D.C. Cronauer, W. Spackmen, H.L. Lovell, A. Davis, B. Biswas, Fuel, 54, 34, 40, 1975.
9. R.E. Guyot, "Influence of Coal Characteristics on the Yields and Properties of Hydrogenation Products", Aust. Coal Ind. Res. Laboratories, Report PR 78-8, June 1978.
10. J.F. Cudmore, Fuel Processing Technology, 1, 227, 1978.
11. I.W. Smith, R.J. Tyler - CSIRO Division of Process Technology, private communication.
12. G.H. Taylor, M. Shibaoka and S. Ueda - CSIRO Fuel Geosciences Unit, private communication.
13. D. Jones, H. Rottendorf, M. Wilson - CSIRO Division of Process Technology, unpublished results.
14. R.A. Durie and M. Shibaoka - unpublished results.
15. K.McG. Bowling and P.L. Waters, "Fluidized-Bed, Low Temperature Carbonization: Effect of Coal Type on the Yields and Properties of Products", CSIRO Division of Coal Research, Investigation Report 74, September 1968.
16. N.Y. Kirov and T.P. Maher, "The Tailoring of Products from Pyrolysis of Coal", Paper 11, Institute of Fuel (Australian Membership) Conference on "The Changing Technology of Fuel", Adelaide, November 1974.
17. E.H. Boomer, A.W. Saddington, and J. Edwards, Can. J. Res. 13B, 11, 1935.
18. N. White, The Broken Hill Proprietary Co. Ltd., Melbourne Research Laboratories - private communication.
19. D.K. Mukherjee, J.K. Sama, P.B. Choudhury, and A. Lahiri, Proc. Symp. Chemicals and Oil from Coal, CFRI India, 1972.
20. H.R. Brown and D.J. Swaine, J. Inst. Fuel 37, 422, 1964.
21. R.A. Durie, Fuel, Lond. 40, 407, 1961.
22. G.F. Baragwanath, Proc. Aust. I.M.M. (202), 131, 1962.
23. M.S. Burns, R.A. Durie and D.J. Swaine, Fuel, Lond. 41, 373, 1962.
24. H.N.S. Schafer, CSIRO Division of Process Technology, unpublished results.
25. H.R. Appell, I. Wender, and R.D. Miller, "Liquefaction of Lignite with Carbon Monoxide and Water", US Bureau of Mines, I.C. 8543, 1972.
26. H.N.S. Schafer, Fuel, Lond. 49, 271, 1970.

TABLE 1: AUSTRALIA'S FOSSIL FUEL ENERGY RESOURCES (1)

| <u>Resource</u> | <u>Quantity</u> (Demonstrated) | <u>Specific Energy</u> (10 ¹⁸ Joules) | <u>(Percentage)</u> |
|--------------------------|--------------------------------------|---|---------------------|
| Black Coal* | | | |
| In Situ | 36.30 x 10 ⁹ t | 1040 | 69.8 |
| Recoverable | 20.26 x 10 ⁹ t | 580 | 58.9 |
| Brown Coal | | | |
| In Situ | 40.93 x 10 ⁹ t | 400 | 26.8 |
| Recoverable | 39.00 x 10 ⁹ t | 380 | 38.6 |
| Crude Oil and Condensate | | | |
| In Situ | 49.00 x 10 ⁹ bb1 | 29.7 | 1.99 |
| Recoverable | 20.70 x 10 ⁹ bb1 | 12.4 | 1.26 |
| Natural Gas + LPG | | | |
| In Situ | 545 x 10 ⁹ m ³ | 21.0 | 1.40 |
| Recoverable | 327 x 10 ⁹ m ³ | 12.6 | 1.28 |
| Total | | | |
| In Situ | | 1,685.7 | 100 |
| Recoverable | | 1,145.0 | 100 |

*Demonstrated + Inferred in situ black coal resources are estimated to be 5600 x 10¹⁸J with 55% recoverable - inferred resources of crude oil and natural gas are relatively minor representing only 1% and 8%, respectively, of the demonstrated resources.

TABLE 2: PATTERN OF AUSTRALIAN USE OF FOSSIL FUELS 1974-75 (2)

Total primary energy demand 2512 x 10¹⁵J consisting of:
coal 1035 x 10¹⁵J; oil 1318 x 10¹⁵J; natural gas 159 x 10¹⁵J

| | <u>% of Fuel Type</u> | <u>% Total Primary Energy</u> |
|------------------------|-----------------------|-------------------------------|
| <u>Coal</u> | | |
| Electricity generation | 61 | 26) |
| Iron and steel | 25 | 10) 42 |
| Other | 14 | 6) |
| <u>Oil</u> | | |
| Transport* | 61 | 32) |
| Fuel oil | 15 | 8) 52 |
| Other | 24 | 12) |
| <u>Natural Gas</u> | | |
| Electricity generation | 20 | 1) |
| Other | 80 | 5) 6 |

*Includes fuel oil for bunkering

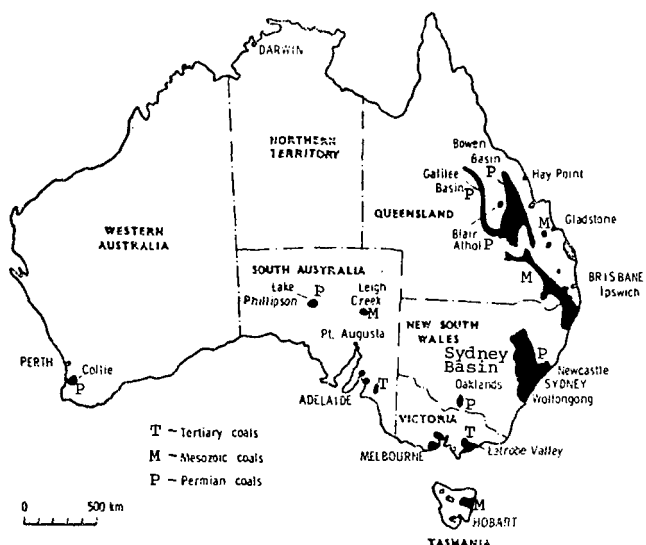


FIG.1. AUSTRALIAN COALFIELDS (3)

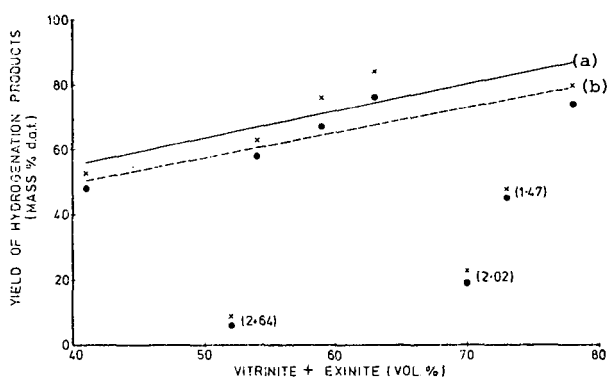


Fig.2. Non catalytic hydrogenation - Product yields versus vitrinite + exinite content. Curve (a) total conversion (x) (b) extract (●) (11)
 Note: Lines (a) & (b) relate to rank range R_0 max. 0.43 - 0.68%. Values in parenthesis refer R_0 max. for higher rank coals.

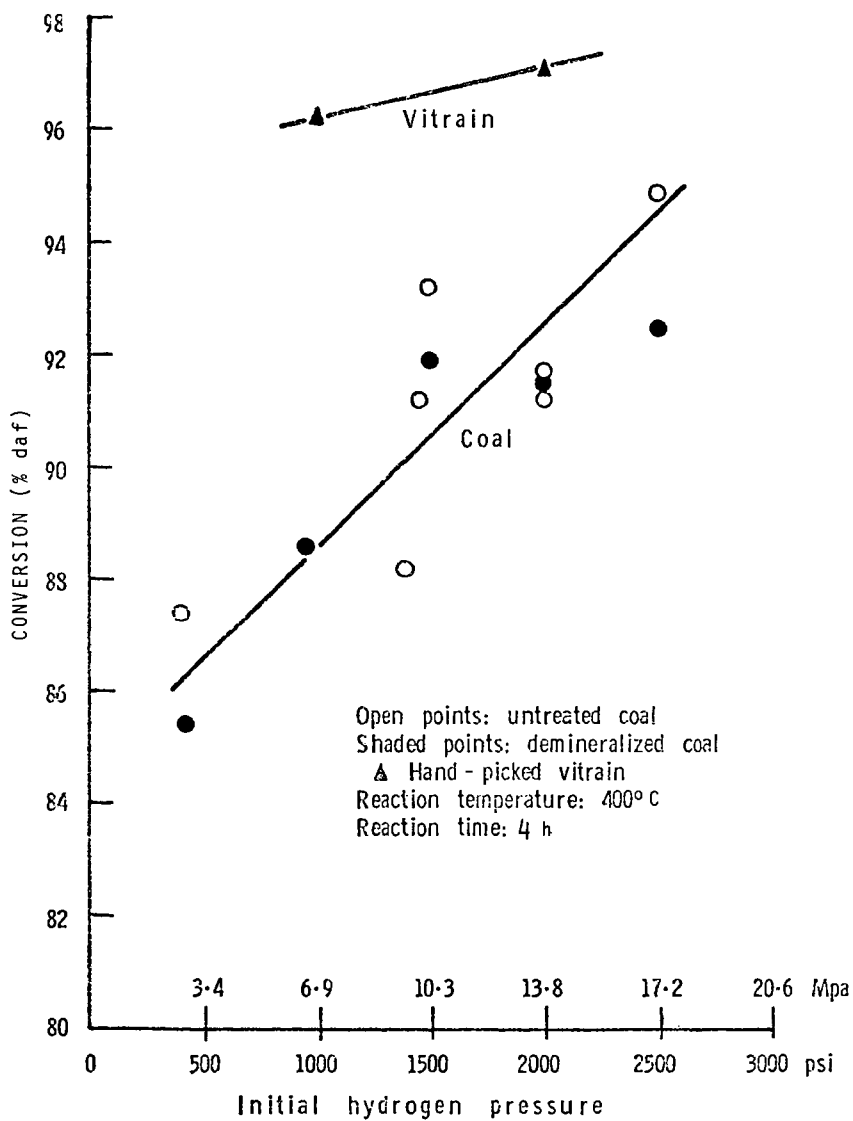


FIG. 3. EFFECT OF HYDROGEN PRESSURE ON CONVERSION OF LIDDELL COAL (13).

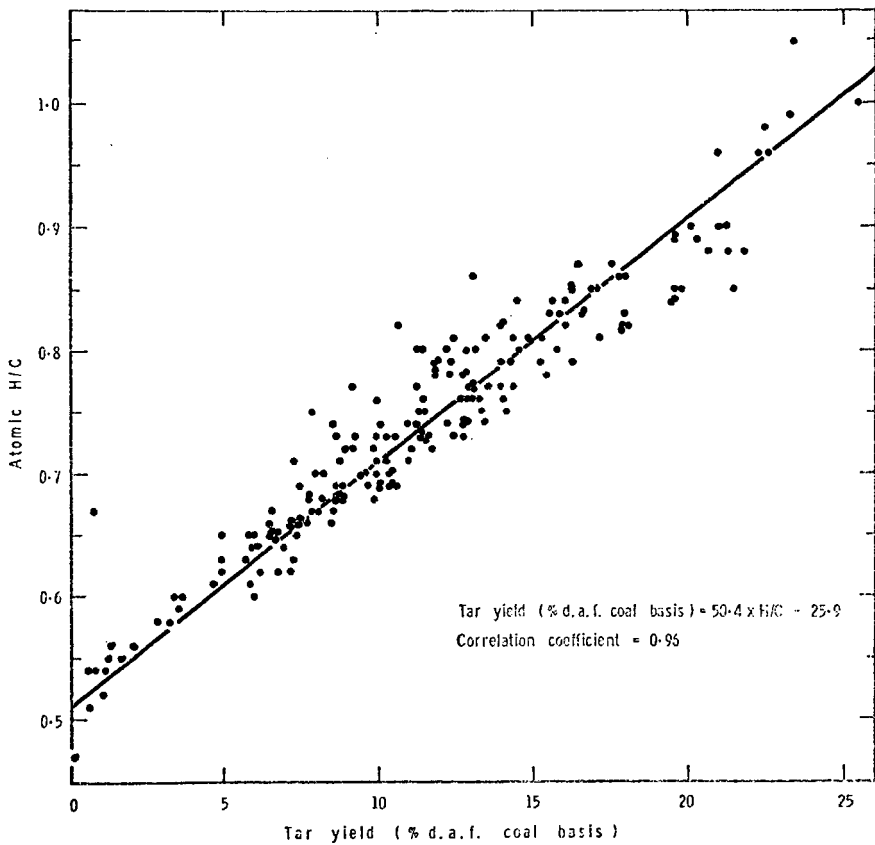


FIG.4 DEPENDENCE OF TAR YIELD, DETERMINED BY LOW-TEMPERATURE GRAY-KING CARBONIZATION ASSAY, ON ATOMIC HYDROGEN-TO-CARBON RATIO FOR A WIDE RANGE OF AUSTRALIAN COALS (14)

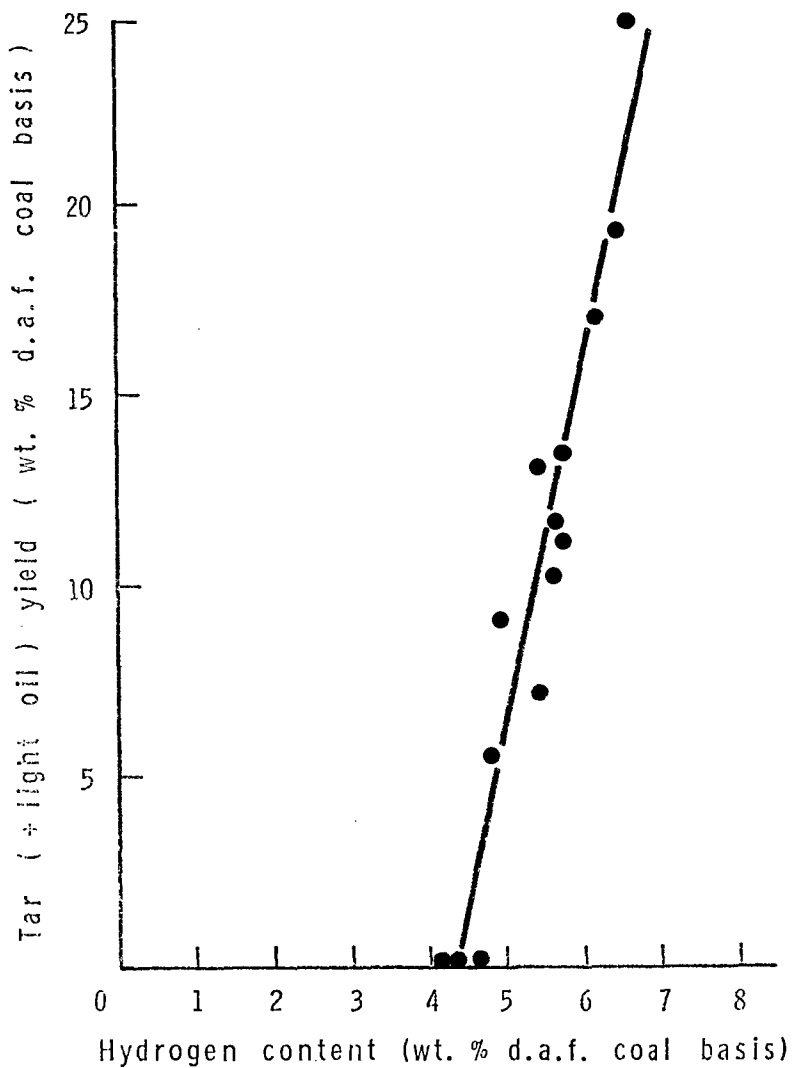


FIG. 5. DEPENDENCE OF TAR YIELDS FROM LOW TEMPERATURE (500°C) FLUIDIZED-BED CARBONIZATION ON HYDROGEN CONTENT FOR SOME AUSTRALIAN COALS (15,16)

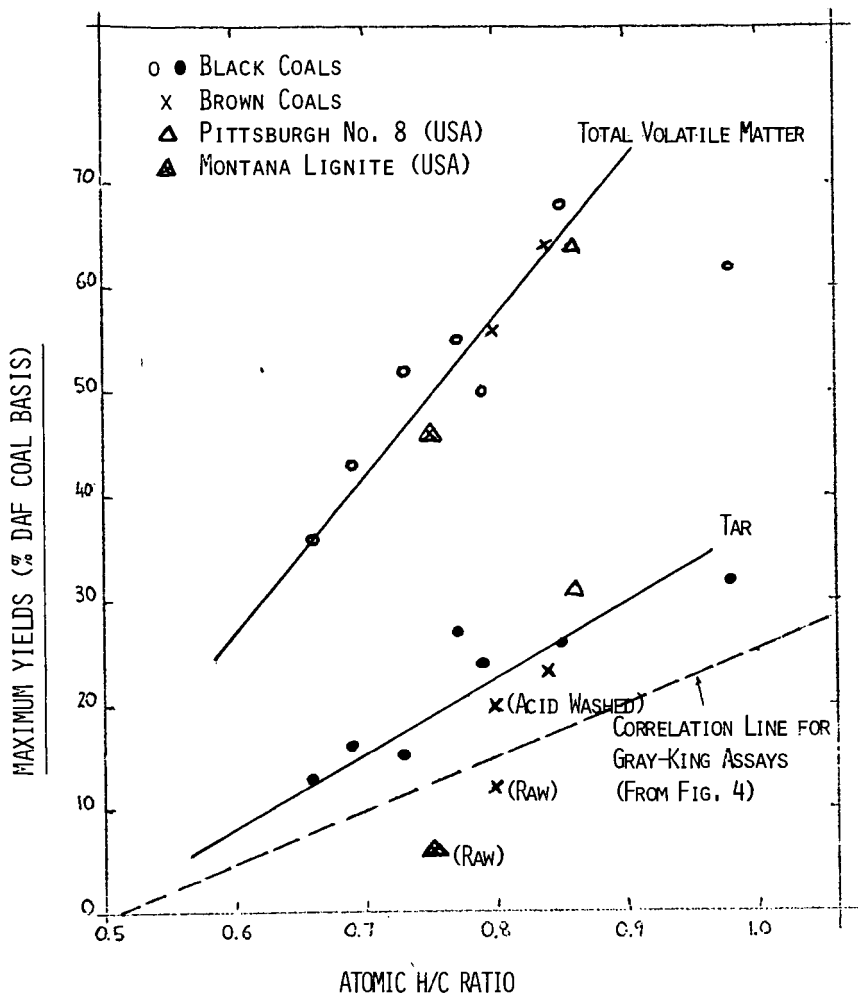


FIG. 6. DEPENDENCE OF MAXIMUM TAR YIELDS AND CORRESPONDING TOTAL VOLATILE MATTER YIELDS DURING FLASH PYROLYSIS ON ATOMIC HYDROGEN-TO-CARBON RATIO FOR SOME AUSTRALIAN AND USA COALS (11,27)

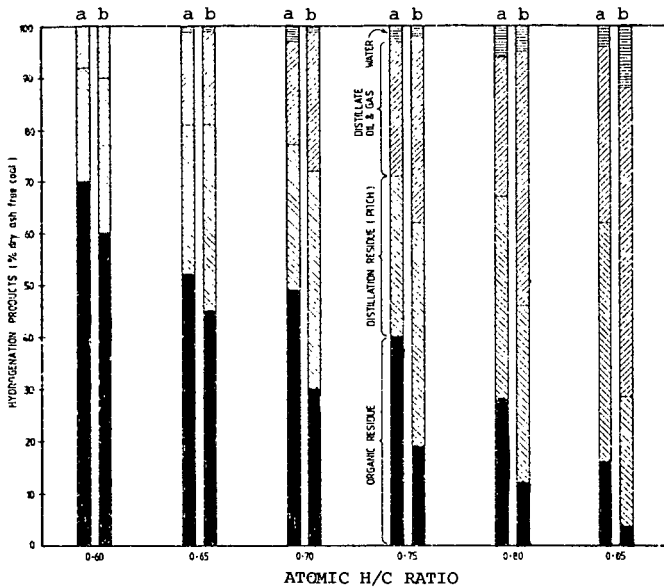


Fig. 7. Dependence of yields of hydrogenation products on the atomic hydrogen-to-carbon ratio.
 (a) Australian coals - non catalytic conditions (10)
 (b) Canadian coals - catalytic conditions (17)

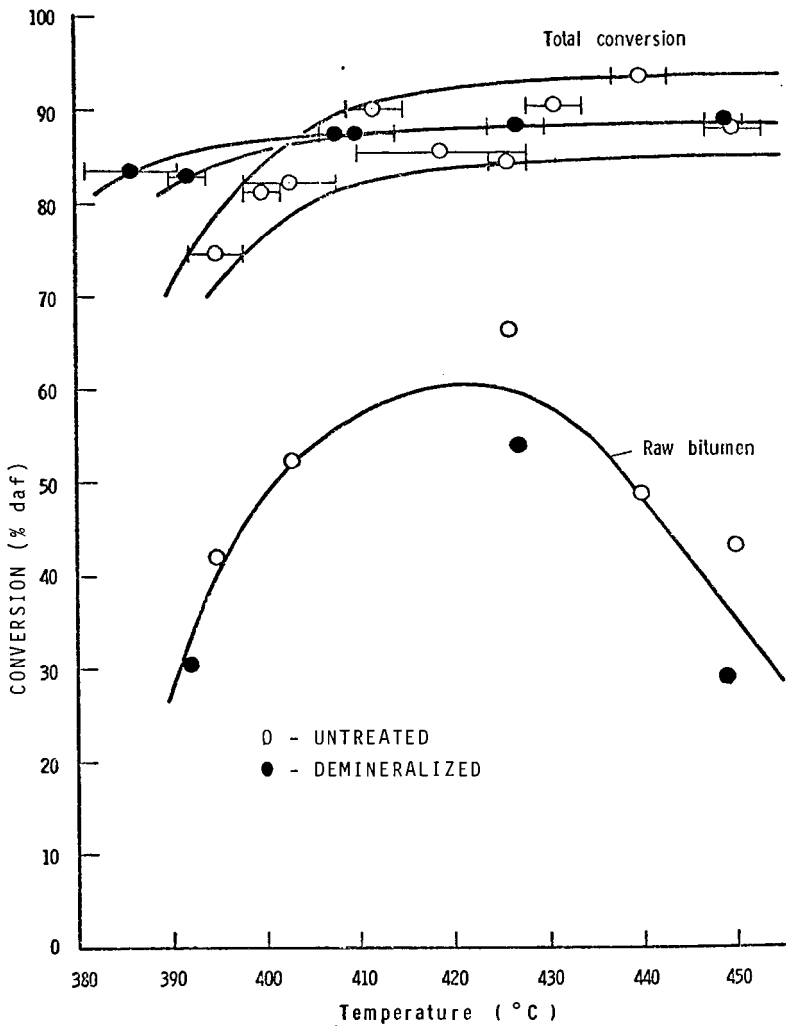


FIG. 8. EFFECT OF TEMPERATURE ON CONVERSION OF UNTREATED AND DEMINERALIZED LIDDELL COAL (13) (300 ml autoclave, 6.9 MPa, 4 h)

RELATIONSHIP BETWEEN COAL CHARACTERISTICS AND ITS REACTIVITY ON HYDROLIQUEFACTION

K. Mori, M. Taniuchi, A. Kawashima, O. Okuma, and T. Takahashi,
Mechanical Engineering Laboratory, Kobe Steel, Ltd., Nada-ku,
Kobe 657, Japan.

INTRODUCTION

The reactivity of coal during hydroliquefaction should be related to the characteristics of coal as are determined by ultimate, proximate and petrographic analyses, etc.

The relationship between the characteristics of coal and its reactivity has been studied by several researchers. As a result, several typical parameters are purported to be in this relationship (1,2,3). Among these parameters, carbon content, mean reflectance, volatile matter, H/C atomic ratio, reactive macerals, etc. are reported to be related to coal reactivity. However, it is generally known that these are usually applied only in limited conditions of hydroliquefaction. Therefore, attempts to find better parameters still continue.

In this study the most closely related parameter to coal reactivity, as represented by conversion, has been selected by liquefying several types of coals covering a wide range from lignite to bituminous coals as well as samples from a narrow range collected at different mining sites. Selected coals from the wide range of rank are located in the coal band shown in Fig. 1. The resulting parameters are compared with other parameters reported by other papers (2,3).

EXPERIMENTS AND RESULTS

The liquefaction of coals was studied in a 500 ml magnetically stirred stainless steel autoclave. Analytical data on coals used in this study are presented in Tables 1 and 2. Hydroliquefaction data on coals used in this study are summarized in Tables 3 and 4.

The experimental methods and procedures were carried out by conventional methods.

Conversion was calculated as follows.

$$\text{Conversion \%} = \frac{\text{Coal charged (d.a.f.)} - \text{Insoluble residue (d.a.f.)}}{\text{Coal charged (d.a.f.)}} \times 100$$

The relations between coal reactivity and several parameters representing coal characteristics are shown in Figs. 2 to 7. In these figures the reactivity of coal is measured by conversion. In the results, volatile carbon % is selected as a more closely related parameter than the common parameters, such as C %, H %, O %, H/C atomic ratio, volatile matter, etc.

Volatile carbon % is defined by the equation as follows.

$$\text{Volatile carbon \%} = \text{C \% (d.a.f.)} - \frac{\text{Fixed carbon \%}}{\text{Volatile matter \%} + \text{Fixed carbon \%}} \times 100$$

This parameter is derived from the following basis. It is generally considered that the first step of coal hydroliquefaction is the thermal decomposition of C-C and C-O bonds, etc. in coal structure. Thus, it is presumed that the volatile matter in coal is closely related, as a parameter to coal reactivity (conversion). But, the amounts of oxygen containing compounds, such as carbon dioxide, water, etc. in volatile matter vary greatly with the rank of coal. Therefore, the carbon % in volatile matter (Volatile carbon %) will be considered as the parameter representing reactivity.

DISCUSSION

It is well known that coal reactivity depends on the solvent, the conditions of hydroliquefaction, and the composition of the coal. Thus, it is desirable that the parameter representing coal reactivity shows essentially the same tendency, despite the conditions of hydroliquefaction. Accordingly comparison of parameters were carried out, using some previously reported results (2,3).

The following results were obtained as shown in the example below. The relationship between conversion and C % in coal (d.a.f.) is shown in Fig. 2. In this figure, the relatively close relationship between conversion and C % is observed, but at the same time it is found also that there are exceptions in this relationship. The behaviour of abnormal coals could possibly be explained by inert content of the coal at the same carbon level. That is, in Yamakawa's data, the inert content of Miike and Yubari coals are lower, while Griffin coal is higher. The same result can be observed in our results. The inert content of Lithgow coal is high. Furthermore, in P. H. Given's data, the lignite sample, PSOC 87 coal deviated considerably from the general tendency. This seems to indicate that this coal was chemically treated (3). It is found also that the consequences of this relationship depend on the conditions of liquefaction and coal quality used (Fig. 2). Thus, C % in coal is not appreciably useful as a parameter. Similar consequences are found in the relationship between conversion and other parameters, such as H %, O % in coal.

The relationship between conversion and the H/C atomic ratio of coal is shown in Fig. 3. In this figure, a good relationship is found to hold in some restricted conditions of liquefaction, but the consequences of this relationship are not general.

The relationship between conversion and volatile matter % (d.a.f.) in coal is shown in Fig. 4. The consequences of this relationship are found to differ greatly from one another in the conditions of liquefaction and the coals used.

The relationship between conversion and volatile carbon % in coal is shown in Fig. 5. According to this relationship as shown in Fig. 5, conversion of almost all coals in our research can be expressed exclusively under the same experimental conditions. It was further found that the effect of a catalyst was larger in coals of lower volatile carbon %. In Yamakawa's data, a fairly good relationship is found except for abnormal coals of high sulphur content (Kentucky No. 11) and of high inert content (Griffin), though the behaviour of Taiheiyo coal can not be explained. In addition, in Given's data, a similar good relationship is found except for an abnormal coal (PSOC 99).

In spite of the differences of liquefaction conditions and coals used, the consequences of this relationship are almost the same except for some abnormal coals. Therefore, it is safe to say that coals of higher volatile carbon % are more reactive than those of lower volatile carbon %. Thus, volatile carbon % seems to be a better parameter to estimate coal reactivity.

The relationship between conversion and the mean maximum reflectance of coal is shown in Fig. 6. In Yamakawa's data, a fairly good relationship is found except for abnormal coals of high inert content (Griffin, Grose valley) and low inert content (Miike). And a similar good relationship is found also in Given's data. However, the consequences of this relationship are the reverse in both cases.

The relationship between conversion and petrographic components % in coal is shown in Fig. 7. In this figure, a good relationship between conversion and reactive macerals % in coals is observed. Furthermore, fairly good relationships between conversion and inert ingredients % in coal are also observed. And the consequences of this relationship are essentially the same in two different liquefaction conditions. Thus, it is concluded that the reactive macerals % or inert ingredients % in coal are better parameters to estimate coal reactivity.

In coals of the narrow range of rank (Morwell brown coal) volatile carbon % and other parameters are in relation to the color tone of brown coal as shown in

Table 2. Thus, the reactivity of Morwell brown coal is roughly represented by the color tone of the coal (lithotype). That is, "Light" coal is more reactive than "Dark" coal.

The experimental results described above seem to demonstrate that volatile carbon % in coal (a new parameter) is very useful as a parameter to estimate coal reactivity. However, further study is necessary to clarify the validity of this parameter.

CONCLUSION

A good correlation between volatile carbon % in coal (a new parameter) and coal reactivity was observed. That is, conversion increases with the increasing volatile carbon %. Further, the effect of a catalyst is larger in coals of lower volatile carbon %. In addition, a similar good correlation between petrographic components % in coal (reactive macerals %, inert ingredients % in coal) and coal reactivity was confirmed. In coals of the narrow range (Morwell brown coal), a lithotype, distinguishing the color tone of the coal, is valuable as a parameter. "Light" coal is more reactive than "Dark" coal.

ACKNOWLEDGEMENT

Victorian brown coals (Yallourn, Morwell) used here and their data on coal characteristics were offered by the Herman Research Laboratory of State Electricity Commission of Victoria, to whom the authors wish to express their appreciation. In addition, they wish to thank Nissho-Iwai Co. Ltd. who kindly acted as intermediary with respect to Victorian brown coals studied.

REFERENCES

- (1) I.G.C. Dryden, Chemistry of Coal Utilization, John Wiley and Sons, New York London, 1962, Supplementary Volume, P.237-244.
- (2) T. Yamakawa, K. Imuta, K. Ouchi, K. Tsukada, H. Morotomi, M. Shimura and T. Miyazu : Preprints, the 13th Coal Science Conference, Japan, October, 1976, P. 40.
- (3) P.H. Given, D.C. Cronaner, W. Spackman, H.L. Lovell, A. Davis and B. Biswas: Fuel, 54, No. 1 (1975) 40 ; O C R R&D Report No. 61 / Int. 9.

Table 1. Analytical data on coals used in the study of the wide range

| Coal type | Coal quality | Ultimate analysis (d.a.f.) | | | | | | | Proximate analysis* | | | Volatile carbon content% | |
|---------------------|--------------|----------------------------|-----|------|-----|-----|-------|-------|---------------------|------|-----------------|--------------------------|--------------|
| | | C | H | O | N | S | H/C | O/C | Moisture | Ash | Volatile Matter | | Fixed Carbon |
| Yallourn brown coal | | 62.4 | 4.2 | 32.6 | 0.6 | 0.2 | 0.800 | 0.392 | 11.4 | 0.8 | 45.5 | 42.3 | 14.2 |
| Taiheiyō coal | | 73.0 | 5.6 | 19.4 | 1.6 | 0.4 | 0.912 | 0.199 | 6.3 | 13.6 | 40.2 | 39.9 | 23.2 |
| Lithgow coal | | 81.5 | 5.1 | 11.0 | 1.6 | 0.8 | 0.744 | 0.101 | 1.7 | 12.1 | 32.6 | 53.6 | 19.3 |
| Miike coal | | 81.5 | 5.7 | 8.3 | 1.3 | 3.2 | 0.832 | 0.076 | 0.7 | 13.4 | 39.8 | 46.1 | 27.8 |

* Equilibrium moisture content

Table 2. Analytical data on Morwell brown coals used in the study of the narrow range

| Coal sample | Coal quality | Ultimate analysis (d.a.f.) | | | | | | | Proximate analysis(dry) | | | Litho-type | | |
|-------------|--------------|----------------------------|------|-------|------|------|-------|-------|-------------------------|-----|-----------------|------------|--------------|--------------------------|
| | | C | H | O | N | S | H/C | O/C | Moisture* | Ash | Volatile matter | | Fixed carbon | Volatile carbon content% |
| A | | 67.05 | 3.70 | 28.36 | 0.58 | 0.31 | 0.656 | 0.317 | 23.3 | 2.4 | 49.4 | 48.2 | 17.66 | Dark |
| B | | 69.36 | 4.12 | 25.45 | 0.82 | 0.26 | 0.713 | 0.275 | 15.2 | 2.3 | 45.8 | 51.9 | 16.24 | Medium Dark |
| C | | 69.82 | 4.45 | 24.49 | 0.92 | 0.32 | 0.765 | 0.263 | 15.7 | 2.7 | 47.3 | 50.0 | 18.43 | Medium Light |
| D | | 69.49 | 4.72 | 24.79 | 0.76 | 0.27 | 0.815 | 0.267 | 14.5 | 2.9 | 53.7 | 43.4 | 24.79 | Light |
| E | | 71.85 | 4.90 | 21.95 | 0.87 | 0.43 | 0.811 | 0.229 | 21.2 | 2.7 | 51.2 | 46.0 | 24.52 | Light |

* Equilibrium moisture content

Table 3. Reaction conditions and results of hydroliquefaction on coals used in the study of the wide range

| Feed Coal | Yallourn coal | Lithgow coal | Taiheyo coal | Mike coal |
|---|--------------------------------|--------------|--------------|-----------|
| Feed Coal (g. as d.a.f.) | 43.9 | 43.1 | 40.1 | 43.0 |
| Solvent* | 150 | 150 | 150 | 150 |
| Catalyst (g) | 0 | 0 | 0 | 0 |
| | Fe ₂ O ₃ | | | |
| | S | | | |
| Hydrogen initial pressure (kg/cm ²) | 60 | 60 | 60 | 60 |
| Reaction Temperature (°C) | 450 | 450 | 450 | 450 |
| Holding Time at Reaction Temp. (hr.) | 2 | 2 | 2 | 2 |
| Conversion** (%) | 28.5 | 55.0 | 41.8 | 58.9 |
| | | | 60.3 | 65.2 |
| | | | | 91.1 |
| | | | | 97.4 |

* Solvent consists of creosote oil and recovered solvent.

** Conversion was calculated by benzene insoluble residue.

Table 4. Reaction conditions and results of hydroliquefaction on Morwell brown coal used in the study of the narrow range

| Feed coal sample | A | B | C | D | E |
|---|--------------------------------|-------|-------|-------|-------|
| Feed coal (g. as d.a.f.) | 37.5 | 37.5 | 37.5 | 37.5 | 37.5 |
| Solvent* | 112.5 | 112.5 | 112.5 | 112.5 | 112.5 |
| Catalyst (g) | 0.54 | 0.54 | 0.54 | 0.54 | 0.54 |
| | Fe ₂ O ₃ | | | | |
| | S | | | | |
| Hydrogen initial pressure (kg/cm ²) | 80 | 80 | 80 | 80 | 80 |
| Reaction Temperature (°C) | 430 | 430 | 430 | 430 | 430 |
| Holding Time at Reaction Temp. (hr.) | 1.0 | 1.0 | 1.0 | 1.0 | 1.0 |
| Conversion** | 59.0 | 75.8 | 81.6 | 87.7 | 80.8 |

* Solvent means creosote oil.

** Conversion was calculated by pyridin insoluble residue.

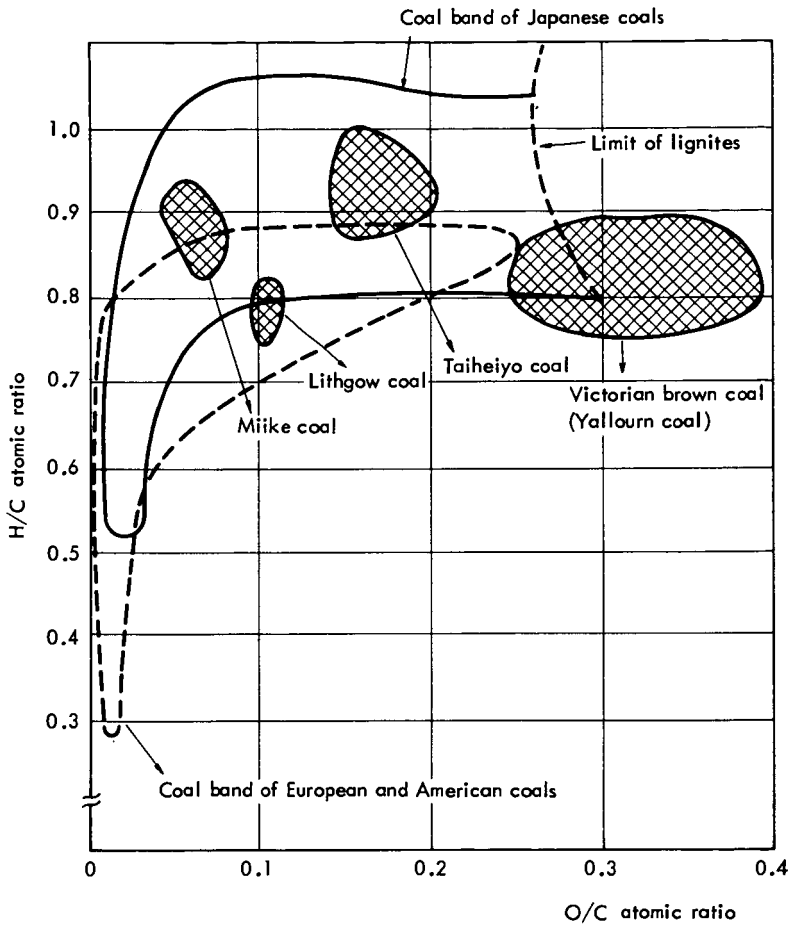


Fig. 1 Relationship between coals used and coal bands

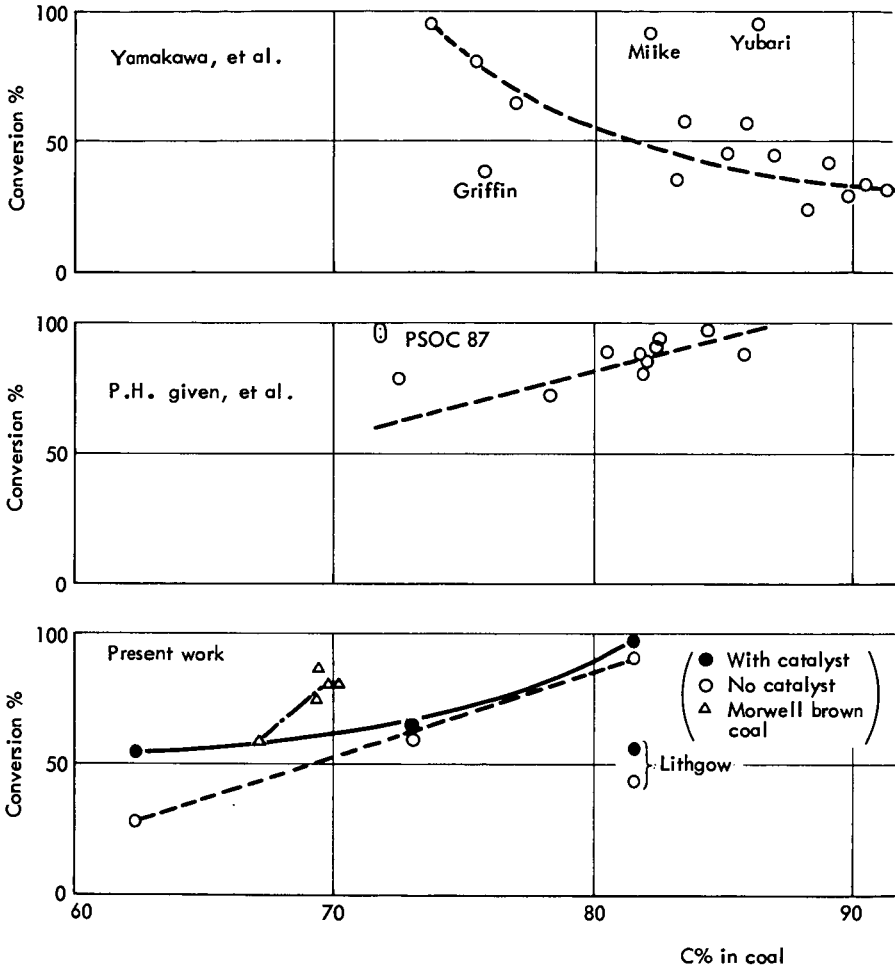


Fig. 2 Relationship between conversion and C% in coal

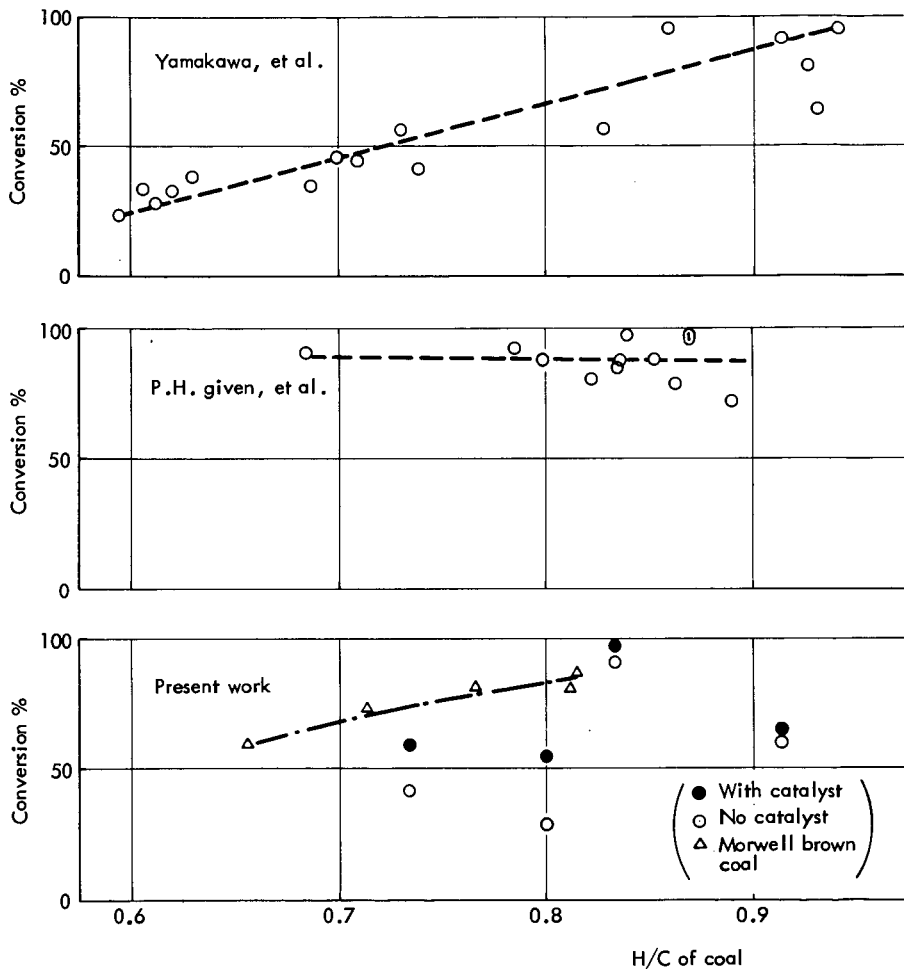


Fig. 3 Relationship between conversion and H/C of coal

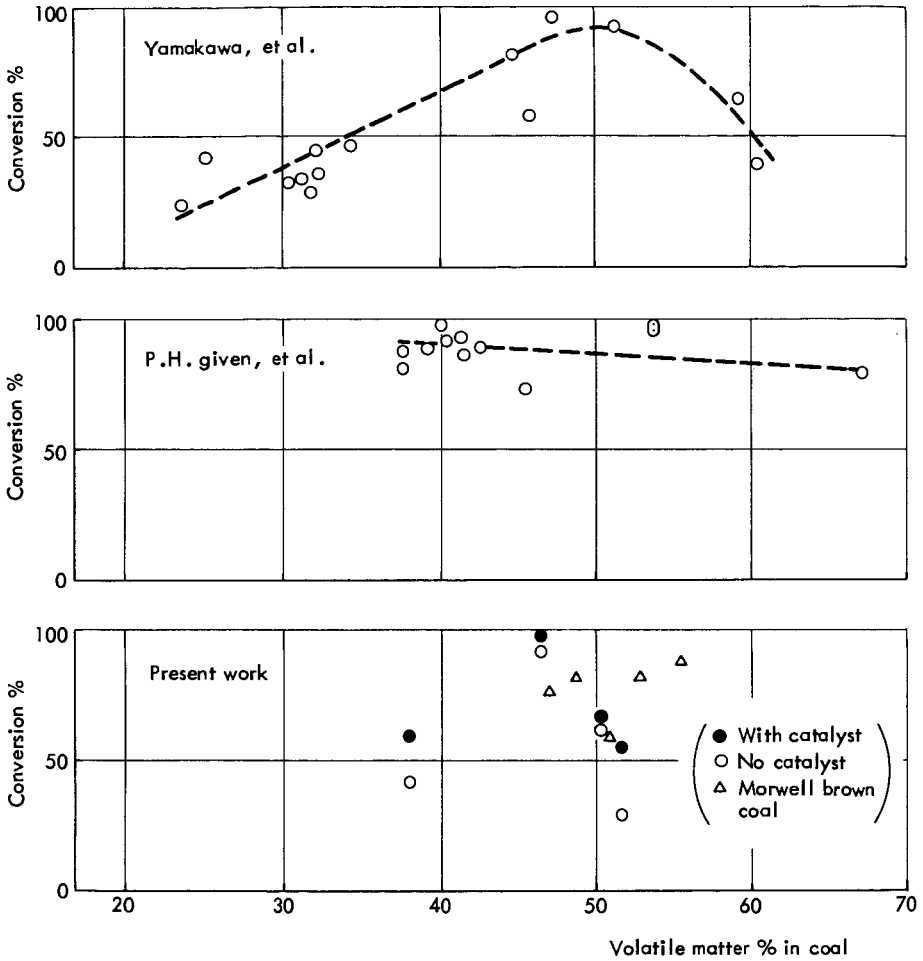


Fig. 4 Relationship between conversion and volatile matter % in coal

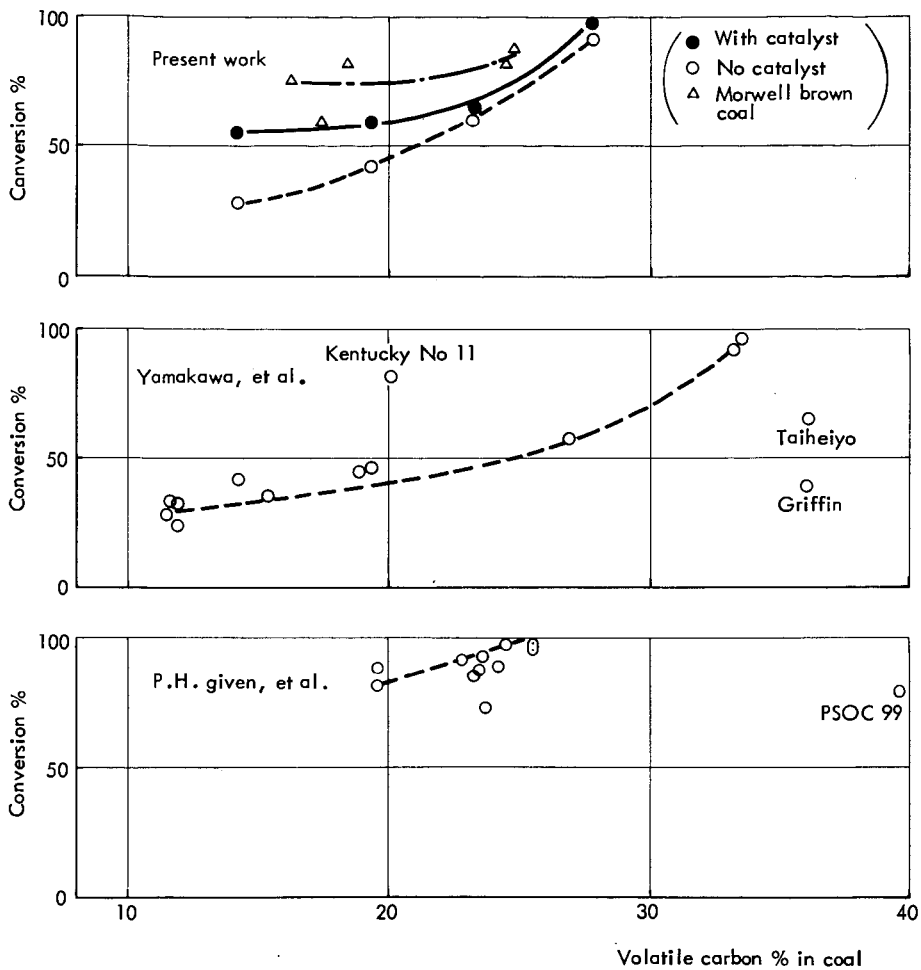


Fig. 5 Relationship between conversion and volatile carbon % in coal

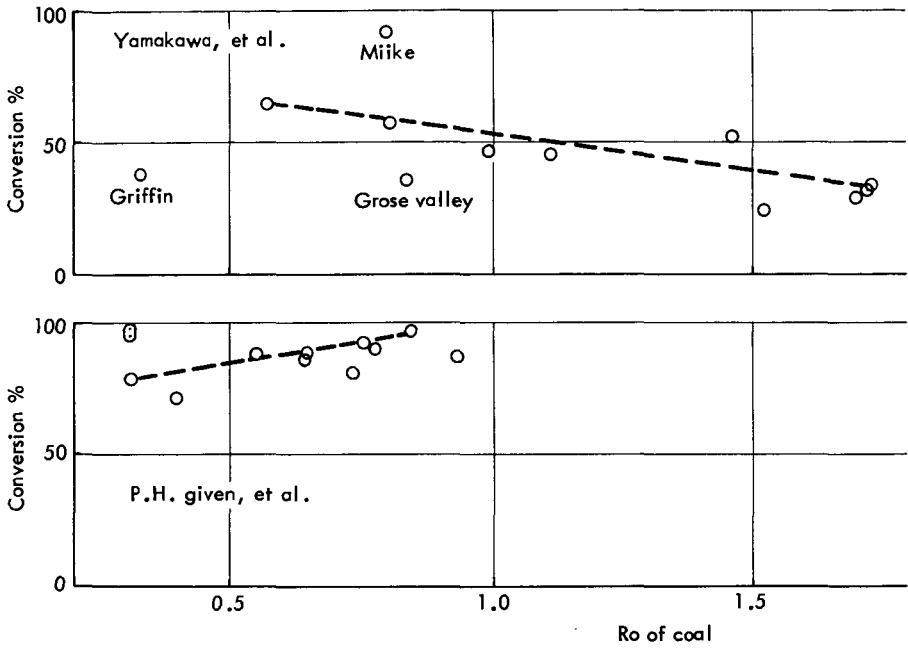


Fig. 6 Relationship between conversion and mean maximum reflectance

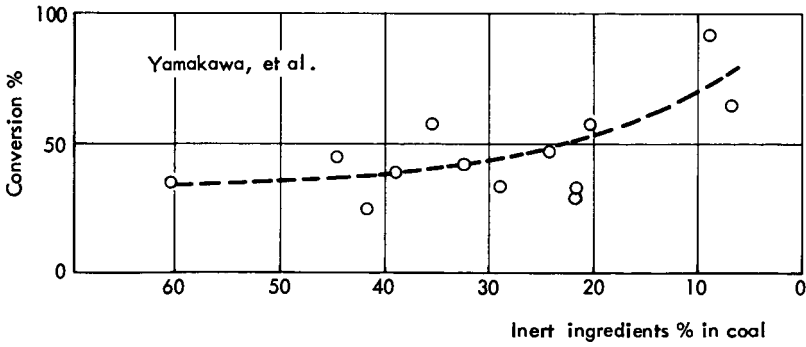
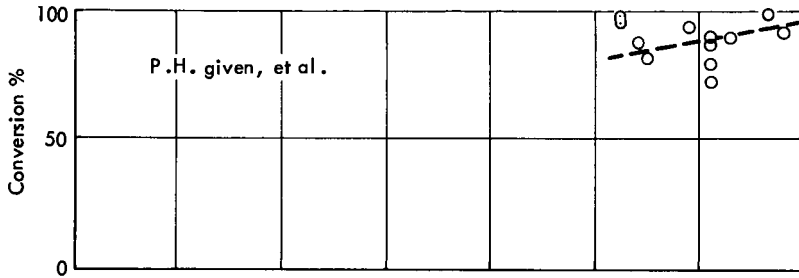
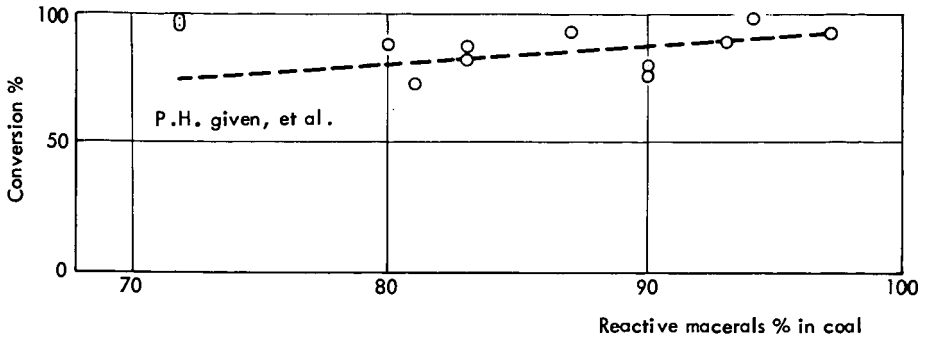


Fig. 7 Relationship between conversion and petrographic components % in coal

STUDIES ON NON-CATALYTIC LIQUEFACTION
OF WESTERN CANADIAN COALS

by

B. Ignasiak, D. Carson, A. J. Szladow* and N. Berkowitz
Alberta Research Council, Edmonton, Alberta, Canada

Though still only very incompletely explored, and subject to major revisions, Canada's coal resources are so extensive as to place this country among the half-dozen most richly coal-endowed nations (1-3). Recent appraisals (Table 1) set ultimate in-place resources in >2 1/2ft thick seams under less than 2500 ft of cover at some 518 billion tons; and preliminary estimates from deeper testhole logs suggest that similar, if not even larger, tonnages may lie in coal occurrences at depths between 2500 and 4500 feet.

But there are wide regional disparities with respect to distribution and coal type.

Except for a relatively small (<500 million ton) lignite deposit in northern Ontario's James Bay area, the Central region (i.e., Quebec, Ontario and Manitoba) which accommodates some 70% of the country's population and the greater part of its industry, is devoid of coal; and the Maritime Provinces (principally Nova Scotia) contain less than 2% of Canada's total coal - mostly Carboniferous hvb coal which closely resembles its Eastern US counterparts.

The great bulk of Canadian coal is concentrated in the three Western provinces (Saskatchewan, Alberta and British Columbia). In this region, it is of Cretaceous and/or Tertiary age, with rank generally increasing in a westerly direction toward the Rocky Mountains. Although contained in different geological formations (which, in Alberta, form three partially overlapping coal zones), the lignites of Saskatchewan thus give way to subbituminous coals in the Alberta Plains, and the latter successively to hvb, mvb and lvb coals in the Mountain regions further west.

Table 1 summarizes latest available data respecting reserves of these classes of coal.

As matters stand, the low-rank coals of Western Canada (as well as some hvb coal in the Maritimes) are now being increasingly used for

* Presently at Pennsylvania State University.

generation of electric energy, and metallurgical (mvb and lvb) coals are being primarily produced for export (notably Japan, though other markets are being developed in Korea, South America and Western Europe). But the large reserves of near-surface subbituminous coals and lignites are also being looked upon as future sources of synthetic fuel gases and liquid hydrocarbons, and could therefore augment production of synthetic crude oils from, e.g., Northern Alberta's oil sands (4).

A notable feature of the Western Canadian coals is their low sulphur content (usually, <0.5%) which tends, however, to be partly offset by higher mineral matter contents than are associated with the Eastern coals. As well, the bituminous coals in the mountain belts are typically deficient in vitrinite, which often represents less than 50% of the coal "substance" and only occasionally reaches 70-75%, but this is compensated by the fact that micrinites and semifusinites tend to be "reactive" constituents when the coals are carbonized. Notwithstanding their low fluidity (rarely >1000 dd/min), Western mvb coals therefore make excellent metallurgical cokes when carbonized in suitably proportioned blends.

But, perhaps reflecting their unique petrographic make-up as much as a more basic chemistry which may set them apart from their Carboniferous equivalents, the Western coals also tend to respond differently to, e.g., oxidation and the action of solvents on them. Air-oxidation at 150°C, instead of developing acid oxygen functions, incorporates much of the chemisorbed oxygen in carbonyl groups, and solubility in CHCl_3 (after shock-heating to ~400°C) is substantially smaller than the FSI would lead one to expect from correlations for Carboniferous coals (5).

These, and other, behaviour differences have prompted initiation of several exploratory studies in order to elucidate the response of selected Western coals to liquefaction procedures, and the parameters that affect this response. This paper summarizes some of the more important observations recorded in the course of that work.

1. Liquefaction (Solubilization) by Interaction with H-Donors

To test initial solubilization, ~5 gm samples were reacted with 10-15 gm of tetralin at $390 \pm 2^\circ\text{C}$ and autogenic pressures in helium-purged, sealed heavy-duty Pyrex capsules which were inserted into a stainless steel bomb charged with ~30 ml tetralin in order to counterbalance the pressures generated in the capsules. Reactions were carried to completion over 4 hrs, after which the capsules were cooled to room temperature and opened in a manner that permitted quantitative analysis of all reaction products (including gaseous products).

In one series of experiments, residual tetralin was removed by heating the solvolyzed samples at $70-80^\circ\text{C}$ in vacuo (~0.05 mm Hg) to constant weight, and yields of non-volatile products and their solubilities in pyridine and in benzene were determined.

The solubilities thus recorded for 13 Western (Cretaceous) coals (with 69.6-91.5% carbon, daf) and 8 Carboniferous coals (80.6-90.9% C, daf) are shown in Figure 1, and indicate that

- (a) the pyridine-solubilities of reacted Carboniferous subbituminous and bituminous coals are significantly higher than those of corresponding Cretaceous coals, and
- (b) strongly caking Carboniferous coals (with 86-88% C, daf) tend to generate substantially more benzene-soluble matter under the reaction conditions of these experiments.

What is, however, still unclear is whether these effects arise solely from different chemical compositions (and molecular configurations) or are also, at least in part, a consequence of the Cretaceous coals generally containing almost twice as much mineral matter as the Carboniferous samples.

2. The Role of Ether-Linkages in Solubilization of Low-Rank Carboniferous Coals by H-Donors

There is some consensus that formation of asphaltenes in the early stages of solubilization of low-rank bituminous coals results from cleavage of open ether-bridges (6). But while the presence of such configurations in high- and medium-rank bituminous coals is well established (7), their existence in less mature coals remains to be unequivocally demonstrated. From reactions of low-rank bituminous coals with sodium in liquid ammonia or potassium in tetrahydrofuran, it has, in fact, been concluded that open ether-bonds are absent (8) or only present in negligible concentrations (9).

The failure to detect open ether-linkages through treatment with Na/liq. NH₃ could, of course, be due to formation of non-cleavable phenoxides (10). We note, in this connection, that low-rank coals, which contain much "unreactive" oxygen, are also characterized by relatively high concentrations of hydroxyl groups, and some "unreactive" oxygen could therefore be quite reasonably associated with phenoxy phenol configurations. However, whereas phenoxy phenols would be expected to resist cleavage by hydrogen-donors, low-rank coals are, as a rule, most easily solubilized by them; and in view of this seeming inconsistency, we thought it pertinent to reexamine the behaviour of oxygen-linkages during interaction with H-donors.

The reactions were carried out under the same conditions as solubilization (see sec. 1), except that a constant 2:1 donor:substrate (molar) ratio was used; and in some tests, 1,2,3,4-tetrahydroquinoline was employed instead of tetralin. The results obtained with different ethers are summarized in Table 2.

Detailed discussion of these findings will be presented elsewhere, and here we only wish to point out that responses to a hydrogen donor

tend to be quite critically affected by very minor structural differences (as well as by possible copolymerization of donor and substrate). Thus, while diphenyl ether remains substantially unaffected by exposure to a donor, its hydroxy-derivatives (phenoxy phenols) often display fairly high reactivity. Taken in conjunction with the failure of low-rank coals (7) and phenoxy phenols (10) to suffer reductive cleavage when treated with sodium in liquid ammonia, this lends some support for the existence of phenoxy phenol entities on these coals.

Other observations, however, indicate that this notion will require more direct evidence before it can be accepted.

The inertness of phenols and phenoxy phenols toward Na/liq. NH_3 can be attributed to the fact that phenols are powerful proton-donors in this system; and resistance of the resultant anions toward reduction is believed to result from stabilization by resonance (10). While alkylation of low-rank coals before treatment with Na/liq. NH_3 therefore offers means for establishing the presence of phenoxy phenol ethers in them, an alternative is afforded by the observation that some phenols can be reduced by concentrated solutions of lithium (11): if this latter reaction also reduces phenoxy phenols in coal, a second treatment should then cause ether-cleavage.

We found, however, that even highly concentrated lithium (9M) or sodium (3M) solutions did not reduce coal so that subsequent treatment increased its hydroxyl content; and in parallel tests, 100% unreacted p-phenoxy phenol was always recovered from the lithium solutions.

The failure to cleave p-phenoxy phenol by reduction and subsequent scission of the ether-bond prompted us to examine the possibility of splitting the C-O bond in the alkylated molecule (12). Attempts to alkylate p-phenoxy phenol with $\text{C}_2\text{H}_5\text{Br}$ after treatment with lithium in liquid ammonia proved uniformly abortive; but ethylation in Na/liq. NH_3 yielded nearly 50% of the ethylated product, and ethylation in K/liq. NH_3 led to quantitative conversion - with ~40% of the reaction product recovered as p-diethoxybenzene. Protonation instead of ethylation furnished ~45% of p-dihydroxybenzene. In the light of these results, we believe that the ether-bond in phenoxy phenols can be cleaved without prior alkylation, and consider it significant that treatment of low-rank coal (or of a vitrinite fraction from such coal) with variously concentrated solutions of potassium in liquid ammonia did not cause an increased -OH content in the reacted material. Nor was the hydroxyl content affected by such treatment after prior exhaustive methylation of the coal with dimethyl sulphate and K_2CO_3 in acetone (13).

It appears to us therefore that cleavage of ether-bonds contributes little to solubilization (and consequent reductions of the molecular weight) unless the coal contains an appreciable proportion of open oxygen linkages in the form of dialkyl ethers. And since there are indications that such structures are generally absent (14) one might tentatively conclude that molecular weight reductions during solubilization by H-donors

accrue primarily from C-C bond scission or from structural realignments associated with elimination of oxygen. It should be possible to test this by measuring molecular weight distributions in H-donor liquefied and non-destructively solubilized coal products (see sec. 3).

3. Non-Destructive Solubilization of Low-Rank Bituminous Coal

Present methods for solubilizing coal (including reductive alkylation in tetrahydrofuran (15) or liquid ammonia (8)) entail cleavage of oxygen ethers, scission of C-C bonds in certain polyaryl-substituted ethylenes and, in the case of reactions in tetrahydrofuran, extensive elimination of hetero-atoms (16).

We therefore draw attention to a novel technique which allows solubilization of coal without rupture of covalent bonds. This method utilizes the fact that the acidity of low-rank coals, which is thought to be largely due to their high -OH contents, can be enhanced by proper choice of a medium.

We selected liquid ammonia because of its pronounced solubilizing characteristics and powerful ionizing properties. At -33°C and atmospheric pressure, the pK_a -value for auto-ionization of liquid ammonia [$2\text{NH}_3 \rightleftharpoons \text{NH}_2^{\ominus} + \text{NH}_4^{\oplus}$] is 34; and since the equivalent value for water is only 14, many substances (with pK_a -values between 14 and 34) which are neutral in water should be capable of splitting off protons in liquid ammonia. Acidic properties in liquid ammonia can be further enhanced by increasing the concentration of NH_2^{\ominus} at the expense of protonic NH_4^{\oplus} ; and this can be achieved by adding potassium and/or sodium amides which will then also form the respective coal "salts".

To test this approach, ~ 5 g samples of low-rank vitrinite, each -300 mesh (Tyloer) were stirred for 6 hrs in liquid ammonia (150 ml; -33°C) containing ~ 5 gms of potassium amide and ~ 5 g of sodium amide. (The amides were formed in the medium, before introducing the coal, by action of anhydrous ferric oxide (1 g) or ferric chloride (1.5 g) on alkali metals.) Thereafter, 100 ml of anhydrous ethyl ether was added, the suspended coal material ethylated with $\text{C}_2\text{H}_5\text{Br}$ (32 ml), and the reaction mixture stirred until all ammonia and ether had evaporated. Following acidification of the residue with 10% HCl, the product was thoroughly washed with distilled water, dried at $70-80^{\circ}\text{C}$ in vacuo (0.05 mm Hg) and analysed. Table 3 summarizes the results of three consecutive alkylations, with each datum being the average of four independent test runs. The initial ethylation introduced 7-8 ethyl groups/100 C atoms into the coal, and the results of the second and third ethylations indicate that essentially only -OH groups were ethylated at this stage. Overall, however, over 50% of ethyl groups introduced into coal were not linked to hydroxyl functions. Since in higher-rank vitrinites no atoms other than hydroxyl-oxygens are susceptible to ethylation by this procedure, it is tentatively concluded that acidic carbon atoms exist only in low-rank coals.

The most interesting outcome of this work is the observation that low-rank vitrinites can be rendered substantially soluble in chloroform and pyridine by alkylating coal salts formed in a non-reducing medium and under conditions that effectively preclude cleavage of covalent bonds.

The solubility of coal treated as above can be further enhanced by introducing longer alkyl chains. While, on reductive alkylation, this could lead to dimerization and formation of other by-products, non-reductive alkylation is not accompanied by such side-effects. Moreover, because of a significant reduction in the number of acidic sites, acid-base associations are also essentially excluded, and the alkylated product should, therefore, be amenable to GPC fractionation. Such fractionation, conducted on Bio Beads S-X1 and S-X2, results in separation by molecular weight and indicates that both benzene and chloroform extracts contain substantial amounts of high (~6000) and fairly low (560-640) molecular weight fractions (Figure 2). While the extract yields from non-reductively ethylated vitrinite increase in the order benzene extr. → chloroform extr. → pyrid. extr., the molecular weights, determined by VPO in pyridine, decrease in this order.

Figure 3 shows GPC fractionation of the benzene extract of a vitrinite which, before a single non-reductive ethylation, was treated with tetrahydronaphthalene at 390°C. Although solvolysis reduced the -OH contents (from 4.9 to 1.7%), non-reductive alkylation increased the benzene-solubility of the solvolyzed material from 53% to 80.2%. It appears that this effect is due to ethylation of acidic carbon atoms.

The existence of a substantial number of acidic carbons in a product obtained by thermal treatment of a vitrinite in a reducing medium at 390°C, but absence of such carbons in higher-rank coals raises an interesting question about the role of temperature in coalification.

Analysis of the results presented in Figures 2 and 4 appears to indicate that solvolysis of the vitrinite is also accompanied by polymerization (see pyridine extract, Figure 4). If this can be confirmed, it would be worth investigating whether it involves specific fractions in the original vitrinite or has a random character. Solvolysis of different molecular weight fractions of a non-reductively alkylated vitrinite (or coal) may furnish some insight.

References

1. Ruedisili, L. C. and Firebauch, M. W., Perspectives on Energy, New York-Oxford University Press - London - Toronto, 1975.
2. Reserves of Coal - Province of Alberta, Energy Resources Conservation Board, Calgary, Alberta, Canada, T2P 0T4, Dec. 1976.
3. 1976 Assessment of Canada's Coal Resources and Reserves; Energy, Mines & Resources, Canada, Report EP 77-5.

4. Berkowitz, N. and Speight, J. G., Fuel, 1975, 57, 138.
5. Berkowitz, N., Fryer, J. F., Ignasiak, B. S. and Szladow, A. J., Fuel, 1974, 53, 141.
6. Takegami, Y., Kajiyama, S. and Yokokawa, C., Fuel 1963, 42, 291.
Whitehurst, D. D., Farcasiu, M., Mitchell, T. O. and Dickert, J. J.,
The Nature and Origin of Asphaltene in Processed Coals.
EPRI AF-480 (Research Project 410-1), July 1977.
7. Lazarov, L. and Angelova, G. Fuel 1968, 47, 333.
8. Ignasiak, B. S. and Gawlak, M. Fuel 1977, 56, 216.
9. Wachowska, H. and Pawlak, W. Fuel 1977, 56, 422.
10. Tomita, M., Fujita, E. and Abe, T. J. Pharm. Soc. Japan 1952, 72,
387;
Tomita, M., Fujita, E. and Niva, H., ibid. 1952, 72, 206.
11. Harvey, R. G., Synthesis 1970, No. 4, 161.
12. Tomita, M., Fujita, E. and Murai, F. J. Pharm. Soc. Japan 1951,
71, 226 and 1035;
Tomita, M., Inibushi, Y. and Niva, H., ibid. 1952, 72, 211.
13. Briggs, G. C. and Lawson, G. J. Fuel 1970, 49, 39.
14. Pugmire, R. J., personal communication.
15. Sternberg, H. W., Delle Donne, C. L., Pantages, P., Moroni, E. C.
and Markby, R. E. Fuel 1971, 50, 432.
16. Ignasiak, B. S., Fryer, J. F. and Jadernik, P. Fuel 1978 (in press).

Table 1. Ultimate in-place coal resources in Canada (Energy, Mines & Resources, Canada, Report EP 77-5, 1976 Assessment)

| Region | In-place, billion tons | Principal coal type |
|--------------------|------------------------|---------------------------|
| Maritime Provinces | | |
| Nova Scotia | | |
| New Brunswick | 1.7 | hvb (Carb.) |
| Western Region | | |
| Saskatchewan | 38.8 | lignite (Tert.) |
| Alberta* - Plains | 360.0 | subbit. (U.Cret. & Tert.) |
| Foothills | 10.0 | lvb, mvb, hvb (Cret.) |
| Mountains | 30.0 | lvb, mvb, hvb (Cret.) |
| British Columbia | 77.8 | mvb, lvb (Cret.) |
| | | subbit. (Tert.) |
| Canada Total | 518.3 | |

*After Energy Resources Conservation Board, Report 77-31, December 1976

Table 3. Non-reductive ethylation of Carboniferous vitrinite*
In liquid ammonia

| | Ethyl groups Intr. per 100 mg Cat. | Chloro- form Solub- ility | Pyrioline Solubility | Ult. analysis No of hydro- (daf) xyl groups %C %H %N per 100 mg Cat. | | | |
|----------------|--|------------------------------------|-------------------------|---|-----|-----|--------------------|
| | | | | %C | %H | %N | per 100 mg Cat. |
| I Ethylation | 7-8 | 25 | 45-50 | 81.0 | 6.3 | 1.6 | 2.8 |
| II Ethylation | 8-9 | 45-50 | 55-60 | 81.3 | 6.8 | 1.8 | 2.0 |
| III Ethylation | 9-10 | 55-60 | 60-65 | 81.1 | 7.0 | 1.5 | 1.1 |

*Solubilities of untreated vitrinite: CHCl_3 - 1%; C_5NH_5 - 13%;

Elemental analysis of untreated vitrinite (daf): 80.8%C; 5.2% H;
1.5%N; 0.9% S; 5.0% O_{OH}

Table 2 Reactions of ethers with tetrahydronaphthalene and tetrahydroquinoline at 385°C

| Ether | Structure | 1,2,3,4 Tetrahydronaphthalene | | | | | 1,2,3,4 Tetrahydroquinoline | | | | |
|---------------------------|-----------|-------------------------------|---------------------------------|--------------------------------------|---|--------------------------------|-----------------------------|---------------------------------|---|--|--|
| | | % of Ether Conversion | Hydrogen Consumption Moles/Mole | Recovery of Tetrahydronaphthalene, % | Reaction Identification | Yield [Molar %] | % of Ether Conversion | Hydrogen Consumption Moles/Mole | Recovery of Tetrahydroquinoline, % | Reaction Identification | Yield [Molar %] |
| dibenzyl ether | | 100 | 0.05 | ~100 | toluene benzene benzaldehyde 1-methylindane | 50 29 16 undetermined | 100 | ~1 | 85 | toluene water 3-methylpyridine (1) ethylbenzene (1) high mol. w. product (3) | 51 10 undetermined undetermined |
| | | - | 0.8 | ~100 | toluene | 70 | - | - | 40 | toluene high mol. w. product (3) | 72 undetermined |
| p(benzyloxy)phenol | | - | 0.75 | ~100 | toluene biphenyl 1-naphthol 2-benzyl-naphthalene | 73 7 74 undetermined | - | - | - | - | - |
| | | 2 | 0.0 | ~100 | 1-methylindane (1) 3 unidentified no GC detectable prods. | undetermined | 0 | 0.0 | ~100 | no GC detectable prods. | - |
| p-phenoxyphe- nol | | 7 | 0.04 | 88 | phenol | 7 | 50 | 62 | phenol o-toluidine (1) high mol. w. product (4) | 43 undetermined | |
| | | 0 | 0.0 | ~100 | none | - | 24 | 73 | high mol. w. product (5) | 90 (2) 90 (2) | |
| m-phenoxyphe- nol | | 0 | 0.0 | 100 | none | - | 0 | 100 | none | - | |
| | | 0 | 0.0 | 100 | none | - | 0 | 100 | none | - | |
| p-phenoxylphenyl furan | | 0 | 0.0 | 100 | none | - | 0 | 100 | none | - | |
| | | 0 | 0.0 | 100 | none | - | 0 | 100 | none | - | |
| 2,3-benzofuran | | 0 | 0.0 | ~100 | 1 unidentified | trace | 0 | 0.0 | ~100 | 2 unidentified | traces |
| dibenzofuran | | 0 | 0.0 | ~100 | 1 unidentified | trace | 0 | 0.0 | 100 | none | - |

1. probably originating from donor
 2. % by weight
 3. elemental analysis of the high molecular weight product unknown
 4. elemental analysis: 82.38C; 7.08H; 4.28N; 0.08S; 0.08 ash; 6.580 (by diff.)
 5. elemental analysis: 79.03C; 6.28H; 1.88N; 0.08S; 0.08 ash; 13.080 (by diff.)

Figure 1. Solubilities after treatment with tetrahydronaphthalene at 390°C for 4 hours

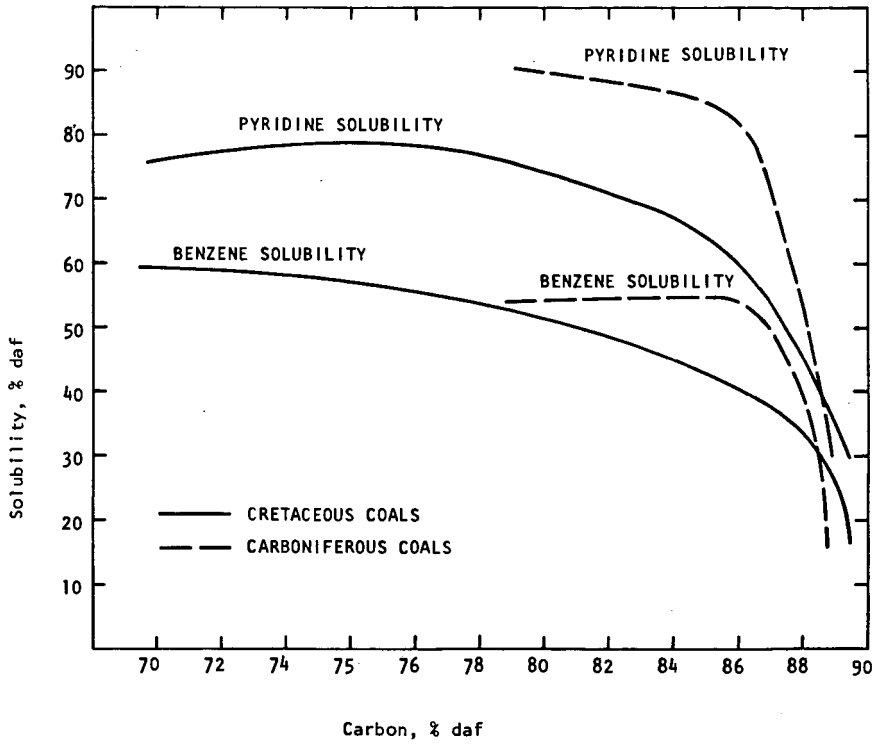
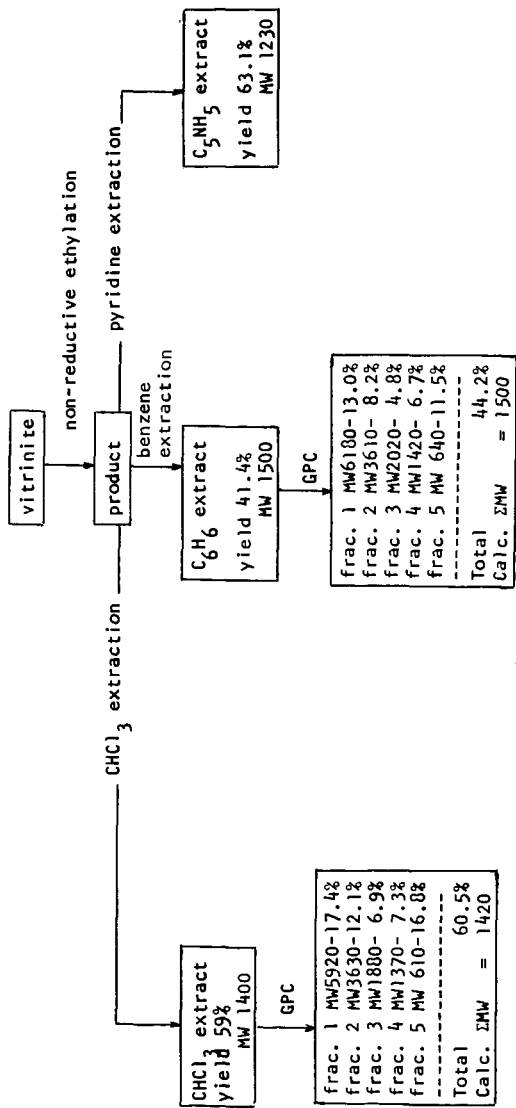
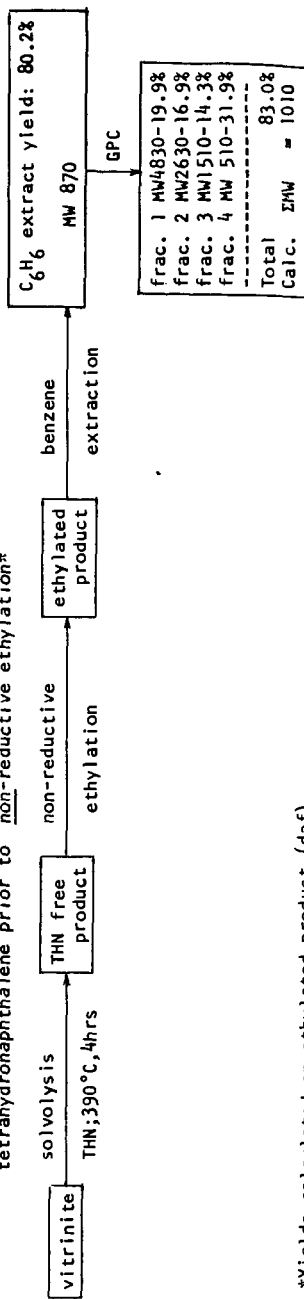


Figure 2. Solubilities and molecular weights of a vitrinite (80.8% C, daf) after non-reductive ethylation*



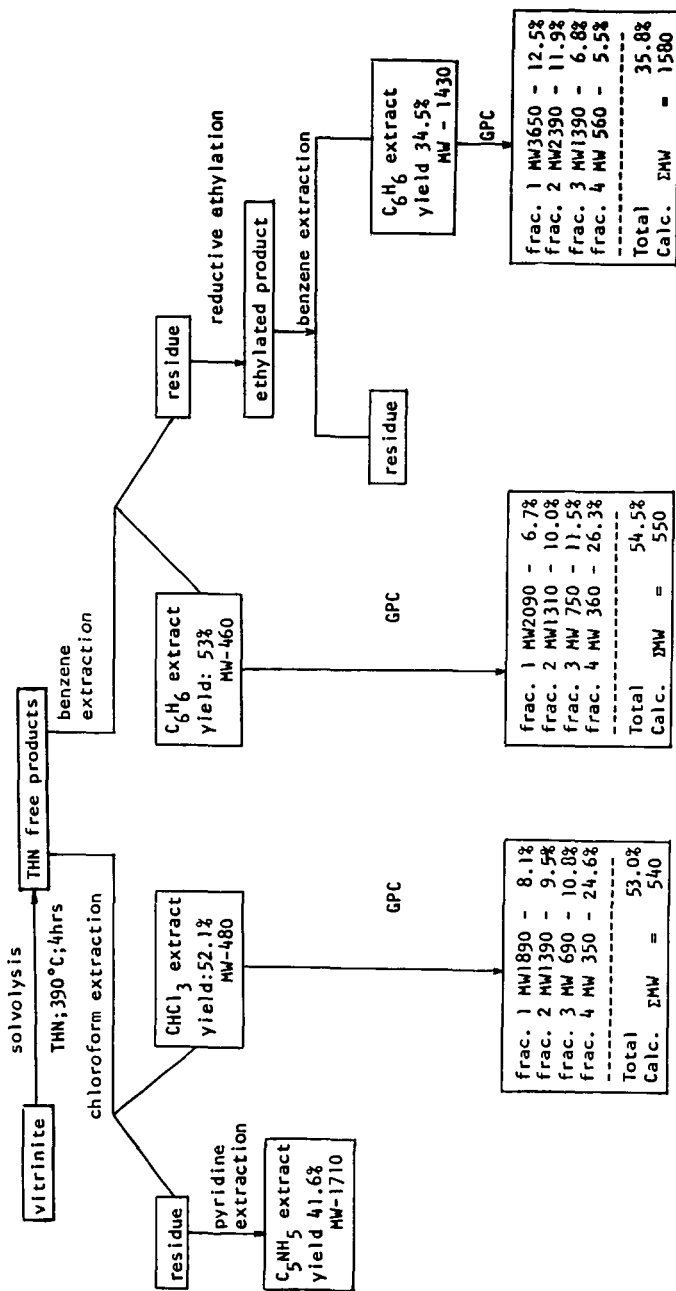
*Yields calculated on ethylated product (daf)

Figure 3. Solubilities and molecular weights of a vitrinite (80.8% C, daf) subjected to solvolysis in tetrahydro-naphthalene prior to non-reductive ethylation*



*Yields calculated on ethylated product (daf)

Figure 4. Solubilities and molecular weights of a vitrinite, subjected to solvolysis in tetrahydronaphthalene*



* Yields calculated on THN free product (daf)

SHORT RESIDENCE TIME COAL LIQUEFACTION

J. R. Longanbach, J. W. Droege and S. P. Chauhan

Battelle's Columbus Laboratories

505 King Avenue

Columbus, Ohio 43201

INTRODUCTION

Based on prior work reported by the Mobil Research and Development Corporation, a two-step coal liquefaction process seems to have potential for savings on hydrogen usage compared to conventional solvent-refined coal (SRC) technology.⁽¹⁾ The first step consists of a short contact time, relatively low temperature, low pressure reaction of coal with a coal derived solvent in the absence of molecular hydrogen. This is followed by a short contact time, high pressure and temperature reaction of the products in the presence of molecular hydrogen. The purpose of the first step is primarily to dissolve the coal. After removal of unreacted coal and mineral matter, the second step is carried out to reduce the sulfur level of the product and to regenerate the solvent. Decreased hydrogen consumption is expected to result from the short contact times and the removal of mineral matter and sulfur before the addition of molecular hydrogen.

EXPERIMENTAL

The apparatus constructed to carry out the experiments consisted of a 1-liter, stirred autoclave (AC1) used to preheat the solvent-coal slurry connected to a 2-liter, stirred autoclave (AC2) equipped with an internal heating coil to bring the solvent-coal slurry rapidly to a constant reaction temperature. The apparatus was later modified by the addition of a third autoclave (AC3) to act as a quench vessel. This allowed direct determination of the material lost in each transfer step and an unambiguous determination of the product yield. Two of the experiments required a high-pressure hydrogen atmosphere. A thermostatted hydrogen cylinder was added with a precise pressure gauge to determine the hydrogen gas balance in these experiments. A drawing of the 3-autoclave apparatus is shown in Figure 1. The slurry transfer lines were heat-traced 1/4-inch tubes equipped with quick-opening valves which could be manually operated through a safety barrier. AC2 was equipped with a thermocouple in the autoclave body as well as in the solution for precise temperature control. During venting, the gas passed through a trap to condense liquids, a gas sample port, an H₂S scrubber, and a wet test meter to measure H₂S free gas volume.

The experimental procedure consisted of preheating the coal-solvent slurry to 250 C in AC1 while AC2 was heated empty to slightly higher than the desired temperature. The slurry was transferred to AC2 and the internal heater was used to bring the slurry rapidly to constant reaction temperature. Typically, heatup required 3.4 ± 0.6 min and the temperature remained constant within ± 1.0 degrees during the reaction period. Small variations in heatup time did not affect the reaction since most of the heatup time was spent below 415 C where the reaction was slow. After the reaction was complete the slurry was transferred back to AC1 or to AC3 where it was quenched to 250 C using an internal cooling coil. After the gases were vented the slurry was transferred to a heated filter and filtered at 250 C.

The product workup consisted of continuously extracting the filter cake with tetrahydrofuran (THF) and combining the proper proportions of THF and filtrate to make up a sample for distillation. The procedure was later modified to include routine extraction of the THF extracted filter cake with pyridine and the inclusion of the pyridine extract in the liquid products. The entire hot filtrate-THF and pyridine extract was distilled to eliminate any questions regarding the use of

a representative sample for distillation. Distillation cuts were made to give the following fractions, THF (b.p. <100 C), light oil (b.p. 100-232 C), solvent (b.p. 232-482 C), and SRC (distillation residue b.p. >482 C).

MATERIALS

The coal used for experiments 1-28 was supplied from the Wilsonville SRC pilot plant, Sample No. 15793. It was a blend of West Kentucky 9 and 14 seam coal from the Colonial Mine of the Pittsburgh and Midway Coal Company. The coal used in experiments 29-37 was similar but contained 0.39 weight percent more organic sulfur than the first coal. Analyses of both coals are shown in Table 1.

TABLE 1. ANALYSES OF STARTING COALS
(As-Received Basis)

| Coal Type | West Kentucky 9/14 | West Kentucky 9/14 |
|---------------------------------|------------------------------|-------------------------------------|
| Source | Colonial Mine ^(a) | Pittsburgh & Midway Coal Company |
| <u>Proximate Analysis, wt %</u> | | |
| Moisture | 5.72 | 2.71 |
| Ash | 12.71 | 8.90 |
| Volatile matter | 34.7 | 36.9 |
| Fixed carbon | 47.5 | 51.49 |
| <u>Ultimate Analysis, wt %</u> | | |
| Carbon | 66.0 | 70.0 |
| Hydrogen | 4.7 | 4.8 |
| Nitrogen | 1.3 | 2.4 |
| Sulfur | 3.75 | 3.16 |
| Oxygen | 12.2 | 10.74 |
| <u>Sulfur Types, wt %</u> | | |
| Total | 3.77 | 3.16 |
| Pyritic | 1.96 | 1.30 |
| Sulfate | 0.64, 0.56 | 0.31 |
| Sulfide | 0.01 | -- |
| Organic (by difference) | 1.16 | 1.55 |

(a) Source of coal used at Wilsonville, SRC Quarterly Report #1, June 25, 1976, p 2.

The solvent used for experiments 1-28 was recycle solvent obtained from the Wilsonville SRC pilot plant, Sample No. 20232. An analysis and distillation data for the solvent are shown in Table 2. The solvent contained 5 percent of material boiling below 232 C, the cutoff point between light oil and SRC in the product distillation and 4-5 percent of material boiling above 482 C, the cutoff point between solvent and SRC.

A blend of Wilsonville recycle solvent (75 weight percent), and 1,2,3,4-tetrahydronaphthalene, J. T. Baker Company Practical Grade (25 weight percent), was prepared for use as the solvent in experiments 29-37. Analyses and distillation data are also given in Table 2. Tetralin boils below 232 C and was collected in the light oil distillation fraction during product workup.

TABLE 2. SOLVENT ANALYSES

| <u>Ultimate Analysis, wt % as received</u> | <u>Wilsonville Recycle Solvent</u> | | <u>3:1 Wilsonville Recycle Solvent-Tetralin</u> | |
|--|------------------------------------|--|---|--|
| | | | | |
| Moisture (benzene azeotrope) | | | | Trace |
| Ash | <0.01 | | | 0.10 |
| Carbon | 87.8 | | | 87.9 |
| Hydrogen | 7.8 | | | 8.3 |
| Nitrogen | 0.7 | | | 0.6 |
| Sulfur | 0.27 | | | 0.21 |
| Oxygen (by difference) | 3.42 | | | 2.89 |
| H/C | 1.07 | | | 1.13 |
| | <u>Corrected Temp, C</u> | <u>Cumulative Volume Distilled % of Sample</u> | <u>Corrected Temp, C</u> | <u>Cumulative Volume Distilled % of Sample</u> |
| | 216 | IBP | 201 | IBP |
| | 248 | 10 | 210 | 4 |
| | 253 | 20 | 214 | 17 |
| | 267 | 30 | 225 | 28 |
| | 281 | 40 | 236 | 36 |
| | 299 | 50 | 260 | 47 |
| | 319 | 60 | 310 | 68 |
| | 356 | 70 | 340 | 76 |
| | 406 | 80 | 390 | 86 |
| | 431 | 90 | 430 | 90 |
| | 444 | 95.5 | 481 | 94.5 |
| | >444 | 4.5 wt % residue | >481 | 4.1 wt % residue |

RESULTS AND DISCUSSION

Four variables were studied in the first part of the experimental program which examined the first step of the proposed two-step process. The variables were reaction temperature (413-454 C) solvent to coal ratio (2:1 and 3:1), residence time, (0-5 minutes), and pressure (300-1800 psi). Recycle solvent from the Wilsonville SRC pilot plant was used in all of these experiments. Later, molecular hydrogen and recycle solvent containing 25 weight percent tetralin were used in four experiments, all at 441 C for 2 minutes. These experiments were designed to simulate the second step, where hydrogenated solvent and molecular hydrogen would be used to lower the sulfur content of the product.

THF Conversion

Tetrahydrofuran (THF) conversion was calculated from the difference between the initial and the final solubilities of the total coal-solvent slurry in THF. THF conversions were calculated on an MAF coal basis and adjusted for the coal not recovered from the autoclaves. The filter cake resulting from filtration of the product at 250 C was continuously extracted with THF for up to three days. The THF soluble conversion figures may be too high however, since hot recycle solvent is probably a better solvent for coal liquids than THF and may have dissolved some material in the hot filtration which would be insoluble in THF.

Figure 2 shows THF conversion plotted as a function of reaction time and temperature at 3:1 solvent/coal ratio. The THF solubles appear to be formed as unstable intermediates in the total reaction sequence. The low molecular weight THF solubles may be able to combine in the absence of hydrogen to form higher molecular weight materials which are insoluble in THF. At 413 C, THF solubles increase ly between 0 and 2 minutes and seem to be only slightly unstable. At 429 C, most

of the THF solubles are produced during the heatup period. The formation of THF solubles is over by the end of the heatup period and decomposition is slowly taking place after "zero" reaction time at 441 C, and at 454 C the production of THF solubles is over before the heatup period is completed and the thermal decomposition reaction is more rapid than at 441 C.

Increasing the solvent to coal ratio might be expected to have the effect of stabilizing the THF soluble materials by making available more hydrogen from the solvent. However the changes in THF conversion as a function of solvent to coal ratio at 1 minute residence time and 427-441 C are relatively small. THF soluble conversion is increased by the presence of both molecular hydrogen in the gas phase and tetralin added to the solvent.

Solubilities of the products in THF followed by pyridine were determined for some of the experiments. The conversions to pyridine solubles averaged 1.6 weight percent more than the conversions to THF solubles.

SRC Yields

SRC yield is defined as the material which is soluble in the hot filtrate plus the material in the filter cake which is soluble in THF with a boiling point above 482 C. All of the SRC yields have been calculated on an MAF coal and MAF SRC basis. The yields of SRC would normally be smaller than the THF soluble conversions were it not for the presence of the solvent. Components of the solvent reported to the SRC fraction either by reacting with the SRC or by polymerizing to higher molecular weight materials which appear in the SRC distillation fraction. In addition, 4-5 weight percent of the starting solvent boiled above 482 C and was included in the SRC during distillation.

Figure 3 is a plot of SRC yield versus time and temperature at 3:1 solvent to coal ratio. SRC yields are shown to decrease at 413 C and 427 C and to increase at 441 C and possibly 454 C as a function of increasing reaction time at temperature. One explanation for these results lies in the thermal instability of the solvent. The product of the interaction of SRC with solvent may decompose at 413 and 427 C releasing solvent molecular weight material while at 441-454 C the solvent may polymerize to heavier molecular weight products which distill with the SRC fraction.

There was a decrease in SRC yield when tetralin was added to the solvent but a slight increase when an overpressure of hydrogen was used. The decrease with added tetralin was probably due to the fact that there was less high boiling solvent present, part of which appeared as SRC when the distillation cut was made at 482 C.

Quality of SRC

The amount of ash and particularly sulfur in the SRC are as important as the yield. If the SRC is to be used as a clean boiler fuel in place of oil, the ash content must be quite low and the sulfur content must be low enough to meet the new source standards for SO₂ emissions during combustion. Average analyses for SRC made from both coals are shown in Table 3. As expected, the average SRC produced in the first step of the two-step process, even using a West Kentucky 9/14 coal blend with an unusually low organic sulfur content (Coal Sample 1) would yield 1.34 lb SO₂/MM Btu during combustion and would not meet the present new source standards.

There appears to be an increase in the sulfur content of the SRC prepared with 25 weight percent added tetralin in the solvent. Again, this may be due to the absence of a sulfur dilution effect which takes place when low sulfur content solvent appears in the SRC fraction. Adding an overpressure of molecular hydrogen did not affect the sulfur level in the SRC when the second step was carried out at 441 C.

Added tetralin, hydrogen overpressure and increased solvent to coal ratios resulted in no measurable increase in gas yield. The results are complicated by and corrected for hydrogen added in the experiments with high-pressure hydrogen.

The average filter cake analysis is also shown in Table 3. Individual filter cake compositions vary widely. As conversion increases, sulfur and ash increase while oxygen and hydrogen and possibly nitrogen concentrations in the filter cakes decrease. The average filter cake yield is 30 weight percent of the as-fed coal. The sulfur present in the filter cake represents 49 percent of the sulfur in the coal feed. This sulfur is made up of the sulfur remaining after partial pyrite decomposition and sulfate sulfur.

Solvent Composition and Recovery

The solvent is defined as the product fraction which is soluble in the hot filtrate and/or during the THF extraction of the filter cake and which boils between 232 C and 482 C at atmospheric pressure. One of the requirements of a commercial liquefaction process is that at least as much solvent be created as is used in the process. In addition, the composition of the solvent must be kept constant if it is to be used as a hydrogen donor and as a solvating agent for the dissolved coal.

The average solvent recovery for these experiments in the absence of hydrogen or tetralin was 89 percent, corrected for solvent lost in the residues which remain in the autoclaves and by normalizing mass balances from 95.4 to 100 percent. Of the 11 percent of the solvent unaccounted for directly during the reaction, 5-6 percent is collected in each of the light oil and SRC fractions as discussed earlier. The recovery of solvent, uncorrected for starting solvent which distilled in the light oil and SRC fractions, is shown as a function of reaction time and temperature in Figure 5. There is no correlation with temperature. However, solvent recovery does increase with reaction time and with decreasing solvent to coal ratio.

Hydrogen Transfer

The data indicate that there was a net consumption of hydrogen in the presence of high pressure hydrogen. A net production of hydrogen in the absence of high pressure hydrogen is well established. During the liquefaction process, the solvent is presumed to donate hydrogen to the dissolved coal molecules to stabilize them and prevent polymerization reactions which lead to coke. In this study, hydrogen transfer was followed by monitoring the elemental analysis of the solvent to see if a change in hydrogen percentage or H/C ratio occurred. Comparison of the average solvent analyses before and after reaction is complicated by the loss of recovered solvent to SRC and light oil fractions which occurs during distillation.

The analyses for hydrogen and carbon are the same within experimental error, however, if as shown in Tables 2 and 3, hydrogen has decreased 0.1 weight percent and the H/C ratio has decreased 0.02 on the average, this means that approximately 1.3 percent of the hydrogen in the solvent transfers to coal during liquefaction at 3:1 solvent to coal ratio. This indicates that up to 85 percent of the coal can be converted to THF soluble materials by transferring hydrogen amounting to less than 0.3 weight percent of the coal charge. The solvent's role in the first step of the process is clearly based as much on dispersing and dissolving the coal molecules resulting from thermal bond breaking as it is on stabilizing the molecules by hydrogen transfer.

Sulfur Balance

The fate of sulfur during the process is also important. The average sulfur balance is shown below.

| <u>Products</u> | <u>Percent of Sulfur in Coal</u> |
|-----------------|----------------------------------|
| Gas | 24.9 |
| Light Oil | 0.4 |
| SRC | 21.2 |
| Filter Cake | 44.4 |
| Solvent | <u>90.9</u> |

About one-quarter of the sulfur in the coal remained in the SRC, one-quarter appeared as H₂S in the gases and nearly one-half remained in the filter cake. Hydrogen introduced in the second step would not see three-quarters of the sulfur contained in the starting coal.

CONCLUSIONS

In step one, conversion of coal to a THF soluble product was rapid. The THF solubles were unstable in the presence of a coal derived solvent, but in the absence of hydrogen. In step two, the addition of molecular hydrogen to the system or of tetralin to the solvent to increase hydrogen transfer to the coal increased the THF soluble conversion but did not lower the sulfur content of the SRC. Higher temperatures were required to remove more sulfur.

SRC yields were greater than 100 percent due to the presence of solvent in the SRC. The average SRC prepared from West Kentucky 9/14 coal blends did not meet new source standards for SO₂ emissions after the first step of the two-step process although all of the inorganic sulfur and an average 12 percent of the organic sulfur was removed.

Hydrogen was produced in the absence of an overpressure of molecular hydrogen and consumed when hydrogen was present in the system. During step one of the two-step process less than 0.3 weight percent hydrogen was transferred from the solvent of the SRC in the absence of hydrogen. The solvent appears to physically stabilize the coal. Solvent recovery from step one was approximately 100 percent when corrected for the amounts of starting solvent which were collected in the light oil and SRC fractions.

ACKNOWLEDGMENT

This work was funded by The Clean Liquid and Solid Fuels Group of EPRI, Contract RP-779-5. (2) William C. Rovesti was the Project Manager.

REFERENCES

1. The Nature and Origin of Asphaltenes in Processed Coals, EPRI AF-252, prepared by Mobil Research and Development Corporation, pp 10-18, February, 1976.
2. "Short Residence Time Coal Liquefaction", EPRI AF-780, prepared by Battelle's Columbus Laboratories, June, 1978.

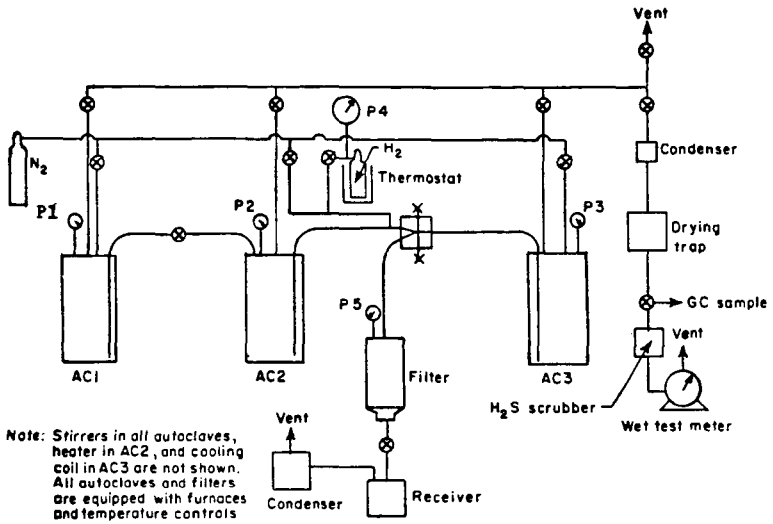


FIGURE 1. SHORT RESIDENCE TIME COAL LIQUEFACTION APPARATUS - 3 AUTOCLAVES

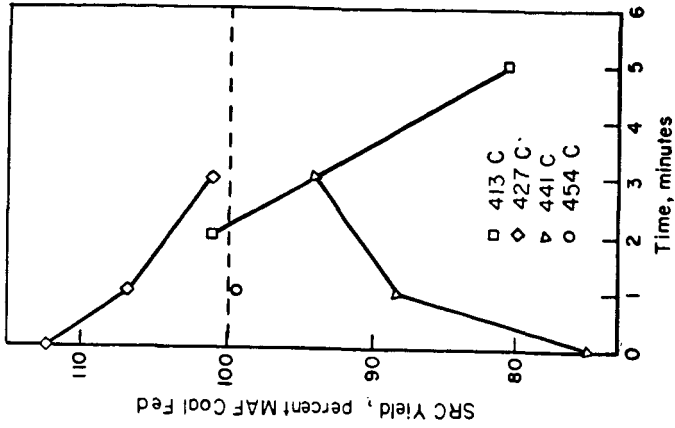


FIGURE 3. SRC YIELD VERSUS TIME AND TEMPERATURE

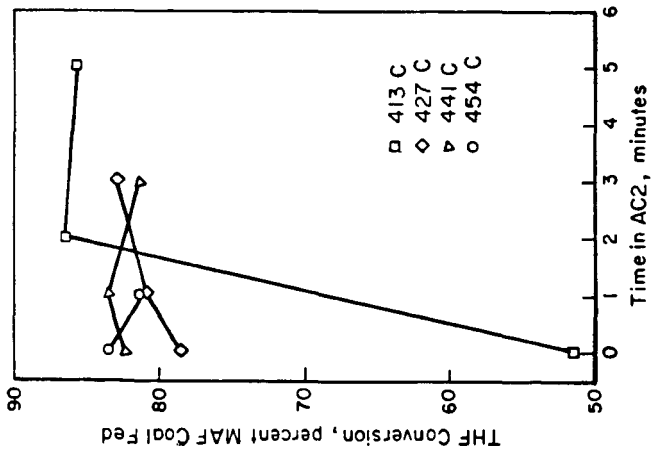


FIGURE 2. THF SOLUBLE CONVERSION VERSUS TIME AND TEMPERATURE

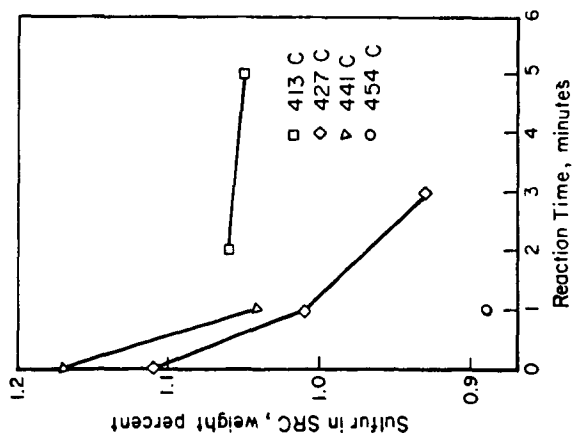


FIGURE 4. SULFUR IN SRC VERSUS TIME AND TEMPERATURE

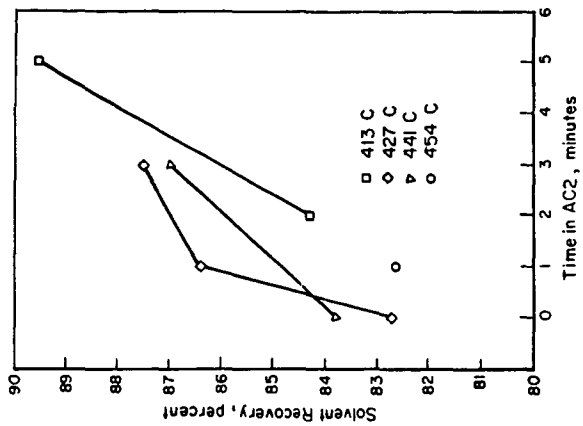


FIGURE 5. SOLVENT RECOVERY VERSUS TIME AND TEMPERATURE

Kinetics of Direct Liquefaction of Coal in the Presence of Mo-Fe Catalyst

Minoru Morita, Shimio Sato and Takao Hashimoto

Department of Chemical Engineering
Yamagata University
Yonezawa 992, Japan

INTRODUCTION

Many studies on direct coal liquefaction have been carried out since the 1910's, and the effects of kinds of coal, pasting oil and catalyst, moisture, ash, temperature, hydrogen pressure, stirring and heating-up rate of paste on coal conversion, asphaltene and oil yields have been also investigated by many workers. However, few kinetic studies on their effects to reaction rate have been reported.

In this present study, the effects of kinds of coal, pasting oil, catalyst and reaction temperature on coal liquefaction are illustrated, and a few kinetic models for catalytic liquefaction of five coals carried out in a autoclave reactor are proposed.

RESULTS and DISCUSSION

(I) Experimentals in catalyst and reaction rate

(I-1) Experimental procedure

Five coal materials were used in this study. These were Miike, Taiheiyo, Hikishima (Japanese coals), Morwell (Australian) and Bukit Asam (Indonesian) coals. The proximate and ultimate analyses of these coals, on a moisture-free basis, are shown in Table 1. All of catalysts were powdered before use. In all of the experiments powdered coal (passed through 80-mesh sieve), 3.3 % of catalyst (calculated on the coal charge), a steel ball (10 mm ϕ) and vehicle were charged to the 0.3 or 0.5-liter autoclave reactor in the required ratio. The reactor was flushed and filled with cold hydrogen to an initial pressure of 100 kg/cm 2 -gauge at room temperature, heated to reaction temperature at a heat-up rate of about 4°C per minute, held at constant temperature for the desired length of time, and cooled to room temperature at a heat-down rate of about 3°C per minute. Then the autoclave residue was extracted with benzene and n-hexane in Soxhlet apparatus, and the proportion of "asphaltene" (defined as the benzene-soluble, n-hexane insoluble material), and "oil" (the benzene, n-hexane soluble material) in the liquefied product was determined.

(I-2) Results of experiments

(A) Effect of pasting oil on liquefaction

(1) Charged ratio of coal to pasting oil

Coal conversion per cent on a moisture- and ash-free was independent of the charged ratio and had constant value about 80-90 %, while liquefaction percentage was decreased with increasing the charged ratio. This result was considered to be responsible for gasification with thermal decomposition and resinifying of coals on inner wall of the reactor; temperature at the wall would be higher due to worse stirring as coal pastes were more viscous when coal concentration was higher. Therefore, well mixing was necessary to obtain a good liquefaction percentage under higher coal concentration.

(2) Kind of pasting oil

Using four pasting oils with boiling temperature of 330°C to 380°C, liquefaction was carried out under the same reaction condition.

When hydrogenated pasting oil were used, reaction rate was greater than that with non-hydrogenated pasting oils. This higher liquefaction rate for the hydrogenated pasting oil was interpreted by the action of greater proton-donner ability with them.

(B) Effect of catalyst on liquefaction

Figs. 1 to 5 were experimental results of Miike coal liquefaction for MoO_3 , $\text{Fe}(\text{OH})_3$ -S, MoO_3 - $\text{Fe}(\text{OH})_3$ -S, $\text{H}_2\text{MoO}_4 \cdot \text{H}_2\text{O}$ and $\text{Fe}(\text{OH})_3$ - $\text{H}_2\text{MoO}_4 \cdot \text{H}_2\text{O}$ -S catalysts. Figs. 6 to 9 were those of Taiheiyo, Hikishima, Morwell and Bikit Asam coals for MoO_3 - $\text{Fe}(\text{OH})_3$ -S. In Figs. 10, 11 and 12, fraction of unreacted coal was plotted as a function of nominal reaction time on semilogarithmic graph paper. Reaction rate was first order with coal concentration in the same way as Takeya et al. (3) showed in Taiheiyo coal liquefaction, since at lower temperature plots gave straight lines. At higher temperatures semilogarithmic plots didn't give only one decreasing straight line. This characteristic was explained from greater gasification and resinification of coal under these temperatures. Specific reaction rates calculated from slope of lines were shown in Table 2. From these results activities of the catalysts were compared. Conclusions were shown as follows;

(a) MoO_3 was more active under lower temperatures, while $\text{Fe}(\text{OH})_3$ -S was more active under higher temperatures.

(b) MoO_3 and $\text{Fe}(\text{OH})_3$ were complements each of the other, MoO_3 - $\text{Fe}(\text{OH})_3$ -S being more active than both under the lower and higher temperatures.

(c) $\text{H}_2\text{MoO}_4 \cdot \text{H}_2\text{O}$ of the catalyst containing H_2O , but having a tendency of resinifying and gasification, $\text{H}_2\text{MoO}_4 \cdot \text{H}_2\text{O}$ - $\text{Fe}(\text{OH})_3$ -S was not so active as expected.

(d) The action of the catalyst to Taiheiyo coal was the same that to Miike coal.

Fig. 3 showed reaction course for Miike coal under several reaction temperatures with nominal reaction time for MoO_3 - $\text{Fe}(\text{OH})_3$ -S which is the most active among the catalysts. This result showed that under temperature range 350°C to 410°C reaction rate increased with increasing temperature and oil yield became greater with increasing nominal reaction time, whereas at the highest temperature 450°C oil yield decreased, and both organic benzene insoluble and asphaltene increased with increasing nominal reaction time. Reaction courses of Hikishima, Morwell and Bukit Asam coals for MoO_3 - $\text{Fe}(\text{OH})_3$ -S catalyst were shown in Figs. 7 to 9, respectively. In Figs. 8 and 9, it was shown that reaction rates and oil yield in the product Morwell and Bukit Asam were larger than ^{any} other tested coal at lower temperatures. Reaction courses for Taiheiyo and Hikishima coals, when the same catalyst was used, were shown in Figs. 6 and 7. They showed that at the highest temperature formed oil degraded to organic benzene insolubles in a similar way to that for Miike coal at the highest temperature. This characteristic was explained from forming of organic benzene insolubles by resinification of produced asphaltene and oil. Degree of resinification were dependent on both reaction temperature and kinds of catalyst, being considerable at the highest temperature. No resinification was observed for $\text{Fe}(\text{OH})_3$ -S.

(II) Mechanism and kinetics of coal liquefaction

Various mechanisms and kinetics of coal liquefaction have been proposed and examined by many investigators (1 to 10).

We assumed the reaction mechanism shown in scheme 1 as a general kinetic model of coal liquefaction. The mechanism in scheme 1 with all reaction rates assumed to be pseudo first order with respect to reacting species and dissolved hydrogen to be in excess, seems to be somewhat similar to those reported in above many literatures. A few typical cases of a general kinetic model are shown in Table 3, and only

the general characteristics for their cases are illustrated on Table 3. When compared these typical figures, the curves are apparently different in shape, but if proper rate constants were selected, the curves would be similar in shape, making it difficult to determine the correct mechanism. Therefore, it is necessary to get initial rate data at lower temperatures (i.e. 350~400°C) in distinguishing between series reactions (case 1, 2, 3) and parallel reactions (case 4, 5), since for series reaction the reaction time-concentration curve for oil (C) has a zero slope and for parallel reaction the time-log(unreacted coal, %) curve does not give a straight line but two ones. A typical curve in Table 3 shows that when the apparent coal and asphaltene concentration begin to increase gradually, a further series reaction, oil→resin→coke, should be assumed. The magnitude of the rate constant of each step is different from kinds of catalyst, and it is possible that the catalyst which is very effective for promoting the reaction rate of any step in a kinetic model is to be found, resulting in the change of mechanism.

In this study oil yield decreased with reaction time, as oil was polymerized at higher temperature for Miike, Taiheiyo and Hikishima coals. Thus a kinetic model (case 2 or 3) in which involves two steps of polymerization and coking, correlated data reasonably well for above coals, whereas for Morwell and Bukit Asam coals, case 5 was more favorable.

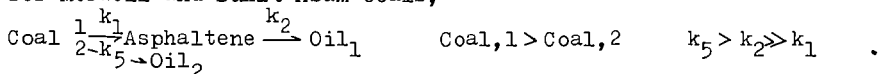
Though kinetic experiments are generally carried out with the autoclave at high temperature and pressure, reaction temperature is not sufficient isothermal but nonisothermal from start of experiment to end. As long as nominal reaction time which consists of heat-up, constant temperature and heat-down periods, is used, it will be difficult for true rate constants to be estimated under isothermal condition. Therefore, the rate constants, k-values were estimated by a non-linear least square which involves minimization of the sum of squares of deviations (between measured and calculated values). The temperature dependence of the rate constants on Miike coal was determined for temperature between 350°C and 450°C. The result was shown in Table 4.

CONCLUSIONS

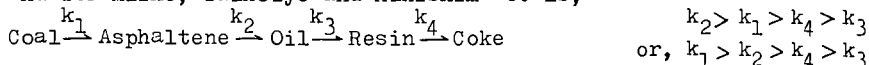
Effects of various reaction conditions on reaction rate and mechanism of coal liquefaction were investigated. Conclusions were summarized as follows;

(1) The order of the reaction, reaction rate, oil yield and composition were affected by kinds of pasting oil and ratio of coal to pasting oil.

(2) Under same reaction conditions, reaction rate and mechanism of coal liquefaction differs from kinds of coal and catalyst. The reaction rate was in the order; Morwell > Bukit Asam > Miike > Taiheiyo = Hikishima coal. Kinetic scheme of coal liquefaction was expressed as follows; for Morwell and Bukit Asam coals,



and for Miike, Taiheiyo and Hikishima coals,



The magnitude of the rate constants is different from kinds of catalyst.

(3) Activities of catalysts were as follows; $\text{H}_2\text{MoO}_4 \cdot \text{H}_2\text{O} > \text{Fe}(\text{OH})_3 - \text{MoO}_3 - \text{S} > \text{MoO}_3 > \text{Fe}(\text{OH})_3 - \text{S}$. The activity of $\text{Fe}(\text{OH})_3 - \text{MoO}_3 - \text{S}$ catalyst may be due to the concerted action with MoO_3 and $\text{Fe}(\text{OH})_3 - \text{S}$, and degrees of resin-

fication and coking were dependent on kinds of catalyst.

(4) In making a kinetic analysis of the experimental data with auto-clave, a non-linear least square method was used to estimate the parameters in the Arrhenius equation under nonisothermal conditions. The theoretical values of component, calculated by substituting the estimated values into the rate equations, were in good agreement with experimental values.

LITERATURE CITED

- 1) Weller et al., Ind. Eng. Chem., 43, 1575 (1951)
- 2) Falkum E. and R. A. Glenn, Fuel, 31, 133 (1952)
- 3) Takeya and Ishii et al., Kagakukogaku, 29, 988 (1965)
- 4) Struck et al., Ind. Eng. Chem. Proc. Des. Develop., 8, 546 (1969)
- 5) Liebenberg B. J. et al., Fuel, 52, 130 (1973)
- 6) Plett et al., paper presented University-ERDA Contractor Conference, Salt Lake City, Utah, Oct 22-23, 1975
- 7) Guin et al., Am. Chem. Soc. Div. Fuel Chem., Prepr., 20(1), 66 (1975), 21(5), 170 (1976)
- 8) Whitehurst et al., EPRI Annual Report No. AF-252, Rp 410-1, (Feb 1976)
- 9) Reuther et al., Ind. Eng. Chem. Process Des. Dev., 16, 249 (1977)
- 10) Shah et al., Ind. Eng. Chem. Process Des. Dev., 17(3), 281, 288 (1978)

Table 1 Analysis of sample coals

| Coal | % | | | % (d.a.f.) | |
|------------|----------|------|------|------------|-----|
| | Moisture | F.C. | V.M. | C | H |
| Miike | 0.9 | 45.9 | 39.8 | 82.9 | 6.2 |
| Taiheiyo | 4.9 | 27.7 | 47.0 | 79.8 | 5.7 |
| Hikishima | 1.2 | 50.7 | 26.0 | 86.2 | 6.2 |
| Morwell | 12.6 | 52.4 | 34.2 | 65.3 | 5.2 |
| Bukit Asam | 9.5 | 44.8 | 45.0 | 68.6 | 5.2 |

Table 2 Rate constants on various catalysts (min^{-1})

| Catalyst \ R.T.(°C) | 350 | 380 | 410 | 450 |
|--|--------|--------|--------|--------|
| MoO ₃ | 0.0145 | 0.0212 | 0.0253 | - |
| Fe(OH) ₃ -S | 0.0039 | 0.0113 | 0.0207 | 0.0338 |
| MoO ₃ -Fe(OH) ₃ -S | 0.0192 | 0.0253 | 0.0305 | - |
| H ₂ MoO ₄ ·H ₂ O | 0.0188 | 0.0322 | - | - |
| Fe(OH) ₃ -S-H ₂ MoO ₄ ·H ₂ O | 0.0023 | 0.0069 | 0.0230 | - |

(Coal:Miike)

Table 4 Rate constant calculated by non-linear least square method under non-isothermal condition (coal:Miike)

| Catalyst | Rate const. (min^{-1}) | Reaction Temperature (°C) | | | |
|--|-----------------------------------|---------------------------|---------|---------|----------|
| | | 350 | 380 | 410 | 450 |
| MoO ₃ | K ₁ | 0.01080 | 0.02000 | 0.03500 | 0.06880 |
| | K ₂ | 0.05040 | 0.09170 | 0.1580 | 0.3060 |
| | K ₃ | — | — | — | — |
| | K ₄ | — | — | — | — |
| Fe(OH) ₃ -S | K ₁ | 0.00785 | 0.01460 | 0.02570 | 0.05080 |
| | K ₂ | 0.01880 | 0.03490 | 0.06130 | 0.1210 |
| | K ₃ | — | — | — | 0.00276 |
| | K ₄ | — | — | — | 0.02910 |
| MoO ₃ -Fe(OH) ₃ -S | K ₁ | 0.01760 | 0.02930 | 0.04660 | 0.08150 |
| | K ₂ | 0.00636 | 0.01140 | 0.01930 | 0.03640 |
| | K ₃ | — | — | 0.00129 | 0.00732 |
| | K ₄ | — | — | 0.00213 | 0.01590 |
| H ₂ MoO ₄ ·H ₂ O | K ₁ | 0.02040 | 0.03420 | 0.05480 | 0.09590 |
| | K ₂ | 0.05020 | 0.1100 | 0.2230 | 0.5190 |
| | K ₃ | — | — | 0.00321 | 0.01710 |
| | K ₄ | — | — | 0.00977 | 0.05730 |
| Fe(OH) ₃ -S-H ₂ MoO ₄ ·H ₂ O | K ₁ | 0.01680 | 0.02020 | 0.02380 | 0.02920 |
| | K ₂ | 0.08120 | 0.1280 | 0.1930 | 0.3180 |
| | K ₃ | — | — | — | 0.000451 |
| | K ₄ | — | — | — | 0.00258 |

Scheme 1 Kinetic Model of Direct Liquefaction of Coal

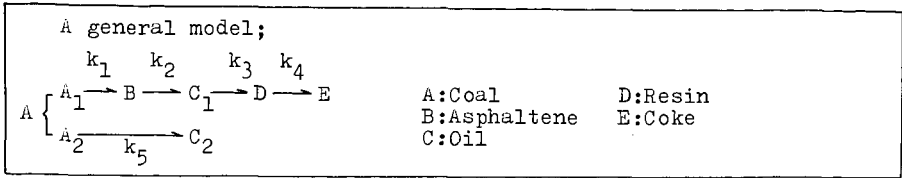
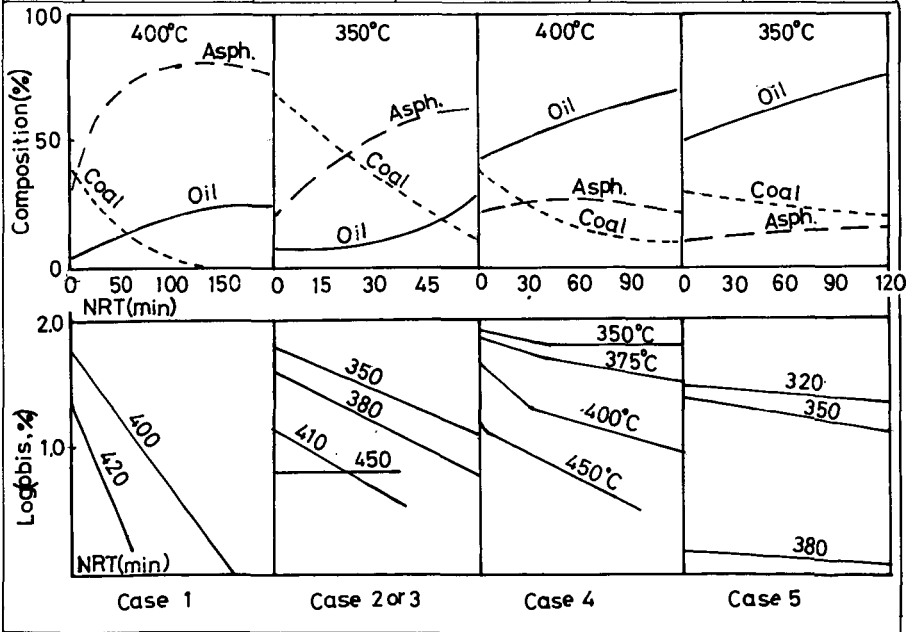


Table 3 Typical Cases of a General Kinetic Model

| Case | Condition | Model | Coal | Catalyst | Worker |
|------|--|--|---------------------------|---|------------------|
| 1 | $A_1 \gg A_2 \neq 0$ $k_1 > k_2 \gg k_3, k_4$ | $A \rightarrow B \rightarrow C$ | Pittsburg Seam | $\text{SnCl}_2\text{-NH}_4\text{Cl}$ | S. Weller et al. |
| 2 | $A_1 \gg A_2 \neq 0$ $k_2 > k_1 > k_4 > k_3$ | $A \rightarrow B \rightarrow C \rightarrow D \rightarrow E$ | Taiheiyo Miike | $\text{Fe(OH)}_3\text{-S}$ $\text{H}_2\text{MoO}_4\text{-S}$ | M. Morita et al. |
| 3 | $A_1 \gg A_2 \neq 0$ $k_1 > k_2 > k_4 > k_3$ | $A \rightarrow B \rightarrow C \rightarrow D \rightarrow E$ | Miike | $\text{Fe(OH)}_3\text{-}$ $\text{MoO}_3\text{-S}$ | M. Morita et al. |
| 4 | $A_1 > A_2$ $k_5 > k_1 > k_2$ | $A \xrightarrow{1} B \rightarrow C_1$ $A_2 \rightarrow C_2$ | Yubari, Soya Sumiyoshi | Red Mud | G. Takeya et al. |
| 5 | $A_1 > A_2$ $k_5 > k_2 \gg k_1$ | $A \xrightarrow{1} (B) \rightarrow C_1$ $(A_2 \rightarrow C_2)$ | Morwell Bukit Asam | $\text{Fe(OH)}_3\text{-}$ $\text{MoO}_3\text{-S}$ | M. Morita et al. |



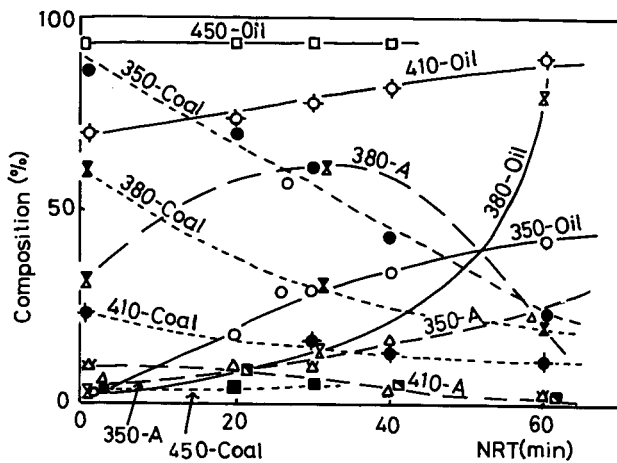


Fig. 1 Change of composition on catalyst MoO_3 at various react. temp. at 350°C (●△○) 410°C (◆◇◇) 380°C (×××) 450°C (■□□)

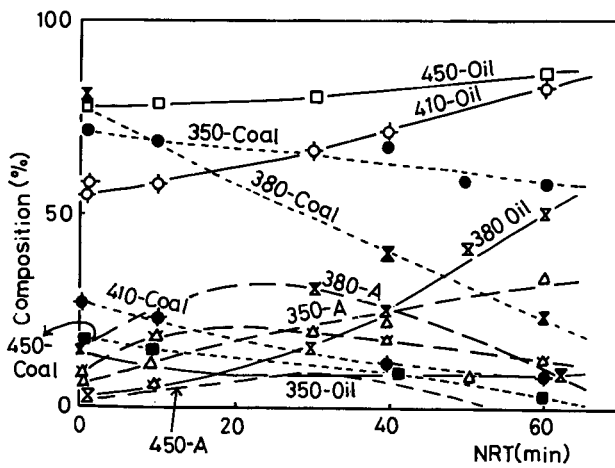


Fig. 2 Change of composition on catalyst $\text{Fe(OH)}_2\text{S}$ at various react. temp. at 350°C (●△○) 410°C (◆◇◇) 380°C (×××) 450°C (■□□)

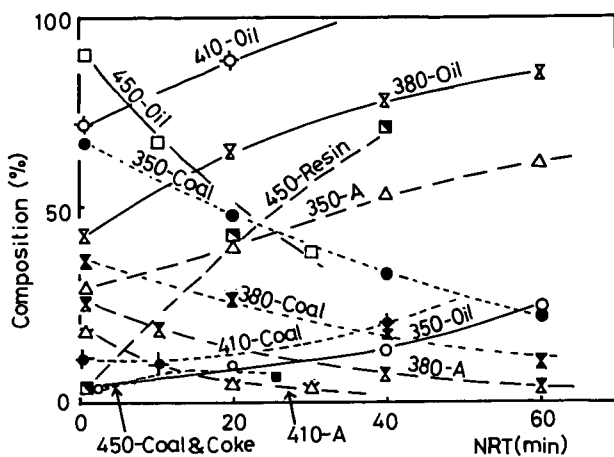


Fig. 3 Change of composition on catalyst $\text{Fe}(\text{OH})_2\text{MoO}_4\text{-S}$ at various R.T. (Miike-coal)
 350°C (●△○) 410°C (◆◇◇)
 380°C (×××) 450°C (■□□)

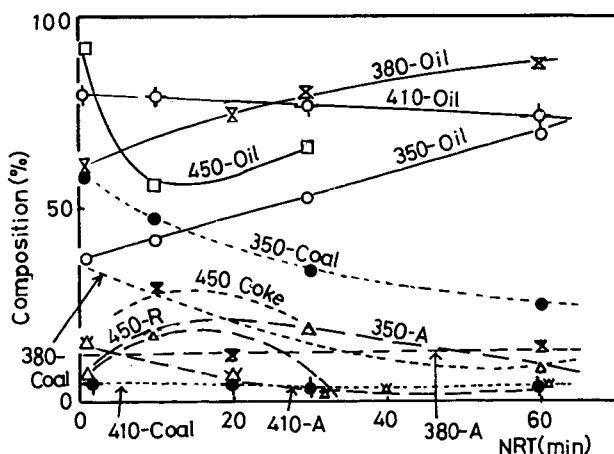


Fig. 4 Change of composition on catalyst H_2MoO_4 at various react. temp.
 at 350°C (●△○) 410°C (◆◇◇)
 380°C (- ××) 450°C (■□□)

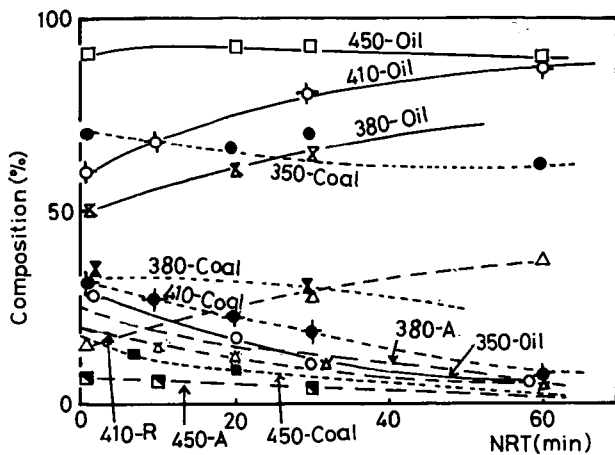


Fig.5 Change of composition on catalyst $\text{Fe(OH)}_2 \cdot \text{H}_2\text{MoO}_4 \cdot \text{H}_2\text{O-S}$ at various react. temp
 at 350°C (●△○) 410°C (◆◇◇)
 380°C (x-x) 450°C (■□□)

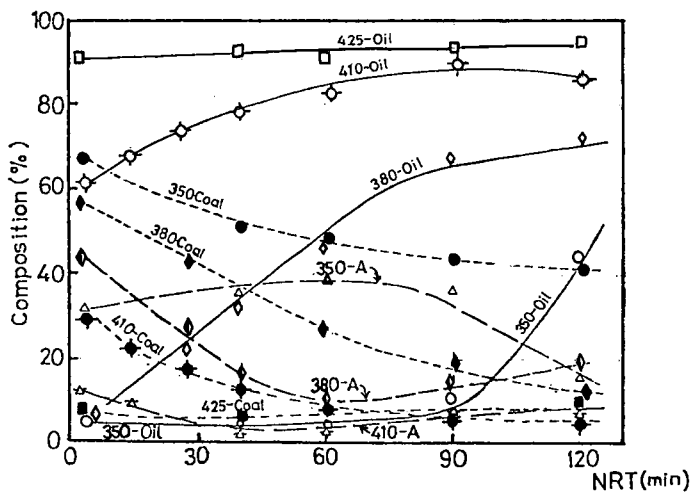


Fig.6 Change of composition on Taiheiyo coal (Numerals; React. temp, A; Asphaltene)
 350°C (●△○) 410°C (◆◇◇)
 380°C (◆◇◇) 425°C (■□□)

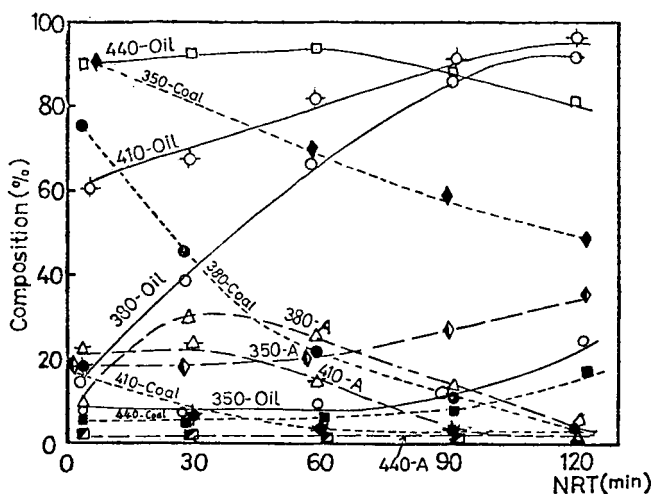


Fig.7 Change of composition on Hikishima coal (Numerals; React. temp., A: Asphaltene) at 350°C (● △ ○) 410°C (◆ ▲ ◇) 380°C (♦ ♦ ♦) or 440°C (■ □ □)

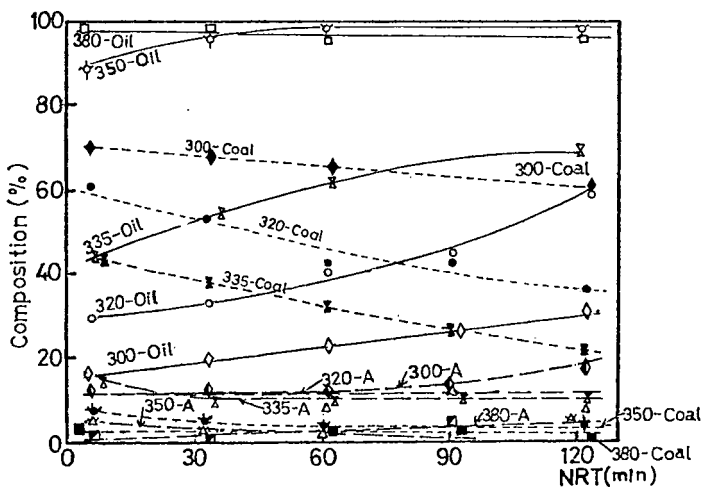


Fig. 8 Change of composition on Morwell coal (Numerals; React. temp., A; Asphaltene) at 300°C (● △ ○) 350°C (▽ ✕ ▽) 320°C (◆ ♦ ♦) or 380°C (■ □ □) 335°C (✕ ✕ ✕)

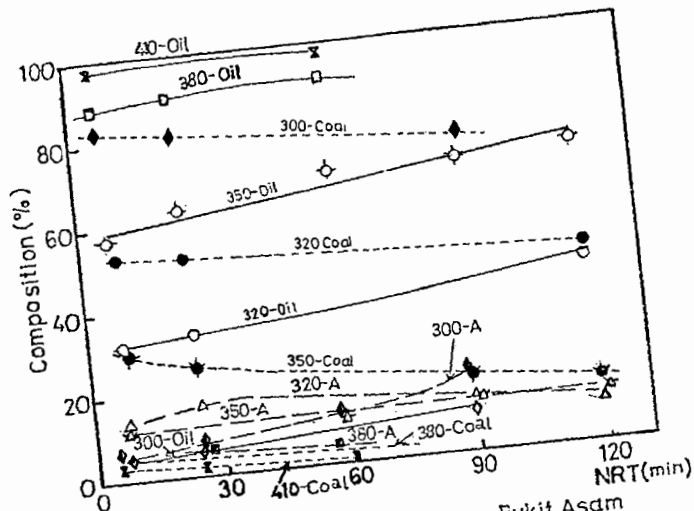


Fig. 9 Change of composition on Bukit Asam coal (Numerals; React. temp, A; Asphaltene) at 300°C (●, △, ○), 350°C (◆, ▲, ◇), 410°C (×, ×, ×), 320°C (♦, ♦, ♦) or 380°C (■, ■, ■)

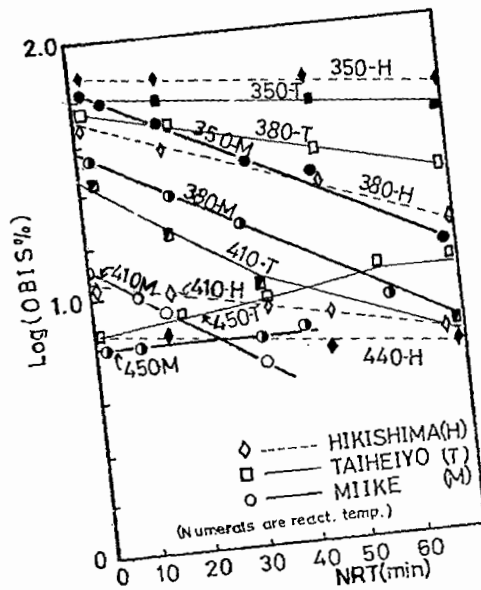


Fig. 10 Log(OBIS%) vs. NRT for various coals

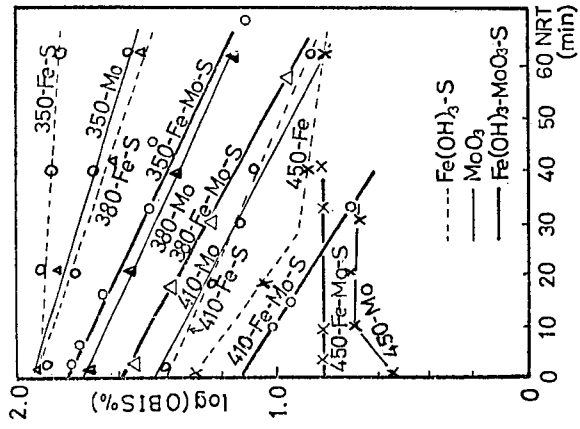


Fig.11 Log(OBIS%) vs. NRT on various temp.(Miike coal)

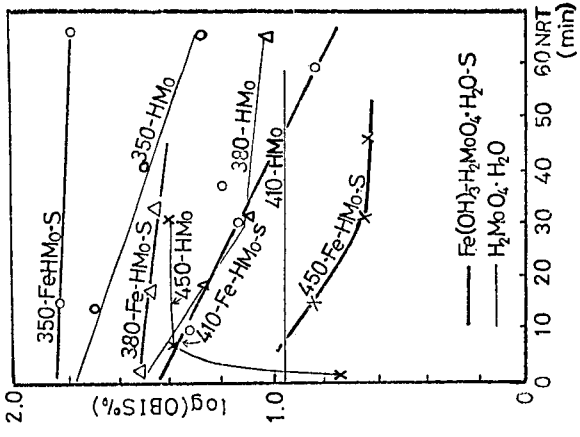


Fig.12 Log(OBIS%) vs. NRT on various temp.(Miike coal)

CARBON MONOXIDE-WATER vs. HYDROGEN FOR LIQUEFACTION:
THE REDUCTION OF DIPHENYLSULFIDE, THIOANISOLE AND DIBENZOTHIOPHENE

R. J. Baltisberger, V. I. Stenberg, J. Wang and N. F. Woolsey

Department of Chemistry
University of North Dakota
Grand Forks, ND 58202

INTRODUCTION

For lignite, several workers have demonstrated a mixture of carbon monoxide and water to be superior to hydrogen for liquefaction when there are no added catalysts(1, 2, 3, 4). The minerals present in lignite are postulated to catalyze the reduction. The relative success of CO is important because it suggests the economics of lignite liquefaction may ultimately favor the use of synthesis gas over hydrogen. If so, the need of the shift reaction section of a hydrogen plant can be eliminated. Carbon dioxide has to be removed at one stage in either process which will probably result in a wash-out of its removal expenses.

There are several important questions which arise from the carbon monoxide results: (1) Which chemical bonds are more easily reduced by CO-H₂O than H₂ under the same conditions? (2) Does the reduction proceed because of "nascent" hydrogen from CO-H₂O? and (3) What materials catalyze the CO-H₂O reaction?

Model compounds are superior to lignite as a material to study to answer the posed questions because the variables can be better controlled. The applicability of the model compound work to lignite liquefaction processes depend upon the relation of the model compounds to the key features of lignite structure and chemistry question examined. The selection of the materials for examination as catalysts depends on the nature of the natural minerals present in the various lignites, available low-cost materials as disposable catalysts and materials to prove or disprove a hypothesis on catalyst activity.

Carbon monoxide and water has proven more effective than hydrogen to convert benzophenone and benzhydrol into products(5). For anthracene, H₂ and CO-H₂O are equally effective for conversion, and for quinoline H₂ is superior to CO-H₂O(6). The product distributions are influenced by catalysts and the presence of a hydrogen-donor solvent.

Thiophene and thiophene derivatives have been desulfurized by tetralin(7), hydrogen over a CoO-MoO₃-Al₂O₃ catalyst(8), an ammonium Y zeolite catalyst(9) and a molybdenum sulfide catalyst(10). Rollman has removed sulfur from model compounds over sulfided CoMo catalysts(11).

EXPERIMENTAL

The reductions are done in a pair of 250-ml rocking Hastelloy C autoclaves. The temperature is maintained at 425°C for two hours. The heat up time is slightly more than an hour, and the cool-down time is done overnight. Initially the autoclaves are charged with 750 psi of reducing gases and 750 psi of argon (1500 psi total). At 425°C, the reactions will achieve a total pressure of about

3,000 psi. After cool-down, the gases are vented and the products removed by decanting.

The water layer is separated from the organic layer by a separatory funnel and filtered through a sintered glass funnel. A 3-ml aliquot of the resultant solution is combined with an appropriate internal standard and analyzed by gas-liquid chromatography. The results were obtained on a Varian Aerograph 90-P instrument and are duplicated with the precision of $\pm 6\%$.

RESULTS AND DISCUSSION

In the absence of possible catalysts, the effectiveness of the reducing gases is $H_2 \approx H_2 - CO - H_2O > CO - H_2O$ for causing conversion of diphenylsulfide (Table 1, runs 1-4) and thioanisole (Table 3, runs 2-4). Hydrogen, with or without carbon monoxide, causes predominantly transformation into benzene, whereas carbon monoxide-water gives a variety of products. The combination of hydrogen with carbon monoxide and water provide results intermediate in percentage yields.

In the absence of reducing gases, neither dibenzothiophene nor diphenylsulfide decompose at 425°C (Tables 1 and 2). However, thioanisole readily decomposes to give diphenylsulfide, toluene and benzene (run 1 of Table 3). Since the latter reaction solution is essentially nonpolar, homolysis of the sulfur-methyl bond is most probably occurring, i.e., reaction 1. The dissociation energy of this bond is 60 kcal/mole¹². Little thiophenol is formed possibly because of the low S-H bond energy. Reactions 2^c and 3 are likely reactions to account for the benzene formed. Reaction 4 illustrates the reaction route to the predominant product, diphenylsulfide. Reaction 5 outlines a possible reaction route to toluene.

For the three sulfur compounds of Tables 1-3, hydrogen is superior to carbon monoxide-water for desulfurization. The CO-H₂O results can be accounted for by the reduction caused by hydrogen from the shift reaction, reaction 6, rather than an interpretation wherein CO directly reacts with the three model compounds.

Since benzoic acid is formed in the reactions of diphenylsulfide and thioanisole only when carbon monoxide is present, it must be the source of the carboxyl group directly or indirectly. The sequence of reactions 7 and 8 are probable for the formation of benzoic acid under these high pressure conditions.

- 1) $Ph-S-CH_3 \rightarrow Ph-S + CH_3$
- 2) $Ph-S \rightarrow Ph + S^{O13}$
- 3) $Ph + PhSCH_3^* \rightarrow PhH + PhSCH_3$
- 4) $Ph + PhSCH_3 \rightarrow PhSPh + CH_3$
- 5) $PhSCH_3 + CH_3 \rightarrow PhCH_3 + SCH_3$
- 6) $CO + H_2O \rightleftharpoons CO_2 + H_2$
- 7) $Ph + CO_2 \rightarrow PhCO_2$
- 8) $PhCO_2 + PhSCH_3^* \rightarrow PhCO_2H + PhSCH_2$

(* or metal -H)

In the diphenylsulfide reductions results described in Table 3, carbon monoxide must be the source of the methyl group of toluene. In support of this, the phenyl ring is unlikely to fragment to a methyl group under these conditions for thermodynamic reasons, and no toluene is formed when hydrogen is used as the sole reducing gas.

The added materials, tetralin, Na_2CO_3 and FeS , inhibit the diphenylsulfide and thioanisole reduction conversions and have little net effect on the dibenzothiophene reactions. Tetralin is not behaving as a good hydrogen donor, but rather as an inert diluent of the reducing gases. Less than 5% of the tetralin is converted into naphthalene.

ACKNOWLEDGEMENTS

We are grateful for the financial support of the United States Department of Energy through Contract No. E (49-18)-2211.

REFERENCES

- (1) Appell, H. R. and Wender, I., *Am. Chem. Soc., Div. Fuel Chem., Prepr.*, 12, 220 (1968).
- (2) Appell, H. R., Wender, I., and Miller, R. D., *Am. Chem. Soc., Div. Fuel Chem., Prepr.*, 13, 39 (1969).
- (3) Appell, H. R., Wender, I., and Miller, R. D., *Chem. Ind. (London)*, No.47, 1703 (1969).
- (4) Appell, H. R., private communication.
- (5) Jones, D., Baltisberger, R. J., Klabunde, K. J., Woolsey, N. F., and Stenberg, V. I., *J. Org. Chem.*, 43, 175 (1978).
- (6) Stenberg, V. I., Wang, J., Baltisberger, R. J., VanBuren, R., and Woolsey, N. F., *J. Org. Chem.*, 43 2991 (1978).
- (7) Doyle, G., *Prepr., Div. Pet. Chem., Am. Chem. Soc.*, 21(1), 165 (1976).
- (8) Bartsch, R., and Tanielian, C., *J. Catal.*, 35(3), 353 (1974).
- (9) Nagai, M., Urinoto, H., and Sakikawa, N., *Nippon Kagaku Kaishi*, (2), 356, *Chem. Abstr.*, (1975), 158438b.
- (10) Urinoto, H., and Sakikawa, N., *Sekiyu Gakkai Shi*, 15(11), 926 *Chem. Abstr.*, (1972), 111042v.
- (11) Rollmann, L. D., *J. Catal.*, 46(3), 243 (1977).
- (12) Franklin, J. L., and Lumpkin, H. E., *J. Amer. Chem. Soc.*, 74, 1023 (1952).
- (13) Bonner, W. A., and Gumim, R. A., "Mechanisms of Raney Nickel Desulfurization," Kharesch, N., and Meyero, C. Y., Ed., Vol.2, *The Chemistry of Organic Sulfur Compounds*, Pergamon Press, Oxford, England, 1966, p.40.

Table 1. Reduction of Diphenyl sulfide¹

| Run | Reducing gases ² | Solvent | Catalyst ³ | Benzene, % ⁴ | Toluene, % ⁴ | Thiophenol, % ⁴ | Thioanisole, % ⁴ | Benzoic acid, % ⁴ | Conversion, % ⁵ |
|-----|-------------------------------------|----------|---------------------------------|-------------------------|-------------------------|----------------------------|-----------------------------|------------------------------|----------------------------|
| 1 | None | None | None | 2.3 | 0.0 | 0.0 | 0.0 | 0.0 | 2.3 |
| 2 | CO-H ₂ O | None | None | 31.0 | 2.4 | 4.3 | 0.0 | 26.7 | 64.4 |
| 3 | H ₂ | None | None | 100.0 | 0.0 | 0.0 | 0.0 | 0.0 | 100.0 |
| 4 | CO-H ₂ O, H ₂ | None | None | 91.4 | 4.0 | 0.0 | 0.0 | 3.8 | 99.2 |
| 5 | CO-H ₂ O | None | Na ₂ CO ₃ | 11.8 | 0.7 | 4.0 | 0.4 | 30.4 | 47.3 |
| 6 | H ₂ | None | Na ₂ CO ₃ | 53.7 | 0.0 | 0.0 | 0.0 | 0.0 | 53.7 |
| 7 | CO-H ₂ O, H ₂ | None | Na ₂ CO ₃ | 41.4 | 0.5 | 0.4 | 0.0 | 1.1 | 43.4 |
| 8 | CO-H ₂ O, H ₂ | Tetralin | Na ₂ CO ₃ | 18.1 | 0.2 | 0.0 | 0.0 | 0.0 | 18.3 |
| 9 | CO-H ₂ O, H ₂ | None | FeS | 52.1 | 2.2 | 3.0 | trace | 11.1 | 68.4 |

1. 0.15 mole total.

2. Each gas is at 750 psi initial pressure except when hydrogen and carbon monoxide are used simultaneously; then each is at 375 psi initial pressure. Argon is added to bring the total pressure to 1500 psi.

3. 0.015 mole.

4. Normalized to converted starting material.

5. Based on recovered starting material.

Table 2: Reduction of Dibenzothiophene¹

| <u>Run</u> | <u>Reducing gases</u> | <u>Catalyst</u> | <u>Solvent</u> | <u>Diphenyl, %</u> | <u>Conversion, %</u> |
|------------|---------------------------------------|---------------------------------|----------------|--------------------|----------------------|
| 1 | H ₂ , H ₂ O | None | None | 2.7 | 2.7 |
| 2 | H ₂ , H ₂ O | Na ₂ CO ₃ | None | 0.6 | 0.6 |
| 3 | CO, H ₂ O | Na ₂ CO ₃ | None | 1.2 | 1.2 |
| 4 | H ₂ , CO, H ₂ O | Na ₂ CO ₃ | None | 0.8 | 0.8 |
| 5 | H ₂ , CO, H ₂ O | Na ₂ CO ₃ | Tetralin | 2.3 | 2.3 |
| 6 | H ₂ , CO, H ₂ O | FeS | None | 1.7 | 1.7 |

1. 0.15 mole and the footnotes of Table 1 apply here also.

Table 3. Reduction of Thioanisole¹

| Run | Reducing gases, ² | Solvent | Catalyst ³ | Benzene, % ⁴ | Toluene, % ⁴ | Diphenyl sulfide, % ⁴ | Thiophenol, % ⁴ | Benzoic acid, % ⁴ | Conversion, % ⁵ |
|-----|---------------------------------------|-----------------------|---------------------------------|-------------------------|-------------------------|----------------------------------|----------------------------|------------------------------|----------------------------|
| 1 | None, H ₂ O ⁶ | None | None | 4.4 | 29.5 | 38.2 | 1.4 | 0.0 | 80.7 |
| 2 | H ₂ , H ₂ O | None | None | 84.1 | 1.1 | 0.0 | 0.0 | 0.0 | 85.2 |
| 3 | CO, H ₂ O | None | None | 10.9 | 6.9 | 9.5 | 0.4 | 12.8 | 40.5 |
| 4 | H ₂ CO, H ₂ O | None | None | 76.1 | 5.7 | 1.8 | trace | 2.5 | 86.1 |
| 5 | H ₂ , H ₂ O | None | Na ₂ CO ₃ | 37.7 | 4.3 | 1.4 | 0.0 | 0.0 | 43.4 |
| 6 | CO, H ₂ O | None | Na ₂ CO ₃ | 24.5 | 10.0 | 7.0 | trace | 1.9 | 43.4 |
| 7 | H ₂ , CO, H ₂ O | None | Na ₂ CO ₃ | 14.0 | 7.3 | 3.0 | 0.0 | 0.0 | 24.3 |
| 8 | H ₂ , CO, H ₂ O | Tetralin ³ | Na ₂ CO ₃ | 9.3 | 0.9 | 1.2 | 0.0 | 0.0 | 11.4 |
| 9 | CO, H ₂ O | None | FeS | 14.9 | 7.8 | 8.9 | 0.0 | 17.8 | 49.4 |
| 10 | H ₂ , CO, H ₂ O | None | FeS | 32.7 | 8.0 | 4.5 | 8.5 | 8.1 | 61.8 |
| 11 | CO | None | None | 2.7 | 44.8 | 15.8 | 0.0 | - | 63.3 |

- 0.15 mole.
- Each gas is at 750 psi initial pressure except when hydrogen and carbon monoxide are used simultaneously; then each is at 375 psi initial pressure. Argon is added to bring the total pressure to 1500 psi.
- 0.015 mole.
- Normalized to converted starting material.
- Based on recovered starting material.
- Contains 7.2% of an unidentified material.

HIGH-YIELD COAL CONVERSION IN A ZINC CHLORIDE/METHANOL MELT UNDER MODERATE CONDITIONS

John H. Shinn and Theodore Vermeulen

Chemical Engineering Department and Lawrence Berkeley Laboratory
University of California, Berkeley, California 94720

INTRODUCTION

Converting coal to soluble material requires cleavage of enough chemical bonds to split the coal into subunits of only moderately high molecular weight. Because coal is inaccessible to conventional solid catalysts, current processing schemes use severe thermal conditions to effect the needed bond scission, with the handicaps of partial fragmentation to gas and partial polymerization of cleaved products.

Hydrogen-donor action involving direct or indirect hydrogenation by solid catalysts has provided minor reductions in the severity of treatment, insufficient to alleviate the wastage of coal and of input hydrogen. To lower the scission temperature adequately requires mobile catalysts which can penetrate thoroughly into the coal. Melts such as zinc chloride are therefore a promising area for study.

Major work on zinc chloride catalysts for hydrogenation and hydrocracking of coal has been carried out by Zielke, Gorin, Struck and coworkers at Consolidation Coal (now Conoco Coal Development Co.)¹. The emphasis there has been on a full boiling-point range of liquid product, from treatment at temperatures between 385 and 425°C and hydrogen pressures of 140 to 200 bars.

In this Laboratory, several potential liquid-phase treating agents have been studied at 225-275°C--that is, at temperatures well below 325°C, which appears to be the initiation temperature for pyrolysis of the coals studied here. Working with Wyodak coal in a ZnCl₂-water melt at 250°C, Holten and coworkers^{2,3} discovered that addition of tetralin increased the pyridine solubility of product to 75%, compared to 25% without tetralin. About 10 wt-% of water is required in the melt, because pure ZnCl₂ melts at 317°C.

We have now found that replacing water in the melt by methanol leads to large increases in pyridine solubility of product from the treatment. In this paper we characterize the effects of temperature, time, hydrogen pressure, reaction stoichiometry, and addition of various inorganic and organic additives. Because oxygen removal from the coal occurs in parallel with solubilization, we conclude that scission of ether-type C-O bonds is the definitive chemical reaction.

EXPERIMENTAL PROCEDURE

The experiments were performed in a 600-ml Hastelloy B stirred Parr autoclave fitted with a 300 ml glass liner. 275 gm of ZnCl₂ (97+% pure from Matheson, Coleman, and Bell) were loaded into the liner with the desired amount of methanol (Mallinkrodt reagent-grade) and heated to about 150°C. At this time, 50 gm of undried Roland seam Wyodak coal (-28 + 100 mesh) and additional solvent (if any) were added to the melt. The autoclave was closed, purged with hydrogen, and pressurized so that it would reach the desired hydrogen pressure at reaction temperature. The contents were heated at approximately 10°C/min with stirring until the desired temperature was reached. After reaction for the desired period, the autoclave was immersed in

a cold-water bath, depressurized, and opened, and the contents were dumped into 2 l. of cold water. The coal was then washed in a Buchner funnel with 6 l. of distilled water at 90°C, and dried to constant weight in a vacuum oven at 110°C under 50 millibars of nitrogen. Some runs were split after water quenching; in these, half of the product was washed with dilute HCl before hot-water rinsing.

Approximately 2 gm of dried product (referred to as melt-treated coal, MTC) were extracted to exhaustion sequentially with benzene and pyridine in an atmospheric soxhlet apparatus. The extracts and residue were dried and weighed to determine solubility of the MTC.

In addition to knowing the total MTC solubility, it was important to determine the amount of methanol or other solvent retained by the MTC. This quantity, the incorporation ratio ($R = \text{gms incorporated organic material/gms coal-derived organic material}$), was determined by a carbon balance on the reaction. By assuming that any solvent retained in the dried MTC is pyridine-soluble, and subtracting it from the total dissolved material, the minimum solubility of the coal-derived material may be calculated. This quantity, the corrected solubility, is an indicator of the true solubilizing effect of a particular run on the coal itself. Based on replicate runs, the standard deviation of the corrected solubility is 6.5% of the reported value.

Additional details on the experimental methods employed are available elsewhere⁴.

RESULTS

Effect of Reaction Conditions on Solubility

Earlier results³ suggested investigation of the ZnCl_2 -methanol system as a coal-liquefaction medium based on high product solubility, low incorporation, and relatively low cost of methanol.

Of primary concern were the effects of temperature, pressure, time, and methanol amount on the solubilizing activity of the melt. Figure 1 presents the effect of hydrogen pressure and temperature on corrected solubility. At 60 min reaction time with 50 gm of methanol, the solubility is roughly linear with hydrogen partial pressure. Even at 225°C there is significant conversion, with 800 psig producing 40% MTC solubility compared to 12% for the raw coal. By 275°C, conversion is rapid with nearly total solubility in one hour at hydrogen pressures as low as 200 psig.

The effect of methanol amount at various hydrogen pressures is shown in Figure 2. At all hydrogen pressures, there is a maximum solubilizing effect near 50 gm methanol (approximately .75/l MeOH/ ZnCl_2 molar). To within experimental error, solubility is linear with hydrogen pressure.

As shown in Figure 3, solubilization proceeds linearly with time at 250°C (800 psig, 50 gm MeOH) with total solubility achieved near 75 minutes. At 275°C, reaction is considerably more rapid, with total conversion possible in less than 30 minutes. Heating alone to 250°C ("zero-time" runs) produces negligible increased solubility, whereas the additional 2-3 minutes between 250 and 275° for heating to 275°C results in almost 40% solubility.

Effect of Reaction Conditions on Incorporation

In addition to solubilizing activity, it is desirable to limit the amount of methanol retained by the MTC. Table 1 shows there is no significant effect of temperature on methanol incorporation at 800 psig, but a rapid rise in incorporation above 250°C at 200 psig hydrogen. There is less incorporation with 25 gm methanol than with 50 gm, and a leveling off of incorporation at higher hydrogen pressures. Also, there is no trend in incorporation with time at 275°C, but a strong increase of incorporation with time at 250°C.

Table 1. Effect of Operating Variables on Incorporation of Methanol and on Corrected H/C Ratios (273 g ZnCl₂, 50 g Wyodak coal)

| Methanol (gm) | Hydrogen (psig) | Temp (°C) | Time (min) | Corrected Solubility (Pct. DAF) | Retained MeOH (gm/gm coal organics) | Atomic H/C Ratio | |
|---------------|-----------------|-----------|------------|---------------------------------|-------------------------------------|------------------|--|
| 50 | 0 | 250 | 60 | 57.3 ¹ | .31 | .53 | |
| | 200 | | | 67.4 ¹ | .16 | .81 | |
| | 500 | | | 70.3 ¹ | .19 | .78 | |
| | 800 | | | 85.0 ¹ | .18 | .85 | |
| 25 | 200 | | | 54.8 | .16 | .70 | |
| | 800 | | | 73.6 | .05 | .96 | |
| 50 | 800 | 250 | 0 | 13.2 | .05 | | |
| | | | 30 | 53.7 | .16 | | |
| | | | 0 | 35.8 | .16 | | |
| | | | 30 | 100.0 | .21 | | |
| | 200 | 225 | 60 | 26.4 | .12 | | |
| | 800 | | | 40.0 | .11 | | |
| | 200 | | | 275 | 95.6 | .32 | |
| | 800 | | | | 99.1 | .17 | |

¹ Average of replicate runs.

Hydrogen-to-Carbon Ratios

An indicator of the quality of the MTC is the hydrogen to carbon ratio (raw coal H/C = .98). Figure 4 shows the effect of methanol amount and hydrogen pressure on the H/C ratio of the coal derived portion of the MTC. Higher hydrogen pressures result in higher H/C ratios regardless of methanol amount. Higher methanol amounts produce lower H/C ratios at all pressures up to 500 psig. At 800 psig, there is a maximum near 25 gm methanol in the H/C ratio with a sharp drop afterward.

Effect of Additives

Table 2 lists the results of runs in which inorganic additives were used in the ZnCl₂-MeOH melt. Addition of 5 mole % ZnO, a noted poison for ZnCl₂, had little effect on solubility and produced a surprising rise in H/C ratio of the MTC. The addition of 1 gm Zn powder had little effect in solubility but slightly improved the H/C

ratio. 100 psig HCl, while producing total solubility, had little more effect than a dilute HCl wash. The hydrated chlorides of tin and cadmium resulted in reduced yields.

Solvent additives to the melt (Table 3) fall into two categories: extractive and reactive. The extractive solvents (decane, perchloroethane, o-dichlorobenzene, and pyrrolidine) had negligible effect on solubility, possibly due to the preferential wetting of the coal by the solvent and exclusion of the ZnCl₂ melt. Reactive solvents (anthracene oil, indoline, cyclohexanol, and tetralin) all incorporated strongly. Donor solvents, tetralin and indoline, increase corrected solubility, whereas anthracene oil and cyclohexanol have negligible effect.

Table 2. Effect of Inorganic Additives to ZnCl₂-Methanol Melt.
273 gm ZnCl₂; 50 gm MeOH; 50 gm coal; T = 250°C; t = 60 min

| Additive (gm) | P _{H₂} (psig) | Corrected Solubility (Pct. daf) | R (gm retained MeOH/gm coal organic) | Corr. Atomic H/C |
|---------------------------------------|-----------------------------------|---------------------------------|--------------------------------------|------------------|
| HCl (100 psig) | 500 | 100.0 | 0.16 | 0.84 |
| ZnO (9.0) ³ | 500 | 69.2 | 0.11 | 1.10 |
| Zn (1.0) | 500 | 73.6 | 0.15 | 0.86 |
| CdCl ₂ (38.5) ¹ | 200 | 44.3 | 0.16 | 0.76 |
| SnCl ₂ (42.1) ² | 200 | 0.0 | 0.19 | 0.55 |
| None ³ | 500 | 70.3 | 0.18 | 0.79 |
| None ³ | 200 | 67.3 | 0.17 | 0.76 |

1 - 11.4 gm water present with CdCl₂

2 - 36.0 gm water present with SnCl₂

3 - Average of two replicate runs

Table 3. Effect of Solvent Additives to ZnCl₂-Methanol Melt.
273 gm ZnCl₂; 50 gm MeOH; 50 gm coal; T = 250°C; t = 60 min

| Solvent (gm) | P _{H₂} (psig) | Corrected Solubility (Pct. daf) | R (gm retained MeOH/gm coal organic) |
|-------------------------------------|-----------------------------------|---------------------------------|--------------------------------------|
| n-Decane (50) | 250 | 41.4 | 0.19 |
| C ₂ Cl ₆ (50) | 200 | 40.5 | 0.43 |
| o-Cl ₂ -benzene (60) | 200 | 33.5 | 0.16 |
| Pyrrolidine (10.5) | 500 | 65.6 | 0.13 |
| Cyclohexanol (10) | 200 | 68.7 | 0.39 |
| Anthracene Oil (10) | 250 | 73.7 | 0.77 |
| Tetralin (10) | 200 | 77.4 | 0.65 |
| Indoline (10) | 500 | 81.5 | 0.27 |
| Methanol only | 500 | 70.3 | 0.18 |

Effect of Wash

Several runs were divided after water quenching of the MTC and 15 ml HCl was added to the cold water wash. Figure 5 shows the increase in benzene and total MTC solubility as a result of the HCl wash. Acid washing produces total pyridine solubility from a 65% soluble water washed MTC. The effect of acid washing on benzene solubility is less marked with a maximum increase of 10-15% at 25% water wash benzene solubility. The maximum benzene solubility with either water or acid wash is 40%.

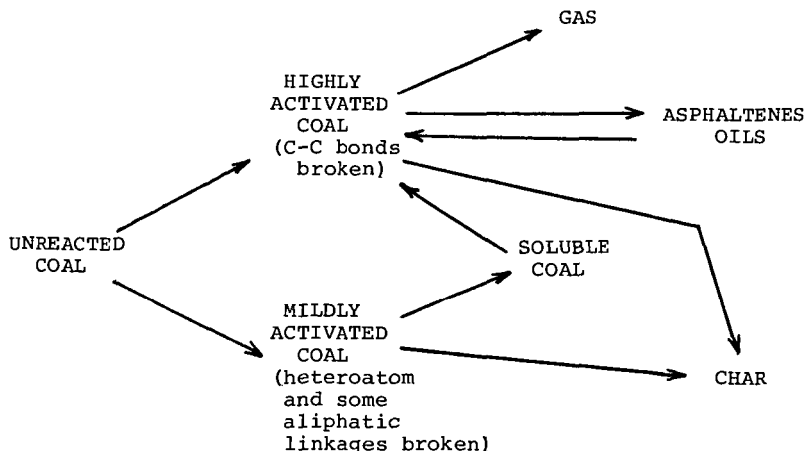
In some runs, a preliminary benzene wash was necessary to make the MTC sufficiently hydrophilic to allow removal of the $ZnCl_2$. The solubilized material from the wash was added to the benzene soxhlet yield for total benzene solubility. As seen in Figure 6, the relationship between benzene solubility and pyridine solubility of the MTC is a function of the type of wash used. Benzene washing produces higher benzene solubility whereas HCl washing produces higher pyridine than water wash.

Oxygen Recovery and Solubility

Earlier work with the $ZnCl_2-H_2O$ system³ had revealed a correlation between the oxygen recovery and the solubility of the MTC. There proved to be a similar relationship in the $ZnCl_2$ -methanol system, as well as a separate relationship for acid-washed runs (Figure 7). Conditions of temperature, hydrogen pressure, reaction time and stoichiometry did not affect the relationship for a particular solvent, whereas additional solvent produced skew points supporting the conclusion that the relationship is solvent dependent. Acid washing produces increased solubility without affecting oxygen removal.

DISCUSSION

The following scheme may be used to explain the conversion of coal to soluble form.



The first step in conversion is activation. This activation may be weak (by using low temperatures and less active catalysts) cleaving only weaker heteroatom bonds or strong (by using higher temperatures and active catalysts such as HCl) cleaving weaker as well as stronger C-C bonds. (Weak bonds include ether and thioether as well as aliphatic linkages with suitably substituted neighboring aromatic centers^{5,6}.) Keys to the mild activation are penetration of the catalyst into the coal, sufficient catalyst activity toward weak bond cleavage and resistance to poisoning. Massive amounts of molten ZnCl₂ provide the proper activation and the correct choice of solvent allows for proper contacting.

Scanning electron micrographs of methanol-treatment MTC show that methanol addition causes massive physical change in the coal particles, presumably enhancing phase contact and removing product during reaction so as to expose unreacted coal⁷.

The cleaved weaker bonds must now be properly "capped" to prevent polymerization to char. Several mechanisms are available for such capping. First, hydroaromatic structures in the coal may exchange hydrogen with the reacted fragments, as noted by Whitehurst et al.⁸ This type of donation may result in a net lowering of H/C ratio of the product as hydrogen is lost forming water upon oxygen removal. Two sources of external hydrogen are also available: from donor solvents and gas-phase hydrogen. The contribution of gas-phase hydrogen is normally small but there is promise for enhancement of this effect through the use of additives with hydrogenation activity still being investigated. Finally, capping may occur without hydrogen, by means of alkylation. Methanol may be important in this step, as its presence may prevent crosslinking subsequent to ZnCl₂ attack.

Conversion of soluble coal to asphaltenes and oils will require further activation of the coal with C-C bond cleavage and further heteroatom removal. Higher temperatures and/or more active catalysts will likely be required with sufficient hydrogen donors and hydrogenation catalysts to reduce char formation. Preliminary investigations on this further conversion are currently under way in our labs. The soluble coal should facilitate contacting, allowing a greater choice of catalysts for upgrading.

CONCLUSIONS

Some preliminary work was done with other solvents which were miscible with the ZnCl₂. We have discovered that replacing water with methanol as a liquefying agent for the ZnCl₂ results in large increases in pyridine solubility of the treated coal. There are several explanations for this effect: improved contacting between the coal and the melt; higher activity of the ZnCl₂ in a methanol media; methylation of cleaved bonds resulting in reduced char formation; extraction of the reaction products, leaving the coal more accessible.

Solubility is linear with hydrogen pressure and time, at constant temperature and methanol charge. There is a strong effect of temperature leading to complete solubility at 275°C in less than 30 minutes. Incorporation is best limited by lower methanol amounts and higher hydrogen pressures.

Extractive solvents reduce solubility; donor solvents increase solubility, but involve incorporation. A relation between benzene and pyridine solubility is dependent on wash conditions. Finally, oxygen recovery and corrected solubility are related, the relationship varying with the solvent used.

REFERENCES

- (1) C. W. Zielke, R. T. Struck, J. M. Evans, C. P. Costanza, and E. Gorin, *Ind. Eng. Chem. Proc. Des. Devel.*, 5, 158 (1966).
- (2) R. R. Holten and T. Vermeulen, Univ. Calif. Lawrence Berkeley Laboratory, Report LBL-5948 (1977).
- (3) J. H. Shinn, F. Hershkowitz, R. R. Holten, T. Vermeulen, and E. A. Grens, "Coal Liquefaction in Inorganic-Organic Liquid Mixtures." Paper presented at Am. Inst. Chem. Engrs. annual meeting, Miami, Florida, November 1977.
- (4) J. H. Shinn and T. Vermeulen, Univ. Calif. Lawrence Berkeley Laboratory, report in preparation.
- (5) N. D. Taylor and A. T. Bell, Univ. Calif. Lawrence Berkeley Laboratory, report in preparation.
- (6) B. M. Benjamin et al., *Fuel*, 57, 269 (1978).
- (7) J. H. Shinn and T. Vermeulen, "Scanning Electron Microscopy Study of the Solubilization of Coal Under Mild Conditions." Paper submitted for presentation at Scanning Electron Microscopy Symposium, Washington, D. C., April 1979.
- (8) D. D. Whitehurst, M. Farcasiu, T. O. Mitchell, and J. J. Dickert, Mobil Res. & Dev. Corp., "Nature and Origin of Asphaltenes in Processed Coals." Electric Power Research Institute, Report AF-252 (February 1976).

ACKNOWLEDGMENT

The work reported was carried out under the auspices of the Division of Chemical Sciences, Office of Basic Energy Sciences, United States Department of Energy.

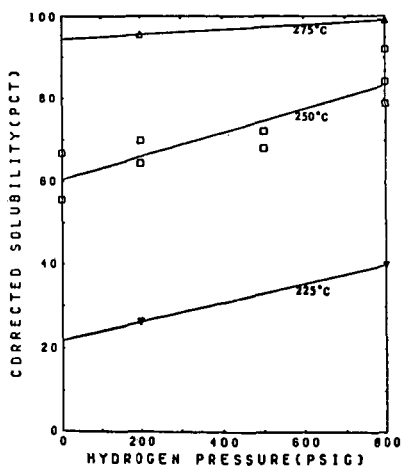


Figure 1.
Effect of Hydrogen Pressure and Temperature on Corrected Solubility. 273 gm $ZnCl_2$; 50 gm coal; 50 gm MeOH; 60 min.

Figure 2.
Effect of Methanol Charge and Hydrogen Pressure on Corrected Solubility.
273 gm $ZnCl_2$; 50 gm coal;
250°C; 60 min.

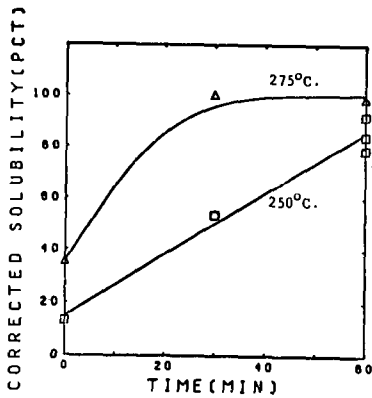
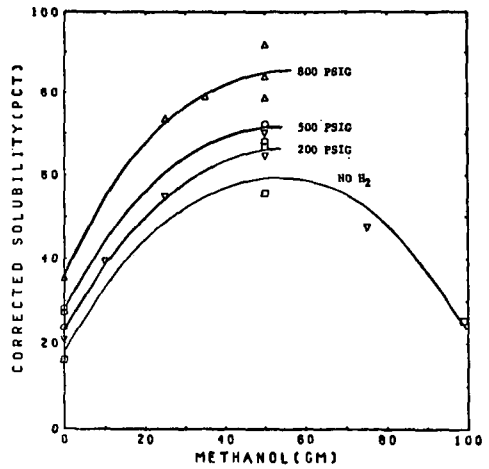
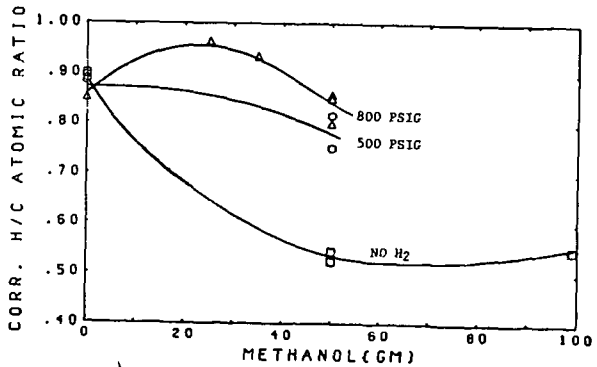


Figure 3.
Effect of Run Time on Corrected Solubility at 250° and 275°C.
273 gm $ZnCl_2$; 50 gm coal;
50 gm MeOH; H_2 , 800 psig.

Figure 4.
Effect of Methanol Charge and Hydrogen Pressure on Atomic H/C Ratio.
273 gm $ZnCl_2$; 50 gm coal;
250°C; 60 min.



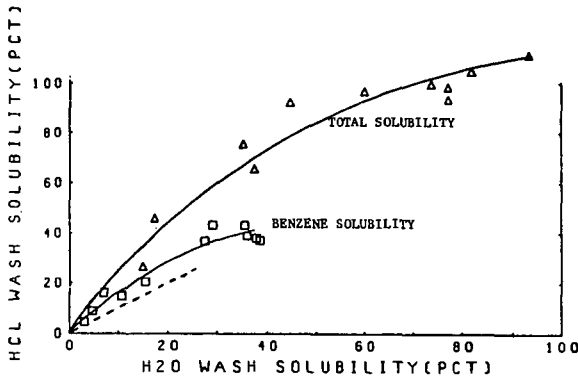


Figure 5.
Effect of Acid Wash
on Solubilities.
273 gm $ZnCl_2$;
50 gm coal.

Figure 6.
Relations Between
Benzene and Total
Solubility.
273 gm $ZnCl_2$;
50 gm coal.

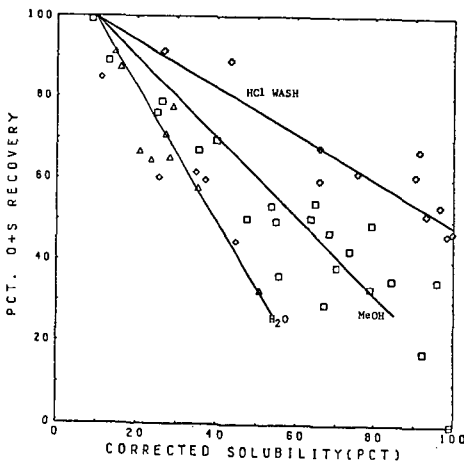
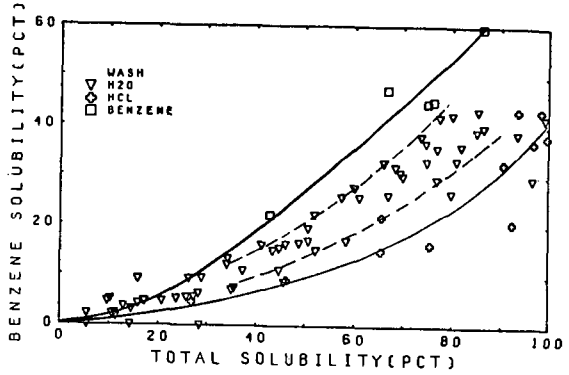


Figure 7.
Oxygen and Sulfur
Recovery in Product
vs Total Solubility.
273 gm $ZnCl_2$; 50 gm coal.

THE EFFECT OF COAL STRUCTURE ON THE
DISSOLUTION OF BROWN COAL IN TETRALIN

Robert J Hooper and David G Evans

DSIR
Industrial Processing Division
Private Bag
Petone
New Zealand

Centre for Environmental Studies
University of Melbourne
Parkville 3052
Victoria
Australia

INTRODUCTION

In much of the literature on coal dissolution in hydrogen donor systems the extent of the hydrogenation processes is assessed in terms of either the yield of liquid product or the conversion of coal to material soluble in a specified solvent, normally a solvent ineffective for coal. However, such approaches can not describe fundamental changes that occur within the coal material. To do this requires an experimental approach that allows coal conversion to be discussed in terms of the chemical changes that occur within the coal. This, in turn, requires a direct method of determining the structural features in coal.

In another paper presented at this Congress (1) we described the use of the acid-catalysed reaction of coal with phenol to study the structure of an Australian brown coal from Morwell, Victoria. The coal was solubilized by reacting it with phenol and then separated into four fractions, the first rich in aliphatics, the second rich in simple aromatics, the third rich in di-aromatics and polar groups, and the fourth rich in polyaromatics.

If these fractions are regarded as models of structural types within the coal, then reacting each fraction separately allows the role played by different chemical structures during the hydrogenation process to be examined. The effect that chemical type has on the coal hydrogenation reaction may then be studied directly and, in addition, the hydrogenation process may be represented by a composite process made up from the individual reactions of the different fractions.

The work now to be reported tested this hypothesis by reacting such fractions individually with tetralin, without any additions of catalyst or gaseous hydrogen. The untreated whole coal was also reacted to test whether phenol, present in the coal fractions as a result of the fractionation procedure, was having any significant effect on the reaction with the fractions.

EXPERIMENTAL

Experimental procedure

Morwell brown coal was solubilized by reacting with phenol, in the presence of para toluene sulfonic acid at 183°C and the reaction product was then separated into four fractions. The structural characteristics of the four fractions, as described in our other paper (1), are summarized in Table 1. As these characteristics are influenced to some extent by the presence of chemically combined phenol, the content of this in each fraction, as estimated in the present work and confirmed by reference to the literature (2,3) is also noted in Table 1.

Approximately 3g samples of the coal fractions and of the whole coal were then reacted separately with 25 - 30 ml of tetralin at 450°C in a type 316 stainless steel, sealed reactor, 13 cm high by 2 cm diameter. The reactor was heated by plunging it into a preheated fluidized sand bath; after 4 hours it was removed and quenched rapidly.

Table 1: Structural Characteristics of Coal Fractions Separated from Solubilized Brown Coal (1)

| Fraction | Mass % Phenol | Structural Characteristics |
|--|---------------|---|
| A A liquid soluble in pentane | 50 | Mostly aliphatic material with some mono-aromatic parts broken off the coal by C-C cleavage. Apart from combined-phenol it has negligible polar material. It contains some free paraffinic material, but exists mostly as alkyl phenols and alkyl-aryl ethers |
| B A liquid insoluble in pentane but soluble in benzene | 50 | A mixture of alkyl side chains and aromatic fragments, predominantly di-aromatic. It exists either as alkyl phenols or as aromatic fragments attached to phenol by methylene bridges. It also contains other oxygen functional groups |
| C A pitch insoluble in benzene but soluble in benzene/ethanol azeotrope | 25 | Consists almost entirely of aromatic fragments attached to phenol by methylene bridges. These fragments are larger than in fraction B as they contain polyaromatic groups. It has more oxygen functional groups than B. |
| D A solid insoluble in ethanol/benzene azeotrope | 10 | Predominantly diaromatic and polynuclear perhaps combined through naphthenic bridges, with negligible aliphatic content |

The temperature of the reaction mix was measured by a stainless steel-sheathed thermocouple inserted through the reactor cap. Heating up and cooling down times were small compared with the total reaction time. In all cases the free space in the reactor was flushed with nitrogen before sealing, and the reaction proceeded under a small initial nitrogen pressure.

After reaction, any solid residue was filtered off and the liquid product was separated by distillation into a bottoms product and a distillate that included unreacted tetralin and low-boiling products from both the coal and the tetralin. As tetralin breaks down under dissolution conditions to form mainly the tetralin isomer 1-methyl indan, naphthalene and alkyl benzenes (4) it was assumed that no compound with a higher boiling point than naphthalene was formed from the solvent, and the distillation to recover solvent was therefore continued until naphthalene stopped subliming. Some residual naphthalene remained in the bottoms product; its mass, as determined from nmr and elemental analysis, was subtracted from the mass of bottoms product recovered and included in the amount of distillate recovered. It was assumed that all naphthalene present came from the tetralin, not the coal. However, as the amount of tetralin reacted was 10 times the amount of coal this assumption appears reasonable.

Material formed from the coal which appears in the distillate is here called solvent-range material, following the terminology used by Whitehurst et al (5). Its mass was estimated by mass balance over the material recovered from the reaction as it could not be

separated from the large excess of tetralin and tetralin breakdown products also contained in the distillate. This procedure includes with the mass of solvent-range material any gases and water formed in the reaction.

Analysis techniques

The contents of the major breakdown products of tetralin (naphthalene and 1-methyl indan) present in the distillate were determined by gas-liquid chromatography using a Hewlett Packard Series 5750 Research Chromatograph with a 62m x 0.5mm diameter glass capillary SCOT column coated with non-polar SE 30 liquid phase (see Ref (4) for details).

Infrared spectra of the original coal, the original coal fractions, and all bottoms product and residues derived from them were measured on a Perkin Elmer 457 Grating Infrared Spectrophotometer. Liquid samples were analysed as a thin film or smear. Solid samples were prepared as a KBr disc containing approximately 0.3% by weight sample. The disc was prepared by grinding the KBr mixture for 2 minutes in a tungsten carbide TEMA grinding barrel, drying for 24 h in a vacuum desiccator over phosphorus pentoxide, then pressing into a disc at 10 tons force, at room temperature, but under vacuum.

Proton nmr spectra of fractions A, B and C and all bottoms products were recorded on a Varian HA 100nmr spectrometer using a solution of the sample dissolved in pyridine-d₅. Spectra were run at room temperature with tetra methyl silane (TMS) as an internal standard, with a sweep width of 0 to 1000 cps from TMS. Fraction D and the whole coal were only partly soluble in pyridine and it was therefore not possible to get representative spectra from them.

Carbon, hydron and oxygen contents of the original coal, original fractions, bottoms and residues were determined microanalytically by the CSIRO Microanalytical Service. Ash contents of samples were determined in a standard ashing oven (6). Phenolic and carboxylic oxygens were measured by the State Electricity Commission, using techniques developed by them for brown coals (7).

RESULTS

Recovery of coal material from the reaction with tetralin

The yields of the different products from the reactions of the various fractions with tetralin are summarized in Table 2.

| Component | Fraction | | | | | Whole Coal | | | | |
|----------------|-----------------|-----------------|-----------------|-----------------|-----------------|-----------------|-----------------|-----------------|-----------------|-----|
| | A | | B | | C | | D | | Composite | |
| | % of frac- tion | g/100g dry coal | % of frac- tion | g/100g dry coal | % of frac- tion | g/100g dry coal | % of frac- tion | g/100g dry coal | g/100g dry coal | |
| bottoms | 47 | 13 | 56 | 37 | 37 | 29 | 30 | 9 | 88 | 46 |
| residue | 0 | 0 | 0 | 0 | 27 | 21 | 61 | 17 | 38 | 40 |
| solvent range | 53 | 15 | 44 | 29 | 36 | 28 | 9 | 2 | 74 | 14 |
| total fraction | 100 | 28 | 100 | 66 | 100 | 78 | 100 | 28 | 200 | 100 |

Table 2: Yields of original coal fractions and their products of reaction with tetralin, g/100g original dry coal.

These yields are also given on the basis of 100 g of original dry coal before fractionation. The bottom line of the table shows the mass of each fraction obtained from 100 g of dry coal. The masses include chemically combined phenol and residual solvent associated with the fraction as a result of the coal preparation and fractionation scheme. (For every 100g of original dry coal an additional 100g of extraneous material was present. Elemental balances and other evidence showed that about 70g of this was phenol and the remainder was excess solvent (benzene) never separated from the original fractions). Note that with fractions A and B no solid residue was obtained.

The amount of residue recovered from the other two fractions is almost the same as that recovered from the whole-coal reaction, suggesting that the combined phenol and residual solvent end up completely in the bottoms product and solvent-range product.

Composition of the coal products

Table 3 shows elemental compositions of the original coal fractions, the solid residues and the bottoms products, together with the portions of the total oxygen present as phenolic and carboxylic groups. Because of dilution with combined phenol and benzene solvent the composite analysis of the original fractions has higher carbon and lower oxygen contents than the original whole coal (note also the higher phenolic oxygen content).

As expected, both the bottoms products and the residues, when formed, have substantially higher carbon and lower oxygen contents than the original fractions, but whereas in the bottoms products the hydrogen contents have increased in the residues they are reduced. The bottoms products, including that from the whole coal, are remarkably similar in composition to each other. Likewise the residues are similar in composition to each other.

Figure 1 shows representative infrared spectra for the fractions before reaction and for bottoms products and residues. Although there were considerable differences in the spectra of the four original fractions the spectra obtained for their bottoms products were quite similar. The spectra show that significant amounts of aliphatic material (2850 and 2920 cm^{-1}) is present in the bottoms. An aromatic content is indicated by the aromatic C-H stretching vibration at 3030 cm^{-1} , but this is due in part, at least, to residual naphthalene and to phenol combined with the original fraction. Absorption at 3400 cm^{-1} (due to hydrogen bonded OH), present in both the coal fractions and the coal before reaction, has almost disappeared in the products from the coal fractions. The absorption does still occur in the bottoms product from the whole coal, although it is greatly reduced.

The spectra show that carbonyl groups (absorption at 1700 cm^{-1}) and the broad absorption in the region $1000 - 1200\text{ cm}^{-1}$ due to oxygen functional groups, both normally present in coal, have been destroyed, indicating, as would be expected, that functional groups are destroyed during the reaction. The absence of a large hydrogen-bonded OH peak at 3400 cm^{-1} indicates that the remaining oxygen absorption at 1250 cm^{-1} is not due to phenol. This absorption may be due to ether absorption, but this assignment is by no means certain, as normally ether absorption in this region is broad whereas the spectra show sharp absorption.

Aliphatic material still remains in the residue from the whole coal, but is virtually eliminated in the residue from fraction C. The absorption at 1170 cm^{-1} in the spectra of both residues may be due to benzofuran type structures (8), but it is felt that the strong absorption in the region $1000-1200\text{ cm}^{-1}$ may have been enhanced by the presence of silica, a major component of the ash content in this coal.

| | fraction | | | | | Whole Coal |
|--------------------------|----------|----|------|----|-----------|---------------|
| | A | B | C | D | composite | |
| <u>original fraction</u> | | | | | | |
| C | 76 | 74 | 69 | 71 | 72 | 63 |
| H | 7 | 6 | 5 | 4 | 5 | 5 |
| O phenolic | 8 | 8 | 7 | 11 | 8 | 5 |
| O carbolic | 0 | 3 | 5 | 4 | 4 | 5 |
| O total | 17 | 16 | 21 | 18 | 18 | 25 |
| ash | - | - | 2 | 3 | 2 | 4 |
| unaccounted | 1 | 4 | 3 | 4 | 3 | 3 |
| <u>residue</u> | | | | | | |
| C | | | 89 | 86 | 88 | 85 |
| H | | | 4 | 4 | 4 | 4 |
| O | | | 3 | 3 | 3 | 5 |
| ash | | | N.D. | 7 | N.D. | 8 |
| unaccounted | | | N.D. | 0 | N.D. | -2 |
| <u>bottoms</u> | | | | | | |
| C | 86 | 83 | 86 | 83 | 85 | 85 |
| H | 7 | 7 | 7 | 7 | 7 | 8 |
| O | 7 | 10 | 7 | 10 | 8 | 7 |

Table 3: Composition of the fractions and their reaction products, mass %. N.D. means not determined (in the case of the residue from fraction C insufficient sample was available for an ash determination). Note that the method for backing out naphthalene from the bottoms involves normalizing the composition to $C + H + O = 100\%$.

Table 4 shows the proton ratios obtained from the nmr spectra on the original fractions A, B and C and all the bottoms products. The proton ratios for the bottoms products have been adjusted to eliminate absorptions due to residual naphthalene. Note that the original fractions contained hydrogen present from combined phenol. Most of this hydrogen appears as monoaromatic hydrogen, but when the phenol -OH is still intact, one proton will appear as OH hydrogen.

| ratio of protons present in various forms to total protons, % | fraction | | | | | | | | |
|---|--------------------|---------|--------------------|---------|--------------------|---------|---------|----------------|---------------|
| | A | | B | | C | | D | comp- osite | Whole Coal |
| | orig frac- tion | bottoms | orig frac- tion | bottoms | orig frac- tion | bottoms | bottoms | btms | bottoms |
| OH hydrogen | 7 | 0 | 17 | 0 | 19 | 0 | 0 | 0 | 0 |
| polyaromatic | 0 | 0 | 0 | 0 | 6 | 0 | 0 | 0 | 0 |
| diaromatic | 6 | 0 | 10 | 0 | 8 | 0 | 0 | 0 | 0 |
| monoaromatic | 63 | 46 | 58 | 54 | 44 | 42 | 43 | 48 | 33 |
| olefinic | 1 | 0 | 0 | 0 | 0 | 0 | 0 | 0 | 0 |
| methylene bridge | 4 | 5 | 9 | 4 | 17 | 1 | 1 | 3 | 0 |
| α methine and methylene | (3 | 15 | 0 | 17 | 0 | 21 | 21 | 18 | 24 |
| α methyl | (| 8 | 1 | 8 | 4 | 11 | 11 | 9 | 8 |
| β methylene | 3 | 10 | 1 | 13 | 0 | 14 | 16 | 13 | 20 |
| β methyl | 13 | 12 | 4 | 5 | 1 | 10 | 7 | 8 | 12 |
| γ aliphatic | 0 | 4 | 0 | 0 | 0 | 0 | 0 | 1 | 4 |
| Har/Hal | 2.8 | 0.9 | 4.5 | 1.2 | 2.7 | 0.7 | 0.8 | 0.9 | 0.5 |

Table 4: Distribution of protons by type and overall aromatic/aliphatic proton ratios for the original fractions and bottoms products, as determined by proton nmr.

The nmr analyses of the bottoms products given in Table 4 show the material to have a large aliphatic content. The aromatic/aliphatic ratios of the fractions are higher than for the whole coal because of the presence of combined phenol and unseparated benzene solvent; reaction with teralin reduces these ratios considerably, presumably by transfer of much of this material to the solvent-range product, but some of it must remain in the bottoms as the aromatic/aliphatic ratio of the composite bottoms product from the fractions is higher than that from the whole coal. It was not possible to calculate the contribution that the diluents, excess solvent and combined phenol, made to the aromatic H, but the large monoaromatic content of the bottoms product must be due, in part, to these.

The remarkable feature in Table 4 is that after the spectra are adjusted for naphthalene, none of the bottoms products show the diaromatic or polyaromatic material which were present in the original materials. In the case of fractions C and D one might expect this material to end up in the solid residue, but in the reactions of fraction A and especially with fraction B, where a large diaromatic content existed before reaction, no residue was formed; thus suggesting that aromatic rings must be broken during the reaction. In addition, none of the OH hydrogen present in the original coal fractions appears in the bottoms product.

The solvent-range product was not separately analysed as it was not able to be separated from the recovered solvent in the distillate. However, GLC examination of the distillate indicated that the solvent-range product was derived mainly from aliphatic side chains

in the coal (9). Note that virtually no solvent-range product was derived from fraction D. Naphthalene and 1-methyl indan contents in the distillate were measured by GLC in order to calculate the amount of hydrogen transferred to the coal material from the solvent. It is beyond the scope of this paper to discuss in detail the results that were obtained, but it is interesting to compare the naphthalene content of the solvent recovered from the reactions between tetralin and the coal fractions with the naphthalene content of the solvent when tetralin is heated alone (Table 5). The large increase in naphthalene content when tetralin is reacted in the presence of coal material can only be explained by a reaction mechanism involving free radicals.

| Fraction | A | B | C | D | Whole Coal | Tetralin heated alone at 450°C 4h.* |
|--------------------------------------|------|------|------|------|------------|-------------------------------------|
| wt% naphthalene in recovered solvent | 12.9 | 16.9 | 23.8 | 17.1 | 11.1 | 4.3 |

* From reference (4)

Table 5: Naphthalene content of recovered solvent from reaction for 4 h at 450°C.

DISCUSSION

The effect of phenol

Three types of phenol compounds have been identified in the fractions derived from the product of the phenolation reaction (1,2): alkyl phenols and alkyl-aryl ethers, both formed by combining phenol with alkyl side chains cleaved from the coal molecule, and compounds made up of aromatic fragments attached to phenol by a methylene bridge, formed by cleaving aromatic-aliphatic linkages in the coal and exchanging the aromatic structures with phenol. For the hydrogenation of coal fractions separated from the phenolated product to simulate the hydrogenation of the whole coal the removal of coal fragments from the coal molecule during the phenolation reaction must involve similar C-C cleavage processes as would occur by the thermal breakdown of coal during a hydrogenation reaction. For example, one would expect alkyl side chains to be cleaved off under hydrogenation conditions, in much the same way as has been seen to occur in the phenolation reaction. Moreover other workers have shown that the molecular weights of coal fragments from the phenolation reaction are in the region 300 - 1000 (3) which is the same molecular weight range as for products from a coal dissolution reaction (4). Thus, both processes, one involving C-C cleavage by phenolation, the other by thermal breakdown, produce coal fragments of the same size. The hydrogenation of the coal fragments can therefore be considered to simulate the reaction of the whole coal, providing appropriate allowance is made for the movement of the phenol groups themselves.

The nature of the products

The composition of the bottoms products from the various reactions were all similar, regardless of the original material. Elemental composition ranged from 83.3% to 86.4% carbon, from 6.6% to 7.2% hydrogen, and from 6.7% to 10.1% oxygen. Infrared and nmr analysis show the material to be largely aliphatic, with hydrogen bonding in the product almost destroyed. Similarly, the residue in a carbon-rich material with very little oxygen were all similar. Its elemental composition ranged from 86.1% to 89.3% carbon, 3.8% to 4.2% hydrogen, and 2.6% to 2.9% oxygen. The material is mainly

aromatic with perhaps some benzofuran type structures, suggesting that condensation reactions may be involved in its formation. Most importantly, a solid residue was shown to form only from fractions C and D. As fraction C was completely soluble in tetralin and the reactor feed before reaction was therefore liquid, the solid material present after reaction was, in the case of fraction C at least, not present in the original coal and must therefore be a product of the reaction.

Although we have followed the usual nomenclature in calling this solid a "residue", such nomenclature is misleading in terms of reaction mechanism. Presumably some of the "residue" formed in the reaction of the whole coal is genuine unreacted residue and some is a reaction product, and one of the aims of liquefaction research must be to learn how to minimize the formation of such solid products (10).

The mechanism of coal dissolution

The classic view of the mechanism for the reaction between coal and a hydrogen-donor solvent involves the thermal breakdown of the single carbon-carbon bonds within the coal to produce reactive fragments in the form of free radicals which are then stabilized by hydrogen transferred from the solvent or elsewhere in the coal. If insufficient hydrogen is available the aromatic fragments can polymerize yielding chars or coke. Another view of coal dissolution, but much less widely held, is that oil is produced from coal via an asphaltene intermediate (11).

A most striking result from the work described above is that the composition of the bottoms product from the dissolution reaction did not depend on the chemical structure of the original coal material; only their relative quantities differed. This supports the view of a free-radical mechanism rather than an asphaltene-intermediate mechanism. The greatly increased formation of naphthalene during the reaction further supports this view.

Perhaps the greatest difference between the present work and more conventional work on higher-rank coals is the important role of the functional-group oxygen. The importance of oxygen groups is stressed, as the predominant process during the dissolution reaction was the destruction of functional groups within the coal. The role of oxygen in the reaction was not clearly defined by the present work, but quinone groups, for example, are thought to play a role in the liquefaction of high-oxygen-content coals (12), and their effectiveness in the free radical abstraction of hydrogen from hydrogen-donor compounds is well known (13).

REFERENCES

1. Evans, D.G., Hooper, R.J., Paper presented to Structure of Coal Symposium, Fuel Chemistry Division, ACS/CSJ Congress, Honolulu, April 1979.
2. Heredy, L.A., et al, Fuel 41, 1962, p221
3. Heredy, L.A., et al, Fuel 44, 1965, p125
4. Hooper, R.J., Battaerd, H.A.J., Evans, D.G., Fuel 57, 1978 in press
5. Whitehurst, D.D., et al, EPRI AF-480, EPRI, California, July 1977
6. B.S. 1076, Part 3, 1973
7. McPhail, I., Murray, J.B., Victoria, State Electricity Commission, Scientific Div. Rep. MR-155, 1969
8. Ouchi, K., Fuel 46, 1967, p319
9. Hooper, R.J., "The Dissolution of a Victorian Brown Coal in a Hydrogen-Donor Solvent", PhD Thesis, University of Melbourne, Australia, April 1978
10. Hooper, R.J., Evans, D.G., Letter submitted to Fuel, 1978
11. Yoshidi, R., et al, Fuel 55, 1976, p337,341
12. Brower, K.R., Fuel 56, 1977, p245
13. Braude, E.A., et al, Journal Chem Soc, 1954, p3574.

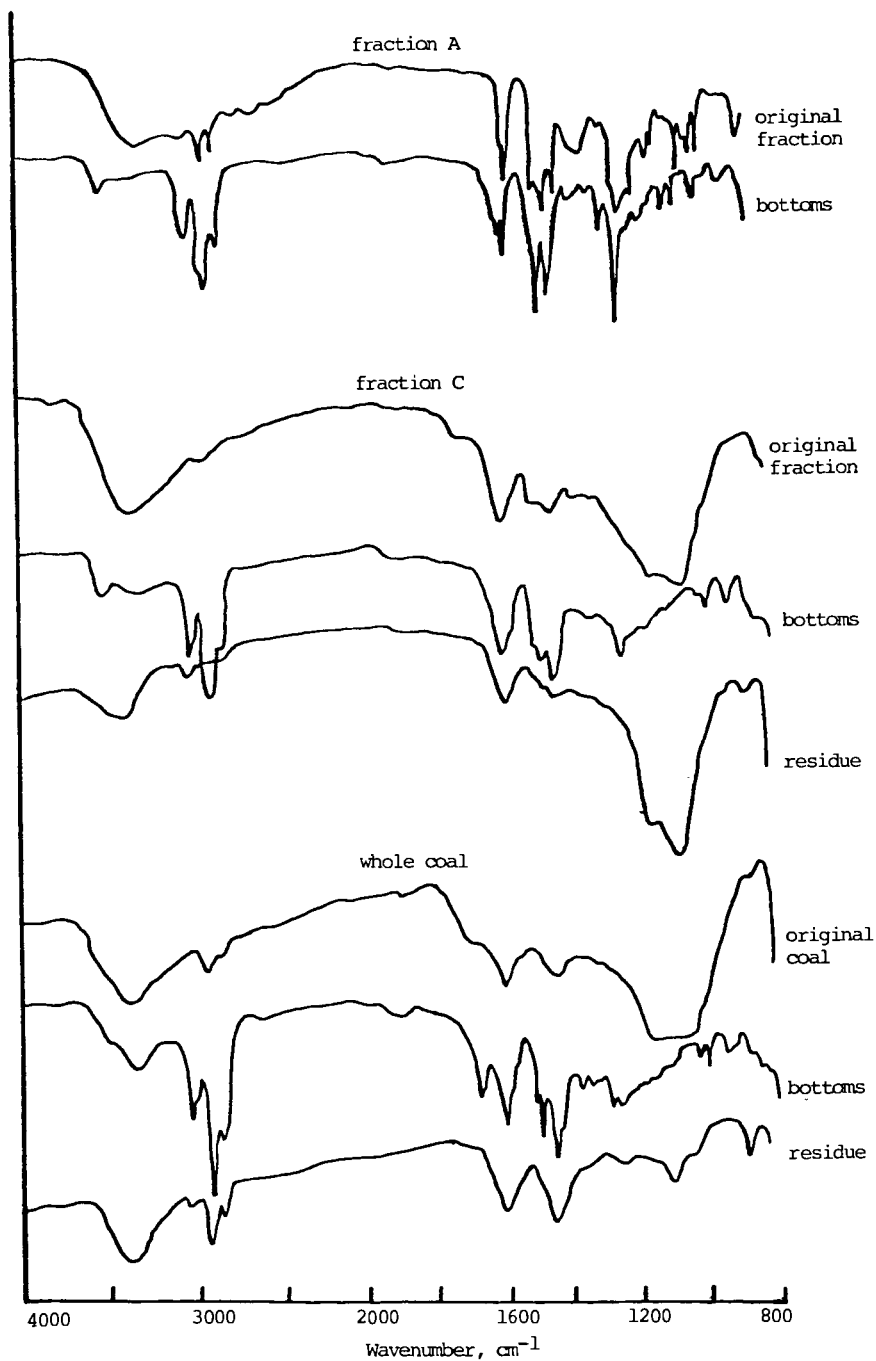


Figure 1: Infrared spectra for typical fractions and their products

Coal Liquefaction under Atmospheric Pressure

I. Mochida and K. Takeshita

Research Institute of Industrial Science, Kyushu University 86,
Fukuoka, JAPAN, 812

INTRODUCTION

Liquefaction of coals has been investigated extensively in the recent time to synthesize liquid fuels of petroleum substituent(1). The processes for liquefaction proposed are classified into three major groups. They are direct hydrogenation of coal under high hydrogen pressure, the solvent refining of coal under medium hydrogen pressure, and the hydrogenation of liquid produced by dry distillation of coal. Among them, the solvent refining may be the most skillful method for the largest yield of coal liquefaction under the moderate conditions(2).

The present authors studied the solvolytic liquefaction process (3,4) from chemical viewpoints as for the solvents and the coals in a previous paper(5). The liquefaction activity of a solvent was revealed to depend not only on its dissolving ability but also on its reactivity for the liquefying reaction according to the nature of the coal. The coal which is non-fusible at liquefaction temperature is scarcely liquefied with the non-reactive aromatic compound. This fact indicates the importance of solvolytic reactivity in the coal liquefaction. This conclusion corresponds to the fact that tetraline or hydrogenated anthracene oil assured the high liquefaction yield(6).

In the present study, the liquefaction activities of pyrene derivatives and decacyclene with coals of several ranks are studied to ascertain the previous ideas of liquefaction mechanism. The coals used in the present study are non-fusible or fusible at relatively high temperature and then gave small liquefaction yield with pyrene of non-solvolytic solvent at 370°C.

EXPERIMENTAL

Coals: The coals used in the present study are listed in Table 1, where some of their properties are also summarized. They were gratefully supplied from Shin Nippon Steel Co., Nippon Kokan Co., and National Industrial Research Laboratory of Kyushu.

Liquefaction Solvents: The solvents used in the present study are listed in Tables 2 and 3. Alkylated and hydrogenated pyrenes were synthesized by Friedel-Crafts and Birch reaction, respectively. Details have been described in else places(7).

Procedure and Analysis: Apparatus used in this experiment consisted of a reactor of pyrex glass(diameter 30 mm, length 250 mm, volume 175 ml) with a stirring bar and a cold-trap. After 1~3 g of coal and described amount of the solvent were added in the reactor, of which weight was previously measured, the reactor was heated in a vertical electric furnace under N₂ gas flow. The temperature was increased at the rate of 4°C/min, and was kept at the prescribed temperature for 1 hr. The weight calculated by subtracting the weight of the reactor cooled from the total weight defined 'residual yield'. The weight of oil and sublimed matter captured in the trap

defined 'oil yield'. The difference between the weight of charged substances and the residue plus oil yields defined 'gas yield', which contained the loss during the experiment. The gas and oil yields were usually less than 20 % under the present conditions.

The residual product in the reaction was ground and stirred in 100 ml of quinoline for 1 hr at room temperature, and filtered after centrifugation. This extraction procedure was repeated until the filtrate became colorless (usually 2~4 times). The quinoline insoluble (QI), thus obtained, was washed with benzene and acetone and then dried for weighing. The collected filtrate was evaporated to dryness in vacuo and washed with acetone for weighing. The degree of the solvolytic liquefaction was described with two ways of expression, liquefaction yield (LY) and liquefying efficiency (LE), which are defined by equations (1) and (2), respectively. QI and the coal fed in these equations were moisture and ash free (maf) weights.

$$\text{Liquefaction Yield (\%)} = \left(1 - \frac{\text{QI}^{\text{P}} - \text{QI}^{\text{S}}}{\text{coal fed}}\right) \times 100 \quad (1)$$

$$\text{Liquefying Efficiency (\%)} = \left(1 - \frac{\text{QI}^{\text{P}} - \text{QI}^{\text{S}}}{\text{QI}^{\text{C}}}\right) \times 100 \quad (2)$$

where QI^{P} , QI^{S} , and QI^{C} are weights of quinoline insoluble in the residual product, in the original solvent, and in the heat-treated coal at the liquefaction temperature without any solvent, respectively. LE describes the increased yield of liquefaction by using the solvent, indicating its efficiency for the liquefaction.

RESULTS

Liquefaction of fusible coal at high temperature

The liquefaction of Itmann coal, of which softening point and maximum fluidity temperature are 417° and 465°C, respectively, was carried out at several temperatures using decacyclene as a liquefaction solvent. The results are shown in Fig. 1, where the QI yield was adopted as a measure of liquefaction extent. Because the solubility of decacyclene in quinoline was rather small, the QI contained a considerable amount of decacyclene. Liquefaction of this coal proceeded scarcely below 420°C of the softening temperature. Above this temperature, the QI yield decreased sharply with the increasing liquefaction temperature until the resolidification temperature of the coal. The maximum LY observed at this temperature was estimated 67 %, decacyclene being assumed uncharged under the conditions. Above the resolidification temperature, the QI yield increased sharply. The carbonization may start. Decacyclene was known unreacted at 470°C in its single heat-treatment(8).

Liquefaction of coals in alkylated and hydrogenated pyrenes

Table 2 shows liquefaction activity of alkylated and hydrogenated pyrenes, respectively. Although hexylpyrene was just same to pyrene, propylation and ethylation certainly improved the liquefaction activity of pyrene with these coals of three different ranks. It is of value to note that ethylpyrene showed LY of 80 % with West-Kentucky coal.

Hydrogenation improved quite significantly the liquefaction activity of pyrene with these coals. The LY values with Taiheiyo

and West-Kentucky coals reached to 80 %.

The effect of hydrogenation extent on the liquefaction activity was summarized in Table 3. As the number of hydrogen atoms introduced per one pyrene molecule varied from 2.2 to 4.7 by using a variable amount of lithium in Birch reduction. The liquefaction activity of hydrogenated pyrene was affected slightly, reaching the maximum at around three of hydrogen atoms. It is obviously observed that LY was always larger with Taiheiyo than Itmann.

Structural change of solvent and coals after the liquefaction reaction

To analyse the structural change of solvents and coals after the liquefaction reaction, the solvent and coal should be separated. Because the separation was rather difficult, it was assumed that the benzene soluble and insoluble fractions after the liquefaction were derived from the solvent and coal, respectively. This assumption was verified by the following fact. The amount of BS recovered in the liquefaction of Taiheiyo coal with pyrene was 73.3 % as shown in Table 4. This value correspond to 97.7 % of the starting amount of pyrene and the BS fraction at the same time showed the same NMR pattern to that of pyrene. The recovery percentages of coal and solvent (BI/coal fed, BS/solvent fed, respectively) calculated based on the above assumption are summarized in Table 4. They were more than 85 % except for the significantly low value for the coal recovery when hydropyrene was used as the solvent. In the latter case, some extent of the coal may be converted into the benzene soluble. Nevertheless, analyses of BS and BI fractions may inform the structural change of coal and solvent after the liquefaction.

Figures 2 and 3 show the NMR spectra of benzene solubles after the liquefaction reaction using hydropyrene and ethylpyrene, respectively, together with those of the solvents before liquefaction for comparison. The BS derived from hydropyrene after the liquefaction lost the resonance peaks at 2.5, 3.2 and 4.0 ppm, extensively, although peaks at 2.0 and 2.8 ppm remained uncharged as shown in Figure 2. In contrast, there was essentially no change in the NMR spectra of ethylpyrene and its BS derivative as shown in Figure 3, indicating that the BS derivative contained unchanged ethylpyrene. However, the relatively low BS recovery of this case suggests that the conversion of this compound into BI may increase the BI yield in comparison with other cases as shown in Table 4.

Table 5 shows the ultimate analysis of benzene insoluble fractions after the liquefaction. H/C ratios of these fractions were similar when no solvent or pyrene was used, however when ethylpyrene and hydropyrene were used, the values were significantly low and high, respectively. The hydrogenation of coal by the hydrogen transfer from the hydrogen donating solvent is strongly suggested in the latter case. The low H/C value in the case of ethylpyrene may be explained in terms of certain extent of carbonization, as suggested by the low recovery of the solvent.

Discussion

In a previous paper(5), the authors described the liquefaction mechanism according to the properties of the coal and the solvent. The coal was classified into two categories,

- (1) fusible at the liquefaction temperature,
- (2) non-fusible at the liquefaction temperature.

The fusible coals can give a high liquefaction yield if the high fluidity during the liquefaction is maintained by the liquefaction solvent to prevent the carbonization. The properties of the solvent required for the high yield with this kind of coal are miscibility, viscosity, radical quenching reactivity and thermal stability not to be carbonized at the liquefaction temperature as reported in literatures (9).

In contrast, the non-fusible coal requires the solvation or solvolytic reaction to give the high liquefaction yield. The solvation of non-polar organic compounds including the pitch is expected low, so that the solvolytic reaction is necessary between the coal and the solvent.

The present results are well understood by the above mechanism. Itmann which is fusible at relatively high temperature was not liquefied below 420°C with a non-solvolytic solvent such as pyrene, however it was significantly liquefied at 480°C in decacyclene of a stable aromatic compound. Decacyclene is reported to be fused but stable for 1 hr heat-treatment at 500°C (8).

With solvolytic solvents, the fluidity of the coal may not be a principal factor any more. Taiheiyō, West-kentucky and Itmann coals of three different ranks were sufficiently liquefied with hydropyrene under atmospheric pressure at 370°C regardless of their fusibility. Lower rank coals show higher reactivity in such liquefaction.

The analyses of hydropyrene and the coal before and after the liquefaction clearly indicate the hydrogen transfer from the solvent to the coal substance. Transalkylation might be expected another kind of the solvolytic reaction. However, the present results suggest low probability with alkylated pyrenes as suggested by the NMR analysis. Instead, the increased polarity by alkyl group and the reactivity of the carbonization precursor from alkylpyrene, especially ethylpyrene, may be responsible for a considerable liquefaction yield. The recovery of the solvent becomes difficult by its latter conversion as observed in the present study

REFERENCES

- (1) (a) P. M. Yavorsky, J. Fuel Inst. Japan, 55, 143 (1976).
(b) D. W. van Kravelen "Coal" Elsevier Amsterdam (1961).
(c) A. G. Oblad, Catal. Rev., 14 (1), 83 (1976).
(d) R. T. Ellington, et al., "Liquid Fuels from Coal", Academic Press Inc. (1977).
- (2) Y. Kamiya, J. Fuel Inst. Japan, 56, 319 (1977).
- (3) Y. Yamada, H. Honda, S. Oi and H. Tsutsui, J. Fuel Inst. Japan, 53, 1052 (1974).
- (4) K. Osafune, H. Honda, et al., J. Fuel Inst. Japan, 55, 173 (1976).
- (5) I. Mochida, A. Takarabe and K. Takeshita, Fuel, in press.
- (6) A. Pott and H. Brock, Fuel, 13, 91, 125, 154 (1934); R. G. Ruberto, et al., Fuel, 56, 25 (1977).
- (7) L. Reggel, R. A. Friedel and I. Wender, J. Org. Chem., 22, 891 (1957); I. Mochida, K. Kudo and K. Takeshita, Fuel, 53, 253 (1974), 55, 70 (1976).
- (8) I. Mochida, H. Miyasaka, H. Fujitsu and K. Takeshita, Carbon (Tanso), No. 92, 7 (1977); I. Mochida and H. Marsh, To be published.

- (9) W. P. Scarah and R. R. Dillon, Ind. Eng. Chem. Process Design Dev., 15, 122 (1975); R. C. Neavall, Fuel, 55, 237 (1976); H. Sato and Y. Kamiya, J. Fuel Inst. Japan, 56, 103 (1977).

Table 1 Coals and their properties

| Properties | coal | Itmann | West Kent.14 | Taiheiyo |
|--------------------------|---------------------|--------|--------------|-------------|
| Proximate analysis (wt%) | ash | 7.3 | 12.8 | 10.1 |
| | volatile matter | 19.9 | 53.0 | 45.9 |
| | fixed carbon | 72.8 | 34.2 | 37.9 |
| ultimate analysis (wt%) | C | 90.1 | 79.0 | 77.8 |
| | H | 4.6 | 5.1 | 6.0 |
| | N | 1.3 | 1.7 | 1.1 |
| | S | 0.5 | 4.6 | 0.2 |
| | O(diff) | 3.5 | 9.6 | 14.9 |
| plasticity analysis | soften.temp.(°C) | 417 | 387 | |
| | max.fluid.temp.(°C) | 465 | 425 | non-fusible |
| | max.fluid.(ddpm) | 64 | 45 | |
| | final temp.(°C) | 487 | 445 | |

Table 2 Coal liquefaction by pyrene derivatives (reaction temp.=370°C, solvent/coal=3/1)

| solvent | n* | coal | residue(%),distillate(%) | | | | L.Y.** | L.E.** |
|---------------------|------|--------------|--------------------------|------|------|------|--------|--------|
| | | | QI | QS | oil | gas | | |
| none | — | West Kent. | 85.1 | 9.2 | 0.8 | 4.9 | 17 | 0 |
| | | Itmann | 97.5 | 0.0 | 0.8 | 1.7 | 3 | 0 |
| | | Taiheiyo | 85.4 | 0.0 | 2.2 | 12.4 | 16 | 0 |
| pyrene | 0 | West Kent*** | 19.9 | 69.9 | 6.0 | 4.2 | 24 | 8 |
| | | Itmann | 20.4 | 75.2 | 3.1 | 1.3 | 23 | 18 |
| | | Taiheiyo | 19.3 | 75.0 | 2.5 | 3.2 | 25 | 11 |
| hydro-pyrene (No.1) | — | West Kent. | 7.6 | 73.4 | 9.6 | 9.4 | 80 | 76 |
| | | Itmann | 9.1 | 79.6 | 5.8 | 5.5 | 69 | 68 |
| | | Taiheiyo | 6.3 | 85.0 | 4.5 | 4.2 | 83 | 80 |
| hexyl-pyrene | 0.83 | West Kent. | 19.3 | 51.3 | 12.8 | 16.5 | 26 | 11 |
| | | Itmann | 20.9 | 63.1 | 8.5 | 7.5 | 17 | 15 |
| | | Taiheiyo | 19.7 | 56.2 | 11.8 | 12.8 | 25 | 9 |
| propyl-pyrene | 0.85 | West Kent. | 14.4 | 66.3 | 3.5 | 16.1 | 49 | 38 |
| | | Itmann | 14.9 | 66.3 | 7.2 | 11.6 | 43 | 42 |
| | | Taiheiyo | 15.7 | 65.7 | 6.7 | 11.9 | 42 | 30 |
| ethyl-pyrene | 0.33 | West Kent. | 7.6 | 79.3 | 12.4 | 0.7 | 80 | 76 |
| | | Itmann | 11.4 | 77.8 | 5.5 | 5.7 | 59 | 58 |
| | | Taiheiyo | 13.4 | 76.8 | 2.9 | 6.9 | 52 | 42 |

* number of alkyl groups introduced/one pyrene molecule

** L.Y.=Liquefaction Yield(%); L.E.=Liquefying Efficiency(%)

*** reaction temp.=390°C

Table 3
Effect of hydrogenation extent on the liquefaction activity
(reaction temp. 370°C, solvent/coal=3/1)

| solvent | n* | Itmann Taiheiyo | | | | |
|------------------|------|-----------------|------|------|------|----|
| | | L.Y. | L.E. | L.Y. | L.E. | |
| | | (%) | (%) | (%) | (%) | |
| hydro- pyrene | No.1 | 2.2 | 69 | 68 | 83 | 80 |
| | No.2 | 2.8 | 78 | 78 | 90 | 88 |
| | No.3 | 4.3 | 72 | 71 | 85 | 82 |
| | No.4 | 4.7 | 72 | 71 | 83 | 79 |

L.Y.=Liquefaction Yield

L.E.=Liquefaying Efficiency

* n = number of hydrogen atoms
introduced one pyrene molecule

Table 4 Benzene extraction of solvolysis pitches
(coal=Taiheiyo, reaction temp. 370°C, solvent/coal=3/1)

| solvent | residue | | distillate | | recovery | |
|----------------------------|---------|--------|------------|---------|----------|-------------|
| | BI (%) | BS (%) | oil (%) | gas (%) | coal (%) | solvent (%) |
| none | 86.4 | 10.0 | 0.5 | 3.2 | 86.4 | - |
| hydro- pyrene (No.2) | 18.4 | 70.6 | 3.6 | 7.4 | 74.6 | 94.1 |
| ethyl- pyrene | 23.9 | 64.0 | 7.9 | 4.2 | 96.0 | 85.3 |
| pyrene | 22.4 | 73.3 | 0.9 | 3.4 | 89.6 | 97.7 |

$$* \text{ recovery coal}(\%) = \frac{\text{BI}}{\text{coal fed}}$$

$$\text{solvent} = \frac{\text{BS in residue}}{\text{solvent fed}}$$

Table 5 Ultimate analysis of benzene
insoluble part of solvolysis pitch
(Coal=Taiheiyo, reaction temp. 370°C, solvent/coal=3/1)

| solvent | C (%) | H (%) | N (%) | others (%) | H/C |
|------------------|-------|-------|-------|------------|-------|
| none | 75.05 | 5.29 | 1.40 | 18.26 | 0.840 |
| pyrene | 76.25 | 5.43 | 1.53 | 16.75 | 0.849 |
| ethyl- pyrene | 82.24 | 4.93 | 1.80 | 11.03 | 0.714 |
| hydro- pyrene | 72.47 | 5.48 | 1.38 | 20.67 | 0.901 |

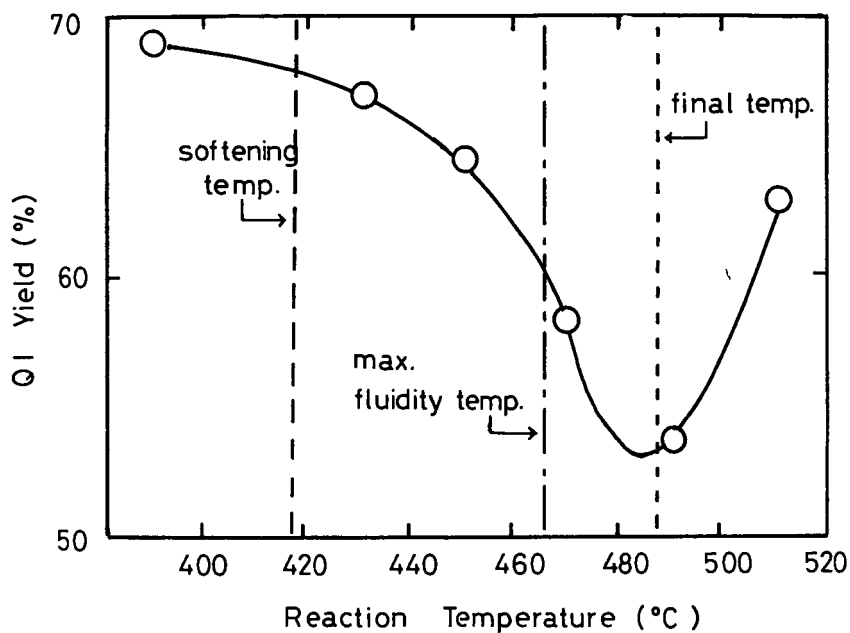


**Fig.1 Effect of Reaction Temperature on
Coal Liquefaction**

(coal : Itmann, solvent : decacyclene
solvent / coal = 3/1)

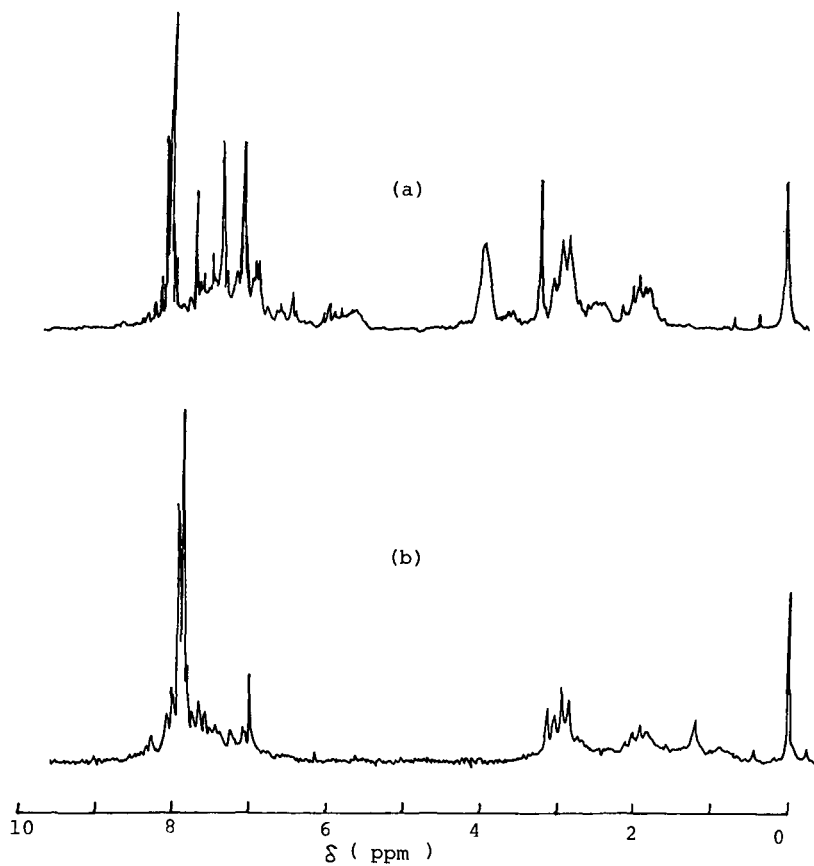


Fig. 2 NMR spectra of hydropyrene (a) and its BS derivative after the liquefaction (b). liquefaction conditions: see Table 4

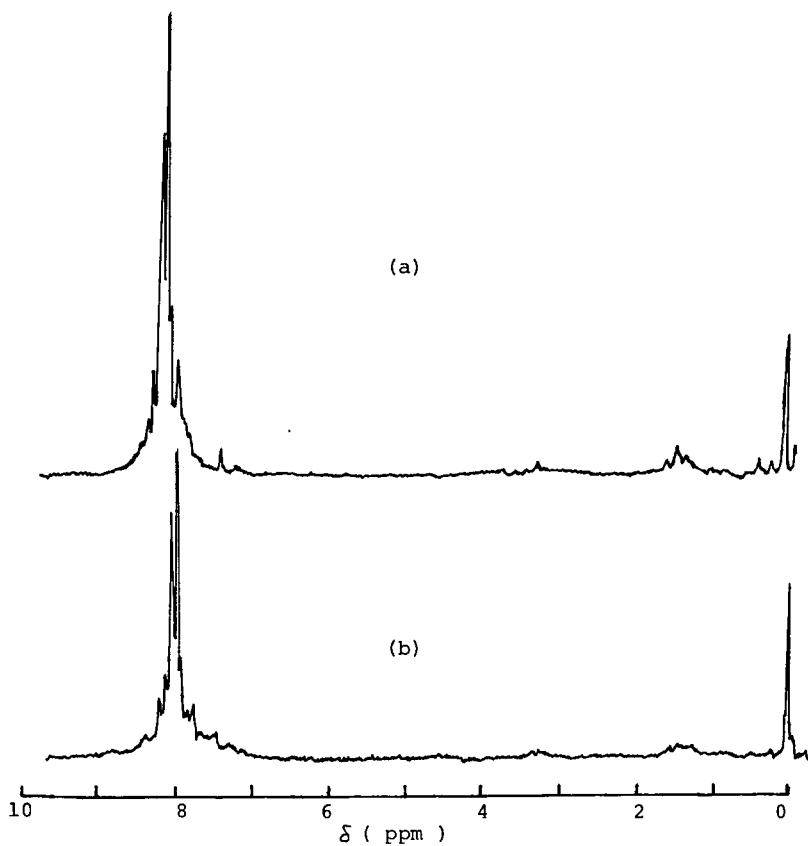


Fig. 3 NMR spectra of ethylpyrene (a) and its BS derivative after the liquefaction (b). liquefaction conditions: see Table 4.

CHANGES IN THE CHEMICAL COMPOSITION OF THE OIL FORMED WITH
VARIATIONS IN HYDROGENATION CONDITIONS

John R. Kershaw and Gordon Barrass

Fuel Research Institute of South Africa, P.O. Box 217, Pretoria,
South Africa

INTRODUCTION

There has been a number of studies of the chemical nature of coal hydrogenation liquids. However, the great majority of the coal hydrogenation liquids studied were produced using a liquid vehicle. The absence of a liquid vehicle may have an effect on the chemical reactions taking place and, therefore, on the chemical composition of the product obtained.

In the work reported here hydrogenation of coal was carried out in the absence of any vehicle oil in a semi-continuous reactor which allowed the volatile product to be swept from the reactor by a continuous stream of hydrogen. We here report our work on the changes found in the chemical composition of the oil (hexane soluble portion) with changes in hydrogenation reaction conditions. The hydrogenation conditions investigated were the catalyst (stannous chloride) concentration and the reaction temperature.

EXPERIMENTAL

Materials

The coal (0.50 to 0.25 mm fraction) used was from the New Wakefield Colliery, Transvaal. Analysis, air dried basis: Moisture 4.9; Ash 14.9; Volatile Matter 32.8%; dry ash-free basis: C, 79.2; H, 5.4; N, 2.1; S, 2.3%.

The catalyst was analytical grade stannous chloride. Stannous chloride was dissolved in water and added to the coal as an aqueous solution. The resultant slurry was mixed by stirring and then dried.

Hydrogenation

Hydrogenation was carried out in a reactor similar to the "hot-rod" reactor (1,2) designed by Hiteshue et al. The heating rate was ca 100°C/minute, and the time at temperature was 15 minutes. Hydrogen, at a flow rate of 22 l/minute, was continuously passed through a fixed bed of coal (25 g) impregnated with catalyst. The volatile products were condensed in a high-pressure cold trap. The other conditions are given in the Results and Discussion section.

The product was removed from the cooled reactor and from the condenser with the aid of toluene. The solid residue was extracted with boiling toluene (250 ml) in a soxhlet extractor for 12 hours. The toluene solutions were combined and the toluene removed under reduced pressure. Hexane (250 ml) was added to the extract and it was allowed to stand for 24 hours with occasional shaking. The solution was filtered to leave a residue (asphaltene) and the hexane was removed from the filtrate under reduced pressure to give the oil.

Fractionation of the oils

The oils were fractionated by adsorption chromatography on silica gel. The column was eluted successively with 40 - 60°C petroleum ether (12 fractions),

40 - 60 petroleum ether / toluene (increasing proportions of toluene, 5 fractions), toluene, chloroform and methanol.

Analysis

I.r. and u.v. spectra were measured for each fraction from the columns. I.r. spectra were measured as smears on sodium chloride plates using a Perkin-Elmer 587 grating spectrophotometer, while u.v. spectra were measured as a solution in hexane (spectroscopic grade) using a Unicam SP 1700 instrument. Fluorescence spectra were recorded as described elsewhere (3).

^1H n.m.r. spectra were recorded for the oils in deuteriochloroform at 90 MHz with tetramethylsilane as an internal standard using a Varian EM 390 instrument. Broad-band proton-decoupled pulse Fourier transform ^{13}C n.m.r. were recorded in deuteriochloroform at 20 MHz using a Varian CFT-20 spectrometer.

Molecular weights were determined by vapour pressure osmometry in benzene solution using a Knauer apparatus. 5 concentrations over the range 1 - 5 g/l were employed and the molecular weight was obtained by extrapolation to infinite dilution.

The viscosities of the oils were measured using a Haake Rotovisco RV3 viscosimeter with a cone and plate sensor at 20°C.

RESULTS AND DISCUSSION

From their i.r. and u.v. spectra, the fractions from column chromatography were grouped as saturate hydrocarbons, aromatic hydrocarbons and polar compounds. The last four fractions from the chromatographic separation were designated as polar compounds. All these fractions showed strong hydroxyl absorption in their i.r. spectra and these fractions contained acidic, basic and neutral compounds.

The effect of catalyst concentration

Four samples impregnated with 1, 5, 10 and 15% tin as stannous chloride were hydrogenated at 450°C and 25 MPa to investigate the effect that increasing catalyst concentration has on the composition of the oil (hexane soluble portion) formed.

Adsorption chromatography of the oils gave the percentage of saturate hydrocarbons, aromatic hydrocarbons and polar compounds in the oil. The percentage of polar compounds in the oil decreased as the catalyst concentration increased (see Figure 1) with mainly an increase in the percentage of aromatic hydrocarbons. The percentage of acids and bases in the oil were obtained by extraction with NaOH and HCl, respectively. There was a decrease in the percentage of acids and bases in the oil as the catalyst concentration increased (see Figure 1).

The i.r. spectra of the first fractions showed that they are aliphatic and contain no double bonds. In the C-H stretching region ($\approx 3000\text{ cm}^{-1}$) the absorption due to methylene groups was much stronger than that due to methyl groups. Weak absorption in the region 720 - 735 cm^{-1} was noticed in all the aliphatic fractions and is attributable to chains having four or more methylene groups (4). G.l.c. analysis of the saturate hydrocarbon fractions showed that the composition was similar to that reported for hydrogenation of a different South African coal (5). There were no noticeable changes with different catalyst concentrations.

The u.v. spectra of the first aromatic fractions of all the oils studied showed the presence of the naphthalenic structure. Strong absorption was seen at ca 224, 226, and 275 nm and weak absorption at 309, 318 and 323 nm. The shape and ratio of the absorbances were similar to those of a number of model naphthalenes recorded under identical conditions, and to the reported spectrum of naphthalene (6). The characteristic naphthalenic odour was also noticed in these fractions. Their i.r. spectra in the 3 000 cm⁻¹ region had strong aliphatic C-H absorption in relation to the aromatic C-H absorption. This may be ascribed to appreciable hydroaromatic and/or alkylaromatic structure.

The later aromatic fractions from the columns were analysed by u.v. and fluorescence spectroscopy. Though u.v. spectroscopy alone was of limited value in the characterization of these fractions, because of the incomplete separation, peaks and even inflections in the spectra were useful as guides for setting the fluorescence excitation wavelength. Full details of the method used, and of the fluorescence emission and excitation spectra of the polyaromatic ring systems identified have been reported elsewhere (3). Ten polyaromatic ring systems were identified by the similarity of their fluorescence excitation and fluorescence emission spectra to those of standard hydrocarbons. These were anthracene, 9,10-dialkylanthracene (model compound, 9,10-dimethylanthracene), pyrene, 1-alkylpyrene (model compound 1-methylpyrene), benzo(a)pyrene, dibenzo(def,mno)chrysene (anthanthrene), perylene, benzo(ghi)perylene, dibenzo(b,def)chrysene (3,4,8,9-dibenzopyrene) and coronene. All the polyaromatic ring systems were identified in all the oils analysed.

The i.r. spectra of the last four fractions of every sample studied showed strong OH absorption. The first of these fractions had sharp bands at ca 3530 and 3420 cm⁻¹, whereas those of the subsequent fractions were broader and at lower frequency, presumably due to increasing hydrogen bonding (4). The aromatic C-H absorption was much weaker than the aliphatic C-H absorption, in the 3000 cm⁻¹ region. All the polar fractions have strong absorption in their u.v. spectra. Considerable absorption above 350 nm showed the aromatic nature of these fractions.

¹H n.m.r. spectra were recorded for the oils produced at the various catalyst concentrations (1, 5, 10 and 15% Sn as SnCl₂). The percentage of hydrogens in aromatic, benzylic and aliphatic environments showed no change with catalyst concentration.

¹³C n.m.r. spectra were also recorded for the oils produced. No discernible differences could be found between the spectra of the four oils. In the aromatic region, using the assignments of Bartle et al. (7), it was noticeable that the aromatic C-H (118 to 129 ppm from TMS) signals were much stronger than those due to aromatic C-C (129 to 148 ppm from TMS). Part of the aromatic C-H band was shifted to higher field (108 - 118 ppm) and may be attributed to aromatic C-H ortho to ether C-O (7). The aliphatic carbon bands extend from 12 to 50 ppm. Superimposed on the aliphatic carbon bands are sharp lines at 14, 23, 32, 29 and 29.5 ppm. These lines have been ascribed by Pugmire et al. (8) to the α, β, γ, δ and ε-carbons of long aliphatic chains. The intensity of the ε-carbon band is approximately four times the intensity of the α or β carbon indicating reasonably long aliphatic chains.

It was obvious on visual examination of the oils that the greater the catalyst concentration used, the less viscous was the oil produced. The decrease in viscosity with catalyst concentration is shown in Figure 2.

It has been reported that the molecular weight of coal liquids affects the viscosity (9,10). However, the decrease in molecular weight that occurred with increasing catalyst concentration was relatively small. (The molecular weights of the oils were 247, 241, 237 and 231 for 1, 5, 10 and 15% catalyst, respectively). We feel that this relatively small change in molecular weight would not cause such a noticeable change in viscosity unless changes in the chemical nature of the oil also contributed to the viscosity reduction.

Sternberg et al. (9) showed that the presence of asphaltenes in coal-derived oils caused a marked increase in the viscosity. This group also showed that these asphaltenes were acid-base complexes and that hydrogen bonding occurs between the acidic and basic components of asphaltenes (11,12). Recent work (10,13) on coal liquefaction bottoms has shown the importance of hydrogen bonding on the viscosity of coal liquids.

The reduction of polar compounds in the oil with increasing catalyst concentration could reduce hydrogen bonding and, therefore, the viscosity of the oil. To further look at this possibility, i.r. spectra were recorded at the same concentration in CCl₄ for each of the oils (see Figure 3). The i.r. spectra showed sharp peaks at 3610 cm⁻¹ (free OH), 3550 cm⁻¹ (2nd free OH?) and 3480 cm⁻¹ (N-H) and a broad peak at ca 3380 cm⁻¹ which is assigned to hydrogen bonded OH. This band decreases with increasing catalyst concentration (see Figure 3) indicating that hydrogen bonding in the oil decreases with increasing catalyst concentration used to produce the oil. The band at ca 3380 cm⁻¹ was shown to be due to intermolecular hydrogen (4, 14) bonding by recording the spectrum of a more dilute solution (using a longer path length cell), the 3380 cm⁻¹ band diminished with an increase in the 3610 cm⁻¹ peak.

It would appear that increasing the amount of stannous chloride catalyst, under our experimental conditions, as well as increasing the amount of oil formed decreases the amount of polar compounds in the oil which decreases the hydrogen bonding and therefore helps to decrease the viscosity of the oil. N.m.r. spectroscopy and evidence from the chromatographic fractions indicates that there is little change in the nature of the hydrocarbon fractions.

The effect of temperature

For this study, the pressure was 25 MPa and tin (1% of the coal) as stannous chloride was used as the catalyst. Some additional runs were also carried out at 15 MPa pressure. The temperature range studied was from 400°C to 650°C.

¹H n.m.r. spectra of the oils were recorded for the range of temperatures and the protons were assigned as aromatic, phenolic OH, benzylic and aliphatic. There was an increase in the percentage of aromatic protons and a decrease in the percentage of aliphatic protons as the temperature increases, while the percentage of benzylic protons remained constant (see Figure 4). It, therefore, appears that as the hydrogenation temperature increases side groups are lost and that the C-C bond directly attached to the aromatic ring is more stable than those further from the ring. The molecular weight of the oil decreases with temperature (see Figure 5) as would be expected if side chains are being removed.

¹³C n.m.r. spectra were recorded for the oils produced at 400°C, 450°C, 550°C and 600°C. As the temperature increased the aromatic carbon bands became much more intense compared to the aliphatic carbon bands (see Figure 6). Quantitative estimation of the peak areas was not attempted due to the effect of variations in spin-lattice relaxation times and nuclear Overhauser enhancement with different carbon atoms. Superimposed on the aliphatic carbon bands were sharp lines

at 14, 23, 32, 29 and 29.5 ppm, which are due to the α , β , γ , δ and ϵ -carbons of long aliphatic chains (8). As the temperature increases, these lines become smaller compared to the other aliphatic bands and this is especially noticeable in the spectrum of the 600°C oil. The ϵ line was approximately four times the intensity of the α and β lines at 400°C and 450°C, at 550°C approximately three times and at 600°C only about twice the intensity. It would seem that as the temperature increases, the long aliphatic chains are reduced in both number and length. (G.l.c. analysis of the saturate fractions from column chromatographic separation showed that as the hydrogenation temperature increases there was a decrease in the percentage of the higher alkanes and an increase in the percentage of their shorter chained analogues in the saturate hydrocarbon fractions). It was also noticeable when comparing the spectrum of the 600°C oil to the spectra of the 400°C and 450°C oils that the intensity of bands due to CH_3 , α to aromatic rings (19 - 23 ppm from TMS (7)) had increased in intensity compared to the other aliphatic bands. This agrees with the ^1H n.m.r. results which showed no change in the percentage of benzylic protons while the percentage of aliphatic protons decreased.

Elution chromatography gave the percentage of aliphatic hydrocarbons, aromatic hydrocarbons and polar compounds in the oil. There was a reduction in the percentage of polar compounds in the oil (see Figure 7) with subsequent increase in the aromatic percentage.

U.v. and fluorescence spectroscopy of the aromatic fractions showed the presence of the same aromatic structures as found in the oils from the catalyst experiments. The i.r. spectra in the 3000 cm^{-1} region of the aromatic fractions varied with temperature. At low temperature the aliphatic C-H absorption was much stronger than the aromatic C-H absorption whereas at high temperature this difference was not so pronounced, which may be ascribed to a decrease in alkyl substitution as was shown by n.m.r. spectroscopy.

The viscosity of the oil decreases considerably with temperature as shown in Figure 8. The viscosity at the lower pressure 15 MPa was 90 mPa.s at 400°C and 9 mPa.s at 650°C. The decrease in viscosity is expected as there was a decrease in molecular weight with increasing temperature and also a decrease in the percentage of polar compounds in the oil.

The effect of increasing the hydrogenation temperature, under the conditions used here, is to give a more aromatic product of lower molecular weight containing fewer long aliphatic chains. The viscosity of the oil and the percentage of polar compounds in the oil also decrease with increasing temperature.

ACKNOWLEDGEMENTS

We are grateful to Mrs. E.W. Esterhuizen and Mrs. K.G. Hermanides for technical assistance, to Mr. F.L.D. Cloete, Chemical Engineering Research Group, C.S.I.R. for viscosity measurements and especially to Dr. K.G.R. Pachler, National Chemical Research Laboratories, C.S.I.R., and his staff for n.m.r. spectra.

REFERENCES

1. R.W. Hiteshue, R.B. Anderson and M.D. Schlessinger, *Ind. Eng. Chem.*, **49**, 2008 (1957).
2. J.A. Gray, P.J. Donatelli and P.M. Yavorsky, *Preprints, Amer. Chem. Soc., Div. of Fuel Chem.*, **20**(4), 103 (1975).
3. J.R. Kershaw, *Fuel*, **57**, 299 (1978).

4. L.J. Bellamy, "The Infrared Spectra of Complex Molecules", 3rd edn., Chapman and Hall, London, 1975.
5. J.R. Kershaw, S. Afr. J. Chem., 30, 205 (1977).
6. E. Clar, "Polycyclic Hydrocarbons", Vol. 1, Academic Press, London, 1964, p.212.
7. K.D. Bartle, T.G. Martin and D.F. Williams, Chem. Ind., 313 (1975).
8. R.J. Pugmire, D.M. Grant, K.W. Zilm, L.L. Anderson, A.G. Oblad and R.E. Wood, Fuel, 56, 295 (1977).
9. H.W. Sternberg, R. Raymond and F.K. Schweighardt, Preprints, Amer. Chem. Soc., Div. of Petrol. Chem., Chicago Meeting, August 24 - 29, 1975.
10. J.E. Schiller, B.W. Farnum and E.A. Sondreal, Amer. Chem. Soc., Div. of Fuel Chem., 22 (6), 33 (1977).
11. H.W. Sternberg, R. Raymond and F. Schweighardt, Science, 188, 49 (1975).
12. F.K. Schweighardt, R.A. Friedel and H.L. Retcofsky, Appl. Spectrosc., 30, 291 (1976).
13. K.A. Gould, M.L. Gorbaty and J.D. Miller, Fuel, 57, 510 (1978).
14. F.K. Brown, S. Friedman, L.E. Makovsky and F.K. Schweighardt, Appl. Spectrosc., 31, 241 (1977).

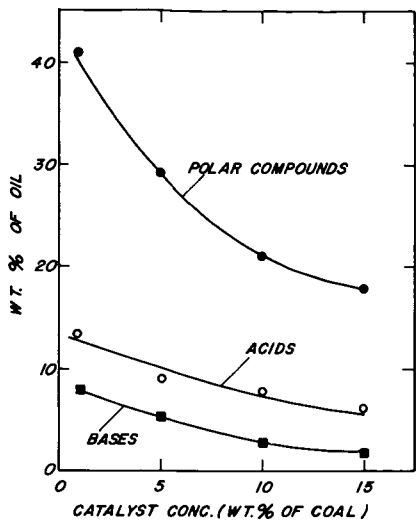


FIGURE 1 VARIATION OF POLAR COMPOUNDS, ACIDS AND BASES IN OIL WITH CATALYST CONCENTRATION.

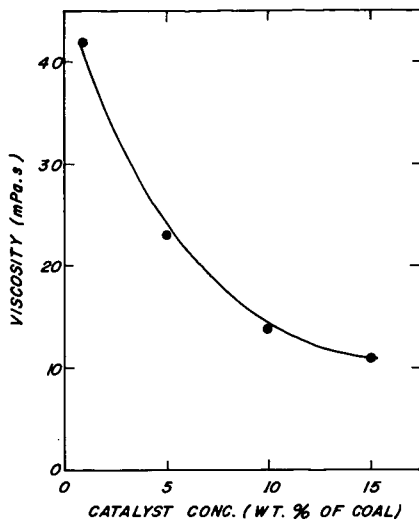


FIGURE 2 VARIATION IN VISCOSITY OF OIL WITH CATALYST CONCENTRATION



FIGURE 3 PARTIAL INFRARED SPECTRA OF OILS (VARIOUS CATALYST CONCENTRATIONS)

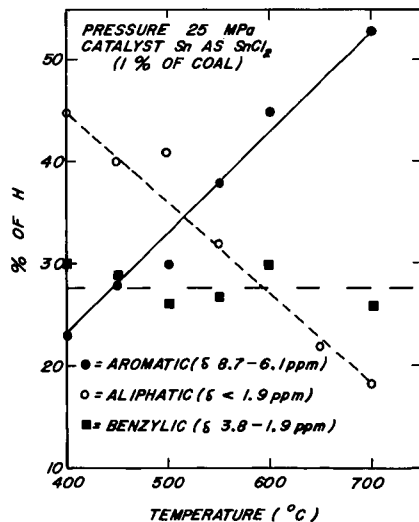


FIGURE 4 VARIATION OF HYDROGEN DISTRIBUTION WITH TEMPERATURE.

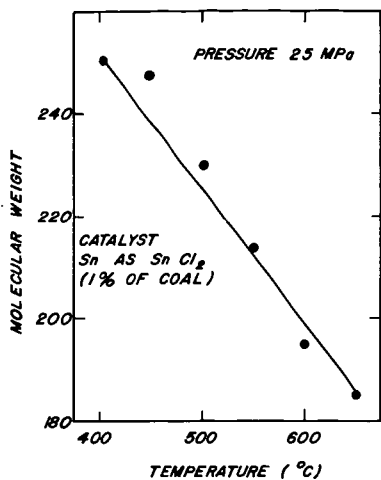


FIGURE 5 VARIATION OF MOLECULAR WEIGHT OF OIL WITH REACTOR TEMPERATURE.

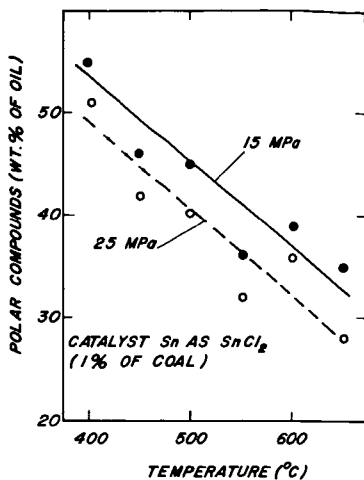


FIGURE 7 VARIATION IN PERCENTAGE OF POLAR COMPOUNDS IN OIL WITH REACTOR TEMPERATURE.

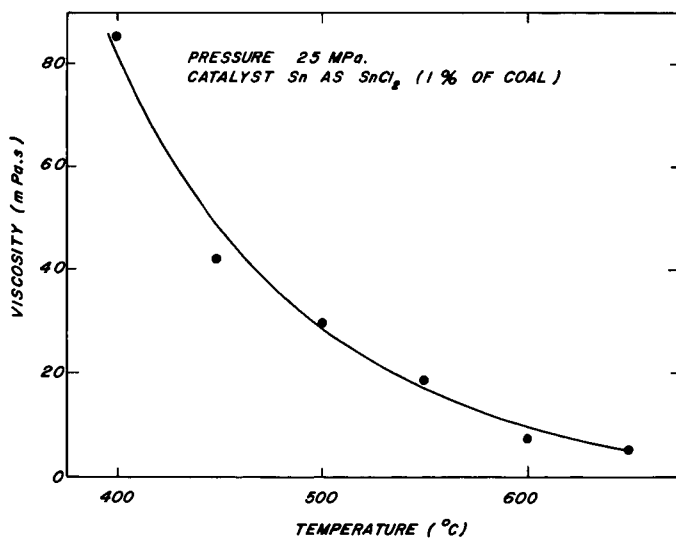


FIGURE 8 VARIATION OF VISCOSITY WITH REACTOR TEMPERATURE.

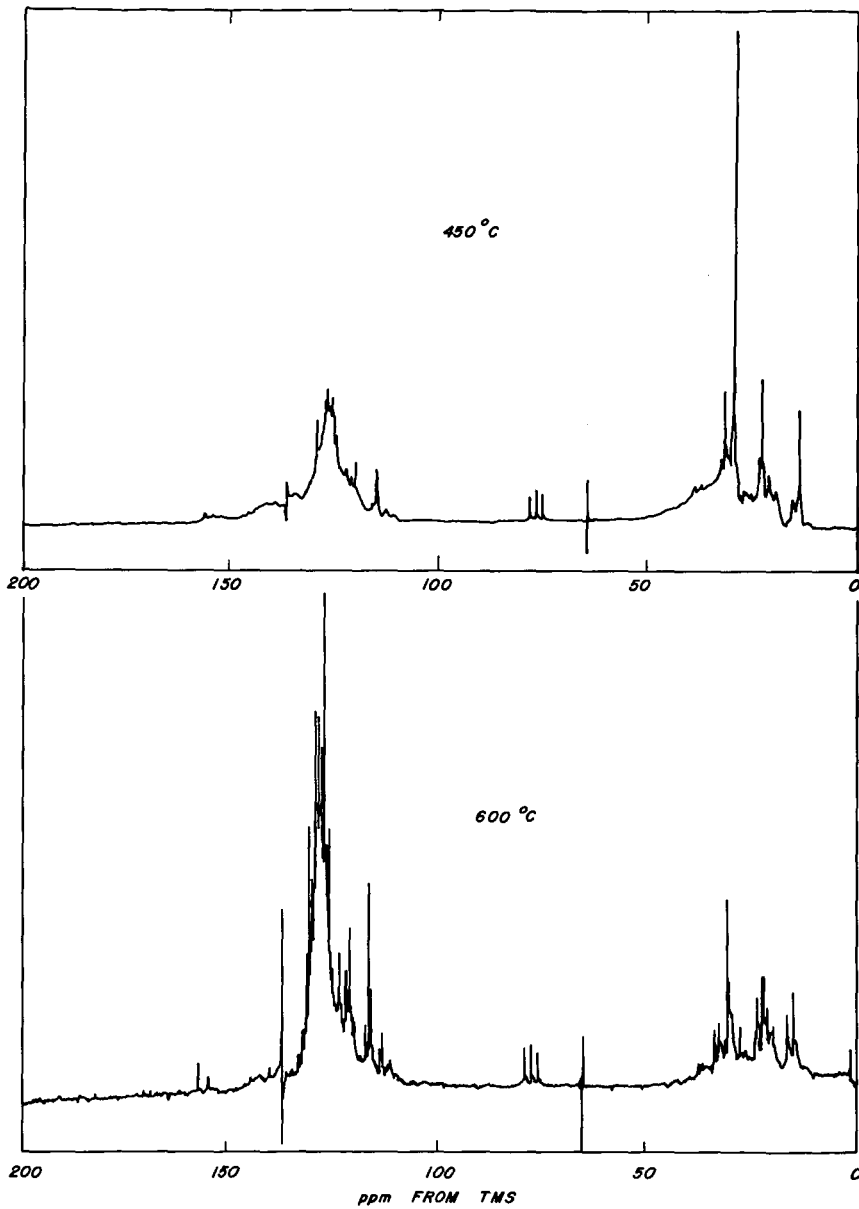


FIGURE 6 ^{13}C n.m.r. SPECTRA OF OILS.

THERMAL TREATMENT OF COAL-RELATED AROMATIC ETHERS IN TETRALIN SOLUTION

Y. Kamiya, T. Yao and S. Oikawa

Faculty of Engineering, University of Tokyo
Hongo, Tokyo 113, Japan

INTRODUCTION

The important elementary reactions of coal liquefaction are the decomposition of coal structure, the stabilization of fragments by the solvent and the dissolution of coal units into the solution.

These reactions proceed smoothly in the presence of hydrogen donating aromatic solvent (1-4) at temperatures from 400°C to 450°C, resulting in the formation of so called solvent refined coal with carbon content of 86-88% on maf basis independent of coalification grade of feed coal.

While, oxygen containing structures of coal must be playing important parts in the course of coal liquefaction. It will be key points that what kinds of oxygen containing structure are decomposed and what kinds of structure are formed in the course of reaction. It has been proposed (5,6) and recently stressed (7-11) that the units of coal structure are linked by ether linkage.

We have studied the thermal decomposition of diaryl ether in detail, since the cleavage of ether linkage must be one of the most responsible reactions for coal liquefaction among the various types of decomposition reaction and we found that the C-O bond of polynucleus aromatic ethers is cleaved considerably at coal liquefaction temperature.

EXPERIMENTAL

Tetralin and 1-methylnaphthalene were reagent grade and were used after washing with sulfuric acid, alkali, and water and the subsequent distillation at 70°C under reduced pressure. Various additives and model compounds were reagent grade, and some of them were used after recrystallization. Phenyl naphthyl ether and phenyl 9-phenanthryl ether were synthesized by refluxing a mixture of aryl bromide, phenol, Cu₂O and γ-collidine (12).

Samples were added to 300 ml or 90 ml magnetic stirring (500 rpm) autoclaves. After pressurizing with hydrogen, the autoclave was heated to the reaction temperature within 45 min. and maintained at the temperature for the desired reaction time.

At the completion of a run, the autoclave was cooled by electric fan to room temperature and the autoclave gases were vented through gas meter and analyzed by gas chromatography. Liquid portions of the samples were subjected to gas chromatographic analysis to determine the composition of products.

RESULTS AND DISCUSSION

Thermal treatment of various aromatic compounds

In order to study the reaction of coal structure, various aromatic compounds were chosen as the coal model and treated at 450°C. The conversion of the reaction along with the detected products were shown in Table 1.

Recently, the thermal decomposition of diaryl alkanes such as dibenzyl and 1,3-diphenylpropane has been studied by Sato and coworkers (13), Collins and coworkers (14). These compounds were confirmed to be decomposed to alkylbenzenes gradually as a function of carbon chain length.

Although diphenyl ether and dibenzofuran were very stable at 450°C, 2,2'-dinaphthyl ether was decomposed slowly and benzyl ethers completely.

The apparent activation energy for the thermal decomposition of phenyl benzyl ether was calculated to be about 50 kcal/mole from the data obtained at 320-350°C.

These results imply that highly aromatic ether linkages will be considerably broken at coal liquefaction temperatures resulting in a main source of phenolic groups of the dissolved coal.

Phenolic compounds were confirmed to be very stable against thermal treatment. Diphenyl methanol and benzophenone were stable against decomposition but hydrogenated to form diphenylmethane quantitatively. Phenyl benzyl ketone was found to be partially hydrogenated or decarbonylated to form diphenyl alkanes.

Naphthoquinone was completely eliminated and hydrogenated to naphthol and dihydroxynaphthalene as reported by Brower (15).

Carboxylic acid and carboxylate were completely decarboxylated to the parent hydrocarbons. According to Brower, carboxylic acid is quite stable in glass apparatus, but decomposed completely in a stainless steel autoclave.

The thermal decomposition of aromatic ethers

According to the results of Table 1, the bond scission of oxygen containing polynucleus aromatic structure of coal at liquefaction temperature of 450°C seems to occur mainly at methylene or ether structures. Therefore, it will be very important to study the characteristics of these structures in the thermolysis.

It has been often proposed that the units of coal structure are linked by ether linkages. Recently, Ruberto and his coworkers (7,8), Ignasiak and Gawlak (9) concluded that a significant portion of the oxygen in coal occurs in ether functional groups.

Thermal decomposition of seven diaryl ethers at various reaction conditions and the composition of reaction products are shown in Table 2.

The decompositions of phenyl benzyl ether and dibenzyl ether proceeded very rapidly at 400°C, and these results corresponded well to the low bond dissociation energy of $\text{PhCH}_2\text{-O}$.

Phenyl benzyl ether was mostly converted to toluene and phenol, but partly isomerized to benzyl phenol.

Dibenzyl ether was entirely converted to toluene and benzaldehyde.

The formation of products can be explained by the following reaction scheme. $\text{PhCH}_2\text{OCH}_2\text{Ph} \longrightarrow \text{PhCH}_2\text{O}\cdot + \cdot\text{CH}_2\text{Ph} \longrightarrow \text{PhCHO} + \text{PhCH}_3$
 $\text{PhCHO} \longrightarrow \text{PhH} + \text{CO}$ $\text{PhCHO} + 2\text{H}_2 \longrightarrow \text{PhCH}_3$

The high yield of toluene over 100% was confirmed to be due to the hydrogenation of benzaldehyde by tetralin. As shown in Figure 1, the yield of toluene increases with increasing reaction time, on the other hand, benzaldehyde decreases gradually after reaching a maximum value, giving toluene as the hydrogenated product and benzene and carbon monoxide as the decomposition products.

Although diphenyl ether and dibenzofuran were very stable for thermolysis at 450°C for 120 min., the rate of decomposition increased with increasing the number of benzene nucleus, that is, phenyl naphthyl ether was converted to the value of 25% and phenyl phenanthryl ether 46% at the same reaction conditions.

These results strongly suggest that in coal structure the covalent bond of benzyl ethers composed of aliphatic carbon and oxygen will be entirely ruptured at temperatures lower than 400°C, and the covalent bond composed of aromatic carbon and oxygen will be considerably decomposed at 450°C, since the unit structure of bituminous coal is considered to be composed of polynucleus of several benzene rings.

The effect of phenolic compounds on the decomposition of diaryl ethers

It has been known that phenolic compounds (16,17) in the presence of hydrogen-donating solvent have a remarkable effect on the dissolution of coal. Therefore, it is important to clarify the fundamental structure of coal being decomposed effectively by the addition of phenol.

The thermal decomposition of dibenzyl was not affected by the addition of phenol or p-cresol. In contrast, the decomposition of 2,2'-dinaphthyl ether increases remarkably in the presence of phenolic compounds as shown in Table 3, and the effect seems to increase with increasing the electron donating property of substituent on the benzene nucleus.

The effect of hydroquinone and p-methoxyphenol is remarkable, but this seems beyond argument at present because considerable parts of them can not be recovered after reaction, suggesting that very complex side reactions are taking place.

Furthermore, we studied the effect of phenolic compounds on the thermolysis of phenyl benzyl ether at 320°C, because even reactive phenols such as p-methoxy phenol are quite stable at this temperature.

As shown in Table 4, all phenols tested were confirmed to accelerate the conversion of phenyl benzyl ether. In this thermolysis, benzyl phenyl ether was decomposed to toluene and phenol (ca. 60%) and also isomerized to benzyl phenol (ca. 40%).

Accelerating effect due to phenols on the rupture of ether linkages

Phenols are weak acids and polar solvent, and so often observed to enhance the thermal decomposition of covalent bond, but we could not observe any accelerating effect due to phenol on the decomposition of dibenzyl.

Therefore, phenols must be participating directly in the course of scission of ether linkage.

Phenolic compounds may enhance the rate of decomposition of aromatic ether by solvating transition state of the scission of ether linkage and by hydrogen transfer to the formed alkoxy radicals.

Previously we have shown that phenolic compounds have a remarkable positive effect (4) on the coal liquefaction in the presence of tetralin, depending strongly on the character of coal as well as on the concentrations of phenols. The effect of phenols on the decomposition of diaryl ethers will give a good explanation for the previous results, because aliphatic ether structures of some young coals will be decomposed rapidly at relatively low temperatures and so the rate of coal dissolution will not be affected by the addition of phenols, on the other hand, the polycondensed aromatic ether structures will be decomposed effectively by the addition of phenols in the course of coal liquefaction.

The effect of mineral matters on the decomposition ethers

Recently, the effect of mineral matters of coal on the coal liquefaction has attracted much attention. It was shown that small amounts of FeS or pyrite are responsible for the hydrogenative liquefaction of coal. Therefore, it is interesting to elucidate the effect of mineral matters of coal on the decomposition rate and products of aromatic ethers, and so three diaryl ethers were thermally treated in the presence of coal ash obtained by low temperature combustion of Illinois No.6 coal.

It was found that the addition of coal ash remarkably accelerates the rate of decomposition of dibenzyl ether and also drastically changes the distribution of reaction products, that is, benzyl tetralin becomes the main reaction product instead of a mixture of toluene and benzaldehyde, as shown in Table 5.

This result is quite surprizing, but can be ascribed to the acidic components of coal ash, since Bell and coworkers (18) reported that benzyl ether acts as an alkylating reagent in the presence of Lewis acid such as $ZnCl_2$.

In the cases of phenyl benzyl ether and phenyl 9-phenanthryl ether, the effect of ash components was not so remarkable.

CONCLUSIONS

Diaryl ether must be one of the important structures responsible for the liquefaction of coal among various oxygen-containing organic structures of coal.

The rate of decomposition of polynucleus aromatic ethers increases with increasing the number of nucleus of aryl structure and are enhanced by the addition of phenolic compounds.

The rate of decomposition and the distribution of products of some diaryl ethers can be affected in the presence of coal ash.

ACKNOWLEDGEMENT

We acknowledge the financial support from the Sunshine Project Headquarters Agency of Industrial Science Technology.

REFERENCE

1. G. P. Curran, R. T. Struck and E. Gorin, Preprints Amer. Chem. Soc. Div. Petrol. Chem., C-130-148 (1966)
2. R. C. Neavel, Fuel, 55, 237 (1976)
3. M. Farcasiu, T. O. Mitchell and D. D. Whitehurst, Preprints Amer. Chem. Soc. Div. Fuel Chem., 21 (7), 11 (1976)
4. Y. Kamiya, H. Sato and T. Yao, Fuel, in press
5. C. H. Fischer and A. Eisner, Ind. Eng. Chem., 29, 1371 (1937)
6. Y. Takegami, S. Kajiyama and C. Yokokawa, Fuel, 42, 291 (1963)
7. R. G. Ruberto, D. C. Cronauer, D. M. Jewell and K. S. Seshadri, Fuel, 56, 17, 25 (1977)
8. R. G. Ruberto and D. C. Cronauer, Preprints Amer. Chem. Soc. Div. Petrol. Chem., 23 (1), 264 (1978)
9. B. S. Ignasiak and M. Gawlak, Fuel, 56, 216 (1977)
10. A. J. Szladow and P. H. Given, Preprints Amer. Chem. Soc. Div. Fuel Chem., 23 (4), 161 (1978)
11. H. Washowska and W. Pawlak, Fuel, 56, 422 (1977)
12. R. G. R. Bacon and D. J. Stewart, J. Chem. Soc., 4953 (1965)
13. Y. Sato, T. Yamakawa, R. Onishi, H. Kameyama and A. Amano, J. Japan Petrol. Inst., 21, 110 (1978)
14. B. M. Benjamin, V. F. Raaen, P. H. Maupin, L. L. Brown and C. J. Collins, Fuel, 57, 269 (1978)
15. K. R. Brower, Fuel, 56, 245 (1977)
16. A. Pott and H. Broche, Fuel in Science and Practice, 13 (4), 125 (1934)
17. M. Orchin and H. H. Storch, Ind. Eng. Chem., 40, 1385 (1948)
18. D. P. Mobley, S. Salim, K. I. Tanner, N. D. Taylor and A. T. Bell, Preprints Amer. Chem. Soc. Div. Fuel Chem., 23 (4), 138 (1978)

TABLE 1 THERMAL TREATMENT OF COAL-RELATED AROMATIC COMPOUNDS IN THE PRESENCE OF TETRALIN
(Tetralin 220 mmole, 1-Methylnaphthalene 140 mmole, Model compounds 10 mmole)

| Model compounds | Reaction conditions | | Conversion(%) | | Products (mole% to reacted model compounds) |
|----------------------------|---------------------|------------|-----------------|-----------------|---|
| | Temp. (°C) | Time (min) | Model compounds | | |
| | | | Model compounds | Model compounds | |
| Diphenylmethane | 450 | 30 | | 1.7 | Benzene 100, Toluene 95 |
| Dibenzyl | 450 | 30 | | 31.1 | Toluene 200 |
| Dibenzyl | 450 | 60 | | 54.1 | Toluene 194 |
| Diphenyl ether | 450 | 30 | | C | |
| Dibenzofuran | 450 | 30 | | 3.3 | |
| Phenyl benzyl ether | 400 | 30 | | 100 | see Table 2 |
| Dibenzyl ether | 400 | 30 | | 65 | see Table 2 |
| 2,2'-Dinaphthyl ether | 450 | 120 | | 23.3 | see Table 2 |
| Phenyl 1-naphthyl ether | 450 | 120 | | 25 | see Table 2 |
| Phenyl 9-phenanthryl ether | 450 | 120 | | 45.5 | see Table 2 |
| Benzyl benzoate | 450 | 30 | | 100 | Benzene 53, Toluene 98 |
| Benzophenone | 450 | 30 | | 29.4 | Diphenylmethane 100 |
| Benzyl phenyl ketone | 450 | 30 | | 25.3 | Dibenzyl 37, Diphenylmethane 37, Benzene 5, Toluene 7 |
| 1-Naphthol | 450 | 30 | | 1.4 | |
| 2-Naphthol | 450 | 30 | | 1.4 | |
| Diphenylmethanol | 450 | 30 | | 79 | Diphenylmethane 96 |
| 1,4-Naphthoquinone | 450 | 30 | | 100 | 1-Naphthol 74, Naphthalene |
| 2-Naphthoic acid | 450 | 30 | | 100 | Naphthalene |
| Diphenyl amine | 450 | 30 | | 8.2 | Benzene 60, Aniline(trace) |
| Diphenyl sulfide | 450 | 30 | | 10.7 | Benzene 183 |

TABLE 2 THERMAL DECOMPOSITION OF DIARYL ETHERS IN TETRALIN

| Diaryl ether | Temp (°C) | Time (min) | Conversion (%) | Products (mole% of reacted ether) |
|----------------------------|-----------|------------|----------------|--|
| Diphenyl ether | 450 | 30 | 0 | — |
| | 450 | 120 | 2 | — |
| Dibenzofuran | 450 | 30 | 3.3 | — |
| Phenyl 1-naphthyl ether | 450 | 120 | 25 | PhOH 66 |
| 2,2'-Dinaphthyl ether | 450 | 60 | 12.5 | 2-Naphthol 84 |
| | 450 | 120 | 23.3 | 2-Naphthol 63 |
| Phenyl 9-phenanthryl ether | 450 | 120 | 45.5 | PhOH 50, Phenanthrene 15 |
| Phenyl benzyl ether | 320 | 30 | 31.4 | PhCH ₃ 55, PhOH 50, Benzylphenol 40 |
| | 400 | 30 | 100 | PhCH ₃ 61, PhOH 66, Benzylphenol 27 |
| Dibenzyl ether | 400 | 30 | 65 | PhCH ₃ 106, PhCHO 73, PhH 12 |

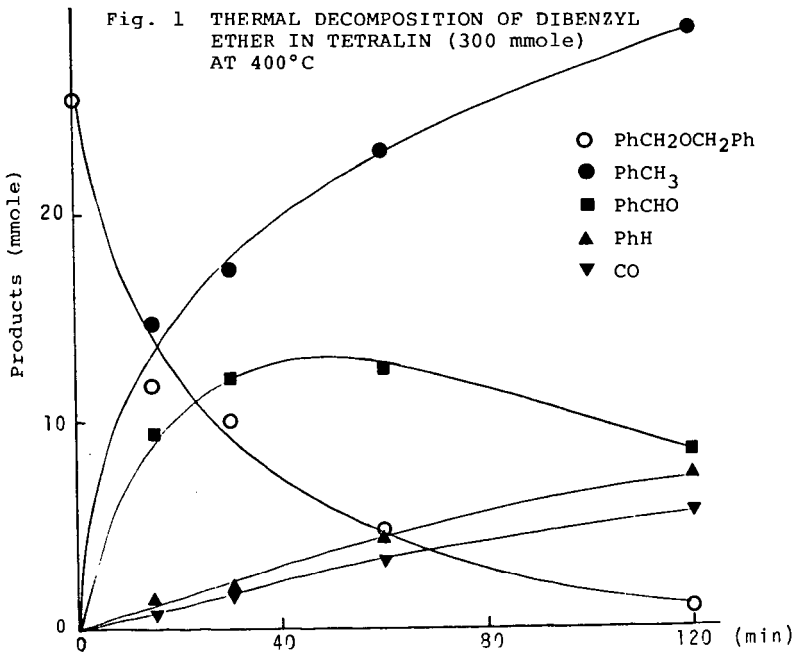


TABLE 3 EFFECT OF PHENOLS ON THE THERMAL DECOMPOSITION 2,2'-DINAPHTHYL ETHER AT 450°C FOR 60 MIN
(2,2'-Dinaphthyl ether 11 mmole, Tetralin 225 mmole, Additive 150 mmole)

| Additive | Conversion (%) | |
|-----------------------|------------------|--------|
| | Dinaphthyl ether | Phenol |
| 1-Methylnaphthalene | 12.6 | — |
| Phenol | 17.1 | 1.5 |
| p-Cresol | 21.0 | 0 |
| 2,4,6-Tremethylphenol | 26.0 | 3.5 |
| 1-Naphthol | 33.7 | 22.1 |
| p-Phenylphenol | 34.1 | 0 |
| p-Methoxyphenol | 49.5 | 100 |
| Hydroquinone | 63.5 | 57.7 |

TABLE 4 EFFECT OF PHENOLS ON THE THERMAL DECOMPOSITION OF PHENYL BENZYL ETHER AT 320°C FOR 30 MIN
(Phenyl benzyl ether 27 mmole, Tetralin 220 mmole, Additive 140 mmole)

| Additive | Conversion (%) | |
|---------------------|---------------------|---------|
| | Beznyl phenyl ether | Phenols |
| 1-Methylnaphthalene | 31.4 | — |
| p-Cresol | 40.2 | 0 |
| p-Methoxyphenol | 44.1 | 1.1 |
| 1-Naphthol | 43.0 | 0 |

TABLE 5 EFFECT OF COAL ASH ON THE THERMAL DECOMPOSITION OF DIARYL ETHERS
(Ethers 4 mmole, Tetralin 40 mmole)

| Ethers | Added Ash(g) | Temp (°C) | Time (min) | Coverision (%) | Products (mole% of reacted ether) |
|----------------------------|--------------|-----------|------------|----------------|---|
| Dibenzyl ether | — | 400 | 30 | 65 | PhCH ₃ 110, PhCHO 77, PhH 13 Benzyltetralin 2.2 |
| | 0.015 | 400 | 30 | 100 | PhCH ₃ 6, PhH trace, Benzyltetralin 152 |
| Phenyl benzyl ether | — | 400 | 30 | 100 | PhCH ₃ 61, PhOH 66, PhCH ₂ Ph 6, Benzylphenol 27, Benzyltetralin 2 |
| | 0.015 | 400 | 30 | 100 | PhCH ₃ 38, PhOH 58, PhCH ₂ Ph 3, Benzylphenol 39, Benzyltetralin 13 |
| Phenyl 9-phenanthryl ether | — | 450 | 120 | 46 | PhOH 50, Phenanthrene 17 |
| | 0.05 | 450 | 120 | 55 | PhOH 45, Phenanthrene 16 |

POSSIBLE HYDRIDE TRANSFER IN COAL CONVERSION PROCESSES

David S. Ross and James E. Blessing

SRI International
Menlo Park, CA 94025

INTRODUCTION

The conversion of coal to liquid fuels is usually carried out in the presence of an H-donor solvent (H-don) such as tetralin. The chemical route commonly suggested for the process is



in which there is initial thermal homolysis of sufficiently weak bonds in the coal structure yielding radical sites. These reactive sites are then "capped" by transfer of hydrogen atoms from the donor solvent. We will discuss here the chemistry of this process, including detailed consideration of the thermochemistry of Steps 1 and 2 above. We will then present some of our recent data, which suggest that there may be an ionic component in the process.

BACKGROUND

Step 1 above requires that there be bonds in coal which are weak enough to break in appropriate numbers at conversion temperatures and times. Table 1 displays some kinetic data for the cleavage of benzylic bonds in a series of increasingly aromatic compounds. In accord with expectation, an extension of the aromatic system increases the resonance stability of the thermally-formed free radical and therefore increases the ease with which the benzylic bond is broken. The phenanthrene system appears to be no more easily cleaved than the naphthalene system; however, ethyl anthracene is clearly destabilized significantly more than the other compounds in the table. The large decrease in bond-dissociation energy for the anthracene system is reflected in the three to four orders of magnitude increase in rate of scission at conversion temperatures as shown in the table.

Also pertinent to discussion of Step 1 is the material in Table 2, which includes bond dissociation energies and kinetic data at conversion temperatures for a series of C-C bonds. For the purposes of this discussion it can be assumed that substitution of -O- for -CH₂- does not change the thermochemistry. Thus, for example, the Ph-OPh bond and the Ph-CH₂Ph bond are similar in strength. Again not surprisingly, double benzylic resonance as present upon the scission of the central bond in bibenzyl results in a significant destabilization, and that compound, as well as benzyl phenyl ether, PhOCH₂Ph, are the only compounds with bonds easily broken under conversion conditions. If the full three to four orders of magnitude increase in rate shown in Table 1 for anthracene systems is applied, we see that perhaps the 1,3-diarylpropane system may also be sufficiently unstable for conversion at 400°-500°C. Thus it would seem that for coal con-

version via Steps 1 and 2, at least at 400°C, the first step can be sufficiently rapid for some structural features. We will discuss below some conversion data at 335°C, however, which suggest that thermally-promoted bond-scission is not fully consistent with experimental observation.

Next, a consideration of the kinetics for Step 2 raises some questions. The transfer of hydrogen in similar reactions has been well studied, and Table 3 presents data for the relative rates of transfer of hydrogen from a number of hydrocarbons to the free radical $\text{Cl}_3\text{C}\cdot$ at 350°C. The donor hydrocarbons are listed in order of increasing ease of H-transfer to the free radical. Tetralin is near the middle of the list. The most reactive donor in the table, 1,4-dihydronaphthalene, is about four times as active as tetralin.

The table also shows the results of experiments with the donors and coal in phenanthrene as solvent. Consistent with the transfer of hydrogen in a radical process, those donors less reactive toward $\text{Cl}_3\text{C}\cdot$ than tetralin are also less effective than tetralin in conversion of coal to a phenanthrene-soluble product. However, in contrast to the chemistry of Step 2 in the above scheme, we see that those donors which are more reactive toward $\text{Cl}_3\text{C}\cdot$ than tetralin are also less effective in their action with coal. Thus this simple conversion scheme is suspect.

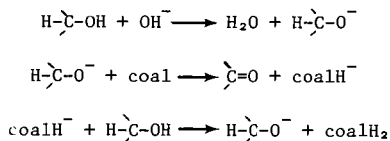
CURRENT RESULTS WITH HYDRIDE-DONORS

We have reported on the use of isopropyl alcohol as an H-donor solvent in coal conversion, and specifically on the effects of the addition of strong bases such as KOH to the system (1). We found that *i*-PrOH brought about a conversion of Illinois No. 6 coal very similar to the conversion level obtained by tetralin under the same conditions. These results are listed in Table 4, along with the results of more recent experiments using methanol as the solvent and adding KOH to the system.

Isopropanol is of course a well known reducing agent under basic conditions, reducing carbonyl compounds via hydride transfer, and becoming oxidized to acetone in the process (2). The table shows that the addition of KOH to the system significantly increases the effectiveness of the coal conversion reaction, and it would seem that such a system would have an advantage over one based on tetralin, where significant catalysis of hydrogen transfer has not been directly demonstrated. We found in our experiments with *i*-PrOH/KOH at 335°C that coal was converted to a product about 60% soluble in *i*-PrOH, that fraction having a number-average molecular weight of about 460.

In some model compound studies with the *i*-PrOH/KOH system we found that anthracene was converted to 9,10-dihydroanthracene in 64% yield. Benzyl phenyl ether was also studied and was converted to a polymeric material under the reaction conditions. There were no traces of phenol nor toluene, the expected reduction products.

We found subsequently that MeOH/KOH media at 400°C were very effective reducing systems, as the results in the table demonstrate. The methanol work yielded products with significant reductions in organic sulfur levels, and moderate reductions in nitrogen levels. We suggest the mechanism of reduction is ionic in nature, involving hydride transfer. Thus



where coalH^- and coalH_2 are an anionic intermediate and reduced coal respectively. The net reaction is

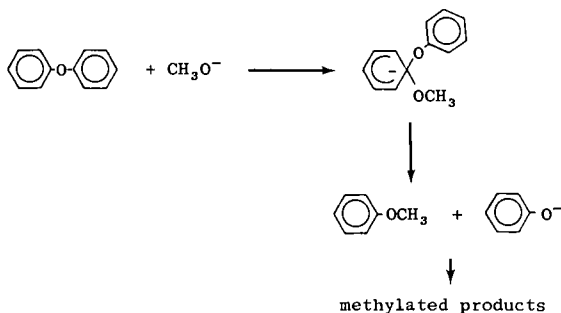


and in fact in the i -PrOH work we isolated acetone in quantities consistent with the quantities of hydrogen transferred to the coal.

The final coal product in the MeOH/KOH experiments was 20%-25% soluble in the methanol. When the methanol was removed, the resultant product was a room temperature liquid with the properties described in Table 5. The polymethylphenol fraction is apparently formed by the cleavage of phenolic ethers and subsequent methylation by the CO present in the reaction mixture as a result of methanol decomposition. The methylation reaction has been observed before for similar systems (3).

The methanol-insoluble product was also upgraded relative to the starting coal. Its H/C ratio was 0.86, its sulfur and nitrogen levels were 0.8% and 1.2% respectively, and it was fully pyridine-soluble.

Model compound studies were carried out in MeOH/KOH also, and the results are shown in Table 6. Phenanthrene and biphenyl were quantitatively recovered unchanged by the reactions, and bibenzyl was recovered in 95% yield, with small amounts of toluene observed. Anthracene and diphenyl ether, on the other hand, were converted respectively to 9,10-dihydroanthracene and a mixture of polymethylphenols similar to that observed in the work with coal. The cleavage of diphenyl ether via hydrogenolysis should yield both benzene and phenol as products; we saw no benzene in our study, and our observation of the polymethylphenols and anisoles thus indicates that nucleophilic ether cleavage is taking place. In other words, it appears that phenoxide is displaced by methoxide.



so that a favorable feature of the MeOH/KOH system in addition to its reducing power is its facility at cleaving otherwise inert ethers.

The alcohol/base chemistry observed here led logically to a system including CO/H₂O/KOH, and accordingly, a series of experiments was performed at 400°C. The COSTEAM Process is of course similar in nature, but without the purposeful addition of base. Also, it is applied primarily to lignite, though the COSTEAM chemistry has

been applied less successfully to bituminous coal also. The results we obtained with the basic system, along with the pertinent citations to earlier work by others, were recently presented (4).

To summarize our effort, we found that CO/H₂O/KOH systems converted Illinois No. 6 coal to a material which was fully pyridine soluble, 51% benzene soluble, and 18% hexane soluble. As with the basic alcoholic systems, there were significant reductions in organic sulfur levels, and moderate reductions in nitrogen levels. The chemistry here is similar to that for the basic alcoholic systems, but with formate (HCO₂⁻) as the hydride-donor, and thus the reducing agent. In control runs with H₂O/KOH or CO/H₂O little or no conversion was observed.

Model compound work with this system showed that anthracene was reduced to its 9,10-dihydro derivative (35% yield). Bibenzyl, on the other hand, was recovered unchanged with only a trace of toluene observed.

The model compound work for the three basic systems is summarized in Figure 1, in which a finding of no significant reduction in the respective system is designated by an x'ed arrow. Our criterion of successful reduction requires that significant quantities of the starting material be converted to reduced products. In the case of benzyl phenyl ether, for example, while little starting ether was recovered, most of it being converted to an intractable polymer, no phenol nor toluene was found. Thus we conclude the system was not effective in reduction of the C-O bond. Similar statements apply regarding the C-C bond in bibenzyl for the MeOH/KOH and CO/H₂O/KOH systems.

A significant conclusion to be drawn from these data is that coal is converted under conditions where the common model compounds benzyl phenyl ether and bibenzyl are not reduced. In explanation, it might be suggested that there are two conversion mechanisms. One would be the commonly considered scheme (eqs 1 and 2), taking place in tetralin-like media, involving free radical chemistry, and reducing both coal and such model compounds as bibenzyl and benzyl phenyl ether through a thermally-promoted initial bond-scission. A second mechanism would be operative in strongly basic media, involve hydride transfer, and would perhaps include the conversion of coal via chemistry related in some way to the reduction of anthracene by these systems.

However, as pointed out above, the commonly proposed free radical mechanism is not entirely consistent with the observed behavior of H-donor solvents and coal. Further, a thermally promoted C-C or C-O bond-scission is inconsistent with our observations in the *i*-PrOH work at 335°C. As also mentioned, a major fraction of the coal was converted in this system to a product with a number-average molecular weight of less than 500. If we consider that the rate constant for the unimolecular scission of the central bond in bibenzyl is expressed (5) as

$$\log k \text{ (sec}^{-1}\text{)} = 14.4 - 57/2.303RT$$

then while the half-life for the reaction at 400°C is about 2 hours, and thus perhaps appropriate for considerations of conversion at those conditions, at 335°C the half-life is about 160 hours, and clearly the reaction cannot play a significant role in the conversion of coal at that temperature.

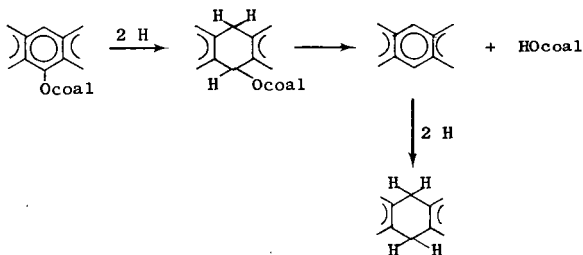
Additionally, it has been noted that tetralin operates via hydride transfer, at least in its reduction of quinones. Thus it has been shown that tetralin readily donates hydrogen to electron-poor systems such as quinones at 50°-160°C. The reaction is accelerated by electron-withdrawing substituents on the H-acceptor and polar sol-

vents, and is unaffected by free radical initiators (6). These observations are consistent with hydride transfer, as is the more recent finding of a tritium isotope effect for the reaction (7).

We propose therefore that the operative mechanisms of coal conversion in both tetralin-like media and our strongly basic systems may be the same, involving hydride donation by the H-donor solvent, followed by proton transfer. Consistent with this surmise are the results for two experiments carried out under the same conditions, utilizing tetralin on the one hand, and CO/H₂O/KOH on the other. The results are presented in Table 7, and show that the products from the two reactions have similar diagnostic characteristics, including benzene solubilities, H/C ratios, and ratios of H_{al}/H_{ar}. Further comparisons are in progress.

Since the proposed conversion process does not include a thermally promoted bond-scission step, the question arises of how the addition of hydrogen results in the bond breaking necessary for significant reduction in molecular weight. We have already noted that the nucleophilic action of the basic methanol system was sufficient to cleave diphenyl ether, and a similar route is available in the basic *i*-PrOH and CO/H₂O systems. On the other hand, we showed in control experiments that strongly basic conditions alone were not sufficient for significant conversion of coal.

Based on the data at hand, we are currently considering two possible modes of molecular weight reduction. The first involves the generation of thermally weak bonds by the initial addition of hydrogen. We suggest that the addition of hydrogen to the structures below may be a key to the cleavage of critical bonds in coal.



It can be shown thermochemically that the addition of hydrogen across structures like those above is favored under conversion conditions (1). In turn it can be suggested that the dihydroether intermediate is rapidly thermalized in the succeeding step, yielding both an oxygen-containing fragment and a rearomatized fragment that is rapidly reduced to a hydroaromatic product. The thermolysis of the intermediate is expected to be rapid at conversion temperatures, in accord with Brower's observation that, in tetralin, anthraquinone is converted all the way to anthracene (8). Moreover, it is recognized that 9-hydroxy-9,10-dihydroanthracenes readily eliminate water at ambient conditions, yielding the aromatized product (9).

The second potential conversion mode takes into consideration the recent observation that hydrogen acceptors such as benzophenone oxidatively couple phenols under

conversion conditions (10). It can thus be suggested that the major role of a reducing component in a coal conversion system is the reduction of quinones and perhaps other oxidants present in the coal rather than direct reduction of the coal. In the absence of an H-donor, then, oxidative crosslinking takes place within the coal upon heating, yielding a product even less soluble in solvents such as pyridine than was the starting coal. On the other hand, in the presence of a reducing agent, either conventional H-donors such as tetralin or our hydride-donating systems, the quinones and other oxidants should be reduced to unreactive material, and the coal then proceeds to liquefy by means of a thermal process involving no addition of hydrogen. We cannot at this time propose a route for purely thermal liquefaction (reverse Diels Alder reactions might be suggested for purposes of example) and the concept currently remains a working hypothesis.

ACKNOWLEDGEMENT

We acknowledge the support of this work by the U.S. Department of Energy under Contract No. EF-76-01-2202.

REFERENCES

1. D. S. Ross and J. E. Blessing, Fuel Division Preprints of the 173rd Meeting of the American Chemical Society, 22, (2), 208 (1977). A full manuscript has been submitted for publication.
2. A Wilds, Organic Reactions, Vol. II, 180 (1947).
3. V. Stenberg, private communication.
4. D. S. Ross and J. E. Blessing, Fuel, 57, 379 (1978).
5. S. W. Benson and H. O'Neal, "Kinetic Data on Gas Phase Unimolecular Reactions," National Bureau of Standards, NSRDS-NBS 21 (1970).
6. R. Linstead et al., J. Chem. Soc., 3548, 3564 (1954).
7. P. van der Jagt, H. de Haan and B. van Zanten, Tetr. 27, 3207 (1971).
8. K. Brower, Fuel, 56, 245 (1977).
9. L. Fieser and R. Hershberg, J. Am. Chem. Soc., 61, 1272 (1939).
10. V. Raaen and W. Roark, in press.

Table 2
THERMOCHEMICAL AND KINETIC FACTORS FOR SOME BONDS IN COAL

| Structure | BD ₀ ^a (kcal/mol) | t _{1/2} ^b | |
|-----------|--|-------------------------------|-------------------------|
| | | 400°C (572°F) | 500°C (932°F) |
| | > 120 | ∞ | ∞ |
| | 116 | 2.6x10 ¹³ yr | 3.7x10 ¹⁰ yr |
| | 82 | 2.7x10 ⁶ yr | 10.2 yr |
| | 81 | 1.3x10 ⁴ yr | 5.3 yr |
| | 69 | 629 days | 19.7 hr |
| | 57 | 2.0 hr | 30 sec |

^aBond dissociation energies. See S. W. Benson, *Thermochemical Kinetics*, John Wiley and Sons, New York (1968).

^bCalculated from the expressions $\log k$ (sec⁻¹) = 14.4 - BDE/4.6T, t_{1/2} = 0.7/k.

Table 1
THERMAL CLEAVAGE OF BENZYLIC BONDS IN AROMATIC SYSTEMS

| Structure | BD ₀ ^a (kcal/mol) | Relative Rate | |
|-----------|--|-------------------|-------------------|
| | | 400°C (572°F) | 500°C (932°F) |
| | 72 (obs.) | 1 | 1 |
| | 68 (obs.) | 20 | 12 |
| | 68 (est.) | 20 | 12 |
| | 60 (est.) | 9x10 ⁵ | 3x10 ³ |

^aBond dissociation energies. See S. Stein and D. Golden, *J. Org. Chem.*, **42**, 839 (1977). The two observed values correspond to estimated values, and are from the unpublished work of D. Golden and D. McMillen, SR1.

Table 3

REACTIVITY OF VARIOUS H-DONOR SOLVENTS WITH CCl_4 AND COAL

| Cosolvent | Relative Reactivity Toward CCl_4^a (350°C) | Relative % Dissolution ^b (2 hr/350°C) |
|--------------------------|---|--|
| None (Phenanthrene) | -- | [33] ^c |
| Toluene | 1.0 | 1 |
| 2-Methylnaphthalene | 2.1 | 0 |
| 1-Methylnaphthalene | 2.6 | 2 |
| Diphenylmethane | 6.0 | 1 |
| Cumene | 8.7 | 0 |
| Fluorene | (20) | 0 |
| Tetralin | 41.0 | 27 |
| 9-Methylanthracene | 56.0 | 0 |
| 1,2-Dihydronaphthalene | (65) | 6 |
| 9,10-Dihydroanthracene | (102) | 24 |
| 9,10-Dihydrophenanthrene | (102) | 22 |
| 1,4-Dihydronaphthalene | (160) | 14 |

^aData from Hendry, D., Mill, T., Piszkiwicz, Howard, J., and Eigenman, H., J. Phys. Chem. Ref. Data, 3, 937 (1974). The values in parenthesis are estimated from other radical data available in the paper. ^bAll reactions carried out in phenanthrene as solvent with 4.0 parts solvent per part coal, and 10 wt % cosolvent. Unpublished data of D. Hendry and G. Hum, SRI. ^cValue for phenanthrene alone.

Table 4

ALCOHOLS AS H-DONOR SOLVENTS IN COAL CONVERSION

| System | T(°C)/min | Pyr. Sol (%) | H/C | ZS _{org} | ZN |
|--------------------|-----------|-----------------|------|-------------------|-----|
| Untreated coal | -- | 13 | 0.73 | 2.1 | 1.7 |
| Tetralin | 335/90 | 48 | 0.81 | 1.8 | 1.6 |
| <i>i</i> -PrOH | 335/90 | 50 | 0.81 | 1.8 | 1.6 |
| <i>i</i> -PrOH/KOH | 335/90 | 96 | 0.88 | 1.6 ^a | 1.6 |
| MeOH/KOH | 400/90 | 99 ⁺ | 0.96 | 0.8 | 1.2 |

^aReduced to 0.5% when product treated further.

Table 5

PROPERTIES OF THE METHANOL-SOLUBLE COAL PRODUCT

| | | | |
|---|------|---|--|
| H/C | 1.37 | } $\xrightarrow[\text{< 0.1 torr}]{\text{distilled}}$ | ~40% polymethylphenols and anisoles |
| ZS _{org} | 0.5 | | ~40% mixture of butyrolactone and heavier materials yielding $\text{CH}_3\text{CH}_2\text{C}=\text{O}^+$ and $\text{HOCH}_2\text{CH}_2\text{CH}_2\text{C}=\text{O}^+$ major fragments by mass spectroscopy |
| ZN | 0.4 | | |
| H _{al} /H _{ar} ^a | 5.1 | | ~20% unidentified |

^aBy nmr

Table 6

MODEL COMPOUNDS IN MeOH/KOH AT 400°C/30 MINUTES

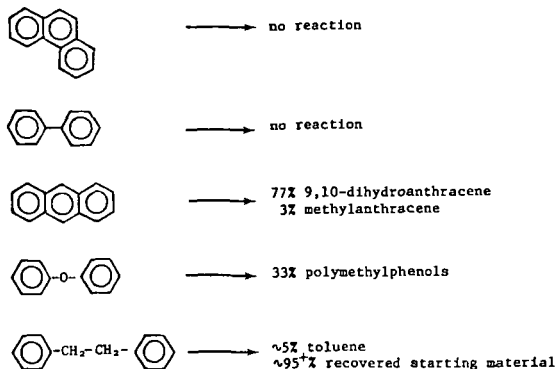


Table 7

COMPARISON OF CO/H₂O/KOH-TREATED AND TETRALIN-TREATED COAL PRODUCTS^a

| Reaction Conditions | Benzene Solubility ^b % | Molar H/C | | ZN | | H _{al} /H _{ar} ^e |
|--------------------------------------|--------------------------------------|-----------------|-----------------|-----------------|-----------------|---|
| | | BS ^c | BI ^d | BS ^c | BI ^d | |
| CO/H ₂ O/KOH ^f | 48 | 1.01 | 0.65 | 1.1 | 1.8 | ~ 3.0 |
| Tetralin ^g | 37 | 1.01 | 0.72 | 0.6 | 1.9 | ~ 2.7 |

^aReactions run at 400°C for 20 min in a stirred, 300 ml Hastelloy "C" reactor. 10.0 g of dried, -60 mesh Illinois No. 6 coal (PSOC-26) used in each case. ^bSolubility of entire product in 50 ml of benzene. ^cBenzene soluble portion of the product. ^dBenzene insoluble portion of the product. ^eRatio of ¹H-NMR areas: H_{al} = 0<δ<5; H_{ar} = 5<δ<10. Contributions from benzene and tetralin were subtracted before calculation. ^f36 g of H₂O, 10 g of KOH, and 700 psig of CO used in a 300 cc reactor. ^g60 g of tetralin.

| IPA/KOH (335°C) | MeOH/KOH (400°C) |
|---|---|
| coal \longrightarrow | coal \longrightarrow |
| anthracene \longrightarrow | anthracene \longrightarrow |
| PhCH ₂ OPh \times | Ph ₂ O \longrightarrow |
| | Phenanthrene \times |
| CO/H ₂ O/KOH (400°C) | PhCH ₂ CH ₂ Ph \times |
| coal \longrightarrow | |
| anthracene \longrightarrow | |
| PhCH ₂ CH ₂ Ph \times | |

FIGURE 1. SUMMARY OF RESULTS FOR COAL AND SELECTED MODEL COMPOUNDS IN SOME STRONGLY BASIC CONVERSION SYSTEMS. Arrows indicate that significant conversion to reduced products was observed. The x'ed arrows indicate that no reduction was observed.

Hydrogenation Mechanism of Coals and Coal Constituents by Structural Analysis of Reaction Products

Y. Maekawa, Y. Nakata, S. Ueda, T. Yoshida and Y. Yoshida

Government Industrial Development Laboratory, Hokkaido
41-2 Higashi-Tsukisamy Toyohiraku,
Sapporo, 061-01, Japan

Introduction

It is generally conceded that in the hydrogenation reaction of coal the following diverse chemical reactions compete in parallel (among and against each other) as the reaction proceeds: namely, thermal decomposition, stabilization of active fragments by hydrogen, cleavage of linkage between structural units, dealkylation, dehydro atom, hydrogenation of aromatic ring, ring opening etc. It is also accepted that the various features of these reactions are strongly influenced and change the type of raw coal, their individual chemical structures, properties of the catalyst employed, type of reducing agents, difference in reaction temperature and pressure and the degree of reaction progress. The resulting reaction products are a complex mixture of compounds and because of the fact that the structural analysis thereof is extremely complicated, it follows that elucidation and clarification of the reaction mechanism involved are extremely difficult and the results are far from satisfactory.

Thus we have conducted work on the structural parameters of coal hydrogenation products using the method of Brown-Ladner¹⁾, and from the results obtained we have conducted a follow up on the changes of structural parameters of product accompanying the reaction course; based on the above the outline of the reaction mechanisms have been previously discussed and our results have been reported^{2,3)}

In the present paper we have selected several kinds of coal samples and using these samples and various reducing agents such as H_2 , $H_2 + CH_4$, D_2 , $D_2 +$ tetralin, $CO + H_2O$, we have carried out hydrogenation reactions. We have made a follow-up of the structural parameters of the reaction products and we have further discussed the reaction mechanisms involved.

Experimental

The results of the analysis of the sample coal used in the experiment are shown in Table 1. Hydrogenation was conducted using a batch type autoclave with an inner volume of 500 ml. The reaction gas after completion of the reaction was analysed by gas chromatography. Further, the produced water was quantitated. The whole of the remaining products was quantitated and fractionated by extraction using n-hexan, benzene and pyridine. The fractionation methods are as shown in Table 2, regarding these when fractionation is completed by benzene extraction the conversion was calculated from organic benzene insolubles (O.B.I.) and when fractionation is carried out by pyridine the same was calculated from organic pyridine insolubles (O.P.I.).

With regards to hydrogenation reducing agents such as H_2 , $H_2 + CH_4$, D_2 , $D_2 +$ tetralin, $CO + H_2O$ were selected and reduction was conducted by varying the reaction time. Each fractionated fraction was subjected to ultimate analysis, H-NMR, C-13 NMR, molecular weight measurement and the structural parameters were calculated. The results of follow up of these structural parameters in the course of the reactions were considered together and the reaction mechanisms thereof were discussed.

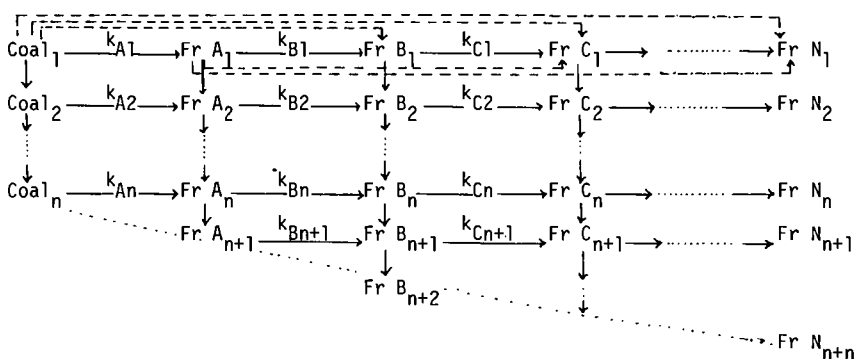
Results and Discussion

Product distribution

Hitherto from a considerable time back high pressure hydrogenation reaction has been dealt with as a consecutive reaction pass through asphaltene as the intermediate⁴⁾⁵⁾⁶⁾. Further it has been pointed out that Py-1, O₂ likewise shows the behavior of intermediates³⁾.

In Fig. 1 the following is depicted; the hydrogenation products of Yubari coal at reaction temperature of 400°C were fractionated by the procedure shown in Table 2, and the changes of these fraction yield by reaction time are shown. Inasmuch as the presence of Py-2 is scarce in coal, the observed results were obtained in the decreasing period, thus it may readily surmized that an increasing period is present in the initial stage of the reaction. Here we consider oil-1 as the final product, and it may be noted that all fraction other than oil-1, show an initial increase and a subsequent decrease in the course of the reaction and it is clear that they show the behavior of intermediate products in a consecutive reaction. A more or less similar reaction was observed in other reducing agents.

Based on previous work⁷⁾⁸⁾ regarding the distribution of molecular weight of these fractions, it is known that these have a wide distribution of molecular weight. It is also known that raw coal itself has a structural distribution⁹⁾¹⁰⁾. Therefore it may be considered that in the high pressure hydrogenation of coal, the reactivity of remained unreacted coal is gradually changed and also consecutive degradation of coal is being conducted. This consideration may be expressed in a schematic diagram as follows.



In other words, coal₁ is raw coal, is reacted and lead to a change to a one step lower molecular fraction Fr A₁, and at the same time as a side reaction Fr B₁ Fr N₁ is directly produced. Coal₂, the remaining coal from which the above constituents have been lost from coal₁, would naturally have a different composition and reactivity of that of coal₁. A similar reaction may be expected when Fr A₁ undergo a change to Fr B₁. The method of dealing with the above indicates the molecular lowering direction of the reaction of hydrogenolysis, and it may be surmized that the chemical reaction of each step would be highly complex.

Based on the above consideration, the mode of kinetic study carried over a wide range, is solely a means to express how the fraction, fractionated by a certain method, changes quantitatively in the reaction course. In other words these experimental results are expressed in equation for convenience sake. And it may be considered that it may be considered as a practical means in applicable form.

Now, each respective fraction shows a structural change along with the reaction course, it may be considered at the same time that it contains transfer material from a higher molecular fraction. In other words, for instance Fr A₂ is produced from coal 2 which changes by hydrogenolysis and at the same time, the residue resulting from the reaction from Fr A₁ to Fr B₁ is transferred and exists in a mixed state.

This should be taken into consideration when the reaction mechanism is to be discussed. In Fig. 1, it may be appropriate to consider that the structural changes of Py-1, Py-2 in the course of the reaction are due to the reaction itself.

Hydrogenolysis by H₂

Hydrogenolysis was conducted using Yubari coal at a reaction temperature of 400°C. The changes of ultimate composition and structural parameters of the Py-1 fraction of the hydrogenolysis products in the reaction course are shown in Fig. 2. Whereas oxygen and sulfur decrease with the proceeding of the reaction, the nitrogen-containing structure is refractory against hydrogenolysis, and a tendency for the nitrogen to be concentrated with the reaction time was recognized. In spite of the Py-1 in the reaction course yield decrease brought about by hydrogenolysis, however the structural parameters are almost the same which suggests that Yubari coal has a uniform unit structure. The decrease in Hau/Ca in the latter part of the reaction, even when considered together with the behavior of other parameters, it cannot be considered that this is the result of growth of the condensed aromatic ring of Py-1. From the results of an investigation of the structural analysis method using C-13 NMR, in spite of the fact that Hau/Ca should increase when saturation of the aromatic rings arises, because of the Brown-Ladner assumption which has it that diphenyl type linkage is lacking, in contrast cases where Hau/Ca decreases in size may be present¹¹⁾. Therefore, it is doubtful the Hau/Ca directly reflects the degree of aromatic ring condensation. From the above in the latter part of the reaction of Py-1, if we could consider that saturation of the aromatic ring has arisen, it may be conceded that an increase in σ al (alkyl group substitution) is present. Although it can be stated that by the decrease of the molecular weight, the Py-1 is transferred to asphaltene, when the structural parameters of Py-1 and asphaltene are compared, it may be conceded that at this molecular weight lowering step deoxygenation reaction, depolymerization, ring saturation (side chain substitution - σ al') and likewise an increase in side chain substitution over C₂ etc are taking place. Similar results may be observed in the hydrogenolysis of Bayswater vitrinite concentrate, and inertinite concentrate.

Hydrogenation by H₂ + CH₄

It was noted that CH₄ is produced as largest gas product in the hydrogenolysis of coal and is found coexisting with reducing hydrogen, the influence thereof on the reaction mechanism was investigated. When methane was added at a pressure of 25 or 50 kg/cm² to the initial hydrogen pressure of 75 kg/cm² and the hydrogenolysis reaction rate constant was measured. The results are as shown in Table 3.

It may be seen that the reaction rate constant mainly depends on the hydrogen

partial pressure. However, as compared with the hydrogen only where methane is added at a pressure of 25 kg/cm², a slightly higher value is seen. But, in the case of 450°C likewise it may be considered that it solely depends on hydrogen partial pressure. The results of an investigation on the change of structural parameters of the reaction products by reaction time are shown in Fig. 3. This, it may be considered that the increase in hydrogen pressure mainly enhances the saturation of aromatic rings (as a result an increase in α -hydrogen is seen).

D₂, D₂ + tetralin reduction of coal

In order to clarify the attack site of the hydrogen used for reduction, D₂ was used as the reducing agent and deuteration of coal was conducted and an investigation of the D distribution of reaction products was carried out. For the measuring distribution of D, D-NMR was used, and determination of D divided in 3 categories namely aromatic D(D_a), D bonded carbon α from aromatic ring (D _{α}), D bonded carbon further β from aromatic carbon was conducted. The results are as shown in Table 4. D_a, D _{α} , D _{β} was converted into H an approximately similar hydrogen type distribution, as seen when H₂ was used, was obtained. However, when compared with the distribution of hydrogen remaining in the reaction products, it was shown that a marked maldistribution of diutrium at the α position was seen. It was also noted that when tetraline is used as the vehicle, this tendency because more pronounced.

In addition to the minute amounts of hydrogen in the produced gas, corresponding to the maxym 34% of hydrogen in coal is present as H-D, and it is known that regarding D in the reaction products, not only D from the reaction but also D arising from the H-D exchange reaction are present. While there is a strong selectivity of H-D exchange reaction^[2], the ratio of D_a, D _{β} is comparatively high in the products of the initial stage and further even with the increase in reaction time, since the D_a, D _{α} , D _{β} ratio does not approach the H_a, H _{α} , H _{β} ratio, it may be considered that a larger portion of D reacts to α carbon from the aromatic rings.

Reduction by CO + H₂O

In Fig. 4 is shown a comparison of changes of the structural parameters of the reaction products in the reaction course where reduction of Soya coal samples is conducted using H₂ and CO + H₂O. The greatest difference between the two, while it is the same fraction under almost the same conversion, in a CO + H₂O system, there is a scarcity of oxygen containing structure. Further when H₂ is used, in asphaltene the α portion (hydrogen bonded α carbon from aromatic carbon) is smaller as compared with the CO + H₂O system. Still further under the present condition the main reaction involved in molecular lowering is depolymerization, so the nacent hydrogen coming from CO + H₂O has a selectivity to attack the ether linkage, in addition it may be considered that H₂ compared with this, has a definite activity for the cleavage of the CH₂ bridge.

Conclusion

The structural parameter changes of products of coal reduction reaction under various reducing reaction conditions were followed up, and a discussion the reaction mechanisms involved was made and the following conclusion were obtained.

- 1) It may be considered that in the hydrogenolysis reaction of coal, the coal is subjected to consecutive changes in components and reactivity which results in a consecutive molecular lowering.
- 2) Regarding the chemical reaction observed under comparatively mild hydrogenolysis,

cleavage of linkage between structural units, saturation of aromatic rings, ring opening, dealkylation, deoxygen, desulfurization were seen.

- 3) When high pressure hydrogen was used as the reducing agent, it could be considered that as a result the addition of hydrogen to α -carbon from the aromatic ring was highest. This was further promoted by increasing the reaction pressure.
- 4) It may be considered that the nascent hydrogen more selectively contributed to the cleavage of ether bridge and that H_2 was more selective than $CO + H_2O$ regarding the cleavage of the CH_2 bridge.

And also recognized that follow up the changes of structural parameters in the course of reaction is effective to elucidate the reaction mechanism of coal hydrogenolysis.

References

- 1) J.K. Brown, W.R. Ladner, Fuel, 39, 87 (1960)
- 2) Y. Maekawa, K. Shimokawa, T. Ishii, G. Takeya, Nenryo Kyokai-shi (J. Fuel Soc. Japan) 46, 928 (1967)
- 3) Y. Maekawa, S. Ueda, S. Yokoyama, Y. Hasegawa, Y. Nakata, Y. Yoshida, ibid, 53, 987 (1974)
- 4) S. Weller, M.G. Pelipetz, S. Friedman, Ind. Eng. Chem., 43, 1572, 1575 (1951)
- 5) E. Falkum, R. A. Glenn. Fuel, 31, 133 (1952)
- 6) T. Ishii, Y. Maekawa, G. Takeya, Kagaku Kogaku (Chem. Eng. Japan) 29, 988 (1965)
- 7) H. Itoh, Y. Yoshino, G. Takeya, Y. Maekawa, Nenryo Kyokai-shi (J. Fuel Soc. Japan) 51, 1215 (1972)
- 8) R. Yoshida, Y. Maekawa, G. Takeya, ibid, 53, 1011 (1974)
- 9) R. Yoshida, Y. Maekawa, G. Takeya, ibid, 51, 1225 (1972)
- 10) R. Yoshida, Y. Maekawa, T. Ishii, G. Takeya, Fuel, 55, 341 (1976)
- 11) T. Yoshida, et al, under contributing
- 12) S. Yokoyama, M. Makabe, M. Itoh, G. Takeya, Nenryo Kyokai-shi (J. Fuel Soc. Japan) 48, 884 (1969)

Table 1 Analytical data on the coals studied

| Sample | Proximate analysis % | | | | Ultimate analysis % | | | | |
|-----------------|----------------------|------|------|------|---------------------|-----|-----|------|------|
| | M. | Ash | V.M. | F.C. | C | H | N | S | O |
| Soya Koishi *1 | 15.5 | 15.7 | 33.6 | 35.3 | 73.0 | 6.6 | 1.5 | 0.04 | 20.0 |
| Bayswater Vi.*2 | 3.4 | 1.6 | 32.9 | 62.1 | 83.0 | 5.3 | 2.0 | 0.5 | 9.2 |
| Bayswater In | 4.5 | 16.2 | 20.8 | 58.5 | 85.0 | 4.1 | 1.9 | 0.3 | 8.7 |
| Yubari | 1.1 | 6.8 | 43.6 | 48.5 | 85.2 | 6.2 | 1.6 | 0.1 | 6.9 |
| Shin Yubari | 1.2 | 7.4 | 34.7 | 56.7 | 87.4 | 6.5 | 1.8 | 0.04 | 4.7 |

*1 Austrarian, Vitrinite 99% concentrate
 *2 " Inertinite 95% concentrate

Table 2 Fractionation of coal hydrogenation product

| Solvent | Fractionation procedure | Fraction | Symbol |
|----------|--------------------------------|---|----------------|
| N-hexane | 1 Room temperature decantation | Oil-1 : n-hexane soluble oil | O ₁ |
| | 2 Soxhlet extraction | Oil-2 : n-hexane extract | O ₂ |
| Benzene | 3 Soxhlet extraction | Asphaltene : benzene soluble, n-hexane insolubles (Organic benzene insolubles) | A (O.B.I.) |
| | 4 Room temperature decantation | Pyridine soluble, benzene insolubles | Py-1 |
| Pyridine | 5 Soxhlet extraction | Pyridine extract | Py-2 |
| | Soxhlet extraction residue | Organic pyridine insolubles | O.P.I. |

Table 3 Reaction rate constant for Shin-Yubari coal hydrogenolysis under different reducing gas composition

| Reaction Temp. | Reducing gas composition (kg/cm ²) | Reaction rate constant min. ⁻¹ | | |
|----------------|--|---|----------------|----------------|
| | | k ₁ + k ₃ | k ₁ | k ₃ |
| 400°C | H ₂ 75 | 0.0115 | 0.0037 | 0.0078 |
| | H ₂ 75 + CH ₄ 25 | 0.0133 | 0.0050 | 0.0083 |
| | H ₂ 75 + CH ₄ 50 | 0.0111 | 0.0033 | 0.0078 |
| | H ₂ 75 + Ar 25 | 0.0109 | 0.0024 | 0.0085 |
| 450°C | H ₂ 50 + CH ₄ 50 | 0.0178 | | |
| | H ₂ 75 + CH ₄ 25 | 0.0230 | | |
| | H ₂ 100 | 0.0258 | | |

Table 4 H and D distribution of hydrogenation and deuteration product of Shin-Yubari coal at 400°C under 50 kg/cm² of initial pressure

| Product | Gas | Rt(min.) | H and D distribution % | | | | | |
|------------|------------------|----------|------------------------|------|------|------|------|------|
| | | | Ha | Hα | Ho | Da | Dα | Do |
| Oil | D ₂ | 60 | 17.5 | 19.5 | 63.0 | 19.4 | 49.5 | 31.1 |
| | D ₂ | 120 | 18.7 | 21.2 | 60.1 | 19.9 | 50.9 | 29.2 |
| | H ₂ | 60 | 21.3 | 29.6 | 49.1 | | | |
| | H ₂ | 120 | 19.8 | 31.2 | 48.9 | | | |
| | D ₂ * | 60 | 28.8 | 29.8 | 41.4 | 20.1 | 54.5 | 25.4 |
| | H ₂ * | 60 | 30.5 | 35.3 | 34.2 | | | |
| Asphaltene | D ₂ | 60 | 30.3 | 29.9 | 39.8 | 12.9 | 61.7 | 25.4 |
| | D ₂ | 120 | 26.5 | 29.9 | 43.5 | 12.5 | 55.1 | 32.4 |
| | H ₂ | 60 | 27.4 | 36.4 | 36.2 | | | |
| | H ₂ | 120 | 30.7 | 34.5 | 34.8 | | | |
| | D ₂ * | 60 | 26.1 | 29.8 | 44.2 | - | 68.3 | 31.7 |
| | H ₂ * | 60 | 29.5 | 34.2 | 36.3 | | | |

* with tetraline

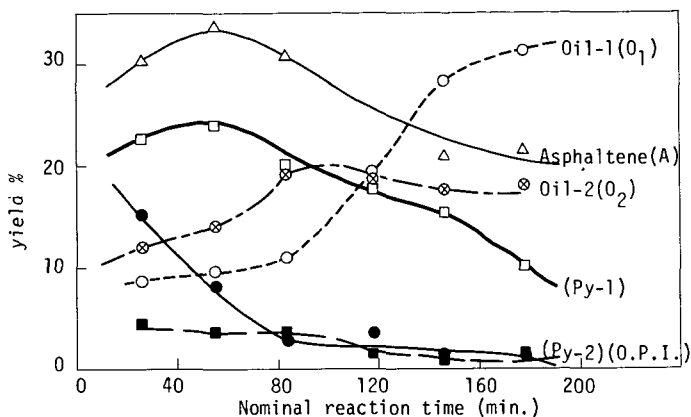


Fig. 1 The distribution of products from Yubari coal hydrogenation at 400°C

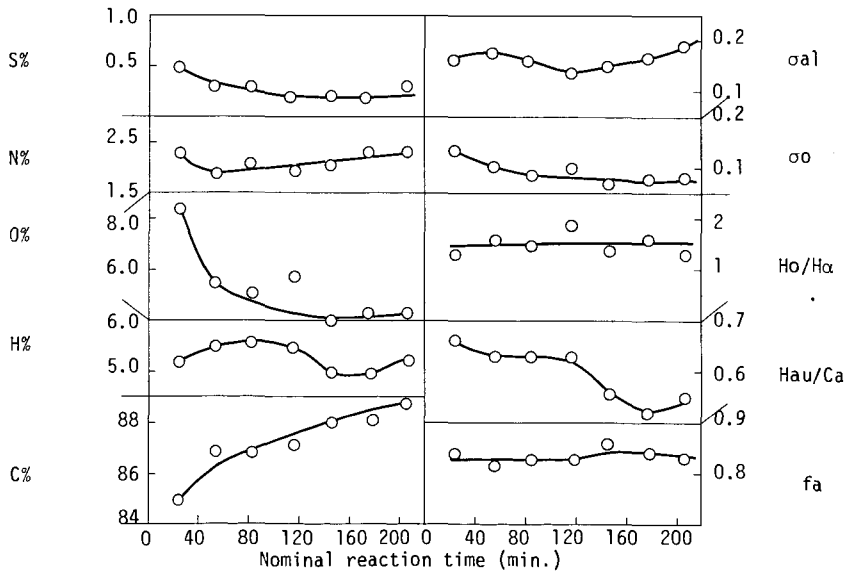


Fig. 2 Ultimate composition and structural parameters of Yubari coal hydrogenolysis product Py-1

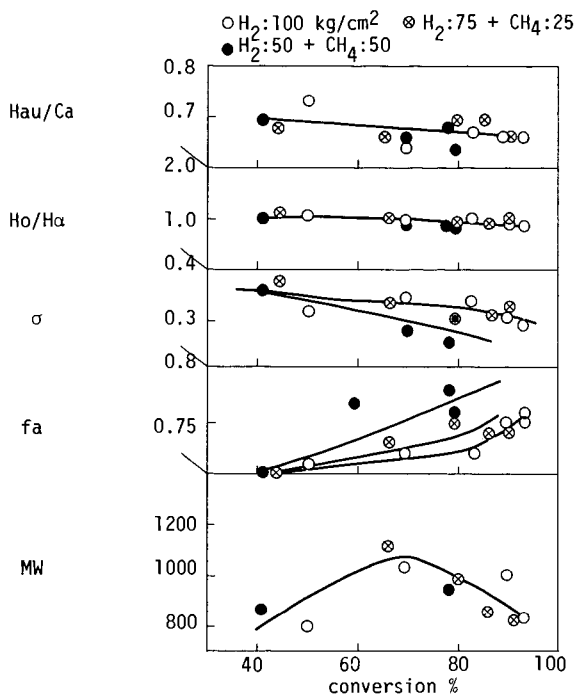


Fig. 3 The distribution of structural parameters of asphaltene from Shin-Yubari coal hydrogenation at 450°C

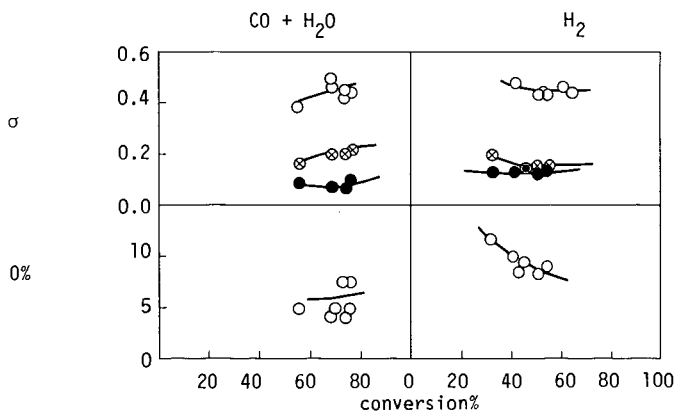


Fig. 4 Structural parameters of asphaltene from Soya Koishi coal by CO + H $_2$ O and H $_2$ reduction at 400°C

FREE RADICAL CHEMISTRY OF COAL LIQUEFACTION. L. W. Vernon. Exxon Research and Engineering Company, P. O. Box 4255, Baytown, Texas, 77520.

In the direct hydrogenation of coal both donor hydrogen and molecular hydrogen play important roles. This report describes some studies which were made on a number of model structures thought to be present in coal, in order to obtain a better understanding of the function of these two hydrogen forms in the chemistry of coal liquefaction. When dibenzyl is pyrolyzed at 450°C, the products produced depend upon the hydrogen environment. In the absence of an external source of hydrogen the major products are toluene and stilbene. In the presence of a donor solvent such as tetralin the only major product is toluene. However, when the pyrolysis is carried out in the presence of molecular hydrogen, the major products are toluene, benzene and ethylbenzene. The product distribution is a function of hydrogen pressure. A simple reaction mechanism is proposed which is consistent with all these results. In this reaction scheme the initial reaction is the thermal cracking of the β bond to form benzyl radicals. The benzyl radical can be stabilized by abstraction of hydrogen from the donor solvent or from dibenzyl. With molecular hydrogen the stabilization reaction produces a hydrogen atom. The hydrogen atom can then promote the cracking of the α bond in dibenzyl to form benzene and ethylbenzene. Experiments with diphenyl give further evidence for the presence of hydrogen atoms in these systems.

PERICYCLIC PATHWAYS IN THE MECHANISM OF COAL LIQUEFACTION

P.S. Virk, D.H. Bass, C.P. Eppig, and D.J. Ekpenyong

Department of Chemical Engineering
Massachusetts Institute of Technology
Cambridge, Massachusetts 02139

1. INTRODUCTION

The object of this paper is to draw attention to the possible importance of concerted molecular reactions, of the type termed pericyclic by Woodward and Hoffman (1), in the mechanism of coal liquefaction.

In outline of what follows we will begin by brief reference to previous work on coal liquefaction. The present approach will then be motivated from considerations of coal structure and hydrogen-donor activity. A theoretical section follows in the form of a pericyclic hypothesis for the coal liquefaction mechanism, with focus on the hydrogen transfer step. Experiments suggested by the theory are then discussed, with presentation of preliminary results for hydrogen transfer among model substrates as well as for the liquefaction of an Illinois No. 6 coal to hexane-, benzene-, and pyridine-solubles by selected hydrogen donors.

Previous literature on coal liquefaction is voluminous (2). Molecular hydrogen at elevated pressures is effective (3) but more recent work has employed hydrogen donor 'solvents', such as tetralin (4), which are capable of liquefying coal at relatively milder conditions. Donor effectiveness is strongly dependent upon chemical structure. Thus, among hydrocarbons, several hydroaromatic compounds related to tetralin  are known to be effective (5,6,7,8), while the corresponding fully aromatic  or fully hydrogenated  compounds are relatively ineffective (7,9). Further, among alcohols, isopropanol HO- and o-cyclohexyl phenol HO- are effective donors (7) whereas t-butanol HO- is not (10). These observations have been theoretically attributed (e.g. 2,9) to a free-radical mechanism according to which, during liquefaction, certain weak bonds break within the coal substrate, forming radical fragments which abstract hydrogen atoms from the donor, thereby becoming stable compounds of lower molecular weight than the original coal. According to this free-radical mechanism, therefore, donor effectiveness is related to the availability of abstractable hydrogen atoms, and this notion seems to have won general acceptance in the literature because it rationalizes the effectiveness of tetralin, which possesses benzylic hydrogen atoms, relative to naphthalene and decalin, which do not. However, the foregoing mechanism is less than satisfactory because indane , which has just as many benzylic hydrogens as tetralin, is relatively ineffective (7) as a donor. Also, the activity of the alcohol donors, like isopropanol, would have to involve abstraction of hydrogen atoms bonded either to oxygen or to an sp³-hybridized carbon; this seems unlikely because both of these bonds are relatively strong compared to any that the hydrogen might form with a coal fragment radical.

The present approach to the coal liquefaction mechanism evolved from contemporary knowledge of coal structure (e.g. 11,12,13), which emphasizes the existence of hetero-atom-containing hydroaromatic structures comprising 2- to 4-ring fused aromatic nuclei joined by short methylene bridges. From this it is apparent that sigma bonds between sp³-hybridized atoms in coal are seldom more than one bond removed from either a pi-electron system or a hetero-atom containing substituent. Such a molecular topology is favorable for pericyclic reactions, which are most prone to occur on skeletons with proximal pi- and sigma-bonds activated by substituents. We therefore hypothesize that the overall interaction between the coal substrate and hydrogen donor, which eventually leads to liquefaction, involves a sequence of concerted, pericyclic steps. (Appropriate steps will be detailed in the next

section.) The novelty of this approach is twofold; first, the mechanistic concept is essentially different from any that has hitherto been proposed in coal-related literature and second, it lends itself to quantitative tests and predictions since the pericyclic reactions envisioned must obey the Woodward-Hoffman rules (1) for the conservation of orbital symmetry. It should also be pointed out that if the present approach proves valid, then it will have the engineering significance that the large volume of recently developed pericyclic reaction theory (14, 15,16) could be applied to the practical problem of defining and improving actual coal liquefaction processes.

2. THEORY

In delineating a coal liquefaction mechanism we distinguish three basic steps, namely rearrangements, hydrogen-transfer, and fragmentation, all of which are hypothesized to occur via thermally-allowed pericyclic reactions. Some typical reactions appropriate for each step are indicated below using Woodward-Hoffman (1) terminology:

Rearrangements: Sigmatropic shifts, electrocyclic reactions
 Hydrogen-Transfer: Group-transfers
 Fragmentation: Group-transfers, retro-ene, cyclo-reversions.

An illustration of how the overall pericyclic mechanism might apply to the decomposition of 1,2 diphenylethane, a model substrate, in the presence of Δ^1 -dihydronaphthalene, a model hydrogen-donor, has recently been given (17). In the present work, attention is focussed on the hydrogen-transfer step.

Hypothesis.

The transfer of hydrogen from donors to the coal substrate during liquefaction occurs by concerted pericyclic reactions of the type termed 'group transfers' by Woodward and Hoffman (1).

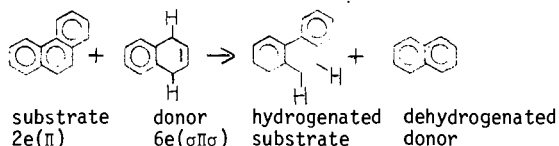
Consequences.

(A) Allowedness.

The Woodward-Hoffman rules (1) state that: A ground state pericyclic change is symmetry allowed when the total number of $(4q + 2)$ suprafacial and $(4r)$ antarafacial components is odd".

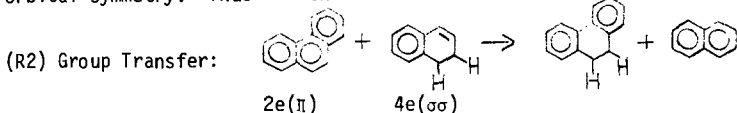
To illustrate how this applies in the present circumstances we consider a possible group transfer reaction between Δ^2 dihydronaphthalene, , a hydrogen donor, and phenanthrene, , a substrate (hydrogen acceptor) which models a polynuclear aromatic moiety commonly found in coal. In the overall group transfer reaction:

(R1) Group Transfer:

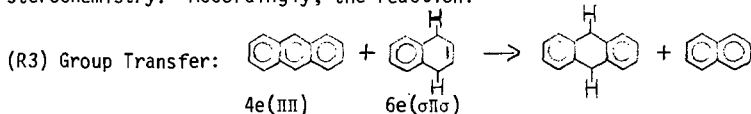


hydrogen is transferred from Δ^2 -dialin to the phenanthrene, producing 9,10 dihydrophenanthrene and naphthalene; this reaction is slightly exothermic, with $\Delta H_p^\circ \sim -8$ kcal as written. The electronic components involved are $2e(\pi)$ on the substrate and $6e(\sigma\pi\sigma)$ on the donor and from the Woodward-Hoffman rules it can be seen that the reaction will be thermally forbidden in either the supra-supra stereochemistry (which is sterically most favorable) or the antara-antara stereochemistry (sterically the most unfavorable) but will be thermally allowed in either the antara-supra or supra-antara modes, both of the latter being possible, but sterically difficult, stereochemistries. A reaction profile for (R1) is sketched in Figure 1, showing energy versus reaction coordinate as well as transition state stereochemistry for both the forbidden supra-supra and the allowed antara-supra modes. We note

next that changing the donor from Δ^2 -dialin  to Δ^1 -dialin , changes the donor electronically from a $6e(\sigma\pi\sigma)$ component to a $4e(\sigma\sigma)$ component, of contrary orbital symmetry. Thus for the overall reaction:



the supra-supra (and antara-antara) modes will be thermally allowed while the antara-supra (and supra-antara) modes are forbidden. The practical upshot of this is that the chemically very similar dialin isomers should exhibit strikingly different reactivities in concerted group transfers with a given substrate, on account of their opposite orbital symmetries. Note that no reasonable free-radical mechanism could predict profound differences in the donor capabilities of these dialin isomers. Orbital symmetry arguments can also be extended to differences in the substrates. Thus anthracene  is a $4e(\pi\pi)$ component, of symmetry opposite to that of phenanthrene , which is a $2e(\pi)$ component; therefore, with a given donor, such as Δ^2 -dialin , group transfers that are symmetry-forbidden with phenanthrene will be symmetry-allowed with anthracene in the same stereochemistry. Accordingly, the reaction:



is a $4e(\pi\pi) + 6e(\sigma\pi\sigma)$ group transfer, which is thermally-allowed in the supra-supra stereochemistry whereas the analogous reaction (R1) with phenanthrene was forbidden.

Generalization of the preceding suggests that there exist two basic classes of donors (and acceptors), of opposite orbital symmetries, which will respectively engage in group transfer reactions either as $(4n+2)$ electron components or as $(4n)$ electron components. Donors with $(4n+2)e$ will, in general, transfer hydrogen to $(4m+2)e$ acceptors, the most favorable supra-supra stereochemistry being presumed in each case. Among the $(4n+2)e$ class of hydrogen donors, the first ($n=0$) member is molecular hydrogen and the second ($n=1$) member is the but-2-ene moiety, while among the $(4n)e$ class of donors, the first ($n=1$) member is the ethane moiety, the second ($n=2$) the hexa-2,4-diene moiety. Among hydrogen acceptors, the $(4m+2)e$ class has the ethylene and hexa-1,3,5-triene moieties as its first two members, while the $(4m)e$ class of acceptors possesses the buta-1,3-diene and octa-1,3,5,7-tetraene moieties as its first two members. Each of the foregoing series can be continued straightforwardly for $n>2$.

Interestingly, the nature of allowed donor-acceptor interactions suggests that donor class will be conserved in any hydrogen transfer sequence. Thus a $(4n+2)e$ donor, say, will transfer hydrogen to a $(4m)e$ acceptor, and the latter, upon accepting the hydrogen, will evidently become a $(4m+2)e$ donor, of the same class as the original donor.

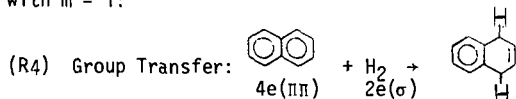
The donor and acceptor classes illustrated with hydrocarbons can be directly extended to include hetero-atoms. For example, the alcohol moiety  would be a $4e$ donor, of the same orbital symmetry as the ethane moiety . Similarly the carbonyl moiety $O=$ would be a $2e$ acceptor, analogous to an ethylene moiety $=$ in terms of orbital symmetry. Thus hydrogen transfer reactions of molecules with hetero-atoms should have the same allowedness as reactions of their iso-electronic hydrocarbon analogues.

(B) Reactivity

The actual rates of thermally-allowed pericyclic reactions vary vastly, and

frontier-orbital theory (14,15,16) has proven to be the primary basis for quantitative understanding and correlation of the factors responsible. It is therefore of interest to find the dominant frontier orbital interactions for the group transfer reactions hypothesized to occur.

The HOMO (highest occupied molecular orbital) and LUMO (lowest unoccupied MO) levels for hydrogen donors used in coal liquefaction are not yet well known, but the principles involved can be illustrated with the group transfer reaction between molecular hydrogen, a $(4n+2)e$ donor with $n = 0$, and naphthalene, a $(4m)e$ acceptor with $m = 1$:



An approximate frontier orbital (FO) interaction diagram for this system is presented in Figure 2. This shows that the dominant FO interaction, i.e., that with the lowest energy gap, is between HOMO(H_2)-LUMO (); details of the interaction are given towards the bottom of the figure showing the respective phases and coefficients involved.

The preceding indications regarding the dominant FO interaction in hydrogen-transfer reactions suggests that they would be facilitated by a reduction in the HOMO (hydrogen donor)-LUMO (hydrogen acceptor) energy separation. Thus donor effectiveness should be enhanced by increasing the donor HOMO energy, e.g., by electron-releasing or conjugative substitution, whereas acceptor effectiveness should be enhanced by lowering the acceptor LUMO level, e.g. by electron-withdrawing or conjugative substitution, or by complexation with Lewis acids. As a practical example relevant to our experiments, we should expect Δ^2 -dialin to be a more effective $(4n+2)e$ type of hydrogen donor than tetralin because vinylic substitution in the former should raise the level of the hydrogen-containing HOMO. For the same reason, Δ^1 -dialin should also be a more effective $(4n)e$ type of donor than tetralin . Note that the Δ^1 - and Δ^2 -dialins have the opposite orbital symmetries; their reactivities cannot therefore be meaningfully compared, inasmuch as their reactions with a common acceptor cannot both be allowed.

3. EXPERIMENTS

(A) Model Compounds

From the theoretical discussion it follows that the present hypothesis for the hydrogen transfer mechanism can be tested by a study of reactions between hydrogen donors and acceptors of opposite orbital symmetries. Our experimental grid is shown in Table 1.1. The coal substrate was modelled by anthracene, a $(4m)e$ acceptor, and by phenanthrene, a $(4m+2)e$ acceptor; both of these aromatic C14 moieties exist in coal and are found in coal-derived liquids. The hydrogen donor solvent was modelled by a number of cyclic C10 compounds derived from naphthalene by hydrogenation. Among these, the Δ^1 - and Δ^2 -dialin isomers were of principal interest, being respectively hydrogen-donors of the $(4n+2)e$ and $(4n)e$ classes; the tetralin and decalin served as control solvents, the former being very commonly used in coal liquefaction experiments. For the 2×2 matrix of possible hydrogen-transfer reactions between the model C14 substrates and C10 dialin solvents, the Woodward-Hoffman rules predict that reaction in the favorable supra-supra stereochemistry should be thermally-allowed for (Δ^1 -dialin + phenanthrene) and (Δ^2 -dialin + anthracene) and thermally-forbidden for (Δ^1 -dialin + anthracene) and (Δ^2 -dialin + phenanthrene). These predictions are shown in Table 1.1 with \checkmark denoting the allowed and x the forbidden reactions.

The experiments were conducted batchwise in small stainless-steel pipe-bombs immersed in a molten-salt bath that was maintained at a desired, constant temperature. Pipe-bomb heat-up and quench times, on the order of 1 min each, were

negligible compared with reaction times, which were on the order of 1 hr. The reagents used were obtained commercially; all were of purity $\geq 98\%$ except for the Δ^2 -dialin which had a composition of (anthracene, phenanthrene, tetralin, decalin) = (7, 9, 20, 64) mol%. The proportions of substrate to solvent were maintained constant, with the C14 substrates as limiting reactants in all cases. The extent of reaction was measured by proton-NMR spectroscopy on samples of the whole reaction batch, as well as of each of the C10 and C14 fractions separated by vacuum distillation and liquid chromatography.

Experimental results are shown in Table 1.2, which quotes the observed percentage conversion of each of the model C14 substrates to their di-hydro derivatives by each of the model C10 solvents. Consider first the column for the anthracene substrate, showing its conversion to 9,10 dihydroanthracene after 2 hr at 300 C in various solvents. The conversion by tetralin (58%), is an order of magnitude greater than that by decalin (5%), in striking accord with the theoretical predictions according to which the reaction with tetralin was allowed while that with decalin was forbidden. Note too that conversions with the control solvents phenanthrene (3%) and anthracene (no reaction) were less than those with the test solvents, verifying that the latter were indeed the more active. Reactions with phenanthrene substrate required rather more severe conditions, namely 2 hr at 400 C, than anthracene. While the lower reactivity of phenanthrene relative to anthracene is generally well known, in the present context it can directly be attributed to the phenanthrene possessing the higher energy LUMO. The conversions observed, tetralin (16%) > decalin (10%), are in accord with theoretical predictions, and appreciably exceed the conversions obtained with the control solvents phenanthrene (2%) and anthracene (no reaction). It is interesting that the observed selectivity of hydrogen-transfer from the Δ^1 - and Δ^2 -dialins to phenanthrene, respectively (0.6/1), is not as great as that to anthracene, respectively (12/1). Possible reasons for this are first that whereas anthracene is essentially always constrained to interact with supra-stereochemistry at its 9,10 positions, the phenanthrene structure admits a possible antarafacial interaction across its 9,10 positions and this latter might have permitted a thermally-allowed (antara-supra) hydrogen-transfer from Δ^2 -dialin. Second, the Δ^2 -dialin used contained some Δ^1 -dialin impurity, which could not contribute to anthracene conversion (forbidden) whereas it might have contributed to the phenanthrene conversion (allowed); third, the dialins have a tendency to disproportionate, to naphthalene and tetralin, at elevated temperatures and this might have influenced the results for phenanthrene, which were at the higher temperature.

In summary, the Δ^1 - and Δ^2 -dialin isomers have been shown to be appreciably more active than tetralin (and decalin) in transferring hydrogen to anthracene and phenanthrene. The observed selectivity of this hydrogen transfer is in accord with the Woodward-Hoffman rules for group transfer reactions, anthracene conversions being in the ratio (tetralin / decalin) = 12/1 \gg 1 while phenanthrene conversions are in the ratio (tetralin / decalin) = 0.6/1 < 1. The quantitative differences in the selectivities observed with anthracene and phenanthrene are being further explored.

(B) Coal Conversion

The dialin donor solvents were also used directly in coal liquefaction studies. Inasmuch as details of coal structure are unknown, the present theory can only be tested in a qualitative way, as follows. First, if the liquefaction of coal occurs under kinetic control with hydrogen-transfer from the donor solvent involved in the rate-determining step, then we should expect the dialin donors to be more effective than the control solvent tetralin (and also decalin). This is suggested by the theory because the dialins possess higher energy HOMOs than tetralin and according to the frontier-orbital analysis given previously, the hydrogen-transfer reactions of the dialins should therefore be kinetically favored relative to those of tetralin. Second, according to the present theory, donor symmetry is preserved during hydrogen transfer, i.e., a donor of a given class is capable only of interaction with acceptors of the complementary class. Now since the coal substrate likely contains hydrogen acceptors of both (4m)e and (4m+2)e classes, a

mixture of solvents containing donors of both (4n+2)e and (4n)e classes should be more effective in hydrogen transfer than a single solvent of either class which could interact with only one of the two possible classes in coal. Thus, in principle, for each coal there should exist an 'optimal' solvent which contains hydrogen donors of opposite symmetries in proportions that are matched to the proportions of the complementary hydrogen acceptors in the coal. For these reasons our theory suggests that a mixture of Δ^1 - and Δ^2 -dialins should be a better donor solvent than either the Δ^1 - or the Δ^2 -dialin alone, with the further indication that there may exist an optimal mixture composition that is characteristic of a given coal.

Liquefaction experiments were performed on a sample (18) of Illinois No. 6 coal, from Sesser, Illinois. Proximate and elemental analyses of this high volatile A bituminous coal are given in Table 2. The coal, of particle size 600-1200 microns (32x16 mesh), was dried at 110 C in a nitrogen blanketed oven prior to liquefaction. A solvent to coal weight ratio of 2.0 was used in all experiments, which were conducted in tubing bomb reactors that were immersed in a constant-temperature bath for the desired time while being rocked to agitate the reactor contents. At the end of each experiment, the reactors were quenched and their contents analyzed to ascertain the amounts of each of hexane-, benzene-, and pyridine-solubles (plus gas) produced from the original coal. The procedure used for all analyses is described for the pyridine-solubles (plus gas). First the reactor contents were extracted with pyridine and the residue dried on a pre-weighed ashless filter paper to provide the gravimetric conversion to pyridine-solubles, defined as $100(1-(\text{daf residue}/\text{daf coal}))$. Second, the residue was ashed in a furnace for 3 hours at 800 C, yielding the ash-balance conversion to pyridine solubles, defined as $100(1-(a/A))/(1-(a/100))$ where A and a were respectively the weight percentages of ash in the residue and in the original coal. The conversions obtained from each of the two methods normally agreed to within ± 2 weight percent and were averaged to provide final values.

Results showing the effectiveness of the Δ^1 - and Δ^2 -dialins in coal liquefaction relative to control solvents, naphthalene, decalin, and tetralin, are presented in Tables 3.1 and 3.2. In both these tables, each row provides the conversion of the coal sample to each of hexane-, benzene-, and pyridine-solubles (plus gases) by the indicated solvent. Table 3.1 contains data derived at a temperature of 400 C and a reaction time of 0.5 hr. Among the control solvents, it can be seen that the naphthalene and decalin give similar results and are both much less effective than tetralin, the yields of each of hexane-, benzene-, and pyridine-solubles obtained with the former being roughly half of those obtained with the latter. The greater effectiveness of tetralin as a donor-solvent relative to naphthalene and decalin is in agreement with previous studies (2,7,9). Further, the absolute conversion to benzene-solubles (plus gases) obtained with tetralin in the present work, namely 44 weight percent, compares favorably with the values of 36 and 47 weight percent reported by Neavel (9) for comparable HVA and HVB bituminous coals at similar reaction conditions. The accord between the control solvent liquefaction data shown in Table 3.1 and the literature permits us to place some confidence in the present experimental procedures. Turning now to the dialin donors, for which coal liquefaction data have not hitherto been reported, it can be seen from Table 3.1 that, relative to tetralin, the Δ^1 -dialin yielded appreciably more hexane-solubles, somewhat less benzene-solubles, and approximately the same pyridine-solubles. Also relative to tetralin, the Δ^2 -dialin yielded appreciably more hexane-solubles, approximately the same benzene-solubles, and appreciably more pyridine-solubles. It is apparent that the dialins, especially the Δ^2 -dialin, were more effective donor solvents than tetralin in liquefaction of the present coal sample. While no precise chemical interpretation can be attached to the quantities used to measure liquefaction, the pyridine-solubles roughly represent the extent to which the coal substrate is converted, whereas the hexane-solubles are a measure of the final, oil, product (the benzene-solubles represent an intermediate). Accordingly, from Table 3.1, the Δ^2 -dialin increased

the coal conversion by 16 percent and product oil formation by 37 percent relative to tetralin. A few liquefaction experiments were also conducted at a temperature of 300 C and a reaction time of 0.5 hr, with results reported in Table 3.2. Of the control solvents, decalin yielded neither hexane- nor benzene-solubles, while tetralin yielded no hexane-solubles but did yield the indicated small amounts of benzene- and pyridine-solubles. The Δ^2 -dialin yielded no hexane-solubles but provided appreciable amounts of benzene- and pyridine-solubles. The conversions seen in Table 3.2 are all much lower than the corresponding conversions in Table 3.1, undoubtedly a consequence of the lower reaction temperature, 300 C versus 400 C, reaction times being equal. Finally, Table 3.2 shows that the Δ^2 -dialin solvent produced 3 times the benzene-solubles and 5 times the pyridine-solubles produced by tetralin, a striking re-inforcement of the indication from Table 3.1 that the dialins were the more effective donors.

A second series of liquefaction experiments were conducted to test the theoretical suggestion that a mixture of Δ^1 - plus Δ^2 -dialin isomers might be a more effective solvent than either one of the dialins alone. Preliminary results at 400 C and 0.5 hr reaction time, are shown in Table 4 which quotes the ratio of the conversion to each of hexane-, benzene-, and pyridine-solubles obtained with a solvent mixture containing equal amounts of Δ^1 - and Δ^2 -dialins relative to the average of the corresponding conversions obtained with each of the Δ^1 -dialin and Δ^2 -dialin solvents separately. (Generally, if P_{MX} was the conversion to say, pyridine-solubles obtained with a solvent mixture containing a fraction x of solvent 1, while p_1 and p_2 were the conversions respectively obtained with the pure solvents 1 and 2 separately, then the departure of the ratio $r_x = P_{MX}/(xp_1 + (1-x)p_2)$ from unity will evidently measure the effectiveness of the solvent mixture relative to the separate pure solvents.) In Table 4 it can be seen that the coal conversion to hexane-, benzene-, and pyridine-solubles with the dialin mixture was respectively 28, 1, and 18 percent greater than the average for the separate solvents. These results are evidently in accord with the theoretical prediction, but further work is being undertaken to seek the generality of this result and to discern an optimum solvent mixture.

4. CONCLUSIONS

At typical coal liquefaction conditions, namely temperatures from 300 to 400 C and reaction times on the order of 1 hr, hydrogen transfer from model C10 donors, the Δ^1 - and Δ^2 -dialins, to model C14 acceptors, anthracene and phenanthrene, occurs in the sense allowed by the Woodward-Hoffman rules for supra-supra group transfer reactions. Thus, in the conversion of the C14 substrates to their 9,10 dihydro derivatives the dialins exhibited a striking reversal of donor activity, the Δ^1 -dialin causing about twice as much conversion of phenanthrene but only one-tenth as much conversion of anthracene as did Δ^2 -dialin.

The dialins were also found to be more effective donor solvents than tetralin in the liquefaction of an Illinois No. 6 HVA bituminous coal. For example, at 400 C and 0.5 hr reaction time, Δ^2 -dialin yielded 16% more pyridine-solubles and 37% more hexane-solubles than tetralin; at 300 C and 0.5 hr reaction time, the Δ^2 -dialin yielded 5 times the pyridine-solubles and 3 times the benzene-solubles yielded by tetralin.

Finally, a mixture containing equal parts of Δ^1 - and Δ^2 -dialin was found to be a more effective donor solvent than either of the Δ^1 - or Δ^2 -dialins separately. At 400 C and 0.5 hr reaction time, the mixture of donors yielded 18% more pyridine-solubles and 28% more hexane-solubles than the average for the separate donors.

The preceding experiments offer preliminary support to our notion that pericyclic pathways might be intimately involved in the mechanism of coal liquefaction. More specifically, the results indicate that pericyclic group transfer reactions constitute a plausible pathway for the transfer of hydrogen from donor solvents to coal during liquefaction.

5. REFERENCES

1. Woodward, R.B., and Hoffmann, R.: "The Conservation of Orbital Symmetry," Verlag Chemie GmbH, Weinheim (1970). Pericyclic reaction terminology defined in this text is used in the present paper.
2. Whitehurst, D.D., et. al.: "Asphaltenes in Processed Coals," Annual Report EPRI-AF-480 (1977) and references therein.
3. Bergius, F.: German Patents 301,231 and 299,783 (1913).
4. Pott, A. and Broche, H., Glückauf 69 903 (1933).
5. Weller, S., Pelipetz, M.G., and Freidman, S., Ind. & Eng. Chem. 43, 1572 (1951).
6. Carlson, C.S., Langer, A.W., Stewart, J., and R.M. Hill, Ind. & Eng. Chem. 50 (7) 1067 (1958).
7. Curran, G.P., Struck, R.T., and Gorin, E., Ind. & Eng. Chem. Proc. Des. & Dev. 6 (2) 166 (1967).
8. Ruberto, R.G., Cronaner, D.C., Jewell, D.M., and Seshadri, K.S., Fuel 56 25 (1977).
9. Neavel, R.C., Fuel 55 161 (1976).
10. Ross, D.S., and Blessing, J.E., ACS Div. of Fuel Chem. Preprints 22 (2) 208 (1977).
11. Given, P.M., Fuel, 39 147 (1960) and 40 427 (1961).
12. Wiser, W.H., in Wolk, R.M. et. al. ACS Div. of Fuel Chem. Preprints 20 (2) 116 (1975).
13. Wender, I., ACS Div. of Fuel Chem. Preprints 20 (4) 16 (1975).
14. Fujimoto, M. and Fukui, D.: "Intermolecular Interactions and Chemical Reactivity," pp 23-54 in "Chemical Reactivity and Reaction Paths," G. Klopman, Ed., Wiley-Interscience, New York (1974).
15. Klopman, G.: "The Generalized Perturbation Theory of Chemical Reactivity and Its Applications," pp 55-166 in "Chemical Reactivity and Reaction Paths", G. Klopman, Ed., Wiley-Interscience, New York (1974).
16. Houk, K.N.: "Application of Frontier Molecular Orbital Theory to Pericyclic Reactions," pp 182-272 in "Pericyclic Reactions", Volume II, A.P. Marchand & R.E. Lehr, Eds., Academic Press, New York (1977).
17. Virk, P.S.: "Pericyclic Pathways in 1,2-Diphenylethane Decomposition," Fuel, 58 000 (1979) (Accepted for publication).
18. Our coal sample was obtained from Inland Steel Company Research Laboratories, Chicago, Ill. through the courtesy of Professor J.B. Howard of the Department of Chemical Engineering, M.I.T., Cambridge, Mass.

ACKNOWLEDGEMENT

This work was supported by the US DOE through the Energy Laboratory at M.I.T.

TABLE 1.1 Model Compound Experimental Grid

| Coal Model C14 |  |  |
|---|---|---|
| Solvent C10 | Supra-Supra Allowedness | |
|  | | |
|  | | |
|  | x | ✓ |
|  | ✓ | x |

TABLE 1.2 Model Compound Experimental Results

| Reaction Conditions | Temp = 300 C Time = 2 Hr | Temp = 400 C Time = 2 Hr |
|---|---|---|
| Coal Model C14 |  |  |
| Solvent C10 | % conversion to 9,10-dihydro-derivative | |
|  | 0 | 0 |
|  | 3 | 2 |
|  | 5 | 16 |
|  | 58 | 10 |

TABLE 2. Coal Sample Characterization

| | | | | | | |
|---------------------|--------------------------------------|------|-----|-------|-----|-------|
| Origin: | Illinois No. 6 from Sesser, Illinois | | | | | |
| Rank: | Bituminous, High Volatile A | | | | | |
| Proximate Analysis: | VM | FC | Ash | Total | | |
| (wt% dry basis) | 37.3 | 56.7 | 6.0 | 100.0 | | |
| Elemental Analysis: | H | C | N | O | S | Total |
| (wt% daf) | 5.4 | 82.0 | 1.6 | 10.2 | 0.8 | 100.0 |

TABLE 3. Coal Liquefaction Results

1. Temperature = 400 C : Reaction Time = 0.5 hr

| Solvent | Coal Conversions to | | |
|--|---------------------|--------------------------------------|-----------|
| | Hexane- Solubles | Benzene- Solubles (plus gas), wt% | Pyridine- |
| Naphthalene  | 8.0 | - | 29.7 |
| Decalin  | 10.8 | 22.5±2.6 | 32.5 |
| Tetralin  | 20.9 | 43.9±1.4 | 70.2 |
| Δ^1 -Dialin  | 27.0 | 39.6±1.9 | 71.3 |
| Δ^2 -Dialin  | 28.6 | 44.9±1.5 | 81.4 |

2. Temperature = 300 C : Reaction Time = 0.5 hr

| | | | |
|--|---|---------|------|
| Decalin  | 0 | 0 | - |
| Tetralin  | 0 | 2.4±0.6 | 3.7 |
| Δ^2 -Dialin  | 0 | 9.0±1.5 | 19.3 |

TABLE 4. Coal Liquefaction by Mixed Dialin Solvent

Temperature = 400 C : Reaction Time = 0.5 hr

Solvent: 1:1 mixture of Δ^1 - and Δ^2 -dialins

| Conversion Ratio r | Hexane- | Benzene- | Pyridine- |
|-----------------------|----------|----------|-----------|
| | Solubles | Solubles | Solubles |
| | 1.28 | 1.01 | 1.18 |

Note: $r = p_m / 0.5(p_1 + p_2)$ where p_m , p_1 , p_2 are respectively the wt% conversions obtained with mixed solvent, Δ^1 -dialin and Δ^2 -dialin.

Fig. 2. FRONTIER ORBITAL ENERGY LEVELS FOR THE REACTION OF H_2 AND NAPHTHALENE

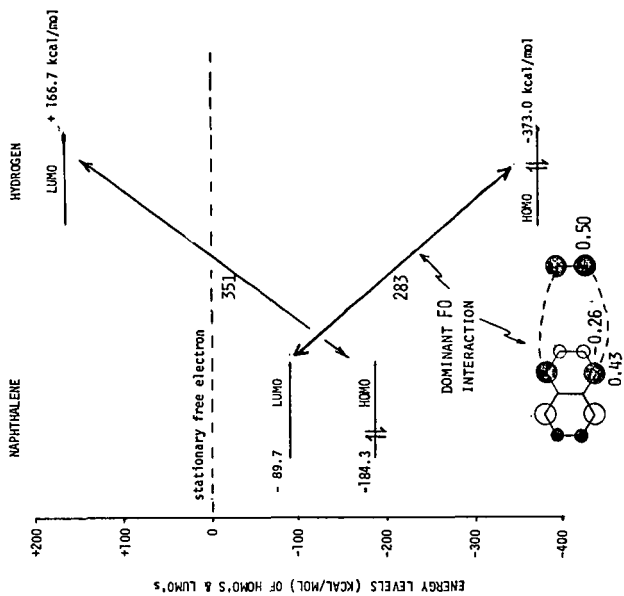
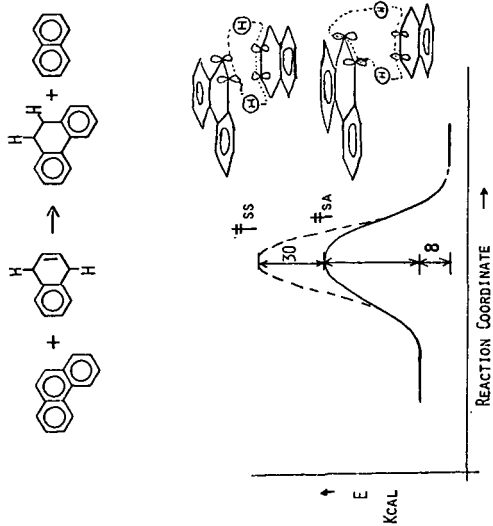


Fig. 1. SCHEMATIC REACTION PROFILE FOR GROUP TRANSFER



AN ISOTOPIC STUDY OF THE ROLE OF A DONOR SOLVENT IN COAL LIQUEFACTION

Joseph J. Ratto

Rockwell International, Corporate Science Center
1049 Camino Dos Rios, Thousand Oaks, California 91360

Laszlo A. Heredy, Raymund P. Skowronski

Rockwell International, Energy Systems Group
8900 De Soto Avenue, Canoga Park, California 91304

INTRODUCTION

For a number of years, laboratory and pilot-scale studies have been conducted in the area of coal liquefaction with hydrogen donor solvents⁽¹⁻⁴⁾. The kinetics of these processes and the composition of the coal products have been studied; however, the mechanism of hydrogen transfer from donor solvent to coal is still not well understood.

Recently we reported on a deuterium tracer method for the investigation of coal hydrogenation⁽⁵⁾. The work involved the use of deuterium gas as a tracer to follow the incorporation of hydrogen into coal during liquefaction. No donor solvent or catalyst was added to the coal in those experiments. Using an isotopic tracer, it was possible to follow the reaction mechanism more closely and to determine the fate of the reactants, without altering the course of the reaction. Two significant results were obtained in that investigation. Deuterium incorporation in solvent-fractionated coal products was found to vary with product fraction and structural type. Deuterium uptake increased from the most soluble oil fraction to the insoluble residue. In each of the three soluble fractions as determined by NMR spectrometry, selective incorporation of deuterium was found in the α -alkyl functional region.

The present work examines the donor solvent process during coal liquefaction. A deuterium labeled donor solvent (tetralin- d_{12}) was prepared to study the chemistry of the solvent during liquefaction. In a separate experiment, naphthalene- d_8 was used to investigate the chemistry of hydrogen transfer between coal and a solvent. In each experiment, the coal products and spent solvent were analyzed for total deuterium content and for deuterium content by structural position.

EXPERIMENTAL

Materials and Apparatus

High volatile A bituminous coal (81.8% C, 5.1% H, dmmf basis), -200 mesh, from the Loveridge Mine, Pittsburgh Seam, was dried at 115°C for 4 hours before use in each experiment. Technical grade deuterium (>98 atom % deuterium and total hydrocarbons <1 ppm) and high-purity nitrogen were utilized. Naphthalene- d_8 was purchased from the Aldrich Chemical Co., and tetralin- d_{12} was prepared in this laboratory⁽⁶⁾. The isotopic purity of tetralin- d_{12} and naphthalene- d_8 were determined by NMR spectrometry. Batch experiments were performed in a 1-liter stirred autoclave (Autoclave Engineers) and a 0.25-liter rocking autoclave (Parr).

Experimental Procedure

In a typical liquefaction experiment, the autoclave was charged at room temperature with tetralin- d_{12} , coal and deuterium gas. The autoclave was heated to 400°C, the reaction was conducted for 1 hour, then the autoclave was cooled to room temperature.

Gaseous products were removed for analysis by GC-MS. The reaction products were distilled at reduced pressure to remove spent donor solvent mixture, and the remaining coal products were solvent-fractionated. The naphthalene extraction experiment was carried out under similar conditions except that nitrogen cover gas was used instead of deuterium.

Product Analyses

The spent solvent mixture was distilled from the coal products, separated by gas chromatography (GC) and analyzed by NMR spectrometry. The solid and liquid coal products were solvent-fractionated into oil (hexane soluble, HS), asphaltene (benzene soluble, BS), benzene-methanol soluble (BMS) and insoluble residue (benzene-methanol insoluble, BMI) fractions. The liquefaction products were solvent-fractionated using three ACS reagent grade solvents: hexane isomer mixture, benzene and methanol. Samples of fractions were combusted, and the resulting water was analyzed by mass spectrometry (Shrader Analytical Labs) to determine the deuterium and protium atom % distribution. Elemental analysis of product fractions was conducted by Galbraith Laboratories.

Proton and deuterium NMR spectra of soluble fractions and spent solvent mixtures were obtained using a JEOL FX60Q FT NMR Spectrometer. A flip angle of 45° was used which corresponds to $14 \mu\text{s}$ for proton and $75 \mu\text{s}$ for deuterium NMR spectra. The pulse repetition times were 6.0 and 9.0 s, respectively. Chloroform-d was used as the proton NMR solvent, and chloroform was used as the deuterium NMR solvent.

RESULTS AND DISCUSSION

The results of two donor solvent hydrogenation experiments and a coal extraction experiment are presented in this paper. The experimental conditions and product yields of the two donor solvent liquefaction experiments (E10 and E19) are summarized in Table 1. These two experiments were conducted under similar conditions except for differences in the type of autoclave and applied pressure. The experiments were designed to investigate hydrogen transfer from a donor solvent to coal. The atom % ^2H values are also shown in Table 1. While in previous hydrogenation experiments made without the use of a donor solvent⁽⁵⁾, it was found that deuterium incorporation increased from the most soluble oil fraction to the insoluble residue, no similar trend was observed in these experiments.

The solvent-fractionated coal products from E10 and E19 were analyzed by proton and deuterium NMR spectrometry. Table 2 lists the integration percentages of the three soluble fractions by functional region. The selective incorporation of deuterium by functional region is demonstrated by taking the ratio of deuterium incorporation over protium incorporation. For example, the E10 HS ^2H percentage of 7% listed in Table 2 is the $^2\text{H}_x/^2\text{H}$ ratio, and the E10 HS ^1H percentage of 11% is the $^1\text{H}_x/^1\text{H}$ ratio. The value 7% represents the number of deuterium atoms in that functional region normalized to a ^2H value of 100%. The $(^2\text{H}_x/^2\text{H})/(^1\text{H}_x/^1\text{H})$ ratios are shown in Table 3. A ratio of unity means that the normalized fraction of protium and deuterium contained in that functional region are equal. Since the ratio is much greater than unity in all of the α -alkyl regions, indications are that in liquefaction experiments conducted with a donor solvent, as well as in liquefaction experiments conducted without a donor solvent or catalyst as was shown in our previous presentation⁽⁵⁾, significant specific incorporation occurs in the α -alkyl position.

One can utilize the isotopic composition and deuterium incorporation by structural position of the spent donor solvent to develop a mechanistic pathway of hydrogen transfer. Attention was focused on two major processes which can occur simultaneously in donor solvent liquefaction. Tetralin- d_{12} can donate four of its transferable deuterium atoms to coal with the formation of naphthalene- d_8 ; tetralin- d_{12} can participate in isotopic exchange of its deuterium with protium in the coal. It is worthwhile to examine the reaction pathways of the donor solvent to assess the importance of each process.

Figure 1 is a summary of the most probable chemical reactions of the donor solvent, tetralin, under liquefaction conditions. Tetralin can be hydrogenated to form decalins, dehydrogenated to form naphthalene, or rearranged to form methylindan. All of the compounds shown in Figure 1 except methylindan were detected in the spent solvent from E10. Figure 2 is the proton NMR spectrum of the spent solvent. Tetralin, naphthalene, and decalin absorption peaks are evident.

In a hydrogen donor reaction, the liquefaction process is generally assumed to occur with the formation of solvent radical intermediates which can accept or donate hydrogen atoms; therefore, in Figure 1 each reversible reaction can be divided into a number of stepwise additions or removals of hydrogen radicals. The initial stage of the dehydrogenation of tetralin to naphthalene is expanded in Figure 3 to include each hydrogen atom transfer pathway. The dihydronaphthalenes are shown as possible intermediates in the formation of naphthalene. The pathway of donation of hydrogen by tetralin requires the abstraction of α - and β -hydrogens by coal or gas phase products, and Reactions 1 and 2 in Figure 2 show the main pathways of hydrogen abstraction. The quantities of hydrogen in the spent solvent can be subtracted from the hydrogen in the starting solvent to determine the net donation.

Table 4 summarizes the composition of the donor solvent before and after completion of E10 and E19. These data have been examined to formulate a mechanism of isotopic exchange. The distilled spent solvent was separated by GC, and the isotopic composition and incorporation by structural position was determined by NMR spectrometry with an internal quantitative standard. In E10, the extent of hydrogen donation to the coal can be calculated from the formation of naphthalene corrected by the amount of hydrogen used in the formation of decalins (Table 4). It is also shown in Table 4 that in addition to the donor mechanism, considerable isotopic exchange occurred between the tetralin- d_{12} and coal; 17.2 atom % of the deuterium in the solvent was exchanged. Tetralin contains four hydrogen atoms in each of three chemically different positions: aromatic (H_{ar}), alpha (H_{α}) and beta (H_{β}) hydrogens. Of the 17.2 atom % replaced by protium, 66% of the protium resided in the H_{α} , 23% in H_{β} and 11% in H_{ar} position. E19 shows a similar effect. Specific protium incorporation occurs in the H_{α} position of tetralin- d_{12} , and this indicates the predominant pathway of hydrogen exchange is Reaction 1. The fact that the α -radical has greater resonance stabilization than the β -radical also supports the choice of Reaction 1 as the predominant pathway. It should be noted that the β -radical can interconvert to the α -radical by a 1,2-hydrogen shift.

An evaluation of the data on the formation of naphthalene- d_8 from tetralin- d_{12} (donation) and protium incorporation into tetralin- d_{12} (exchange) showed that in experiment E10 donation took place to approximately the same extent as did exchange. According to the indicated mechanism (Figure 3) not only hydrogen donation but also hydrogen exchange via the α -radical of the tetralin can have a significant role in stabilizing the primary free radical structures which form by thermal decomposition of the coal.

Table 1 includes the data of an extraction experiment (E21) conducted with naphthalene- d_8 and nitrogen as cover gas. This experiment investigated the transfer of hydrogen taking place during a solvent extraction experiment in the absence of a donor solvent. In the experiment, coal and naphthalene- d_8 with a cover gas of nitrogen were heated at 380°C for 1 hour. The solvent and coal products were analyzed for deuterium loss and incorporation, respectively. The isotopic composition of the starting and spent naphthalene- d_8 is shown in Table 5. The starting naphthalene lost 4 atom % 2H , and the combined coal products gained 11 atom % 2H . It is interesting to note that the H_{α} position of naphthalene exchanged more of its deuterium with the coal than the H_{β} position. This experiment will be discussed in terms of the chemistry of hydrogen transfer between solvent and coal.

In summary, coal hydrogenation and extraction experiments conducted with deuterated tetralin and naphthalene have been discussed. With the use of the deuterium tracer

method, deuterium incorporation was found in specific structural positions of the solvent and soluble coal products. The method has provided insight into the mechanism of hydrogen transfer.

ACKNOWLEDGMENT

This research was supported by the U.S. Department of Energy under Contract EF-77-C-01-2781.

REFERENCES

1. G. R. Pastor, J. M. Angelovich and H. F. Silver, *Ind. Eng. Chem., Process Des. and Develop.* 9 (4) 609 (1970).
2. N. P. Cochran, *Scientific American* 234 (5) 24 (1976).
3. K. R. Brower, *Fuel* 56 (3) 245 (1977).
4. I. Schwager and T. F. Yen, *Fuel* 57 (2) (1978).
5. R. P. Skowronski, L. A. Heredy and J. J. Ratto, *Preprints ACS Fuel Division* 23 (4) 155, Miami (Sept., 1978).
6. R. P. Skowronski, J. J. Ratto and L. A. Heredy, "Deuterium Tracer Method for Investigating the Chemistry of Coal Liquefaction," Annual Report, 1977, Rockwell International, Canoga Park, California, Report FE-232B-13, pp. 53-56.

TABLE 1
SUMMARY OF EXPERIMENTAL CONDITIONS AND PRODUCT YIELDS

| EXPERIMENTAL CONDITIONS | | | |
|--|--------------------------|--------------------------|----------------------------|
| Parameter | E10 | E19 | E21 |
| Cover Gas | D ₂ | D ₂ | N ₂ |
| Solvent | tetralin-d ₁₂ | tetralin-d ₁₂ | naphthalene-d ₈ |
| Coal Weight (g) | 25 | 25 | 25 |
| Solvent Weight (g) | 25 | 25 | 25 |
| Reactor Volume (liter) | 0.25 | 1.0 | 1.0 |
| Stirring Rate or Rocking Rate | 100 osc/min | 100 rpm | 100 rpm |
| Reaction Time (h) | 1.0 | 1.0 | 1.0 |
| Cold Pressure ² H ₂ or N ₂ (psi) | 1200 | 1000 | 1000 |
| Operating Pressure (psi) | 3000 | 2200 | 2200 |
| Temperature (°C) | 400 | 400 | 400 |

| Products | Weight % | | Atom % ² H | | |
|-------------------------------------|----------|-----|-----------------------|-----|-----|
| | E10 | E19 | E10 | E19 | E21 |
| Oil (HS) | 16 | 17 | 38 | 52 | 11* |
| Asphaltene (BS) | 32 | 10 | 45 | 43 | |
| Benzene-methanol Soluble (BMS) | 8 | 2 | 35 | 38 | |
| Benzene-methanol Insoluble (BMI) | 44 | 71 | 37 | 61 | |

* An average value of the combined coal products.

TABLE 2
 ^1H AND ^2H NMR ANALYSES OF PRODUCT FRACTIONS

| E-10 | | | | | | |
|-----------------------|-----------------|----|-----|-----------------|----|-----|
| Functional Region | $\% ^1\text{H}$ | | | $\% ^2\text{H}$ | | |
| | HS | BS | BMS | HS | BS | BMS |
| γ -Alkyl | 11 | 12 | 6 | 7 | 8 | 7 |
| β -Alkyl | 40 | 23 | 20 | 20 | 14 | 16 |
| α -Alkyl | 26 | 25 | 26 | 44 | 42 | 41 |
| Aromatic ⁺ | 23 | 40 | 48 | 29 | 36 | 36 |

| E-19 | | | | | | |
|-----------------------|-----------------|----|-----|-----------------|-----|-----|
| Functional Region | $\% ^1\text{H}$ | | | $\% ^2\text{H}$ | | |
| | HS | BS | BMS | HS | BS* | BMS |
| γ -Alkyl | 9 | 17 | 8 | 5 | - | 4 |
| β -Alkyl | 31 | 33 | 15 | 17 | - | 15 |
| α -Alkyl | 20 | 16 | 33 | 40 | - | 50 |
| Aromatic ⁺ | 40 | 34 | 44 | 38 | - | 31 |

* Sample size was too small for analysis.

⁺ Aromatic region contains phenolic absorbances.

TABLE 3
COMPARISON OF DEUTERIUM AND PROTIIUM DISTRIBUTION
IN E10 AND E19 LIQUEFACTION PRODUCTS

| Functional Region | $(^2\text{H}_x/^2\text{H})/(^1\text{H}_x/^1\text{H})$ Ratio† | | | | | |
|-------------------|--|--------|-----|-----|----------|-----|
| | HS | E10 BS | BMS | HS | E19 BS†† | BMS |
| γ - Alkyl | 0.6 | 0.7 | 1.2 | 0.6 | - | 0.5 |
| β - Alkyl | 0.5 | 0.6 | 0.8 | 0.5 | - | 1.0 |
| α - Alkyl* | 1.7 | 1.7 | 1.6 | 2.0 | - | 1.5 |
| Aromatic** | 1.3 | 0.9 | 0.5 | 1.0 | - | 0.7 |

*Includes α^2 -alkyl region
**Includes phenolic region

†Estimated error: ± 0.1
††Sample size was too small for analysis

TABLE 5
ISOTOPIC COMPOSITION OF HYDROGEN TRANSFER SOLVENT

| <u>STARTING SOLVENT</u> | <u>SPENT SOLVENT</u> |
|-------------------------|----------------------|
| Naphthalene- d_8 | Naphthalene- d_8 |
| 98.5 atom % D | 94.6 atom % D |
| H_α 59% | H_α 78% |
| H_β 41% | H_β 22% |

TABLE 4
ISOTOPIC COMPOSITION OF DONOR SOLVENTS FROM E10 AND E19

| <u>STARTING SOLVENT</u> | | <u>E10 COMPOSITION</u> | <u>SPENT SOLVENT</u> | |
|-------------------------|-----------|------------------------|-----------------------|-----------|
| Tetralin | 94 mole % | → | Tetralin | 70 mole % |
| Naphthalene | 6 mole % | | Naphthalene | 28 mole % |
| | | | <u>Trans</u> -decalin | 1 mole % |
| | | | <u>Cis</u> -decalin | 1 mole % |

| <u>STARTING SOLVENT</u> | | <u>E10 ISOTOPIC DISTRIBUTION</u> | <u>SPENT SOLVENT</u> | |
|--------------------------|---------------|----------------------------------|--------------------------|------------------------------------|
| Tetralin-d ₁₂ | 97.2 atom % D | → | Tetralin-d ₁₂ | H _α 66% ¹ H |
| | | | 80.0 atom % D | H _β 23% ¹ H |
| | | | | H _{ar} 11% ¹ H |

| <u>STARTING SOLVENT</u> | | <u>E19 COMPOSITION</u> | <u>SPENT SOLVENT</u> | |
|-------------------------|-----------|------------------------|-----------------------|-----------|
| Tetralin | 99 mole % | → | Tetralin | 58 mole % |
| | | | Naphthalene | 22 mole % |
| | | | <u>Trans</u> -decalin | 4 mole % |
| | | | <u>Cis</u> -decalin | 16 mole % |

| <u>STARTING SOLVENT</u> | | <u>E19 ISOTOPIC DISTRIBUTION</u> | <u>SPENT SOLVENT</u> | |
|--------------------------|---------------|----------------------------------|--------------------------|------------------------------------|
| Tetralin-d ₁₂ | 99.0 atom % D | → | Tetralin-d ₁₂ | H _α 64% ¹ H |
| | | | 91.6 atom % D | H _β 24% ¹ H |
| | | | | H _{ar} 12% ¹ H |

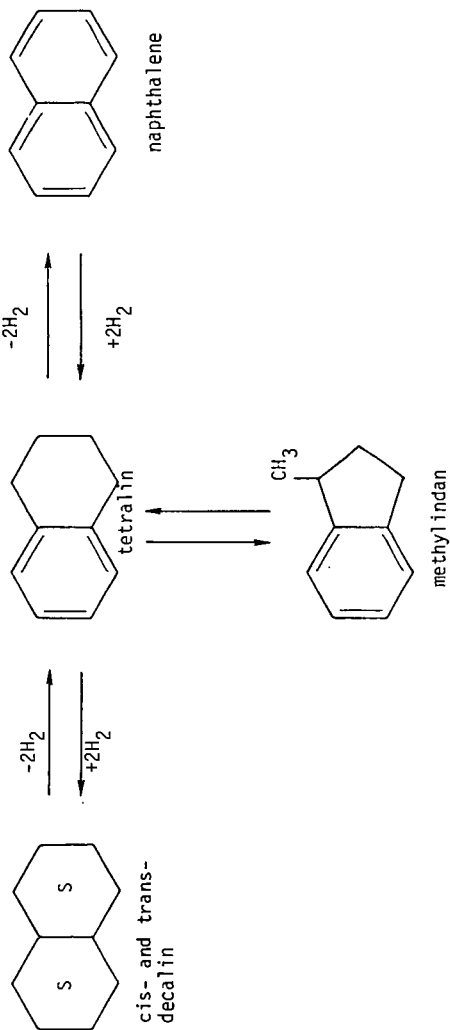


FIGURE 1. REACTION PATHWAYS OF A DONOR SOLVENT DURING LIQUEFACTION

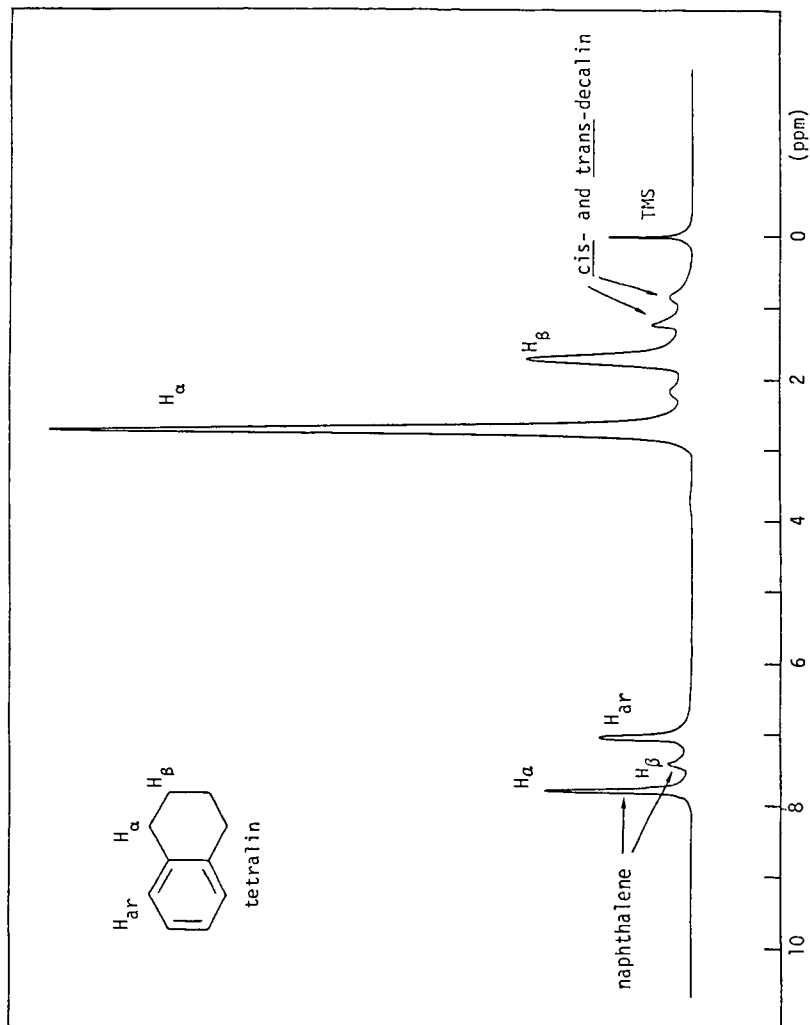


FIGURE 2. PROTON NMR SPECTRUM OF PRODUCT DONOR SOLVENT FROM E10

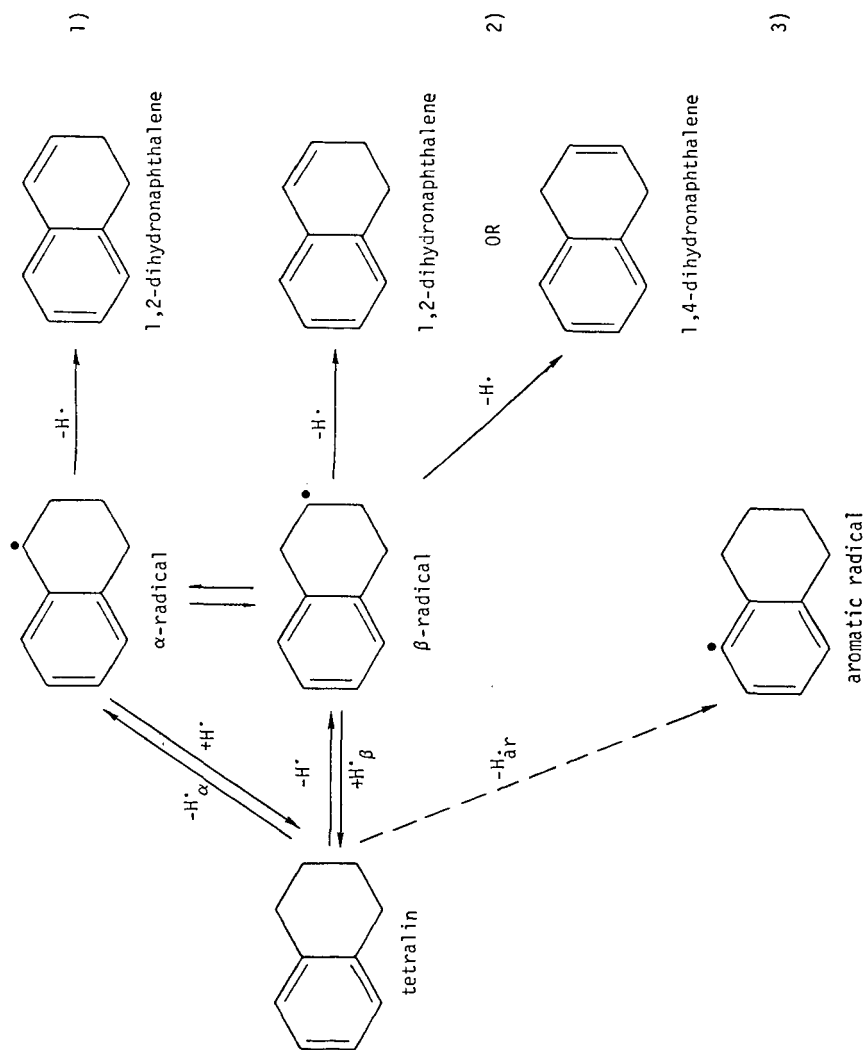


FIGURE 3. STEP-WISE HYDROGEN ATOM TRANSFER FROM TETRALIN

ISOMERIZATION AND ADDUCTION OF HYDROGEN DONOR SOLVENTS UNDER CONDITIONS OF COAL LIQUEFACTION

Donald C. Cronauer
Douglas M. Jewell
Yatish T. Shah
Rajiv J. Modi
K. S. Seshadri

Gulf Research & Development Company
P.O. Drawer 2038
Pittsburgh, PA 15230

INTRODUCTION

Fundamental studies on the chemistry of coal liquefaction have shown that the structure of solvent molecules can determine the nature of liquid yields that result at any particular set of reaction conditions. One approach to understanding this chemistry is to liquefy coal using well-defined solvents or to study reactions of solvents with pure compounds which may represent bond types that are likely present in coal (1). It is postulated that coal liquefaction is initiated by thermal activation to form free radicals which abstract hydrogen from any readily available source. The solvent may, therefore, function as a direct source of hydrogen (donor), indirect source of hydrogen (hydrogen-transfer agent), or may directly react with the coal (adduction). The actual role of solvent thus becomes a significant parameter.

Earlier studies have measured the reactivity of both hydrocarbon (1) and non-hydrocarbon (2) acceptors with good donor solvents (tetralin, hydrophenanthrenes), and poor donors (mesitylene). Although the primary role of solvents was observed to be the stabilization of acceptor radicals, appreciable levels of solvent rearrangement (isomerization), polymerization, and adduction also occurred. Herein, these aspects of solvent chemistry have been pursued with the use of ^{13}C labeling techniques to understand the specific reactions.

EXPERIMENTAL

The experimental procedure to carry out the solvent-acceptor reactions has been described earlier (1,2).

Specifically labeled ^{13}C -octahydrophenanthrene was synthesized by Dr. E. J. Eisenbraun, details of which will be described elsewhere.

REACTIVITY OF HYDROAROMATICS

Background

Due to the relative ease and reversibility of hydrogenation-dehydrogenation of hydroaromatics, they have been used extensively either as a source or agent for placing hydrogen in hydrogen-deficient species, such as coal.⁽³⁾ The assumption has frequently been made that hydroaromatics in the solvents used for this purpose contained the (ideal) six-membered ring while little effort has been directed to determining the isomeric forms. It is known that methyl indanes are essentially stable to hydrogen-transfer as compared to tetralin. Due to difficulties in adequately measuring the concentrations of isomeric structures, the above assumption may not be typically valid.

Tetralin has been shown to undergo thermal dehydrogenation to naphthalene and rearrangement to methylindane in either the absence or presence of free radicals (1). This implies that it may not be valid to assume that hydrogen transfer will be quantitative even in the presence of a large excess of donor solvent. Sym-octahydrophenanthrene (H_0Ph) would be expected to follow the same rearrangement-dehydrogenation reactions as tetralin, except with more isomer and product possibilities (see Figure 1). The kinetics of these reactions will be briefly discussed.

STRUCTURAL FEATURES OF HYDROPHENANTHRENES

The initial indication that hydrophenanthrenes isomerize was the observation of numerous GLC peaks with identical parent ions but different fragment ions in their mass spectra. Compounds with methyl substituents always have more intense $M^+ - 15$ ions than those with unsubstituted six-membered rings. Considering the complexity of the total reaction mixtures, liquid chromatography (HPLC) was used to concentrate more discrete solvent fractions for ^{13}C -NMR study.

Figures 2 and 3 show the partial ^{13}C -NMR spectra of two monoaromatic isomeric octahydrophenanthrenes. The assignments for sym- H_0Ph have been discussed earlier (4). The appearance of new signals at 29 to 21.3 ppm is indicative of methyl groups in a variety of positions on saturated rings and are not present in sym- H_0Ph . The new signals between 30 and 35 ppm are indicative of five-membered rings being formed at the expense of the eight hydroaromatic carbons in the six-membered rings. The absence of a sharp line at approximately 14 ppm indicates that ring opening to a n-butyl substituent did not occur.

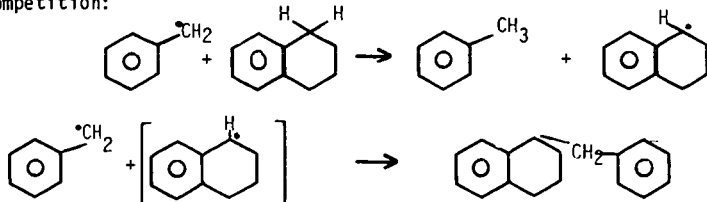
When an acceptor is present, the solvent products are more complex. Reactions were, therefore, performed with 1- ^{13}C -octahydrophenanthrene (10% ^{13}C). The presence of a label provided useful clues as to the real complexity of the structures and pathways for their formation. The products were separated by several liquid chromatographic steps into seven major fractions, arbitrarily designated A through G, and analyzed by ^{13}C -NMR, mass spectrometry, ultraviolet spectroscopy. The partial ^{13}C -NMR stick spectra are shown in Figure 4 where the label appears as an intense broken line. Table 1 illustrates some of the mass spectral data of these fractions. The "best fit" structures deduced from these data will be discussed.

Solvent Adduction

The primary reaction between good donor solvents, such as tetralin and octahydrophenanthrene, and acceptors can give rather ideal products (ex. dibenzyl \longrightarrow toluene in 400-450°C range). However, when poor solvents are introduced secondary reactions become quite important (ex. mesitylene \longrightarrow polymers).

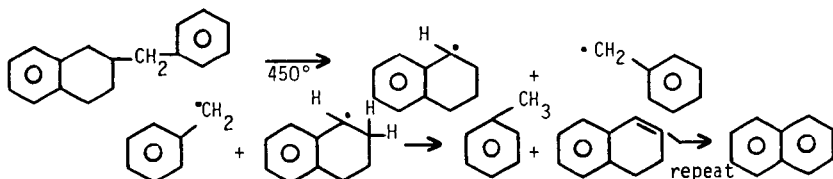
When reactions with oxygen-containing acceptors are performed in the 300-400°C region, the formation of solvent adducts occurs equally well with tetralin and mesitylene. Figure 5 shows a typical GLC curve for products from the reaction of benzyl alcohol and tetralin. These reactions were also done with D_4 -tetralin which permitted the firm identification of the solvent in the adduct. It is noted that several isomers of toluene-tetralin, as well as di-tetralin, were formed. Representative concentrates of total adducts were prepared by HPLC and GPC techniques which permitted their direct study by NMR, MS, and selective reactions.

These analysis indicated that at low temperatures free radical life-times can be reasonably long, thereby permitting competition between H[•] and C[•] for stabilization. The following equations illustrate one representation of this competition:



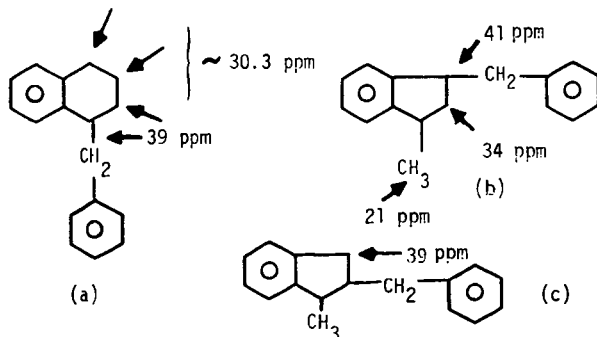
The benzyl free radicals can abstract hydrogen atoms leaving a carbon free radical which has the ability to combine with another benzyl radical. As the reaction proceeds, concentrations of both free radicals increase, creating a greater probability of adduction. Numerous analytical data show increasing concentration of adducts with reaction time and with increasing concentration of acceptor.

It appears that the formation of benzyl tetralin only occurs during the hydrogen transfer reactions at low temperatures (<400°C). If the adduct occurs as shown above, a certain degree of "depolymerization" could be achieved by isolating the adduct fraction and reacting it with fresh tetralin at 450°C. From the previous studies with dibenzyl, diphenylbutane, and phenylhexane, one would predict that cleavage would occur at 450°C as follows:



When this was done, less than 50% of the adduct "depolymerized." The remainder did not react. The remaining adducts had the same molecular weight but much larger M⁻¹⁵ ions indicating the presence of a methyl group. ¹³C-NMR showed that significant rearrangement had occurred.

The following structures were deduced from the NMR spectra:



The strong line at 30.0 ppm in both spectra indicates that the six-membered ring is intact and that, when certain positions are substituted by benzyl groups, they resist cleavage. The fact that lines at 38, 39, and 41 ppm disappear upon heating at 450°C suggests that those particular structures are cleaved (unlikely if they are in a five-membered ring) or rearranged to a more stable form. Finally, the observation that benzyl naphthalenes are also present as reaction products confirms that isomer (a) is present and that it can still function as a donor after adduction.

The adduction reactions discussed are not limited to benzyl-type radicals nor to tetralin solvents. They have been observed with long chain thioether acceptors and donor solvents including dimethyltetralin, octahydro-phenanthrene, and tetrahydroquinoline. Donors using a D or ¹³C label have been used to provide further confirmation that the solvent was incorporated in adducts.

CONCLUSIONS

Implications to Coal Liquefaction

Numerous implications on the fundamental chemistry of coal liquefaction can be drawn from the observed reaction of solvent isomerization and adduction. The literature indicates that recycle solvents from most coal liquefaction processes consist of 2 to 3 aromatic rings with various degrees of saturation, not unlike the model solvents studied. In this system, high levels of effective hydrogen donors can rearrange to isomers having poor donor quality. The following specific points are noted:

1. The isomerization of hydroaromatic donor solvents is a general phenomenon.
2. The rate of rearrangement appears to be first order with respect to donor solvent concentration. (The activation energy of the tetralin reaction is in the range of 26-32 Kcal/g-mole, depending upon whether a free radical precursor is present or not.)
3. The rate of isomerization increases with increasing number of hydroaromatic rings.
4. The rate of rearrangement is increased by order of magnitude when free radicals are present.
5. All solvents have the capability of becoming irreversibly adducted by acceptor free radicals which could arise from the coal.
6. The presence of oxygen and sulfur functions on the free radicals will enhance adduction. Adduction is also enhanced by long reaction times and low temperatures (<400°).
7. At high temperatures (>400°C), adducts are most likely to involve only poor donor solvents; high temperatures will not necessarily cleave adducts formed at low temperatures.
8. Solvent isomerization creates a basic problem in following the progress of liquefaction, namely, measuring the amount of transferred hydrogen. While it is possible to measure the level of "transferable hydrogen" (hydroaromatic six-membered ring

hydrogen) in the feed, recycle, or product liquids by ^{13}C -NMR (5), the present study suggests that it is not possible to isolate the portion contributing to hydrogen transfer alone.

REFERENCES

- 1a. Cronauer, D.C., Jewell, D.M., Shah, Y.T., Kueser, K.A., Ind. Eng. Chem. Fund. (to be issued November, 1978).
- 1b. Benjamin, B.M., Raaen, V.F., Maupin, P.H., Brown, L.L., and Collins, C.J., Fuel 57, 269 (1978).
2. Cronauer, D.C., Jewell, D.M., Shah, Y.T., Modi, R.J., "Mechanism and Kinetics of Selected Hydrogen Transfer Reactions Typical of Coal Liquefaction," paper submitted to Ind. Eng. Chem. Fund., 1978.
- 3a. Ruberto, R.G., Cronauer, D.C., Jewell, D.M., Seshadri, K.S., Fuel 56, 17 (1977).
- 3b. Ibid., 25 (1977)
4. Seshadri, K.S., Ruberto, R.G., Jewell, D.M., Malone, H.P., Fuel 57, 111 (1978).
5. Ibid., 549 (1978).

Table I

MASS SPECTRAL DATA OF ISOLATED HYDROPHENANTHRENES

| Isomer | m/e (% Base Peak) | | | | | | | | | | |
|-------------------------------------|------------------------|--------------------------|------------------------|-----|-----|-----------------------------|-----|-----------------------------|----------------------------|--------------|-----------------------------|
| | 186 | 184 | 182 | 180 | 178 | 171 | 169 | 167 | 158 | 154 | 141 |
| A | P (53) | | | | | P-15 (100) | | | P-28 (18.9) | | |
| B | P ¹ (81) | P ² (34.7) | | | | P ¹ -15 (100) | | | P ¹ -28 (37) | | P ¹ -45 (35) |
| C | P ¹ (93) | P ² (98) | | | | P ¹ -15 (63) | | | | | P ¹ -45 (100) |
| D | | | P (100) | | | | | P-15 (35) | | P-28 (67) | P-41 (27) |
| E | | | P (100) | | | | | P-15 (27) | | P-28 (69) | |
| F | P ² (23) | P ³ (10) | P ¹ (42) | | | | | P ¹ -15 (100) | | | P ¹ -41 (15) |
| G | P (100) | | | | | P-15 (76) | | | P-28 (56) | | |
| Pure tetrahydro- phenanthrene | | | P (100) | | | | | P-15 (15) | | P-28 (78) | P-41 (34) |
| Pure octahydro- phenanthrene | P (100) | | | | | P-15 (68) | | | P-28 (30) | | P-45 ⁱ (33) |

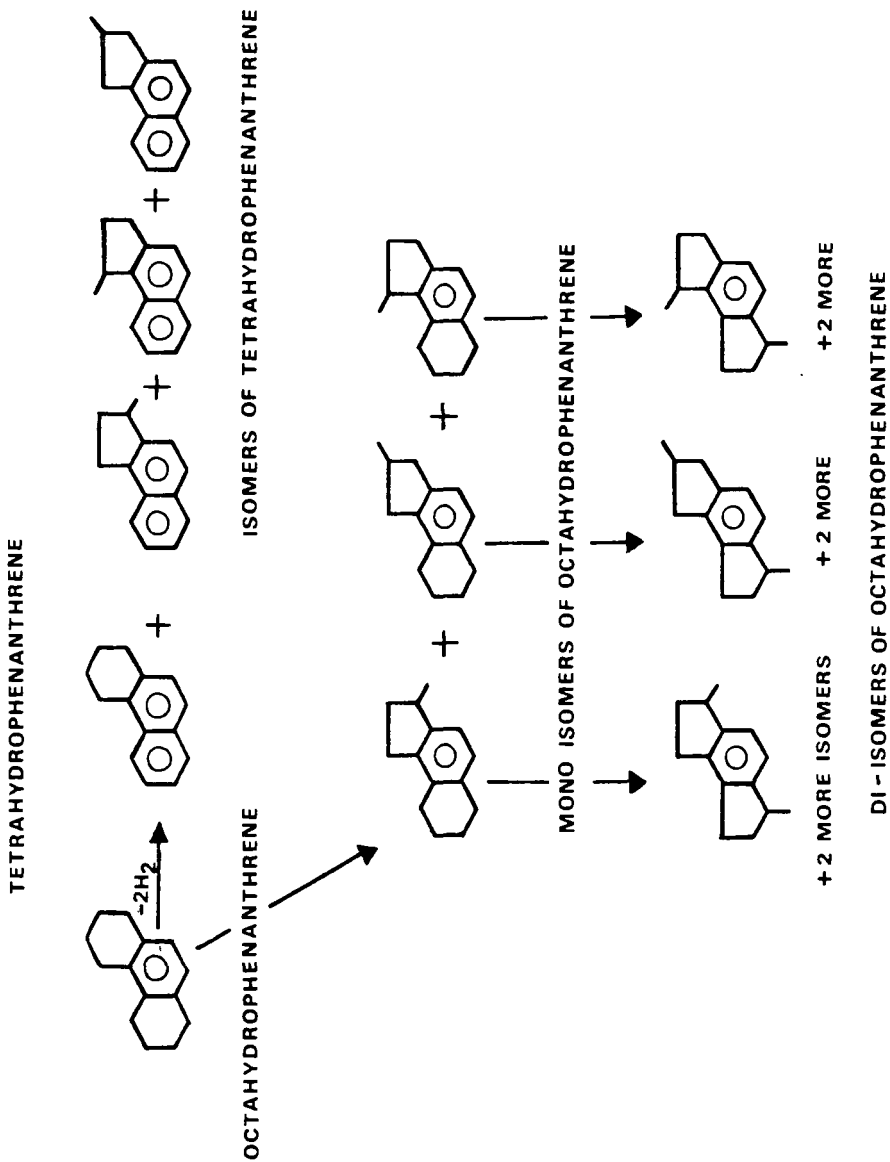


Figure 1: Reactions of Octahydrophenanthrene

Figure 2: ^{13}C -NMR spectrum of monomethyl isomers of rearranged octahydrophenanthrene

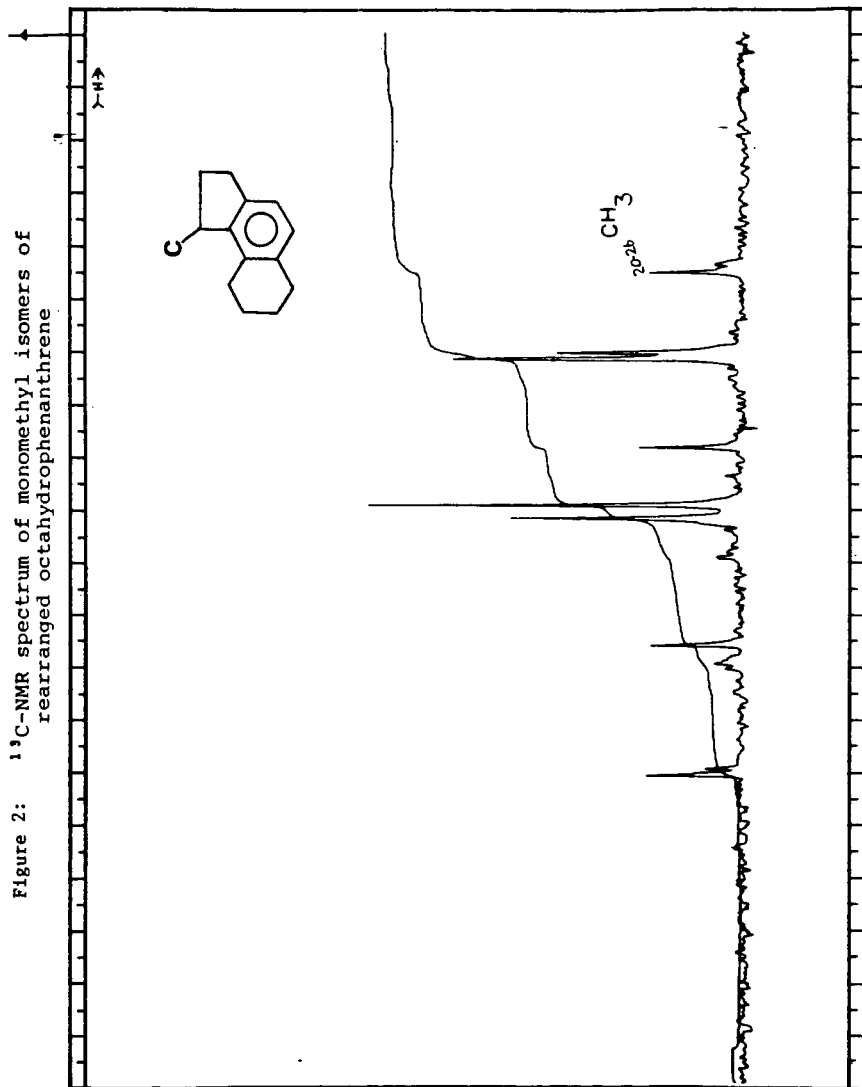
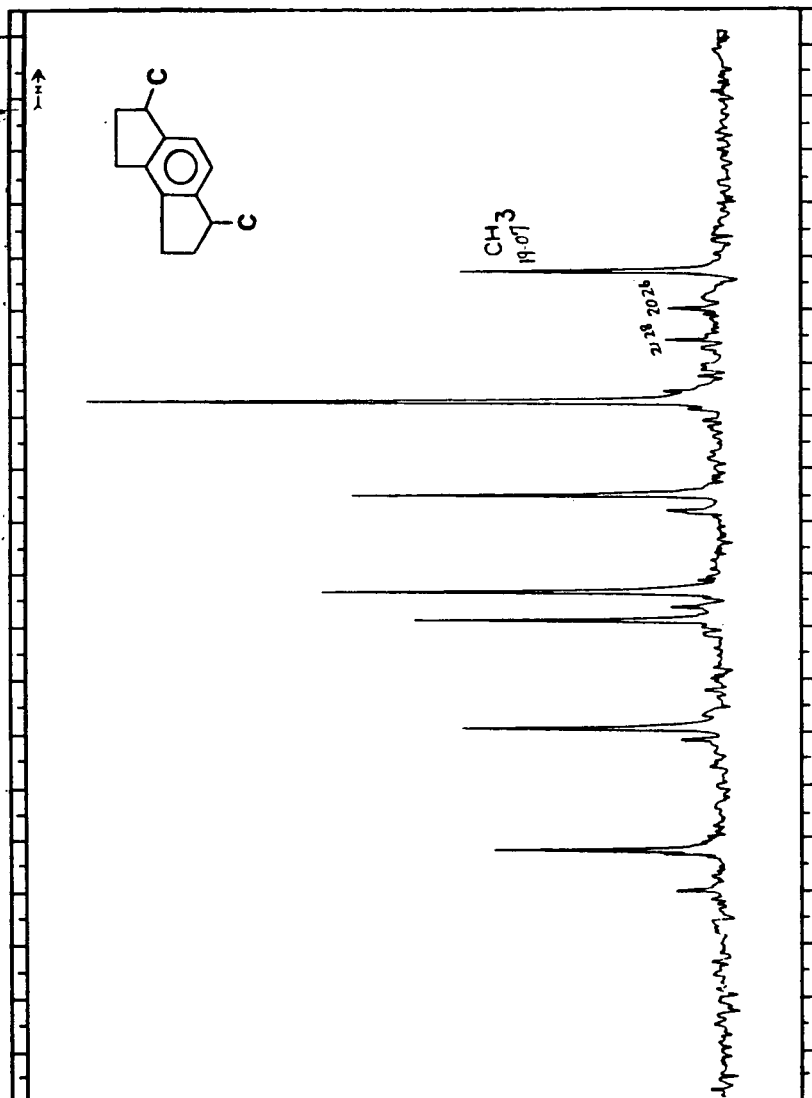


Figure 3: ^{13}C -NMR spectrum of dimethyl isomers of rearranged octahydrophenanthrene



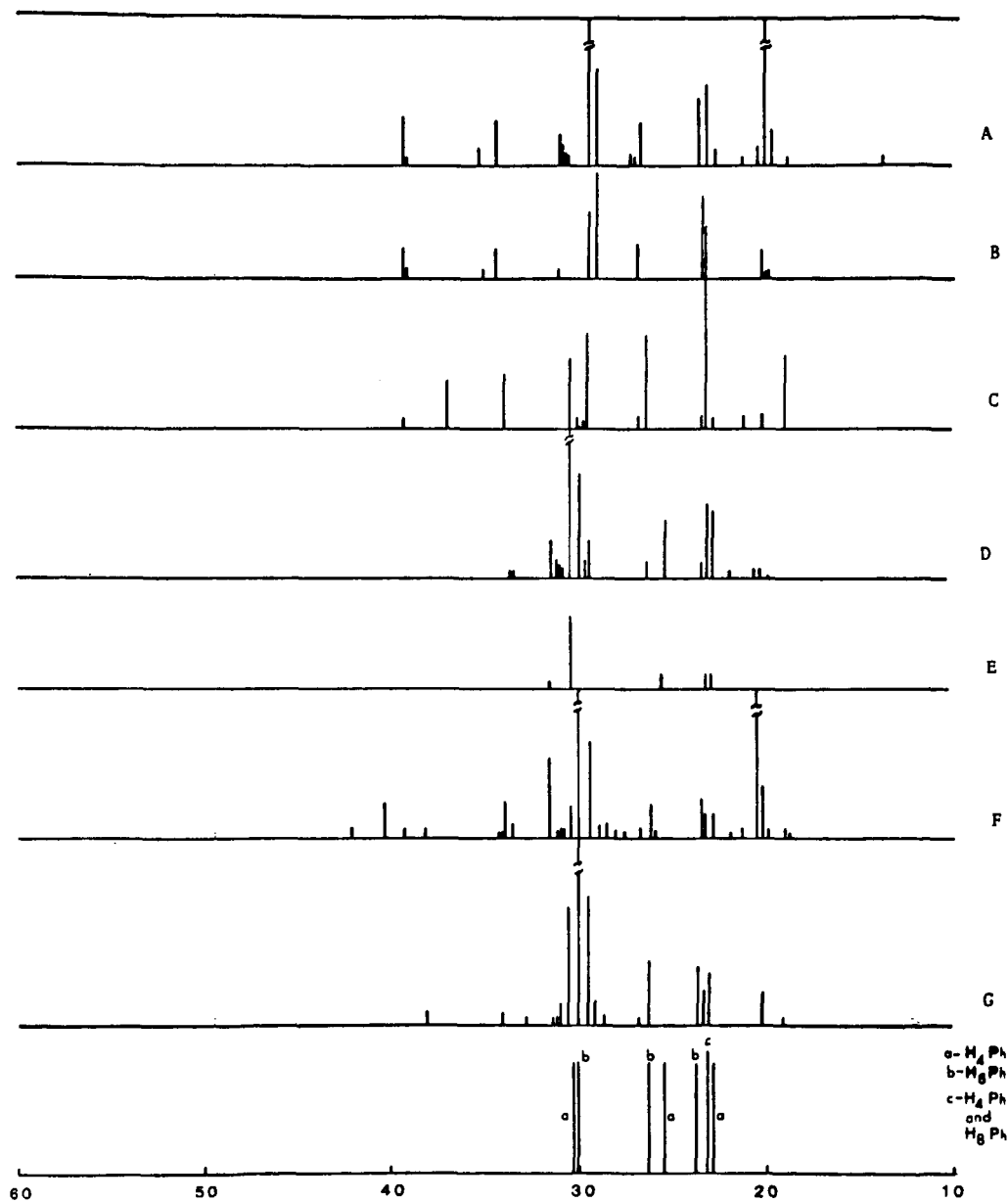


Figure 4: ^{13}C -NMR Spectra of Hydrophenanthrenes:
Saturate Region

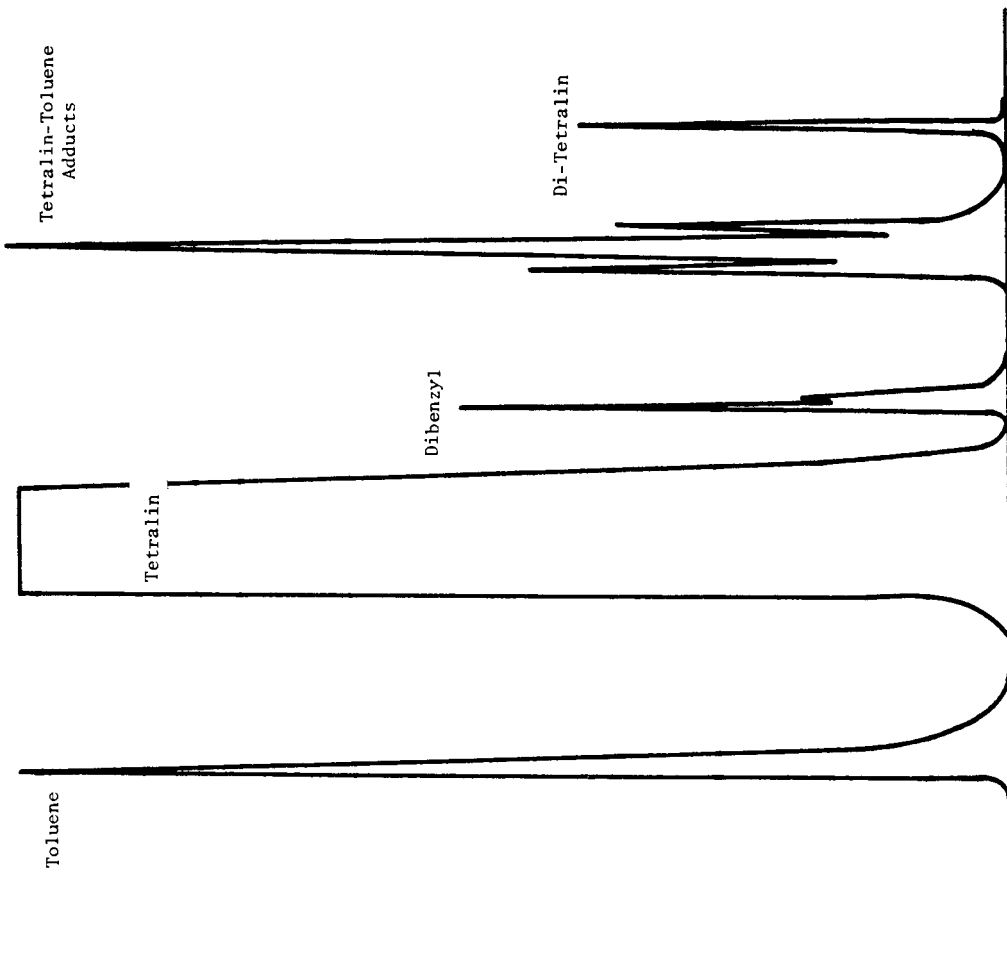


FIGURE 5: GAS-LIQUID CHROMATOGRAM OF PRODUCTS FROM BENZYL ALCOHOL-TETRALIN REACTION AT 400°C

TAR YIELD IN THE OXY FLASH PYROLYSIS PROCESS, K. Durai-swamy, S.C. Che, N.W. Green, E.W. Knell and R.L. Zahradnik. Occidental Research Corporation, 2100 S.E. Main, Irvine, California 92714.

In the Oxy Flash Pyrolysis process, (formerly known as Garrett Flash Pyrolysis Process) coal is heated by direct mixing with circulating hot char and the tar yield is found to be greatly reduced by the presence of char. The tar yield can be increased by using reactive carrier gases such as steam and CO_2 . The tar yield from a subbituminous coal in the ORC flash pyrolysis process was first determined using an electrically-heated bench scale reactor (BSR) where nitrogen was used as the coal transport gas. Later, the tar yield was found to decrease when char was used for heating in a 3 TPD process development unit (PDU). It was hypothesized that the tar vapor adsorbed on the char surface, condensed and cracked to form coke and gas. Further it was proposed to use reactive transport gases such as CO_2 , H_2O , CO and H_2 to inhibit the char surface by adsorption and reduce the tar disappearance. It was experimentally found that the tar yield increased when reactive transport gases were used along with the char heating mode. High tar yields of over 35 MAF wt. % from Hamilton bituminous coal were obtained in the PDU. PDU and BSR results will be reported.

INVESTIGATION OF ALBERTA OIL SAND ASPHALTENES
USING THERMAL DEGRADATION REACTIONS

T. Ignasiak, T.C.S. Ruo and O.P. Strausz

Hydrocarbon Research Centre
Department of Chemistry
University of Alberta
Edmonton, Alberta, Canada T6G 2G2

INTRODUCTION

Thermal breakdown reactions directed toward cracking complex molecules into low molecular weight products constitute an important part of oil sand technologies (1). It is generally accepted that the high asphaltene content of Alberta bitumen is primarily responsible for a large proportion of the coke produced by dehydrogenation and repolymerization reactions that prevail at high temperatures. Moreover, asphaltene obtained from the Alberta oil sands contains appreciable amounts of heteroatoms, mainly sulfur, oxygen and nitrogen, that tend to be associated with coke precursors and as such greatly reduce the marketable value of coke as an energy source. However, our previous results (2-6) suggest that the oxygen-based hydrogen bonding and sulfide linkages play important roles in the molecular size of the sulfur-rich Alberta oil sand asphaltene. These observations are significant because the energy requirement for the cleavage of sulfide bonds is generally lower than that required for coke formation. We have therefore undertaken a study of the thermal behaviour of asphaltene under moderate conditions aimed at high product recoveries and low coke yields.

EXPERIMENTAL

The origin of the samples and the preparation of asphaltenes have been described (2,3).

Thermal degradation

The pyrolysis of asphaltene (1.5 g) was carried out in a vacuum (0.1 torr) sealed tube (vol. 40 ml) inserted in a furnace maintained at a preset temperature. After the heating period the tube was cooled to -15°C, opened, and the product Soxhlet extracted with *n*-pentane to yield the pentane-soluble (maltene) fraction. Subsequent extraction with benzene yielded the benzene soluble (retrieved asphaltene) fraction.

Reduction

A one gram sample of asphaltene dissolved in 15 ml dry THF was introduced to 100 ml liquid ammonia, followed by 45 ml of 98% ethanol and then lithium metal (6 g) cut into small pieces was gradually added over a period of about 1 hour. The mixture was stirred for another 2 hours and finally quenched with 15 ml ethanol. Ammonia was allowed to evaporate overnight. The reduced product was recovered by the usual procedure involving acidification with aqueous HCl, filtration, removal of inorganic salts by water extraction, and was then dried *in vacuo* at 60°C for 24 hours.

Chromatography separation of pentane soluble fractions

A compound class separation was performed on a glass column, 100 cm x 1 cm (i.d.) packed with silica gel Woelm (activated overnight at 140°C). The sample to solvent ratio was 1:65 (for elution solvents, see Table 5). To assure purity of the fractions, they were monitored by HPLC on a μ -Porasil column using a UV detector.

A clear-cut separation of saturates from olefins was achieved by semipreparative HPLC on a silver aluminum silicate column (column, 6 cm x 0.9 cm (i.d.); solvent, heptane; flow rate, 9 ml/min; pressures, ~8-900 psi).

The molecular weights were determined by vapor pressure osmometry at a nominal concentration of 20 mg/ml in benzene.

RESULTS AND DISCUSSION

1. Thermal degradation of asphaltene

Athabasca asphaltene was heated either at constant temperature for various periods of time or at different temperatures for constant time periods (Table 1).

The yield of the pentane-soluble (maltene) fraction does not seem to increase significantly either during prolonged heating or with increasing temperature but high temperature leads to coke formation. Volatiles and coke are produced at the expense of residual asphaltene.

The elemental analyses of maltene, residual asphaltene and insoluble residue, if any, are given in Table 2. The chemical composition of the maltene fraction does not show much variation with either time of heating or temperature; it is more saturated than the residual asphaltene and distinctly lower in nitrogen content than both the original and residual asphaltenes. In the residual asphaltene, the lower H/C ratios indicate that aromatization increases with either reaction time or increased temperature. The insoluble residue produced at 390°C is the most unsaturated portion of pyrolyzed asphaltene and contains the highest concentration of heteroatoms. Under the conditions used, the overall desulfurization does not exceed 22% in terms of the sulfur present in the parent asphaltene.

In earlier studies (3,6) it was found that the amount of sulfur in bridges susceptible to cleavage in potassium-THF solution varies for Athabasca, Cold Lake, Peace River and Lloydminster asphaltenes. To estimate to what extent these structural variations in the Alberta oil sand asphaltenes are reflected in their thermal behaviour, these asphaltenes were heated under conditions where thermolysis of the Athabasca asphaltene gives optimal conversion and no coke.

At 300°C, after 72 hours, (Table 3), all these sulfur-rich asphaltenes retain full solubility in benzene. Some variations are, however, indicated by the yield of pentane solubles which is the highest for Athabasca and significantly lower for the remaining asphaltenes. This roughly corresponds to the decrease in the molecular weight of the heated asphaltenes. Desulfurization accounts for up to 15% of the original sulfur content and deoxygenation varies from 20 to 40%.

2. Thermal degradation of reduced asphaltene

According to the previous results, (2,7) depolymerization of asphaltene depends to a large extent on the cleavage of C-S bonds and thermolysis at 300°C will involve only the most unstable ones. Any structural changes in the asphaltene molecule which would lower the energy of activation for cleavage of the C-S bonds present may enhance the degradation under the same conditions. It was therefore of interest to investigate the thermal behaviour of asphaltene that had been chemically modified by reduction with alkali metals. The reductive systems applied were potassium in tetrahydrofuran with naphthalene as a charge transfer catalyst (2) and lithium in liquid ammonia in the presence of ethanol. In both cases simple protonation results in partial insolubilization which accounts for up to 60% of reduced asphaltene.

a) Potassium-THF-naphthalene reduced Alberta sulfur-rich asphaltenes

When heated at 300°C for 72 hours these reduced and protonated asphaltenes (Table 4) exhibit thermal properties which are distinctly different from those of naturally occurring asphaltenes, cf. Table 3. Thus thermally treated reduced asphaltenes became almost fully soluble in benzene; the yield of pentane solubles was doubled (except for the case of the Athabasca sample) and the loss of sulfur upon conversion was also twice that observed for unreduced asphaltenes, cf. Table 3. The overall desulfurization upon reduction and thermolysis, about 50%, is comparable for all four asphaltenes.

b) Lithium-liquid ammonia reduced Athabasca asphaltene

The treatment with lithium in liquid ammonia in the presence of ethanol enhances the thermal reactivity of Athabasca asphaltene to an even larger extent than that with potassium in THF. The rate of conversion into pentane solubles and desulfurization have been found to be directly related to the amount of hydrogen introduced to asphaltene on reduction. This again seems to depend on the lithium and ethanol concentrations. The enhanced degree of hydrogenation of asphaltene in the presence of ethanol is apparently due to the fact that ethanol as a proton source is more acidic than ammonia and facilitates the reduction of aromatic systems such as benzene derivatives having high negative reduction potentials.

The results (Table 4) show that at 300°C lithium reduced Athabasca asphaltene yielded close to 50% of pentane solubles, and the sulfur content was depleted by about 50%. It is interesting to note that the proportion of hydrogen to carbon in the reduced and heated asphaltene is more favorable than in the original asphaltene. The conversion rate is distinctly higher than in the case of potassium-THF pretreatment and comparable with that obtained in the case of the tetralin reaction at 390°C (7).

It is apparent that the high thermal reactivity of reduced asphaltenes as compared to the original asphaltene and reflected by appreciable conversion and desulfurization, is related to the cleavage of carbon-sulfur bonds and to partial saturation of double bonds. This leads to the formation of thermally unstable thiols which are easily removed at temperatures as low as 300°C.

3. Characterization of the pentane-soluble fraction obtained from thermal degradation of Athabasca asphaltene

The appreciable yields and relatively low molecular weights of the pentane soluble fractions obtained from thermal treatments of asphaltene make them amenable to chromatographic separation. The pentane-soluble products of Athabasca asphaltene, pyrolyzed neat at 300° and 390°C, and in the presence of tetralin at 390°C, and of lithium reduced and pyrolyzed asphaltene at 300°C, have been separated into compound classes on silica gel. The results (Table 5) indicate that the yields of saturates and aromatics increase with increasing temperature of thermolysis at the expense of the polar I and polar II fractions. Significantly, pretreatment with lithium in liquid ammonia in the presence of ethanol promotes the formation of saturates and aromatics I, the yields of which, at 300°C, approximate those obtained at 390°C.

CONCLUSIONS

It is clear from the data presented here that the early stage of low temperature degradation is a gradual depolymerization, where the crosslinking bonds in the asphaltene molecule are preferentially broken with the formation of lower molecular weight, pentane-soluble polar materials. Polar fractions can readily undergo thermolysis to generate hydrocarbons (e.g., saturates and aromatics).

The alkali metal pretreatment activates certain C-S bonds, most likely by generation of thiols which can be easily removed, thus affording an appreciable overall desulfurization on subsequent pyrolysis. The reduction using lithium/liquid ammonia in the presence of ethanol represents a situation in which the hydrogen added to asphaltene molecule reacts with the free radicals produced during thermolysis, thus stabilizing the fragments and resulting in a remarkable conversion into pentane-soluble materials.

ACKNOWLEDGMENTS

This work was supported by the National Research Council of Canada and the Alberta Oil Sands Technology and Research Authority. We thank Dr. E.M. Lown for reading the manuscript.

REFERENCES

- (1) Watson, W.T., *Energ. Processing, Canada*, 62 (1974).
- (2) Ignasiak, T., Kemp-Jones, A.V. and Strausz, O.P., *J. Org.*, 42, 312 (1977).
- (3) Ignasiak, T., Kemp-Jones, A.V. and Strausz, O.P., Preprints, Div. Fuel Chem., ACS, Symposium on Oil Sand and Oil Shale, 2nd Annual Joint Meeting, Chemical Institute of Canada/American Chemical Society, Montreal, Canada, May 29-June 2, 1977, Vol. 22, No. 3, pp.126-131.
- (4) Kemp-Jones, A.V. and Strausz, O.P., Preprints, Div. Fuel Chem., ACS, Symposium on Oil Sand and Oil Shale, 2nd Annual Joint Meeting, Chemical Institute of Canada/American Chemical Society, Montreal, Canada, May 29-June 2, 1977, Vol. 22, No. 3, pp.132-139.
- (5) Ignasiak, T., Strausz, O.P. and Montgomery, D.S., *Fuel*, 56, 359 (1977).
- (6) Kemp-Jones, A.V., Ignasiak, T. and Strausz, O.P., in "Oil Sand and Oil Shale Chemistry", O.P. Strausz and E.M. Lown, Eds., Verlag Chemie International, 1978, p.211.
- (7) Ignasiak, T. and Strausz, O.P., *Fuel*, in press.

Table 1. Thermolysis of Athabasca Asphaltene

| Temp., °C | Time, hrs | Yield, % Wt Asphaltene | | | Residue | Desulfurization % |
|--------------|--------------|------------------------|------------------|---------|---------|----------------------|
| | | Volatiles | Soluble fraction | | | |
| | | | Pentane | Benzene | | |
| 300 | 4 | 0 | 20 | 80 | 0 | 9 |
| 300 | 30 | 1 | 22 | 77 | 0 | 9 |
| 300 | 72 | 5 | 28 | 67 | 0 | 14 |
| 300 | 114 | 5 | 26 | 69 | 0 | 14 |
| 348 | 4 | 4 | 24 | 72 | 0 | 14 |
| 390 | 4 | 10 | 32 | 38 | 20 | 22 |

Table 2. Elemental analyses of maltene and residual asphaltene obtained from thermolysis of Athabasca asphaltene

| Temp., °C | Time, hrs | MW | H/C | % | | |
|----------------------------|--------------|------|------|------|------|------|
| | | | | N | O | S |
| <u>Maltene fraction</u> | | | | | | |
| 300 | 4 | 690 | 1.36 | 0.60 | 2.02 | 7.00 |
| 300 | 30 | 680 | 1.38 | 0.51 | 1.59 | 6.75 |
| 300 | 72 | 530 | 1.38 | 0.55 | 1.23 | 6.39 |
| 300 | 114 | 570 | 1.40 | 0.65 | 1.30 | 6.40 |
| 348 | 4 | 620 | 1.40 | 0.51 | 1.60 | 6.58 |
| 390 | 4 | 430 | 1.42 | 0.50 | 1.16 | 6.10 |
| <u>Residual asphaltene</u> | | | | | | |
| 300 | 4 | 6100 | 1.18 | 1.29 | 1.90 | 7.00 |
| 300 | 30 | 5500 | 1.16 | 1.33 | 1.84 | 7.20 |
| 300 | 72 | 6600 | 1.07 | 1.37 | 1.80 | 7.21 |
| 300 | 114 | 4500 | 1.04 | 1.34 | 1.90 | 7.15 |
| 348 | 4 | 5300 | 1.11 | 1.34 | 2.00 | 7.05 |
| 390 | 4 | 2400 | 1.06 | 1.40 | 1.80 | 6.88 |
| <u>Residue</u> | | | | | | |
| 390 | 4 | - | 0.89 | 1.63 | 2.16 | 7.16 |

Table 3. Thermolysis of Alberta asphaltenes at 300°C/72 hrs.

| Asphaltene | | Conversion Wt % | Product | | MW |
|--------------|------|--------------------|------------|--------|------|
| Source | MW | | Loss, Wt % | | |
| | | | Sulfur | Oxygen | |
| Athabasca | 6000 | 28 | 14 | 40 | 1300 |
| Cold Lake | 8100 | 7 | 5 | 30 | 5500 |
| Peace River | 9500 | 14 | 14 | 40 | 2500 |
| Lloydminster | 9300 | 14 | 15 | 20 | 3500 |

Table 4 - See following page.

Table 5. Chromatographic separation of the pentane soluble products from thermally treated Athabasca asphaltene

| Eluate | Fraction | Yield, wt % (pentane solubles = 100%) | | | |
|--------------------------|--------------------------------|---------------------------------------|----------|-------|-----------------|
| | | 390°C | | 390°C | |
| | | neat | tetralin | neat | Lithium reduced |
| n-C ₅ | Saturates | 12.1 | 15.1 | 3.2 | 11.3 |
| | Olefins | 2.7 | 1.9 | 0.8 | 1.3 |
| n-C ₅ /15% Bz | Aromatic I (mono-, di-) | 13.7 | 13.2 | 5.8 | 10.9 |
| n-C ₅ /15% Bz | Aromatic II (> di-to poly-) | 30.6 | 27.5 | 17.8 | 19.9 |
| 100% Bz | Polar I | 22.5 | 26.3 | 47.3 | 30.9 |
| THF | Polar II | 15.5 | 18.4 | 29.9 | 24.6 |

Table 4. Thermolysis of reduced asphaltenes at 300°C/72 hrs.

| Asphaltene | Volatiles by weight loss | Solubility in benzene | H/C ratio | MW | Conversion (pentane solubility) | Sulfur content (wt %) | | Overall Desulfurization % | |
|--|--------------------------------|--------------------------|--------------|------|---------------------------------------|--------------------------|-----------------------|---------------------------------|----|
| | | | | | | Original | Reduced and Heated | | |
| | wt % | wt % | | | wt % | | | | |
| <u>K/THF/Nap reduction</u> | | | | | | | | | |
| Athabasca | 6 | 94 | 1.19 | 1300 | 32 | 8.00 | 5.75 | 4.05 | 49 |
| Cold Lake | 5 | 95 | 1.19 | 2500 | 18 | 7.97 | 5.22 | 4.21 | 47 |
| Peace River | 7 | 93 | 1.22 | 1500 | 28 | 8.75 | 6.11 | 4.25 | 51 |
| Lloydminster | 7 | 93 | 1.19 | 1500 | 25 | 8.30 | 5.20 | 3.87 | 53 |
| <u>Li/NH₃/Eth reduction^a</u> | | | | | | | | | |
| Athabasca | 9 | 91 | 1.35 | 1000 | 48 | 8.00 | 6.48 | 3.91 | 51 |

^a H/C of reduced asphaltene = 1.48.

RELATION BETWEEN COAL STRUCTURE AND THERMAL DECOMPOSITION PRODUCTS

P. R. Solomon

United Technologies Research Center
East Hartford, CT 06108

INTRODUCTION

In a recent study, the thermal decomposition of 13 coals was examined in over 600 vacuum devolatilization experiments (1). The results for all 13 coals were successfully simulated in a model which assumes the evolution of tar "monomers" from the coal "polymer" and the parallel evolution of smaller molecular species produced by further cracking of the molecular structure (2,3). The evolution of each species is characterized by rate constants which do not vary with coal rank. The differences between coals are due to differences in the mix of sources in the coal for the evolved species. The sources were tentatively related to the functional group concentrations in the coal.

This paper reports a study to verify the relationship between functional group distribution and thermal decomposition behavior. A Fourier Transform Infrared Spectrometer (FTIR) has been employed to obtain quantitative infrared spectra of the coals, chars and tars produced in the devolatilization experiments. The spectra have been deconvoluted using a computerized spectral synthesis routine to obtain functional group distributions, which are compared to the model parameters.

MODEL

The thermal decomposition model is illustrated in Fig. 1. The initial coal composition (Fig. 1a) is described by the fraction Y_i^0 of each functional group present ($\sum_i Y_i^0 = 1$) and the fraction of coal X^0 which is potentially tar forming. During decomposition each component may evolve as an independent species into the gas or may evolve with the tar. The evolution of a component into the tar is described by the diminishing of the X dimension and into the gas by the diminishing of the Y_i dimensions according to

$$X = X^0 \exp(-k_X t) \quad \text{and} \quad Y_i = Y_i^0 \exp(-k_i t)$$

where k_i and k_X are rate constants given in Table I.

According to this model the tar contains a mix of functional groups similar to that in the parent coal. This concept is based on the strong similarity between vacuum devolatilized tar and the parent coal observed in chemical composition (1,2,3), infrared spectra (1,3,4,5), and nmr spectra (1,3). The similarity of the infrared spectra is illustrated in Fig. 2 for four coals. The resemblance of the tar and parent coal suggests that the tar consists of "monomers" released from the coal "polymer". The major difference observed in the ir spectra between tar and parent coal is the higher quantity of aliphatic* CH_2 and CH_3 . This is presumably

* No attempt has been made in this paper to distinguish between aliphatic and alicyclic CH.

because the monomers abstract hydrogen to stabilize the free radical sites produced when the monomer was freed. Similar arguments were given for pyrolysis of model compounds by Wolfs, van Krevelen and Waterman (6).

TABLE I KINETIC CONSTANTS FOR LIGNITE AND BITUMINOUS COALS (2)

| Functional Group | Kinetic Rates |
|------------------|--|
| carboxyl | $k_1 = 6 \exp(-4000/T) \text{ sec}^{-1}$ |
| hydroxyl | $k_2 = 15 \exp(-4950/T)$ |
| ether | $k_3 = 890 \exp(-12000/T)$ |
| aliphatic | $k_4 = 4200 \exp(-9000/T)$ |
| aromatic H | $k_5 = 3600 \exp(-12700/T)$ |
| aromatic C | $k_6 = 0$ |
| tar | $k_X = 750 \exp(-8000/T)$ |

Figure 1b illustrates the initial stage of thermal decomposition during which the volatile components H_2O and CO_2 evolve from the hydroxyl and carboxyl groups respectively along with aliphatics and tar. At a later stage (Fig. 1c) CO and H_2 are evolved from the ether and aromatic H.

To simulate the abstraction of H by the tar, the aliphatic fraction in the tar is assumed to be retained together with some additional aliphatic material which may be added directly or may contribute its hydrogen. When hydrogen from the aliphatic material is contributed, its associated carbons remain with the aromatic carbon fraction which eventually forms the char (Fig. 1d).

INFRARED SPECTRA

Infrared Spectra of coals, tars and chars were obtained on a Nicolet FTIR. KBr pellets of coals and chars were prepared by mixing 1 mg of dry, finely ground (20 min in a "Wig-L-Bug") sample with 300 mg of KBr. Thirteen mm diameter pellets were pressed in an evacuated die under 20,000 lbs pressure for one minute and dried at 110°C overnight to remove water. Since the heating process destroyed similarly prepared tar pellets, the water correction was obtained by subtracting the spectrum of a blank disk prepared under the same conditions. The H_2O corrected spectra matched those from samples prepared by allowing the tar produced in thermal decomposition to fall directly onto a water free blank KBr disk.

The FTIR obtains spectra in digital form and corrections for particle scattering, mineral content and water may be easily made. A typical correction sequence is illustrated in Fig. 3. The lower curve is the uncorrected spectrum of a dried coal. It has a slope due to particle scattering and peaks from the mineral components near 1000 and 450 cm^{-1} . In the middle figure a straight line scattering spectrum has been subtracted. In the top the spectrum for a mixture of kaolin and illite has been subtracted (7) and the spectrum scaled to give the absorbance for 1 mg of coal dmmf.

Much previous work has been done to identify the functional groups responsible for the observed peaks. Extensive references may be found in Lowry (8) and van Krevelen (9). To get a quantitative measure of the functional group concentrations, a curve analysis program (CAP) available in the Nicolet library was used to synthesize the ir spectra. The synthesis is accomplished by adding 26 absorption peaks

with Gaussian shapes and variable position, width, and height as shown in Fig. 4. The peaks are separated according to the identified functional group. It has been determined that all the coals, chars, and tars which were studied could be synthesized by varying only the magnitudes of a set of Gaussians whose widths and positions were held constant. These samples could therefore be analyzed in terms of a fixed mix of functional groups.

Peak O at 1600 cm^{-1} has been included with the hydroxyl group. The identity of this peak has caused much speculation in the literature (8,9). Fujii et al. (10), showed that the intensity of the 1600 cm^{-1} peak varied linearly with oxygen content in the coal. The present study narrows the correlation still further. Figure 5 shows a linear relation between the intensity of the O peak at 1600 cm^{-1} and the hydroxyl content measured by peaks L, M, N and Q. The correlation includes chars which have a high oxygen content in ether groups but very low hydroxyl so that the correlation with total oxygen would no longer hold. It has, therefore, been concluded that the sharp line at 1600 cm^{-1} is caused mainly by hydroxyl oxygen probably in the form of phenols.

The calibration of the aliphatic peaks near 2900 cm^{-1} (lines A-E) and the aromatic peaks near 800 cm^{-1} (lines I-K) is shown in Fig. 6. The objective is to determine the values of the constants a and b, which relate peak areas to the corresponding hydrogen concentration, i.e.,

$$H_{\text{ali}} = a A_{\text{ABCDE}} \quad \text{and} \quad H_{\text{aro}} = b A_{\text{IJK}}$$

where A_{ABCDE} is the area under the aliphatic peaks A-E, A_{IJK} is the area under the aromatic peaks I-K, and H_{ali} and H_{ar} the aliphatic (or alicyclic) and aromatic hydrogen concentrations, respectively. The equation for total hydrogen concentration $H_{\text{total}} = H_{\text{ali}} + H_{\text{ar}} + H_{\text{hydroxyl}}$ may be combined with the above equations to yield

$$a \left[\frac{A_{\text{ABCDE}}}{H_{\text{total}} - H_{\text{hydroxyl}}} \right] = 1 - b \left[\frac{A_{\text{IJK}}}{H_{\text{total}} - H_{\text{hydroxyl}}} \right]$$

where H_{hydroxyl} is the hydrogen content in hydroxyl groups obtained from

$$H_{\text{hydroxyl}} = c A_{\text{LMNQ}}$$

where c has been determined using the relation between hydroxyl content and specific extinction coefficient at 3450 cm^{-1} derived by Ōsawa and Shih (11).

The hydrogen distribution computed using the determined values of $a = .075$ and $b = .071$ are shown in Table II. In the present investigation it was felt that the determination of peak areas rather than peak intensities would be more accurate method for determining quantitative functional group concentrations. For comparison to other infrared investigations more useful relations are

$$H_{\text{ali}} = 11.5 \times D_{\text{ali}} \text{ A/M \%} \quad \text{and} \quad H_{\text{aro}} = 19.2 \times D_{\text{aro}} \text{ A/M \%}$$

where A is the area of the pellet in cm^2 , m the sample weight in mg, D_{ali} is the optical density of the peak at 2920^{-1} and D_{aro} is the average optical density of the I, J, and K peaks near 800 cm^{-1} .

TABLE II HYDROGEN DISTRIBUTION IN COALS (dmmf)

| COAL | PLOTING SYMBOL | C | H | O | From IR | | | |
|-----------------|----------------|------|------|-------|------------------|------------------|-------------------|------------------------------------|
| | | | | | H _{aro} | H _{ali} | H _{hydr} | H _{aro} /H _{ali} |
| PSOC 268 | M | 86.2 | 5.24 | 6.13 | 2.2 | 2.8 | .28 | .79 |
| PSOC 124 | B | 84.8 | 7.17 | 6.35 | 1.6 | 6.0 | .42 | .27 |
| PSOC 170 | G | 81.8 | 5.37 | 9.12 | 1.8 | 3.2 | .31 | .56 |
| PSOC 103 | A | 82.9 | 5.11 | 10.04 | 2.0 | 2.4 | .36 | .83 |
| Bu Mi 40660 | Z | 79.9 | 5.32 | 11.74 | 2.0 | 3.1 | .42 | .65 |
| PSOC 330 | V | 80.4 | 5.09 | 12.21 | 1.9 | 2.8 | .42 | .68 |
| PSOC 212 | J | 76.2 | 4.81 | 16.81 | 1.5 | 2.5 | .58 | .60 |
| PSOC 308 | T | 74.0 | 5.11 | 18.14 | 1.7 | 3.0 | .58 | .57 |
| Montana Lignite | 4 | 65.2 | 3.60 | 29.44 | 1.1 | 1.7 | .71 | .65 |

The aromatic hydrogen values are in agreement with those determined by van Krevelen (8) and by Mazumdar, et al. (11), from pyrolysis measurements but are larger (by about a factor of 2) than those determined by Brown (12) using ir techniques. Brown measured the ratio of extinction coefficients at 3030 cm^{-1} (line H) and 2920 cm^{-1} (line D) and used an assumed value of 2 (this value has been open to question) for the ratio of absorption strength for aliphatic and aromatic C-H bonds. The ratio of extinction coefficients determined in the present study are in reasonable agreement with those determined by Brown thus the absorption strength ratio must be approximately 4 to produce the measured values of H_{aro}/H_{ali}.

THERMAL DECOMPOSITION

The progress of thermal decomposition is illustrated by the series of spectra for chars in Fig. 7. The chars were produced by devolatilizing coal PSOC 212 for 80 sec at the indicated temperature. The results are similar to those observed by Brown (13) and Oelert (14). The rapid disappearance of the aliphatic and hydroxyl peaks is apparent. The temperature and time dependence of the decrease in these groups is in agreement with the kinetic constants of Table I obtained from analysis of the gas components and elemental composition of the char and tar in thermal decomposition. The aromatic peaks remain to high temperature and the ether peaks are observed to increase in intensity possibly from the creation of new ether linkages by



For high temperature chars whose carbon content exceeds 92 percent a broad absorption begins to dominate the spectrum. This is similar to the effect observed in high rank coals (above 92% C) which has been attributed to electronic absorption (8,9).

Figure 8 shows the quantitative determination of the hydrogen functional group distribution for the chars in Fig. 7. Figure 9 shows the measured hydrogen content and model prediction. The agreement is good. Comparison of Figs. 8 and 9 clearly shows how the low temperature loss of aliphatic material and tar and the retention

of aromatic hydrogen produced the observed shape for the curve of total hydrogen content vs. temperature. The distribution of other products of thermal decomposition for the same coal is shown in Figs. 10 and 11.

The thermal decomposition model was developed using model parameters derived from the decomposition experiments (1,2,3). The observed relationship between the products and the functional group compositions determined from ir measurements indicates that several of these model parameters may be obtained directly from the ir spectra. A comparison of parameters determined from the thermal decomposition experiments with those determined from the ir measurements is made in Fig. 12. Additional parameters may also be determined in the same way.

CONCLUSIONS

The results of the present investigation have yielded the following conclusions:

1. FTIR provides a convenient tool for obtaining quantitative infrared spectra of coals, chars and tars on a dry mineral matter free basis.
2. The spectra of all the coals, chars and tars studied could be deconvoluted by varying the magnitudes of a set of 26 Gaussians whose width and position were held constant. This provides a good way for determining magnitudes of individual peaks.
3. Correlation of the magnitudes of the 1600 cm^{-1} peak with the hydroxyl content of a variety of coals, tars and chars indicates that hydroxyl, probably in the form of phenols, contributes strongly to this peak.
4. A regression analysis applied to a series of coals, chars and tars with widely differing ratios of aliphatic to aromatic hydrogen has been used to calibrate the aliphatic and aromatic C-H absorption intensities.
5. The values of aromatic hydrogen for coals derived from the infrared analysis are in reasonable agreement with those of van Krevelen (8) and Mazumdar (11) but are roughly a factor of 2 larger than those derived by Brown (12).
6. Infrared spectra of a series of coals and tars demonstrate the very close similarity of tars to their parent coals providing further evidence that the tar consists of hydrogen stabilized "monomers" derived from decomposition of the coal "polymer".
7. The variation of functional group concentrations in the products of thermal decomposition is in good agreement with the predictions of a detailed thermal decomposition model (1,2,3).
8. Most of the coal parameters used in the thermal decomposition model may be obtained directly from an infrared, ultimate and proximate analysis of the coal allowing prediction of thermal decomposition behavior from a general set of kinetic constants applicable to lignite and bituminous coals.

ACKNOWLEDGEMENT

The author wishes to acknowledge the able technical assistance of David Santos and Gerald Wagner and helpful discussions with Med Colket and Daniel Seery. The thermal decomposition studies upon which this work was based was supported in part by Grant #AER75-17247 from the National Science Foundation under the technical supervision of the Department of Energy.

REFERENCES

1. Solomon, P. R., "The Evolution of Pollutants During the Rapid Devolatilization of Coal," Report NSF/RA-770422, NTIS #PB278496/AS.
2. Solomon, P. R., and Colket, M. B.: Seventeenth Symposium (International) on Combustion, the Combustion Institute (to be published).
3. Solomon, P. R., and Colket, M. B.: Fuel, to be published.
4. Orning, A. A., Greifer, B.: Fuel 35, 381 (1956).
5. Brown, J. K., Dryden, I. G. C., Dunevein, D. H., Joy, W. K., and Pankhurst, K. S.: J. Inst. Fuels 31, 259 (1958).
6. Wolfs, P. M. J., van Krevelen, D. W. and Waterman, H. I.: Fuel 39 25, (1960).
7. Painter, P. C., Coleman, M. M., Jenkins, R. G., and Walker, P. L., Jr.: Fuel 57 124 (1978).
8. Lowry, H. H.: Chemistry of Coal Utilization (Supplementary Volume), Wiley, NY (1963).
9. van Krevelen, D. W., and Schuyer, J.: Coal Science, Elsevier, Amsterdam (1957).
10. Fujii, S., Ōsawa, Y., and Sugimura, H.: Fuel 49 68 (1970).
11. Ōsawa, Y., and Shih, J. W.: Fuel 50 53 (1971).
12. Brown, J. K.: J. Chem. Soc. 744 (1955).
13. Brown, J. K.: J. Chem. Soc. 752 (1955).
14. Oelert, H. H.: Fuel 47 433 (1968).

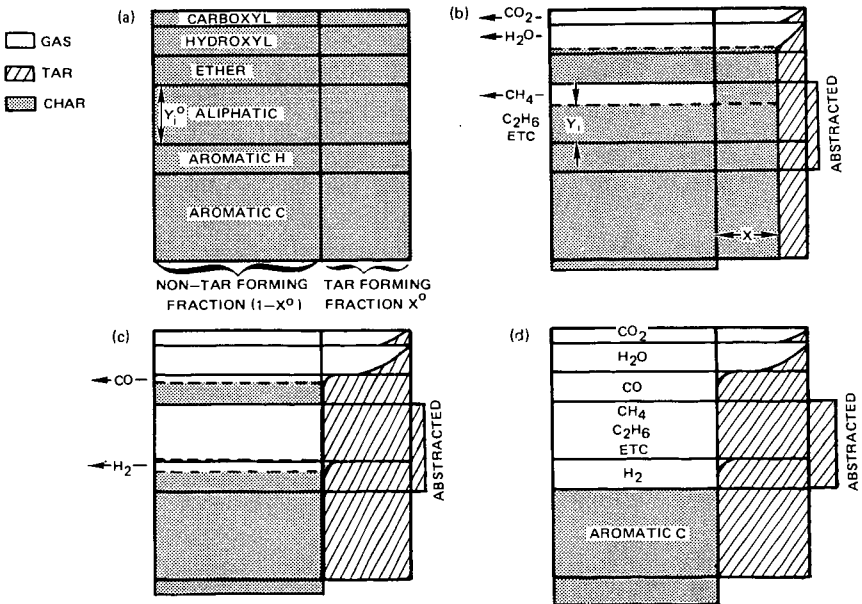


Figure 1 Progress of Thermal Decomposition a) Functional Group Composition of Coal
 b) Initial Stage of Decomposition c) Later Stage of Decomposition
 d) Completion of Decomposition

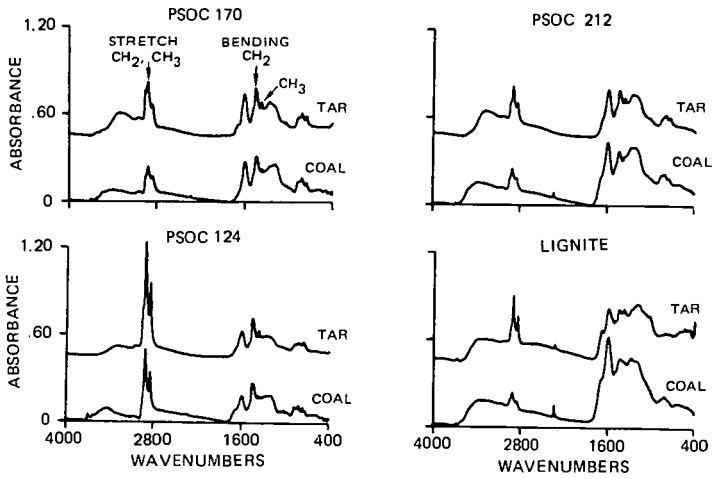


Figure 2. Infrared Spectra of Coals and Tars

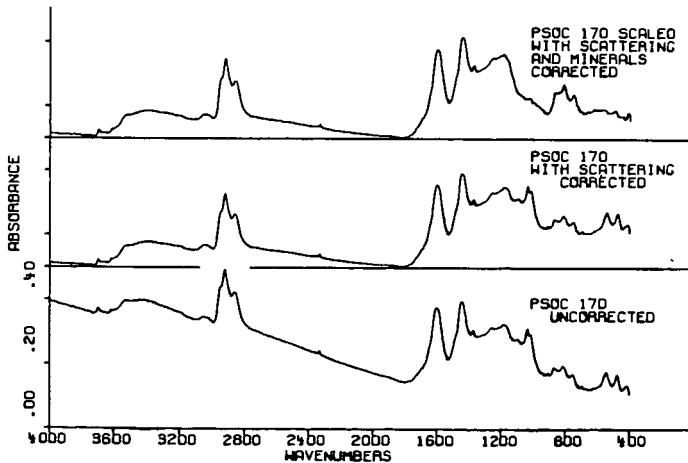


Figure 3. Correction of Coal Spectrum for Scattering and Minerals

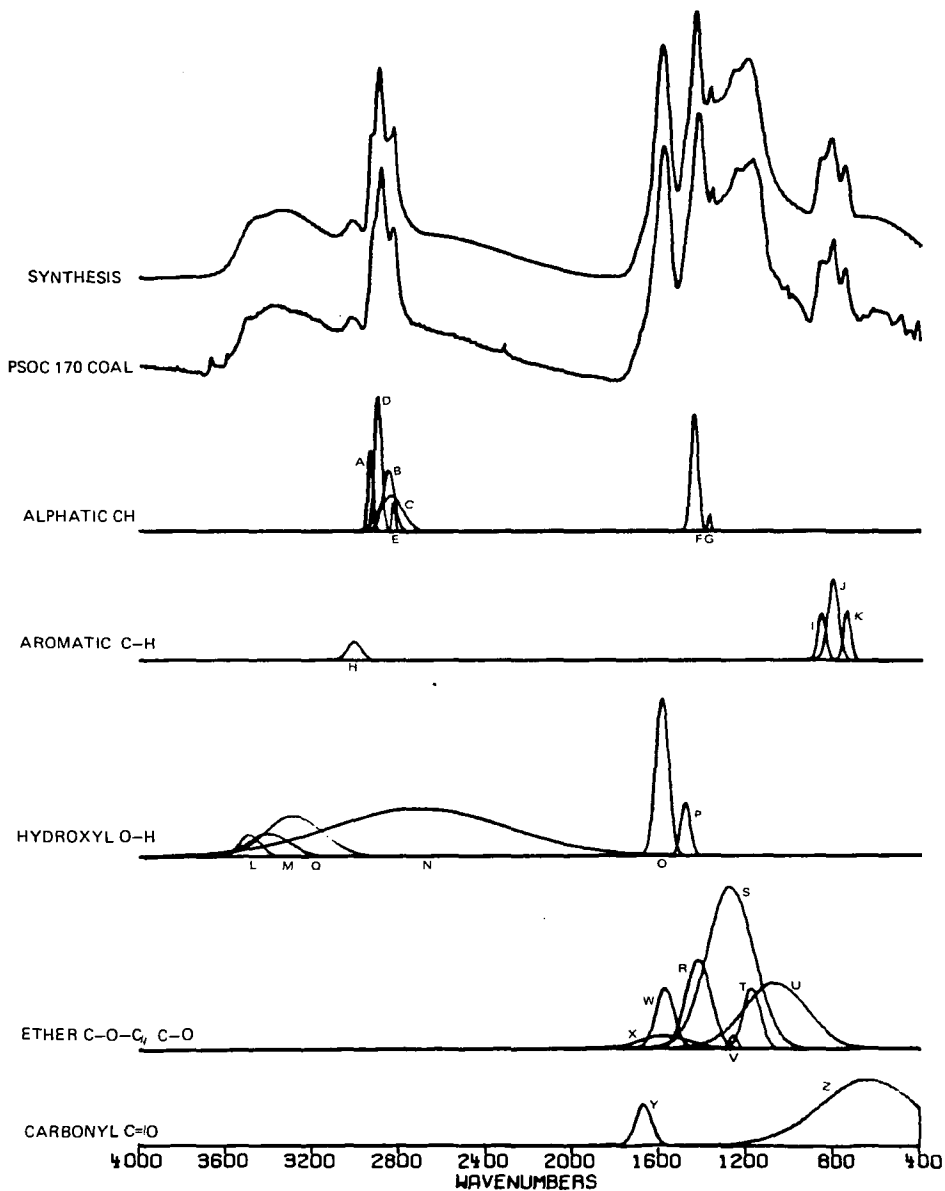


Figure 4. Synthesis of Infrared Spectrum

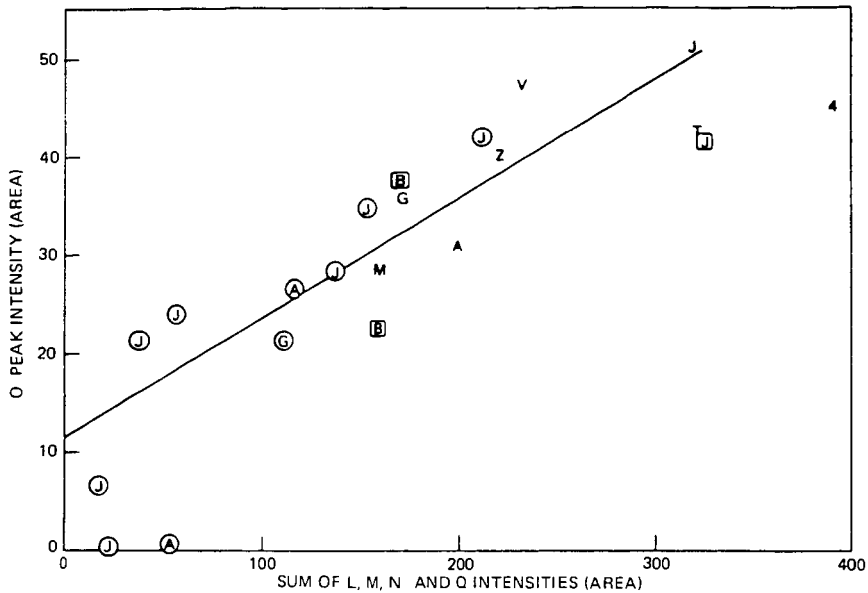


Figure 5. Correlation of 1600 cm^{-1} Absorption with OH Absorption Intensity. Letters Designate Coals; See Table II. \circ Chars \square Tars

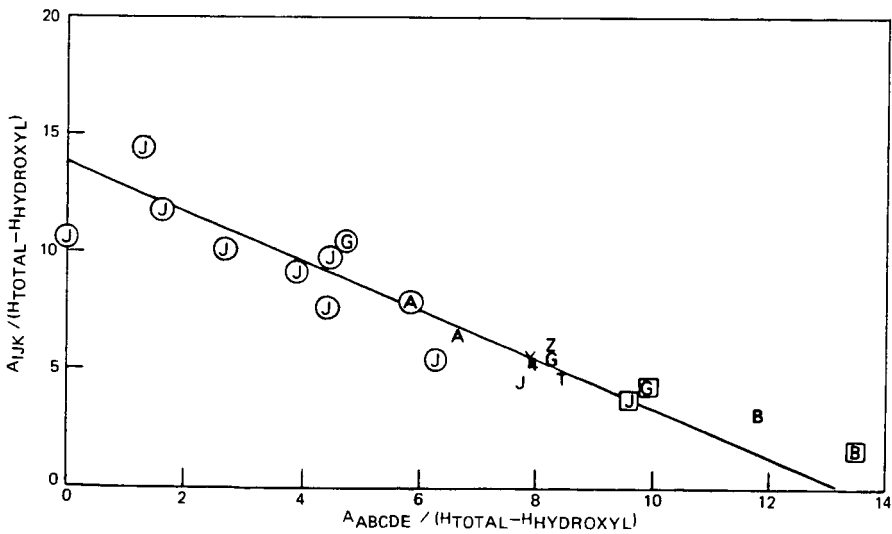


Figure 6. Calibration of Aromatic and Aliphatic Absorption Peaks. Letters Designate Coals; See Table II. \circ Chars \square Tars

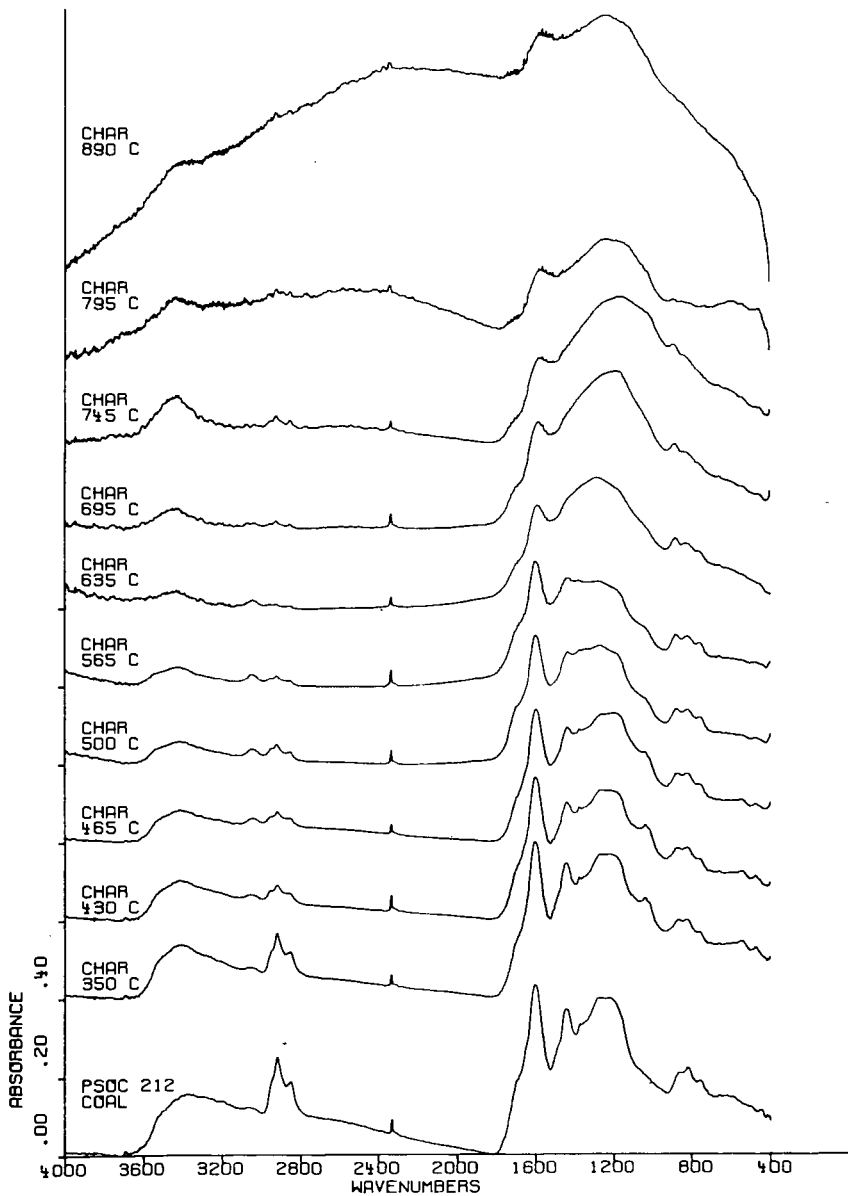


Figure 7. Spectra of Chars

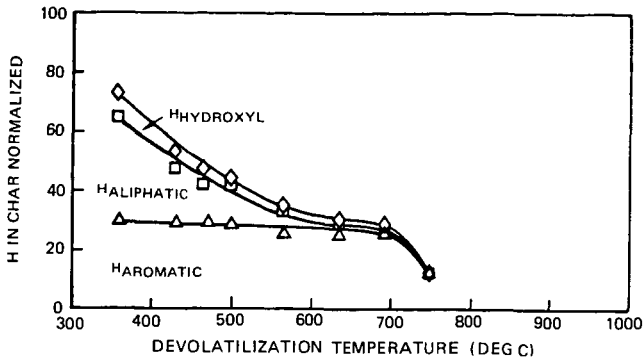


Figure 8. Hydrogen Distribution in Char from Infrared Analysis – The Hydrogen in the Char is Normalized by the Amount of Hydrogen in the Starting Coal Sample

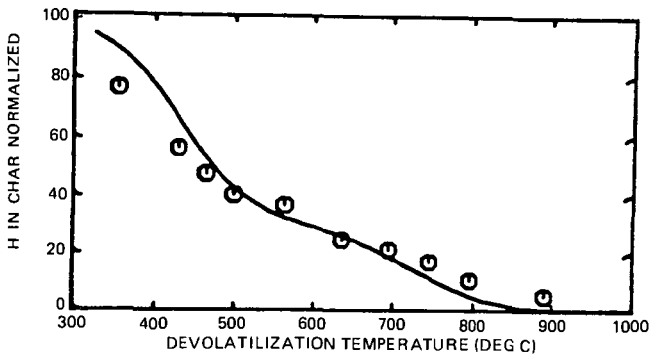


Figure 9. Hydrogen in Char—Experiment and Theory – The Hydrogen in the Char is Normalized by the Amount of Hydrogen in the Starting Coal Sample.

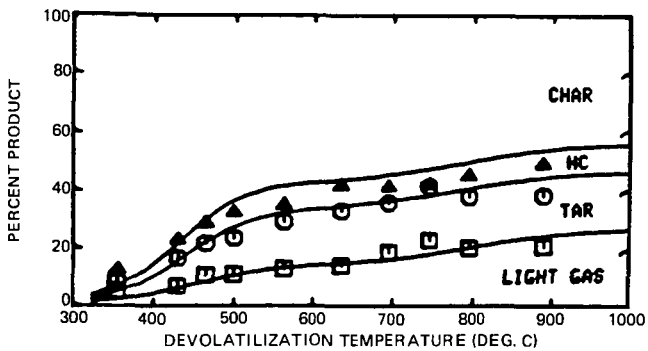


Figure 10. Products of Thermal Decomposition – Experiment and Theory

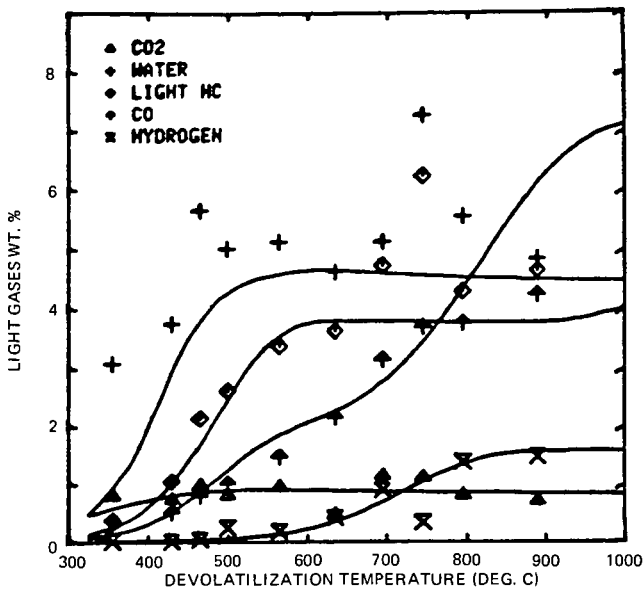


Figure 11. Products of Thermal Decomposition - Experiment and Theory

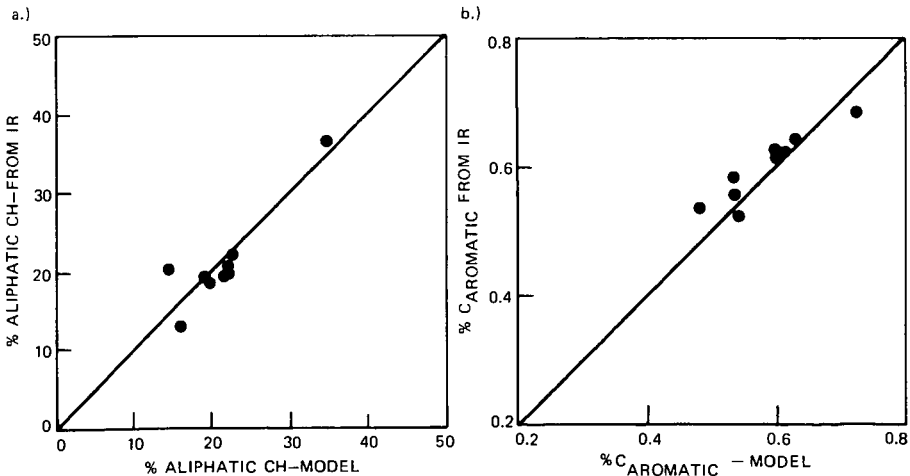


Figure 12. Comparison of Model Parameters with IR Intensity

Characterization of Hydrolytically Solubilized Coal

Randall E. Winans, Ryoichi Hayatsu, Robert L. McBeth,
Robert G. Scott, Leon P. Moore, and Martin H. Studier

Chemistry Division
Argonne National Laboratory, Argonne, Illinois 60439

INTRODUCTION

In a search for relatively mild methods for solubilizing coal, we have found that treating a bituminous coal with potassium hydroxide in ethylene glycol at 250°C is quite effective. The use of alkali in protic solvents is not new. Recently, Ouchi and co-workers (1) have reported in detail the reaction of coal with ethanolic KOH from 260° to 450°C. Also, Ross and Blessing have looked at both iPROH/iPROK (2) and MeOH/KOH systems at 400°C (3). In an early study Pew and Withrow found that the yield of 2-ethoxyethanol extract at 135°C for a bituminous coal increased from 9.4% to 31.3% with the addition of KOH (4). In general at lower temperatures (< 250°C) it has been found that only low rank coals are appreciably solubilized (1). We feel that the glycol is playing a special role in producing a soluble product and have characterized this product in order to understand the chemistry involved. Our conclusions are similar to those given by Ouchi (1).

We decided to use glycol as a solvent for several reasons. First, the results of Pew and Withrow (4) indicate that glycol and KOH have special properties and therefore more drastic conditions could give improved extract yields. It is easier to obtain higher reaction temperatures with glycols without using an autoclave. Finally, cleavage of C-C bonds has occurred as side reactions in Wolf-Kishner reductions (5). Also, alkaline hydrolysis at high temperatures (> 200°C) will cleave ethers (6,7) and carbonyls (7). The original objective of these experiments was to cleave these linkages and to determine their importance in the structure of coal. However, as observed by Ouchi (1) and Ross (2,3) apparently reduction is involved also as seen in the increased H/C ratio and decrease in aromatic carbons. We shall show that this is a true reduction of aromatic rings in the coal, not just an attachment of the solvent.

In the analysis of the glycol solubilized coal we have applied all the techniques used in our studies on coals, SRC and SRL products (8). The effect of the reaction on the aromatic units was shown by comparing selective oxidation products from the coal and its hydrolytic product. These results were compared with the aromaticity of the product determined by C-13 nmr. The molecular size distribution was determined using gel permeation chromatography (GPC). Also, we compared the products from glycols to those from water and alcohol alkaline hydrolysis.

EXPERIMENTAL

In a typical reaction 15 g of Illinois #2 high volatile bituminous coal [73.9% C, 5.2% H, 1.4% N, 3.4% total S (1.2% organic S), 16.1% O (by difference) on a maf basis] which was extracted by refluxing

with benzene/MeOH (3/1) was mixed with 20 g potassium hydroxide and 200 g of solvent and heated at 250°C in a rocking autoclave for 2-3 hours. With triethylene glycol the reaction was also run at atmospheric pressure under a nitrogen sweep. The autoclave was cooled and the gases produced were collected for mass spectrometric analysis. The homogeneous, alkaline, reaction mixture was poured into water, acidified with conc. HCl, filtered and dried *in vacuo* at 100°C. The product was successively extracted with hexane, benzene-methanol (1:1) and pyridine under reflux with the results shown in Table 1.

The hexane insoluble product from Reaction No. 1 and the original coal were derivatized with d₆-dimethylsulfate and oxidized with aq. Na₂Cr₂O₇ at 250°C for 38-48 hours (8). The resulting aromatic acids were derivatized with diazomethane and analyzed by gas chromatography mass spectrometry. The identifications of the esters were confirmed from retention times and mass spectra of authentic compounds, from published data and from high resolution mass spectrometric analysis of the mixture.

The molecular size distribution was determined using gel permeation chromatography with a series of four μ-styragel columns (500 Å, 3 x 100 Å). Tetrahydrofuran was used as the elution solvent with a UV detector set at 254 nm (see Fig. 1, Reaction 1 product). Calibration curves (Figure 2) were obtained under the same conditions for linear polymers and a series of aromatic hydrocarbons.

The C-13 nmr spectra were obtained on a Bruker WP-60 at 15.08 MHz, with 3 sec delays, no decoupling and typically 50,000 scans. The samples of chloroform soluble product were made up to 50% (w/v) in deuteriochloroform.

RESULTS AND DISCUSSION

In the initial experiments with triethylene glycol (TEG) it was noticed that the H/C of the product (1.08) was significantly higher than that of the coal (0.84). This would indicate that either reduction or solvent attachment or both were occurring. Also, the yield of solid product was greater than the amount of the original coal. The hexane extract, which was significant in this case (11.9%), was shown by solid probe MS and GCMS to be mostly glycol degradation products. When ethylene glycol was used there was no increase in weight and the amount of hexane extractable material was reduced. Both Ouchi (1) and Ross (2,3) observed an H/C increase with the alcohols.

With the increase in H/C ratio one would expect a decrease in the fraction of aromatic carbons (fa). From the C-13 nmr spectra (Fig. 3) the fa for product #1 was determined to be 0.50. This same coal has been shown by fluorination to have an fa of approximately 0.69 (9). The attachment of ethylene glycol groups (ROCH₂CH₂-O-COAL) has been determined to be 5.1% of carbons from the integration of the peaks from 55-65 ppm. We have found these peaks to be absent in other coal products such as SRC. Also, the importance of the carbonyl carbon peak at 215 ppm will be discussed later. However, these data do not exclude the reaction of ethylene (CH₂=CH₂) with the coal as mentioned by Ouchi (1).

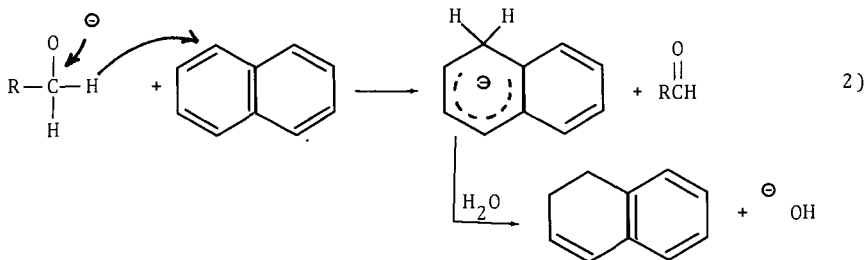
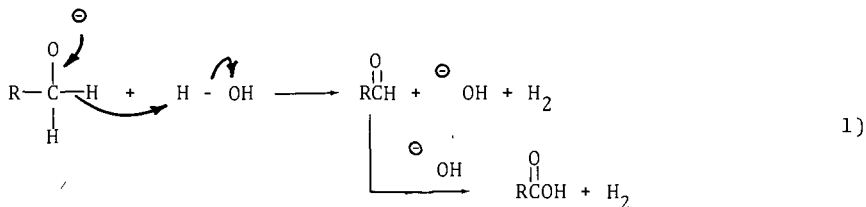
The best evidence for the occurrence of polycyclic aromatic ring reduction is the comparison of the aq. Na₂Cr₂O₇ oxidation products of the hydrolytic product with those of the original coal (Table 2).

The gas chromatogram for the volatile methyl esters from the original coal oxidation is shown in Figure 4 with identification in Table 3. As we have shown before a significant amount of polycyclic aromatics such as phenanthrene and naphthalene carboxylic acids and hetero-aromatics including dibenzofuran and xanthone carboxylic acids were isolated (8). Figure 5 is the gas chromatogram for the oxidation products from the hydrolytic product with peak identification in Table 3. The major products are benzene, methoxybenzene, and methylbenzenecarboxylic acids. The acids from the coal and hydrolytic product are compared in Table 2. It is obvious that the polycyclic aromatics and heteroaromatics have been reduced and degraded. As expected the furan ring in dibenzofuran was destroyed. Since aqueous alkali treatment has been used as a method for removal of sulfur from coal (10), it is not surprising that in Reaction #1 the total sulfur was reduced from 3.5% (1.2% organic) to 0.72%. Most of the loss was due to the removal of inorganic sulfur, but a significant amount of organic sulfur including dibenzothiophene was removed. The yield of phenanthrene and anthracene (isolated as anthraquinones) carboxylic acids has been reduced to a nondetectable level. We and Ross (3) have observed independently that anthracenes are reduced with alcoholic alkali. The greater amount of hydroxybenzene compounds in the product indicate that as expected aryl and arylalkyl ethers have been cleaved. The exception to this is the aryl methyl ethers which from the labeling experiments with d_6 -dimethylsulfate appear to be stable.

Other characteristics of the hydrolytic product can be seen in the gel permeation chromatogram shown in Figure 1. For comparison it has been superimposed on a chromatogram for a SRC (11) using the same amount of sample. The hydrolytic product has a higher molecular weight distribution than the SRC. Using the aromatic hydrocarbon curve from Figure 1, the M.W. runs from approximately 350 to 1500. Because of the lower temperature of the reaction (250° compared to 450°C), this coal has not been so extensively fragmented. The lower UV absorption of the hydrolytic product (HSC) again indicates a lower aromaticity compared with the SRC which has an $f_a = 0.85$ from C-13 nmr data. Figure 2 demonstrates a problem encountered in using GPC for coal product analysis, that is which standards should be used. We chose the aromatic hydrocarbons because they were more representative of the hydrolytic product than linear polymers.

From examination of Table 1 it is evident that glycol is superior to other protic solvents for hydrolysis. There are at least two possible reasons for this. First, the glycol is better at solvating the positive ion. Secondly, the glycol may be more effective for reducing the aromatics in coal. Even in a nonpolar solvent such as toluene (Reaction #3) TEG brought the KOH into solution and gave a substantial yield of soluble product. The effects of base strengths were examined by changing the alkali metal using Li^+ , Na^+ , K^+ , Rb^+ and Cs^+ . However, no trends were found in the extraction yields and the GPC indicated a possible increase in M.W. with increase in size of the ion.

The alkaline oxidation of alcohols and glycols is thought to involve hydride transfer with the intermediate formation of the corresponding aldehyde (7,12) (Eq. 1).



Therefore, a possible pathway for reduction is by a hydride transfer to an activated aromatic ring (Eq. 2). Hydrogenation with H_2 can be ruled out for two reasons. First, there are no active catalysts available. Secondly, the triethylene glycol reactions were conducted in an open system so that the H_2 could escape and yet the decrease in aromatic carbon was observed. Also alkaline oxidation of reduced phenols and alcohols could account for the carbonyls seen in the C-13 nmr spectra.

CONCLUSIONS

From the characterization of the hydrolytically solubilized coal with glycols the following observations can be made: 1. The polycyclic aromatic rings are being reduced. A possible mechanism is hydride transfer from the solvent. Also oxygen heteroaromatics are destroyed. 2. Arylalkyl ethers are being cleaved by this process. 3. The ability of the glycols to chelate the positive alkali metal ion could contribute to the enhanced yields of soluble coal compared to other protic solvents.

This study demonstrates the utility of using a multi-pronged analytical and chemical approach to the study of non-volatile coal products.

ACKNOWLEDGEMENTS

This work was supported by the Department of Energy-Fossil Energy, Division of Coal Conversion-Liquefaction. Chemical and instrumental techniques used were developed with support from the Office of Basic Energy Sciences.

REFERENCES

1. Makabe, M., Hirano, Y., and Ouchi, K., *Fuel*, 57, 289 (1978).
2. Ross, D. S., and Blessing, J. E., Preprints, *Div. of Fuel Chemistry, Am. Chem. Soc.*, 22(2), 208 (1977).
3. Ross, D. S., and Blessing, J. E., Homogeneous Catalytic Hydrocracking Processes for Conversion of Coal To Liquid Fuels: Basic and Exploratory Research, ERDA-FE-2202-21, Quarter ending July 31, 1977 SRI.
4. Pew, J. C., and Withrow, J. R., *Fuel*, 10, 44 (1931).
5. Reusch, W., in "Reduction," R. L. Augustine, Ed., Marcel Dekker, N. Y., p. 184 (1968).
6. Staude, E., and Patat, F., in "The Chemistry of the Ether Linkage," S. Patai, Ed., Interscience, N.Y., p. 47 (1967).
7. Weedon, B. C. L., Alkali fusion and some related processes in Elucidation of Organic Structures by Physical and Chemical Methods (Eds. by K. W. Bentley and G. W. Kirby), Part II, Wiley-Interscience, N. Y. (1973).
8. Hayatsu, R., Winans, R. E., Scott, R. G., Moore, L. P., and Studier, M. H., *Fuel*, 57, 541 (1978).
9. Huston, J. L., Scott, R. G., and Studier, M. H., *Fuel*, 55, 281 (1976).
10. "Liquefaction and Chemical Refining of Coal," Battelle Energy Program Report, Battelle Columbus, Columbus, Ohio (1974).
11. A solvent refined Pittsburgh #8 bituminous coal from Wilsonville, Alabama.
12. Dytham, R. A., and Weedon, B. C. L., *Tetrahedron*, 9, 246 (1960).

Table 1
Yields and Solubilities of the Hydrolytic Coal Products in Weight Percent^a

| Reaction # | Solvent | Yield | Hexane | Benzene/ MEOH(1/1) | Pyridine | Insoluble |
|------------|--------------------------|-------|--------|-----------------------|----------|-----------|
| 1 | Triethylene glycol (TEG) | 123 | 11.9 | 46.8 | 37.3 | 4.1 |
| 2 | Ethylene glycol | 90 | 1.3 | 48.9 | 42.2 | 7.4 |
| 3 | Toluene-TEG ^b | 124 | 0.6 | 46.6 ^c | 35.1 | 17.7 |
| 4 | Water | 86 | --- | 18.5 | 12.0 | 69.7 |
| 5 | Methanol | 90 | 0.8 | 37.3 ^c | 7.8 | 54.0 |

^aAll reactions at 250°C; ^b1:1 mole ratio of TEG and KOH; ^cIncludes solids soluble in the reaction solvent.

Table 2
Relative Mole Abundances from the GC Data of the Volatile Aromatic Carboxylic Acids from the Oxidation of the Coal and its Hydrolytic Product

| Carboxylic acids of: | Illionois #2 Bituminous Coal | Hydrolytic Product from Reaction #1 (Table 1) |
|-----------------------|---------------------------------|--|
| Benzene | 100 | 100 |
| Hydroxybenzene | 1.4 | 10 |
| Methylbenzene | 2.3 | 7 |
| Naphthalene | 7.2 | 1 |
| Phenanthrene | 1.1 | --- |
| Dibenzofuran | 1.5 | 0.4 |
| Xanthone | 1.3 | --- |
| Dibenzothiophene | 0.5 | --- |
| Other Heteroaromatics | 2.8 | <1 |

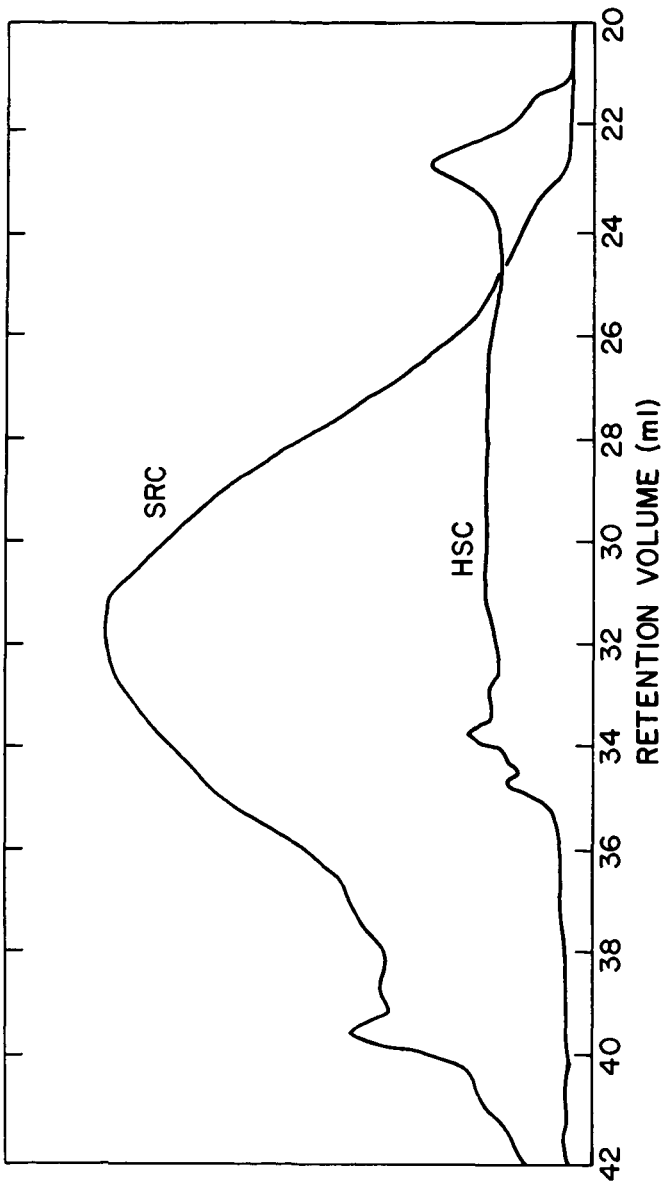
--- not detected.

Table 3
Methyl Esters of the Oxidation Products from Coal (Figure 4) and the Hydrolytic Product (Figure 5)

| Peak No. | | Compound | | |
|----------|---------|----------|---|--|
| Coal | Product | | | |
| | 1 | Methyl | succinate | |
| | 2 | Methyl | methylsuccinate | |
| | 3 | Methyl | benzoate | |
| | 4 | Methyl | methylfurancarboxylate | |
| | 5 | Methyl | methylbenzoate | |
| | 9 | Methyl | methoxybenzoate (+d ₃ -methoxy) | |
| | 11 | Methyl | methoxymethylbenzoate | |
| | 12 | 1 | Methyl | furandicarboxylate |
| | 13 | 2 | Methyl | 1,2-benzenedicarboxylate |
| | 14 | 3 | Methyl | 1,4-benzenedicarboxylate |
| | 15 | 4 | Methyl | 1,3-benzenedicarboxylate |
| | 5,7,8 | Methyl | methoxy-(methoxy-d ₃)-benzoate(T) | |
| | 16 | 6,9,10 | Methyl | methylbenzenedicarboxylate |
| | 17 | Methyl | naphthalenecarboxylate | |
| | 11 | Methyl | pyridinedicarboxylate | |
| | 19 | 13 | Methyl | methoxybenzenedicarboxylate (+d ₃ -methoxy) |
| | 12,14 | Methyl | (methoxy-d ₃)-benzenedicarboxylate | |
| | | Methyl | dimethylfurandicarboxylate | |
| | | Methyl | biphenylcarboxylate | |
| | 16 | Methyl | 1,2,4-benzenetricarboxylate | |
| | 17 | Methyl | 1,2,3-benzenetricarboxylate | |
| | 18 | Methyl | unidentified m/e 261,230 | |
| | 19 | Methyl | 1,3,5-benzenetricarboxylate | |
| | 20-23 | Methyl | methylbenzenetricarboxylate | |
| | 26 | Methyl | dibenzofurancarboxylate | |
| | 24,25 | Methyl | naphthalenedicarboxylate | |
| | | Methyl | pyridinetricarboxylate | |
| | 26 | Methyl | methoxybenzenetricarboxylate (+d ₃ -methoxy) | |
| | 27-29 | Methyl | (methoxy-d ₃)-benzenetricarboxylate | |
| | | Methyl | fluorenonecarboxylate | |
| | 30 | Methyl | 1,2,4,5-benzenetetracarboxylate | |
| | 31 | Methyl | 1,2,3,4-benzenetetracarboxylate | |
| | 32 | Methyl | 1,2,3,5-benzenetetracarboxylate | |
| | 33,34 | Methyl | methylbenzenetetracarboxylate | |
| | | Methyl | phenanthrenecarboxylate | |
| | | Methyl | dibenzothiophenecarboxylate | |
| | | Methyl | xanthonecarboxylate | |
| | | Methyl | anthraquinonecarboxylate | |
| | 35,36 | Methyl | naphthalenetricarboxylate | |
| | | Methyl | methylxanthonecarboxylate | |
| | 37 | Methyl | dibenzofurandicarboxylate | |
| | 38 | Methyl | benzenepentacarboxylate | |
| | | Methyl | benzoquinolinecarboxylate | |
| | | Methyl | phenanthrenedicarboxylate | |
| | | Methyl | carbazolecarboxylate | |
| | | Methyl | xanthonecarboxylate | |

T indicates that identification is tentative.

Figure 1. Gel permeation chromatogram of hydrolytic product (HSC) from Reaction #1 and of a solvent refined coal (SRC) from Wilsonville, Alabama.



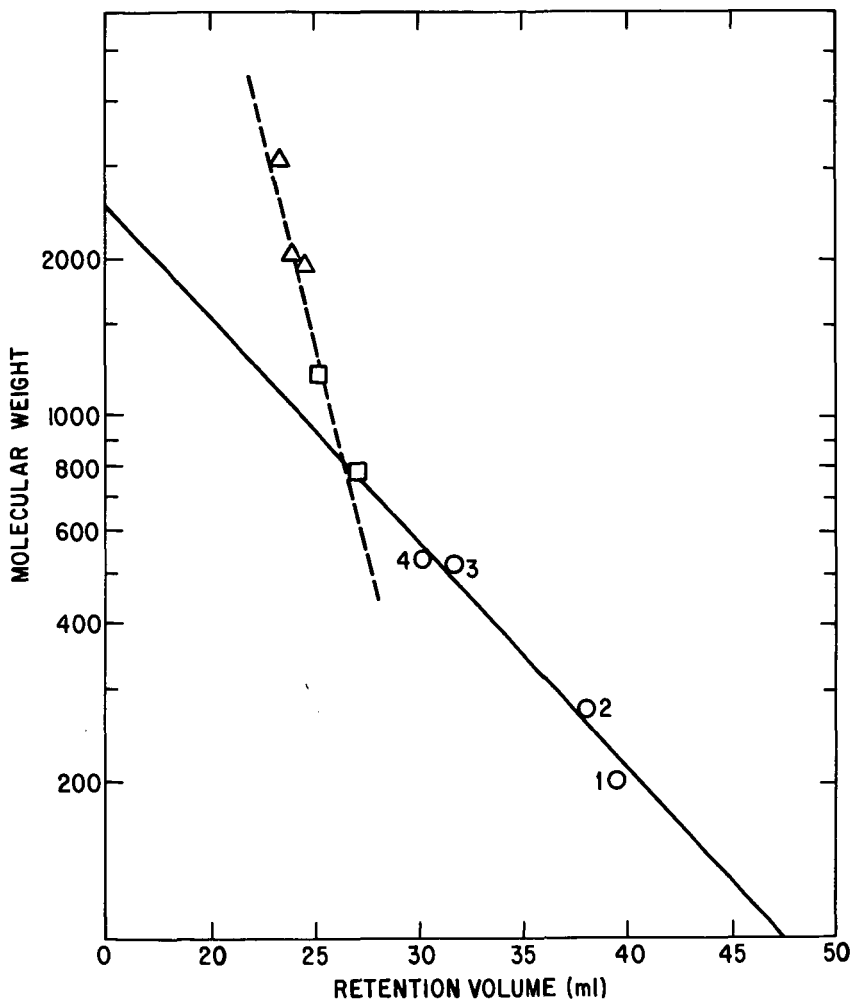


Figure 2. Calibration curves for GPC. \circ - aromatics, \square polyethylene standard, and \triangle polystyrene standard.

Figure 3. C-13 nmr spectra of hydrolytic product from Reaction #1, in ppm from TMS.

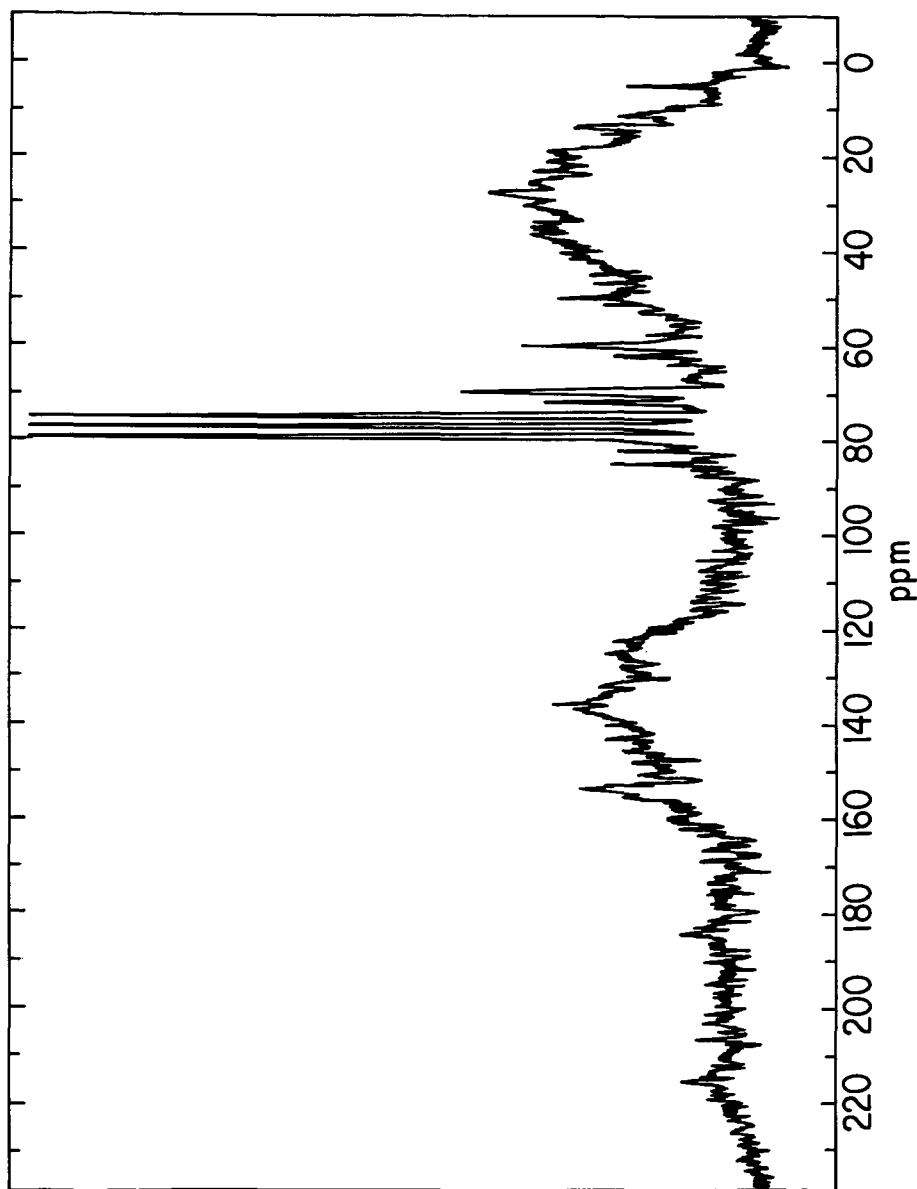


Figure 4. Gas chromatogram of methyl esters from the oxidation of Illinois #2 bituminous coal. Separated on an OV-17 support coated open tubular column (SCOT), temperature programmed at 100-250°C at 4°/min.

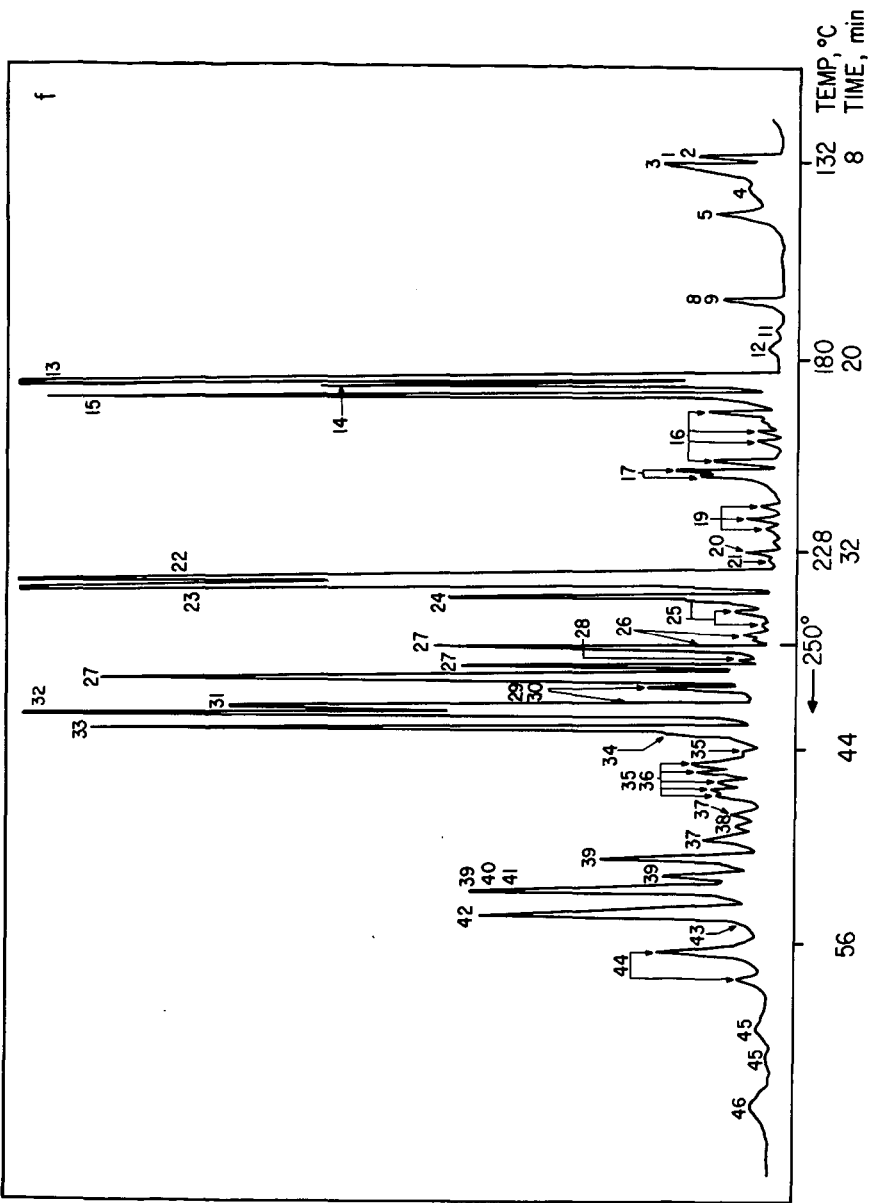
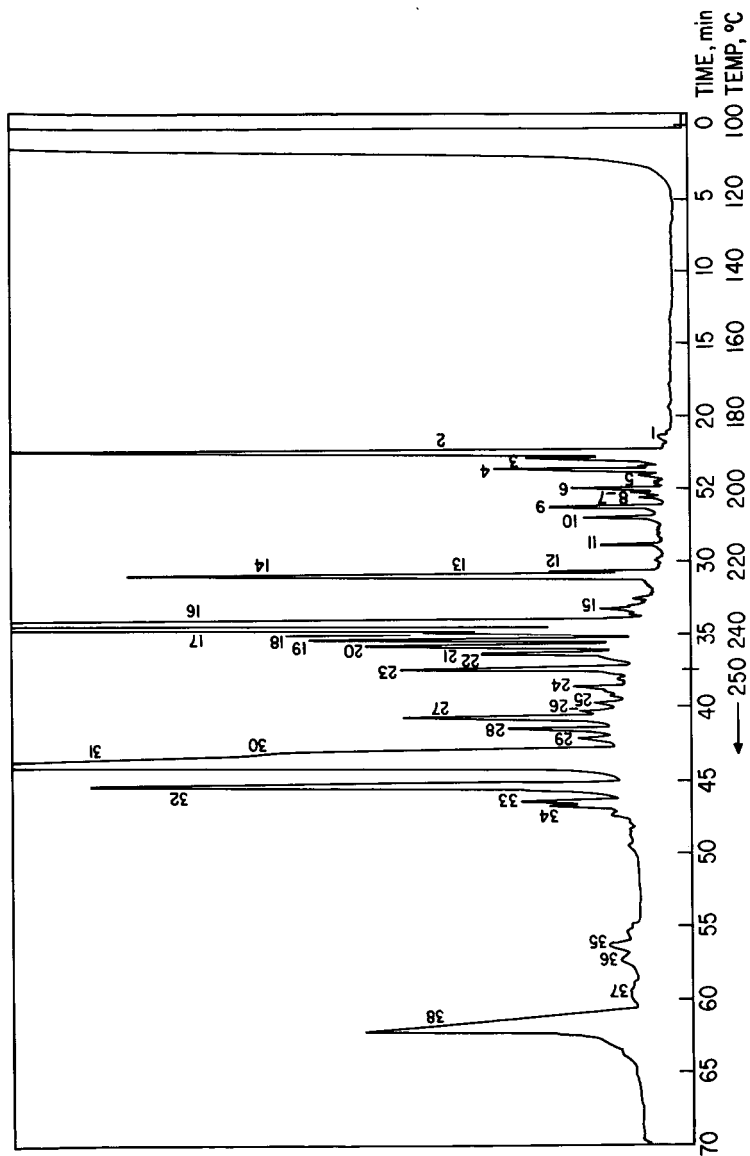


Figure 5. Gas chromatogram of methyl esters from the oxidation of the hydrolytic product from Reaction #1. Same conditions as Figure 4.



OXIDATION OF COALS WITH NITRATE IN CONCENTRATED CAUSTIC SODA SOLUTIONS AT ELEVATED TEMPERATURES.

H. Kawamura, A. Okuwaki, O. Horie, A. Amano and T. Okabe

Department of Applied Chemistry, Faculty of Engineering, Tohoku University, Sendai 980, Japan.

Introduction

Molten alkali nitrate, a strong oxidizing agent having low melting point, is interesting to use as an oxidizing agent and solvent in the oxidation reactions of both inorganic and organic compounds. Previously, we have applied caustic soda-sodium nitrate melt to the production of chromate or oxyacids of manganese. In the present paper, we have examined it for the oxidation of coals, thereby studying the effects of rank, reaction temperature, concentrations of caustic soda and sodium nitrate, and pre-oxidation on the yields of oxidation products. Benzene-carboxylic acids in the products are currently noted as important raw chemicals.

Experiment

Three kinds of foreign coals, Latrobe coal(Australia), Amax coal(U.S.A.), and Goonyella coal(Australia) were used. Their properties are shown in Table 1. Coal(100-150mesh) 5g, caustic soda 150g, sodium nitrate 0-38g, and water 40g were placed in an autoclave(SUS 304) equipped with a mechanical stirrer, were maintained at 150-300°C for 3 hrs. Alkaline solutions of reaction products were analysed for residue, humic acids(water soluble acids of high molecular weight), and aromatic acids obtained by two stages methyl ethyl ketone extraction from acidified solutions of oxidation products. Nitrate and nitrite in the alkaline solutions were also determined. Aromatic acids were first esterified by diazomethane. Benzenepolycarboxylic acids were then determined as esters by temperature programmed gas chromatography using a SE-30 column.

Table 1. Analyses of sample coals

| Sample | Ultimate analyses(% d.a.f.) | | | | Ash (%d) |
|------------------------|-----------------------------|------|------|-------|-------------|
| | C | H | N | O | |
| Latrobe coal(Victoria) | 64.10 | 4.85 | 0.09 | 30.96 | 1.06 |
| Amax coal(Utah) | 76.53 | 5.22 | 1.77 | 16.48 | 8.87 |
| Goonyella coal(Q'land) | 85.49 | 5.05 | 2.07 | 7.39 | 7.04 |

Results and Discussion

Listed in Table 2 are the results obtained for Latrobe coal. Latrobe coal was found to be easily soluble in the concentrated alkaline solutions leaving a small amount of residue. Aromatic acids as well as humic acids was formed in good yield even in the absence of sodium nitrate. Upon further oxidation at raising temperature and increasing amount of nitrate, however, humic acids gave rise to aromatic acids. The maximum yield of aromatic acids was thus reached at 200°C and 7g of sodium nitrate. The ratio of aromatic acids/humic acids reached maximum at 250°C and 18-38g of sodium nitrate, but the yield of aromatic acids became much higher at the amount of sodium nitrate less than 18-38g. On the other hand, nitrate was reduced by the carbonaceous materials to nitrite and further to nitrogen and ammonia depending on the reaction conditions. In the absence of water, the coal was converted to carbon dioxide and water with the concurrent reduction of nitrate to nitrogen as shown in Table 3. The maximum yield of aromatic acids was

Table 2. Oxidation of Latrobe coal

| Temp. (°C) | Coal (g) | NaNO ₃ (g) | Yields to coal(wt%) | | | Mol ratios to initial NO ₃ (%) | | |
|---------------|------------------|--------------------------|---------------------|-------------|----------------|--|-----------------|------|
| | | | Residue | Humic acids | Aromatic acids | NO ₃ | NO ₂ | |
| L-1 | 150 ^a | 10.43 | 17.36 | 8 | 30 | 30 | 46.6 | 46.1 |
| L-2 | | 12.58 | 44.74 | 8 | 43 | 25 | 79.7 | 18.4 |
| L-3 | | 12.58 | 94.37 | 2 | 43 | 28 | 74.8 | 16.4 |
| L-4 | 200 | 5.035 | 0 | 9 | 40 | 30 | - | - |
| L-5 | | 5.019 | 6.97 | 4 | 30 | 63 | 0 | 48.8 |
| L-6 | | 5.084 | 17.79 | 3 | 20 | 60 | 17.6 | 74.3 |
| L-7 | | 5.034 | 37.80 | 3 | 17 | 35 | 46.3 | 49.2 |
| L-8 | b | 5.029 | 17.97 | 2 | 11 | 53 | 0 | 85.8 |
| L-9 | c | 5.008 | 17.94 | 5 | 10 | 36 | 0 | 89.1 |
| L-10 | 250 | 5.024 | 0 | 4 | 29 | 38 | - | - |
| L-11 | | 5.020 | 6.95 | 3 | 17 | 55 | 0 | 19.5 |
| L-12 | | 5.024 | 17.92 | 2 | 6 | 50 | 3.8 | 86.3 |
| L-13 | | 5.029 | 37.82 | 2 | 2 | 19 | 10.1 | 82.0 |

a; NaOH 400g, b; 6hr, c; 9hr

Table 3. Effect of caustic soda concentration on oxidation of Latrobe coal
(Temp. 250°C. NaOH 5.5g, NaNO₃ 6.3g, time 3hr in a 15ml autoclave)

| | Coal (g) | Water (g) | Yields to coal(wt%) | | | Mol ratios to initial NO ₃ (%) | |
|------|-------------|--------------|---------------------|-------------|----------------|--|-----------------|
| | | | Residue | Humic acids | Aromatic acids | NO ₃ | NO ₂ |
| L-14 | 2.013 | 0 | 1 | 0 | 1 | 0.6 | 5.6 |
| L-15 | 2.032 | 1.4 | 1 | 15 | 40 | 13.7 | 52.7 |
| L-16 | 2.012 | 2.6 | 2 | 16 | 49 | 21.4 | 50.4 |
| L-17 | 2.015 | 3.4 | 3 | 15 | 52 | 29.6 | 46.8 |
| L-18 | 2.032 | 6.4 | 5 | 15 | 40 | 42.4 | 29.5 |

reached at caustic soda concentration of about 60-70% under which the ratios of aromatic acids/humic acids were about 3. It was confirmed that even under the high ratio of coal to the solvent shown in Table 3, Latrobe coal underwent the oxidation by nitrate.

Amax coal was only poorly soluble in concentrated caustic soda solutions and the yields of humic acids and aromatic acids were very low in the absence of sodium nitrate. The amounts of the intermediates increased with increasing amount of sodium nitrate as shown in Table 4.

Table 4. Oxidation of Amax coal

| Temp. (°C) | Coal (g) | NaNO ₃ (g) | Yields to coal(wt%) | | | Mol ratios to initial NO ₃ (%) | | |
|---------------|-------------|--------------------------|---------------------|-------------|----------------|--|-----------------|------|
| | | | Residue | Humic acids | Aromatic acids | NO ₃ | NO ₂ | |
| A-1 | 150 | 5.082 | 21.95 | 83 | 1 | 0 | 94.1 | 5.9 |
| A-2 | 200 | 4.935 | 0 | 78 | 2 | 4 | - | - |
| A-3 | | 5.167 | 7.07 | 41 | 14 | 12 | 18.1 | 70.4 |
| A-4 | | 5.294 | 14.20 | 22 | 15 | 9 | 39.3 | 50.5 |
| A-5 | | 5.192 | 21.18 | 14 | 42 | 23 | 41.4 | 54.2 |
| A-6 | | 5.295 | 38.05 | 16 | 25 | 13 | 72.5 | 27.5 |
| A-7 | a | 4.983 | 22.18 | 70 | 4 | 4 | 92.2 | 5.9 |
| A-8 | b | 5.084 | 21.49 | 14 | 23 | 14 | 49.8 | 43.9 |
| A-9 | c | 5.014 | 21.60 | 16 | 45 | 21 | 38.6 | 56.3 |
| A-10 | 250 | 5.091 | 0 | 78 | 4 | 6 | - | - |
| A-11 | | 5.123 | 7.11 | 13 | 33 | 25 | 0 | 55.5 |
| A-12 | | 5.138 | 21.72 | 5 | 36 | 29 | 0.8 | 95.3 |
| A-13 | | 5.100 | 37.83 | 10 | 20 | 27 | 19.3 | 71.5 |

a; 1hr, b; 6hr, c; 9hr

The formation of the intermediates reached at its maximum with 21g sodium nitrate. The maximum yield of aromatic acids was reached at 250°C, but lower than that observed for Latrobe coal. The ratios of aromatic acids/humic acids were consistently lower than those for Latrobe coal.

Goonyella coal, sparingly soluble under the hydrothermal conditions, was treated in caustic soda-sodium nitrate melts at 300°C. More than 50% of Goonyella coal was recovered as residue giving rise to only as low as 2-6% of intermediary formation of humic acids and aromatic acids, since the latter were readily oxidized. Consequently, it seems difficult to obtain aromatic acids in good yield directly from a higher rank coal such as Goonyella coal by the oxidation with nitrate in caustic melts.

When Goonyella coal and Amax coal preoxidized in air were reacted with nitrate in concentrated caustic soda solutions at 250°C for 3hrs, the yields of the oxidation products were improved remarkably as shown in Table 5.

Table 5. Oxidation of the coals pre-oxidized in air
Goonyella coal: Air oxidation; 300°C, 5hr

| | Coal | | Temp. (°C) | NaNO ₃ (g) | Yields to coal (wt%) | | | Mol ratios to initial NO ₃ ⁻ (%) | |
|--------------------------------------|------------------------------|-------|---------------|--------------------------|----------------------|-------------|----------------|--|-----------------|
| | Wt. loss on oxidn. (g) | (wt%) | | | Residue | Humic acids | Aromatic acids | NO ₃ ⁻ | NO ₂ |
| G-1 | 5.320 | 5.4 | 250 | 0 | 21 | 36 | 10 | - | - |
| G-2 | 5.321 | 4.8 | | 6.59 | 18 | 30 | 28 | 0 | 68.5 |
| G-3 | 5.319 | 2.8 | | 17.94 | 6 | 27 | 42 | 0 | 90.0 |
| G-4 | 5.318 | 4.9 | | 37.72 | 6 | 8 | 24 | 22.5 | 65.9 |
| G-5 | 5.492 | 5.4 | 300 | 17.90 | 4 | 19 | 25 | 0 | 62.8 |
| Amax coal: Air oxidation; 300°C, 5hr | | | | | | | | | |
| A-14 | 5.529 | 17.5 | 250 | 17.91 | 6 | 12 | 42 | 0 | 90.1 |
| Amax coal: Air oxidation; 250°C, 5hr | | | | | | | | | |
| A-15 | 5.507 | 4.9 | 250 | 17.93 | 4 | 20 | 53 | 0 | 82.9 |

Air-preoxidized Goonyella coal dissolved appreciably in the alkaline solutions and formed the intermediates. Humic acids decreased with increasing amount of sodium nitrate. Aromatic acids, however, reached maximum at 18g of sodium nitrate. When air-preoxidized Amax coal was used, the yields of aromatic acids were considerably improved. The drastic increase in the oxygen content from 7.4 to 28.3% and the appearance of carbonyl absorption in IR range upon the preoxidation of Goonyella coal suggest the significant structural and constitutional changes in a manner suitable for the oxidation.

From the results described it was made clear that the oxidation became more difficult for coals of higher rank. In general, it is well known in the oxidation of coal that the following stages proceed successively and the constitution of coal is closely related to its reactivity.

coal-I-water insoluble acids-II-water soluble acids-III- CO₂, H₂O

Latrobe coal is very active as it contains a large amount of oxygen in the form of active functional groups such as phenolic hydroxide and carboxylic acid. The rate of dissolution in concentrated caustic soda solutions was very fast. The reactions I and II thus take place smoothly, and humic acids and aromatic acids could be obtained in good yield. When Amax coal, being higher rank than Latrobe coal, was used, the rate of dissolution was slow, but the rates of oxidations of humic acids and aromatic acids were relatively fast resulting in a lower yield of the intermediate oxygen compounds. The trend was found re-

markable in the case of Goonyella coal which was placed at the highest rank among the samples tested.

The composition of benzenepolycarboxylic acids in aromatic acids was shown in Table 6.

Table 6. Determination of benzenecarboxylic acids in aromatic acids

| Specimen | Ratios of benzenecarboxylic acids in aromatic acids | | | | | | | | | Yield to coal (wt%) |
|----------|---|-----|-----------------------|-----|---------------------------|-----|-----------------------|-----|------|---------------------|
| | Di- 1,3- 1,2- 1,4- | | Tri- 1,2,3- 1,2,4- | | Tetra- 1,3,5- 1,2,3,4- | | 1,2,3,5-1,2,4,5-(wt%) | | | |
| L-6 | 0.8 | 0.3 | 0.7 | 2.2 | 0.5 | 1.1 | 1.5 | 2.1 | 9.2 | 5.5 |
| L-8 | 0.7 | 0.4 | 0.5 | 1.7 | 0.5 | 0.8 | 1.1 | 1.7 | 7.4 | 3.9 |
| L-12 | 1.2 | 1.0 | 0.8 | 3.6 | 1.2 | 1.2 | 1.3 | 2.6 | 12.9 | 6.5 |
| L-13 | 2.6 | 0.8 | 0.6 | 3.9 | 2.3 | 1.3 | 2.1 | 4.8 | 18.4 | 3.5 |
| A-5 | 1.7 | 1.2 | 1.0 | 3.8 | 0.8 | 1.1 | 1.3 | 2.0 | 12.9 | 3.0 |
| A-12 | 0.8 | 1.3 | 1.4 | 5.0 | 1.2 | 1.5 | 1.4 | 2.5 | 15.1 | 4.4 |
| A-15 | 1.6 | 1.7 | 1.6 | 5.6 | 1.3 | 1.7 | 1.5 | 2.5 | 17.5 | 9.3 |
| G-8 | 1.9 | 2.0 | 1.8 | 6.9 | 1.4 | 1.9 | 2.0 | 2.8 | 20.7 | 8.7 |
| G-10 | 1.5 | 0.6 | 0.8 | 3.4 | 0.8 | 0.9 | 1.0 | 1.2 | 10.2 | 2.6 |

Neither benzoic acid was detected by gas chromatographic analysis, nor was detected water-soluble acids such as citric acid in the raffinates on the methyl ethyl ketone extraction by permanganate titration. The sum of the contents of the benzenecarboxylic acids reached a maximum of 20.7% in the air-preoxidized Goonyella coal. However, the best yield of benzenecarboxylic acids was obtained in the case of similarly treated Amax coal. When Latrobe coal was used, both the content of benzenecarboxylic acids in aromatic acids and the yield of benzenecarboxylic acids to the raw coal were not high. Furthermore, the content of benzenetetracarboxylic acids was the highest in the benzenecarboxylic acids for Latrobe coal, that of tri-carboxylic acids, however, was the highest for air-preoxidized Amax coal and Goonyella coal.

Concentrations of caustic soda used in the present study might be too high to obtain benzenecarboxylic acids in good yield. But the following results are concluded. In the oxidation of coals with the present method, a low rank coal such as Latrobe coal dissolves easily and forms humic acids and aromatic acids in good yield. In order to obtain benzenecarboxylic acids, however, it is profitable to use an air-preoxidized high ranked coal such as Amax coal and Goonyella coal.

Selective Bond Cleavage of Coal by Controlled Low-Temperature Air Oxidation

by J. Solash, R.N. Hazlett, J.C. Burnett, P.A. Climenson and J.R. Levine

Naval Research Laboratory, Combustion and Fuels Branch-Code 6180, Washington, DC 20375

Recent efforts to find low temperature routes to liquefy coal have led to a renewal of interest in oxidative methods. Air oxidation of coal has been used to effect desulfurization(1). Application of low temperature air oxidation to SRC (Solvent Refined Coal)(2) and some coals(3) have shown that coal is easily oxidized in solvent with radical initiators at 50° and without initiators at 100-200°C. Subsequent thermolysis of the oxidized SRC for instance, leads to significant production of low molecular weight compounds(2). The attraction of the air oxidation routes to coal liquids are two fold: inexpensive reagent(air) and low-temperature and pressure conditions. However, the oxidation must be controlled or severe loss of C and H can occur. It is worthwhile to note that the well known basic water oxidations of coal(4,5) produced high yields of benzene carboxylic acids but also gave CO₂ amounting to approximately 50% of the available carbon.

Under mild conditions, oxidation of coal in pyridine should proceed principally at benzylic positions. Many organic sulfur forms should also oxidize readily near 100°C(1,6,7). Upon thermolysis, as noted above, SRC which was oxidized in quinoline has been shown to produce as much as 32% by wt. of compounds with molecular weights less than 210. Thus a two step scheme which involves first low-temperature air oxidation followed by a higher temperature pyrolysis step could lead to significant yields of low molecular weight compounds. We would now like to present our results which extend the two step oxidation-thermolysis scheme to SRC and several raw coals using pyridine as solvent. It should be noted that all of our work thus far has been performed using small batch scale reactors and greater control over reactive intermediates might be achieved using flow reactors(9).

Experimental

The coals used in this work were obtained courtesy of the Pennsylvania State University, College of Earth and Mineral Sciences. Ultimate analyses (performed by Pennsylvania State University) are shown in Table I. Also shown are the total quantity of pyridine solubles of each coal used determined by soxhlet extraction. SRC was obtained from a Western Kentucky coal (Lot No. AL-3-35-77) and was supplied courtesy of Catalytic, Inc.

Complete details of the apparatus, experimental details and analytical methods have been reported elsewhere(2). Briefly, air is passed through a solution (SRC) or suspension (coal) of substrate in pyridine which is maintained at approx. 100°C. At the end of the oxidation period, the solution and the remaining residue are thermolyzed in the absence of air. The coals were oxidized and thermolyzed as 10% (wt/wt) slurries. Low molecular weight products (below 210) are quantitatively analyzed by gas chromatography using an internal standard.

Results

All coals and SRC oxidized smoothly at 100°C in pyridine. By monitoring the vent gases from our oxidation reactor for O₂, CO₂, CO and H₂O (2) we can determine how much oxygen reacted with the coal. The oxygen gas balance data for six coals and SRC oxidized in pyridine are presented in Table II. The vent gas from our

oxidation reactor passes through a condenser which is maintained at 0°C prior to gas analysis. Consequently very little water vapor escapes the condenser to be analyzed. While the water vapor content of the vent gases can be measured in all cases the total oxygen content represented by this water vapor is negligible and is therefore not reported in Table II. Water analysis of the pyridine solvent both before and after oxidation must be performed to close the oxygen balance. It seems unlikely however that all of the remaining oxygen can be accounted for by water.

It should be noted that these oxidations are quite mild. The evolved carbon (as carbon oxides) from the Sub-Bituminous B coal for instance, represents 0.001% of the available carbon on a mmf basis (Table I). The extent of oxidation, assuming negligible water production, is only 0.6% by weight for the Hi Volatile C bituminous coal. The extent of oxidation of the raw coals in this work is less than that observed for SRC in quinoline (2) or in pyridine at 100° (Table II). Thus, these are indeed mild, controlled oxidation conditions and should be compared again with the much more severe base catalyzed oxidations performed by others (4,5).

While sulfur moieties should oxidize readily under these conditions we do not expect SO₂ to be evolved at these temperatures (1,6,7). In prior work (2) in quinoline solution, SRC showed no evidence of sulfur dioxide evolution while oxidizing at temperatures as high as 180°C (10). While the substrate in the above case was low in sulfur and therefore evolved SO₂ might have gone undetected, it appears most unlikely that 180° is sufficient to cause appreciable SO₂ extrusion from sulfones (7).

The oxidized solutions and recovered residue were then placed in small stainless steel tubes which were fitted with Swagelok valves. The tubes were subjected to several freeze (-78°)-pump-thaw cycles then pressurized to 500 psig (room temperature) with hydrogen. The slurries were then heated to 415° for 3 hours. After cooling, the recovered solutions were quantitatively analyzed by gas chromatography. The results are reported in Table III. The conversion represents the yield, on a weight basis, of compounds whose molecular weight is less than approximately 210. In runs performed with raw coals, but not with SRC, some formation of pyridine (solvent) dimers was observed. The coals which gave the higher yields of low molecular weight compounds also appear to produce more pyridine dimer. Oxidized SRC was heated at two different temperatures. As observed previously using quinoline as solvent (2), only when the thermolysis temperature is above 400° are appreciable yields of low molecular weight compounds observed (Table III).

Discussion

All coals and SRC used in this work oxidized smoothly at 100° in pyridine. The coals of higher rank absorbed more oxygen than those of lower rank (Table II). The SRC absorbed more oxygen than any coal and appeared to be as reactive in pyridine at 100° as in quinoline at temperatures up to 150° (2). This difference in reactivity toward liquid phase air oxidation between SRC and the coals listed in Table I is probably not connected with oxygen transport within coal pores (9). Rather the difference in reactivity appears to be structure related. SRC has a lower oxygen content than any of our coals (11) and probably a lower phenolic oxygen content (12). Similarly, higher rank coals which absorb more oxygen than lower rank coals (Table II) appear also to have a lower content of phenolic oxygen. Hindered phenols are well known liquid phase oxidation inhibitors (13) so that this explanation is consistent with the observed oxidation behavior of the coals and SRC.

The oxidized solutions and recovered residue (coals only) were then thermolyzed in stainless steel tubes for 3 hours. Initial experiments with SRC at 350° showed that only small amounts of low molecular weight compounds were produced. At 415°

a dramatic increase in the observed production of low molecular weight products was observed. In an earlier paper we suggested that at temperatures over 400° thermal decarboxylation of acids, which were produced during oxidation, followed by rapid quenching of the radicals could account for the observed results (2). The same pattern of reactivity is exhibited by SRC in the present work. Recently, Campbell (14) has shown that CO₂ is evolved from the organic portion of sub-bituminous coal only at temperature above 400°. Presumably, thermal decarboxylation also explains this data.

Thermolysis of some of the oxidized coals produced some interesting results. The two higher rank coals (Table III) produced more low molecular weight compounds than the lower rank coal studied. The yields of low molecular weight material were always higher if the substrate were subjected to the mild oxidation prior to thermolysis. However, thermolysis of the raw coals at 415 induced dimerization and some trimerization (15) of the solvent, pyridine. The quantity of bipyridine formed roughly follows the pattern of oxidative reactivity of the coals- more oxygen absorbed, more bipyridine formed. Interestingly, no bipyridine was observed from the thermolysis of any SRC at 415 but biquinolines formed at 450° with SRC in quinoline.

The degree of solvent involvement reported in Table III is significant. Bipyridines distill in the same region as major products and if not removed would lead to high N content of the product. One way in which the bipyridines could be formed is by H atom abstraction from a solvent molecule in a coal pore by a 'hot' radical. Self-reaction with another solvent molecule in close proximity rather than quenching with hydrogen might be the preferred reaction pathway. We attempted to suppress bipyridine formation by addition of some tetrahydropyridine to the thermolysis slurries. The observed formation of bipyridines was reduced by a factor of about 2 when tetrahydropyridine was present in 10 wt % in the oxidized or unoxidized (raw coal + pyridine) slurries of the Hi Vol A and Hi Vol C coals. The observed yields of low molecular weight material were also reduced. However, the substrates used in the latter experiments had inadvertently been allowed to remain at room temperature for approximately two months. We had observed that these solutions and residues are easily degraded even at freezer temperatures in short periods of time.

The data presented in Table III demonstrate that coal can be fragmented to yield significant quantities of low molecular weight material. Since the reported yields from the oxidized and thermolyzed runs are all higher than the pyridine soxhlet extracts, on a weight basis, we can say that the two step process employed here definitely attacks some of the polymeric coal structure. Work is now in progress to replicate these results but on a much larger scale so that the yield of distillate (not gc yield) material can be reported. Similarly the residue after thermolysis will be examined for sulfur content. Finally it should be noted that the soxhlet extractable material from the Hi Vol A coal contains about 1% by weight of low molecular weight (less than 210) compounds.

References

1. A. Attar and W. H. Corcoran, *Ind. Eng. Chem., Prod. Res. Dev.*, 17, 102 (1978); S. Friedman and R. P. Warzinski, *Eng. Power*, 99, 361 (1977).
2. R. N. Hazlett, J. Solash, G. H. Fielding and J. C. Burnett, *Fuel*, 57, 631 (1978).
3. J. G. Huntington, F. R. Mayo and N. A. Kirshen, *Fuel*, in press.
4. R. C. Smith, R. C. Tomarelli and H. C. Howard, *J. Amer. Chem. Soc.*, 61, 2398 (1939).
5. R. S. Montgomery and E. D. Holly, *Fuel*, 36, 63 (1957).
6. R. B. LaCount and S. Friedman, *J. Org. Chem.*, 42, 2751 (1977).
7. T. J. Wallace and B. N. Heimlich, *Tetrahedron*, 24, 1311 (1968); T. G. Squires, Presentation at Confab '78 Meeting, Saratoga, Wyo., July 28, 1978.
8. R. N. Hazlett, J. M. Hall and M. Matson, *Ind. Eng. Chem., Prod. Res. Dev.*, 16, 171 (1977).
9. G. Kapo, Ph.D. Dissertation, Case Institute of Technology, 1964.
10. R. N. Hazlett, unpublished data.
11. M. Farcasiu, T. O. Mitchell and D. D. Whitehurst, *Amer. Chem. Soc., Div. Fuel Chem., Preprints*, 21(07), 11 (1976).
12. Generally, phenolic oxygen content decreases with rank but can be as high as approximately 4% for coals that are 85% carbon; eg, L. Blom, L. Edelhausen and D. W. van Krevelen, *Fuel*, 36, 135 (1957).
13. N. M. Emanuel, E. T. Denisov and Z. K. Maizus, Liquid-Phase Oxidation of Hydrocarbons, Plenum Press, New York, 1967, Chap. 7.
14. J. H. Campbell, *Fuel*, 57, 217 (1978).
15. Field ionization mass spectrometric analysis of some of these thermolyzed samples demonstrated the presence of pyridine trimers.

Table I

Elemental Analyses of Coals

| Coal, PSU No. - Type | Ultimate Analysis ¹ | | | Soxhlet Extract, wt % | | |
|--------------------------------|--------------------------------|-----|-----|-----------------------|-------------------|-----------------|
| | C | H | N | | | |
| PSOC 314 - Hi Vol A bituminous | 81.5 | 6.1 | 1.7 | 0.72 | 10.2 ³ | 24 ⁴ |
| PSOC 237 - Hi Vol B Bituminous | 81.9 | 5.5 | 1.8 | 0.6 | 10.2 | 15 |
| PSOC 316 - Hi Vol C Bituminous | 78.3 | 5.4 | 2.3 | 0.5 | 13.5 | 11 |
| PSOC 230 - Sub Bituminous B | 76.3 | 5.0 | 1.1 | 0.5 | 17.1 | 7 |
| PSOC 101 - Sub Bituminous C | 75.7 | 5.1 | 0.9 | 0.3 | 18.1 | ----- |
| PSOC 247 - Lignite | 75.5 | 4.8 | 1.5 | 0.5 | 17.6 | 6 |

1, wt %; elemental analysis data (dmf basis - direct basis) were kindly provided by the Pennsylvania State University, College of Earth and Mineral Sciences. 2, Organic sulfur. 3, Oxygen by difference. 4, wt % extracted, in pyridine, based on weight of raw coal (coals were allowed to air dry to constant weight at room temperature prior to extraction); conditions - N₂ atmosphere, exhaustive extraction (> 12 hrs).

Table II

Partial Oxygen Balances for Oxidation of SRC and Various Coals in Pyridine at 100°C⁴

| <u>Substrate</u> | <u>O₂Absorbed, mmoles</u> | <u>Evolved Gases, mmoles³</u> | |
|---------------------|--------------------------------------|--|------------------------|
| | | <u>CO₂</u> | <u>CO</u> |
| SRC | 5.1 | 0.5(.4) ² | -nm ¹ |
| Hi Vol A Bituminous | 2.8 | 0.5(.4) | 0.04(.01) ² |
| Hi Vol B Bituminous | 4.0 | 0.6(.4) | 0.06(.02) |
| Hi Vol C Bituminous | 4.1 | 0.6(.4) | 0.05(.01) |
| Sub Bituminous B | 3.1 | 0.9(.6) | 0.05(.01) |
| Sub Bituminous C | 2.5 | 0.9(.7) | 0.05(.01) |
| Lignite | 2.3 | 0.8(.6) | 0.04(.01) |

¹, Not measured. ², Numbers in parenthesis in this column refer to the calculated amount of O₂ in mmoles, accounted for in this gas. ³, A negligible amount of water was evolved in the oxidation gases. Karl-Fischer water analysis of the suspensions before and after oxidation remain to be performed. ⁴, Oxidation conditions: 100°C, 250 ml/min air flow, 3 hours, pyridine solvent.

Table III

Liquefaction Yields from SRC and Various Coals

| <u>Substrate</u> | <u>Oxidized¹</u> | <u>Thermolyzed², °C</u> | <u>Conversion, %³</u> | <u>Wt % Bipyridines Formed⁴</u> |
|------------------|-----------------------------|------------------------------------|----------------------------------|--|
| SRC | No | 415 | 1 | n.f. ⁵ |
| SRC | Yes | 350 | 7 | n.f. |
| SRC | Yes | 415 | 36 | n.f. |
| Hi Vol A Bit. | No | 415 | 15 | 0.9 |
| Hi Vol A Bit. | Yes | 415 | 32 | 0.4 |
| Hi Vol C Bit. | No | 415 | 12 | 0.3 |
| Hi Vol C Bit. | Yes | 415 | 19 | 1.8 |
| Sub-Bit. B | No | 415 | 4 | 0.2 |
| Sub-Bit. B | Yes | 415 | 10 | 0.2 |

1, Oxidized in pyridine maintained at 100°C, for 3 hours with air. 2, Oxidized solution and residue (for raw coals) heated for 3 hours at indicated temperature in Swagelok sealed stainless steel tubes. Tubes pressurized to approx. 500 psig (r.t.) with H₂ after several freeze (-78°C)-pump-thaw cycles. 3, Based on amount of coal and corrected for bipyridines formed. 4, Identified by retention time on two different columns; based on total amount of pyridine present. 5, Not found.

Hydrogasification of Carbon Catalyzed by Nickel

Yoshiyuki Nishiyama and Yasukatsu Tamai

Chemical Research Institute of Non-Aqueous Solutions,
Tohoku University, Katahira, Sendai, 980 Japan

Introduction

Gasification of coals to produce high-Btu gases is receiving extensive attentions. Catalysis at gasification stage is investigated by several workers(1), but the catalytic processes, especially the interaction between coal and catalyst, are not well understood. In the preceding report from this laboratory, it was shown that some of the transition metals catalyze the hydrogasification of active carbons and that methane was formed in two or three stages. When Ni was used, the first stage reaction occurred at a temperature region around 550°C and the second one above 800°C. It would be interesting if the low temperature reaction can be incorporated in a coal conversion process. In this presentation, a study to clarify the nature of the reactions is described, putting emphasis on the behavior of Ni.

Experimentals

Two types of activated carbon were used; one in a granular form (AC-G) and the other a powder(AC-P). They were impregnated with a Ni salt, normally $Ni(NO_3)_2$, if not stated otherwise, from aqueous solution. Gasification was conducted mainly in a thermobalance and the specimen, 0.1-0.5 g, was heated in an atmospheric flow of hydrogen at a constant heating rate(denoted as HR) up to 1000°C and the amount of methane formed was analyzed by a gas chromatograph. Gasification at elevated pressures were done in a fixed bed reactor. In this case, the temperature was raised to 900°C in 80 min and kept for 1 hr.

The dispersion of Ni on carbon surface was examined using X-ray diffraction, scanning electron microscope and a magnetic measurement. In the last one, the magnetization of the specimen was measured in hydrogen atmosphere by Faraday method using a permanent magnet. The apparant magnetic susceptibility given below, χ_a , is supposed to be proportional to the magnitude of magnetization at a constant field.

Results

Types of reactions concerned

A typical methane formation profile is illustrated in Fig. 1. Of the two active regions, the lower one between 400 and 700°C is referred to as R-1 and the other, the higher one above 800°C, as R-2. In the results given below, conversion to methane is denoted by X.

Features of R-1 reaction

[1] Temperature dependence. One of the marked character of R-1 is its transient nature, i.e., the specimen lost its activity when heated above 650°C whether the heating accompanied gasification or not, but a re-impregnation of Ni to the deactivated specimen restored the reactivity(Table 1). Even when the temperature was kept within the active region, the rate decreased rather rapidly, as shown by one of the broken lines, A, in Fig. 1, as if a limited portion of carbon could be gasified.

[2] Pressure dependence. R-1 had a negative dependence on the hydrogen pressure above 1 atm(Fig. 2).

[3] Dependence on Ni content. Fig. 3 shows that X(R-1) is small up to 2 % of Ni for AC-P and beyond this limit, the conversion increases steeply with Ni content. For another carbon, similar patterns were

observed, but the extent of Ni content within which the activity was insignificant depended on surface state of carbon. For example, a nitric acid treatment of AC-G (in 13.5 N acid at 20°C for 3 hr) increased the amount of inactive Ni to 4 % when this was 1.5 % for untreated specimen (AC-G). The concentrations of surface acidic sites titrated with NaOH were 52 and 9 mmol/100g for treated and untreated carbon, respectively. This suggests that the inactive Ni atoms are trapped at active sites.

[4] Effect of Ni salts. Table 2 shows a comparison of Ni salts used as Ni source. $\text{Ni}_2\text{CO}_7(\text{OH})_4$ from aqueous ammonia solution and $\text{Ni}(\text{NO}_2)_2$ were active for R-1, whereas NiCl_2 was almost inactive under normal conditions. Interestingly, X(R-1) of NiCl_2 -impregnated specimen varied with the condition to reduce the salt. The activity increased by a prolonged reduction at lower temperatures (Table 3). These results can be understood by a variation in the dispersion of Ni.

Features of R-2 reaction

[1] Dependence on temperature and pressure. R-2 is an ordinal reaction in that it proceeds at nearly constant rate at a constant temperature though the rate increased somewhat at the initial period and decreased gradually with the carbon burn-off and that the rate varied reversibly with temperature. R-2 had a positive order with respect to hydrogen pressure (Fig. 2).

[2] Dependence on Ni content. In contrast to R-1, X(R-2) increased with Ni content at first but leveled-off soon, as shown in Fig. 3.

[3] Effect of Ni salt and the surface state of carbon. R-2 had no preference to the species of Ni salt to be impregnated (Table 2). Also, the surface treatment of carbon had negligible effect on X(R-2).

Dispersion of Ni on carbon surface

[1] X-ray diffraction. The breadth of (111) diffraction of Ni showed a trend that the smaller the average crystallite size, the larger the X(R-1), and that growth of Ni crystallites occurred after R-2 took place (Table 2), but this method is insensitive to the smaller part of crystallite and is inappropriate to follow the changes during R-1.

[2] Microscopic observation. From observations by a SEM, slight change in the distribution of Ni was noted after the completion of R-1. Upon heating to R-2 region, visible Ni particles appeared on the whole surface (Fig. 4).

[3] Magnetic measurement. Fig. 5 demonstrates typical changes in χ_a at the initial and the final stage of R-1. The turns at 70-200°C was ascribed to the adsorption of hydrogen at lower temperatures. The figure indicates that Ni in unreacted specimen is in a superparamagnetic state (3), which was converted into a ferromagnetic state by heating. The χ_a at 100°C from descending curve or its extrapolation was used as a measure of the dispersion of Ni and is given as χ° in Table 4, together with the activity in R-1. The conversion into a ferromagnetic state occurred even without gasification reaction. If a plot is made from Table 4, it can be shown that the remaining activity of specimens preheated to various degrees is nearly proportional to the change in χ° by further heating. In another experiment, a specimen was heated repeatedly to the predetermined temperature which was raised in succession and the weight and χ_a were measured at room temperature (Fig. 6). Both of these changed concurrently at the same temperature regions. The χ_a decreased during or after R-2, which seems to suggest a change in the bonding state of Ni, probably due to the dissolution of carbon or some component of ash concentrated on carbon surface.

Discussions

From the results given above, it can be concluded that the deactivation by heating above the R-1 region is due to a change in the dispersion of Ni, i.e., an aggregation to a larger particles. Fig. 6 and Table 4 seem to suggest that the catalytic action is related to the migration of Ni atoms and smaller particles on carbon surface. The migration itself is, perhaps, a thermal motion, not associated with the gasification reaction. The dependence of R-1 activity on Ni content indicates that those atoms strongly held at active sites are immobile and are inactive for R-1. Ni particles continue to grow during R-2, but this seems to be caused by the disappearance of the substrate.

Two types of possible mechanism of catalytic gasification are frequently discussed: (A) hydrogen dissociates on the catalyst surface and spills over to carbon surface, and (B) catalyst modifies the C-C bonds to enhance the reactivity. The present results are insufficient to draw a conclusion about the mechanism, but it seems improbable that (A) type action is working in R-1, as this has negative dependence on hydrogen pressure. For R-2, on the other hand, (A) type action can account the pressure dependence as well as the insensitiveness to Ni content and to the state of dispersion, although other possible explanations may exist. The decrease in χ_c at R-2 region need further study and it is not clear at present whether this change has any correlation with the gasification reaction.

References

- (1) J. L. Johnson, *Cat. Rev.*, **14**, 131 (1976).
- (2) A. Tomita and Y. Tamai, *J. Cat.*, **27**, 293 (1972).
- (3) P. W. Selwood, "Adsorption and Collective Paramagnetism", Academic Press, New York (1962).

Table 1 Activities in R-1*

| Specimen | X(R-1) |
|-------------------|--------|
| Unreacted | 30.2 % |
| Reacted once | 0.7 |
| Re-impregnated | 27.7 |
| Preheated in He** | 3.1 |

* AC-P, 5 % Ni. HR=5°C/min.
 ** at 600°C for 2 hr.

Table 2 Comparison of Ni salts*

| Salt | Ni content | X(R-1) | X(R-2) | Crystallite size after reduction | |
|--|------------|--------|--------|----------------------------------|------------|
| | | | | R-1 | R-2 |
| Ni(NO ₃) ₂ | 4.3 % | 5.8 % | 7.0 % | 35 Å | 40 Å 260 Å |
| NiCl ₂ | 4.1 | 0.8 | 6.4 | 200 | 200 230 |
| NiBr ₂ | 4.3 | 0.9 | 5.4 | 200 | - 490 |
| Ni ₃ CO ₃ (OH) ₄ ** | 4.1 | 6.3 | 4.8 | 260 | 300 320 |
| (CH ₃ COO) ₂ Ni** | 3.9 | 1.2 | 6.8 | 165 | - 190 |

* AC-G, HR=2.3°C/min.

** Impregnated from aqueous ammonia solution.

Table 3 Effect of reduction temperature

| Conditions | X(R-1) | Crystallite size |
|----------------|--------|------------------|
| 240°C, 5 hr | 1.2 % | - Å |
| 257°C, 14.7 hr | 2.7 | 125 |
| 263°C, 8 hr | 1.1 | 135 |
| 284°C, 3 hr | 0.8 | 140 |
| const. rise** | 0.9 | 200 |

* AC-G impregnated with NiCl₂ (4.1 % Ni).

** HR=2.3°C/min.

Table 4 \bar{X}° and R-1 reactivity*

| Ni content | Treatment** | \bar{X}° | X(R-1) |
|------------|-------------------|-----------------|--------|
| 1 % | 300°C, 2 hr | 3.2 esu/g Ni | 1.2 % |
| 1 | 450°C, 2 hr | 3.7 | 0.5 |
| 1 | 600°C, 2 hr | 5.5 | 0.1 |
| 5 | 300°C, 2 hr | 2.3 | 30.2 |
| 5 | 450°C, 0 hr | 3.9 | 25.2 |
| 5 | 450°C, 2 hr | 4.2 | 24.0 |
| 5 | 600°C, 2 hr | 8.0 | 0.7 |
| 5 | 600°C, 2 hr in He | 8.9 | 3.1 |

* AC-P, HR=5°C/min.

** In hydrogen except for the last line.

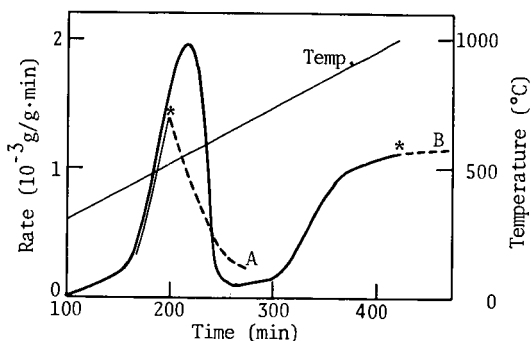


Fig. 1 Methane formation profile (AC-G)

Solid line: HR=2.3°C/min,

Broken lines: Temperature was kept constant

from the points marked by asterisks. A at

560°C and B at 1000°C.

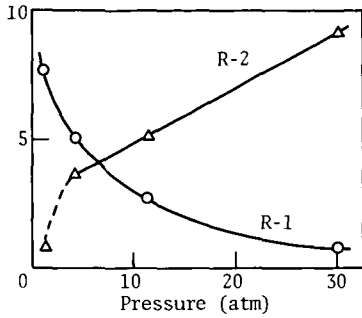


Fig. 2 Pressure dependence (AC-G, 7%Ni)
 R-1: conversion in %.
 R-2: maximum rate at 900°C in 10^{-5} g/g.min.

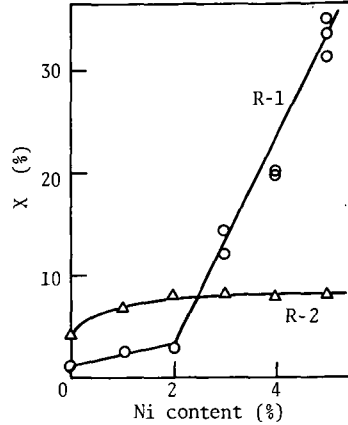


Fig. 3 Conversion vs. Ni content
 Specimen: AC-P, HR=5°C/min.

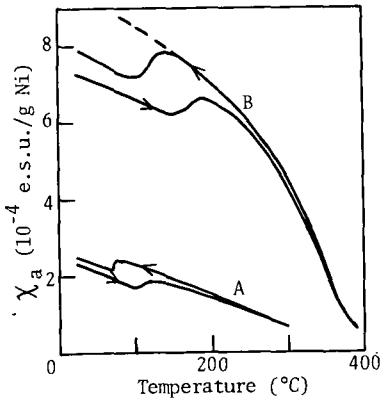


Fig. 5 Apparent magnetic susceptibility of AC-P with 5% Ni
 Specimens were heated in hydrogen for 2 h, A: at 300°C, B: at 600°C before measurement.

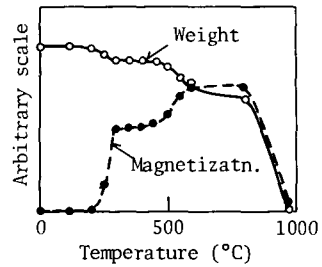


Fig. 6 Changes in weight and magnetization
 Specimen: NiCl₂-impregnated (5% Ni)

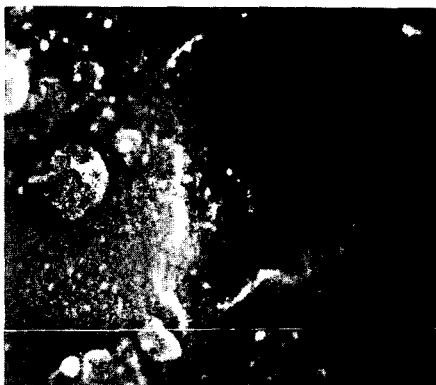
1 μ



(a) Heated to 350°C.



(b) Heated to 670°C.
X=5.1 %



(c) Heated to 1000°C.
X=11.4 %



(d) Kept at 1000°C for 25 min.
X=18.9 %

Fig. 4 Photographs of an AC-G specimen with 7 % Ni (as an average for a batch of the specimen), heated repeatedly in hydrogen HR=5°C/min.

SCANNING ELECTRON MICROSCOPE STUDY
ON THE CATALYTIC GASIFICATION OF COAL

Akira Tomita, Kazutoshi Higashiyama and Yasukatsu Tamai

Chemical Research Institute of Non-Aqueous Solutions,
Tohoku University, Katahira, Sendai 980, Japan

INTRODUCTION

In previous papers (1,2), it has been reported that coals pretreated with liquid ammonia can be gasified more easily than untreated coals, especially when they are impregnated with nickel catalysts. The effectiveness of nickel catalyst varies with such parameters as the method of nickel loading, the kind of nickel salt, the condition of reduction of salt to metallic state, and others. According to circumstances, nickel does not necessarily act as effective catalyst. In order to obtain a higher catalytic activity, it is essential to understand how a nickel particle catalyzes the gasification reaction. Some particles may be active, and others may be less active. We then have to find the way of nickel loading to produce only such active particles. Thus, we can maximize the catalytic activity of nickel for coal gasification. The microscopic observation is known to be one of the most useful tool for understanding the behavior of metal catalyst on carbon gasification (3,4,5). Scanning electron microscope (SEM) studies on catalytic coal gasification have been made by several groups of workers in recent years (6, 7). These studies have dealt almost exclusively with the static state of catalyst. We wish to report here dynamic behaviors of catalyst on coal gasification observed by the SEM coupled with the energy dispersive analysis of X-rays (EDAX).

This technique would be useful in the following aspects. The movement of nickel particles can be monitored by examining the specimens before and after gasification. The relationship between the catalytic activity and the size or shape of nickel particle can be checked. A semi-quantitative analysis is possible with respects to the presence of mineral matter and its catalytic activity on the gasification. The interaction of nickel with other elements can be examined. The sulfur poisoning of nickel catalyst is the most important interaction among all. The present method, however, has some limitations in addition to the dangers implicit in the use of microscopy, which Thomas called as the twin evils of electricity and tendentiousness (3). The first limitation is that we did not observe the change of coal surface at reaction conditions, but at room temperature. Some changes might occur during the cooling stage. The second one is the neglect of possible catalytic activities of fine particles of diameter less than 100 nm. In spite of these limitations, we believe that this technique may give useful informations about the catalytic behavior of nickel particles.

EXPERIMENTAL

Coal samples used in this study were the same as in the earlier work (2). Ammonia treatment was carried out at 373 K and 10 MPa for 1 hr. About 1 wt% of nickel was impregnated on coal from an aqueous solution of hexaamminenickel(II) carbonate. Details on these pretreatments and analyses of coals were reported elsewhere (8). We would like to use the abbreviations for coal samples with different pretreatments; UN for raw coal, UC for raw coal with nickel catalyst, and TC for ammonia treated coal with nickel catalyst. The same nomenclatures are also used for the chars therefrom. For the SEM observations, five coal particles of 1 - 2 mm in size were mounted on a cylindrical graphite holder which is fit for the SEM equipment. Graphite paste was used to adhere the coal particles to the holder.

Figure 1 illustrates the reactor assembly. Two graphite sample holders were put on a rectangle quartz dish with a size of 20 by 40 mm. The dish can be moved horizontally by a quartz tube with a hook. In this quartz tube, a thermocouple was inserted to monitor the reaction temperature. The temperature difference between the tip of this thermocouple and the coal sample was less than 5 K. The furnace temperature was controlled by another thermocouple. For steam generation, a small evaporator with an electric heating wire was utilized. It evaporates water fed from a microfeeder at a constant rate. Exposed parts of tubings were also wound with a heating wire in order to prevent a steam condensation.

Coal samples on a graphite holder were examined under an SEM, a Hitachi-Akashi MSM 4C-101, to which an EDAX, a Horiba EMAX-1500, was attached. Then, the holder was put on a quartz dish and placed in the reactor. The initial position of the dish was outside of the furnace. After an evacuation of the system, nitrogen gas was introduced at the flow rate of 200 cm³(STP)/min. When the furnace temperature reached 773 K, the quartz dish was pushed into the center of the furnace. It was pulled out after the devolatilization for 1 hr. Samples were then carefully examined by SEM and EDAX. The graphite holder were returned to the quartz dish in the reactor. The evacuation of the system was followed by the introduction of nitrogen and reacting gas. In case of steam gasification, the flow rate of nitrogen was kept at 40 cm³(STP)/min and the flow rate of steam was 150 cm³(STP)/min. When the temperature and the gas flow rate became stationary, the quartz dish was pushed in. After the required time of gasification, the coal sample was pulled out to be examined. Similar procedures were repeated for several times to follow the morphological changes at the same sights on char surface. In case of hydrogasification, the flow rate of hydrogen was 200 cm³(STP)/min. Some photographs were taken for coal samples gasified in the thermobalance reported earlier (2).

The conversion of coal at each stage was determined in a different series of experiments. Coal particles of about 200 mg were placed on a quartz dish without graphite holders. The devolatilization and gasification were carried out under the same reaction conditions as before. At the end of each stage, the weight was measured and the conversion was calculated on a dry ash free basis.

RESULTS AND DISCUSSIONS

We would like to mention first about the result of observation on coals without any heat treatment. Figure 2 shows the surface of Shin-Yubari coal cut by a microtome in order to check whether the nickel salt penetrated into the inside of particle. Three points should be noted here. First, the ammonia treated coal has cracks of various widths, whereas the untreated coal has no cracks. We present here only one particle for each, but this tendency was quite general one. The crack formation was particularly remarkable for lower rank coals. Second, the presence of nickel salt was recognized either on the external surface as in (b) or along the cracks as in (d). In these two photographs, the concentration of nickel was analyzed along the upper straight line, and it was shown as a notched line. These facts indicate that the nickel salt on a UC sample exists mainly on the external surface, whereas that on a TC sample exists not only on the external surface but also in the inside of coal particle. Third, there were many ellipsoidal holes of a diameter of about 10 μm on the cut surface. Flakes with a thickness of 1 μm were made during the course of cutting by a microtome, and it was also examined on SEM. We found that the flake consisted of many granular particles supported on a thin film. These particles might come out from the holes mentioned above. It can therefore be presumed that these holes are made because of the heterogeneity of coal in mechanical strength. Similar holes were observed for all other types of coal.

Table I. Successive Gasification of Leopold Coal

| Stage | Gas | Temperature (K) | Reaction Time (hr) | Conversion (% daf) | | |
|-------|------------------|--------------------|-----------------------|--------------------|----|----|
| | | | | UN | UC | TC |
| 1 | N ₂ | 773 | 1.0 | 26 | 25 | 23 |
| 2 | H ₂ O | 1023 | 0.5 | 37 | 37 | 37 |
| 3 | H ₂ O | 1023 | 0.5 | 40 | 41 | 42 |
| 4 | H ₂ O | 1023 | 0.5 | 42 | 45 | 47 |
| 5 | H ₂ O | 1073 | 0.5 | 49 | 55 | 56 |
| 6 | H ₂ O | 1073 | 1.0 | 60 | 67 | 71 |

As an example of catalytic coal gasification, we present here the result on steam gasification of Leopold coal. The heat treatment procedures and the conversion on a dry ash free basis are summarized in Table I. The conversion was in accordance with that obtained earlier in a thermobalance (2). Figure 3 shows a typical behavior of nickel catalysts during steam gasification. At the first stage, where the coal was devolatilized in nitrogen, most nickel exist as flakes. Some granular nickel particles are seen in Figure 3(a). An X-ray diffraction analysis revealed that the state of nickel at this stage was already metallic. The dispersion of nickel is not homogeneous, and the accumulation of nickel along cracks is observed. A lesser amount of nickel is found on the flat surface at the upper left side of the photograph. At the second stage, most of flakes have changed to particles. The size of particle seems to be around a few microns so far as judging from Figure 3(b). However, in fact, each particle consists of a number of much smaller particles which are bundled in a wooly substance. In the upper left corner, many nickel particles appeared and they catalyzed the gasification around them, resulting in the formation of holes. Most of these particles disappeared in their own holes at the third stage (c). At the fifth stage (d), the surface becomes rough and rough. The nickel particles start to agglomerate. The ditch becomes wide. EDAX examined the nickel and sulfur concentration for the whole field of view in this series. It can be said that the nickel content decreased at the third stage perhaps due to the submersion of particles into holes. The sulfur content also decreased at this stage. The mechanism whereby this occurs is unclear. One possible explanation may be the desulfurization by an excess amount of steam and/or hydrogen. Figure 4 shows somewhat less common example. At the devolatilization stage, fine particles with diameters of less than 0.1 μm gather to form a long, narrow strip. Fine cracks were observed on and near this strip. Some of them were perpendicular to the strip. After the gasification for 0.5 hr, a deep ditch appeared where fine particles had existed. Comparing with the depth of holes dug by an ordinal spherical particle shown on a flat surface, we may presume that the fine particle is much more active as a gasification catalyst. After the second stage, the gasification reaction proceeds in a similar manner as shown in Figure 3. In some cases, needle crystals containing nickel and a considerable amount of sulfur were observed after devolatilization. These were not so active.

Low magnification photographs of Leopold-UC coal and the first stage char are shown in Figure 5. A cubic particle swells upon devolatilization. The degree of swelling can be estimated by measuring the size of particle before and after the heat treatment. Usually, TC samples do not swell and some of UC samples swell as this particle does. Most of UN coal particles swell to some extent (FSI is $1\frac{1}{2}$). Such suppression effect on caking property by the present pretreatment has been found for a variety of coals. Almost no nickel particles were observed on the hemispherical portion of char in Figure 5(b), which had bubbled out from the inside of coal. In order to check the uncatalyzed gasification rate, the change in this portion was followed throughout the series of steam gasification shown in

Table I. Practically no change was observed. Ash particles containing iron catalyzed the gasification, although the effect as catalyst was much smaller than that of nickel. Other ash particles containing aluminum, silicon, potassium, or calcium were found to be catalytically inactive.

Figure 6 shows two examples of the fate of nickel catalyst. Both samples are Leopold TC char gasified in steam at 1123 K for 2 hr. The conversion was 92 %. The first photograph indicates the accumulation of nickel and ash on the external surface of char particle at such a high conversion. Spot analyses by EDAX revealed the composition of ash as follows: A, nickel; B, nickel and sulfur; C, nickel; D and E; aluminum, silicon, nickel, iron and sulfur; F, iron; G, little sulfur, which means the main element is carbon. The blackish part which can be seen through the cleavage of ash layer is nearly pure carbon. The contact of this carbonaceous portion with nickel catalysts seems to be poor. The ash layer may be a resistance for gas diffusion. These facts imply the difficulty of catalyst utilization at high conversion. The second photograph shows the interior of Leopold char. This surface was exposed by cutting a char particle by a razor blade. The inside of char is very porous. In these macropores, few nickel particles were recognized. In accord with the observation in Figure 2, some nickel particles were found in the inside of TC char, but none in the inside of UC char. Anyhow, the amount was quite small compared with that present on the external surface. All other chars from different coals also have similar macropores. The amount of nickel in these macropores are also limited. In order to utilize nickel catalyst efficaciously, we should make all possible efforts to impregnate nickel salt not only on the external surface but also in the inside of coal particle.

Figure 7 exhibits some reactions of nickel with other elements in coal. A somewhat peculiar form of nickel is shown in the first photograph which was taken from Zollverein TC char. The intensity of EDAX tells us that a stick-shaped part is made from iron with a small amount of nickel, and that a ball-shaped part is made from nearly an equal amount of nickel and iron. The slender the stick, the larger the ratio of iron to nickel. The bigger the ball, the larger the nickel content. We think these are some compound resulted from the reaction of nickel and iron, although an X-ray diffraction study of char could not identify it. There is no evidence so far that they catalyze the gasification reaction. The reaction with sulfur is more important in connection with the catalyst poisoning (7). Sulfur exists all over the coal particle, and this reaction was observed quite frequently in case of steam gasification. As is shown in the line profiles of nickel and sulfur in Figure 7(b), some nickel particles contain a considerable amount of sulfur, while the others do not. The concentration of sulfur is not homogeneous even in a single particle. The catalytic activity of nickel does not seem to have a strong dependence on the sulfur content. We can find many nickel particles which is still active in spite of the contamination with sulfur. In the case of hydrogasification at 1273 K, the sulfur on nickel was quickly taken away as hydrogen sulfide. Essentially no sulfur remained after a few stages of hydrogasification.

CONCLUSIONS

A nickel catalyzed gasification of coal has been investigated by means of SEM and EDAX. We followed the movement of catalyst by observing the fixed sight before and after gasification. The most important finding is that nickel particles do not exist in the interior of coal particle so far as the present method of impregnation is utilized. Nickel particles on the external surface are found to be very active as catalysts. In other words, true reaction rate for catalytic gasification is much greater than non-catalytic reaction rate. If we can only find an appropriate method of impregnation to put nickel salt into the inside of

coal, the catalytic effect would be significantly improved. The next important result is the fact that the catalytic activity of nickel varies with the form of nickel particle. Very fine particle, for example, are much more active than the others. Thus, the second subject that we should challenge is to find an impregnation method which can disperse most nickel in the form of such very fine particles.

REFERENCES

1. Matida, M., Nishiyama, Y., and Tamai, Y., "Gasification of Coals Treated with Non-Aqueous Solvents. 1. Liquid Ammonia Treatment of a Bituminous Coal," Fuel, 56, 171 (1977).
2. Tomita, A., Oikawa, Y., Kanai, T., and Tamai, Y., "Gasification of Coals Treated with Non-Aqueous Solvents. 6. Catalytic Steam Gasification at Atmospheric Pressure," presented at the Annual Meeting of CSJ, Yokohama, April, 1978.
3. Thomas, J. M., "Microscopic Studies of Graphite Oxidation," in P. L. Walker, Jr., Ed., "Chemistry and Physics of Carbon," Vol. 1, Marcel Dekker, New York (1965), p 121.
4. Tomita, A. and Tamai, Y., "An Optical Microscopic Study on the Catalytic Hydrogenation of Graphite," J. Phys. Chem., 78, 2254 (1974).
5. Baker, R. T. K., "Catalysis in Action," Chem. Eng. Prog., April 97 (1977).
6. Gardner, N., Samuels, E., and Wilks, K., "Catalyzed Hydrogasification of Coal Chars," in L. G. Massey, Ed., "Coal Gasification," American Chemical Society, Washington, D. C. (1974), p 217.
7. Rai, C. and Hoodmaker, F., "Effect of Coal Sulfur on Catalyst Activity in the Direct Production of Hydrocarbons from Coal-Steam Systems," AIChE Symposium Series, 72, 332 (1976).
8. Tomita, A., Tano, T., Oikawa, Y., and Tamai, Y., "Gasification of Coals Treated with Non-Aqueous Solvents. 5. Properties of Coals Treated with Liquid Ammonia," presented at the Annual Meeting of CSJ, Yokohama, April, 1978.

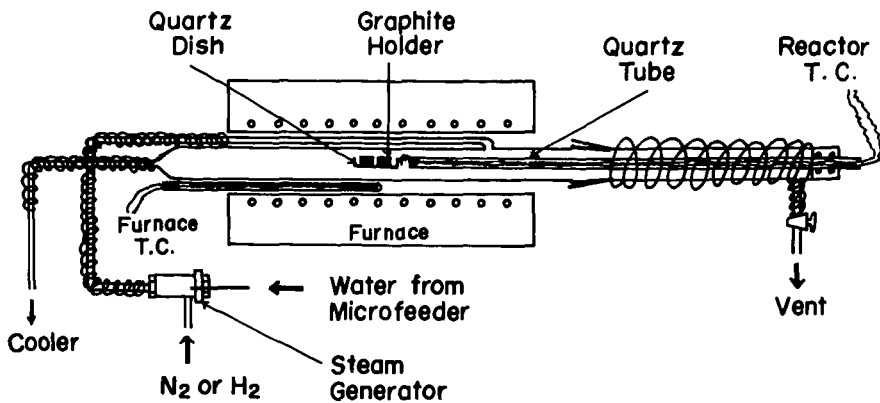
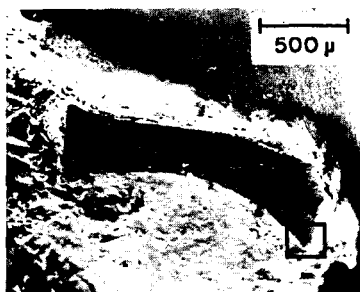
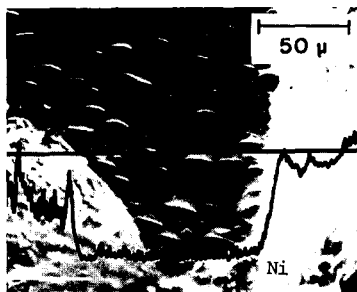


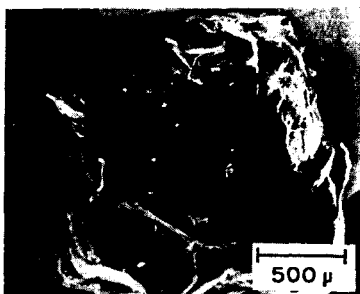
Fig. 1. Schematic diagram of apparatus



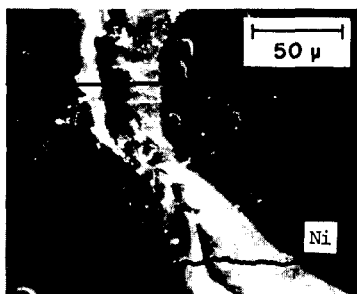
(a) UC Coal



(b) UC Coal

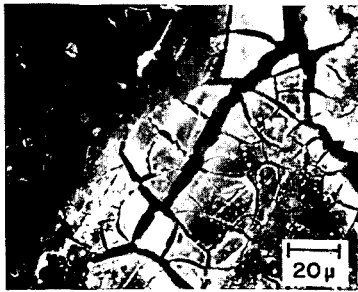


(c) TC Coal

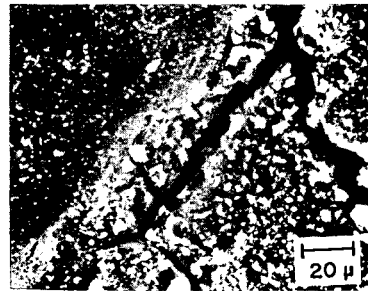


(d) TC Coal

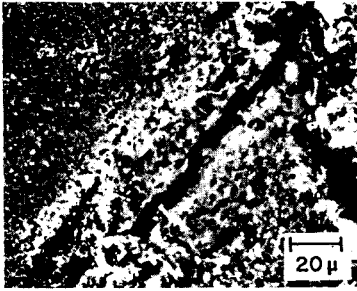
Fig. 2. Nickel Impregnated Shin-Yubari Coal



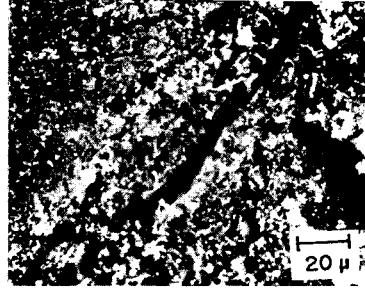
(a) 1st Stage



(b) 2nd Stage

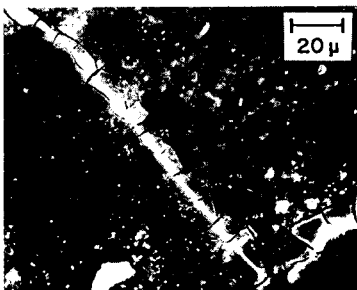


(c) 3rd Stage



(d) 5th Stage

Fig. 3. Leopold TC Char (1)

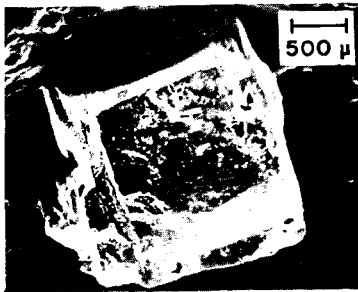


(a) 1st Stage

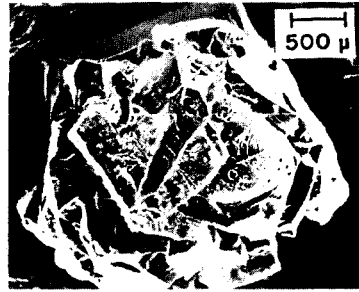


(b) 2nd Stage

Fig. 4. Leopold TC Char (2)

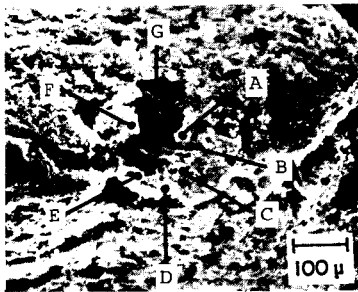


(a) Raw Coal

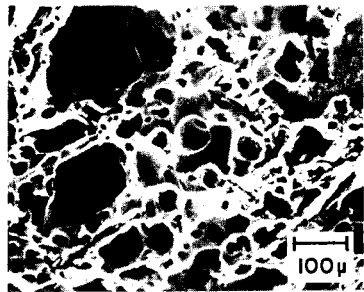


(b) 1st Stage Char

Fig. 5. Leopold UC Coal and Char



(a) Accumulation of Ash

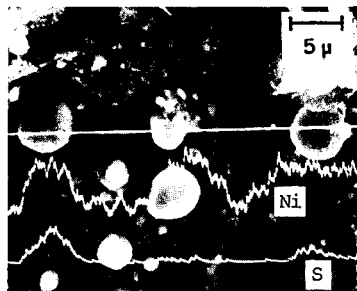


(b) Interior of Char

Fig. 6. Leopold Char at a Conversion of 92%



(a) Reaction with Fe



(b) Reaction with S

Fig. 7. Reaction of Nickel

COAL LIQUIDS HYDROGASIFICATION: EXPERIMENTS AND MECHANISM

H. N. Woebecke, P. E. Koppel, and P. S. Virk

Stone & Webster Engineering Corporation, P.O. Box 2325, Boston, MA 02107

Experimental data are presented for the hydrogasification of coal-derived liquids at conditions of temperature, pressure and residence time respectively 1200-1700F, 740-1500 psig, and 10-120 s, with hydrogen-to-substrate ratios from 0.8 to 2.0 times stoichiometric. The coal liquids originated from hydroliquefaction of Pennsylvania and Wyoming coals; both full range 300-1200F and low boiling 400-650F fractions were employed, all samples being characterized by elemental analysis and NMR spectroscopy. Hydrogasification was performed in a packed tubular flow reactor with sequential effluent quenching and analysis by GCMS to yield information on products from C1(methane) to C14(phenanthrene). Theoretically, it was postulated that the hydrogasification mechanism involves two steps, namely (i) hydrodealkylation of substituted alkyl-aromatics to their nude polynuclear aromatic parent plus gas and (ii) fragmentation of the unsubstituted polynuclear aromatics to progressively smaller aromatic molecules and further gas. The theory predicts that the kinetics of both steps should be governed by the delocalization energy of the aromatic nuclei involved; at the conditions of the present experiments, step (i) should be appreciably faster than step (ii). The experimental data for gas, benzene and naphthalene yields were well rationalized by the theory. Further, the present theoretical framework can be applied to infer hydrogasification behavior of any aromatic feedstock from its NMR analysis, using the aromaticity and ring-breakdowns provided by the latter.

METHOD FOR REACTIVATION OF A CATALYST USED IN STEAM REFORMING OF HYDROCARBONS

J. Kimoto, K. Yamauchi, M. Morimoto, M. Yamada and F. Noguchi

Research Center, Osaka Gas Co., Ltd., 6-19-9 Torishima
Konohana-ku Osaka 554, Japan

1. Introduction

Osaka Gas Company, Ltd. has been bringing in LNG, a clean fuel, from overseas since late 1972. With the necessity of the fact that our company smoothly converts its system from manufactured gas to natural gas distribution, the establishment of SNG (Substitute Natural Gas) production technology is essential if any possibility of a short supply of LNG is taken into account.

We have already developed the MRG (Methane Rich Gas) process, a low temperature steam reforming process, jointly with Japan Gasoline Company (JGC). Although this process, a SNG process using LPG or Naphtha with a nickel type reforming catalyst, is of good efficiency, it is considered that a SNG process with a better reforming catalyst can be expected to be of higher efficiency. As the result of extensive investigation, we have recently succeeded in developing a new steam reforming catalyst completely different from conventional catalysts. This catalyst, SN-108, has many excellent characteristics as compared with conventional steam reforming catalysts. In particular, it is a great advantage that this catalyst can be reactivated perfectly by the newly developed method.

It is our intention to explain principally about the characteristics of SN-108 and the method for reactivation.

2. Catalyst

The conventional catalysts used in low temperature steam reforming of hydrocarbons are usually nickel type. On the other hand, SN-108 has a γ -Alumina oxide core impregnated with active metal which is not nickel. The characteristics of SN-108 are as follows.

- (1) High activity and long life.
 - (2) Resistance to the deposition of carbonaceous materials.
 - (3) Operable in the low temperature range and with a low steam to carbon ratio, such as 1.5 and 0.7 respectively at 1st and 2nd stage of two stages reactors.
 - (4) Handling is simple and no hydrogen reduction is required.
- In addition to these characteristics, SN-108 can be completely reactivated by the specified method which we have recently developed. Furthermore, it has been found that SN-108 has a good performance in gasifying heavier distillates such as kerosene, gas oil, V.G.O. etc.

SN-108 has already been used for three winter seasons in a commercial plant of a daily output of 200,000 Nm³/day to reform straight run naphtha having an end point 180 °C (Test Naphtha) and also subjecting to reactivation during this period. In these operations, the characteristics of SN-108 has been confirmed. Fig.1 shows the catalyst deterioration with passing of time in the third operation. The reaction conditions are as follows.

steam / carbon ratio : 1.5

reaction pressure and temperature : 12 Kg/cm² G, 490 °C

3. Reactivation

3.1 Method of reactivation

Typical conventional procedures for reactivation are treatments with hydrogen, steam or oxygen, which are mainly effective for the elimination of carbonaceous materials deposited on the catalysts. Our new reactivation system consists of two stages of chemical treatment essentially different from conventional ones. It is particularly noted that the combination of two chemical treatments is essential for the performance of reactivation. The system cycle may be repeated depending on the extent of catalytic activity deterioration. Even if the catalytic activity deteriorates completely after being used, it is recovered to the state of fresh catalyst by 6 to 8 treatments.

Fig.2 shows the general process flow.

3.2 Effect of reactivation

1. Sample

The sample to be reactivated is the catalyst which had been used in a commercial plant for 4300 hours to reform Test Naphtha with steam and whose activity deteriorated completely.

2. Catalytic activity

Fig.3 shows the temperature profiles of steam reforming reaction using Test Naphtha. It can be found that the catalytic activity is recovered depending on the number of treatment.

3. Catalytic properties

Table 1 shows the typical catalytic properties of fresh catalyst, used catalyst and reactivated catalyst.

Table 1. Typical property of the catalyst

| sample property | | fresh cat. | used cat. | reactivated cat. |
|--------------------|-------------------------------------|------------|-----------|---------------------|
| | | | | |
| catalyst | carbon content (wt%) | 0.2 | 6.0 | 3.0 |
| | sulfur content (wt%) | 0.00 | 0.09 | 0.00 |
| | relative active metal content | 1 | 1 | 1 |
| carrier | crush strength (kg) | 20 | 7.3 | 7.0 |
| | surface area (m ² /g) | 140 | 90 | 95 |
| | pore volume (cc/g) | 0.46 | 0.38 | 0.38 |

4. Chemical state of active metal

Fig.4 shows XPS spectra of the three kinds of catalysts. It became clear that the active metal consists of three kinds of chemical state, the relative ratios of three states change after being used and the chemical state of used catalyst is recovered to the almost same state of fresh catalyst by reactivation.

3.3 Mechanism of reactivation

In general, catalytic steam reforming reactions of hydrocarbons result in deposition of various materials such as carbonaceous and sulfurous materials on the catalyst. In addition, these reactions often result in a sintering of active metal particles causing their mutual cohesion, whereby the size of active metal particles enlarged and the dispersibility consequently lowered. Further, the physical or chemical constitution and behaviour of active metal may be gradually changed during the catalytic reactions. From the results in Table 1, it became clear that carbonaceous and sulfurous materials on the catalyst were eliminated by reactivation. Especially sulfurous materials was removed completely. Moreover, the observations by transparent electron-microscope gave the fact that there existed some sintered active metal particles on the catalyst after being used which disappeared after reactivation. Furthermore, as indicated in Fig.4, active metal of used catalyst was recovered to the chemical state of active metal of fresh catalyst. Consequently it may be concluded from these facts that our reactivation method is effective for the reduction or elimination of all of these adverse factors.

It may be noted, as stated in section 3.1, that conventional reactivation treatment with hydrogen, steam or oxygen is effective for the removal of carbonaceous material deposited on the catalysts, but not for the elimination of sulfurous materials and the recovery of chemical constitution of active metal. We have already found that conventional reactivation method has completely no effect on the recovery of the catalytic activity of SN-108 and furthermore our reactivation method is not effective for the recovery of the activity of conventional nickel type catalysts.

4. Summary and Conclusions

We have developed the new catalyst, SN-108, for low temperature steam reforming of hydrocarbons which has various excellent characteristics as compared with conventional nickel type catalysts. In particular, SN-108 is operable with a extremely low steam to carbon ratio, which enables SNG process with the catalyst to be of much higher efficiency. Furthermore, we have developed the new reactivation method for SN-108 essentially different from conventional methods and succeeded in commercializing this method. We believe that the process with SN-108 can make the great many of advantages in the field of steam reforming of hydrocarbons.

In Japan where stringent environmental protection regulations are being enforced, there has been a trend of using lighter fuel oil and it is considered inevitable that there will be greater surplus hereafter of residual oil. With this background, we will continue to investigate the catalytic activity and the reactivation method for SN-108 with residual oil.

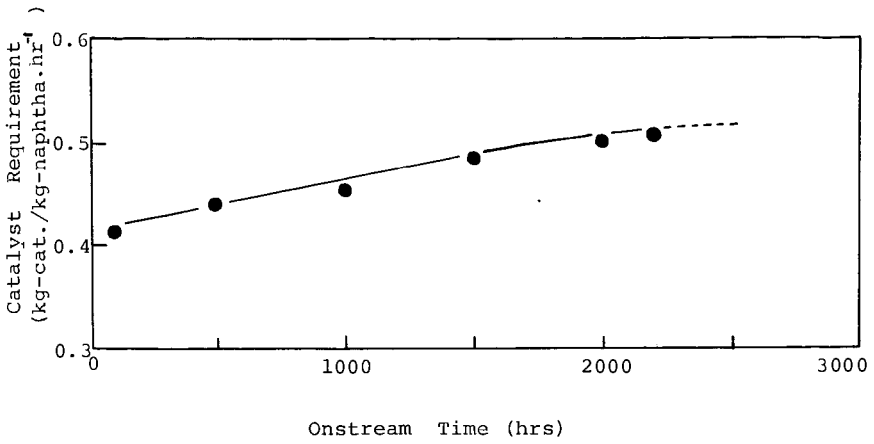


Fig.1 Activity deterioration curve of SN-108

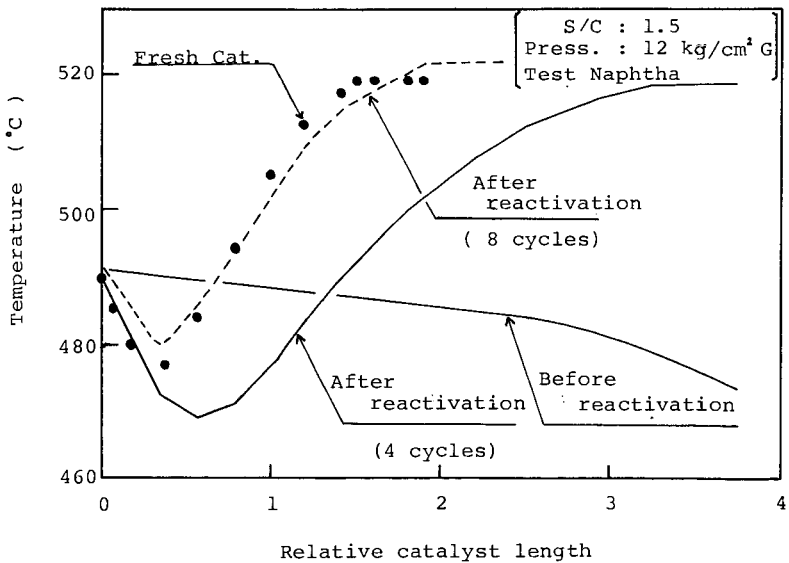


Fig.2 Recovery of the catalytic activity

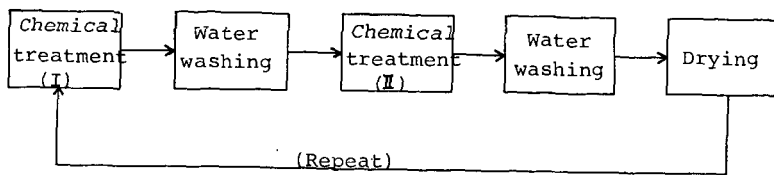


Fig.3 General process of reactivation

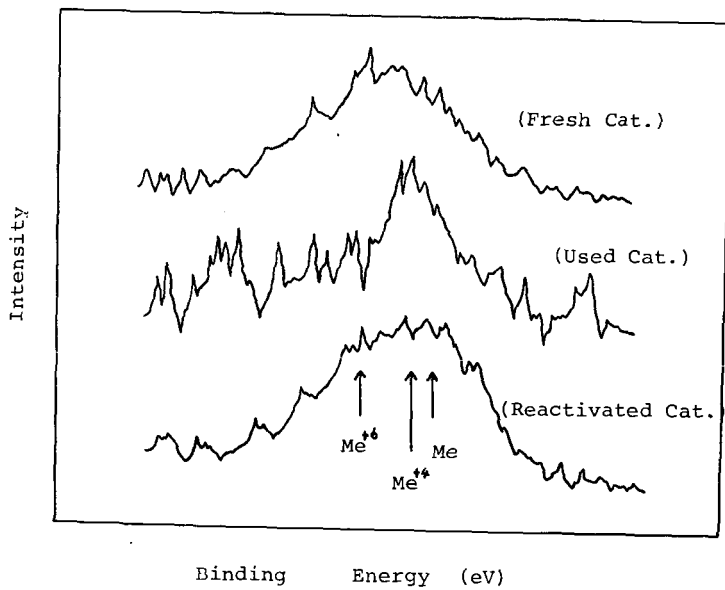


Fig.4 XPS spectra of active metal

Fluidized Bed Combustion of Residual Oils

Y. Morita, T. Kimura, H. Ikeda, Y. Kondo and E. Kikuchi

Department of Applied Chemistry, School of Science and Engineering, Waseda University, 3-4-1 Okubo, Shinjuku-ku, Tokyo 160, Japan.

INTRODUCTION

Shortage of crude oil plus the lack of progress in the development of stack gas clean up systems have sparked interest in processes that generate electric power by the fluidized bed combustion of residual oil and coal with high sulfur and nitrogen content. Many development works on the fluidized bed combustion of fossil fuels have been carried out by various organizations in U.S.A. and other countries. In all of these works, dolomite or limestone has been used as a bed material because these substances have ability to absorb H_2S or SO_2 released during combustion. Furthermore, reduced NO_x emission can be achieved by the lower operating temperature in fluidized bed combustion than conventional combustors(1,2).

The authors have investigated the combustion of various residual oils in the fluidized bed of a dolomite at $700 \sim 1000^\circ C$ and atmospheric pressure. By use of the dolomite, heavy residual oils of low reactivity such as an Arabian Light vacuum residue could be burnt with combustion efficiency higher than 98% above $850^\circ C$. It was also shown that the dolomite was effective to reduce the concentration of SO_x and H_2S in flue gases to very low levels at temperatures below $900^\circ C$. The purpose of the present work was to investigate catalytic reduction of NO_x (mostly fuel NO_x) by ammonia using a fluidized bed of the dolomite loading various kinds of metal oxide.

EXPERIMENTAL

Figure 1 shows a schematic diagram of the fluidized bed combustion system. The combustor was made of 50 mm ϕ i.d. SUS 27 stainless steel tube and its bed depth was 400 mm. Stainless steel beads (3 mm ϕ) were packed at the conical-bottom of the combustor as bed support and gas distributor. Feed oil (Arabian Light vacuum residue) was introduced at the bottom of the fluidized bed through an atomizer from a microfeeder. To prevent coke plugging in the feed pipe, the atomizer was cooled by circulating a coolant. The bed material was first heated externally to a desired temperature in a stream of air and then the residual oil was fed. After combustion started, external heating was cut off. To remove the heat evolved, water was circulated in a coil of 6 mm ϕ o.d. SUS 27 stainless steel tube which was immersed in the fluidized bed. After a certain period of combustion, ammonia was admitted to the combustion system at the upper level of fluidized bed from a cylinder which contained 5% ammonia in nitrogen.

After the condensation of steam in an ice-trap, the flue gas passed through a solution of 3% hydrogen peroxide to absorb SO_x and through a solution of ammine complex of zinc to absorb H_2S . The SO_x in the solution was titrated by barium acetate using Arsenazo III as an indicator. The H_2S concentration in the solution was determined by I_2 titration using sodium thiosulfate. The flue gases were periodically sampled to determine their compositions. The NO_x concentrations were measured as nitrous ions by means of photometric analyzer using naphthyl ethylene diamine. Compositions of gaseous products, methane, carbon monoxide and dioxide were determined by means of gas chromatography.

Dolomite from Kuzuo (Tochigi Prefecture) was used after calcined at 700°C (CaCO₃·MgO). Its composition (wt%) was as follows: CaO 65.4, MgO 33.4, SiO₂ 0.8, Al₂O₃ 0.3, and Fe₂O₃ 0.1. The dolomite was impregnated with an aqueous solution of Fe, Co, Cu, or Cr nitrate. These were finally calcined at 900°C prior to reaction.

RESULTS AND DISCUSSION

Table I shows the catalytic activity of some typical bed materials for the reduction of NO_x emitted during combustion of the residual oil. The concentration of added NH₃ (1050 ppm) was calculated from the volume of flue gases (wet basis) and feed rates of ammonia. Combustion was carried out at the optimum operating conditions for the dolomite: bed temperature, 850°C; excess air, 20%; residence time, 0.57 sec. The concentrations of NO_x in the absence of ammonia were almost independent of the kind of bed materials (near 320 ppm). The NO_x concentrations decreased on addition of NH₃ to the combustion system. As shown in Table I, Fe₂O₃-dolomite was the most active among the bed materials tested.

Table I. Catalytic Activity of Some Bed Materials for the Reduction of NO_x by NH₃

| | Dolomite | Fe ₂ O ₃ - Dolomite | CuO- Dolomite | Cr ₂ O ₃ - Dolomite | CoO- Dolomite |
|-------|----------|--|------------------|--|------------------|
| C(a) | 328 | 305 | 313 | 348 | 303 |
| C(b) | 246 | 149 | 184 | 246 | 192 |
| X (%) | 25.0 | 51.1 | 41.2 | 29.3 | 36.6 |

C(a) and C(b) are the concentrations of NO_x in flue gases in the absence and presence (1050 ppm) of ammonia, respectively. And X is % reduction of NO_x defined by $[C(a)-C(b)] \times 100 / C(a)$. The content of metal oxides was 10 wt%.

Figure 2 shows the effect of bed temperature on the reduction of NO_x by ammonia in the fluidized bed combustion using Fe₂O₃-dolomite containing 7.5 wt% of Fe₂O₃. When NH₃ was absent, the NO_x emission increased with increasing bed temperature. The NO_x emission, however, decreased in the temperature range of 700 ~ 950°C in the combustion with NH₃ added. The catalytic reduction of NO_x by NH₃ was enhanced remarkably as the bed temperature increased. At 950°C, the NO_x concentration was reduced from 337 to 116 ppm by the catalytic reduction with NH₃.

Excess air was found to be a critical factor for the catalytic reduction of NO_x on the Fe₂O₃-dolomite. With stoichiometric amount of air, the NO_x concentration was not reduced by the addition of NH₃. However, the NO_x concentration decreased with increasing amount of excess air and it was leveled off at about 10% excess air.

Figure 3 shows the effect of NH₃ concentration on the NO_x emission. The NO_x concentration decreased with increasing concentration of added NH₃. The lowest NO_x emission of 57 ppm was attained when 2000 ppm NH₃ was added at 850°C, 10% excess air and 0.61 sec residence time.

Figure 4 shows that combustion efficiency was also improved by loading Fe₂O₃ on the dolomite in the range of combustion temperature from 700 to 950°C. Here combustion efficiency was defined as percent carbon in the oil converted to carbon dioxide. Combustion efficiency increased with increasing bed temperature and reached 100% at 950°C on both bed materials. The Fe₂O₃-dolomite was more effective

for combustion at lower temperatures than the dolomite. Combustion efficiency also increased with increasing excess air and it exceeded 99% at 10% excess air without formation of carbon monoxide and methane.

Figure 5 shows the effect of bed temperature on the emission of SOx and H₂S during combustion in the fluidized bed of the Fe₂O₃-dolomite. The results on the dolomite fluidizing were also shown in Figure 5. Concentrations of (SOx + H₂S) in flue gases were as low as 10 ppm in the temperature range of 700 ~ 900°C but they increased abruptly as the bed temperature further increased as described by Moss (3) and Roberts (4). The mode in variation of (SOx + H₂S) emission with bed temperature in the Fe₂O₃-dolomite and the dolomite bed were similar. This suggests that the sulfur removing efficacy of the Fe₂O₃-dolomite is completely due to the dolomite.

CONCLUSION

The concentration of NOx emitted during the combustion of the vacuum residual oil was reduced when NH₃ was added to the fluidized bed of Fe₂O₃-dolomite. Furthermore, combustion efficiency higher than 99% was attained above 800°C. Simultaneously concentrations of (SOx + H₂S) in the flue gases were kept at very low level by the action of dolomite which might absorb SOx and H₂S. The optimum operating conditions for the Fe₂O₃-dolomite fluidized bed were determined as follows: bed temperature, 850°C; excess air, 10%; residence time, 0.61 sec. Under these conditions, the concentrations of (SOx + H₂S) and NOx were as low as 10 ppm and 57 ppm, respectively.

REFERENCES

- (1) Nack, H., Kiang, K.D., Liu, K.T., Murthy, K.S., Smithson, G.R., and Oxley, J.H., Int. Fluid. Conf. (U.S.A.) 2, 339 (1976).
- (2) Beer, J.M., Sym. Int. Combust. (U.S.A.) 16, 439 (1977).
- (3) Moss, G., Int. Conf. Fluid. Combust. D2-1 (1975).
- (4) Roberts, A.G., Stantan, J.E., Wilkins, D.M., Beacham, B., and Hoy, H.R., Int. Conf. Fluid. Combust. D4-1 (1975).

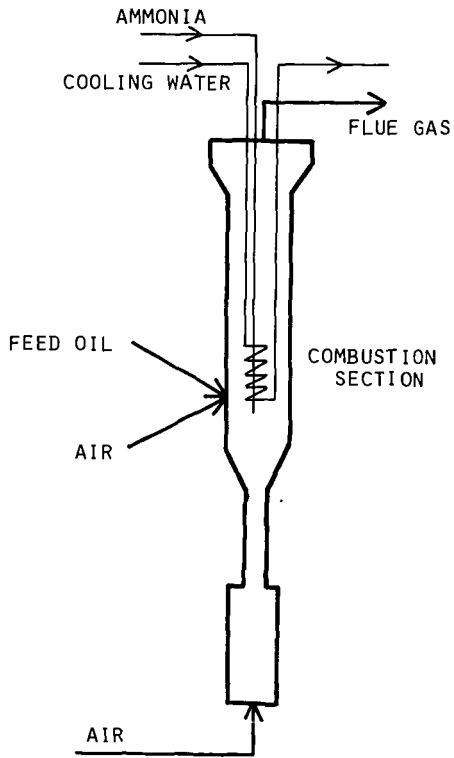
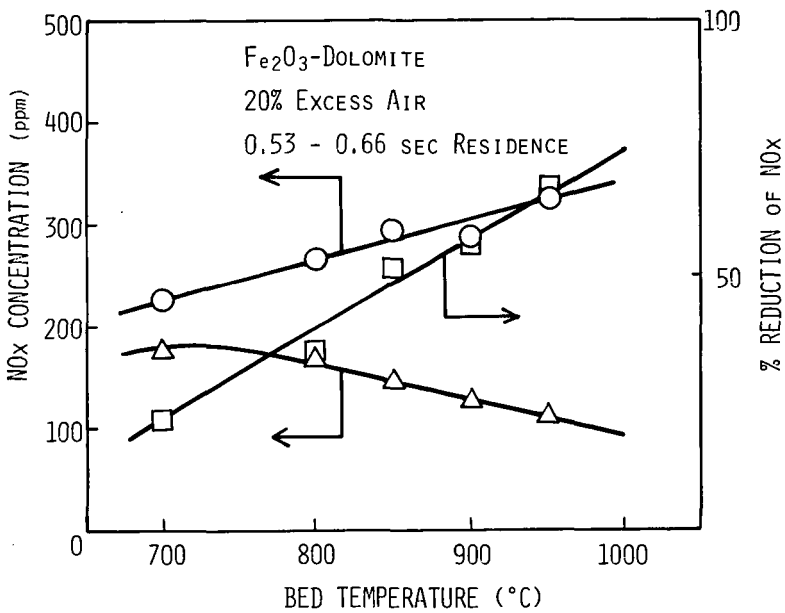


Figure 1. Diagram of Combustor Assembly



- IN THE ABSENCE OF AMMONIA
- △ IN THE PRESENCE OF AMMONIA (1050 ppm)
- % REDUCTION OF NO_x

Figure 2. The Effect of Bed Temperature on the Reduction of NO_x by NH₃.

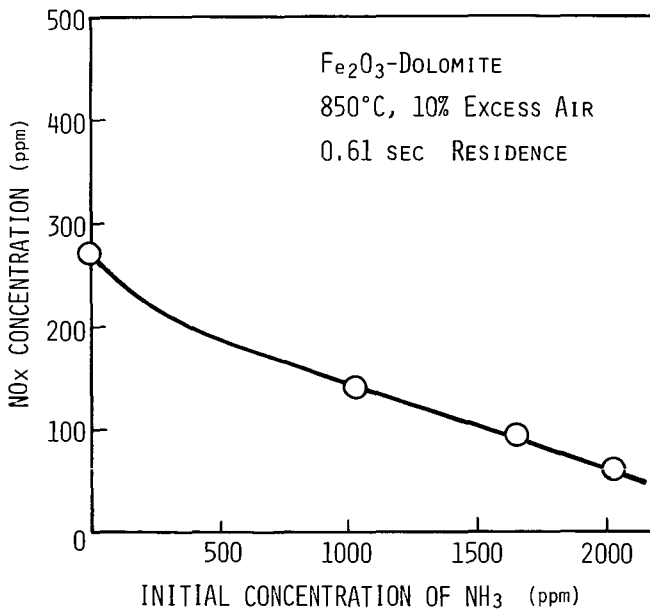


Figure 3. The Effect of NH₃ Concentration on the Reduction of NO_x by NH₃.

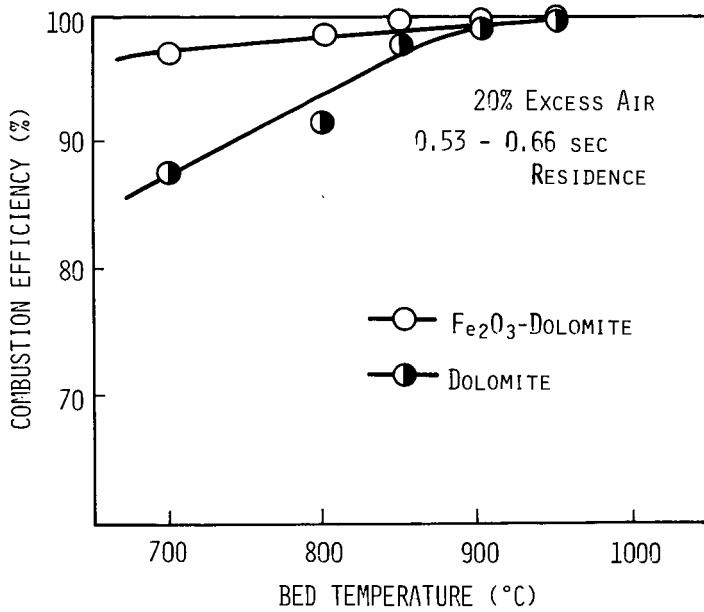


Figure 4. Relationships between Combustion Efficiency and Bed Temperature

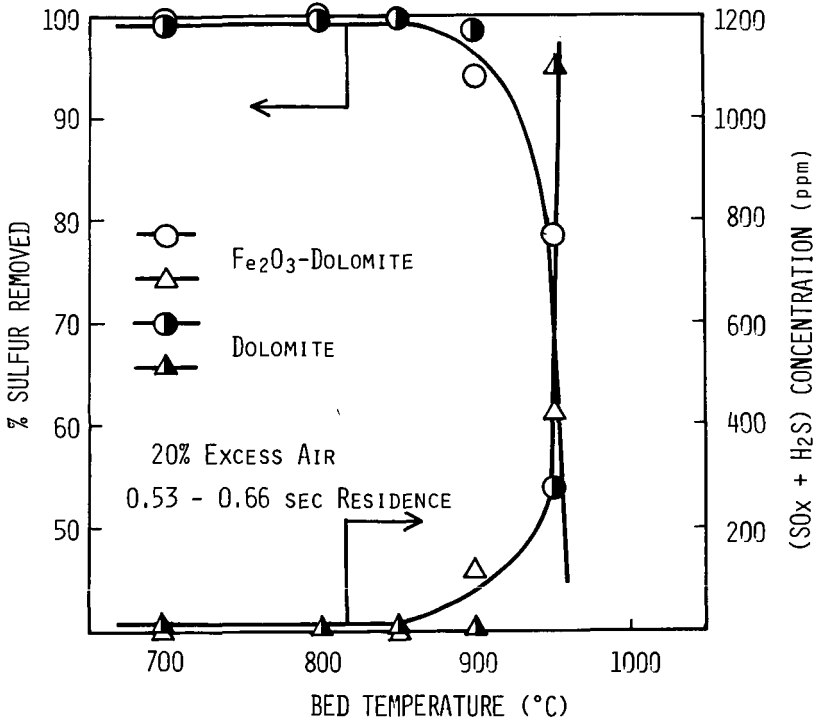


Figure 5. Sulfur Removing Efficacy of Fe₂O₃-Dolomite and Dolomite as a Function of Bed Temperature.

CHEMISTRY OF COAL ASH MELTING IN GASIFICATION AND COMBUSTION

Karl S. Vorres

Institute of Gas Technology
3424 South State Street
Chicago, IL 60616

INTRODUCTION

Coal deposits occur in a number of localities within the United States. The mineral matter in the coal varies with the location but is usually made up of quartz, pyrite, clay, shale and smaller amounts of other materials. The relative amounts of the mineral matter in the parent coal will vary from one region to another and within regions, as well as individual coal seams. During combustion or gasification, the mineral matter will contact other types of mineral matter resulting in a coal ash of different properties than the parent mineral species.

Our reliance on coal for production of energy via combustion or synthetic fuels will necessitate the ability to operate under a wide range of conditions. The boilers that generate electric power are in some cases designed to reject coal ash in the form of a molten slag. Some gasifiers are intended to operate with a continuous flow of molten ash from the gasifier to a collection zone. Continuing reliable operation of this equipment requires the ability to sustain an ash viscosity within a range to permit the ready removal of the ash material.

The determination of viscosity of the ash from coal is an expensive and time-consuming operation. A number of efforts have been made to correlate this property with the chemical composition. Different types of correlation have been suggested for use with coal ash of different ranges of compositions. It is desirable to have some understanding of the chemistry of the interactions that occur within the melt in order to more fully understand the melting behavior of this material and to make effective predictions of that behavior from the chemical composition.

ASH CATION PROPERTIES

The species that make up a coal ash after it has been in the reactor are usually metal oxides. This discussion assumes the coal ash materials are, or have been, converted to oxides. In a general way the behavior of the different ions can be viewed as the result of the important properties of charge and size that the positive ions or cations possess.

One of the more important properties is that of the size or radius. A listing of cation radii is given below for the important metal ion species in coal ash.

| | | | |
|------------------|------|------------------|------|
| Si ⁺⁴ | 0.42 | Fe ⁺² | 0.74 |
| Al ⁺³ | 0.51 | Na ⁺¹ | 0.94 |
| Fe ⁺³ | 0.64 | Ca ⁺² | 0.99 |
| Mg ⁺² | 0.67 | K ⁺¹ | 1.33 |
| Ti ⁺⁴ | 0.68 | | |

These cation radii according to Ahrens (1) are given in angstrom units, Å (10^{-8} cm). The largest ion is roughly three times the size of the smallest.

A number of correlations of behavior have been made with the base-to-acid ratio of the oxide mixtures. The acids have been defined as oxides of Si, Al, and Ti. The bases have been identified as the oxides of Fe, Ca, Mg, Na, and K. The listing of radii does not readily divide the group into acids and bases. Iron is listed twice because it can occur in melts in two oxidation states.

In melts and other liquid solutions there is a tendency for the smaller more highly charged positive ions to draw the larger negatively charged ions into a complex ion. For coal ash this complex could have a general formula, MO_x^{-n} , where x oxide ions are coordinated around an M ion and the overall negative charge is n units. The coordination number, x, is determined primarily by the ratio of the radii of the M and O ions. The value of 1.40 angstroms was assigned to the oxide ion. A coordination number of 4 is observed for Si and Al. The coordination number of 6 is observed for the rest of the ions except K which has the number of 8 in these systems. In some cases Al may also be found with a coordination number of 6.

The other property of importance in the coal ash cations is that of charge. The charge affects the relative capacity to attract the negative ions to the cation. The capacity is also affected by the size of the ion. The ionic potential, defined as the ratio of cation oxidation state or valence to the ionic radius, gives a measure of the ability of the cation to attract the anion. A high ionic potential indicates an ability to compete effectively with other ions of lower ionic potential for a limited supply of oppositely charged ions. The values of the ionic potentials calculated from the ionic radii given earlier are listed below.

| | | | |
|------------------|-----|------------------|------|
| Si ⁺⁴ | 9.5 | Fe ⁺² | 2.7 |
| Al ⁺³ | 5.9 | Ca ⁺² | 2.0 |
| Ti ⁺⁴ | 5.9 | Na ⁺¹ | 1.1 |
| Fe ⁺³ | 4.7 | K ⁺¹ | 0.75 |
| Mg ⁺² | 3.0 | | |

Examination of these values quickly indicates that the highest values belong to the acid group of Si, Al, and Ti, while the lower values are associated with the bases. This grouping and the physical interpretation of the ionic potential lead to the suggestion that this parameter is a physical characteristic which can be useful in quantifying acid and base behavior. To the extent that this is true, then this parameter should also be useful in further efforts to correlate coal ash chemical compositions with melting, viscosity and other properties associated with ash deposition in the process.

The ionic potential is an indication of a cation's capacity to form a complex ion such as SiO_4^{-4} . This capacity may be limited by the availability of oxide ions as in coal ash systems. In the compound SiO_2 each Si is expected to have

four oxide ions around it. This can only be accomplished if oxygen ions are shared between different Si ions. This tetrahedral coordination occurs both in the solid and liquid state and requires sharing of oxide ions in all cases. The sharing of oxide ions leads to the formation of polymeric aggregates in the liquid state. Individual angular SiO_2 groups may join in chains, sheets, or other arrangements. These groupings require additional oxide ions for termination of the polymer. Oxides of ions of lower ionic potential than Si can provide these oxide ions. The groupings will terminate more frequently and the average polymer or aggregate size would decrease as more oxide ions became available. Al ions occur in many mineral species with Si and are able to take the place of Si in the polymeric groupings. In a similar fashion it is expected that they would be able to participate in the polymer formation in the melt. Alkali metal oxides could most readily supply oxide ions since they have the lowest ionic potentials. The alkali cations would find positions between the polymeric chains or other groupings involving Si and Al. At equilibrium, complexes will be formed due to attractive forces and disrupted by thermal energy. A population of complexes of various sizes would be expected for a given composition. The larger the aggregates, especially chain types, the greater the number of opportunities for interaction between them and to increase the viscosity.

The effectiveness of the addition of other cations to reduce the viscosity for reliable slag formation depends on the rate of mixing of the additives, the dissociation of the cations and oxide ions and the diffusion of these ions into the melt. These steps are typically much slower than the acid-base reaction in water solutions typified by titration.

A flux such as fluorite, CaF_2 , is added in some cases to decrease the viscosity of a melt. This material provides a supply of F^- anions with a size comparable with oxide ions. The fluoride radius is 1.36 Å compared to 1.40 for oxides. Fluorite is even more electronegative than oxide and both can serve as chain terminators. The addition of calcium fluorite instead of the oxide provides twice as many anions for each calcium ion, effectively doubling the capacity to limit polymer formation.

In coal ash melts, the role of an acid is that of a complex ion or polymer former. The tendency for polymer formation increases with ionic potential. The bases serve as oxide ion donors. The tendency to yield oxide ions is greatest for those with lowest ionic potential. The oxide ions are attracted by cations with the highest ionic potential in the system to form polymers, terminate polymer groupings and diminish viscosity. The cations with low ionic potentials exist as unattached hard spheres and can facilitate slippage between the polymer groups.

THE ROLE OF IRON

Ferric and ferrous ions have significantly different ionic potentials (4.7 and 2.7). The ferric ion falls between the values for the acid group and the basic group. The importance of iron is associated with its unique ability to alternate between the two valence states, the different behavior associated with

each state and its significant contribution to the composition of many coal ashes. Iron acts as either an acid or a base depending on its charge. The intermediate values for ionic potential indicates that ferric iron would be a weak acid and ferrous would be a moderate base.

The combustion process in boilers produces a coal ash with a mixture of the two states. Analyses have indicated that about 20% is present as ferric ion while the remainder was ferrous. In some slagging gasifiers elemental iron has been observed. Since the majority of the iron was present as ferrous ion it was appropriate to classify the iron oxides with the bases (assuming that a single classification had to be made) even though the oxide is identified as Fe_2O_3 in earlier correlations. The gaseous environment determines the equilibrium oxidation state of the iron in coal ash systems. Iron is an important component of most Eastern coal ashes, usually following Si and Al in abundance. The behavior of the coal ash system depends on the oxidation state of the iron. Viscosity studies show a reduction of coal ash viscosity for reducing conditions with a reduction of the ratio of ferric to ferrous iron. (2) This observation is consistent with the role of a complex former for the acidic ferric iron and an oxide donor role for the ferrous iron.

Figure 1 (3) indicates the liquidous relationships in the alkali and alkaline earth-silica systems. A comparison of the depression of the melting point for different alkali metal oxides indicates that the depression is greatest for the ions with lowest ionic potential or strongest bases. A similar relationship holds for the alkaline earths. In general, for this series of bases the melting point depression increases with decreasing ionic potential.

Table 1 (4) indicates the analysis of a series of coal ashes and gives the ash fusion temperatures. The indicated initial deformation temperature of 2900°F is just below 1600°C for the low-volatile bituminous coal. This material is essentially a two-thirds SiO_2 /one-third Al_2O_3 mixture. An examination of the Al_2O_3 - SiO_2 equilibrium diagram indicates that this softening temperature would be close to the eutectic melting temperature. One would then expect a very much higher liquid temperature.

Table 1 also gives the ash analyses of a series of high-volatile bituminous coal taken from three Eastern fields and one Western field. The SiO_2 contents of three of the four are close to 48%. The Al_2O_3 contents diminish from about 23% to 11%. The TiO_2 remains relatively constant in the range 0.6 to 1.0%. The Fe_2O_3 content is indicated from about 29.3 down to 7% which would indicate a wide range of behavior depending on the gaseous environment. The sum of SiO_2 and Al_2O_3 , the dominant acid species, is greatest for the Ohio coal and the highest oxidizing fluid temperature is observed for this material. The next highest sum is for the Illinois coal and this one has the next highest oxidizing fluid temperature. The remaining two (Utah and West Virginia) have similar total Si and Al contents. However, the iron content is much lower for the Utah coal than for the West Virginia coal. In an oxidizing environment this means that the total acid content would be higher for this coal and a higher oxidizing fluid temperature is observed for the West Virginia fuel.

An examination of the phase equilibrium diagram for the system $\text{FeO-Al}_2\text{O}_3\text{-SiO}_2$, Figure 2 (5), shows that in the region of about 50% SiO_2 , 25% Al_2O_3 , 25% FeO , which corresponds fairly closely to the Ohio coal, one would expect a liquidus temperature of about 1450°C (2642°F) which is in good agreement with the fluid temperature in the reducing environment for the Ohio coal ash. The lowest temperature on the diagram is at the eutectic between fayalite, tridymite and iron cordierite. The indicated temperature is 1083°C or 1980°F which is in general agreement with the observed initial deformation temperature for the reducing environment. The minimum temperature would correspond to a localized region in a sample where this phase could form through diffusion of different constituents with the required composition for formation of that material.

The composition of the Illinois coal ash is similar; however, this material does contain a significant amount of calcium oxide which is expected to reduce the melting temperature below that observed for the Ohio coal. The two temperatures are similar but are somewhat less for the Illinois material.

The West Virginia coal is richer in Fe_2O_3 according to the analysis. Again, referring to the $\text{FeO-Al}_2\text{O}_3\text{-SiO}_2$ phase equilibrium diagram and normalizing the content of these three constituents, the material falls in the same general region in the phase diagrams as the Ohio and Illinois coals. However, the melting temperature expected appears to be about 1540°C or about 2430°F . This temperature is somewhat higher than the observed reducing fluid temperature, however there is also about 4% calcium oxide, 1.2% magnesium oxide, and smaller amounts of other bases which contribute to the reduction in observed temperature.

The observed reducing initial deformation temperature is similar for the three coals from Ohio, West Virginia and Illinois. The same equilibrium phase diagram would apply to all three and would reflect the earlier mentioned minimum temperature.

The Utah coal is richest in SiO_2 , CaO , and Al_2O_3 . In the phase equilibrium diagram for this system, Figure 3 (6), the normalized composition for this ash lies in the pseudo-wollastonite region. From this normalized composition the melting temperature to be expected is about 1280°C or 2336°F . The solid species would be a wollastonite ($\text{CaO} \cdot \text{SiO}_2$). This temperature is about 80° above the observed fluid temperature in a reducing environment, indicating that the iron has the ability to depress the melting point by this amount in conjunction with the other basic materials. The oxidation of the iron is able to elevate the fluid temperature as indicated, through production of the acid ferric ions and associated change in oxide ion availability.

BIBLIOGRAPHY

1. Ahrens, L. H., *Geochim. Cosmochim. Acta.*, 2, 155 (1952).
2. *Steam, Its Generation and Use*, Publ. by the Babcock & Wilcox Co., N.Y., pp. 15-16 (1978).
3. *Phase Diagrams for Ceramists*, E. M. Levin, H. F. McMurdie & F. P. Hall, Fig. 128, pp. 66 (1956). Am. Ceram. Soc., Columbus, Ohio.

4. Ref. 2, pp. 15-20.
5. Ref. 3, Fig. 696, pp. 241 (1964 edition).
6. Ref. 3, Fig. 631, pp. 220 (1964 edition).

Table 1

Ash content and ash fusion temperatures of some U.S. coals

| Rank: | Low Volatile Bituminous | High Volatile Bituminous | | | |
|--------------------------------------|-----------------------------------|--------------------------|-----------------------------|-------------------|------|
| | Pocahontas No. 3 West Virginia | No. 9 Ohio | Pittsburgh West Virginia | No. 6 Illinois | Utah |
| Seam | | | | | |
| Location | | | | | |
| Ash, dry basis, % | 12.3 | 14.10 | 10.87 | 17.36 | 6.6 |
| Sulfur, dry basis, % | 0.7 | 3.30 | 3.53 | 4.17 | 0.5 |
| Analysis of ash, % by wt | | | | | |
| SiO ₂ | 60.0 | 47.27 | 37.64 | 47.52 | 48.0 |
| Al ₂ O ₃ | 30.0 | 22.96 | 20.11 | 17.87 | 11.5 |
| TiO ₂ | 1.6 | 1.00 | 0.81 | 0.78 | 0.6 |
| Fe ₂ O ₃ | 4.0 | 22.81 | 29.28 | 20.13 | 7.0 |
| CaO | 0.6 | 1.30 | 4.25 | 5.75 | 25.0 |
| MgO | 0.6 | 0.85 | 1.25 | 1.02 | 4.0 |
| Na ₂ O | 0.5 | 0.28 | 0.80 | 0.36 | 1.2 |
| K ₂ O | 1.5 | 1.97 | 1.60 | 1.77 | 0.2 |
| Total | 98.8 | 98.44 | 95.74 | 95.20 | 97.5 |
| Ash fusibility | | | | | |
| Initial deformation temperature, F | | | | | |
| Reducing | 2900+ | 2030 | 2030 | 2000 | 2060 |
| Oxidizing | 2900+ | 2420 | 2265 | 2300 | 2120 |
| Softening temperature, F | | | | | |
| Reducing | | 2450 | 2175 | 2160 | |
| Oxidizing | | 2605 | 2385 | 2430 | |
| Hemispherical temperature, F | | | | | |
| Reducing | | 2480 | 2225 | 2180 | 2140 |
| Oxidizing | | 2620 | 2450 | 2450 | 2220 |
| Fluid temperature, F | | | | | |
| Reducing | | 2620 | 2370 | 2320 | 2250 |
| Oxidizing | | 2670 | 2540 | 2610 | 2460 |

SiO₂-R₂O, RO

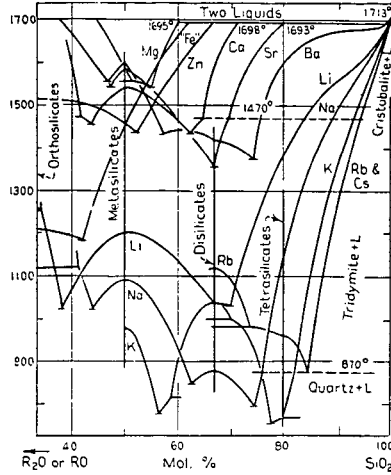


Figure 1. Liquidus Relations in the Alkali and Alkaline Earth-Oxide-SiO₂ Systems

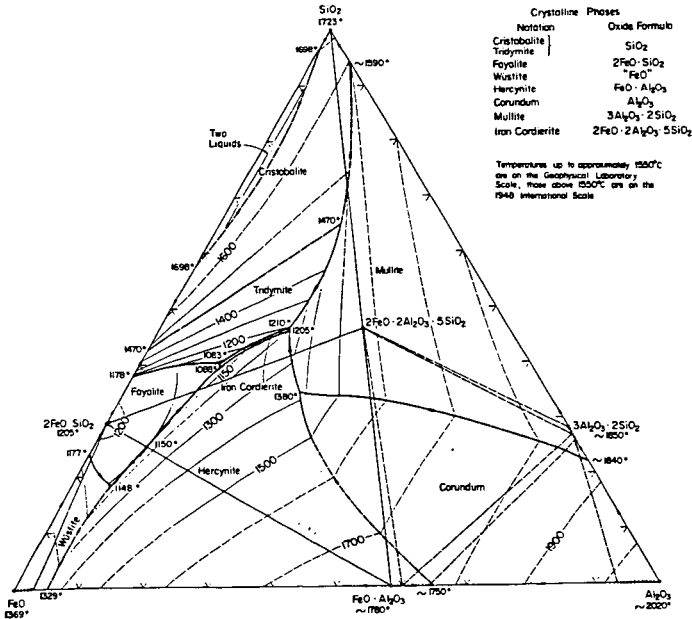


Figure 2. Composite "FeO"-Al₂O₃-SiO₂ System

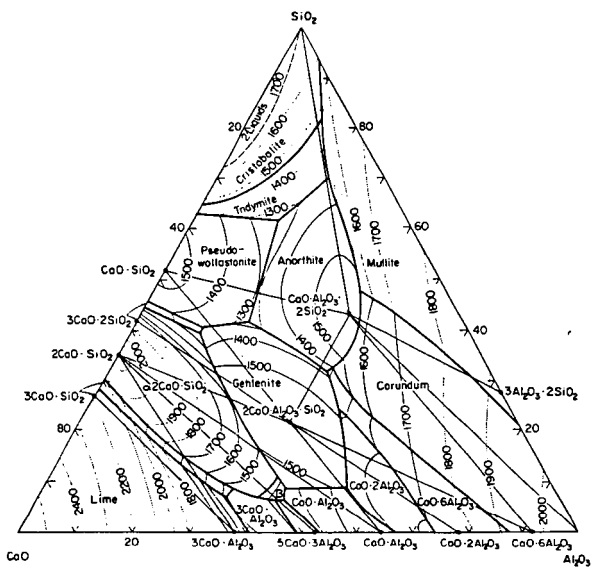


Figure 3. $\text{CaO}-\text{Al}_2\text{O}_3-\text{SiO}_2$ System

CALCIUM CARBONATE DEPOSIT FORMATION DURING THE LIQUEFACTION OF LOW RANK COALS

J. B. Stone, K. L. Trachte and S. K. Poddar

Exxon Research and Engineering Company
P. O. Box 4255; Baytown, Texas 77520

Introduction

During the liquefaction of low rank coals, that is subbituminous or lower, the calcium humates in the coal decompose to form calcium carbonate solids. These solids have been identified in the reactor solids from pilot plant runs and could be a significant operational problem in commercial sized equipment. The purpose of this paper is to present our operating experience and proposed solutions to this problem as it applies to the Exxon Donor Solvent, or EDS, Process. The units used in the EDS development program range from 3 gram batch reactors to a one ton-per-day process development unit.

In the EDS Process, which is shown in Figure 1, crushed coal is slurried with a hydrogen donor recycle solvent and liquefied in a tubular upflow reactor to which molecular hydrogen has been added. The liquefaction operating conditions are about 840°F and 2000 psig. The liquefaction reactor product is separated into a light hydrocarbon gas stream, the spent solvent, which is recycled and upgraded in a catalytic hydrogenation unit, the total liquid product and a residual bottoms slurry which is processed in a Flexicoker to produce process fuel and some additional liquid product. The ash residue from the Flexicoker is landfilled. The plant is balanced in that the solvent, hydrogen and process fuel needed are generated by the process. For an Illinois No. 6 bituminous coal approximately 2.7 barrels of liquid are produced per ton of dry coal. Liquid yields from a balanced plant processing lower rank coals are less because of their lower carbon content.

Source of Calcium Carbonate Deposits

Most of the calcium in low rank coals is in the form of salts of humic acids. These calcium humates are represented in Figure 2. These humates decompose in the liquefaction reactor to form calcium carbonate. The exact mechanism for calcium carbonate formation is not known, but all of the components of the calcium carbonate within the dashed lines are readily available. The calcium is ionically bonded to carboxylic acid and sometimes phenolic groups in the coal. Since these groups are weak acids, the calcium can be ion-exchanged. There are also other calcium salts present in coal. Calcite and gypsum are found predominately in higher rank coals, bituminous and above, and are stable under liquefaction conditions. The three coals studied in greatest detail for calcium carbonate deposition are: a Wyoming subbituminous coal from the Wyodak mine, a North Dakota lignite from the Indian Head Mine and a Texas lignite from the Big Brown Mine.

Identification of Calcium Carbonate Problem

During the second quarter of 1975, a screening study was completed on the Wyoming subbituminous coal. Inspection of the reactors used in these runs revealed calcium carbonate deposition as wall scale. Since this was not a problem specific to the pilot units used, calcium carbonate deposition could have a significant impact on the operation of a commercial unit. A study was then initiated to identify the magnitude of this deposition problem.

The bench scale and pilot units used in the calcium carbonate deposition study range from 3 gram batch tube autoclave reactors to a one ton-per-day Pilot Plant. Each of these units plays an integral part in the testing of solutions to the calcium carbonate problem. Some solutions can easily be tested in the batch reactor; whereas other solutions must be tested in a flow unit. The liquefaction product from the batch reactor is separated with a hydrocarbon solvent wash and the residue is analyzed for calcium carbonate by X-ray diffraction and thermo-gravimetric analysis. In the flow units, the residual bottoms can be tested similarly as in the batch case. But more importantly, the reactor solids from these units can be analyzed for particle size, calcium carbonate content and calcium carbonate growth patterns and crystal forms. The larger units, the 50- and 100-pound-per-day Recycle Coal Liquefaction Units (RCLU) and the one ton-per-day Coal Liquefaction Pilot Plant (CLPP), are completely integrated pilot plants with distillation and recycle solvent hydrogenation sections. A smaller Once-Through Coal Liquefaction Unit (OTCLU) uses a simulated recycle solvent and has no distillation or solvent hydrogenation facilities.

Types of Deposit Forms

Calcium carbonate deposition occurs as scale on the liquefaction reactor wall and free-flowing solids or oolites. Wall scale is very easy to detect in the liquefaction reactor solids by its characteristic shape. Oolite solids are particles of the coal mineral matter, clays, silicas, etc., which have a uniform layer of calcium carbonate growing around them. These oolites are predominately concentrated in mesh size fraction one size larger than the feed coal. For example, in the small pilot plants which use minus 100 mesh coal, the oolites are concentrated in the 50 to 100 mesh size. Similarly, for the large pilot plant using minus 30 mesh coal, the oolites are concentrated in the 16 to 30 mesh range. These oolites would be expected to grow larger during much longer runs, because they would not be swept out of the reactor by the normal fluid flow.

The predominant form of the calcium carbonate growth does depend on the coal from which it was formed. With the Wyoming subbituminous coal, the wall scale formed is primarily vaterite which is rarely found in nature. The growth on the oolites is primarily calcite and some wall scale, at times, is also calcite. For North Dakota lignite, on the other hand, scale and oolites in the first stages of the reactor are always calcite and in the latter stages of the reactor sodium magnesium carbonate (eitelite). The forms of the calcium carbonate deposits for the Texas lignite are essentially the same as those for the Wyoming coal.

Most of our operating experience with low rank coals has been the processing of Wyoming coal in the 50 pound-per-day RCLU pilot plant. After a run in this unit the reactor is removed and drained of solids and residual coal slurry. Methyl ethyl ketone washes and sometimes mechanical scraping are needed to remove the scale. The total solids are toluene washed to remove excess solvent, dried and sieved. For the RCLU unit, the wall scale is plus 50 mesh. Oolites are 50 to 100 mesh. Minus 100 mesh material is unreacted feed coal or coal mineral matter which has not yet formed oolites. The ranges of accumulation of calcium carbonate containing solids for the three coals studied are shown in Table 1. The accumulation is reported as pounds per 100 pounds of coal fed to compensate for the variations in run length. The only significant difference in the three coals is that the Texas lignite produces more oolites than the Wyoming coal. The oolite accumulation for the North Dakota lignite is not available because it was not possible to accurately sieve the reactor solids. The deposit accumulation is unaffected by changes in most liquefaction process variables, such as, temperature, space velocity, solvent quality, solvent boiling range and hydrogen gas rate. During high pressure operations (2500 vs. 1500 psig) there was a significant increase in oolite and wall scale accumulation.

Scanning Electron Microscope (SEM) photographs have provided invaluable information about the reactor solids recovered from the flow units. Most of the oolites have surfaces of calcium carbonate. This is identified by an X-ray spectrometer which is an integral part of the SEM. Some oolites have surfaces of iron sulfide crystals which are again identified by the X-ray. The iron sulfide surface is much more irregular in appearance than the calcium carbonate surface. Cross sections of these oolites reveal more information about the calcium carbonate growth. These cross sections show that calcium carbonate growth occurs on seeds of the coal mineral matter. There is also evidence of iron sulfide growth on the mineral matter seeds. The seed material can be iron sulfide itself, silica or clays or any part of the coal mineral matter. The iron sulfide growth is very regular and crystalline whereas the calcium carbonate growth is more evenly distributed.

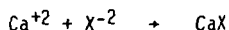
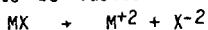
The other type of calcium carbonate growth is wall scale. The reactor used in the 15 pound-per-day OTCLU is very amenable for detecting scale. It is a vertical hairpin tubing reactor which can be split along its length for a detailed inspection of any scale present. The reactor which is shown schematically in Figure 3 has eleven sections: six upflow and five downflow. The graph at the bottom of Figure 3 is a plot of the amount of calcium in the wall scale versus the reactor section number. Almost all of the calcium carbonate scale is in the first half of the reactor with the heaviest concentration in the 15 to 25 minute residence time range. This finding has been verified directionally in the pilot plants, although it is very difficult to detect the exact location of scale in the pilot plants. The SEM can also be used to detect the structure of the scale. The surface of the scale which is next to the reactor is smooth and is mostly iron sulfide and a slight amount of nickel sulfide. This is indicative of the fact that the sulfidation products of the wall are providing growth sites for calcium carbonate. The process side of the scale has a surface which is very similar to that of the oolites.

Solutions to Deposition Problem

Potential solutions to calcium carbonate deposition that we have investigated are mechanical or chemical in nature. The mechanical solutions tried are solids withdrawal and acid washing. The theory behind solids withdrawal is that since the oolites are free-flowing solids it should be very easy to withdraw them from the liquefaction reactor. Oolite growth can be controlled if the withdrawal rate is high enough so that the oolites do not have sufficient residence time for growth. Solids withdrawal has been very effective in controlling the growth of oolites in the one ton-per-day unit. A way to control wall scale growth is periodic acid washing of the reactor walls during reactor shutdowns. Several chemicals have been identified as ones which can effectively dissolve the calcium carbonate scale. A combination of solids withdrawal and acid washing is a very cost effective way of controlling calcium carbonate deposits. An uncertainty here is whether the scale would flake off the reactor walls and cause operational problems during the extended runs (6-12 months) in a commercial plant. This uncertainty will be tested during the operation of our 250 ton-per-day pilot plant now under construction.

The effect of solids withdrawal on solids accumulation and oolite growth in the one ton-per-day unit is shown in Table 2. During a four-day run without solids withdrawal, 1/4 percent of the coal fed remained in the reactor and of this amount, about one-third was larger than the feed coal, that is, plus 30 mesh. During a 16-day run with solids withdrawal, only nine-hundredths of one percent of the coal remained in the reactor, and essentially none of the oolites grew larger than the feed coal. Wall scale growth rates were about the same for both runs. This scale growth would amount to about 1/2 inch per year.

Chemical solutions to the calcium carbonate deposition problem can be classified as coal pretreatments or reactor additives. Coal pretreatments are ion exchanges in which the humate calcium which is the source of the calcium carbonate deposition is reacted with acids or metal salts. The resulting calcium salt would, of course, need to be stable in the liquefaction reactor for the exchange to be successful. A generalized mechanism for the ion exchange is:



Where the $\overset{\sim}{Ca}$ is a representation of the humate calcium.

The acids that we have concentrated most on and have been successful in ion exchanging with the calcium are sulfuric acid and sulfur dioxide. The sulfur dioxide readily dissolves in the coal's moisture and forms sulfurous acid. The HSO_3^- ion then diffuses through the coal pores to the site of the humate calcium where it exchanges with the calcium. Various metal salts have also been tried. In general, bivalent metal salts exchange very effectively with the humate calcium. Monovalent metal salts will also exchange if the resultant calcium (CaX) salt is very insoluble. For example, sodium carbonate will exchange more effectively than sodium sulfate because the resulting calcium carbonate is more insoluble than calcium sulfate. This insolubility provides an added driving force for the exchange. The metal salts would have an added advantage if the metal were catalytically active in liquefaction.

Coal pretreatments can be tested in the batch tube autoclave reactor because the form of the calcium has been changed, and it is only necessary to determine the amount of calcium carbonate in the liquefaction residue. Untreated Wyoming coal forms about 40% calcium carbonate on ash. Sodium sulfate is only partially effective in ion-exchanging with the calcium. The liquefaction residue contained about 20% calcium carbonate on ash (the remaining calcium is calcium sulfate). A run in the 15 pound-per-day unit did produce scale which confirms that sodium sulfate is only partially effective. Sulfur dioxide treated coal has only about 8% calcium carbonate on the ash of the residue. Ferrous sulfate and sulfuric acid are even more effective in exchanging with the calcium. After these pretreatments there is only 1% calcium carbonate in the residue ash. Reactor inspections after runs in the 15 pound-per-day unit revealed no scale for the sulfur dioxide, ferrous sulfate and sulfuric acid pretreatments. Sulfur dioxide and sulfuric acid treatments were also successful in preventing scale and oolite growth in the 50 pound-per-day RCLU.

Liquefaction reactor additives have different proposed mechanisms for success, but in general are not fully effective. Surfactants theoretically will disperse the calcium carbonate into a fine size so that it will flow out of the reactor before forming scale. It was difficult to find a surfactant that was stable under liquefaction conditions, but when we tried one that was, it had no effect on scale growth. There are two types of scavengers used: One to tie up the calcium, for example, colloidal silica to form calcium silicate, and another to scavenge the carbon dioxide, for example magnesium oxide. Neither of these materials was effective in preventing calcium carbonate growth. Another possible mechanism for the colloidal silica to work is by providing many small sites for the calcium carbonate growth. This could prevent wall scale growth. Addition of two weight percent colloidal silica on coal did reduce scale formation in the 15 pound-per-day unit but did not eliminate it. Crystal modifiers have been used to shift the crystal form from vaterite to calcite but have had no effect on scale growth. Some reactor additives which have shifted the Wyoming coal wall scale from

vaterite to calcite are water, hydrogen sulfide and various chelating agents. The basic reason for the failure of these reactor additives is that the calcium carbonate formation occurs in the pores of the coal, and reactor additives reach only the coal particle surface at best.

SUMMARY

The major findings in our liquefaction work with low rank coals are that oolite formation and wall scale growth are primarily related to coal rank. We have detected both forms of calcium carbonate deposits with every low rank coal tested. As long as the calcium in the coal is present in the humate form, calcium carbonate deposition will occur. The physical withdrawal of solids from the liquefaction reactor can effectively control oolite accumulation and growth but not wall scale. Wall scale can be removed during reactor shutdowns by acid washing. Liquefaction reactor additives are generally ineffective in controlling calcium carbonate deposition. Coal pretreatment, that is, ion-exchange, can be very effective in altering the form of the calcium salt and thus prevent any type of calcium carbonate deposition in the liquefaction reactor.

ACKNOWLEDGEMENT

This work was performed at Exxon Research and Engineering Company's Baytown Research and Development Division in cooperation with the Corporate Research Laboratories as part of the Exxon Donor Solvent Coal Liquefaction Development Program. Funding for this program is shared by the U.S. Department of Energy, The Carter Oil Company (an Exxon affiliate), Electric Power Research Institute, Japan Coal Liquefaction Development Company, Ltd., Phillips Petroleum Company, and Atlantic Richfield Company. The authors gratefully acknowledge this support.

TABLE 1
RANGES OF CALCIUM CARBONATE SOLIDS ACCUMULATION

| COAL TYPE | WYOMING SUBBITUMINOUS | NORTH DAKOTA LIGNITE | TEXAS LIGNITE |
|---|--------------------------|-------------------------|----------------------|
| MINE | WYODAK | INDIAN HEAD | BIG BROWN |
| <u>COAL COMPOSITION,</u> WT% DRY COAL | | | |
| CALCIUM | 1.22 | 1.31 | 2.2 |
| SODIUM | .05 | .84 | .05 |
| <u>SOLIDS ACCUMULATION,</u> LBS/100 LBS COAL FED | | | |
| TOTAL SOLIDS | 0.35-0.57 | 0.22-1.1 | 0.49-2.0 |
| OOLITES | 0.07-0.27 | NA | 0.39-0.49 |
| WALL SCALE | 0.002-0.007 | 0.005-0.035 | 0.002-0.010 |
| <u>TOTAL SOLIDS COMPOSITION,</u> WT% | | | |
| ASH | 56-70 | 57-67 | 78-82 |
| CaCO ₃ | 24-83 | 17-49 | 67-74 |
| Na ₂ Mg(CO ₃) ₂ | - | 24-46 | - |
| CaCO ₃ FORMS | CALCITE, VATERITE | CALCITE | CALCITE, VATERITE |

TABLE 2
EFFECT OF SOLIDS WITHDRAWAL ON SOLIDS ACCUMULATION
ONE TON-PER-DAY UNIT, WYOMING COAL

| | WITHOUT SOLIDS WITHDRAWAL | WITH SOLIDS WITHDRAWAL |
|--|------------------------------|---------------------------|
| <u>INITIAL SOLIDS ACCUMULATION,</u> WT% OF FEED COAL | 0.25 | 0.09 |
| <u>PARTICLE GROWTH</u> WT% OF REACTOR SOLIDS LARGER THAN FEED COAL | 33 | 1 |
| <u>WALL SCALE GROWTH</u> INCHES/DAY | .001 | .0011-.0015 |

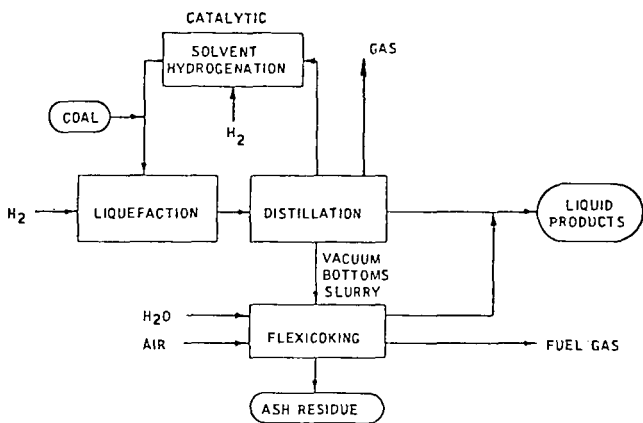


FIGURE 1. EDS PROCESS SCHEMATIC

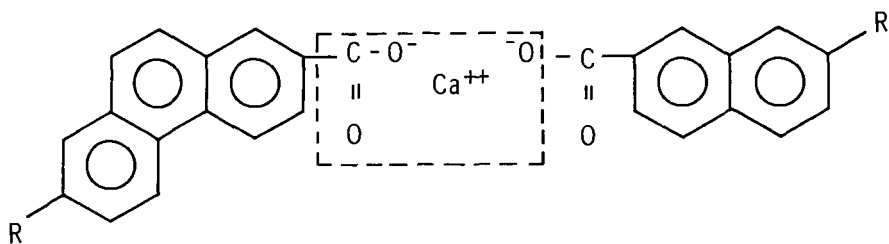


FIGURE 2. REPRESENTATION OF CALCIUM HUMATES

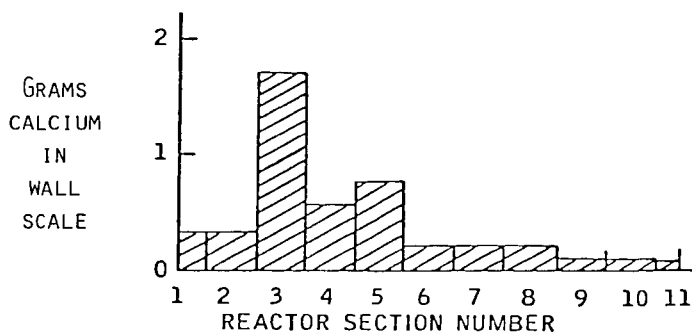
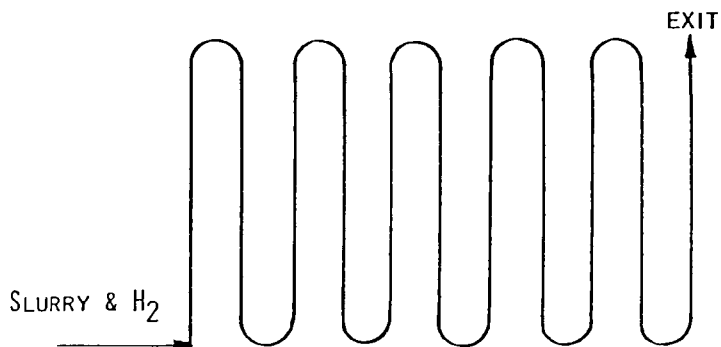


FIGURE 3. SCALE DISTRIBUTION IN A 15 LB/DAY UNIT

A ^{13}C , ^2H , ^1H NMR AND GPC STUDY OF STRUCTURAL EVOLUTION
OF A SUBBITUMINOUS COAL DURING TREATMENT WITH TETRALIN AT 427°C
James A. Franz
Pacific Northwest Laboratory, P.O. Box 999, Richland, WA 99352

The recently developed magic angle/cross polarization Waugh-Pines techniques⁽¹⁾ promise to significantly advance the state of understanding of the statistical structure of coals. However, much work remains to be done in the area of detailed product characterization before predictable models of coal reactivity can be constructed. Although tetralin and other donor systems have been utilized in numerous studies, the results of Neavel⁽²⁾ were among the first to demonstrate that certain coals can be rendered soluble in pyridine in >90% conversion in <5 min. Very little effort to characterize the evolution of coal structure over time during reductive thermolysis of coal has been made.

In this work the products from the thermal dissolution of subbituminous Kaiparowitz coal at 427°C in tetralin are examined by spectroscopic (^{13}C , ^1H , ^2H NMR, IR) molecular weight (gel permeation chromatography and vapor pressure osmometry) and elemental analysis and hydroxyl group analysis. The use of 1, 1-dideuteriotetralin in conjunction with ^2H NMR to monitor the time dependence of introduction of deuterium into aliphatic and aromatic structures is presented. The tetralin-derived products were monitored versus time by glpc to determine the relationship between hydrogen uptake and coal product yields.

Reactions of Coal and Tetralin or 1,1-dideuteriotetralin

The procedure for these sections is similar to that of Neavel⁽²⁾: A 0.6 cm x 6.3 cm stainless steel tube equipped with threaded caps was charged with 0.15 g tetralin and 0.25 g coal or a 0.95 cm x 6.3 cm tube was charged with 1 g coal and 2 g tetralin. One or more tubes attached to a compressed air vibrator were plunged into a molten lead bath maintained at a temperature which would compensate for the heat uptake by the reaction vessel and stabilized as rapidly as possible at 427°C or 500°C. The sample tubes were withdrawn from the bath at various times from 2.5 min to 2 hr and quenched in water, the contents were washed out with 50 ml of THF and filtered through a 25 μm millipore filter. The insoluble material was dried and weighed. The THF soluble portions were analyzed directly by GPC in THF and the entire reaction mixture analyzed by gas chromatography (GLPC) to determine tetralin, naphthalene, methyl indane et al. The THF solutions were concentrated to 1-3 ml and combined with ~ 50 ml pentane. The resulting precipitate was repeatedly washed until no tetralin or naphthalene was detectable by GLPC of the pentane wash. This fractionation provides an excellent separation of coal from solvent-derived material. The pentane-insoluble, THF-soluble fractions were examined by vapor pressure osmometry, elemental analysis, GPC, hydroxyl group analysis and ^{13}C , ^2H and ^1H FTNMR.

Results and Discussion

As shown by Figure 1, subbituminous Kaiparowitz coal is rapidly converted to THF-soluble products at 427°C. The ultimate yield of 80% of THF-soluble products plus gases is achieved after approximately 35 min with most (75%) of the ultimate product forming within 10 min. A correction for ash content in the residues would increase the yields by approximately 8%. Vapor pressure osmometry of pyridine solutions of the THF-soluble fraction

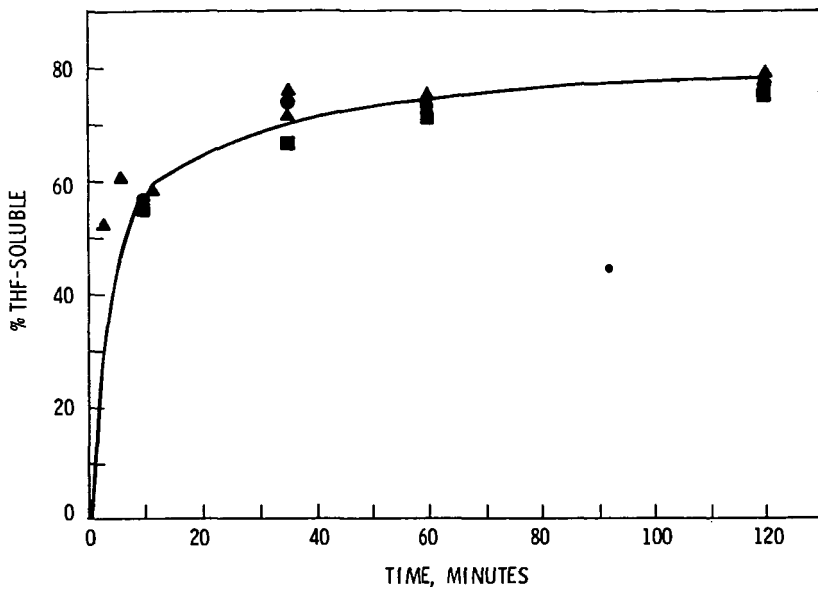


FIGURE 1. Percent THF-Soluble Product plus Gases from 427°C Reaction of Kaiparowitz Coal and Tetralin ■ = Total carbon rendered soluble ● = 1°/sec heatup rate ▲ = 15°C/sec heatup rate

shows a drop in number average molecular weight from approximately 1200 at 10 min to about 500 at 30 min and longer with a slight but reproducible increase after 2 hr reaction. Gel permeation chromatography of the entire reaction mixture in THF (including tetralin and tetralin derived products) shows the molecular size behavior versus time (Figures 2 and 3). Consistent with the vpo results, the principal peak occurs at molecular weight 1000 (polystyrene and polyethylene glycol standards). This peak decreases in size relative to major peaks at MW < 500 so that by 35 min, molecular weights less than 500 dominate weight distribution occur in the first 15-20 min of reaction. After 35 min, the growth of the CA. 300 MW peak occurs only very gradually. The vpo results show an increase in molecular weight from CA. 500 to 600 between 1 and 2 hr. At 500°C the conversion of the higher molecular weight constituents to lower molecular weight products occurs more rapidly than at 427°C. Constituents with MW >10,000 are not observed at 500°C; however, even after 2 hr at 500°C there remains a substantial fraction of material of molecular weight >1000.

The conversion of aliphatic to aromatic structure occurs throughout the reaction. Figure 4 shows the ratio of aliphatic/aromatic hydrogen, deuterium and carbon versus time from integrals corrected for solvent absorptions. The carbon values are not quantitative, but qualitatively exhibit the same trend shown by the proton and deuterium data, with a decrease in C_{ali}/C_{arom} from 0.9 to 0.6 over a 2 hr reaction. The IR spectra of successive THF-soluble fractions shows the expected growth in aromatic CH stretch ($3000-3100\text{ cm}^{-1}$) relative to aliphatic CH stretch ($2900-3000\text{ cm}^{-1}$), and a notable increase in aromatic CH out-of-plane bending motion ($700-850\text{ cm}^{-1}$).

^{13}C NMR spectra for 10, 35, 60 and 120 min reactions were similar in most respects except for small changes in aromatic/aliphatic integrals. The aromatic region of a typical ^{13}C NMR spectrum (Figure 5) revealed a distinct region of absorption at δ 150-160 consistent with aryl ether and phenolic CO and a shoulder at 110-120 ppm, typical of aromatic carbons adjacent to aromatic carbons bearing oxygen atoms.^(3,4,5) The aryl ether and phenolic absorption accounts for 11%, 11%, 7% and 8% of the total aromatic integral of 10, 35, 60 and 120 min reactions, respectively. Since these are quaternary carbons with low or no NOEs, these percentages represent less than half of the actual percentages of aromatic carbons possessing oxygen substituents. Elemental analysis of the THF-soluble fractions (Table 1) reveals a rapid initial drop in oxygen content from CA. 17% in the coal to 14% in the THF-soluble fraction. The %O about 2% over a 2 hr reaction time in the THF-soluble fraction. The percent of oxygen in hydroxyl groups drops from CA. 30% to CA.15% over a 2 hr. reaction time indicating the incursion of dehydrocyclization-type reactions, consistent with the drop in aromatic CO observed by ^{13}C NMR.

Table 1. Elemental Analyses of THF-Soluble Fractions and Coal from the Reaction of 500 mg Tetralin and 250 mg Coal in 0.65 x 6.3 cm Reaction Vessels at 427°C

| | Reaction Time, | %C | %H | %N | %S | %O(diff) ^(a) | % ash | %OH ^(b) |
|--------------------------|----------------|-------|------|------|------|-------------------------|-------|--------------------|
| | min | | | | | | | |
| Coal | -- | 71.0 | 5.19 | 1.1 | 0.3 | 17.11 ^(a) | 8.6 | -- |
| | 10 | 75.45 | 6.19 | 1.3 | 0.3 | 14.0 | 1.2 | 4.8 |
| THF-Soluble Fractions | 35 | 76.22 | 6.32 | 1.43 | 0.2 | 13.9 | 1.0 | 4.2 |
| | 60 | 77.81 | 6.09 | 1.5 | 0.3 | 13.5 | 0.6 | 1.8 |
| | 120 | 79.49 | 6.01 | 1.7 | 0.12 | 13.3 | 0.8 | 2.2 |

(a) Oxygen analyses by difference in the presence of large ash residues are not reliable.

(b) Hydroxyl uncertainty is $\pm 1\%$.

Hydrogen transfer during the reaction is very rapid during the first 15 min of reaction but levels off and becomes sluggish after 30 minutes, after the low energy processes of conversion of coal to preasphaltenes is succeeded by slower bond breaking processes leading to asphaltenes.

The analysis of tetralin, methylindane, and naphthalene by GLPC during the reaction revealed that for every six carbon atoms in the total coal, 1.0, 1.2, 1.7 and 2.4 hydrogen atoms are transferred from tetralin at 5.5, 10, 35 and 60 minutes reaction time. Thus the hydrogen uptake per incremental increase in product yield is much lower in the initial 5 min of reaction than at succeeding times. This is consistent with the breaking of fewer bonds per weight of solvated material yielding radicals or ions which may abstract hydrogen or hydride from tetralin during the early stages of reaction.

The ^2H NMR results⁽⁶⁾ (Figure 4) qualitatively support the concept of a rapid initial disruption of aliphatic structure in the early stages of conversion of coal to preasphaltenes. About 55% of the coal is dissolved within 10 minutes, deuterium incorporation occurring much more rapidly at aliphatic sites.

The ^1H NMR results reveal that the bulk of aliphatic hydrogen occurs at position β to aromatic rings ($\text{ArCH}_2\text{CH}_2\text{CH}_3$) and cyclohexyl or internal methylenes of normal paraffins (δ 1-1.9) and at positions adjacent (α) to aromatic rings ($\text{ArCH}_2\text{CH}_2\text{CH}_3$) (δ 1.9-3.2). Aliphatic hydrogen is detectable in modest amounts assigned to diaryl substituted methylenes (α^2) (δ 3.2 - 4). As shown by Table 2, the percent of α and α^2 hydrogen doubles from 2.5 to 35 min, consistent with a significant increase in aromatic structure during the reaction.

TABLE 2. Distributions of Aliphatic Hydrogen versus Time from ^1H NMR Integrals of THF-Soluble Products (427°C) in Pyridine- d_5

| Reaction Time (min) | Chemical Shift Ranges, δ (ppm) | | | |
|------------------------|---------------------------------------|------------------|------------------|------------------|
| | δ 0-1.0 | δ 1.0-1.9 | δ 1.9-3.2 | δ 3.2-4.0 |
| 2.5 | 18% | 55% | 24% | 3% |
| 10 | 13% | 48% | 34% | 5% |
| 35 | 10% | 38% | 44% | 7% |
| 60 | 9% | 45% | 39% | 8% |

Summary

The dissolution of subbituminous coal occurs very rapidly to produce predominantly phenolic aromatic or aryl ether structures associated with about an equivalent amount of aliphatic structure with molecular weights typically around 1000, and as high as 30,000. The ^{13}C NMR spectra show the products to possess a wide variety of structures in the chemical shift regions of diaryl and triaryl methanes and ethanes, cyclic and acyclic saturated hydrocarbons, with insignificant oxygenated aliphatic, carbonyl or quinoidal structure. Oxygenated aliphatics, if present, are destroyed in the first 10 min of reaction.⁽⁷⁾ The hydrogen transfer process occurs initially at aliphatic sites but is soon incorporated in aromatic structure, as indicated by ^2H NMR results. The ^1H NMR results confirm the gradual production of aromatic structure during the reaction. The incursion of condensation reactions is reflected in a gradual upswing of average molecular weights beyond 1 hr reaction times, as well as a small but definite drop in hydroxyl group content in the coal products.

Acknowledgment

This work was supported by the Department of Energy, Division of Energy Research, Basic Energy Sciences Program, under contract EY-76-C-06-1830 with Battelle Memorial Institute. The author wishes to especially acknowledge the help of Mr. Gary L. Roberts for sample preparation, glpc and gpc analysis.

References

1. Bartuska, V. J., G. E. Maciel, J. Schaefer, and E. O. Stejskal, Fuel **56**:354, 1977 and references therein.
2. Neavel, R. C., Fuel **55**:237, 1976. For review of related earlier work, see loc. cit.
3. Levy, G. C. and G. L. Nelson, Carbon-13 Nuclear Magnetic Resonance for Organic Chemists, Wiley-Interscience, New York, N.Y., 1972.
4. Stothers, J. B., Carbon-13 NMR Spectroscopy, Academic Press, New York, N.Y., 1972.
5. Emsley, J. W., J. Feeney and L. H. Sutcliffe, High Resolution Nuclear Magnetic Resonance, Pergamon Press, New York, N.Y., vol 2, 1966.
6. For recent work in the use of ^2H nmr for characterization of batch hydrogenation, see Skowronski, R. P., J. J. Ratto, and L. A. Heredy, "Deuterium Tracer Method for Investigating the Chemistry of Coal Liquefaction - Annual Technical Progress Report for the Period July 1976 - June 1977," FE-2328-13, Atomic International Division, Rockwell International, Canoga Park, CA 91304, February 1978.
7. (a) Similar decreased in oxygen content have been reported in experiments using naphthalene or phenanthrene as a reaction medium: Whitehurst, D. D., M. Farcasiu, and T. O. Mitchell, "The Nature and Origin of Asphaltenes in Processed Coals," Electric Power Research Institute Report AF-252, Annual Report, February, 1976, Ch. 10, and references therein. (b) See ibid., p. 6-46 for comments on quinoidal functions.

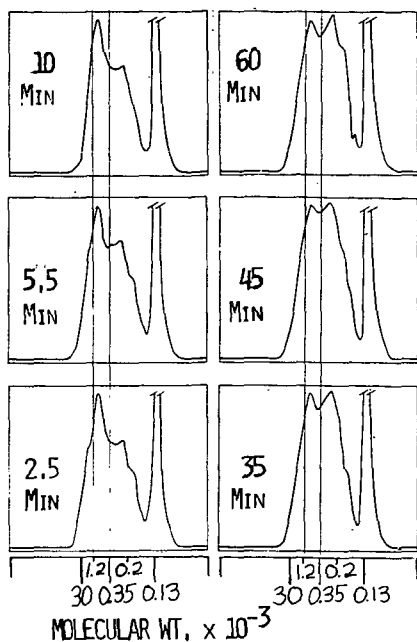


FIGURE 2. GPC trace of the THF solutions of products from the reaction of tetralin and coal at 427°C for varying periods of time. Tetralin and tetralin-derived products appear at MW 130.

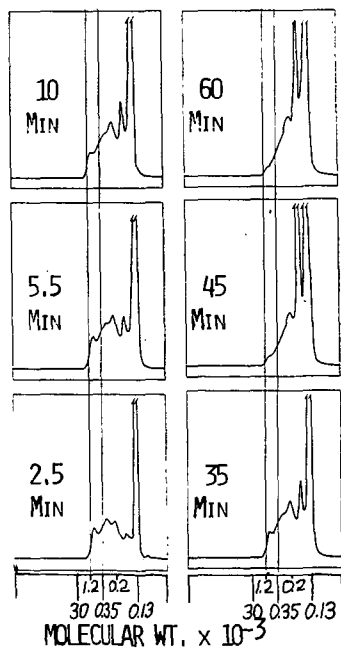


FIGURE 3. GPC trace of the THF solutions of products from the reaction of tetralin and coal at 500°C for varying periods of time. Tetralin and tetralin-derived products appear at MW 130.

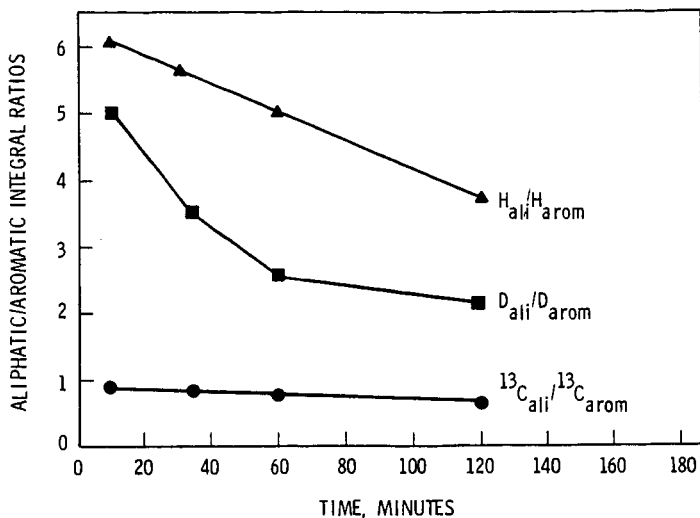


FIGURE 4. Aliphatic/Aromatic FTNMR Integral Ratios vs. Time for Reactions of Coal and Tetralin at 427°C. FTNMR spectra were determined at 79.54 MHz (1H), 20.000 MHz (^{13}C) and 12.211 MHz (2H) with a Varian model FT-80 multinuclear FTNMR spectrometer.

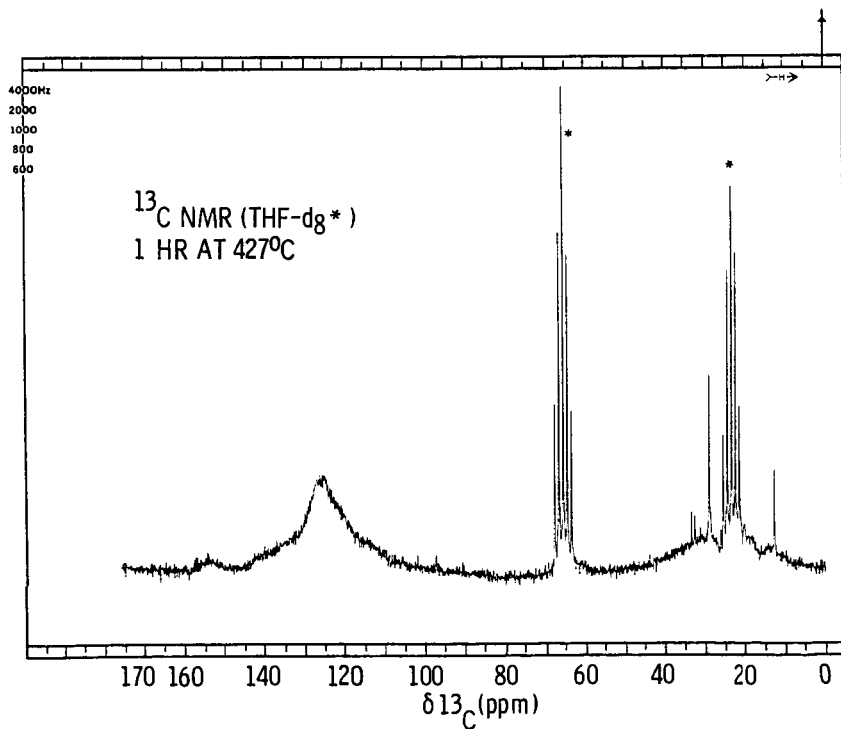


FIGURE 5. ^{13}C FTNMR Spectrum of the Pentane-Insoluble, THF-Soluble Products from the reaction of Tetralin and Coal in THF- d_8 at 427°C for 1 hr.

Effect of Hydrogen Pressure on Rate of Direct Coal Liquefaction

Minoru Morita
Shimio Sato
Takao Hashimoto

Department of Chemical Engineering
Yamagata University
Yonezawa, Japan 992

Introduction

There have been numbers of studies for direct coal liquefaction. Many of them have been carried out with batch autoclaves, which are heated up to a designed temperature (hereinafter called nominal reaction temperature), followed by holding at that temperature for a desired time (hereinafter called nominal reaction time) and cooling down. Then total pressure inside the autoclaves changes with the temperature varying and consuming of hydrogen by the reaction. Thus the hydrogenation of coal is non-isothermal and non-isobaric. Workers, however, have analysed kinetics conventionally considering experimental results by the autoclave as those under isothermal and isobaric conditions at a reaction time according to a nominal reaction time (NRT) (1-6)

The authors pointed out that the conventional analysis (hereinafter called isothermal analysis) was unsuitable for not only investigation of reaction kinetics represented by a scheme including a unobservable species but also calculation of the real value of rate parameters (7). Effect of hydrogen pressure on a rate of the reaction has been investigated by some workers (1-3). They examined dependence of initial hydrogen pressure or average pressure during period of NRT on rate constants which are calculated by the isothermal analysis using data obtained under different initial pressures at same nominal reaction temperature (NRTM). From the same reason as above mentioned, however, it may be doubtful for these studies to be calculated a accurate value of rate parameters.

In this report, hydrogen pressure effect on the rate and rate parameters values was estimated by non-isothermal analysis, in which experimental results with a batch autoclave were allowed to remain non-isothermal and non-isobaric.

Apparatus and Procedure

The experiments were carried out with a shaking type 0.5-liter autoclave. The apparatus and procedure were identical with those previously described (7). Experiments were made under the following conditions: from 350°C to 440°C NRTM, from 2-minutes to about 2-hours NRT and from 50 atm to 110 atm initial hydrogen pressure. 12 grms of powdered coal and 28 grms hydrogenated and decrystallized anthracene oil as vehicle were used. A catalyst, consisting powdered sulphur, ferrous hydride and molybdenic oxide in 1:1:1 at weight ratio, was prepared in this laboratory. Taiheiyo coal (Japanese) and Morwell coal (Australian) were studied. Ultimate analysis, on a moisture-free basis, showed that Taiheiyo coal had a higher carbon-to-hydrogen ratio of 1.17 (79.8%C and 5.7%H) than that of 1.05 (65.3%C and 5.2%H) in

Morwell coal. Proximate analysis showed that moisture, fixed carbon and volatile materials contents (%) were 12.6, 52.4 and 34.2 for Morwell coal, and being 4.9, 27.7 and 47.0% for Taiheiyo coal, respectively.

Extents of reaction were determined by measuring product solubility in two solvents, benzene and n-hexane. Then organic benzene insolubles (OBIS), in which unconverted coal and cokes produced by side reactions were contained, asphaltene and oil were separated and weighed by the general procedure (6)

Experimental Results and Discussions

Examples of process time-temperature and process time-pressure curves, at different NRT's, are given in Fig. 1. The changes in pressure indicates that the absorption of hydrogen apparently is initiated about 250°C, and after the temperature has been reached at the NRTM of 440°C, the pressure begins to decrease at almost constant rate by consuming of hydrogen with the hydrogenation, follows by rapid decreasing as the temperature decreases. Fig. 2 and 3 represent the experimental results of Morwell coal liquefaction under various initial hydrogen pressures at 350°C of NRTM. Those represent that dependence of reaction course and the rate on the initial hydrogen pressure is not very sharp; under any pressure the courses show similar trends—i.e., an increased NRT increases oil formation from coal, while it has less influence on asphaltene production. Compared with the reaction extent at zero NRT (that during pre-heating and quenching period), the extent for NRT period is little. Liquefaction, moreover, progresses to fair degree in spite of low NRTM of 350°C. These hydrogenation characteristics may be explained from Morwell coal's properties: pyrolysis accompanying deoxygenation from groups containing oxygen will precede hydrogenation, because Morwell coal have much oxygen contents of 30% (by difference) as indicated from the ultimate analysis; this coal is converted into oil and asphaltene to appreciable degree by the pyrolysis through the pre-heating and quenching period, and remaining unreacted coal is reacted to form oil. Fig. 4 and 5 show the experimental results for Taiheiyo coal. From those it is found that there is a tendency to increase reaction rate with increasing initial hydrogen pressure, and being a marked one at the higher NRTM; moreover, the higher initial hydrogen pressure prevents cokes formation from occurring; under the lowest initial hydrogen pressure at NRTM of 440°C, oil yield decreases against OBIS fraction increasing with increasing NRT. This can be expressed as produced oil is degraded to make cokes, which is measured as OBIS. On the other hand, under higher initial hydrogen pressures there is little influence of oil degradation.

Hydrogenation Rate Analysis

From previously reported facts (1-6) it may be considered that coal is liquefied through the following two-step process as the main reaction, coal → asphaltene → oil. Then under severe reaction conditions of higher temperature, or under the influence of a active catalyst, gasification and cokes formation is accompanied with the main reaction simultaneously. For a case where the oil is degraded to an appreciable degree, the authors proposed the following four-step scheme taking into account cokes formation from polymerization of the oil, coal → asphaltene → oil → resin → cokes (7). With this scheme Miike coal (Japanese) liquefaction behaviors were investigated using

the non-isothermal analysis method to be well expressed. To describe the Morwell coal liquefaction properties, however, the above mentioned scheme must be modified by addition of another reaction process such as one step oil formation, coal→oil. Therefore, in this study a reaction scheme was derived so as to express the experimental hydrogenolysis courses, and its kinetic parameters values including reaction order with respect to hydrogen pressure were estimated so that simulated courses might have close agreement with the experimental ones. On estimation of the rate parameters values in the derived reaction scheme, as its rate equations was so complicated that an analytical method might be unsuitable, a numerical analysis based on the non-linear least sum of squares method was used; Marquardt method was adopted because of its good convergency. A estimation procedure is illustrated with flow chart. Its detail is as follows: experimental reaction temperatures and pressures values at ten or fifteen process times in each run were stored up; from these storage reaction temperature and pressure-process time curves of each run were described by a spline function (9); reaction courses of each run were simulated using the rate equations; from this function and values of rate parameters, i.e., reaction orders, activation energies and frequency factors, the parameters values were optimally estimated from comparing the simulated courses with experimental ones. To remove interference with the optimum estimation by compensation effect between frequency factor and activation energy, variables were transformed (10). A detail of investigated results will be presented in the meeting.

Conclusions

Effect of hydrogen pressure on coal hydrogenation properties was investigated. It was found that for liquefaction of Morwell coal in which oxygen contents appears to be considerable, hydrogen pressure little effect. In the case of Taiheiyo coal liquefaction hydrogen pressure had effects: higher pressure gave higher oil yield and prevented cokes formation from occurring.

A reaction scheme was derived so as to express the experimental liquefaction courses, and kinetics was analysed by the proposed non-isothermal method using the batch autoclave data which is non-isothermal and non-isobaric ones.

Reference

1. Weller S., M. G. Pelipetz and S. Friedman, "Kinetics of Coal Hydrogenation (Conversion of Asphaltene)" *Ind. Eng. Chem.*, 43, 1572(1951)
2. Pelipetz M. G., J. R. Salmon, J. Bayer and E. L. Clark, "Catalyst-Pressure Relationship in Hydrogenolysis of Coal" *Ind. Eng. Chem.*, 45, 806(1953)
3. Maekawa Y., T. Ishii and G. Yakeya, "The Effect of Hydrogen Pressure on the Hydrogen Reaction of Coal" *J. Chem. Eng. Japan*, 10, 101(1977)
4. Pelipetz M. G., E. M. Kuhn, S. Friedman and H. H. Storch, "Effect of Catalysts on the Hydrogenolysis of Coal" *Ind. Eng. Chem.*, 40, 1259(1948)
5. John A. Ruether, "Kinetics of Heterogeneously Catalyzed Coal Hydroliquefaction" *Ind. Eng. Chem., Process Des. Dev.*, 16, 249(1977)
6. Falkum E. and R. A. Glenn, "Coal Hydrogenation Process Studies (Effects of Time on Restricted Hydrogenolysis of Spitzbergen Coal with Adkins Catalyst)" *Fuel*, 31, 133(1951)
7. Morita M., S. Sato and T. Hashimoto, "Rate Analysis of Direct Coal Liquefaction under Non-isothermal Conditions" Preprint of the 14th Congress for Coal Science , Japan, Tokyo Nov. 2 (1978)
8. Marquardt, D. W., "An Algorithm for Least-Sum-Squares Estimation of Nonlinear Parameters" *J. Soc. Ind. Appl. Math.*, 11, 431 (1963)
9. Greville T. N. E., "Introduction to Spline Functions" pl, Academic Press, (1969)
10. Himmelbrau D. M., "Process Analysis by Statistical Method" pl94, John Wiley & Sons, Inc., (1968)

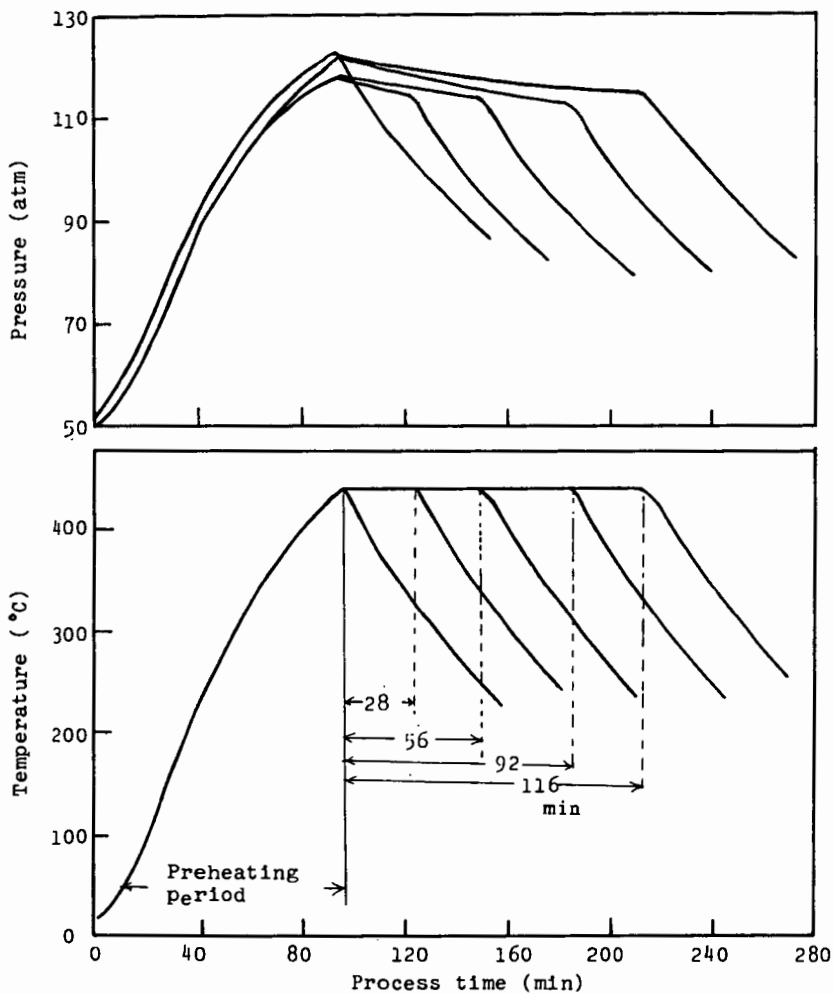


Fig. 1 Examples of the experimental pressure- and temperature-
 curves at the nominal reaction temperature (NRTM) of
 40 °C under several nominal reaction times (NRT)

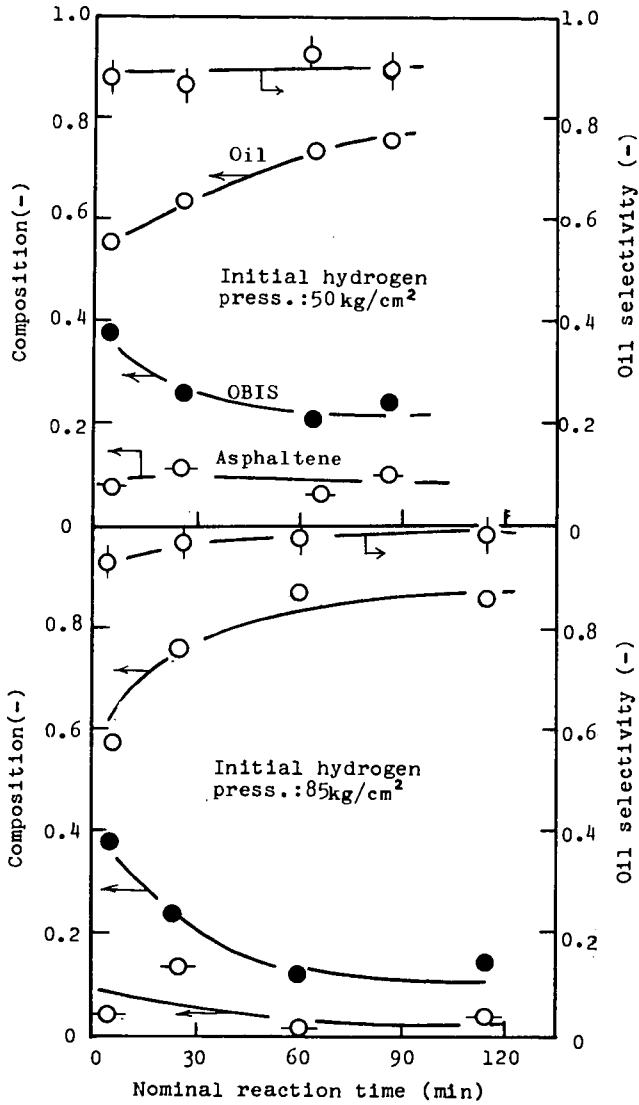


Fig. 2 Liquefaction course of Morwell coal under lower initial hydrogen pressure at NRTM of 350°C

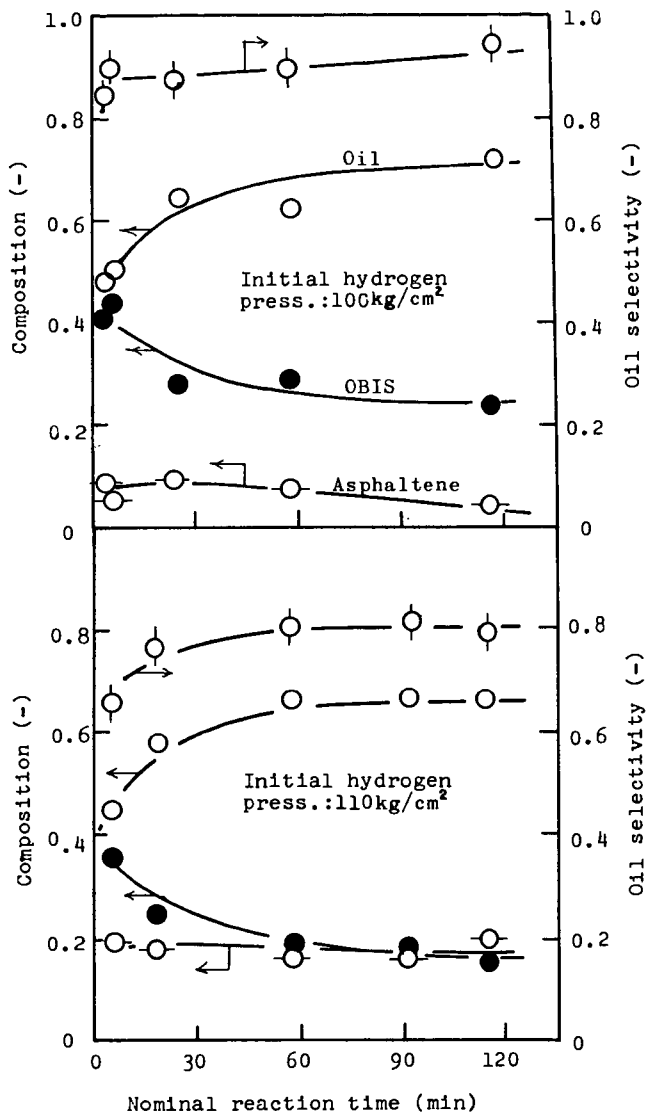


Fig. 3 Liquefaction course of Morwell coal under higher initial hydrogen pressure at NRTM of 350°C

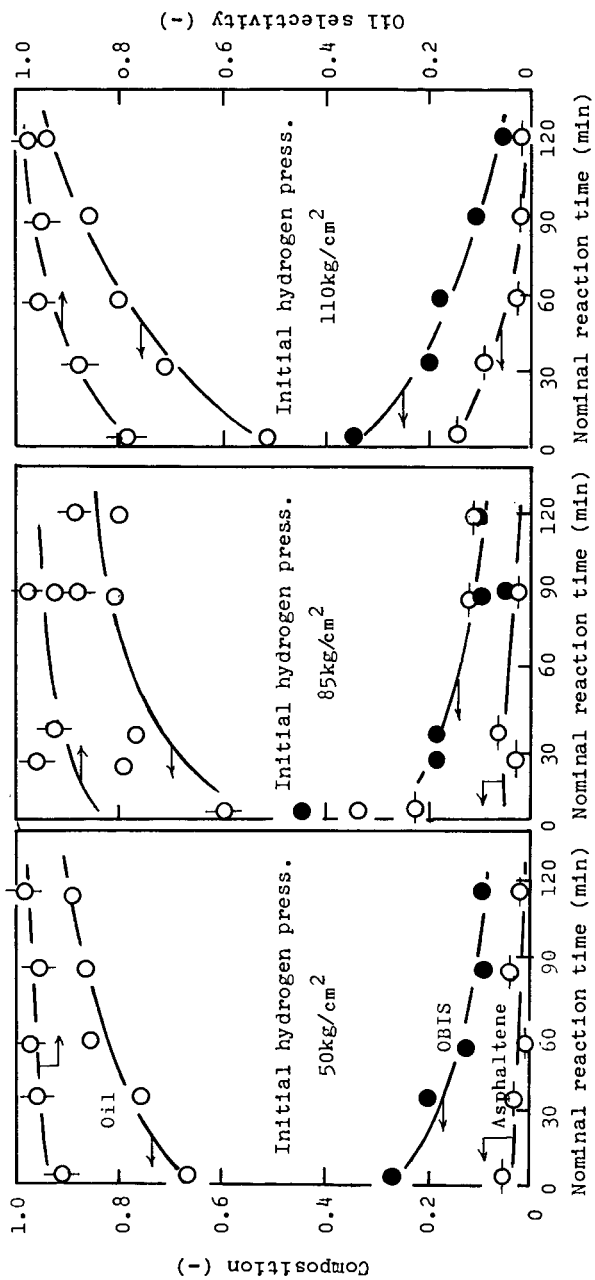


Fig. 4 Dependence of initial hydrogen pressure on liquefaction course of Taiheiyō coal at lower NRTM of 380°C

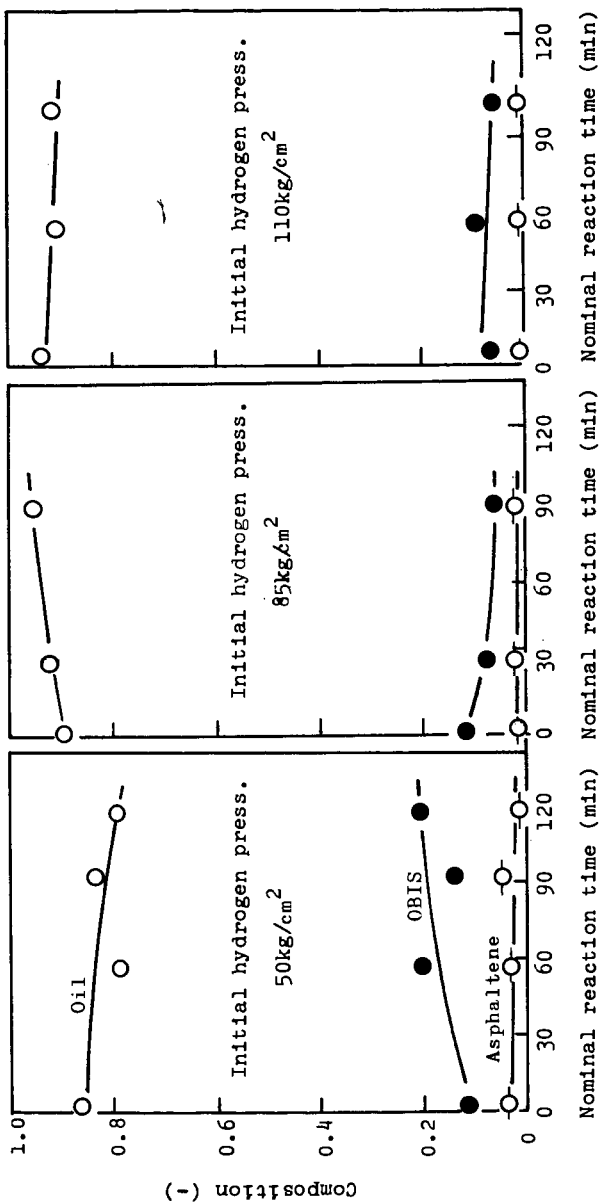
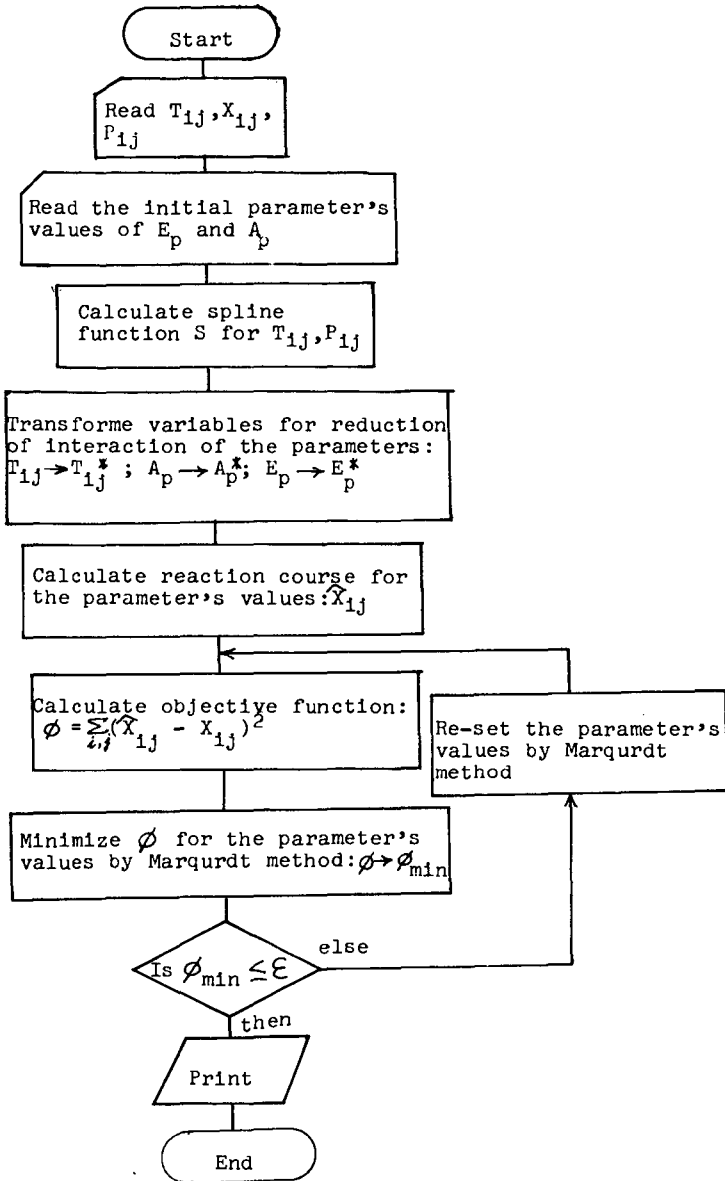


Fig. 5 Dependency of initial hydrogen pressure on liquefaction course of Taiheiyo coal at higher NRTM of 440°C

Flow chart



HYDROGENATION OF COAL LIQUIDS
IN THE PRESENCE OF SULFIDED Ni-Mo/Al₂O₃

L. Veluswamy*, J. Shabtai[†] and A. G. Oblad

Department of Mining and Fuels Engineering
University of Utah, Salt Lake City, Utah 84112

INTRODUCTION

Hydrogenation is one of the most important catalytic processing techniques applied to the petroleum industry. Although considerable work has been done on the hydrotreating of petroleum feedstocks(1,2) and model compounds(3), relatively few studies have been reported on hydrogenation of coal-derived liquids(4-9). Coal liquids contain much less hydrogen (6-8% b. wt.) and considerably more nitrogen (1-2%) and oxygen (4-5%) as compared to petroleum crudes and residua (hydrogen, 11%; nitrogen, <1%)(10). Coal liquids have much higher concentration of asphaltenes than petroleum residua (25-35% b. wt. vs 5-6% b. wt.), as well as higher overall aromaticity than the latter (60-75% b. wt. vs 20-35% b. wt. of aromatic carbon). This high concentration of condensed aromatic ring structures in coal liquids causes coke formation to a large extent in refining processes such as catalytic cracking. The heteroatoms, particularly nitrogen and sulfur, are severe poisons for many of the catalysts employed in petroleum refining. Hence, hydrotreatment of such liquids may be necessary to upgrade their quality and make them suitable for further refining processes. In this study, the hydrogenation of Synthoil and fractions derived from it, in the presence of sulfided Ni-Mo/Al₂O₃ and Ni-W/Al₂O₃ systems, was systematically investigated as a function of experimental conditions, such as, reaction temperature, pressure and process time. Results obtained with model compounds (11-13) were correlated with results of this study to elucidate the hydrogenation behavior of syncrudes.

EXPERIMENTAL

Feedstock

The Synthoil (from West Virginia coal) used in this study was supplied by the Pittsburgh Energy Research Center. The cyclohexane soluble fraction (maltene) and cyclohexane insoluble fraction (A-P) of Synthoil were prepared according to the following procedure. Synthoil was mixed with cyclohexane in a ratio of 1:40 and the mixture was heated to near the boiling point of cyclohexane with magnetic stirring for about 40 minutes. The mixture was cooled to room temperature and kept overnight with continued stirring. The maltene fraction with cyclohexane was separated from A-P by vacuum filtration. The maltene fraction of Synthoil was separated from cyclohexane by evaporating cyclohexane under slight vacuum. The A-P fraction was dried in an oven kept at 80°C. Data on properties of the Synthoil and fractions derived from it are given in Table 1.

*Presently with Exxon Research and Engineering Company, Baytown, Texas

[†]Weizmann Institute of Science, Rehovot, Israel

Table 1

Analysis and some Properties of Synthoil and Synthoil Fractions

| <u>Material</u> | <u>C</u> | <u>H</u> | <u>N</u> | <u>S</u> | <u>O</u> | <u>H-aromaticity %</u> |
|--------------------------------------|----------|----------|----------|----------|----------|------------------------|
| Synthoil ^a | 86.4 | 7.2 | 1.3 | 0.7 | 4.4 | 30.7 |
| Cyclohexane-soluble fr. ^b | 88.3 | 7.5 | 1.2 | 0.6 | 2.4 | 28.1 |
| Cyclohexane-insoluble fr. | 88.1 | 6.1 | 1.9 | 0.3 | 3.6 | 36.4 |

(Asphaltene^c-Preasphaltene^d)

(a) Specific gravity, 1.14; viscosity SSF @ 82°C, 104; ash 1.6% b. wt.

(b) Represents 64.7% b. wt. of the total Synthoil; (c) Represents 28.1% b. wt. of the total Synthoil; (d) Represents 7.2% b. wt. of the total Synthoil

Catalyst

The catalysts used in this study were (i) HT100E, manufactured by Harshaw Chemical Company and (ii) Sphercat 550, manufactured by Nalco Chemical Company. The 1/16 inch HT100E extrudates contain 3.0% NiO and 15.0% MoO₃ on alumina. The 1/16 inch Sphercat 550 spheres contain 5.1% NiO and 20.2% WO₃ on alumina. These catalysts were chosen from several commercial catalysts for our study because of their high hydrogenation activity and low cracking characteristics in the hydrogenation of model compounds(11). Both catalysts were sulfided before use.

Hydrogenation Technique

All the experiments on hydrogenation of Synthoil were carried out in a fixed bed flow reactor (36" L. x 1.25" I.D. x 0.5" W.T.) system. An autoclave (11) of 300cc capacity was used in all the experiments on hydrogenation of maltene and A-P fractions of Synthoil.

The fixed-bed hydrotreating unit (11) was flushed with hydrogen to remove air, and the system was brought to reaction temperature and pressure. Synthoil was heated to about 80°C and pumped at a rate of 30 cc/hr. to maintain a LHSV of 0.5 hr⁻¹ (catalyst:60cc) in each experiment. A hydrogen flow rate of 2 litres/min. was used. The product was cooled in the condenser and the liquid product was collected from the low pressure separator. The gaseous product was passed through a series of scrubbers (to remove H₂S and NH₃) and wet test meter. The liquid product was dissolved in CCl₄, filtered and analyzed.

The hydrogenation procedure in the autoclave unit is as follows. After placing known amounts of Synthoil fraction and catalyst in the autoclave, the autoclave was purged with H₂ and then pressurized with H₂ to half the reaction pressure. The reactor was heated to the reaction temperature and the pressure was adjusted to the experimental pressure. The total pressure in the system was maintained constant throughout the reaction period by the automatic addition of hydrogen whenever necessary from the cylinder through the regulator and check valve. At the end of each experiment, the reactor was cooled rapidly, and the pressure was released. The product was mixed with CCl₄, filtered to remove the catalyst and analyzed.

Due to the complex nature of coal-derived liquids and their products of hydrogenation, no attempt of structural analysis of the liquid products was made. Elemental analysis was done for all samples. A simple analytical method, using PMR (Proton Magnetic Resonance), was developed(11) to determine the overall aromatic saturation. The extent of saturation was estimated as

$$\% \text{ decrease in H-aromaticity} = \frac{(\text{H-aromaticity})_{\text{feed}} - (\text{H-aromaticity})_{\text{product}}}{(\text{H-aromaticity})_{\text{feed}}} \times 100$$

RESULTS AND DISCUSSION

Effect of Experimental Conditions upon the Hydrogenation of Synthoil

Coal derived liquids consist of condensed polycyclic aromatic hydrocarbons (mainly 3 to 5 rings), as well as aromatic-naphthenic, aromatic-heterocyclic and aromatic-naphthenic heterocyclic systems. The extent of hydrogenation and heteroatom removal depend on several factors, e.g., (a) reaction temperature, (b) reaction pressure, (c) hydrogen/substrate ratio, (d) liquid hourly space velocity (LHSV), (e) catalyst structure and type, and (f) composition of the feedstock (structural characteristics of the starting substrate components and of partially hydrogenated intermediates). The effect of some of these variables upon hydrogenation of Synthoil over Ni-Mo/Al₂O₃ was studied in a fixed bed reactor, using a hydrogen flow rate of 2 litres/min., and a LHSV of 0.5 hr⁻¹.

Effect of Process Time

Figure 1 summarizes the observed hydrogen uptake, viz. the % decrease in H-aromaticity, in the product from hydrogenation of Synthoil as a function of process time (between 60-260 min.). Initially (process time, 60-140 min.), a rapid decrease in hydrogen uptake, is observed. However, as the process time is extended (140-300 min.), the % decrease in H-aromaticity and the hydrogen uptake reach a plateau. This indicates that the catalyst deactivates appreciably at the beginning of the experiment, but subsequently its activity is stabilized. Product analysis shows a hydrogen content of ca 10% b.wt., and a 55-60% decrease in H-aromaticity under steady state conditions (Figure 1).

Effect of Temperature

Figure 2 shows the observed change in hydrogen content and in H-aromaticity of the product from hydrogenation of Synthoil as a function of temperature (between 300-400°C at 2900 psig). As seen, the hydrogen uptake increases with increase in temperature up to ca 370°C (maximal % decrease in H-aromaticity, 62.4%; and maximal hydrogen content, ca 10%). Above 370°C, there is apparently a tendency of decrease in the hydrogen uptake. Experimental and calculated data (14,15) on hydrogenation equilibria of polycyclic aromatics indicate that at high hydrogen pressures, e.g., above 2000 psig and temperatures below 390°C, the equilibrium is displaced almost entirely in the direction of hydrogenation. On the other hand, at temperatures above 390°C (this temperature may vary depending upon the type of aromatics), there should be some of the free aromatic reactant at equilibrium. The concentration of this aromatic component increases with increase in temperature. For example, upon hydrogenation of phenanthrene, the concentration of the latter at equilibrium decreases with increase in temperature up to 375°C, but then increases with further increase in temperature (14). Hence, this provides a plausible explanation for the observed hydrogenation behavior of Synthoil. The observed increase in aromatic content of the product from hydrogenation of Synthoil at temperatures above 370°C may be also due to some increase in the extent of cracking reactions.

Figure 3 shows the change in nitrogen and sulfur content of the product from hydrogenation of Synthoil as a function of temperature (between 300-400°C). As expected, the extent of N and S removal increases with increase in temperature,

since the equilibrium data indicate that heteroatom removal proceeds irreversibly and is, therefore, not equilibrium controlled. Nitrogen removal ranges from 18% to 70% whereas the S removal ranges from 45% to 86%. This indicates that the former process is generally a slower one. The observed incomplete removal of heteroatoms may be due to the stereochemical characteristics of some more complex nitrogen-and sulfur-containing heterocyclics, and of partially hydrogenated intermediates (11,13). Another reason for incomplete saturation of polyaromatics and incomplete removal of heteroatoms in feedstocks such as Synthoil and their fractions may be due to diffusion effects (1,16).

Effect of Pressure

Figure 4 shows the observed change in H-aromaticity of the product from hydrogenation of Synthoil as a function of pressure (between 2500-2900 psig). As seen, the saturation of aromatics increases with increase in pressure. It is indicated(11) that nitrogen removal increases with increase in pressure (51% at 2500 psig and 70% at 2900 psig), but the extent of S removal changes only to a small extent (83 to 89%) with increase in pressure (between 2500-2900 psig). A similar behavior was observed in the Texaco work on hydrodesulfurization of heavier intermediate cracked gas oil(1).

Hydrogenation of Maltene (Cyclohexane-Soluble) and Asphaltene-Preasphaltene (Cyclohexane-Insoluble) Fractions of Synthoil

A Synthoil sample was separated into a maltene (cyclohexane-soluble) fraction and an asphaltene-preasphaltene (cyclohexane-insoluble) fraction as described in experimental section. These fractions derived from Synthoil were hydrogenated in an autoclave under severe conditions (pressure, 2900 psig; temperature, 288-377°C; reaction time, 7 hr.) using sulfided Ni-W/Al₂O₃ catalyst and the results are summarized in Table 2. As seen from experiment 1, the cyclohexane-soluble fraction is readily hydrogenated (% decrease in H-aromaticity=71.2%, corresponding to a residual H-aromaticity of only 8.1%). On the other hand, hydrogenation of the cyclohexane insoluble fraction (asphaltenes plus preasphaltenes), under the same set of conditions, (expt. 3) is very limited (% decrease in H-aromaticity of 23.6% corresponding to a residual H-aromaticity of 27.8%). Table 2 also shows that the saturation of the cyclohexane-insoluble fraction increases with increase in temperature.

Table 2

Change of Quality in the Product from Hydrogenation of Synthoil Fractions^{a-c}

| <u>Expt. No.</u> | <u>Cyclohexane soluble fr.^d</u> | <u>Cyclohexaneinsoluble fr.^e (asphaltenes-preasphaltenes)</u> | | |
|-----------------------------|--|--|----------|----------|
| | <u>1</u> | <u>2</u> | <u>3</u> | <u>4</u> |
| Reaction temperature, °C | 341 | 288 | 341 | 377 |
| H-aromaticity, % | | | | |
| in feed | 28.1 | 36.4 | 36.4 | 36.4 |
| in product | 8.1 | 34.5 | 27.8 | 25.3 |
| % decrease in H-aromaticity | 71.2 | 5.6 | 23.6 | 30.5 |
| % heteroatom removed | | | | |
| N | 86.1 | 8.5 | 31.9 | 51.6 |
| S | 62.9 | -- | -- | 62.5 |
| O | 96.7 | 33.1 | 63.6 | 82.4 |

(a) Catalyst: sulfided Ni-W/Al₂O₃; (b) Pressure: 2900 psig; (c) Reaction time: 7 hr.; (d,e) For elemental composition of reactant, see Table 1.

A probable reason for the difficulty of completely hydrogenating the maltene fraction of Synthoil is indicated by results obtained from hydrogenation of model compounds, e.g. phenanthrene and pyrene(11,12) using commercial hydrogenation catalysts (Ni-Mo/Al₂O₃, Ni-W/Al₂O₃, etc.). It was found that hydrogenation of the outer rings in phenanthrene is a fast reaction. But, once the two outer rings are saturated, the subsequent step of hydrogenating the sterically hindered inner ring is much slower. It should be expected in the case of condensed polycyclic compounds present in the maltene fraction, at least a part of the inner rings become sterically hindered by adjacent hydroaromatic rings during the step-wise hydrogenation process. This would be more probable in tetracyclic and pentacyclic systems, e.g., triphenylene. In the latter compound, for instance, there is one inner ring which is fully substituted by three terminal benzene rings which upon hydrogenation form a steric barrier around the residual inner benzene ring. Examination of molecular models show that flatwise adsorption of this inner benzene ring on the catalyst surface is very difficult while edgewise adsorption is excluded. The residual 8.1% of H-aromaticity in the hydrogenated maltene fraction corresponds roughly to 15-20% of residual non-hydrogenated aromatic rings, *viz.* approximately one residual aromatic ring per 5-6 hydroaromatic rings, in line with the above suggested model. The relatively higher resistance to hydrogenation shown by the asphaltene-preasphaltene fraction (Table 2; expt. 2, 3, and 4) may be due to the higher complexity and proportionally higher concentration of sterically hindered inner rings in the polycyclic systems present in this fraction. For instance, in 1,2,3,4,5,6,7,8-tetrabenzonaphthalene which is a hexacyclic system, the completely substituted rings represent 33% (one out of three) of the condensed system.

The products of hydrogenation of the asphaltene-preasphaltene fraction (expts. 2,3, and 4) were analyzed for cyclohexane solubility. Results obtained are plotted in Figure 5. As seen, solubility increases sharply with gradual decrease in the H-aromaticity of the asphaltene fraction, reaching a level of about 85% at a point of 31% decrease in H-aromaticity. This important result can be rationalized by considering three possible factors affecting solubility: (a) polar compounds such as O, S, and N-containing compounds undergo heteroatom removal (Table 2) making the product less polar, *viz.*, more soluble in a non-polar solvent, e.g., cyclohexane, (b) decrease in the complexity and molecular weight of the asphaltene molecules resulting from splitting reactions, (c) the partial hydrogenation of the polycyclic aromatic system could also contribute to the observed increase in solubility.

CONCLUSIONS

Results obtained from this study of hydrogenation of Synthoil and its fractions indicate the following:

(i) Even under severe hydrogenation conditions where the aromatic saturation equilibria favor in the direction of complete saturation, coal-derived liquids show marked resistance to complete hydrogenation. It is concluded, in line with the results obtained with model compounds, that the resistance to complete hydrogenation may be due to sterically hindered aromatic rings.

(ii) Hydrodenitrogenation is relatively more difficult when compared to hydrodesulfurization in coal-derived liquids.

(iii) The rate and depth of hydrodenitrogenation and hydrodesulfurization of coal-derived liquids may strongly depend on the steric characteristics of condensed N and S heterocyclic aromatic feed components, or of partially hydrogenated intermediates.

(iv) The asphaltene-preasphaltene fraction of Synthoil shows higher resistance to hydrogenation than the maltene fraction of Synthoil.

(v) The solubility of the hydrogenated product of asphaltene-preasphaltene fraction of Synthoil in cyclohexane increases with decrease in H-aromaticity and heteroatom content.

REFERENCES

1. Gully, A. J. and Ballard, W. P., *Advances in Petroleum Chemistry and Refining*, Interscience Publishers, Wiley, N.Y., 1960, 7, Chapter 4.
2. Horne, W. A. and McAfee, J., *Advances in Petroleum Chemistry and Refining*, Interscience Publishers, Wiley, N.Y., 1960, 2, Chapter 5.
3. Weisser, O. and Landa, S., "Sulfide Catalysts, their properties and application", Pergamon Press, Oxford, N.Y., 1973.
4. White, P. J., Jones, J. F., and Eddinger, R. T., *Hydrocarbon Processing*, 1968, 47, No. 12, p. 97.
5. Jacobs, H. E., Jones, J. F., and Eddinger, R. T., *Ind. Eng. Chem. Process Des. Devel.*, 1971, 10, No. 4, p. 558.
6. Catalytic Hydrotreating of Coal Derived Liquids - Project Seacoke, Phase II, Final report to OCR, ARCO Chemical Co., Aug., 1963-Dec., 1966.
7. John, J. J., Jones, J. F. and McMunn, B. D., *Am. Chem. Soc., Div. Fuel Chem., Prepr.*, 1972, 16, No. 1, p. 216.
8. Heck, R. H. and Stein, T. R., *ACS, Div. Petr. Chem., Prepr.*, 1977, 22, No. 3, p. 948.
9. de Rosset, A. J., Tan, G. and Gatsis, J. G., *ACS, Div. Petr. Chem., Prepr.*, 1977, 22, No. 3, p. 962.
10. Stein, T. R., Voltz, S. E. and Callen, R. B., *Ind. Eng. Chem. Prod. Res. Dev.*, 1977, 16, No. 1, p. 61.
11. Veluswamy, L. R., "Catalytic Hydrogenation of Coal-Derived Liquids and Related Polycyclic Aromatic and Heterocyclic Compounds," Ph.D. thesis, University of Utah, 1977.
12. Shabtai, J., Veluswamy, L. and Oblad, A. G., *ACS, Div. Fuel Chem. Prepr.*, 1978, 23, No. 1, p. 107.
13. Shabtai, J., Veluswamy, L. and Oblad, A. G., *ACS Div. Fuel Chem. Prepr.*, 1978, 23, No. 1, p. 114.
14. Frye, C. G., *ACS, Div. Petr. Chem. Prepr.*, 1961, 6, B157.
15. Bondi, A., *Petr. Refiner*, 1959, 38, No. 2, p. 161.
16. Smith, J. M., "Chemical Engineering Kinetics", Second Edition, McGraw Hill Book Company, N.Y., 1970, p. 365.

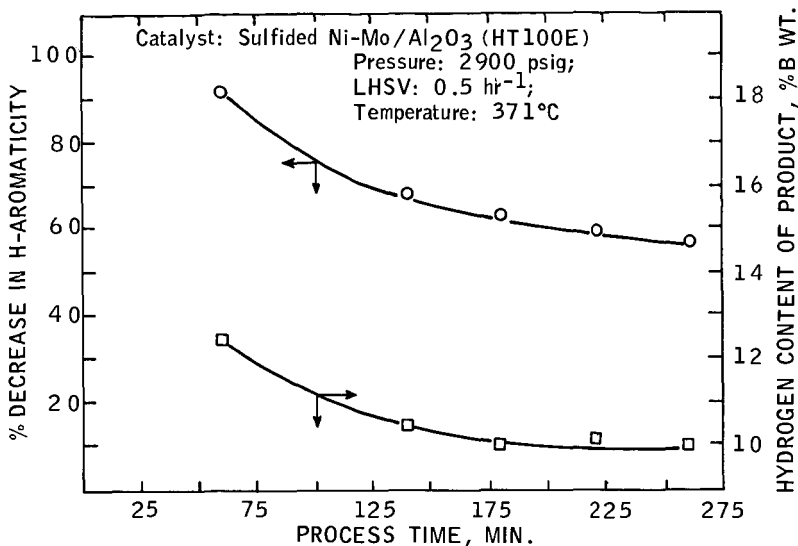


Fig. 1. Change in hydrogen content and H-aromaticity of the product from hydrogenation of Synthoil as a function of process time.

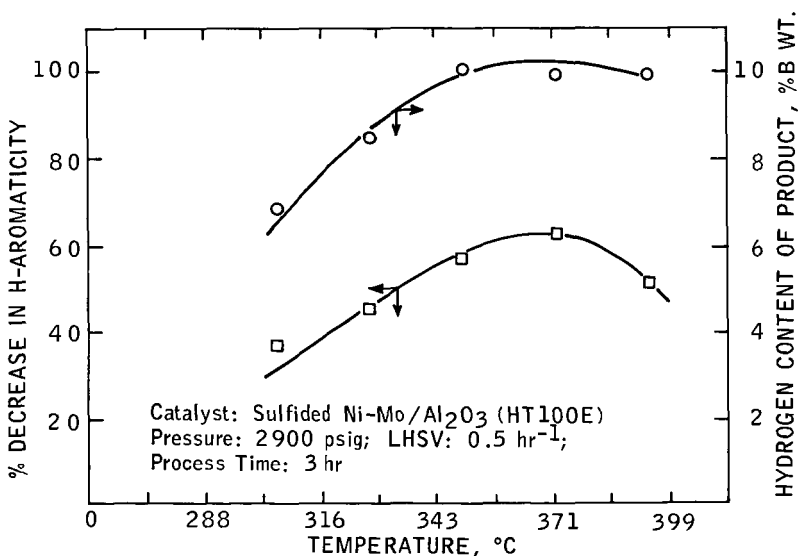


Fig. 2. Change in hydrogen content and H-aromaticity of the products from hydrogenation of Synthoil as a function of temperature.

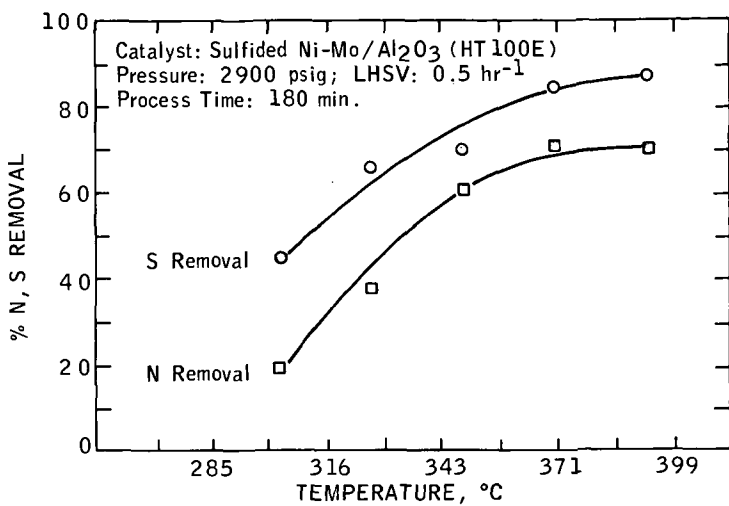


Fig. 3. Change in nitrogen and sulfur content of the product from hydrogenation of Synthoil as a function of temperature.

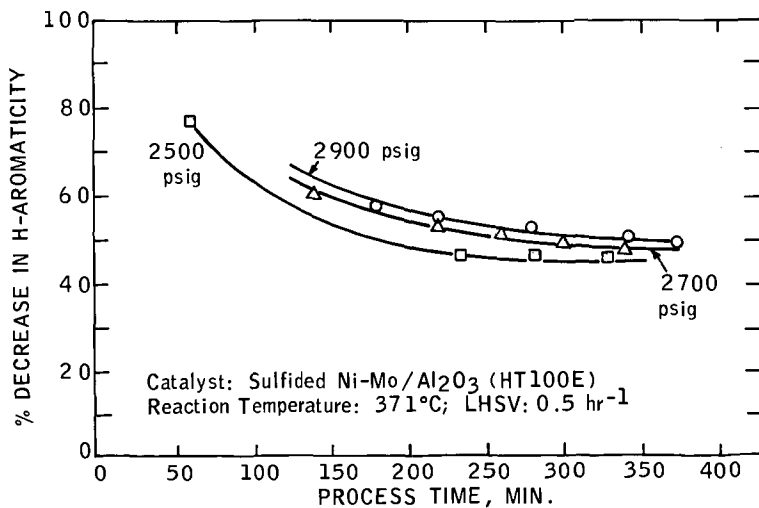


Fig. 4. Change in H-aromaticity of the product from hydrogenation of Synthoil as a function of pressure.

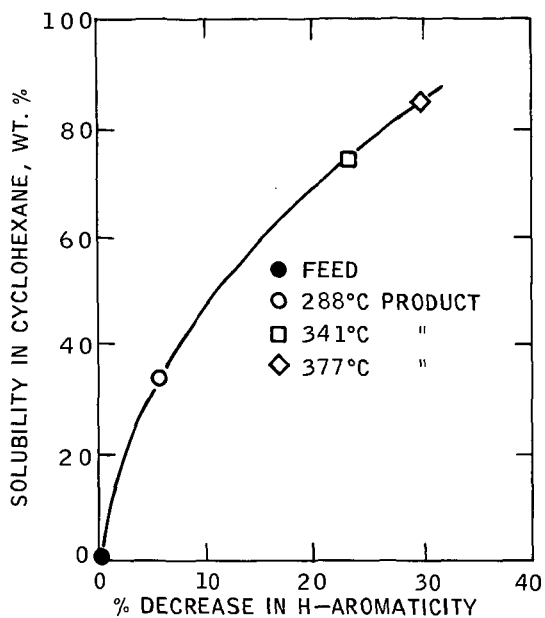


Fig. 5. Change in solubility of asphaltene fraction in cyclohexane as a function of decrease in H-aromaticity.

Pressure: 2900 psig
 Reaction time in each run, 7 hr.
 Catalyst: Sulfided Ni-W/ Al_2O_3

Studies on Coal Hydrogenation Reaction Using High Pressure Differential Thermal Analysis

S. Yokoyama*, S. Ueda*, Y. Maekawa* and M. Shibaoka**

*Government Industrial Development Laboratory, Hokkaido
41-2, Higashi-Tsukisamu, Toyohiraku,
Sapporo, 061-01, Japan

**CSIRO, Fuel Geoscience Unit, P.O.Box 136, North Ryde,
N. S. W. Australia 2113

Introduction

High pressure hydrogenation reaction of coal is an exothermic reaction accompanied by heat generation and hydrogen consumption. As compared against autoclave experiments, when high pressure DTA is applied it is possible to conduct a rapid and simple follow up of the course of reaction over a wide thermal range, and the results obtained are of considerable interest.

Up till the present, utilizing a 2 cell high pressure DTA apparatus developed by the present workers¹⁾, we have conducted measurements of the heat of coal hydrogenation²⁾ and desulfurization reaction of heavy oil³⁾. Following the above we have carried out comparative studies of catalytic activity and reactivity with regard to hydrogenation of aromatic compounds and coals⁴⁾⁻⁶⁾.

In the present paper, first we will describe a newly developed single cell DTA apparatus. This single cell apparatus, as compared against the conventional 2 cell DTA apparatus, was designed in such a way as to have a simpler heating rate control and a higher measurement sensitivity.

Next, in the hydrogenation reaction of coal, generally it is not quite so easy to maintain or obtain a contact of hydrogen and the coal sample. Thus, in the present work we did not use stirring, but instead we made an even mixture of the unreacted solid, namely $\alpha\text{-Al}_2\text{O}_3$ was mixed at various rates with the coal sample, and by gradually changing the hydrogen availability, we investigated the relationship of mesophase formation and hydrogenation.

Next, under the condition of a sufficient hydrogen availability necessary for the coal hydrogenation reaction, the exothermic peaks were measured and the reaction course of coal hydrogenation was investigated.

Experimental

Sample

The present work was undertaken as part of a series of studies on hydrogenation of the petrographic composition of coal, in the study vitrinite concentrate hand-picked from Bayswater and Liddell seam coal (N.S.W., Australia) with a high volatile bituminous rank were used. The particle size was under 100 mesh. The petrographic and chemical analysis of the hand-picked samples are given in Table 1.

Apparatus

The essential part of the single-cell DTA apparatus comprises two sheath thermoconples (1.6 mm diameter) and a heat-sink, which are placed in an ordinary autoclave (25 mm i.d., 50 ml capacity). One thermocouple is inserted into a hole

in the heat-sink and the other into the sample. Exothermic or endothermic reactions can be detected by measuring the temperature difference between the heat-sink and the sample. This temperature difference can be recorded on a chart as a DTA curve. The pressure change can also be recorded on a chart simultaneously by using a pressure transducer and an amplifier.

Experimental conditions

The sample coal was impregnated with accurate 10% ZnCl_2 using an ethanol solution and was subsequently evaporated to dryness in a vacuum dryer. 5.5 g of this sample was used for each high pressure DTA experiment. In order to vary the hydrogen availability, to each sample 0~5.5 g of unreacted solid, namely $\alpha\text{-Al}_2\text{O}_3$ of 80 mesh was mixed in evenly. Hydrogen initial pressure 100 kg/cm^2 was charged into the autoclave, and at a heating rate of 3°C/min , the temperature was raised to a given point and the DTA and pressure change curve was measured. After reaching a given temperature, the autoclave was immediately removed from the furnace and allowed to cool in air and the temperature was lowered at a rate of 35°C/min . After cooling down to room temperature, the reaction products were analysed using a Soxhlet extractor and a gaschromatography. Oil is defined here as a hexane-soluble fraction and asphaltene as benzene-soluble, hexane-insoluble fraction. The solid residues were examined under a reflected light microscope.

Results and discussion

1. The effect of hydrogen availability on coal hydrogenation and DTA

Previous work⁷⁾ by the present author showed that the formation of the mesophase during coal hydrogenation was controlled not only by temperature and time but also by hydrogen availability.

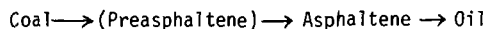
In the cases where coal hydrogenation was carried without the use of vehicle oil, since stirring is difficult, in the present case a new technic was attempted, namely by mixing unreacted solid, $\alpha\text{-Al}_2\text{O}_3$, evenly into the sample under various ratios, the hydrogen availability was gradually changed. In Fig. 1, the DTA curve and pressure change curve obtained by mixing in 0~5.5g of $\alpha\text{-Al}_2\text{O}_3$, and raising the temperature to 450°C , are shown. Fig. 2 shows the results of analyses of the reaction products after cooling down to room temperature. From microscopic observations of the extraction residues, in the case where less than 2.5 g of $\alpha\text{-Al}_2\text{O}_3$ is mixed in, it was shown that while the mesophase formed, when the addition of $\alpha\text{-Al}_2\text{O}_3$ was increased over 3.3 g the mesophase was not formed. In the former, from microscopic observations during the exothermic peak formation, it was considered that the reaction proceeds in the following manner. In the former half of the exothermic peak on the lower temperature side, the coal particles are independent of each other, and since the contact with hydrogen is good, the hydrogenation reaction proceeds rapidly accompanied by heat generation and hydrogen consumption. However, on the high temperature side of the exothermic peak, because of the melting point aided by a slight liquefaction, it was noted that the coal particles melted and agglomerated. Because of this, the contact of coal and hydrogen became poor and the hydrogenation was terminated. As the temperature is raised higher, mesophase formation proceeds accompanied by dehydrogenation and the evolution of carbon dioxide. In the case where more than 3.3 g of $\alpha\text{-Al}_2\text{O}_3$ is mixed in, from the results of DTA and microscopic observation together with analyses of the products, it was shown that hydrogen availability was in sufficient quantity.

2. Reaction course of coal hydrogenation

In order to investigate the reaction course of coal hydrogenation, the temperature rise was terminated at 10 points of the exothermic peak and after cooling down to room temperature, the reaction products were analysed as shown in Fig. 3. These

exothermic peaks were measured under the conditions of an adequate hydrogen availability necessary for the coal hydrogenation reaction, produced by an addition 4 g of α -Al₂O₃.

From these results, the following reaction course was derived.



References

- 1) Takeya,G., Ishii,T., Makino,K., and Ueda,S., J. Chem. Soc. Japan, Ind. Chem. Sect., 69, 1654 (1966)
- 2) Itho,H., Makino,K., Umeda,N., Takeya,G., and Ueda,S., J. Fuel Soc. Japan, 50, 919 (1971)
- 3) Ueda,S., Yokoyama,S., Ishii,T., Makino,K., and Takeya,G., Ind. Eng. Chem., Process Des. Dev., 14, 493 (1975)
- 4) Ishii,T., Sanada,U., and Takeya,G., J. Chem. Soc. Japan, Ind. Chem. Sect., 71, 1783 (1968)
- 5) Ueda,S., Yokoyama,S., Ishii,T., and Takeya,G., *ibid*, 74, 1377 (1971)
- 6) Ueda,S., Yokoyama,S., Nakata,Y., Hasegawa,Y., Maekawa,Y., Yoshida,Y., and Takeya,G., J. Fuel Soc. Japan, 53, 977 (1974)
- 7) Shibaoka,M., and Ueda,S., Fuel In Press

Table 1 Petrographic, Proximate and Ultimate Analyses of Sample Coals

| Sample | Maceral analysis (%) | | | | Proximate analysis (%) | | | | Ultimate analysis (% d.a.f.) | | | | | |
|----------------------------------|----------------------|---------|-----------|---------------|------------------------|----------|-----|-----------------|------------------------------|------|-----|-----|-----|-----|
| | Vitrinite | Exinite | Miorinite | Semi-fusinite | Fusinite | Moisture | Ash | Volatile matter | Fixed carbon | C | H | N | S | O |
| Bayswater, Vitrinite concentrate | 99 | 0.5 | 0.5 | tr | tr | 3.4 | 1.6 | 32.9 | 62.1 | 83.0 | 5.3 | 2.0 | 0.5 | 9.2 |
| Liddell, Vitrinite concentrate | 99 | 0.5 | tr | 0.5 | tr | 7.3 | 0.7 | 31.6 | 60.4 | 84.0 | 5.3 | 1.8 | 0.6 | 8.3 |

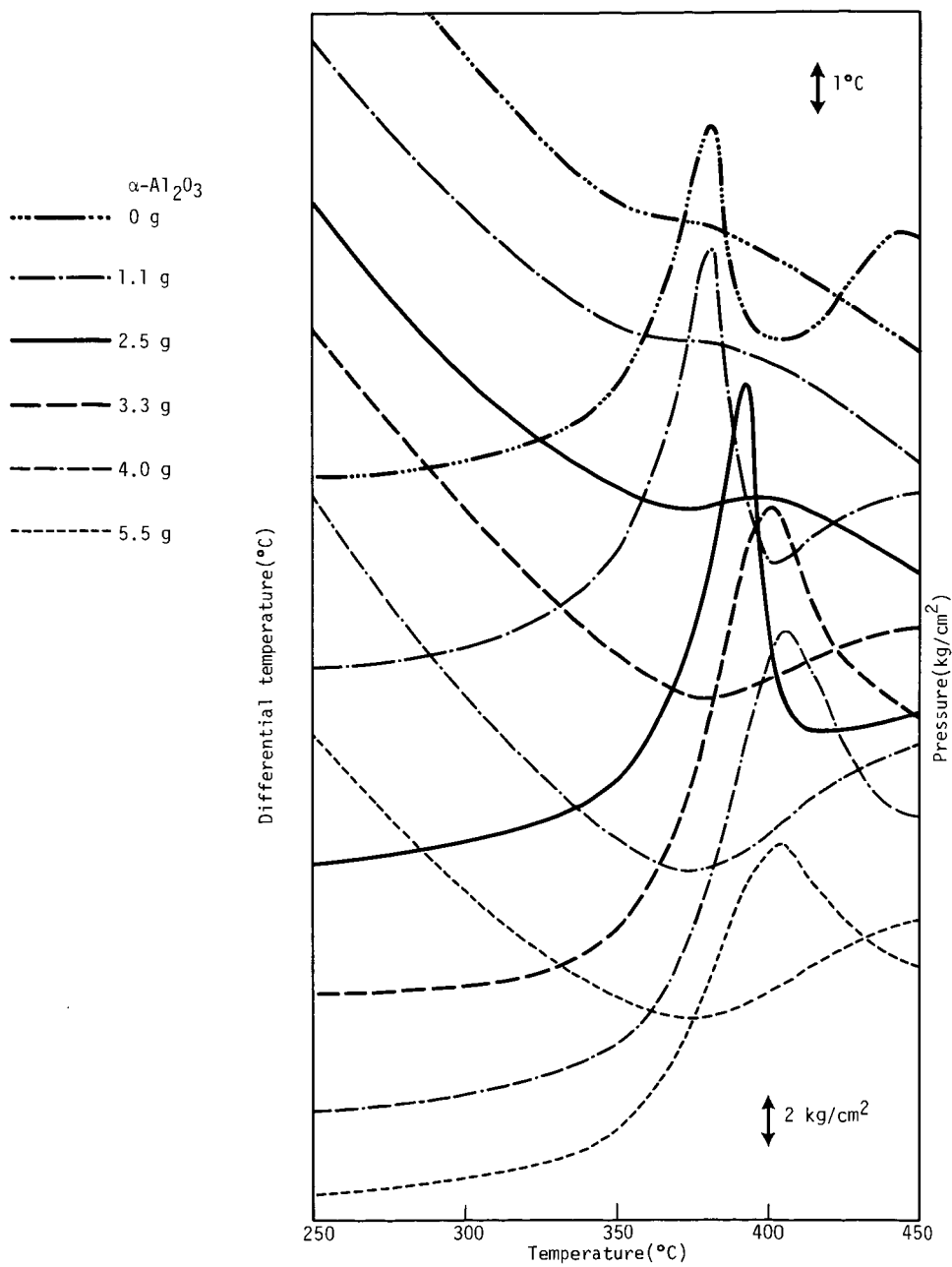


Fig. 1 DTA and pressure change curves in hydrogenation reaction of Bayswater seam coal

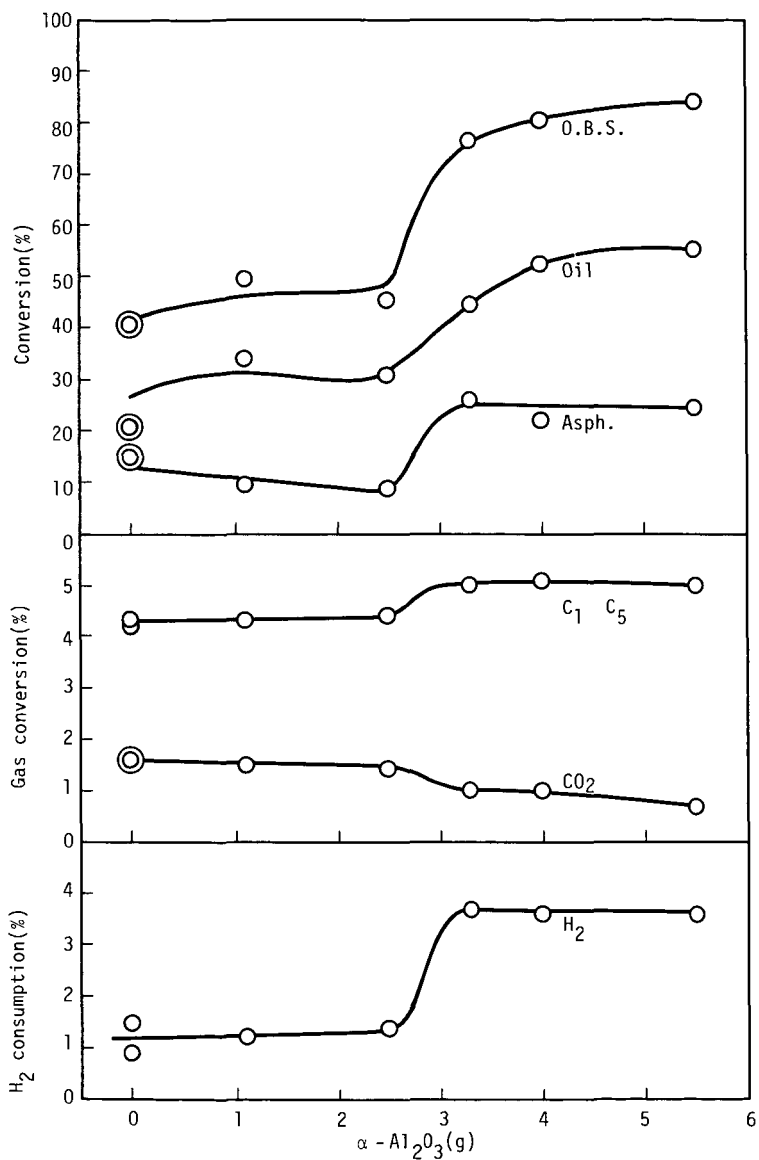


Fig. 2 Relationship between hydrogenation products and mixed $\alpha\text{-Al}_2\text{O}_3$ for Bayswater seam coal

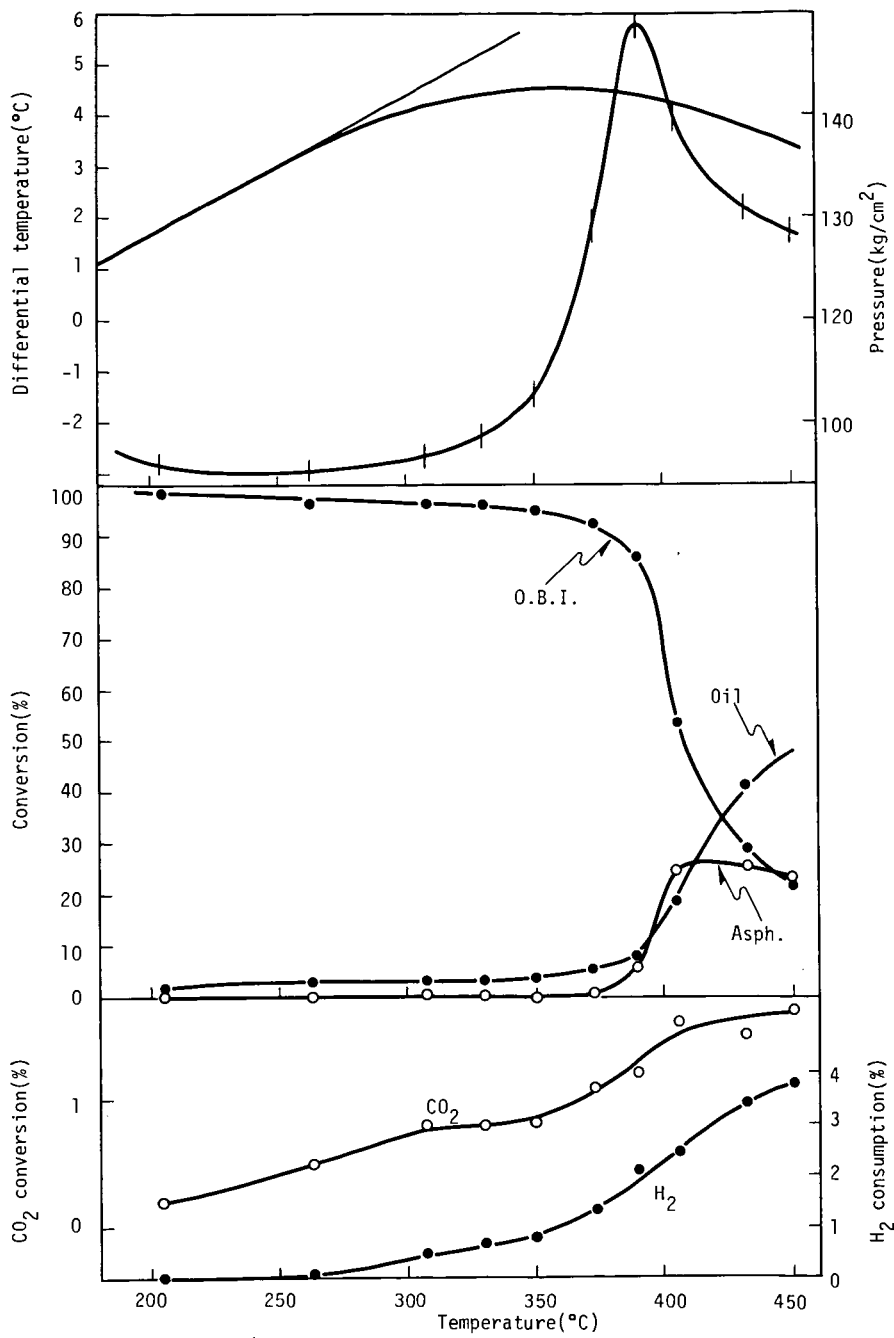


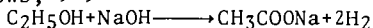
Fig. 3 DTA curve and products in hydrogenation reaction of Liddell seam coal

EFFECT OF HYDROGEN PRESSURE ON THE REACTION OF NaOH-ALCOHOL-COAL.

Masataka Makabe and Koji Ouchi.

Faculty of Engineering, Hokkaido University, Kita 13, Nishi 8, Sapporo, Japan, 060.

The reaction of coals with alcohol-NaOH has been studied in detail¹⁾²⁾ and the younger coals with less than 82%C could be dissolved nearly completely in pyridine after the reaction at 300°C for 1 hour. Even a coal of 87%C could be nearly completely dissolved by the reaction at 350°C for 1 hour. Other reaction conditions, temperature, time and the concentration of NaOH, were also examined in detail. The species of alkalis was examined, which revealed that NaOH and LiOH were most effective³⁾. Reaction mechanism was pursued by the structural analysis for the pyridine extracts of which yield were more than 90%⁴⁾. The results show that the main reaction is the hydrolysis and partly associated with hydrogenation by the hydrogen produced from the reaction between alcohol and NaOH as follows,¹⁾²⁾



The structural analysis of pyridine extracts which represent the almost all the reaction products, that is to say the original coals themselves, revealed that the aromatic ring numbers in the structural unit (cluster unit) of the younger coals consist of 1 with 0.5 naphthenic ring and the bituminous coals have the aromatic ring number of 4 with 1 naphthenic rings. The younger coals have more of ether linkages and constitute higher molecular weight structure.

As the nascent hydrogen atoms can contribute to the hydrogenation of coal molecules, probably the atmospheric pressure affects the reaction degree and the hydrogen pressure will give more effects. This report treats the effect of hydrogen pressure on this reaction.

Experiments

Coal sample is the vitrinite of Taiheiyo coal (C:77.5%, H:6.3%, N:1.1%, S:0.2%, O_{diff}:14.5%) prepared by the float-and-sink method. The crushed coal of 1g, NaOH of 1g and 10ml of alcohol were placed in an autoclave of 38ml with the magnetic stirrer and the atmosphere was replaced with pressurized nitrogen or hydrogen. Then they were reacted at 300~430°C, for 1 hour. After reaction the gas was analyzed with GC and the product was acidified with 2N HCl. The precipitate was centrifuged, filtered, washed and dried. The extraction was carried out by shaking the product with pyridine, alcohol or benzene for 10 hours at room temperature.

At the higher reaction temperature than 400°C, the product becomes oily. Therefore benzene was added to the product and small amount of water was also added to dissolve the block of sodium acetate. The mixture of two phase solution with the unreacted powder was filtered to eliminate the unreacted part and the benzene phase was separated from aqueous phase. The benzene solution was washed well with water and dried with sodium sulfate, then benzene was recovered by distillation. The residue was extracted with benzene by shaking at room temperature as above.

IR spectra were recorded by KBr pellet with the special care to

eliminate the humidity.

Results and discussion

The reaction condition, products yield and solvent extraction yield are listed in Table 1~2 and Fig 1~2. Under the nitrogen pressure the yield of ethanol extraction increases with the pressure. The main reaction of NaOH-alcohol-coal system is the hydrolysis which results the splitting of ether linkages and contributes the reduction of molecular weight¹⁾³⁾⁴⁾. But as pointed out in the previous papers a slight hydrogenation takes place with the hydrogen produced from the reaction of alcohol with NaOH. This hydrogen is expected to act as a nascent hydrogen and under the pressure it may be confined in the solution, which contributes to the rise of reactivity.

The yield of extraction with ethanol for the products under hydrogen pressure has the higher values than those under nitrogen. The dissolution of atmospheric hydrogen into the solution may contribute to the hydrogenation.

The rise of temperature also increases the extraction yield. The yield of extraction with ethanol under hydrogen pressure always has the higher values than those under nitrogen pressure. The yield of extraction with benzene under nitrogen has the higher values than those under hydrogen at the lower temperature, but at the higher temperature the yield of extraction under hydrogen becomes higher. This can not be explained well. The possibility is that under hydrogen ether linkages split more than under nitrogen and the product contains more of OH groups, which favors the solubility into ethanol and limits the solubility into benzene.

(references)

- 1) K. Ouchi, M. Makabe, Nenryokyokaishi (J. Fuel Soc Hapan), 57, 249 (1978)
- 2) M. Makabe, K. Ouchi, Fuel, 57, 289. (1978)
- 3) M. Makabe, K. Ouchi, Fuel, in press.
- 4) M. Makabe, K. Ouchi, Fuel Proc, Tech in press.
- 5) M. Makabe, K. Ouchi, Fuel, in press.

Table 1. Reaction conditions, product yield and solvent extraction yield at 300°C

| Initial pressure, MPa | Species* of gas | Product yield % | Solvent extraction yield% | |
|-----------------------|-----------------|-----------------|---------------------------|---------|
| | | | Pyridine | Ethanol |
| 0.1 | N | 84.1 | 98.1 | 47.7 |
| | H | 87.0 | 95.6 | 83.5 |
| 2 | N | 89.1 | 93.7 | 68.4 |
| | H | 89.7 | 95.6 | 86.8 |
| 5 | N | 87.9 | 91.9 | 69.3 |
| | H | 86.4 | 97.0 | 91.0 |
| 8 | N | 87.9 | 95.9 | 74.5 |
| | H | 88.5 | 95.0 | 88.1 |

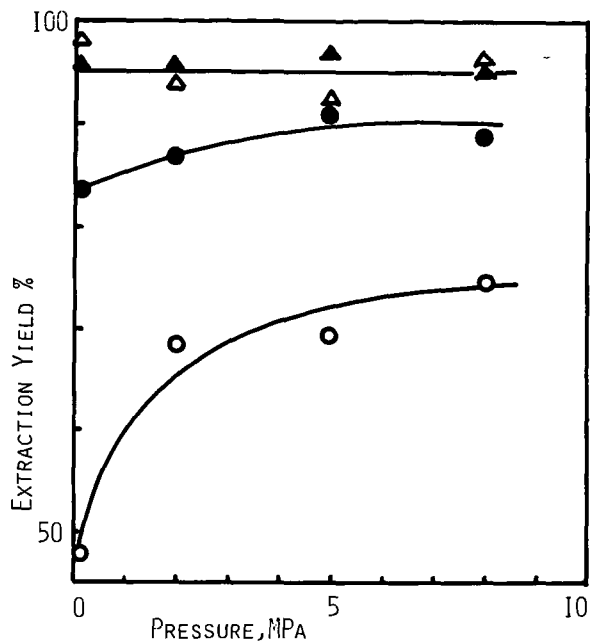
* N:nitrogen, H:hydrogen

Table 2. Reaction conditions, product yield and solvent extraction yield.

| Reaction temperature °C | Species of gas | Product yield% | Solvent extraction yield% | | |
|-------------------------|----------------|----------------|---------------------------|---------|---------|
| | | | Pyridine | Ethanol | Benzene |
| 300 | N | 87.4 | 98.1 | 47.7 | 35.7 |
| | H | 89.7 | 95.6 | 86.8 | 18.4 |
| 350 | N | 89.2 | 97.5 | 51.1 | 42.9 |
| | H | 91.0 | 98.6 | 72.2 | 38.4 |
| 400 | N | 93.0 | 98.4 | 72.9 | 74.7 |
| | H | — | — | 85.5 | 85.0 |
| 430 | H | — | — | — | 70.8 |

* N:nitrogen 0.1MPa, H:hydrogen 2MPa(initial pressure)

FIG 1. PRESSURE DEPENDENCY OF SOLVENT
EXTRACTION YIELD



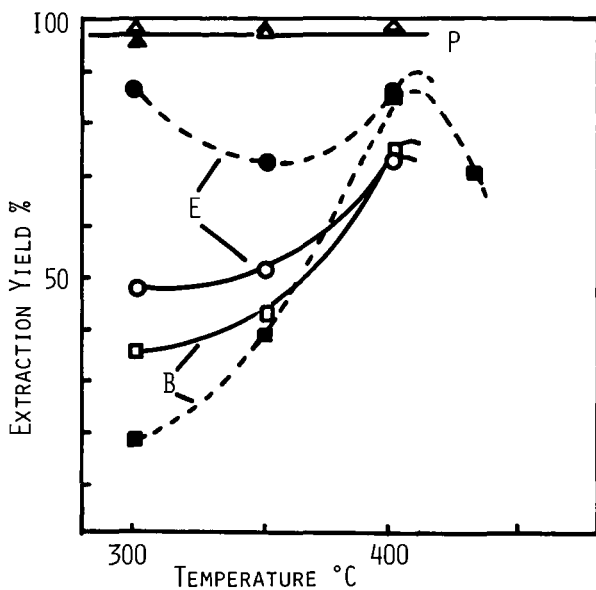
○ △ N₂

● ▲ H₂

○ ● ETHANOL EXTRACTION

△ ▲ PYRIDINE EXTRACTION

FIG 2. TEMPERATURE DEPENDENCY OF SOLVENT EXTRACTION YIELD



△ □ ○ N₂, 0.1MPa
 ▲ ■ ● H₂, 2MPa

P:PYRIDINE
 B:BENZENE
 E:ETHANOL

Characterization of Organic Functional Groups in
Model Systems for Coaly Matter Employing ^{19}F NMR

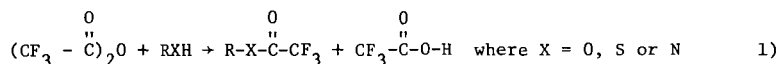
H. C. Dorn, P. S. Sleevi, K. Koller and T. Glass

Dept. of Chemistry, Virginia Polytechnic Institute and State University
Blacksburg, Virginia 24061

INTRODUCTION

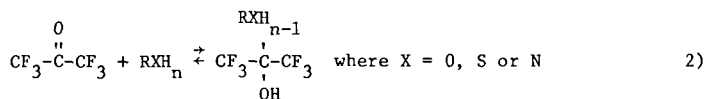
The characterization of complex organic mixtures has been explored using ^{19}F NMR to introduce a fluorine "tag" into molecules containing hetero atom functional groups. The ^{19}F NMR approach was suggested because it is nearly as sensitive as ^1H NMR and has a much wider range of chemical shifts (~375 ppm vs. ~15 ppm for ^1H). This range indicates that fluorine chemical shifts are more sensitive to subtle changes in molecular structure when compared to ^1H . An added advantage of ^{19}F NMR is that most analytical samples of interest (e.g., coal products) contain no fluorine alleviating the inherent background problem when compared with ^1H and ^{13}C NMR techniques.

The use of ^{19}F nmr to characterize organic functional groups was first suggested by Manatt (1), who used trifluoroacetic anhydride as the reagent for the introduction of a "fluorine tag" into the molecules of interest. Manatt examined various trifluoroacetic acid esters formed from various alcohols which have characteristic ^{19}F nmr chemical shifts dependent upon whether the substrate was a primary, secondary or tertiary alcohol. The general reaction for this reagent is indicated below.



Later, other studies extended the trifluoroacetic anhydride approach to other organic functional groups including phenols (2), steroids (3), and hydroxy groups in poly(propylene oxides) (4).

Another ^{19}F reagent, hexafluoroacetone, was suggested by Leader (5) for the characterization of various functional groups. The adduct (formation of hexafluoroacetone with active hydrogen compounds) is indicated below.



This reagent has been utilized for characterization of alcohols, amines, mercaptans and other active hydrogen containing compounds (5-9). Preparation of the adducts is easily accomplished *in situ* by bubbling the reagent gas (hexafluoroacetone) into a solution of the sample and solvent. Although the equilibrium indicated in equation 2 strongly favors the adduct product on the right for most primary alcohols and many other simple systems, the equilibrium tends to shift to the left for more complex and/or sterically hindered active hydrogen containing functional groups (10). Obviously, this feature limits the scope of this reagent if quantitative data is desired.

By comparison, it should be mentioned that ^1H nmr reagents (i.e. hexamethyl-disilazane (11), acetic anhydride (12), dichloroacetic anhydride (13), etc.) have also been developed for characterizing functional groups. Unfortunately, most of

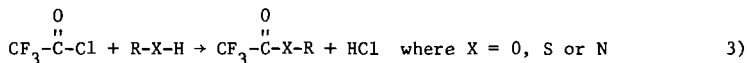
these reagents typically yield ^1H nmr spectra with relatively small chemical shift ranges (0.1 - 0.4 ppm). That is, for even partial characterization of the various possible functional groups encountered in coal product samples (e.g., phenols, carboxylic acids, alcohols, etc.), the highest available nmr field strengths (super-conducting magnets) are normally employed (14) with the ^1H nmr reagents presently available. In contrast, the range of ^{19}F chemical shifts for numerous model systems observed for the hexafluoroacetone adducts and trifluoroacetyl derivatives are -10 ppm and -1-2 ppm, respectively. These results reinforce the basic premise that ^{19}F nmr chemical shifts are usually more sensitive than ^1H shifts to subtle changes in molecular structure.

RESULTS AND DISCUSSION

In the present study, preliminary nmr examination of the reaction products of the trifluoroacetic anhydride (^{19}F nmr), hexafluoroacetone (^{19}F nmr), and hexamethyldisilazane (^1H and ^{13}C nmr) reagents discussed in the Introduction with typical model compounds and actual solvent refined coal fractions indicate a number of limitations with these reagents. This point is particularly true in utilizing these reagents for relatively complex coal product samples. Based on these initial findings, it was deemed appropriate to establish certain criteria necessary for an "ideal" nmr reagent for general characterization of a wide range of different functional groups. These criteria are listed below.

- 1) The ideal nmr reagent should not require harsh preparation conditions and only very limited manipulations should be involved in the preparation procedure.
- 2) The nmr reagent should react quantitatively and side reactions should be kept to a minimum.
- 3) The scope of the nmr reagent would be enhanced if derivative preparation could be accomplished in various solvents.
- 4) The nmr "probe nuclei" for the reagent should be very sensitive to subtle changes in molecular structure.
- 5) Ideally, a complimentary feature of item 4 would be the availability of selective nmr reagents. That is, reagents which would only detect the presence of certain specific functional groups.

With these criteria in mind, new ^{19}F nmr reagents have been examined. The first of these is trifluoroacetyl chloride which yields the same derivatives as the trifluoroacetic anhydride reagent (1-4) (Equation 3).



This reagent is a gas (b.p. -18°C) and derivatives are easily prepared in situ by bubbling the reagent into a solution consisting of the sample and solvent at temperatures from -50°C to -10°C . Various solvents have been utilized including chloroform or chloroform-d, tetrahydrofuran, and methylene chloride. The entire preparation procedure can be carried out in the sample nmr tube. This represents a distinct advantage in the derivative preparation when compared with the trifluoroacetic anhydride reagent. In addition, the by-product of this reaction is HCl compared with $\text{CF}_3\text{CO}_2\text{H}$, the by-product formed with the trifluoroacetic anhydride reagent, which in many cases causes a large interfering peak in the ^{19}F spectra of these derivatives. It should be noted, however, that if water is present in the sample, the trifluoroacetic acid peak also appears in the ^{19}F nmr spectrum when trifluoroacetyl chloride is the reagent.

The initial phase of the trifluoroacetyl chloride study was an examination of suitable trifluoroacetyl derivative preparation procedures, the range of ^{19}F chemical shifts for model systems, and typical yield data for this reagent. A typical ^{19}F spectrum for the trifluoroacetyl derivative obtained from benzyl alcohol is indicated in Figure 1. The reference at 0.0 ppm in these spectra is 1,2-difluorotetrachloroethane ($\text{CFCl}_2\text{CFCl}_2$) and was the ^{19}F reference employed in most of this work. The trifluoroacetyl chloride reagent reacts with primary, secondary, tertiary alcohols, benzyl alcohols, amines, phenols and thiols. The by-product of the reaction, HCl , does not interfere in the ^{19}F NMR spectrum.

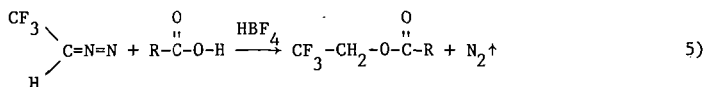
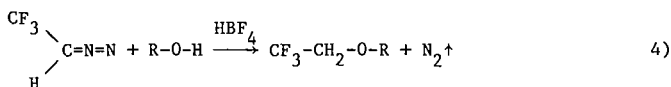
Certain reactions, particularly those of phenols and amines were quite slow. A study was conducted to see if using a nucleophilic base would improve the reactions. Those bases which were tried were pyridine, triethyl amine, 2,6-lutidine, and 4-dimethylaminopyridine (DMAP). Based on reaction yields, 2,6-lutidine and DMAP appear to be the best catalysts. It has been shown previously that DMAP is an excellent acylation catalyst (17).

A side reaction which can occur using this reagent is the formation of trifluoroacetic acid. This interference, however, can easily be removed by allowing the reaction mixture to stand over a small amount of K_2CO_3 . The acid peak is entirely removed from the spectrum. The peak which occurs from excess trifluoroacetyl chloride is also readily removed by degassing the sample with N_2 .

It appears that the derivatives formed using trifluoroacetyl chloride are well-resolved in the ^{19}F NMR spectra as indicated by figure 2 with only a couple of regions of overlap. The overall chemical shift range is about 2 ppm. It appears that this reagent will be useful as an analytical tool for characterization of functional groups. All interferences in the spectrum can be removed and the reactions occur in high yield with the proper choice of catalyst.

A second and entirely new class of ^{19}F nmr reagents under examination is fluorinated diazoalkanes. Diazomethane with and without a Lewis acid catalyst has been extensively used in organic chemistry for preparation of methyl ester and methyl ether derivatives (15). An obvious extension of this approach would be the use of a fluorine containing diazo reagent.

The first fluorinated diazoalkane examined in this study was trifluorodiazomethane (16). We have found that this reagent reacts smoothly with alcohols, phenols and carboxylic acids at room temperature to -10°C in the presence of a catalyst (typically HBF_4) to yield fluorinated ethers and esters according to equations 4 and 5.



One of the disadvantages of this reagent using our present reaction conditions is the water present in the added catalyst (50% water solution of HBF_4). The trifluorodiazomethane reacts with the water to yield 1,1,1-trifluoroethanol and bis(1,1,1-trifluoroethyl)ether.

The ^{19}F spectra for these derivatives appear as triplets (^{19}F - ^1H coupling to methylene protons). However, singlet spectra can be obtained by ^1H decoupling.

Figures 2 and 3 indicate the range of ^{19}F chemical shifts observed for a number of model compounds using the trifluoroacetyl chloride and trifluorodiazethane reagent, respectively. In general, the yields are somewhat higher for the trifluorodiazethane reagent. The chemical shift range, however, appears to be slightly larger for the trifluoroacetyl derivatives. Nevertheless, both of these reagents have potential advantages over other reagents previously employed.

Figure 4 is the first spectrum obtained from the acid fraction of an Amax solvent refined coal (SRC) sample using the trifluoroacetyl chloride reagent. The large peak at ~ 8.5 ppm is trifluoroacetic acid. The peak centered at ~ 7.6 ppm with fine structure is undoubtedly due to phenols and perhaps benzyl alcohols. The peaks between 7.7 ppm and 8.4 ppm indicate limited presence of aliphatic alcohols. The broad peak centered at ~ 7.4 ppm has not been assigned at the present time. Although these are only the first results obtained from the ^{19}F nmr reagents, the number of resolved lines in several SRC fractions indicate that the ^{19}F nmr approach is indeed a promising technique. Results applying the ^{19}F nmr approach to additional coal products will be discussed in this presentation.

REFERENCES

1. Manatt, S.L., J. Amer. Chem. Soc., 88, 1323 (1966).
2. Konishi, K., Y. Mori and N. Taniguchi, Analyst, 94, 1002 (1969).
- 3a. Jung, G., W. Voelter, E. Brietmaier and E. Bayer, Anal. Chem. Acta, 52, 382, (1970);
- b. Voelter, W., W. Brietmaier, G. Jung and E. Bayer, Org. Mag. Res., 2, 251, (1970).
4. Manatt, S.L., D.D. Lawson, J.D. Ingham, J.D. Rapp and J.D. Hardy, Anal. Chem., 38, 1036 (1966).
5. Leader, G.R., Anal. Chem., 42, 16 (1970).
6. Leader, G.R., Anal. Chem., 45, 1700 (1973).
7. Ho, F.F.-L, Anal. Chem., 45, 603 (1973).
8. Ho, F.F.-L, Anal. Chem., 46, 496 (1974).
9. Ho, F.F.-L and R.R. Kohler, Anal. Chem., 46, 1302 (1974).
10. Leader, G.R., Appl. Spect. Reviews, 11, 287 (1976).
11. Friedman, S., M.L. Kaufman, W.A. Steiner and I. Wender, Fuel, 40, 33 (1961).
12. Mathias, I.A., Anal. Chem. Acta, 31, 598 (1964).
13. Vickers, G.D., Anal. Chem., 40, 610 (1968).
14. Schweighardt, F.K., H.L. Retcofsky, S. Friedman and M. Hough, Anal. Chem., 50, 368 (1978).
15. M.C. Casserio, J.D. Roberts, M. Neeman, and J.S. Johnson, J. Amer. Chem. Soc., 80, 2584 (1958); M. Neeman, M.C. Casserio, J.D. Roberts, and W.S. Johnson, Tetrahedron, 6, 36 (1959).
16. Preparation of trifluorodiazethane was by a procedure described by, R. Fields and R.N. Hazeldine, J. Chem. Soc., 1881 (1964).
17. G. Hofle, W. Steglich, H. Vorbrüggen, Angew. Chem. Int. Ed. (Eng.), 17, 569 (1978).

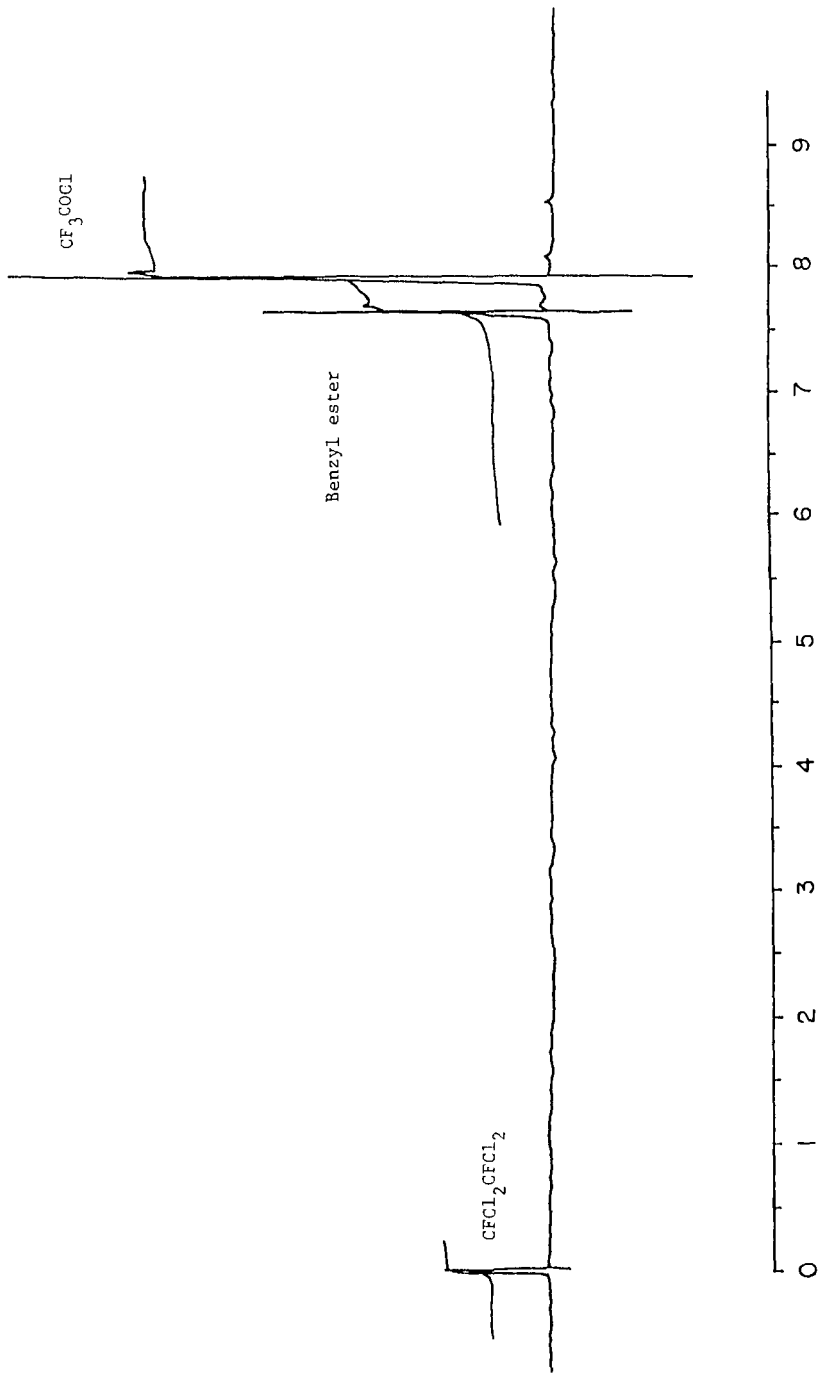


Fig. 1. ^{19}F nmr spectrum of solution prepared by reacting benzyl alcohol with trifluoroacetyl chloride, solvent is chloroform-d with 1,2-difluorotetrachloroethane used as the reference.

^{19}F CHEMICAL SHIFTS OF DERIVATIVES

USING $\text{CF}_3\text{-C}(=\text{O})\text{-Cl}$

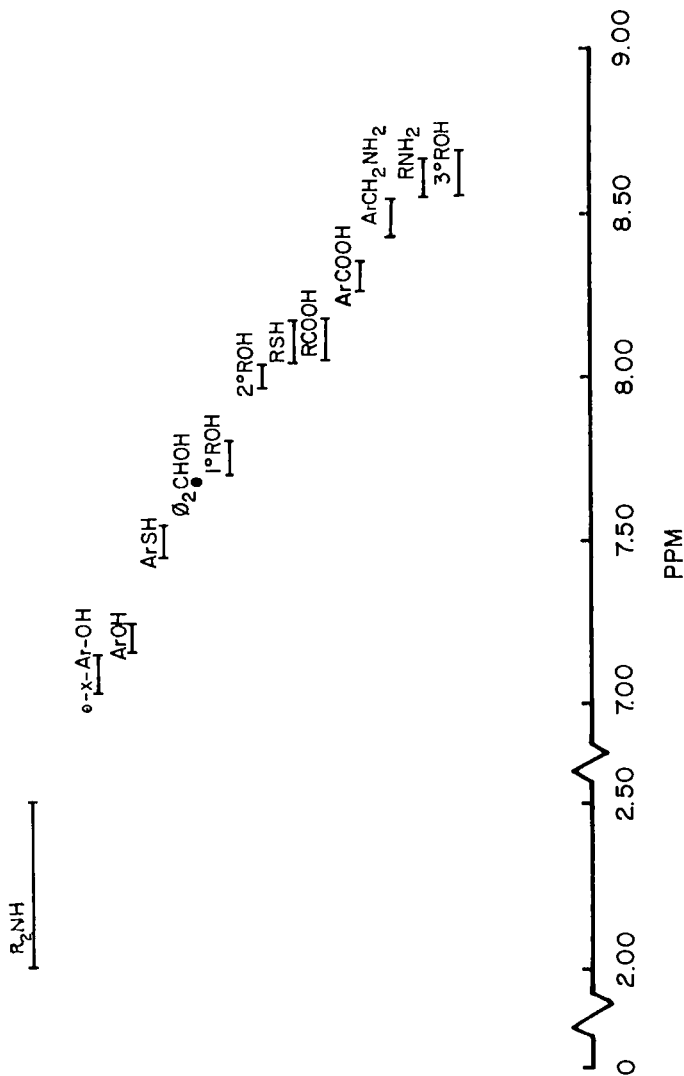


Fig. 2. Range of ^{19}F nmr chemical shifts observed for trifluoroacetyl derivatives of model compounds with 1,2-difluorotetraethane used as the reference.

¹⁹F CHEMICAL SHIFTS OF
TRIFLUOROETHYL ESTERS AND ETHERS

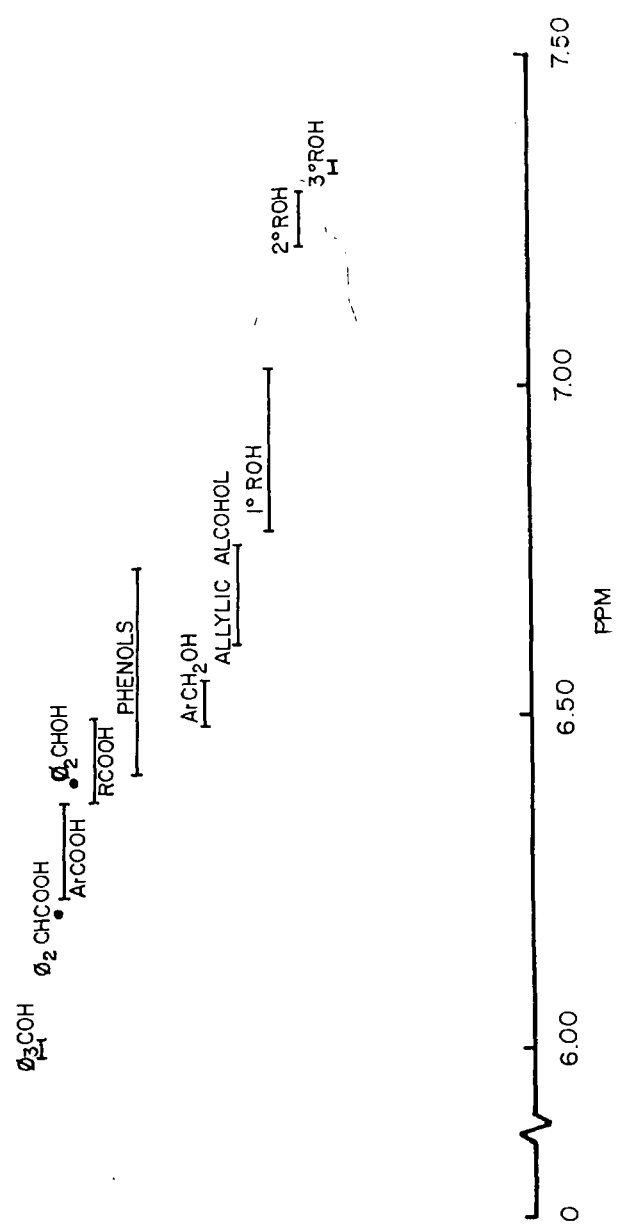


Fig. 3. Range of ¹⁹F nmr chemical shifts observed for trifluorodiazoethane derivatives of model compounds with 1,2-difluoroethane used as the reference.

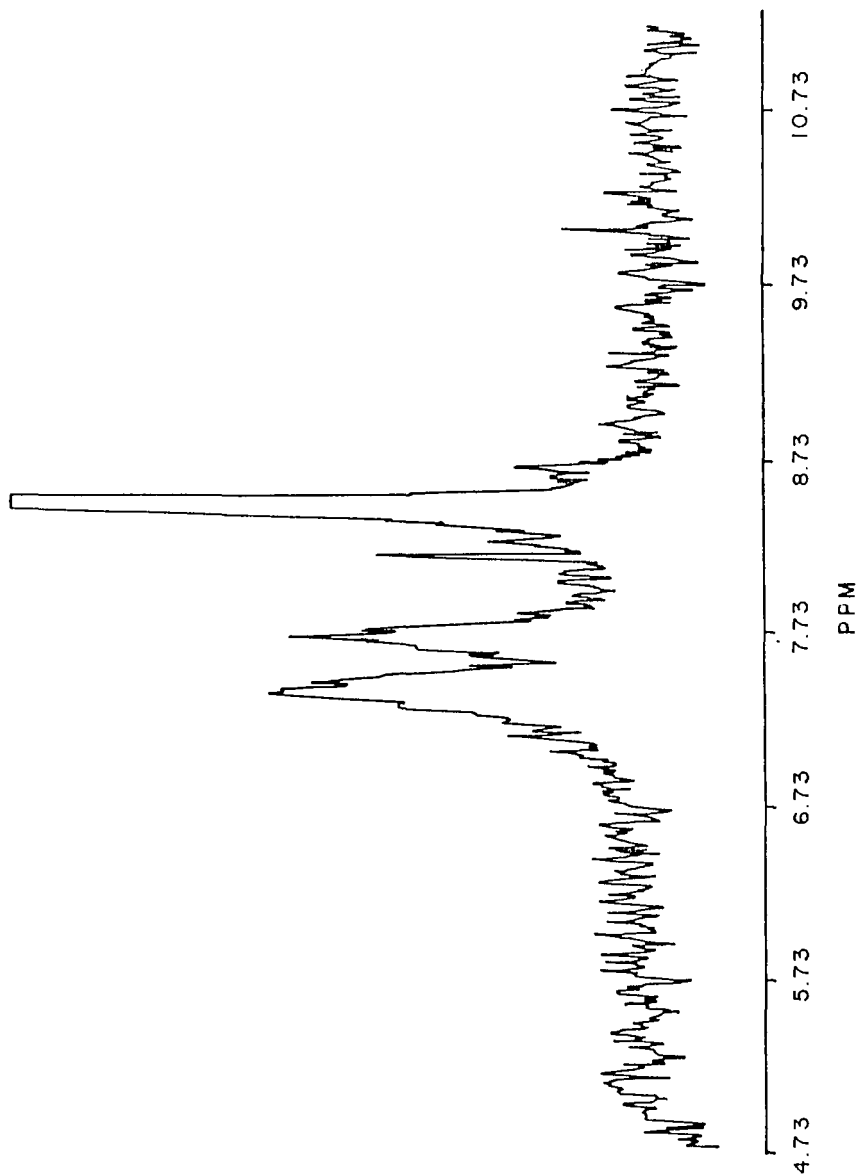


Fig. 4. ^{19}F FT nmr spectrum of reaction mixture of trifluoroacetyl chloride and Amax SRC acids fraction, solvent is chloroform-d with 1,2-difluoroethane used as the reference.

The Use of Acetylation to Quantitate Acid Groups in Coal Derived Liquids

R. J. Baltisberger, K. M. Patel,
V. I. Stenberg, and N. F. Woolsey

Department of Chemistry
University of North Dakota
Grand Forks, North Dakota 58202

The determination of types of nitrogen and oxygen species in coal derived products is an important problem to be solved in liquefaction research. Methods are needed which can rapidly isolate or characterize the nitrogen and oxygen heteromolecules in complex mixtures. Two major types of problems need to be solved. First, the types of functional groups can be identified by specific chemical reactions, but such reactions must be quantitative to be of use. Secondly, a large portion of coal derived products formed in the early stages of a liquefaction process are preasphaltenes, which limit any subsequent chromatographic procedures used to isolate compound types or molecular fractions. In this paper we shall describe the use of acetylation as a means of measuring quantitatively the fraction of acidic protons in coal derived products.

The similarity of the fractions of acidic protons measured by acetylation techniques with those of acid-base titration data suggest that no alcoholic groups are present in the SRL and SRC samples selected for this study. In addition, the acetylation process greatly increased the dissolubility of the coal derived substances in benzene and chloroform. Such dissolubility would give the opportunity for studies not accessible in pyridine. For example, the use of NMR shift reagents in chloroform could be employed in structural analysis.

Experimental

Materials

Three solvent refined lignite (M11-A, M34-A and M39-A) and two solvent refined coal (AMAX and Tacoma) samples were obtained and ground to about 40 mesh for this study (1). Elemental analysis of the samples was performed by Spang Micro-Analytical Laboratory.

NMR Spectra

Proton NMR spectra were obtained using a Varian EM-390 spectrometer. Samples were dissolved in pyridine- d_5 containing a calibrated amount of s-trioxane as standard. Correction for pyridine was based on a standard versus residual pyridine integration. Generally, seven integrations were run and averaged. Carbon 13 PFT-NMR were measured in a JOEL JNM-FX60 spectrometer. Chloroform- d_1 was used as the solvent with TMS as an internal standard.

Non Aqueous Titration

Non-aqueous potentiometric titration of the acidic groups was carried out in pyridine using 0.05 M of tetra-n-butylammonium hydroxide in benzene as the titrant (2). The emf was measured by a Beckman Zeromatic -pH meter with a glass electrode and a simple side arm column reference electrode connected by a salt bridge of KCl-dry methanol through a medium porosity filter to the titration solution (3).

Acetylation

Samples of SRL or SRC (1.0 g) were acetylated by refluxing for 24 h with 15 ml acetic anhydride-pyridine mixture (1:3) under an inert atmosphere of argon. Subsequently, the reaction mixture was concentrated by rotovap to about 5 ml. The mixture was added to 250 ml water and the precipitated derivative filtered. The residue on the filter was washed with water until the effluent was free of acid. The acetylated sample was freeze dried with benzene to remove the last portion of residual pyridine. Finally, the sample was vacuum dried at 80° in an abderhalden apparatus.

Acidic Proton Analyses

The acetylated samples were analyzed for acidic proton content by saponification-titration, and by NMR measurement. The saponification of a dried acetylated sample was carried out with 1.5 g potassium hydroxide in 100 ml water-pyridine (3:1) by refluxing for 20 h. The mixture was then acidified (pH 3.0) with concentrated sulfuric acid. The liberated acetic acid was collected by distillation and titrated with standard sodium hydroxide.

Proton NMR measurements of the sample in pyridine- d_5 before and after acetylation were used to measure the fraction of acid groups in the sample. Prior to acetylation the acidic proton signals are located under the aromatic region. After acetylation the methyl group of the acetyl group signals are in the aliphatic region. The percentage H as acidic hydrogens can be calculated

from (equation 1),

$$\% \text{H as acidic H} = \frac{R_2 - R_1}{2R_1 + 1} \times 10^2 \quad (1)$$

where R_1 is the fraction of the aromatic protons (area) in the acetylated SRC and SRL samples and R_2 is the fraction of aromatic protons (area) in the non-acetylated samples.

Measurement of the percentages of acidic protons by C^{13} NMR was calculated from the relative area of the carbonyl carbon (169 ppm) to the total carbon atoms and from the carbon-hydrogen elemental analysis (equation 2).

$$\% \text{H as acidic H} = \frac{(\text{C=O Area}) \times (\text{Wt \% C}) \times 10^2}{[\text{Total Carbon Area} - 2 (\text{C=O Area})] \times 12 \times (\text{Wt \% H})} \quad (2)$$

Results and Discussion

Dissolubility

Table I shows the chemical analysis of the SRL and SRC samples studied in this work. The increased dissolubility of the coal derived products in several solvents due to acetylation is shown in Table 2. The dissolubility in this work was not run in the necessary manner to define the percentage of pre-asphaltenes, asphaltenes and oils in the samples, but rather to demonstrate the increased dissolubility obtained through the acetylation reactions. The dissolubility was measured by mixing 1 gm of sample in 10 ml of solvent for 20h at room temperature. The mixture was filtered through Whatman number one filter paper. The resulting filtrate and residue was dried and weighed. The total recovery varied from 97 to 99%. One immediate benefit of this increased dissolubility is that C^{13} NMR techniques could be used to measure the percentage of acetyl groups using chloroform- d_1 as the solvent. The remarkable increase in dissolubility after derivatization of the acidic groups can be attributed to the breaking of intermolecular hydrogen bonding (4,5). Gould, *et. al.* have recently reported the silylation of coal liquefaction bottoms which resulted in a four to seven fold decrease in viscosity and 0 to 26% increase in extrability in heptane (6).

Acid Content

Nonaqueous titration for acidity gave a range of 1.34 to 2.22 meq/gm for the corresponding to 2.5 to 4.0% protons as acidic protons. The pure com-

pounds, carbazole and phenol, can be titrated with a precision of $\pm 3\%$. The actual SRL and SRC samples give a wider range of uncertainty as shown in Table 3. This is due to the presence of a wide range of weak acids which give a poor titration break.

The acetyl group content of a derivatized sample was measured by different methods. The saponification-titration procedure gave the same meq/gm as the nonaqueous titration results. The results were converted to %H as acidic H in Table 3 for comparison. The number of acetyl groups determined by proton NMR (equation 1) agreed with both types of titration data. Acetylation of model compounds (phenol, carbazole, and several hindered phenols) gave complete acetylation of the acidic groups as determined by NMR measurement of the products. The agreement between the three types of data would be consistent with the following. 1) No acylation of the aromatic carbon of the aromatic rings in coal was apparent. The acylation of an aromatic carbon seems remote under the reaction conditions, but in any case the agreement between the saponification-titration and proton NMR data eliminates that possibility. 2) The presence of alcoholic hydrogens in the samples can be ruled out because of the agreement between the acetylation and nonaqueous titration data. If alcohol acetylation had occurred a similar quantity of phenolic groups would have to remain unreacted for comparable results. That this would occur to the same extent to agree with the nonaqueous titration seems extremely remote. To check this point we are planning to measure total replaceable hydrogen content by LAH reduction in pyridine. 3) The location of the acidic protons lies under the aromatic portion of NMR spectra when the samples are dissolved in pyridine. In our study of several model compounds, the chemical shifts of OH (phenols) and NH (carbazole) hydrogens in pyridine- d_5 are generally downfield (between 9.5 to 6.3 ppm, aromatic region) depending upon the concentration (7).

Carbon-13 NMR integration data were generally lower than the other two types of acetyl analyses as shown in Table 3. The precision also is poorer as noted in Table 3. The reason for this is due to the small percentage of C=O groups relative to the total number of carbons and the inability to properly phase the baseline in the C=O region of the NMR experiment.

Acknowledgement

We acknowledge the support of the Department of Energy in this work.

References

1. Samples were obtained as follows:
M11-A prepared by the University of North Dakota Chemical Engineering Department under Project Lignite, from North Dakota Lignite. Conditions: 2500 psi of 1:1 CO; H₂ at 479°C (max); M34-A, 2500 psi of 1:1 CO; H₂ at 426°C (max); M39-A, 2500 psi of hydrogen at 426°C (max).
Tacoma prepared by Pittsburg and Midway Coal Co. at their Fort Lewis PDU from a blend of Kentucky No. 9 and No. 14 bituminous coals from the Colonial Mine. Conditions: 1500 psi of H₂ (85% min) at 450°C (max) using recycle solvent.
Amax Catalytic Inc., Wilsonville, Alabama from Amax subbituminous coal from Bel Ayr Mine, Wyoming. Conditions: 2500 psi H₂ and recycle gases at 460°C (max) using recycle solvent heavy in phenols and 1,2 and 3 ring aromatics.
2. Woolsey, N. F., Baltisberger, R. J., Klabunde, K., Stenberg, V., and Kaba, R., Am. Chem. Soc., Fuel Div. Preprints, 21 (7), 33 (1976).
3. Adams, R. N., in "Electrochemistry of Solid Electrodes", Marcel Dekkar, New York, p 288 (1969).
4. Sternberg, H. W.; Raymond, R. and Schweighardt, F. K., Science, 188, 49 (1975).
5. Schweighardt, F. K., Friedel, R. A. and Retcofsky, H. L., Applied Spectroscopy, 30, 291 (1976).
6. Gould, K. A., Gorbaty, M. L., and Miller, S. D., Fuel, 57, 510 (1978).
7. See for the chemical shifts of phenols in DMSO, Chapman, O. L, and King, R. W., J. Am. Chem. Soc., 86, 1256 (1964).

Table 1

Comparison of Coal and Lignite Derived Samples

| | <u>M11-A</u> | <u>M34-A</u> | <u>M39-A</u> | <u>Tacoma</u> | <u>Amax</u> |
|-----------|-------------------|-------------------|-------------------|-------------------|-------------------|
| C% | 89.31 | 86.74 | 87.47 | 87.31 | 88.29 |
| H% | 5.80 | 6.73 | 6.09 | 5.59 | 5.65 |
| N% | 1.11 | 1.63 | 1.11 | 2.36 | 1.65 |
| S% | 0.86 | 1.15 | 0.74 | 0.30 | < 0.1 |
| O% | 2.35 ^a | 2.10 ^b | 3.57 ^b | 3.22 ^a | 3.37 ^a |
| H% (Acid) | 2.6 | 2.70 | 3.3 | 3.7 | 4.0 |
| Ash % | < 0.1 | 1.7 | 1.0 | < 0.1 | < 0.1 |

^a measured by neutron activation analysis^b measured by difference

Table 2

Dissolubility in Various Solvents

| | <u>Pyridine</u> | <u>Benzene</u> | <u>Chloroform</u> |
|--------|-----------------|----------------------|-----------------------|
| M11-A | 96.8 | 50 (90) ^a | 60 (100) ^a |
| Tacoma | 95.4 | 25 (80) | 40 (100) |
| M39-A | 96.5 | 48 (85) | 62 (99) |

^a The number in parenthesis indicates the dissolubility after acetylation.

Table 3

Acid Proton Contents of Various Samples

| Samples | Acetylated Samples and | | Saponification/ Titration | Direct Nonaqueous Titration |
|-----------|--------------------------------|---------------------|--------------------------------|-----------------------------------|
| | ^1H - nmr | ^{13}C nmr | | |
| M11-A | $2.65 \pm 0.06\%$ ^a | 2.0, 2.3 % | $2.57 \pm 0.05\%$ ^a | $2.6 \pm 0.3\%$ ^a |
| M34-A | 2.7 ± 0.2 | 2.8 | 2.7 ± 0.2 | 2.5 ± 0.2 |
| M39-A | 3.1 ± 0.2 | 3.1, 3.3 | 3.3 ± 0.1 | 3.3 ± 0.1 |
| Tacoma II | 3.9 ± 0.2 | 3.1, 3.4, 3.5, 3.7 | 3.7 ± 0.2 | 3.7 ± 0.1 |
| AMAX | 4.1 ± 0.2 | 3.6, 3.9 | 4.0 ± 0.2 | 4.0 ± 0.2 |

^a The uncertainty reported is the standard derivation (1σ) for four to five determinations.

DETERMINATION OF PROTONATED AND QUATERNARY CARBONS IN H-COAL LIQUIDS FROM
QUATERNARY CARBON SUPPRESSED AND NONSUPPRESSED CMR SPECTRA

Joseph T. Joseph and John L. Wong*

Department of Chemistry, University of Louisville
Louisville, Kentucky 40208

INTRODUCTION

The potentially rapid and accurate measurement of the carbon distribution by structural types in a coal liquid is an attractive application of ^{13}C FT-NMR spectroscopy. Extensive CMR work has been carried out in many laboratories⁽¹⁾ on coal-derived liquids. As part of a continuing program to study the physicochemical properties of the H-Coal liquids to provide analytical support for the commercial development of the H-Coal process⁽²⁾, we have made further application of quantitative FT-CMR technique to determine the distribution of several types of aliphatic and aromatic carbons in three H-Coal liquids. In order to confirm the interpretation of the highly complex spectra based on chemical shifts, use has been made of the difference in CMR absorptivity of protonated and quaternary carbons as a means to distinguish between them. We have demonstrated the reliability of this difference by comparing the quantitative CMR spectrum of a simulated coal liquid containing 30 peaks (15 each in the aliphatic and aromatic region) with the spectrum of the same mixture obtained with a Fourier transform parameter set wherein the quaternary carbons are suppressed. This difference CMR technique has been applied to three H-Coal liquids: atmospheric still overhead (ASO), atmospheric still bottom (ASB), and vacuum still overhead (VSO). There is no discernible amount of aliphatic quaternary carbon found in these liquids. In the aromatic region, the ring carbons are divided into six subgroups by ring substitutions. The three liquids are thus compared by structural classification and quantitation of their CMR spectra.

EXPERIMENTAL

The liquefied coal samples under investigation were received from the Institute for Mining and Minerals Research, University of Kentucky. The liquefaction was performed by the H-Coal process involving a catalyst in the "syncrude" mode with reactor temperature at 454°C, exit reactor partial pressure of hydrogen at 2245 psig. The samples were designated atmospheric still overhead (ASO), atmospheric still bottom (ASB), and vacuum still overhead (VSO). The nominal boiling ranges of these samples are ASO $C_4 - 200^\circ\text{C}$, ASB 200-350°C, VSO 350-520°C⁽²⁾. Chemicals were purchased from Aldrich Chemical Co.

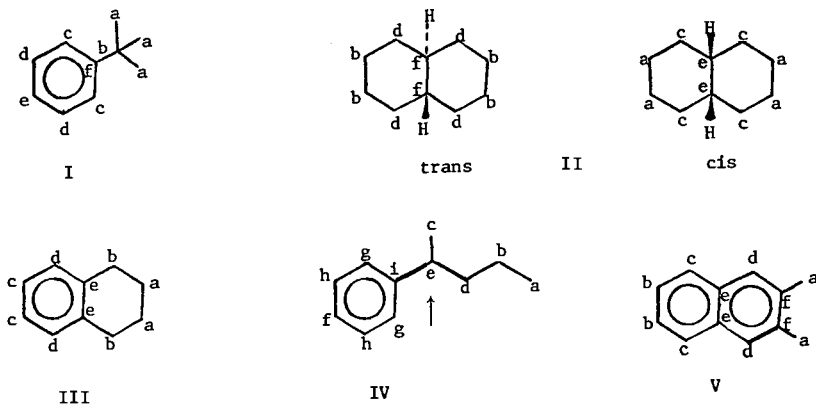
A Bruker WH-90DS nuclear magnetic resonance spectrometer with a 10 mm probe and a Nicolet BNC 1180 computer (16 K memory) was used in the Fourier transform mode to obtain the ^{13}C spectra at 22.63 MHz. The FIDs were accumulated on 8K memory, using an acquisition time of 0.819s. A 5000 Hz spectral width with 200 microseconds dwell time was used in all spectra. The quantitative spectra were obtained at 30° pulse width with 5s delay between the end of data acquisition and the beginning of the next pulse for ~10,000 pulses. During the delay, the proton spin decoupler was gated off, but a 5.0 watt decoupling power was applied while scanning. The relaxation agent $\text{Cr}(\text{acac})_3$ was used at 20 mg/g of sample. For the quaternary carbon-suppressed spectra, the following FT parameters were adopted: 90° pulse width, no pulse delay, broad band proton decoupling at 5.0 watt for ~10,000 scans, and no paramagnetic relaxation agent added.

The H-Coal samples were prepared by adding 1.0 g of the respective coal liquid to 1 ml of CDCl_3 containing 1% of tetramethylsilane. The solvent CDCl_3 also served the purpose of internal deuterium lock. For the simulated coal liquid, the following mixture was made up: t-butylbenzene (69.0 mg, 0.515 mmol), decalin (77.2 mg, 0.559 mmol), tetralin (77.5 mg, 0.587 mmol), 2-phenylpentane (76.4 mg, 0.516

mmol), and 2,3-dimethylnaphthalene (75.9 mg, 0.487 mmol), and CDCl_3 was added to make a 2 ml solution. When the spectra were calibrated for integration, a weighed amount of dioxane in a sealed capillary tube was placed along the axis of the 10 mm nmr tube with the aid of a vortex-type plug.

RESULTS AND DISCUSSION

The quaternary carbons which are devoid of protons in their immediate vicinity, hence lacking the $^{13}\text{C} - ^1\text{H}$ dipole-dipole relaxation mechanism, are expected to have long spin-lattice relaxation recovery times (T_1). This makes the signal intensity very dependent on the pulse repetition rate. The presence of nuclear Overhauser enhancement (NOE) for the protonated carbons further accentuates the difference in absorptivity between these two types of carbons. Thus, in a normal broad band proton decoupled CMR spectrum, the quaternary carbons show much reduced signal intensities relative to others. We have quantitated the differences in absorptivity for carbons with various levels of proton attachment (1° , 2° , 3° , and 4°) using a simulated coal liquid (Cf. Experimental). This mixture is comprised of 25 aliphatic carbons (primary 7, secondary 14, tertiary 3, and quaternary 1) and 28 aromatic carbons (protonated 20 and quaternary 8) as shown below. The aromatic and aliphatic



regions of this spectrum are shown in Figures 1A and 2A respectively. This set of FT parameters tend to equalize all signal intensities per carbon unit irrespective of their molecular environment. Thus, the one aliphatic and eight aromatic quaternary carbons were separately integrated to yield absolute value within 5% deviation from the theoretical. On the other hand, when the spectrum was taken in the absence of $\text{Cr}(\text{acac})_3$ using broad band decoupling at 90° pulse width and no delay, vast variations of the signal intensities including suppression of the quaternary carbons were registered. The respective aromatic and aliphatic regions shown in Figures 1B and 2B reveal the differences from those in Figures 1A and 2A. In order to quantitate these changes, the height of each peak in both spectra was normalized to either the tallest peak at $\delta 125.47$ (protonated carbons IIIc and Vb) or to an internal standard of dioxane. The normalized peak height of each peak in the quantitative spectrum is expressed as a ratio to that of the same derived from the quaternary carbon suppressed spectrum to show the signal intensity changes in the latter spectrum. These results are shown in Table I. It can be seen that the two columns of peak height ratios point to the same trend and agree to within 7% of deviation. Thus, the dioxane methylene carbons and the aromatic methine carbons IIIc and Vb exhibit similar relaxation characteristics and are both adequate as integral references. In the

nonquantitative spectrum, the eight quaternary aromatic carbons appearing in 5 peaks average a 5 fold decline. The twenty protonated carbons in ten peaks increase by ~20% per carbon. The single aliphatic quaternary carbon is suppressed 4.7 fold, while the 14 peaks representing 3 tertiary, 14 secondary, and 7 primary aliphatic carbons average an increase of 0%, 37%, and 43% per carbon respectively. Although these peak enhancements of various protonated carbons are similar, hence not diagnostic of the extent of proton attachment, it is demonstrably clear that the quaternary carbons can be confirmed by this difference CMR method due to their pronounced peak height changes.

Thus, the H-Coal liquids ASO, ASB, and VSO were submitted to close examination by the difference CMR technique. The comparisons for the aromatic and aliphatic regions are shown in Figures 3 and 4 respectively for ASO, Figures 5 and 6 for ASB, and Figures 7 and 8 for VSO. In each figure, spectrum A is the quantitative type and B the quaternary carbon-suppressed type. Those peaks which have disappeared or declined in intensity by at least 3.8 fold for ASO and ASB and at least 2 fold for VSO are assigned to the quaternary aromatic compounds either as bridge carbons in a condensed ring system or carbons to which alkyl or aryl substituents are attached. The remainder of the aromatic resonances therefore belong to the protonated carbons. It is interesting to note that the aliphatic regions for all three liquids show no discernible difference when the two types of spectrum are compared, indicating the absence of quaternary branching in the saturated carbon skeletons.

The chemical shifts of unsubstituted carbons in mono, di, tri, and tetra aromatic ring systems fall in a narrow range of 123 - 130 ppm^(3,4). When the benzene ring bears heteroatom substituent such as OH or OR, the protonated carbons are shifted upfield considerably, e.g. to 113 ppm in *m*-cresol and to 106 ppm in benzofuran⁽⁵⁾. In the region of 130-133.8 ppm, most of the condensed-ring bridge carbons can be found^(3,4). However, in a highly condensed system such as pyrene, the interior bridge carbons resonate at 125 ppm due to the anisotropic ring current effect⁽³⁾. The 133.8 - 137.3 ppm region is appropriate for substituted carbons in tetralin and methylbenzenes^(3,5). Short chains (Et, Pr, *i*Pr, etc.) tend to shift the substituted carbons downfield to 149 ppm^(3,5). Also, an alkyl substituent at C-8 in tetralin and particularly gem-substituted tetralins can bring the bridge carbon C-8a to the 140's⁽³⁾. Biphenyls also appear in this region⁽⁵⁾. Beyond 149 ppm, the aromatic carbons carrying a heteroatom group such as OH or OR appear^(1c,5). Such chemical shift analysis in combination with the difference CMR method to determine the quaternary and protonated carbons permit a reasonable interpretation of the aromatic resonances in the H-Coal liquids. In Table II, the distribution of the aromatic carbons in ASO, ASB, and VSO are shown as obtained from the integration of the chemical shift regions indicated. The one quaternary carbon detected in ASO at 127.1, at 124.4 in ASB and at 124.7 in VSO may be attributed to highly condensed interior carbon. The absence of other reduced signals in the 123 - 130 ppm region confirms the assignment of this region to the protonated carbons. The patterns of the distribution of aromatic carbons in the three liquids generally denote the more condensed ring systems with higher branchings in the VSO liquid, whereas ASO and ASB are more similar.

ACKNOWLEDGEMENT

This investigation was supported by Grant S 3688, awarded by the Institute for Mining and Minerals Research, University of Kentucky. The authors also wish to acknowledge the consultation with Professor Stanford L. Smith, Department of Chemistry, University of Kentucky on FT-CMR spectroscopy.

REFERENCES

1. (a) H. L. Retcofsky and R. A. Friedel, Fuel, 55, 363 (1976); (b) H. L. Retcofsky, Appl. Spectroscopy, 31, 116 (1977); (c) R. J. Pugmire, D. M. Grant, K. W. Zilm, L. L. Anderson, A. G. Oblad and R. E. Wood, Fuel, 56, 295 (1977); (d) R. J. Pugmire, K. W. Zilm, D. H. Bodily, D. M. Grant, H. Ito and S. Yokoyama, Am. Chem. Soc. Div. Fuel Chem., Preprints, 23, No. 2, 24 (1978); (e) D. L. Wooten, W. M. Coleman, L. T. Taylor and H. C. Dorn, Fuel, 57, 17 (1978).
2. (a) D. L. Katz, "Evaluation of Coal Conversion Processes to Provide Clean Fuels", EPRI 206-0-0 Final Report, Parts II, III, Feb. 1974; (b) R. I. Kermodé, Institute for Mining and Minerals Research Annual Report, Sept. 1973.
3. K. S. Seshadri, R. G. Ruberto, D. M. Jewell and H. P. Malone, Fuel, 57, 17 (1978).
4. H. C. Dorn and D. L. Wooten, Analyt. Chem., 48, 2146 (1976).
5. (a) J. N. Shoolery and W. L. Budde, Analyt. Chem., 48, 1458 (1976); (b) The Sadtler Standard Carbon-13 NMR Spectra, Sadtler Research Laboratories, Philadelphia, PA.

Table I. Ratios of Carbon Peak Heights from Quantitative and Quaternary Carbon Suppressed CMR Spectra of the Simulated Coal Liquid^a

| Peak No | δ TMS = 0 | Assignment ^b | | Peak Height Ratios | |
|---------------------|---------------------|-------------------------|---------------------------------|---------------------------------|--------------------------------|
| | | Notation | Carbon Type | Internal Reference ^c | Dioxane Reference ^d |
| 1 | 151.0 | If | 4 ^o | 6.4 | 6.1 |
| 2 | 147.9 | IVi | 4 ^o | 5.7 | 5.4 |
| 3 | 137.1 | IIIe | 4 ^o | 4.5 | 4.2 |
| 4 | 135.4 | Vf | 4 ^o | 4.2 | 3.9 |
| 5 | 132.5 | Ve | 4 ^o | 5.4 | 5.1 |
| 6 | 129.1 | IIIId | 3 ^o | 1.0 | 1.0 |
| 7 | 128.3 | IVh | 3 ^o | 0.8 | 0.7 |
| 8 | 128.1 | Ie | 3 ^o | 1.0 | 1.0 |
| 9 | 127.4 | Vd | 3 ^o | 0.8 | 0.7 |
| 10 | 127.0 | IVg | 3 ^o | 0.9 | 0.8 |
| 11 | 126.9 | Vc | 3 ^o | 0.8 | 0.8 |
| 12 | 125.8 | IVf | 3 ^o | 0.9 | 0.9 |
| 13 | 125.5 | IIIc, Vb | 3 ^o , 3 ^o | 1.0 | 0.9 |
| 14 | 125.3 | Id | 3 ^o | 1.0 | 1.0 |
| 15 | 125.0 | Ic | 3 ^o | 0.8 | 0.8 |
| | | | | | |
| B. Aliphatic Region | | | | | |
| 16 | 43.5 | IIIf | 3 ^o | 1.2 | 1.1 |
| 17 | 40.8 | IVe | 3 ^o | 0.8 | 0.7 |
| 18 | 39.7 | IVd | 2 ^o | 0.9 | 0.6 |
| 19 | 35.4 | IIe | 3 ^o | 1.3 | 1.2 |
| 20 | 34.6 | Ib | 4 ^o | 5.0 | 4.7 |
| 21 | 34.3 | IIId | 2 ^o | 0.8 | 0.8 |
| 22 | 31.3 | Ia | 1 ^o | 0.7 | 0.7 |
| 23 | 29.4 | IIb, IIc | 2 ^o , 2 ^o | 0.8 | 0.7 |
| 24 | 26.8 | IIb | 2 ^o | 0.9 | 0.8 |
| 25 | 24.8 | IIa | 2 ^o | 0.9 | 0.9 |
| 26 | 23.3 | IIIa | 2 ^o | 0.7 | 0.6 |
| 27 | 22.3 | IVc | 1 ^o | 0.7 | 0.6 |
| 28 | 20.9 | IVb | 2 ^o | 0.7 | 0.7 |
| 29 | 20.1 | Va | 1 ^o | 1.0 | 0.9 |
| 30 | 14.2 | IVa | 1 ^o | 0.7 | 0.6 |

^a A mixture of t-butylbenzene (I), decalin (II, cis:trans 1:4) tetralin (III), 2-phenylpentane (IV) and 2,3-dimethylnaphthalene (V) was made up in mole fractions of 0.1955, 0.2105, 0.2180, 0.1955 and 0.1805 respectively.

^b According to The Sadtler Standard Carbon-13 NMR Spectra^{6b}

^c Peak heights are normalized to the tallest peak at δ 125.47 (protonated carbons, IIIc and Vb)

^d Peak heights are normalized to the capillary dioxane peak. Refer to footnote a in Table I.

Table II. Distribution of Aromatic Carbons in H-Coal Liquids by Structural Types

| Benzene Ring Carbon Types | Chemical Shift Range, ppm | % Distribution | | |
|------------------------------|------------------------------|----------------|------|------|
| | | ASO | ASB | VSO |
| CH, OR subst. | 111-123 | 3.4 | 12.0 | 9.7 |
| CH, Unsubst. | 123-130 | 53.0 | 49.2 | 46.1 |
| CR, Condensed bridge | 130-133.8 | 11.7 | 11.4 | 14.9 |
| CR, Tetralin & Me Subst. | 133.8-137.3 | 13.4 | 11.5 | 10.4 |
| CR, Aryl & Branched Alkyl | 137.3-149 | 18.5 | 15.9 | 18.8 |
| C-OR | 149-160 | a | b | b |

^a No discernible signals are found.

^b A few low intensity signals are observed but they are too small to integrate.

Figure 1 Aromatic Regions of the Quantitative (A) and Quaternary Carbon Suppressed (B) CMR Spectra of the Simulated Coal Liquid.

Figure 2 Aliphatic Regions of the Quantitative (A) and the Quaternary Carbon Suppressed (B) CMR Spectra of the Simulated Coal Liquid.

Figure 3 Aromatic Regions of Quantitative (A) and Quaternary Carbon Suppressed (B) CMR Spectra of ASO.

Figure 4 Aliphatic Regions of Quantitative (A) and Quaternary Carbon Suppressed (B) CMR Spectra of ASO.

Figure 5 Aromatic Regions of the Quantitative (A) and Quaternary Carbon Suppressed (B) Spectra of ASB

Figure 6 Aliphatic Regions of the Quantitative (A) and Quaternary Carbon Suppressed (B) CMR Spectra of ASB

Figure 7 Aromatic Regions of the Quantitative (A) and Quaternary Carbon Suppressed (B) CMR Spectra of VSO

Figure 8 Aliphatic Regions of the Quantitative (A) and Quaternary Carbon Suppressed (B) CMR Spectra of VSO

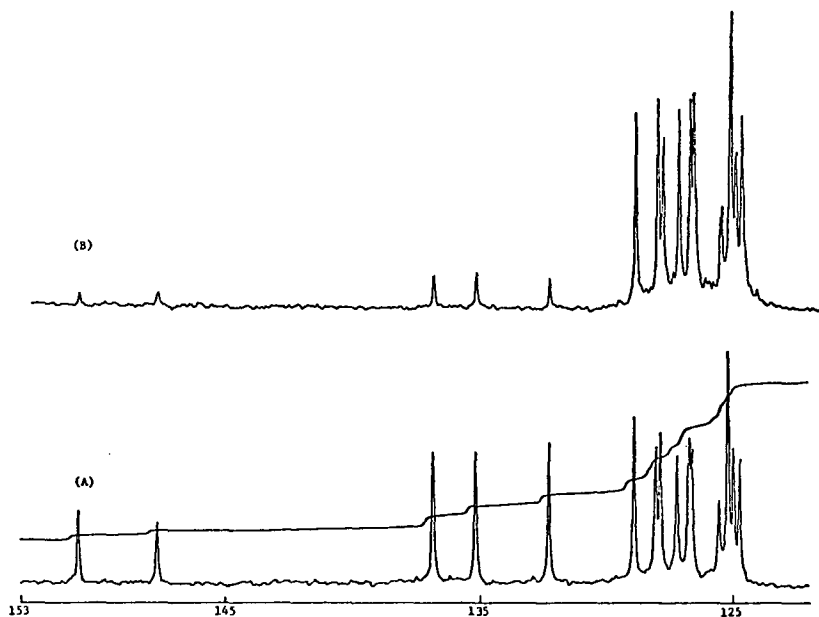


Figure 1

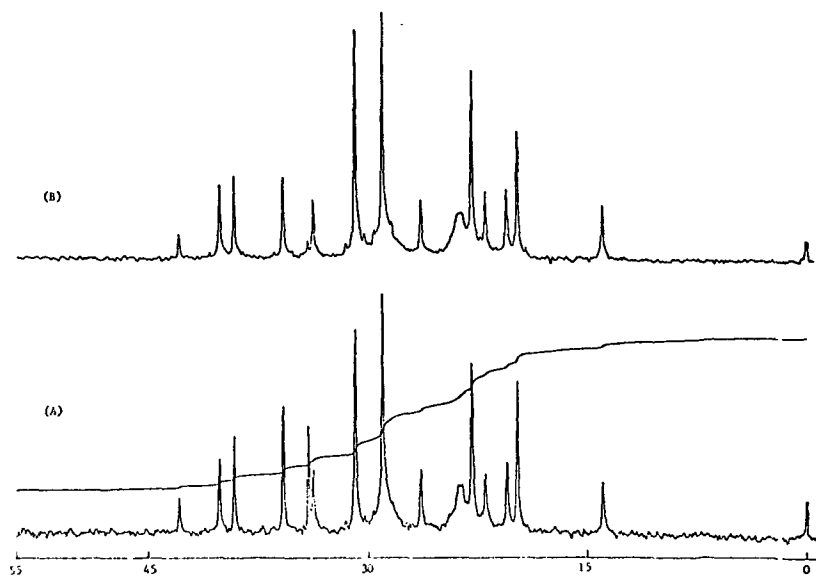


Figure 2

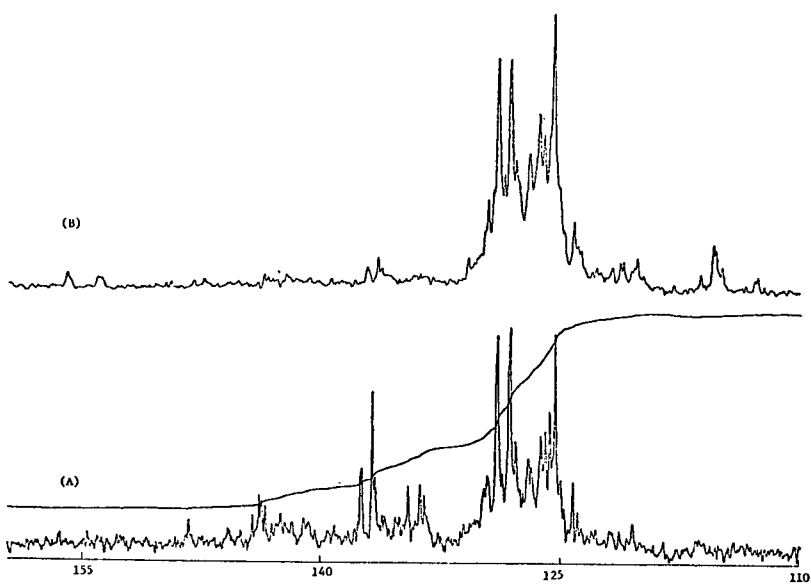


Figure 3

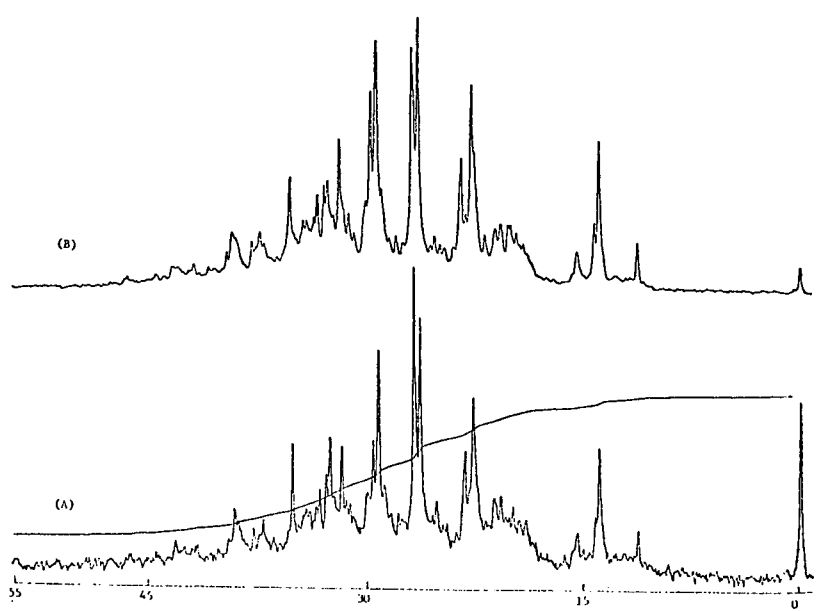


Figure 4

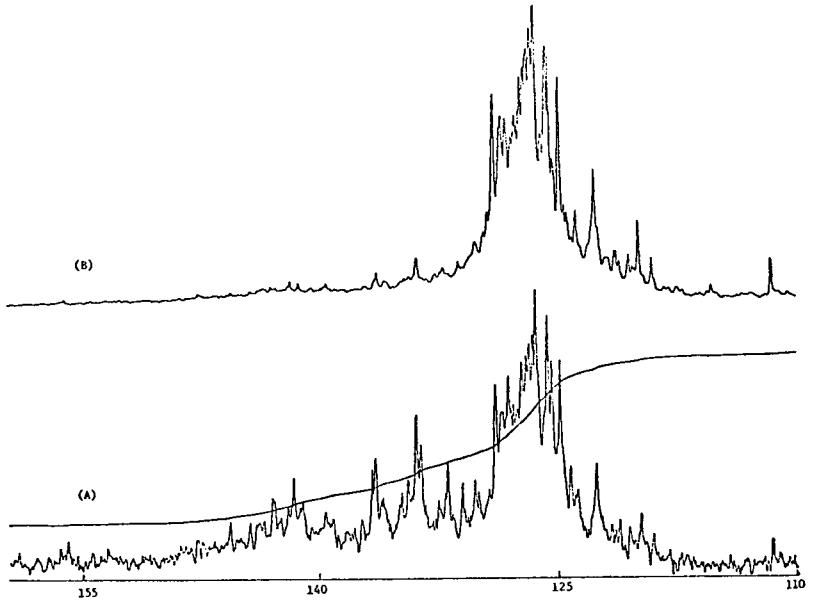


Figure 5

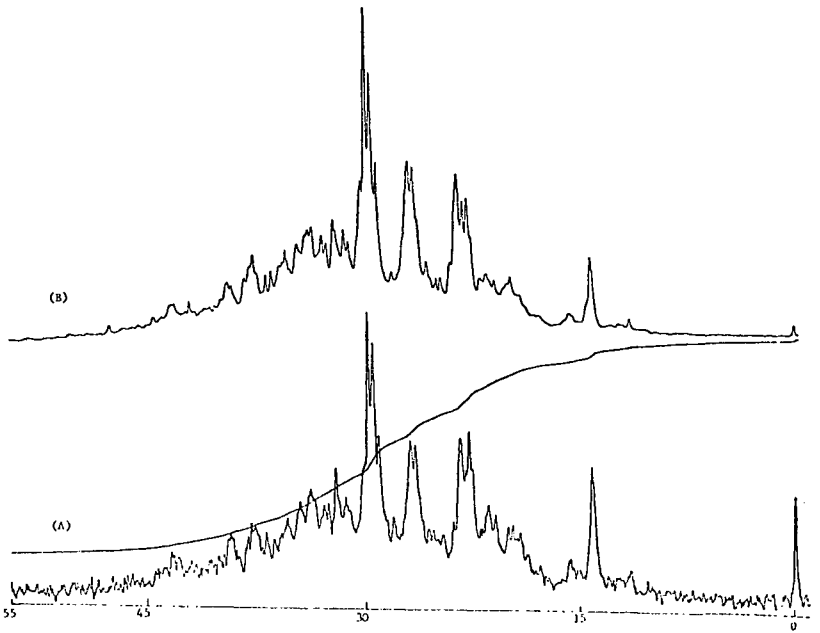


Figure 6

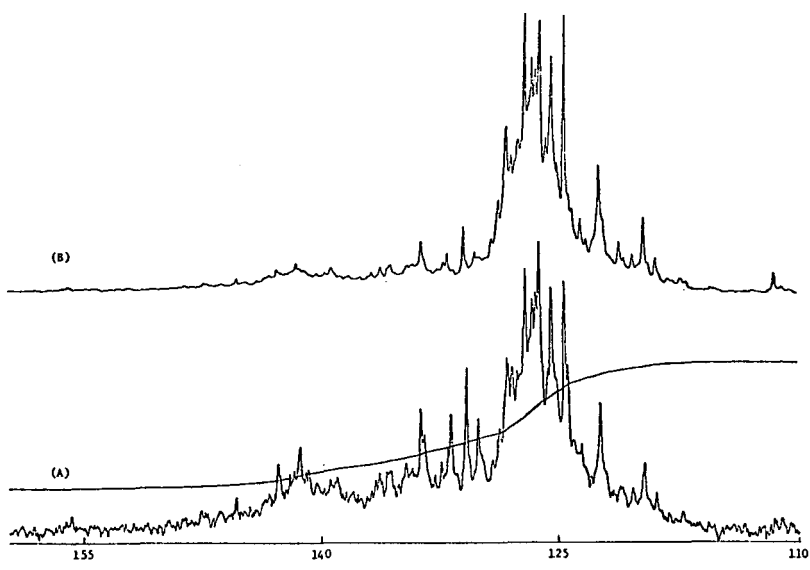


Figure 7

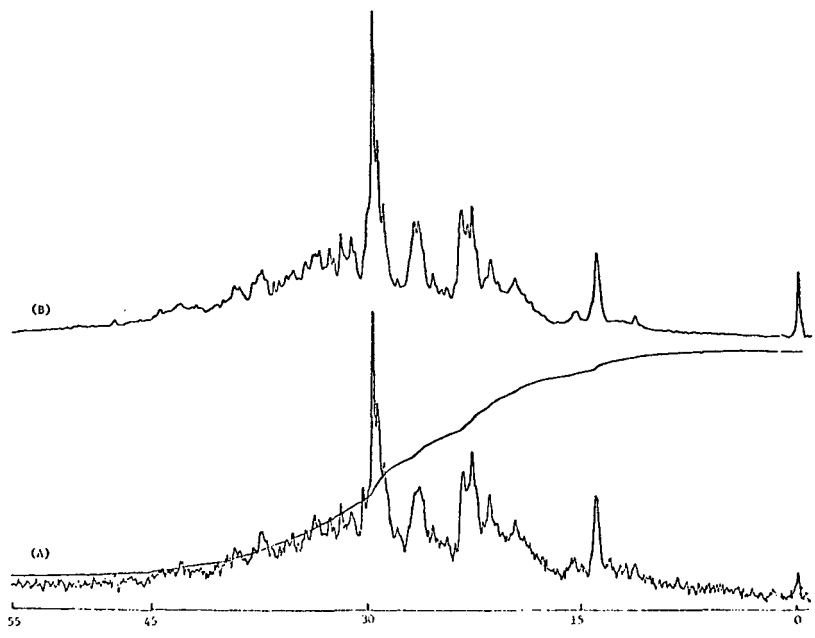


Figure 8

CARBON-13 NMR STUDIES OF COALS BY CROSS POLARIZATION AND
MAGIC-ANGLE SPINNING

F. P. Miknis

U.S. Department of Energy, Laramie Energy Technology Center
P.O. Box 3395, University Station, Laramie WY 82071

and

G. E. Maciel and V. J. Bartuska

Department of Chemistry, Colorado State University
Fort Collins CO 80523

INTRODUCTION

Knowledge of the chemical structures of the organic compounds in fossil fuels is essential for a fundamental understanding of these important materials and how to utilize them most effectively. For solid fossil fuels (e.g., oil shales and coals) this kind of chemical characterization has been difficult because many of the most powerful analytical techniques for organic structure determination, including conventional nuclear magnetic resonance (NMR) have required liquid samples. However, for coals and oil shales only small fractions of the organic constituents can be dissolved under conditions for which one can be confident that the structural integrity of the organic compounds is retained.

Until recently NMR spectra of solid samples have usually consisted of featureless, broad resonances with little or no useful information available regarding molecular structure. Recently, it has been demonstrated that useful ^{13}C NMR spectra can be obtained on solid samples by using some newly developed techniques.

Standard continuous wave or pulse Fourier transform NMR approaches on powdered or amorphous samples give very broad lines of generally low intensity. The breadth of ^{13}C resonances is due to the manifold of ^1H - ^{13}C dipole-dipole interactions and the chemical shift anisotropy resulting from random orientation of the molecules in the sample. The low signal-to-noise ratio found in such ^{13}C NMR spectra is at least partly due to the long ^{13}C spin-lattice relaxation times (T_1) characteristic of solids and the fact that repetitions of the experiment are thereby constrained to long time intervals. Pines, Gibby and Waugh^{1,2} have shown how the ^1H - ^{13}C dipole-dipole problem can be eliminated by a high-power ^1H decoupling method which also provides an enhancement in the ^{13}C NMR signal and effectively deals with the problem of long T_1 's. This approach has previously been applied to coal samples.^{3,4,5}

The remaining line broadening source one would like to remove, chemical shift anisotropy, can be eliminated by rapidly spinning the sample about an axis at an angle of 54° ^{6,7,8}, the "magic-angle," with respect to the axis of the static magnetic field. A combination of cross polarization and magic-angle spinning techniques has provided promising spectra for coals and oil shales.

While anticipated improvements in the ^{13}C techniques--e.g., using larger static magnetic fields--may provide more detailed structural information, valuable information on the aromatic/aliphatic character of coals is presently obtainable using CP-MAS techniques. This paper provides information at that level on some representative coals and coal-derived materials.

EXPERIMENTAL

The coals on which ^{13}C NMR measurements were made include a Texas lignite, three Wyoming subbituminous coals (two from Hanna, one Wyodak), an Illinois bituminous, two Indiana bituminous, two eastern bituminous coals and an anthracite. In addition, the following coal-derived materials were studied: metallurgical coke; a Hanna coal that had been subjected to reverse combustion; and a solvent refined coal derived from the Wyodak coal. Each sample was studied as a powder, about 1.4 cm^3 in each case.

The ^{13}C NMR measurements were based upon the single-contact cross polarization method.^{1,2} A 90° ^1H pulse is applied, followed by a 90° phase shift, after which ^1H rf power is maintained during the ^{13}C cross polarization and for ^1H decoupling during data acquisition. Radio frequency power at the ^{13}C resonance frequency is applied according to the Hartmann-Hahn condition during the contact period and then turned off during the period in which the ^{13}C resonance frequency of 15.1 MHz on a home-built spectrometer, using a 14 kgauss magnet, and a commercially available ^{13}C Fourier transform data system. The H_1 field for ^1H was 10 gauss and that for ^{13}C was 40 gauss. Magic-angle spinning rates of 1.9 to 2.4 kHz were achieved with a spinner of the Andrew type, using air pressure of 13 to 20 lb/in². All spectra obtained using magic-angle spinning resulted from data accumulated from 4000 scans.

RESULTS

Before truly quantitative results can be reported from ^{13}C NMR techniques of the type employed in this study, a great deal of calibration work will be required with standards, and the detailed dynamics of the cross polarization phenomenon will have to be characterized for each coal type. Such work is not yet completed, but was not considered a prerequisite for reporting the essence and qualitative significance of the present results. VanderHart and Retcofsky⁴ and Bartuska et al.⁵ have previously discussed the problems of obtaining quantitative analytical data from cross polarization experiments.

In order to choose a reasonable set of experimental parameters, which could be expected to give integrated intensities of at least semiquantitative significance, parameter variations were carried out in experiments on the Illinois bituminous sample. The contact (cross polarization) time, which must be chosen to conform with the dynamics of ^{13}C - ^1H cross polarization and ^1H T_1 constraints, was varied over the following values: 0.5 msec, 1.0 msec, 3.0 msec, and 5.0 msec. Using a repetition time of 4.0 sec, we measured the integrated signal intensity of the "aromatic" and "nonaromatic" carbon resonances and the apparent carbon fraction found in the aromatic region, f_a (aromaticity); these values were found to be 0.75 and 0.76 for 1 msec and 3 msec, and 0.72 and 0.68 for 5 msec and 0.5 msec, respectively, for the contact time. The best signal-to-noise ratio (S/N) was found for the 1 msec contact time; S/N deteriorated badly at 5 msec. Choosing the 1 msec contact period, we repeated the experiment with a repetition time of 8.0 sec, obtaining a 0.74 value for f_a . Settling on 1 msec and 4 sec contact and repetition times, respectively, all cross polarization results reported in this paper were obtained using these parameters.

In order to check that by using the above-mentioned experimental parameters reasonable f_a values would be obtained in cross polarization experiments, we made ^{13}C NMR measurements on the Illinois bituminous sample by using the pulse Fourier transform method, with magic-angle spinning and high-power ^1H decoupling, but without cross polarization. Intensity data of such experiments are still subject to uncertainties associated with nuclear Overhauser effects and differing relaxation times,¹⁵ but such uncertainties are entirely different from those associated with the cross polarization approach. When pulse repetition times of 30 and 99 sec were employed, f_a values of 0.71 and 0.77, respectively, were obtained. Hence, while

there is no guarantee that the same cross polarization parameter set (1.0 msec and 4.0 sec) will serve equally well for all of the coal samples, indications are that this set leads to no major intensity distortions for the Illinois bituminous sample, and is a reasonable set to employ in the present survey.

DISCUSSION

An example of the advantages of magic-angle spinning in conjunction with cross polarization and high-power decoupling is shown in Figure 1a and b for the Hanna subbituminous coal. Clearly, the main structural distinction that can be made is between aliphatic and aromatic carbons. The spinning case shows much better resolution because the chemical shift anisotropy, which is evident in the aromatic region of Fig. 1a, has been eliminated. Aromaticity values are determined by dividing the integrated intensity of the aromatic band by the integrated intensity of the complete spectrum.

A ^{13}C spectrum of the Hanna coal which had been subjected to reverse combustion at 500°C is shown in Fig. 1c. The spectra clearly show depletion of the aliphatic carbons, relative to the aromatic carbons. Similarly, the CP-MAS spectra of a Wyodak coal (Fig. 2a) and its solvent refined product (Fig. 2b) show that the solvent refining process increases the aromaticity of subbituminous coals. These examples suggest the use of CP-MAS techniques for studies of coal combustion and processing.

^{13}C NMR spectra of a series of coals of varying rank are shown in Fig. 3a-f. This simple montage of ^{13}C spectra shows quite graphically that the aromaticity of coals increases with increasing rank. The metallurgical coke is included because it had a measured f_a of 1.00. A matter of concern regarding quantitative measurements in CP-NMR of solids is whether all the carbon types in the sample are being polarized equally, particularly aromatic carbons in condensed systems. The fact that the f_a of the coke yielded a very reasonable value of 1.00 implies that all of the carbons in the coal are being observed. Recent work on oil shales also addresses this problem.^{12,13}

One fuel property that would be interesting to relate to structural features is the heating value. Figure 4 shows a plot of the heating values of the coals vs. the f_a values derived from the ^{13}C spectra. That a simple correlation is not found is not surprising, as a variety of variations occur within these samples. In progressing from a lignite to a bituminous coal to an anthracite, the percent organic carbon of the material increases, which tends to increase the heating value.

An increase in f_a , by itself, would tend to decrease the heating value, as can be seen from the following heats of combustion: benzene, 782.3 kcal/mole; cyclohexane, 937.8 kcal/mole; n-hexane, 989.8 kcal/mole; phenol, 732.2 kcal/mole; cyclohexanol, 890.7 kcal/mole. In addition, within a collection of coal samples there are substantial variations in the percent oxygen, nitrogen and sulfur--i.e., in the occurrence of oxygen-, nitrogen- or sulfur-containing organics. Oxygen-containing species tends to decrease the heating value of a coal, for a given amount of carbon, as seen from the following heats of combustion: benzene, 782.3 kcal/mole; phenol, 732.2 kcal/mole; cyclohexane, 937.8 kcal/mole; cyclohexanol, 890.7 kcal/mole; toluene, 934.3 kcal/mole; benzyl alcohol, 894.3 kcal/mole; benzoic acid, 771.2 kcal/mole.

In viewing variations of heating values of coals, if one wishes to eliminate the factor due to percent organic carbon in the coal, the heating value per pound of carbon (maf) is of interest. Figure 5 shows a plot of this heating value vs. f_a . Note that, if the organic constituents of coal were strictly hydrocarbons, such a plot would be expected to show a decrease in BTU/lbc as f_a increases, reflecting the heat of combustion pattern stated above. Instead, Figure 5 shows a nearly

constant value of about 1.75×10^4 BTU/lbC for coals with apparent aromatic fractions ranging from 0.70 to 0.75 and a fall off on both sides of that f_a range.

This pattern can be understood as follows: As stated above, if coal were composed of only hydrocarbons, the trend would be to lower BTU/lbC for higher f_a values. This trend is responsible for the fall off of the curve for the highest three f_a values. However, organic compounds containing oxygen, but equivalent numbers of carbon atoms have lower heats of combustion than analogous hydrocarbons. The coals with the lowest observed f_a values, which might have been expected have the highest BTU/lbC values, also have the highest total oxygen contents (maf), and their lower BTU/lbC values may be associated with these high oxygen contents. The coals with highest f_a values (0.81, 0.95, and 1.0) have very low oxygen contents, and there is a roughly decreasing progression of oxygen contents as f_a increases from 0.59 to 1.0. Hence, there are two competing influences on the BTU/lbC parameter, giving rise to the broad maximum at about 1.75×10^4 BTU/lbC.

REFERENCES

1. Pines, A., Gibby, M. G., and Waugh, J. S. J. Chem. Phys., v. 56, 1972, p. 1779.
2. Pines, A., Gibby, M. G., and Waugh, J. S. J. Chem. Phys., v. 59, 1973, p. 569.
3. Bartuska, V. J., Maciel, G. E., Schaefer, J., and Stejskal, E. O. Fuel, v. 56, 1977, p. 354.
4. VanderHart, D. L., and Retcofsky, H. L. Fuel, v. 55, 1976, p. 202.
5. Retcofsky, H. L. and VanderHart, D. L. Fuel, v. 57, 1978, p. 421.
6. a) Lowe, I. J. Phys. Rev. Letters, v. 2, 1959, p. 285.
b) Kessemeyer, H., and Norberg, R. E. Phys. Rev., v. 155, 1967, p. 321.
7. Andrew, E. R. Progr. Nucl. Magn. Reson. Spectrosc., v. 8, 1971, p. 1.
8. Schaefer, J., and Stejskal, E. O. J. Amer. Chem. Soc., v. 98, 1976, p. 1031.
9. Maciel, G. E., Bartuska, V. J., and Miknis, F. P. Fuel (in press).
10. Maciel, G. E., Bartuska, V. J., and Miknis, F. P. Fuel, v. 57, 1978, p. 505.
11. Maciel, G. E., Bartuska, V. J., and Miknis, F. P. Fuel (in press).
12. Miknis, F. P., Maciel, G. E., and Bartuska, V. J. Org. Geochem. (in press).
13. Resing, H. A., Garroway, A. N., and Hazlett, R. N. Fuel, v. 57, 1978, p. 450.
14. Noggle, J. H., and Schirmer, R. E. The Nuclear Overhauser Effect, Academic Press, New York, 1971.
15. Farrar, T. C., and Becker, E. D. Pulse and Fourier Transform NMR, Academic Press, New York, 1971.
16. Whitehurst, D. D. "Organic Chemistry of Coal," J. W. Larsen, Ed., ACS Symposium Series, v. 71, Amer. Chem. Soc., Wash., D.C., 1978.

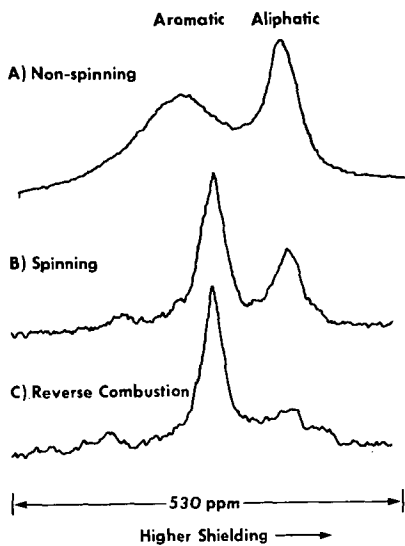


Figure 1. ^{13}C NMR Spectra of Hanna, Wyoming Coal

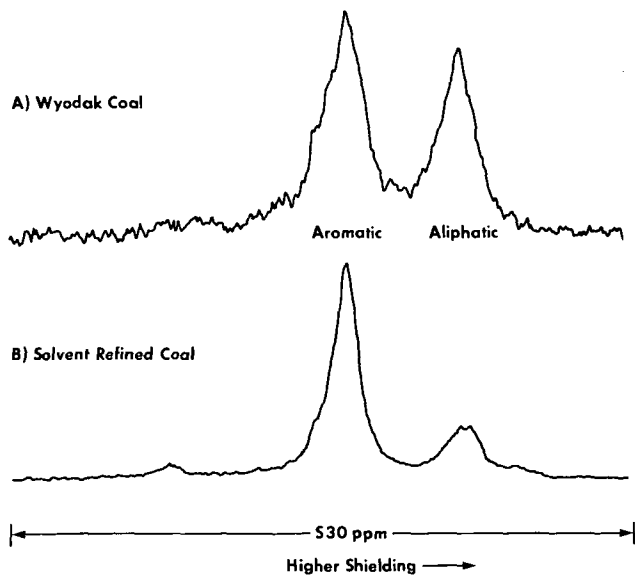


Figure 2. ^{13}C NMR Spectra of Wyodak Coal and SRC Product

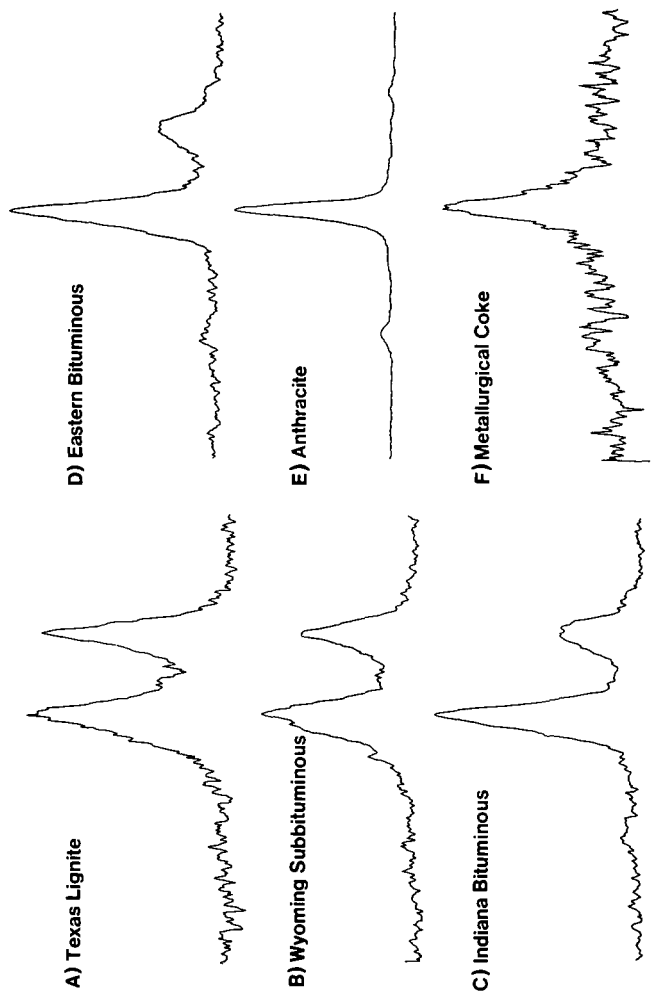


Figure 3. ^{13}C NMR Spectra of Coals of varying rank

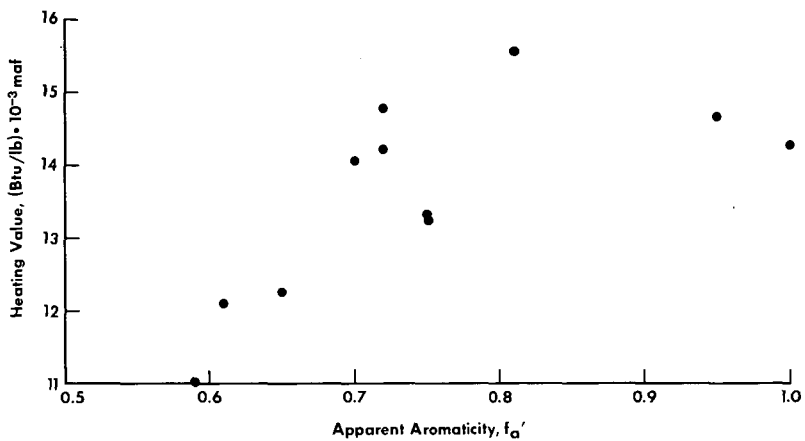


Figure 4. Plot of heating value versus aromaticity

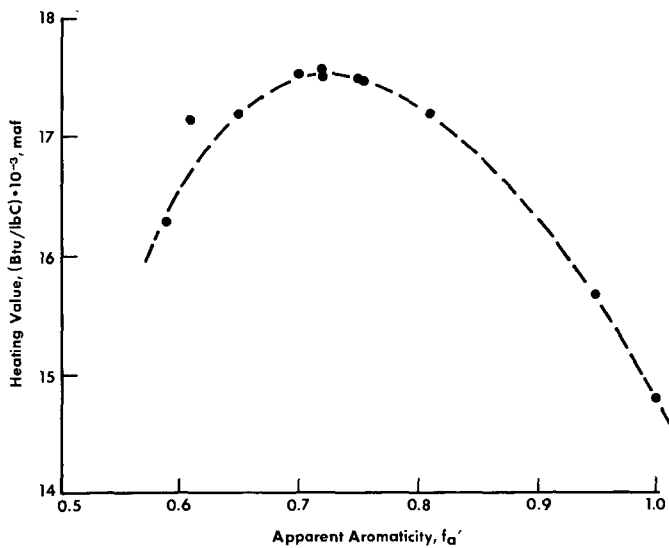


Figure 5. Plot of heating value/pound of carbon versus aromaticity

THE EFFECTS OF T_1 AND NOE CONSIDERATIONS IN QUANTITATIVE APPLICATIONS OF CARBON-13 NMR TO THE ANALYSIS OF COMPLEX HYDROCARBON MIXTURES

Terry D. Alger, Ronald J. Pugmire, W. David Hamill, Jr., and David M. Grant

Departments of Chemistry and Mining and Fuels Engineering, University of Utah,
Salt Lake City, Utah 84112

I. Introduction

Since the signal intensities of a nuclear magnetic resonance spectrum are dependent upon the number of given nuclei present in a compound, nuclear magnetic resonance can be a strong analytical tool for quantifying the amounts of material present in a sample. In many compounds of interest which contain carbon, carbon-13 magnetic resonance (cmr) spectra are of particular value as an analytical tool since the spectra can be void of multiplet structure due to ^{13}C - ^{13}C splittings (if carbon is in natural abundance only) and can be void of multiplet structure due to ^1H - ^{13}C splittings (if noise-modulated proton decoupling techniques are used). Moreover, a range of chemical shifts of over 200 ppm for common functional groups assist greatly in resolving individual peaks in any given spectrum (1). Thus under such experimental conditions, each ^{13}C nuclear environment is represented by a single ^{13}C resonance. In complex mixtures of hydrocarbons resulting from coal liquification, these qualities of cmr make ^{13}C spectra particularly useful. Such coal mixtures can contain hundreds of compounds, and may be quite viscous. In such mixtures, ^{13}C spectra have been used by various workers to quantify the amount of a given compound, as well as to quantify the amount of aromaticity in given coal derivative samples (2-4).

Nevertheless, there are some problems attendant with the ^{13}C nmr technique and the usefulness of the ^{13}C signal intensity as a quantifiable parameter. To begin with, ^{13}C nuclei in natural abundance amount to only about 1.1%. In complex mixtures of multiple compounds, signal sensitivity therefore becomes a problem. Fourier transform methods of data acquisition with repeated pulse sequences and data storage for signal averaging, has somewhat overcome such complications (4). However, such Fourier techniques themselves lead to other problems. To ensure that the time necessary to store sufficient transients is not inordinately long, it is desirable to repeat the pulse sequence as rapidly as possible. Nevertheless, the delay time between successive pulse sequences (individual transients) is dependent upon the spin-lattice relaxation times (T_1) of the ^{13}C system. If the next pulse sequence is begun before any given ^{13}C signal has had an opportunity to relax to its thermal equilibrium value, saturation effects occur, and the resultant ^{13}C signal intensity is not maximized. For hydrocarbon systems which contain a wide variety of carbon-13 relaxation times from fairly short (2 sec) to fairly long (200 sec), this creates a problem. Reasonable delay times of 1-10 seconds between successive 90° pulses would most likely saturate the ^{13}C signals with long relaxation times (200 sec) so that less than 10% of the possible signal would be observed. In contrast, delay times of 1-10 seconds with 90° pulses could permit nearly 90% of the signals to be observed if the relaxation times were short (2 sec). Under such variable saturation effects, the ^{13}C signal intensities would be difficult to relate to quantifiable results (4).

For hydrocarbon systems which result from coal derivatives, such wide variations in relaxation times are a reality. Spin-lattice relaxation times in acenaphthene have been reported to vary from 3.1 seconds for the ^{13}C nuclei with two protons attached, to about 150 seconds (5a,5b,5c) at the internal bridgehead carbon. A similar range of the spin-lattice relaxation times for the protonated and non-protonated carbons in pyrene has been observed. Since delay times of $5T_1$ are necessary to ensure complete relaxation following a 90° or 180° pulse (6), some other method must be found for taking ^{13}C signal intensities in

hydrocarbon systems with long relaxation times. Repeated pulse sequences (1,000 to 10,000 transients) with delay times of 1,000 seconds ($5T_1$) become prohibitively long to run (for example, 10,000 transients with delay times of 1,000 sec between transients would take 116 days per spectrum).

Another problem inherent in the proton-decoupled ^{13}C spectra relates to the Nuclear Overhauser Effect (NOE) experienced by the ^{13}C signals when the coupled ^1H nuclei are doubly irradiated. It has been observed that ^{13}C intensities are enhanced when coupled ^1H signals are irradiated by a saturating second frequency. The value of the NOE is determined by the ratio of $S \approx S_0$. (The ^{13}C signal intensity after the proton decoupler has been on long enough to establish equilibrium is $S \approx S_0$ is the signal intensity without proton decoupling) (7). Depending upon whether a given nucleus is dominated by dipole-dipole relaxation, or by other relaxation mechanisms, the value of NOE can vary from 3 to 1, respectively (8,9). In the hydrocarbon systems of coal derivatives, it appears that the NOE factors can vary over the maximum ranges (being about 3 if protons are directly attached, and as low as 1-2 if no protons are attached). Hence, variations in NOE enhancements of ^{13}C signal intensities representing the same number of ^{13}C nuclei could vary over a magnitude of 1-3 (8). This is hardly acceptable for quantitative studies. Thus, some means of either quickly determining the NOE factors for each ^{13}C signal must be found, or else some means of eliminating the NOE enhancement must be used.

In an effort to address the preceding problems we have obtained T_1 and NOE values on a number of model compounds (polycyclicaromatic hydroaromatic, and alkylated aromatic hydrocarbons) which are thought to have representative values similar to those found in complex hydrocarbon mixtures. The T_1 and NOE values thus obtained provide valuable information on relaxation processes, range of values expected, and details of molecular motion.

II. Experimental

The T_1 and NOE data were taken at 25 MHz and 75 MHz on Varian XL-100-15 and SC-300 FT spectrometers, respectively. T_1 's were obtained by the inversion recovery method (10) while NOE values were obtained by a two point gated decoupling method.

III. Results and Discussion

We have obtained T_1 and NOE data on naphthalene, tetralin, acenaphthene, pyrene, symmetrical hexahdropyrene, phenanthrene, 1,2,3,4,5,6,7,8, octahydro-phenanthrene, xanthone, and phenyloctane. This group of compounds represent a set of structural types representative of many moieties known to occur in coal derived liquids. In terms of general relaxation considerations the data can be considered, for convenience, in terms of protonated and non-protonated carbons. Protonated carbons are found, within experimental error, to exhibit essentially a full nuclear overhauser effect and the dipolar relaxation mechanism thus is dominant (11). The T_1 values at 25 MHz for all protonated carbons examined fall in the range of 2-11 second. Similar values are observed at 75 MHz. The non-protonated carbons, however, fall in the range 28-240 seconds at 25 MHz with the higher numbers associated with the PAH's where the $1/r_{\text{C-H}}^6$ term in the relaxation expression rapidly alternates the efficient carbon-hydrogen intramolecular dipolar relaxation mechanism.

Some very interesting results are observed for the non-protonated carbons at 75 MHz. The T_1 values are shortened considerably indicating significant contributions made by chemical shift anisotropy at high fields. Using the rate expression (11)

$$\frac{1}{T_1} = \frac{1}{T_1^D} + \frac{1}{T_1^{\text{CSA}}} + \frac{1}{T_1^0} \quad (1)$$

and assuming that $1/T_1^0$ approaches zero for the systems in question (which, based on the low and high field data, is justified), one can readily calculate dipolar

contributions of 88, 413, and 127 seconds, to the relaxation rates at C-9,10,C-11, and C-12, respectively by assuming isotropic motion of the molecules. The chemical shift anisotropy term is 88, 73, and 54 seconds, respectively for these carbons. In the case of pyrene the contribution from chemical shift anisotropy is even greater with contribution of 35 and 38 seconds for carbons 11,12,13,14 and 15,16 respectively. Hence, relaxation constraints are much less severe at high fields than those encountered using iron core magnet NMR technology.

Based on the data obtained to date, we estimate that the non-protonated carbons at C-15,16 in pyrene represent the longest T_1 values one would expect to encounter. Using mixtures of these compounds we have varied spectrometer operating conditions in order to arrive at an optimal set of parameters for use on coal derived liquids. Details of the results of these studies at 25 and 75 MHz will be forthcoming.

Acknowledgment

We gratefully acknowledge support for this work from the Department of Energy under contract ER-78-S-02-5006 and a National Institutes of Health Regional Resources grant RR-574.

REFERENCES

1. J. Strothers Carbon-13 NMR Spectroscopy, Academic press, New York, London 1972.
2. H. L. Retcofsky, F. K. Schweighardt and M. Hough, *Anal. Chem.*, **49** 585 (1977).
3. R. J. Pugmire, D. M. Grant, K. W. Zilm, L. L. Anderson, A. G. Oblad, and R. E. Wood, *Fuel*, **56**, 295 (1977).
4. a) R. G. Ruberto, D. C. Cronauer, D. M. Jewell, and K. S. Seshadr, *Fuel*, **56**, 25 (1977); b) *Ibid.*, **56**, 17 (1977); c) K. S. Seshadri, R. G. Ruberto, D. M. Jewell, and H. R. Malone, *Div. Fuel Chem.*, **20**, 38 (1977).
5. a) J. N. Shoolery and W. C. Jankowski, *Varian Applications Note NMR-73-4*, August, 1973; b) J. N. Shoolery, *Varian Instrument Applications*, Vol. 10, Number 3, 1976; c) J. N. Shoolery, "Some Quantitative Applications of ¹³C NMR Spectroscopy," in *Progress in Nuclear Magnetic Resonance Spectroscopy*, Pergamon Press Ltd., Oxford, England (1977).
6. R. K. Harris, and R. H. Newman, *Journal of Magnetic Resonance* **24** 449 (1976).
7. J. R. Lyerla and D. M. Grant, *MPT International Review of Science Physical Chemistry, Series One*, **4** 155 (1972).
8. a) T. D. Alger, D. M. Grant, and R. K. Harris, *Journal Physical Chemistry*, **76**, 281 (1972); b) A. J. Jones, D. M. Grant, and K. F. Kuhlmann, *J. Amer. Chem. Soc.*, **91**, 5013 (1969).
9. It should be noted, see Ref. 7 for a complete description, that if the liquid is not in the region of motional narrowing,

$$\text{i.e., } (\omega_{\alpha\beta}^2 \tau_C^2 \ll 1),$$

the NOE will not be equal to 3 even if the relaxation is totally dipole-dipole dependent (transition probabilities and hence relaxation mechanisms are related to:

$$W_{\alpha\beta} = \gamma^2 H^* \text{Loc}(t) H_{\text{Loc}}(t) \left(\frac{\tau_C^2}{1 + \omega_{\alpha\beta}^2 \tau_C^2} \right)$$

10. R. Freeman and H. D. W. Hill, *J. Chem. Phys.*, **53**, 4103 (1970).
11. K. F. Kuhlmann and D. M. Grant, *J. Chem. Phys.*, **55**, 2998 (1971).

TABLE I

Relaxation Parameters in Pyrene and Acenaphthene

| COMPOUND | POSITION | T_1 $\frac{25 \text{ MHz}}{\eta}$ (± 0.2) | | T_1 $\frac{75 \text{ MHz}}{\eta}$ (± 0.2) | |
|--------------|-------------|---|-----|---|------|
| Acenaphthene | 1,2 | 3.1 ± 0.2 | 3.0 | 3.1 | 1.95 |
| | 3,8 | 5.6 ± 0.8 | 2.8 | 6.0 ± 0.4 | 1.85 |
| | 4,7 | 5.6 ± 0.8 | 2.8 | 6.6 ± 0.5 | 1.85 |
| | 5,6 | 6.4 ± 0.9 | 2.8 | 6.5 ± 0.4 | 1.85 |
| | 9,10 | 87 ± 10 | 2.3 | 44 ± 2 | 1.0 |
| | 11 | 208 ± 30 | 1.8 | 62 ± 7 | 0.4 |
| | 12 | 128 ± 10 | 2.1 | 38 ± 3 | 0.4 |
| Pyrene | 1,3,6,8 | 8.0 ± 0.4 | 1.9 | 4.9 ± 0.4 | 2.0 |
| | 2,7 | 6.8 ± 0.2 | 1.9 | 4.5 ± 0.3 | 2.0 |
| | 4,5,9,10 | 7.2 ± 0.8 | 1.9 | 5.4 ± 0.2 | 2.0 |
| | 11,12,13,14 | 135 ± 10 | 1.2 | 26.2 ± 1.4 | 0.51 |
| | 15,16 | 240 ± 30 | 0.6 | 35.1 ± 3.5 | 0.17 |

Hydrogenation Reactivity of Petrographic Composition of Coal

Y. Nakata*, S. Ueda*, Y. Maekawa* and M. Shibaoka**

*Government Industrial Development Laboratory, Hokkaido
41-2, Higashi-Tsukisamu, Toyohiraku,
Sapporo, 061-01, Japan

**CSIRO, Fuel Geoscience Unit, P.O.Box 136, North Ryde,
N. S. W., Australia 2113

Introduction

With special regard to the characteristics of high pressure hydrogenation of the petrographic composition of coal, in the past reports by Bergius¹⁾, Wright et al²⁾, Fisher et al³⁾ are available, and more recently we have reports on the results of work by Given, Davis and Mitchell et al⁴⁾⁻⁷⁾. According to these reports, among the 3 maceral groups of coal, namely vitrinite, exinite and inertinite, it has been pointed out that the reactivity of vitrinite and exinite are high.

Among the coals produced in Australia, while there are rather large number of coals with a relatively high inertinite content, and whereas the main component of inertinite is semifusinite, generally the scarcity of fusinite is characteristic. While it is generally accepted that the hydrogenation reactivity of fusinite is low, no reports regarding semifusinite seen to be available.

In the present report we conducted liquefaction experiments by hydrogenation reaction on hand picked vitrinite concentrates and inertinite concentrates of Bayswater seam coal (N.S.W., Australia), and the respective features of liquefaction reaction were clarified and a comparative investigation was made between the two.

Experimental

The samples used in the experiments were vitrinite concentrates and inertinite concentrates hand picked from Bayswater seam coal of high volatile bituminous rank. The petrographic, proximate and ultimate analyses of the hand-picked samples are given in Table 1. In the experiments we used a batch type autoclave with an inner volume of 500 cc as the hydrogenation apparatus. In the once experiment, we inserted 10 g of dry sample coal, 1 g of red mud catalyst, 0.1 g sulfur promoter together with 10 steel balls for agitation, and the hydrogenation reaction was conducted under an initial hydrogen pressure of 100 kg/cm² at reaction temperatures of 400°C and 450°C respectively and by changing the reaction time from 0-150 minutes. In the case where vehicle oil was used, we applied decrystallized anthracene oil.

Among the reaction products, the gas was dealt with gas chromatography and the composition thereof was measured. Regarding the liquid and solid products, using n-hexane, benzene were fractionated into oil-1(O₁), oil-2(O₂), asphaltene(A), and organic benzene insolubles (O.B.I). The conversion was calculated from total product(gas+O₁+O₂+A). In addition O.B.I. was subjected to extracting tests using pyridine. The details of the above are as seen in our previous report⁸⁾.

Results and discussion

In Fig. 1 is shown the changes by reaction time of the yield of each fraction

of hydrogenation products of vitrinite and those of inertinite are shown in Fig. 2.

Even at a reaction temperature of 400°C the reaction of vitrinite proceeds and the conversion increases with the reaction time however the conversion of inertinite does not exceed 15% or thereabouts. However, in the case where vehicle oil is added to inertinite, even under identical reaction conditions the conversion increases markedly to 45% or thereabouts.

When this vehicle oil is used, this conversion is attained by the nominal reaction time zero. From the previous paper⁹), it may be considered that the coal hydrogenation reaction with vehicle oil proceeds by the chemical reaction controlling. Therefore, it may be understood that the initial stage reaction rate of inertinite is very fast. However, thereafter ever what the reaction time is increased, no increase in the conversion was recognized, and it is surmized that the portion which can react under certain given conditions is restricted. Whereas the equilibrium conversion is higher than 400°C a similar tendency is seen when the reaction temperature is 450°C. This point is that which differs from vitrinite in which a gradual increase is seen with the increase in reaction time. However, when the distribution of reaction products is viewed, the distribution of gas, oil and asphaltene in both cases is relatively similar.

Further, hydrogen consumption of both cases in hydrogenation is as shown in Table 2, it may be seen that in the case of inertinite approximately 2 fold values are seen. The molecular weight of the reaction products of both cases are as seen in Table 3. When the reaction temperature becomes 450°C, a relative fairly good coincidence is seen between the vitrinite and inertinite, however when the reaction temperature is 400°C, it may be noted that the reaction products from inertinite show higher values. The H-NMR spectra of oil-1 and oil-2 of inertinite at 400°C are shown in Fig. 3; as may be seen an approximately similar pattern is recognized. Similarly the H-NMR spectra of oil-1 of inertinite at 150 minutes, 400°C, and oil-1, oil-2 of vitrinite at 30 minutes, 400°C as shown in Fig. 4 show a similar pattern.

Thus from the above, it may be surmized that product from the liquefaction of the main parts of both sample coal have a relatively similar composition.

Conclusion

- 1) The reaction rate of vitrinite shows a gradual increase with the reaction time, however in the case of inertinite, the reaction does not proceed beyond a given value. This given value shows an increase with the rise in reaction temperature and the reaction rate is fast up till the time that this value is attained.
- 2) The hydrogen consumption is larger in inertinite.
- 3) It may be surmized that the liquefaction products from the main part of both sample coal have a relatively similar composition.

References

- 1) Bergius, F., Gluckauf, 61, 1317 (1925)
- 2) Wright, C.C., and Sprunk, G.C., Penn. State Coll. Min. Ind. Exp. Stat. Bull. 26 (1939)
- 3) Fisher, C.H., Sprunk, G.C., Eisner, A., O'Donnell, H.J., Clarke, L., and Storch, H. H., U.S. Bureau Mines Tech. Paper 642 (1942)
- 4) Given, P.H., Cronauer, D.C., Spackman, W., Lovell, H.L., Davis, A., and Biswas, B., Fuel, 54, 34 (1975)
- 5) Given, P.H., Cronauer, D.C., Spackman, W., Lovell, H.L., Davis, A., and Biswas, B., ibid, 54, 40 (1975)

- 6) Davis,A., Spackman,W., and Given,P.H., Energy Sources, 3, 55 (1976)
- 7) Mitchell,G.D., Davis,A., and Spackman,W., Liquid Fuels From Coal, Academic Press, p.p 255-270 (1977)
- 8) Maekawa,Y., Ueda, S., Hasegawa,Y., Yokoyama,Y., Hiroki,E., Yoshida,Y., Nenryo Kyokai-Shi (J. Fuel Soc. Japan) 49, 908 (1970)
- 9) Maekawa,Y., Shimokawa,K., Ishii,T., Takeya,G., Kogyo Kagaku Zasshi (J. Chem. Soc. Japan, Ind. Chem. Section), 73, 2347 (1970)

Table 1 Petrographic, Proximate and Ultimate Analysis of Bayswater Seam Coal

| Sample | Maceral analysis (%) | | | | | Proximate analysis (%) | | | | Ultimate analysis (%) | | | | |
|------------------------|----------------------|---------|-----------|---------------|----------|------------------------|------|------------------|--------------|-----------------------|-----|-----|-----|-----|
| | Vitrinite | Exinite | Miorinite | Semi-fusinite | Fusinite | Moisture | Ash | Volatiles matter | Fixed carbon | C | H | N | S | O |
| Vitrinite concentrate | 99 | 0.5 | 0.5 | tr | tr | 3.4 | 1.6 | 32.9 | 62.1 | 83.0 | 5.3 | 2.0 | 0.5 | 9.2 |
| Inertinite concentrate | 0.5 | 5 | 4 | 90 | 0.5 | 4.5 | 16.2 | 20.8 | 58.5 | 85.0 | 4.1 | 1.9 | 0.3 | 8.7 |

Table 2 Hydrogen consumption of vitrinite and inertinite hydrogenation

| Sample | R.T °C | Rt min. | H ₂ consumption | |
|------------|--------|---------|----------------------------|-------------------------|
| | | | wt % of coal | wt % of coal/conversion |
| Vitrinite | 400 | 0 | 0.75 | 6.1 x 10 ⁻² |
| " | " | 30 | 1.24 | 5.6 " |
| " | " | 60 | 3.42 | 7.0 " |
| " | " | 90 | 2.95 | 4.5 " |
| " | " | 120 | 3.52 | 4.9 " |
| " | " | 150 | 4.22 | 5.4 " |
| " | 425 | 60 | 4.84 | 6.9 " |
| " | 450 | 0 | 1.37 | 2.7 " |
| " | " | 30 | 4.20 | 5.4 " |
| " | " | 60 | 5.40 | 6.1 " |
| Inertinite | 400 | 0 | 2.05 | 1.8 x 10 ⁻¹ |
| " | " | 30 | 2.64 | 1.6 " |
| " | " | 60 | 1.39 | 1.4 " |
| " | " | 150 | 2.95 | 2.5 " |
| " | 410 | 60 | 1.30 | 1.3 " |
| " | 425 | 60 | 2.80 | 1.4 " |
| " | 435 | 60 | 2.23 | 0.6 " |
| " | 450 | 0 | 1.38 | 1.1 " |
| " | " | 30 | 1.67 | 4.9 " |
| " | " | 60 | 5.05 | 0.9 " |
| " | " | 90 | 4.72 | 0.9 " |
| " | " | 120 | 4.99 | 0.9 " |
| " | " | 150 | 5.86 | 1.0 " |

Table 3 Molecular weight of inertinite and vitrinite hydrogenation product

| Raw Sample | R.T °C | Rt min. | oil-1 | Product oil-2 | Asphaltene |
|------------|-----------|------------|-------|------------------|------------|
| Vitrinite | 400 | 0 | 340 | 500 | - |
| " | " | 30 | - | - | 680 |
| " | " | 60 | 320 | 450 | 660 |
| " | " | 90 | 300 | 360 | 700 |
| " | " | 120 | - | 420 | 760 |
| " | " | 150 | 420 | 530 | 770 |
| " | 425 | 60 | 290 | 450 | 750 |
| " | 450 | 0 | 340 | 460 | 580 |
| " | " | 30 | 280 | 480 | 800 |
| " | " | 60 | 300 | 370 | 850 |
| <hr/> | | | | | |
| Inertinite | 400 | 0 | 490 | 460 | 470 |
| " | " | 30 | 470 | 500 | 520 |
| " | " | 60 | 420 | 530 | 530 |
| " | " | 150 | 400 | 580 | - |
| " | 410 | 60 | 440 | 550 | 630 |
| " | 425 | 60 | 340 | 440 | 580 |
| " | 435 | 60 | - | 370 | 620 |
| " | 450 | 0 | 370 | 630 | 590 |
| " | " | 30 | 350 | 420 | 590 |
| " | " | 60 | 340 | 510 | 830 |
| " | " | 90 | 350 | 370 | 650 |
| " | " | 120 | 350 | 440 | 690 |
| " | " | 150 | 320 | 420 | 690 |

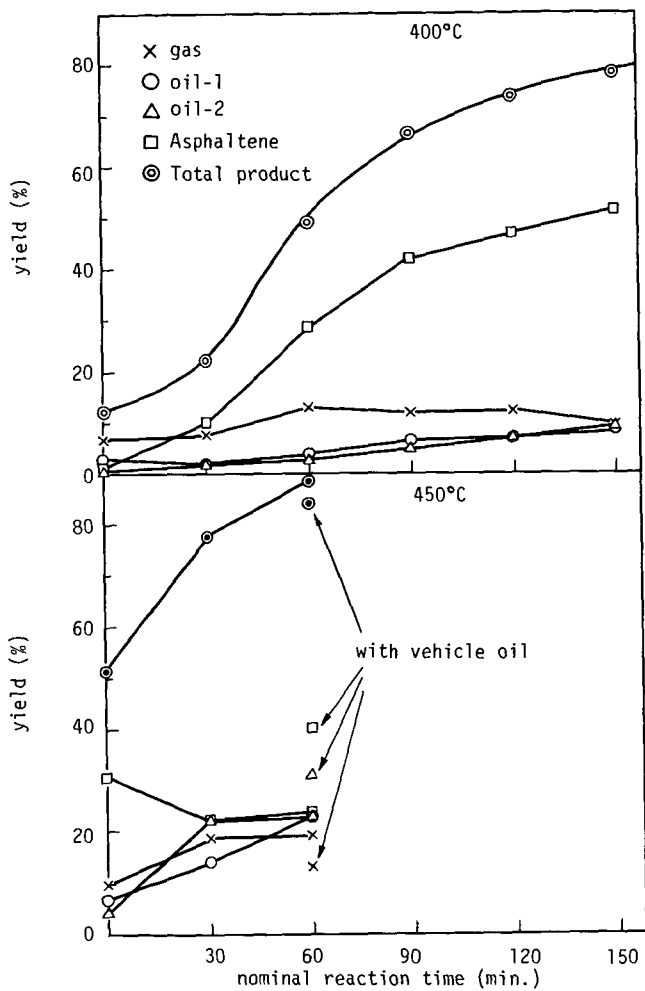


Fig. 1 Distribution of hydrogenation products from Bayswater vitrinite at 400°C, 450°C

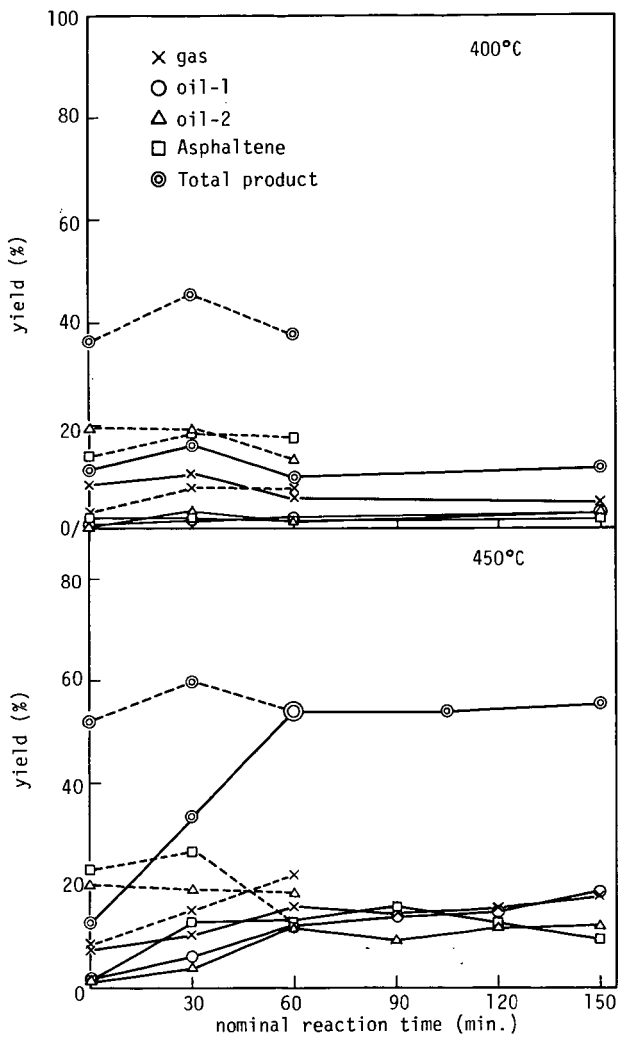


Fig. 2 Distribution of hydrogenation products from Bayswater inertinite at 400°C, 450°C

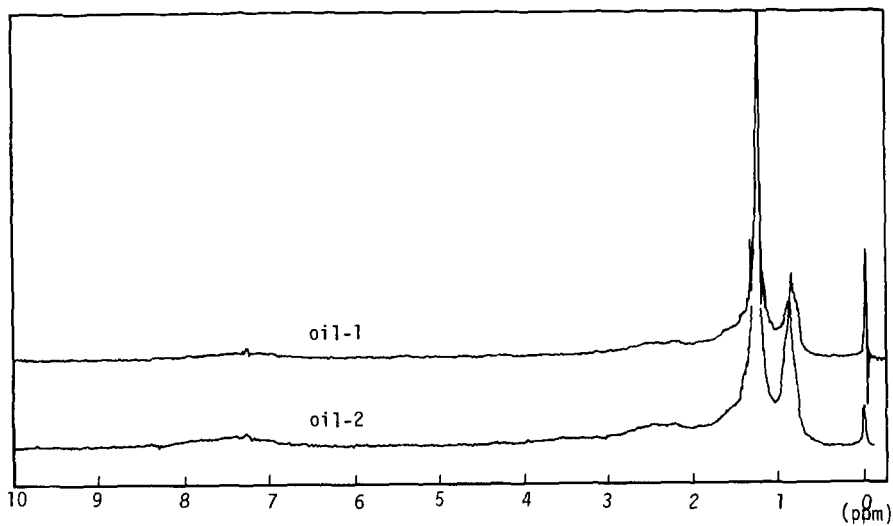


Fig. 3 H-NMR spectra of oils from inertinite hydrogenation at 400°C(Rt:30 min.)

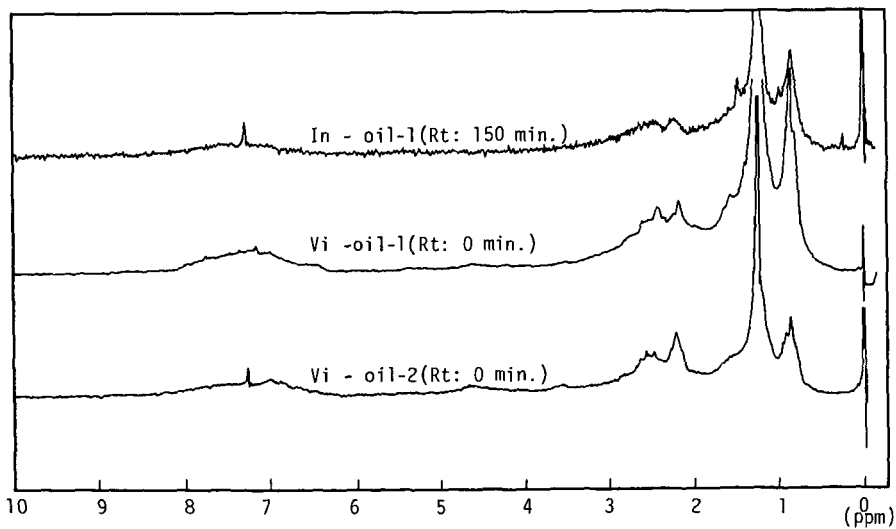


Fig. 4 H-NMR spectra of oils from inertinite and vitrinite hydrogenation at 400°C

STRUCTURAL ANALYSIS OF COALS AND COAL DERIVATIVES USING
REFERENCE POLYMERS AND THE C-H-O TERNARY DIAGRAM

J.F. Stephens

CSIRO Fuel Geoscience Unit
North Ryde, N.S.W., Australia 2113

INTRODUCTION

The C-H-O ternary diagram is a most effective tool for dealing with the complexities of the chemical structure and reactivity of coals and coal derivatives. Three papers submitted recently discuss the geochemistry of coals(1), the structure of coals(2) and an overview of the conversion of brown coal to oil(3) with its aid. Previously there has been only limited use of the ternary diagram in coal chemistry(4,5) except in the form of the van Krevelen H/C vs O/C diagram(6) which is a simplified version of the C-H-O ternary diagram.

The full C-H-O ternary diagram has been found to offer a clearer and more quantitative approach to problems in coal chemistry than the van Krevelen diagram. It has been of particular value in conceptualizing model molecules of coals and coal derivatives. In the theoretical approach described here these model molecules are in essence 'hybrid polymers' assembled from a wide range of reference polymers which report in the same general area of the C-H-O ternary diagram as coals(2). The reference polymers are based upon the structures of benzene, naphthalene, anthracene (phenanthrene), pyrene and dibenzanthracene as representative of the likely benzenoid structures in coal. These aromatic structures have been modified by a variety of substituents such as aliphatic chains of various lengths and hydroxyl groups as well as ortho-attached alicyclics, furan and cyclopentadiene, and the monomer structures have been linked together either directly or via ether or carbonyl groups. Varying degrees of polymerization, from the dimer to the infinite polymer of these structures, were plotted on C-H-O ternary diagrams as shown in Figure 1, where, as an example, the disposition within a segment of the C-H-O ternary diagram of reference polymers incorporating the furan structure is shown. Each inverted triangle, such as JKL, indicates the distribution of a family of polymers with the same substituent/s on each monomer unit. From right to left in Figure 1 the substituents associated with each triangle are: none, methyl, alicyclic ring plus hydroxyl, alicyclic ring and lastly hexyl aliphatic chain. The relative positions of the individuals in each family are the same within their respective triangles as illustrated in greater detail for the unsubstituted family of the triangle JKL on the right of Figure 1. The simplest individual in the family, the dimer of furan, reports at the left hand end of the baseline (J) while the infinite polymer of furan reports at the right hand end (K), with polymers of intermediate degree reporting at points along the baseline, the distance between them getting smaller with each increase in degree of polymerization. The lines within the triangle give the locations of the corresponding polymers incorporating benzene, naphthalene, anthracene (phenanthrene) and dibenzanthracene, each group occupying a line further and further removed from the base of the triangle. The polymers incorporating pyrene report on a line to the right of the triangle. The data given in Figure 1 also do duty for the corresponding thiophen structures, the difficulty of the presence of nitrogen and sulphur in coal composition being overcome by replacing them with their valence equivalents, C+H for N and O for S.

The 'law of levers' is used to assemble model coal molecules(1,7). This 'law' is the formal expression of the observation that when two or more substances are compounded together then the product has a composition that is intermediate to those of the contributing substances. Moreover the composition of the product is closer to that of the major contributor than to that of any of the others. Thus as it applies here: the total product of compounding together any quantities of any

numbers of members of a ternary system lies at the centre of gravity of their distribution on the ternary diagram. This also holds in reverse, for the decomposition of a member of a ternary system into its constituent parts.

The simplest example of the 'law of levers' is the compounding of two substances D and E into a product F in the C-H-O ternary system. This is expressed as follows.

$$\alpha \begin{pmatrix} C \\ H \\ O_D \end{pmatrix} + (1-\alpha) \begin{pmatrix} C \\ H \\ O_E \end{pmatrix} = \begin{pmatrix} C \\ H \\ O_F \end{pmatrix}$$

D and E lie at the end of a line given unit length in the ternary diagram; F, the product of their compounding, lies on the line between them at the fractional distance α from E and $(1-\alpha)$ from D. If F lies close to E then α is small and D makes only a small contribution to the composition of F while E makes a correspondingly larger contribution.

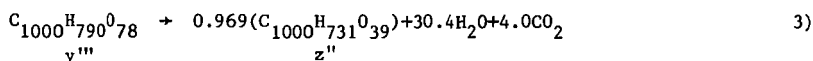
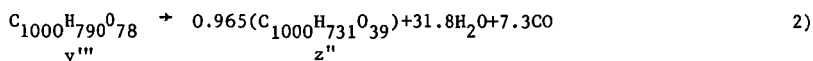
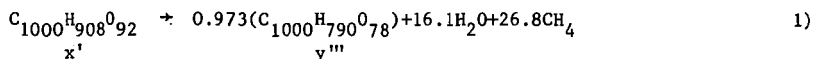
In this communication the 'law of levers' is used both notionally and by way of calculation in the application of the C-H-O ternary diagram and reference polymers to three aspects of coal science and technology.

THE CHEMICAL AND STRUCTURAL MATURATION OF AUSTRALIAN VITRINITES

It has been found that concentrates of Australian vitrinites cluster into three major compositional groups labelled x, y and z in order of increasing maturity(1). Model structures x', y', y'' and z' with compositions corresponding to the median values of each of these groups were assembled by linking together reference polymers in linear assemblies, it being assumed that the required molecular masses were infinite.

The application of these procedures led to each model coal structure having its maximum or close-to maximum possible aromatic character. These model structures are presented as lists of relative proportions of structural components per 1000 carbon atoms in Table 1. Their ternary coordinates and the coordinates of the median compositions of the corresponding cluster of vitrinites are also listed. Structures y' and y'' were assembled to demonstrate the effect on aromaticity of changing proportions of alicyclic to aliphatic structures.

The compositions of the models were expressed as molecular formulae, each containing 1000 carbon atoms. The ternary diagram and the 'law of levers' were then used to establish the reactions of Equations 1 to 3 by which coal of composition x could mature to y and then to z, forming the new structures y''' and z'' from x'.



The elimination of methane and water in these reactions leads to an increase in bonding in the residues so that the formation of y''' proceeds via the introduction of 43 new bonds into the residue of x' while further maturation to z'' requires the formation of a further 30 to 33 bonds. The structure x' contains 69 linearly linked substructures per 1000 carbon atoms so that each of the substructures of x' forms on average 1.25 new bonds on changing to y''', increasing to 2.12 to 2.17 on changing to z''.

X-ray diffraction studies of coals by Cartz and Hirsch(8) and by Hirsch(9) suggest that there is only a slow increase in aromatic character in the bituminous coal range until the rank of ~89% carbon is attained when a comparatively abrupt change in molecular structure, including a rapid increase in aromatic character, occurs.

Coupling this X-ray diffraction data with the above structure modelling based solely on compositional data suggests

(a) that the substructures in bituminous vitrinite molecules consist principally of two or three-ring aromatic structures often including furan or cyclopentadiene moieties, and

(b) that in high rank bituminous vitrinites each substructure can be bonded on average to as many as four other neighboring substructures.

COAL HYDROGENATION

The Australian Coal Industry Research Laboratories have surveyed the hydrogenation potential of a wide range of Australian coals in recent years using a batch autoclave procedure(10). Their work can be divided into two parts, an initial small program in which carbon black feed stock oil was used as the hydrogenation vehicle and a second larger program in which tetralin was the vehicle. The essential differences between these two programs can be seen in Figure 2 where the positions of the average atomic compositions of the feed coals, the vehicles and the products of both series of experiments are plotted.

The first program was characterized by the use of some high rank feed coals and probably a limited transfer of hydrogen to the coals via the carbon black feed stock oil. Indeed application of the 'law of levers' to the relative dispositions of the reaction components on the ternary diagram suggests strongly that redistribution of the hydrogen already in the coals was a most significant aspect of the reactions. Thus both the insoluble residues and the distillation residues are significantly depleted in hydrogen relative to the feed coals while the hydrogen enriched fraction of the coals, the oil and the recovered solvent, probably also enriched in hydrogen, could not be separated by distillation.

In the second program, in which tetralin was employed as the vehicle, all reaction products except the insoluble matter contained more hydrogen and less oxygen than the feed coals. The tetralin vehicle was also recovered at the end of these reactions with only slight changes to its composition. While a significant proportion of the hydrogen consumed in these reactions was lost in by-product molecules such as water and methane, another substantial proportion contributed to the formation of the coal extracts. As can be seen by further application of the 'law of levers' to Figure 2 most of this hydrogen formed part of the 42 atomic percent of the coal extract which in the average case distilled as oil, leaving a distillation residue only marginally enriched in hydrogen with respect to the parent coal.

This analysis highlights the role that the vehicle plays in reactions designed to obtain liquid fuels from coals.

ASPECTS OF THE SUPERCRITICAL-GAS EXTRACTION OF A COAL

Bartle, Martin and Williams(11) have examined the chemical nature of a supercritical-gas (toluene) extract of a low rank coal (~83% carbon) from the Markham Main seam, United Kingdom. The extract was obtained at the Coal Research Establishment of the British National Coal Board. This work is significant for the insight it permits into the structure of coal as well as for the opportunity it opens up of liquefying coal under mild conditions.

The extract, which constituted 17% of the original coal, was first fractionated by solution and chromatographic techniques. The fractions were then characterized by

elemental and functional group analysis, ^1H nmr spectroscopy and isopiestic molecular weight determinations. These data were supplemented by ^{13}C nmr, mass and ir spectroscopy. Within the frameworks of empirical formulae provided by the elemental analysis and the molecular weight determinations, the ^1H nmr spectroscopy data were used to generate structural models for the various fractions of the extract. The method of model building used by Bartle, Martin and Williams(11) was based principally on nine factors (derived from the ^1H nmr data) of which five are referred to here. These are

- i) AlkC - the number of aliphatic and alicyclic carbon atoms in a structure.
- ii) $\text{RJ}(\text{CH}_2)$ - the number of ring joining CH_2 groups in a structure.
- iii) C_R - the number of aromatic ring carbons in the 'average equivalent hydrocarbon' (aeh) corresponding to a structure.
- iv) C_J - the number of ring joining carbons in the aeh,
- v) H_R - the number of hydrogen atoms in the unsubstituted nucleus of the aeh.

Complete understanding of the meaning of these definitions requires reference to the work of Bartle, Martin and Williams(11) and to that of Bartle and Smith(12,13) who originated much of this technique when studying the structure of tars.

In the present study these factors were divided by \bar{C} , the number of carbon atoms in the formula of the structure in question. This enabled ready comparison of the factors between structures of different composition, organization and size.

The factors C_R , C_J and H_R were used by Bartle, Martin and Williams(11) to define aromatic nuclei for their model structures. This was achieved by using a three dimensional rectangular graph on which these three factors for the various fractions of the extracts were compared with those for a wide range of representative aromatic hydrocarbon types. The representative aromatic hydrocarbon type selected by this comparison was then made into a complete model structure by the addition of other structural details defined by the other factors. Two aspects of this work have been reexamined by the present author with the aid of the C-H-O ternary diagram. First the composition of the various fractions of the extract are compared with those of the macerals of the parent coal using the analytical data of Given, Peover and Wyss(14). Second, new model structures are suggested for the largest fraction of the extract, Band A_1 .

Origins of Fractions of Extract

In Figure 3 the four fractions known as Bands A, B, A_1 and B_1 , which constitute over 80% of the extract, are shown to cluster around the position of exinite while the remainder of the extract, the benzene insoluble fraction, reports near the position of the vitrinite. In fact the weighted mean composition of Bands A, B, A_1 and B_1 reports at almost the same position as that of the exinite, the two sets of C-H-O ternary coordinates being 0.46759, 0.49686, 0.03555 and 0.46728, 0.49837 and 0.03435 respectively. This close match may be somewhat fortuitous as the petrographic purity of the exinite used for elemental analysis was given as 88%. Nevertheless, it is very probable that the greater part of the supercritical-gas extract came from the exinite of the parent coal.

The benzene insoluble fraction lies on the line joining the position of the vitrinite to that of the benzyl radical $\text{C}_6\text{H}_5\text{CH}_2$ (0.500,0.500,0.0), suggesting strongly that this fraction was derived from the vitrinite by reaction with benzyl radicals from the toluene solvent. Application of the 'law of levers' gives a 13.5 atomic percent benzyl contribution to the composition of the benzene insoluble fraction, that is ~2.2 atomic % of the whole extract. While Bartle, Martin and Williams expressed the opinion that the extract was formed from the coal by mild pyrolysis during the supercritical-gas extraction process, they also reported the formation of a minor amount of bibenzyl which they attributed to some pyrolysis of the toluene used as solvent. In these circumstances some reaction of the coal with the hydrogen and benzyl radicals from the toluene must occur. The minor amount of hydrogen released may well

have played a significant but as yet unidentified role in the process, just as the benzyl radicals apparently did.

The Chemical Structure of Band A₁ Fraction

The factors derived from ¹H nmr data by Bartle, Martin and Williams(11) provide a close specification of molecular structure, particularly when combined with compositional and molecular weight data.

The C-H-O ternary diagram and the reference polymers have been used to evaluate the structure suggested for the average molecule of the Band A₁ fraction by Bartle, Martin and Williams as well as to suggest other structures that meet the specifications either alone or in mixtures with other structures.

The procedure used by the present author to assemble the model structures from the reference polymers depended on knowing the distribution of the reference polymers on the C-H-O ternary diagram and the use of the 'law of levers' for guidance in choosing combinations likely to have the right composition. In order that the somewhat indefinite molecular weight specifications were met, the model molecules were assembled mainly from halves of reference dimers though, in a few cases, the model molecules were assembled from thirds of trimers. On several occasions, when the compositions of the model molecules so assembled were not quite as required, minor structural changes such as the addition or subtraction of substitutional groups (e.g. -CH₂- and -O-) were made so that compositional requirements were met. Once a model molecule had been assembled, its five structural factors AlkC, RJ(CH₂), C_R, C_J and H_R were compared with the experimental values for the Band A₁ fraction. On some occasions the model molecules were rearranged in attempts to improve the agreement between the calculated and experimental values. This, however, was never a straightforward matter as the factors are not independent but are related in a complex manner. After some initial exploration four satisfactory results were obtained quite rapidly, two being individual model molecules and the two others being groups of four different model molecules with satisfactory average factors. The structures of these model molecules are given in Figures 4 and 5 and their compliance with the experimentally determined values of the factors are indicated by the error bar graphs in Figure 6. These model molecules satisfy the constraints as well, and probably better than, the model molecule proposed by Bartle, Martin and Williams, particularly with respect to composition. A moderate change in the structure, namely the replacement of four alicyclic carbon atoms and their hydrogens with four aliphatic carbon atoms and their hydrogens virtually eliminates this comparatively small compositional defect in the Bartle, Martin and Williams model molecule, a simplified version of which appears in Figure 5.

All the model molecules have a certain general similarity confirming that the factors derived from the ¹H nmr data coupled with compositional and molecular weight data can only arise from a narrow range of molecular structures. Improvement in molecular weight determinations would appear to be the major need for further restricting and thus improving the choice of structures. The structural features of these model molecules are most easily appreciated by inspection of those labelled M and N in Figure 5. These were formed by 'averaging' the previously formed model molecules. Both M and N are needed as the 'average' includes only half of an alicyclic ring. Two features stand out. First, the dominance of aliphatic over alicyclic components in the non-aromatic part of the structures. Second, the extended nature of the aromatic cores of the molecules which, however, would probably yield derivatives of mainly naphthalene and benzene on degradation because they incorporate pentacyclic structures.

The aliphatic portions of all the model molecules are shown in Figures 4 and 5 as single chains for convenience only. Their real distribution would be quite diverse(11) and could well extend to cross-linking. This could occur either

between otherwise unattached aromatic sub-structures or within a single structure, taking a partly alicyclic form incorporating some other number of carbon atoms than the usual five or six. Either of these possibilities would probably require a simplification of the aromatic portion of the structure, such as the opening of a pentacyclic ring, for the maintenance of the structural factors near the required values.

CONCLUDING REMARKS

The C-H-O ternary diagram has been shown previously to provide most useful insights into the chemistry of fossil fuels. Here it has been employed in conjunction with a series of reference polymers to generate information on the structural aspects of both coal maturation and the derivation of liquid fuels from coal.

The use of the C-H-O ternary diagram with the reference polymers provides a planar system of analysis which reduces the need for the three dimensional rectangular system used by Bartle, Martin and Williams(11) to interpret the structural factors derived from their ^1H nmr data. It is both easy and useful to work out the structural factors as each model molecule of correct composition is formed. Often the results indicate the changes needed to a trial model to produce a better one. Alternatively the results may indicate plainly that particular types of trial models cannot be improved. The molecular structures suggested both in this communication and by Bartle, Martin and Williams are remarkably specific. They should be accepted with a modicum of caution as no allowance has been made for the normal uncertainty of compositional data or for some assumptions made of necessity by Bartle, Martin and Williams in the interpretation of their ^1H nmr data.

REFERENCES

1. J.F. Stephens, Fuel, submitted (1978).
2. J.F. Stephens, Fuel, in preparation.
3. H.A.J. Battaerd, and D.G. Evans, Fuel, submitted (1978).
4. W. Francis, "Coal : Its Formation and Composition", E. Arnold, London, 1954, p.304.
5. T.K. Ghosh, Fuel, 50, 218 (1971).
6. D.W. van Krevelen, "Coal, Typology, Chemistry, Physics, Constitution", Elsevier, Amsterdam, 1961.
7. G. Masing, "Ternary Systems" (Trans by B.A. Rogers), Dover, New York, 1944.
8. L. Cartz, and P.B. Hirsch, Trans. Roy. Soc., 252(A), 557 (1960).
9. P.B. Hirsch, Proc. Roy. Soc., 226(A), 143 (1954).
10. Australian Coal Industry Research Laboratories, Reports No. PR75-6, PR75-14, PR76-8, PR77-1, PR77-8, PR77-15 (1975-77).
11. K.D. Bartle, T.G. Martin and D.F. Williams, Fuel, 54, 226 (1975).
12. K.D. Bartle and J.A.S. Smith, Fuel, 44, 109 (1965).
13. K.D. Bartle and J.A.S. Smith, Fuel, 46, 29 (1967).
14. P.H. Given, M.E. Peover and W.F. Wyss, Fuel, 39, 323 (1960).

Table 1

Proportions of Structural Features Constituting C₁₀₀₀ Linearly
Linked Model Coal Molecules Together with Their Ternary
Coordinates and Those of the Median Coals Aimed At

| Structural features | x' | y' | y'' | z' |
|-----------------------------|---------|-------------|---------|---------|
| benzene | 27.3 | 13.5 | 15.7 | 0 |
| naphthalene | 30.3 | 18.9 | 23.6 | 0 |
| anthracene | 6.1 | 18.9 | 18.3 | 6.4 |
| dibenzanthracene | 3.0 | 8.1 | 7.9 | 32.1 |
| cyclopentadiene | 12.1 | 8.1 | 10.5 | 9.6 |
| furan | 9.1 | 10.8 | 10.5 | 9.6 |
| aliphatic - CH ₂ | 142.4 | 56.8 | 162.3 | 118.6 |
| alicyclic - CH ₂ | 157.6 | 162.2 | 0 | 25.6 |
| -O-as hydroxyl and ether | 48.5 | 46.0 | 41.9 | 16.0 |
| >C = O groups | 27.3 | 21.6 | 26.2 | 12.8 |
| quinone oxygens | 6.1 | 0 | 0 | 0 |
| | | Coordinates | | |
| Model coal molecule | | | | |
| C | 0.50000 | 0.53546 | 0.53501 | 0.56522 |
| H | 0.45455 | 0.42258 | 0.42297 | 0.41304 |
| O | 0.04545 | 0.04197 | 0.04202 | 0.02174 |
| Median coal | | | | |
| C | 0.50000 | 0.53500 | 0.53500 | 0.56500 |
| H | 0.45400 | 0.42300 | 0.42300 | 0.41300 |
| O | 0.04600 | 0.04200 | 0.04200 | 0.02200 |

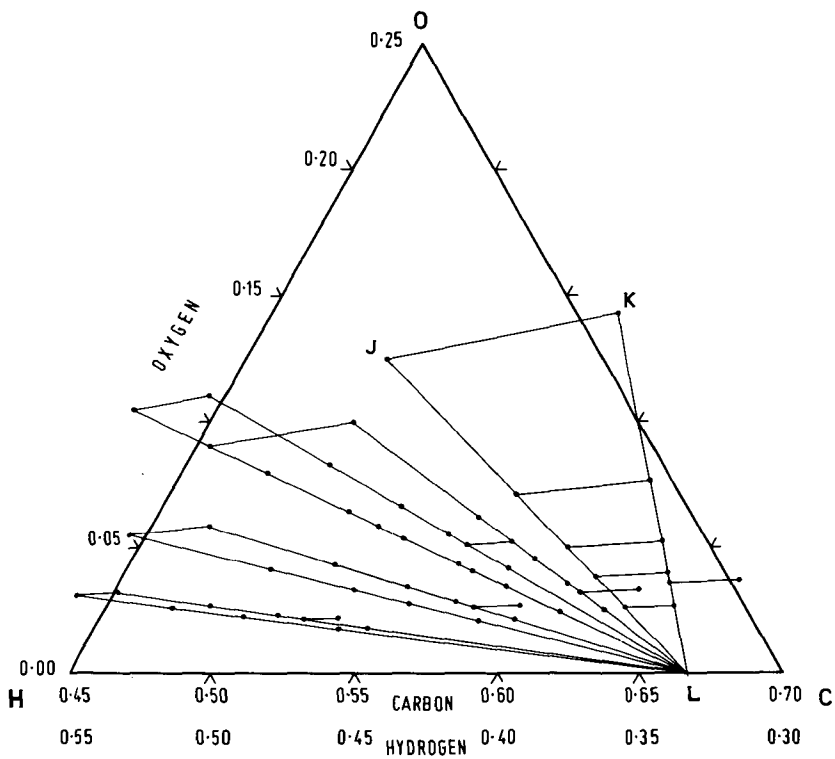


Figure 1. The distribution of the furan-containing reference polymers on a segment of the C-H-O ternary diagram. C, H and O values given as atomic fractions.

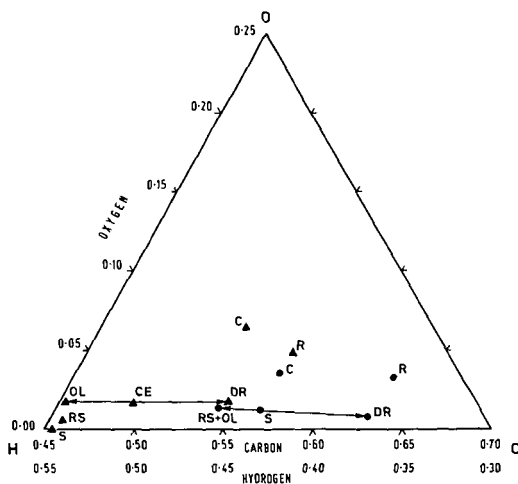


Figure 2. ACIRL coal hydrogenation results. ▲, components in tetralin experiments; ●, components in carbon black feed stock experiments; CF, coalfeed; S, solvent; RS, recovered solvent; CE, coal extract; OL, oil; DR, distillation residue; R, insoluble residue.

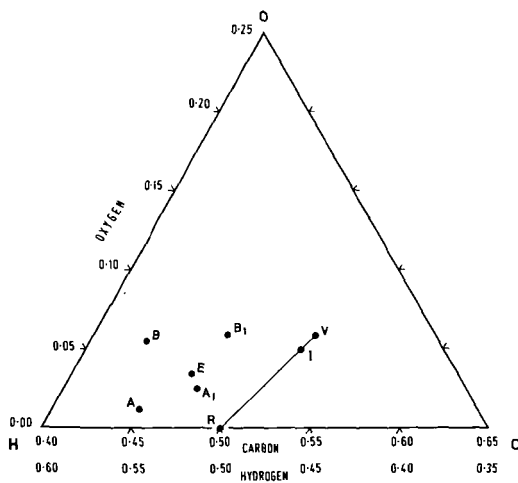
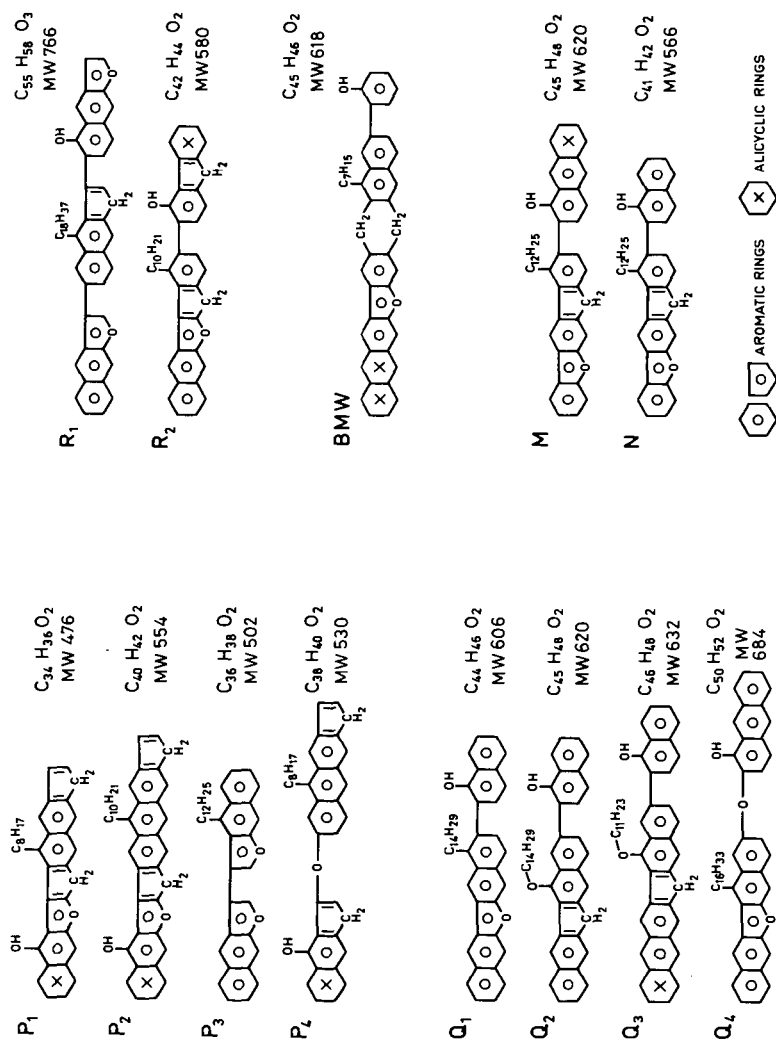


Figure 3. Super critical-gas extraction of coal. Locations of Bands A, B, A₁, B₁, I, benzene insolubles; R, benzyl radical; E, Markham Main exinite; V, Markham Main vitrinite.



Figures 4 and 5. Structures of model molecules with compositions approaching that of Band A1.

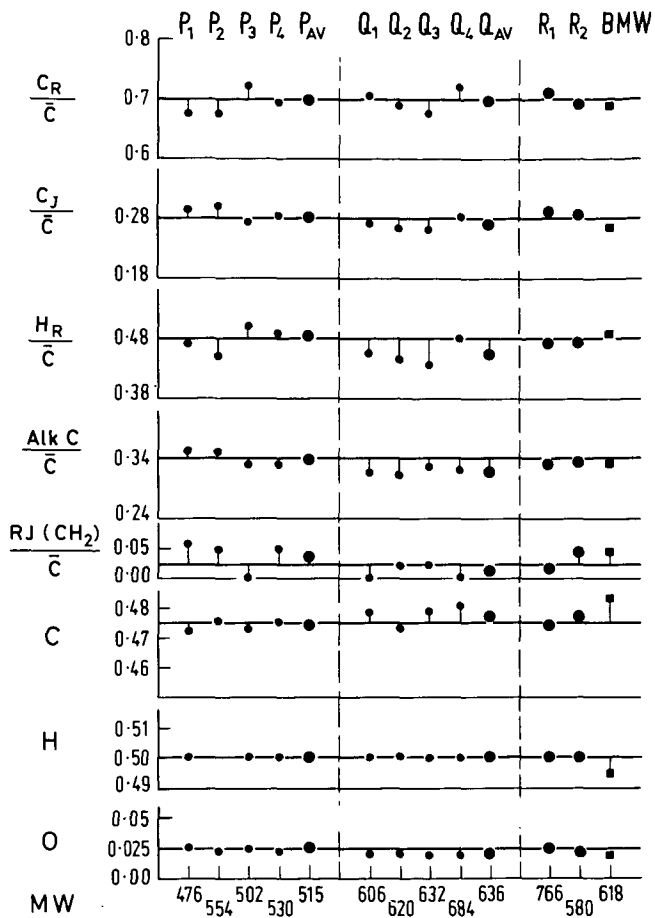


Figure 6. Error bar graphs of structural factors and compositions for the model molecules of Figures 4 and 5 and the averages, P_{AV} and Q_{AV} , for two groups of them.

THE INTERACTIONS OF GASES WITH COAL: STRUCTURAL INFERENCES*

E. L. Fuller, Jr.

Chemistry Division
Oak Ridge National Laboratory
Oak Ridge, Tennessee 37830

Current and proposed efficient uses of coal involve the interaction of fluid phases with coal or coal chars. This study deals with the mode of interaction of gases with coal from the standpoint of analyses related to the structure of coal and implications pertinent to mechanisms of fluid phase reactions. "Coal is an amorphous substance and it is difficult to define its structure.... The fundamental chemistry of coal liquefaction will probably remain poorly understood until coal structure is better defined." (1) There is considerable effort to define this structure in terms of internal surface area and microporosity in studies of vapor (2) (3) (4) and liquid (5) interactions. Microgravimetric sorption equipment and techniques (6) have been used to elaborate the thermodynamics and kinetics described in this text. The coal, high-volatile A-bituminous Illinois No. 6, was obtained at the mine face and stored in argon prior to grinding (< 200 mesh) in argon.

Sorption-desorption isotherms are given in Figures 1-3 for (a) N₂ [classical vapor for surface area determinations], (7) (b) CO₂ [often suggested as a means of determining the "effective area" of coal], (2) and (c) H₂O [of interest because of its inherent content in coal and its potential use as a reactant at elevated temperatures]. Classical BET (7) analyses of the data indicate a marked disparity in the apparent specific surface area of this coal: 2.8, 128, and 68.2 m²/gm for N₂, CO₂, and H₂O respectively. (The N₂ value is consistent with the predominant 1-10 μm size distribution observed microscopically.) These values vary markedly and seem to be "dominated by dipolar and London forces" as noted in related studies. (5)

Alternate analyses of the isotherms can be performed in terms of the sorption potential: $\epsilon = -RT \ln P/P_0$ (Polyani, circa 1914). (8) Various relationships between this quantity and the sorbate concentration, Γ , have been used. (8)

In terms of the chemical (9) and physical structure (10) of coal [polynuclear aromatic rings with methylenic linkages with numerous polar functional groups, oriented to some extent in parallel layers] one can readily envision the energetics of the sorption process to follow a distribution of the type (11) (12) $\epsilon = \epsilon^0 e^{-a\Gamma}$. If we were to view the substrate as a yielding "soft" electronic structure (extensive pi bond network with the polar entities rather randomly distributed), we would anticipate considerable energetic (electronic) perturbation by the sorption processes. Then a distribution like that above would be expected to apply. Such a model is akin to the image forces induced in the mobile electrons when sorption occurs on metals. (13) Our experimental results follow the trends inherent in this model for each of the gases. The data for water is shown in Figure 4. Many have attributed the variation of sorption capacity to temperature effects on the diffusion rate by virtue of very large activation energy for diffusion into the coal matrix. (14) Our kinetic results were not amenable to interpretation in terms of diffusion mechanisms. However good adherence to a mass action second order (15) was noted. An example is given in Figure 5 for one incremental pressure change employed in the construction of the water isotherm. One should note that this data was obtained under isobaric, controlled pressure, conditions ($\pm 0.0001 P_0$) for the time required to evaluate the steady state condition at each chosen pressure. The technique and evaluation

*Research sponsored by the Office of Basic Energy Sciences, Division of Material Sciences, U. S. Department of Energy under contract W-7405-eng-26 with the Union Carbide Corporation.

procedures are outlined elsewhere.(16) Carbon dioxide results were more complex and indicated that there were two second order processes in play.

With such assurance that we are dealing with steady state conditions, based on this kinetic continuity and accountability, we can confidently attribute the desorption retention to structural changes induced in the coal matrix. This retention is totally removed in vacuo [10^{-10} P₀] albeit quite slowly [24+ hours]. Such behavior could arise if trace amounts of a second vapor, i.e., H₂O in N₂, were adsorbed. We have employed 99.9995% N₂ and have not noted the retention phenomena on rigid substrates in this microgravimetric system. Many related systems show a similar retention where there is a "change in 'structural' arrangement in the molecular network".(17)

We can gain further insight into the process in terms of the molecular properties of the sorbate molecules. If there are induced effects in the substrate, one would anticipate the magnitude of the energy of interaction to be proportional to energy arising from the intermolecular forces between two sorbate molecules in the gas phase.(18) There is good correlation between the dispersion ($\frac{3}{4} a^2 h\nu$) and electrostatic ($\frac{2}{3} \frac{\mu^2}{kT}$) energies and the ϵ° term inherently evaluated in our treatment of the sorption isotherms in the form of Figure 4. The correlation is shown in Figure 6.

These results are to be contrasted with that predicted for sorption onto a rigid ("hard") electrostatic field (13) and noted experimentally as a first power relation (19) in polarizability (α) and second power in dipole moment (μ).

In light of these studies and the marked swelling properties of coal, even on CO₂ and CH₄ sorption,(20) we must question the existence of a fixed definable pore structure and/or internal surface area of coal. Further analyses on this and coals of varied rank are warranted. One would anticipate that the results might range from the marked sorption swelling of cellulosic materials to the intercalation phenomena noted for graphite.(17)

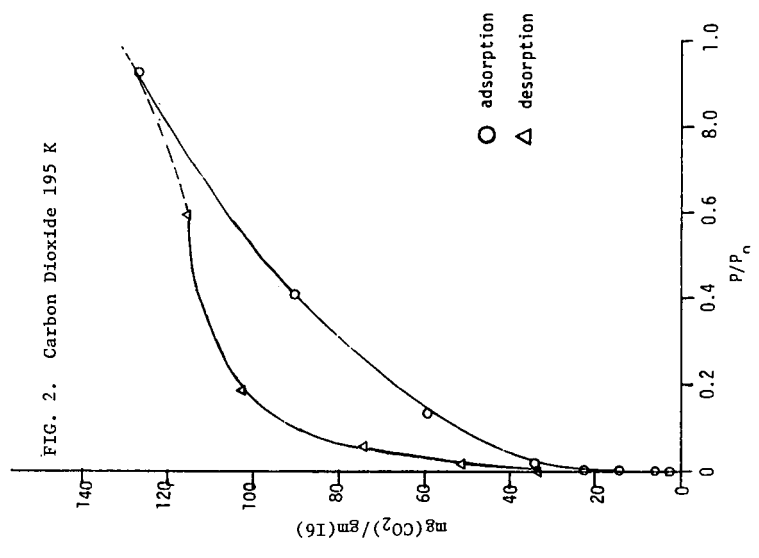
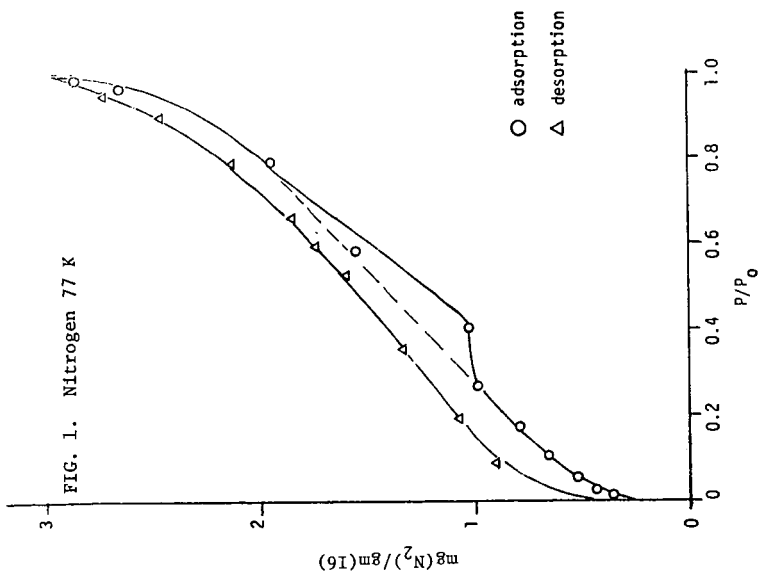
Acknowledgment: This work is the result of the diligent and conscientious efforts of the members of the Massachusetts Institute of Technology School of Chemical Engineering Practice, M. M. Alger, O. K. Chow, M. Z. Khan, and S. M. Senkan.

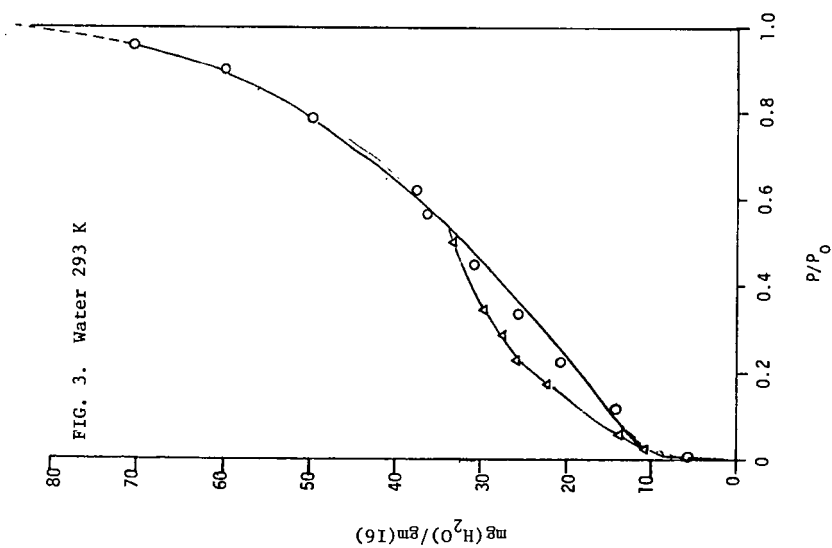
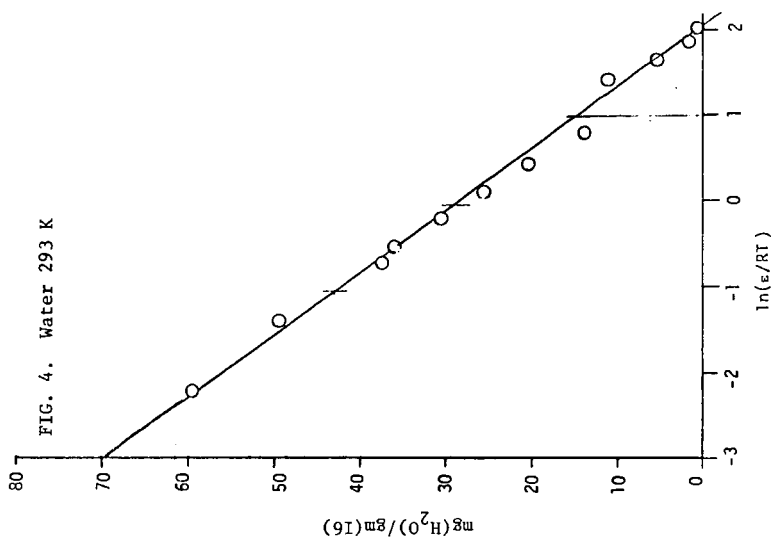
References

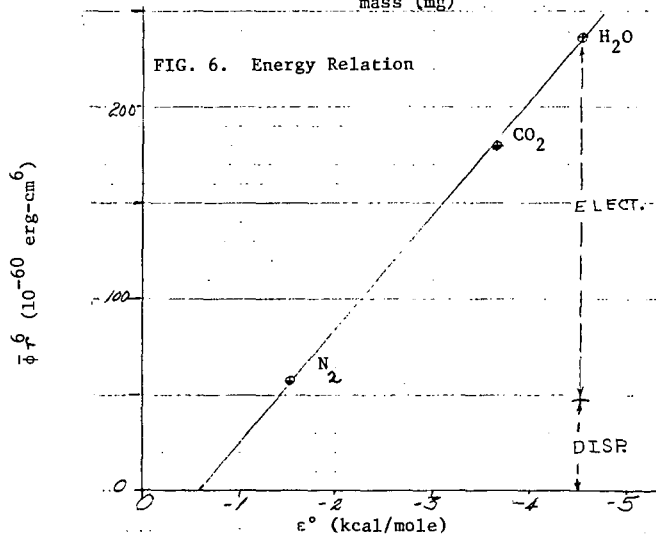
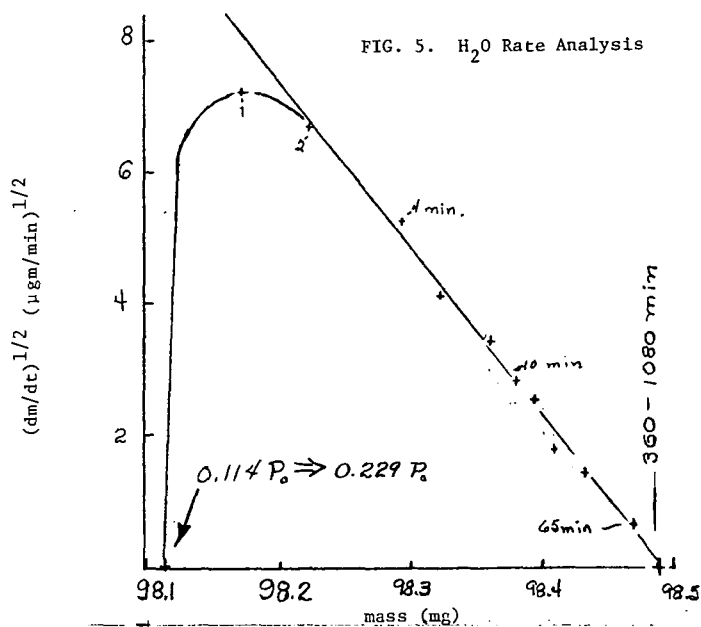
1. W. H. Wisler and L. L. Anderson, *Ann. Rev. Phys. Chem.* 26 339 (1975).
2. J. Medik, *Fuel* 56 131 (1977).
3. K. Tomkow et al., *Fuel* 56 101 (1977).
4. Z. Spitzer et al., *Fuel* 56 313 (1977).
5. J. W. Larson et al., *Fuel* 57 309 (1978).
6. E. L. Fuller, Jr. et al., *Prog. Vac. Sci. Tech.* 3 71 (1974) and 1 265 (1972).
7. S. Brunaur, P. H. Emmett and E. Teller, *J. Am. Chem. Soc.* 60 309 (1938).
8. A. W. Adamson, "Physical Chemistry of Surfaces," Wiley, p. 575 (1976).
9. (a) G. R. Hall and L. B. Lyon, *Ind. Eng. Chem.* 56 36 (1962); (b) W. H. Wisler, *Ref. 1* (1975).
10. P. B. Hirsch, *Proc. Roy. Soc.* 226A 143 (1955).

11. J. H. deBoer and C. Zwikker, Z. Phys. Chem. B3 407 (1929).
12. R. S. Bradley, J. Chem. Soc. (1936) 1799.
13. W. A. Steele, "The Interactions of Gases with Solid Surfaces," Ch. 2, Pergamon (1974).
14. S. P. Nandi and P. L. Walker, Fuel 43 385 (1964).
15. S. W. Benson, "The Foundations of Chemical Kinetics," McGraw-Hill (1960).
16. E. L. Fuller, Jr., "Microgravimetric Studies of Catalysts in Microweighing in Vacuum and Controlled Environments," editor, A. W. Czanderna, Elsevier (in press, 1978).
17. P. J. Sereda and R. F. Fedlman, Ch. 24 in "The Solid-Gas Interface," editor, E. A. Flood, Vol. II, Marcel Dekker (1967).
18. J. O. Hirschfelder et al., "Molecular Theory of Gases and Liquids," Ch. 13, Wiley (1954).
19. E. L. Fuller, Jr. and P. A. Agron, "Reactions of Atmospheric Vapors with Lunar Soils," ORNL-5129, March 1976.
20. (a) H. Briggs and R. P. Sinha, Proc. Royal Soc. Edin. 53 48 (1933); (b) A. Czaplinski, Arch. Gorn. 16 227 (1971); (c) E. A. Flood and R. H. Heyding, Can. J. Chem. 32 660 (1954).

By acceptance of this article, the publisher or recipient acknowledges the U.S. Government's right to retain a non-exclusive, non-transferable license in and to any copyright covering this article.







Coal Hydrogenation Char as Blending Agents for Coke Production

Ralph E. Wood and David M. Bodily

Department of Mining and Fuels Engineering
University of Utah
Salt Lake City, Ut 84112

Metallurgical coke, necessary in the production of "hot metal" in the conventional blast furnace, requires large quantities of coal with specific physical properties. These coals are expensive because of their relative scarcity in comparison with non- or marginally coking coal. For many years blast furnace practice, the world over, has utilized minimum amounts of premium coals by blending coals with different properties to produce a mix that will give an acceptably strong and porous coke.⁽¹⁾ In some areas of the world, Japan for example, as many as 15 different coals may be blended to provide an acceptable mix.⁽²⁾ These coals are purchased in Canada, Australia and the United States and only small quantities of Japanese coals are used because of their marginal coking quality. Practice in the United States requires the use of minimum quantities of premium coals and maximum use of marginally coking coals.

As an example of the U.S. situation, U.S. Steel's Geneva Works, near Provo, Utah, uses a blend of three coals to produce coke with a stability factor (percentage of the original coke remaining at a preselected screen size, following a fixed tumbling sequence) that is known to be required for iron production with a fixed blast furnace ore, limestone and coke feed. Captive coal from U.S. Steel's Geneva, Utah, and Somerset, Colo., mines (nearly equivalent in coking properties) are blended with 20% to 30% of coal from the Mid-Continent Coal & Coke Co. mine at Coal Basin, Colo. The Geneva and Somerset coals are high volatile bituminous in rank, with very low fluidity (1-5 dial divisions per minute in a Grissler Plastometer) and only minimum coking character as evidenced by a Free-Swelling Index of no more than 1. The Coal Basin coal is a medium volatile bituminous material with plasticity of more than 20,000 dial divisions per minute and a Free-Swelling Index of 3 or 4.

The present study is a laboratory scale examination of the possibility of using coal liquefaction char residues as a blending material with marginally coking coals to enhance the desired properties of the resulting coke.

Experimental

Standard blends of U.S. Steel, Geneva, Utah, coal and Mid-Continent Coal & Coke Co., Coal Basin coal were used as the base case for comparison with cokes produced using Geneva coal with added amounts of residual chars produced in the University of Utah's entrained-flow coal liquefaction reactor.⁽³⁾ Proximate and ultimate analyses of the reference coals and the tested chars are shown in Table 1 and 2. The hydrogenation reactor conditions, as well as pertinent information with respect to the production of chars are included in Table 3. Properties of resultant cokes tested were Free-Swelling Index, strength, CO₂ burnoff rate and combustion temperature. Because only small quantities of char are available it was not possible to make strength or stability tests at the scale ordinarily required. Free-Swelling Index measurements were made on coke buttons resulting from ASTM test D720 applied to coals and blends.⁽⁴⁾ Strength comparisons were made by measuring the pressure in pounds required to break the coke buttons produced in ASTM test D720, a dead weight gage was used for this measurement. Since this test was performed at such a small scale the results can be considered to be qualitative in nature and large-scale tests would be required for actual extrapolation to blast furnace operation.

Carbon dioxide burnoff rates were measured by heating coke samples (1 gram) at

900° C in a flowing stream of CO₂ for 1 hour⁽⁵⁾. Traces of oxygen were removed from the gas by passing it over a bed of hot copper turnings. The combustion temperatures were measured by heating a 1-gram coke sample in a stream of oxygen and noting the temperature at which a sudden increase in temperature was observed⁽⁶⁾.

For each of the measurements made, a series of 3 to 6 replicates were made in an effort to improve the confidence in the final answer.

Results and Discussion

The original impetus for this study followed observation that some coal liquefaction chars show extreme swelling in the standard volatile matter test (ASTM Test D-3175-77). Some of these chars swell sufficiently to fill the entire crucible and thus indicate high fluidity in the plastic temperature zone. Figure 1 shows the Free-Swelling Index (FSI) of a variety of residual coal hydrogenation liquefaction chars as a function of the conversion level. These measurements were made with a single starting coal, Clear Creek, Utah, from Island Creek Coal Co.'s Utah #2 mine. The indication is that higher conversion leads to higher FSI numbers. Obviously, this function must peak out and descend with very high conversion when the remaining organic matter is insufficient to provide fluidity. However, in the 60- to 80%-conversion range the FSI numbers approach those of acceptable blending coals.

Figure 2 shows the effect on FSI of blending Coal Basin coal and two different chars with Geneva Coal. R-71 and R-85 chars were produced from the same starting coal. R-71 represents a conversion of 75% of the coal matter to liquids and gases while R-85 represents a conversion of 25%. The lower conversion char does not affect the FSI while the high conversion char produces the same change in FSI and as does the addition of the accepted blending coal. If FSI were the only criterion required for blending material then R-71 would make a good substitute for Coal Basin coal in the Geneva coke starting material.

In Figure 3 are shown the pressures required to break the coke buttons prepared in the FSI tests. In this case the low conversion char (R-85) produces coke buttons that are harder than those produced by the reference coal. The high conversion char (R-71) produces coke buttons that are weaker. It is tempting to say that a high conversion char should be added for increasing the plasticity of the blend and that a low conversion char should be added for strength. However, these tests are yet to be performed.

Table 4 contains the CO₂ burnoff rates of cokes produced at 70, 80 and 90% Geneva coal concentration for the reference coal and the two chars. The low conversion char approximates the standard blend in burnoff rate at 70% but is higher at 80 and 90%. The high conversion char is higher in burnoff rate at all concentrations.

Table 5 contains a similar comparison for combustion temperatures. At 70% concentration of Geneva coal the standard additive is considerably better (has a higher combustion temperature). At 80 and 90% the low conversion char has no advantage but the high conversion char is at least equal to the standard additive.

Addition of a high conversion char such as R-71 would result in addition of ash materials to the product coke. This is not desirable because of the additional slag produced in the blast furnace as well as the additional heat required from the coke to melt the slag produced by the ash. Considering the material of this study, a 20%-addition of Coal Basin coal would increase the ash from 5.0 to 5.3%. A 20%-addition of R-71 (22.1% ash) would increase this from 5.0 to 8.4%.

A formidable problem with the addition of these particular chars to coals for production of metallurgical coke is that ZnCl₂ was used as a catalyst in the hydrogenation-liquefaction procedure. Zinc is a very troublesome element

if present in blast furnace feed materials. Its compounds are reduced in the hot portion of the blast furnace, the metal is volatilized to the cooler portions of the upper area of the furnace. It tends to condense as ZnO and blocks small passageways such that the flow of gases may be seriously restricted. The oxide also tends to react chemically with Al₂O₃ in the firebrick lining of the furnace. This causes expansion and spalling of the brick surface. Chlorine is likewise an undesirable component of blast furnace materials because of its corrosive effects⁷⁾.

The data of Table 6 show the effect of successive leaching steps on the zinc content of the high conversion char (R-71). Seven leaches with HCl will reduce the ZnCl₂ equivalent concentration to 0.3% or 0.15% Zn. As a 20% component of the coal blend this would constitute only 0.03% Zn and would be quite acceptable.

It is apparent that some coal liquefaction chars do possess physical and chemical characteristics that would be desirable in coal blends used for the production of metallurgical grade coke. These are fluidity, strength and combustion temperature. The CO₂ burnoff rate was not improved by the addition of the chars used in this study.

ACKNOWLEDGEMENT

This work was supported by the U.S. Department of Energy, contracts EE-77-5-03-1484 and E(49-18)-2006.

REFERENCES

1. W. Beimann, H.S. Auvil and D. C. Coleman, High Temperature Carbonization, H. H. Lowry, Ed., "Chemistry of Coal Utilization, Wiley, N.Y., 1963, Ch. 11.
2. T. Miyazu, Y. Okuyama, N. Suzuki, T. Fukuyama and T. Mori, Nippon Kokan Technical Report--Overseas, December 1975, p. 1.
3. R. E. Wood and W. H. Wiser, Ind. Eng. Chem., Process Des. Devel., 15 (1), 144, (1976).
4. American Society for Testing and Materials, 1977 Annual Book of ASTM Standards, Part 26, 1977, p. 244.
5. W. K. Kinzer and R. E. Kusner, Proc. Ironmaking Conf., Iron & Steel Soc., AIME, Vol. 34, 2 (1975).
6. General Motors Corp., Test Methods for Coke, GM 4444-P.
7. H. E. McGannon, Ed., The Making, Shaping and Treating of Steel, U.S. Steel Corp., Pittsburgh, PA, 1971., Ch. 15.

Table 1. - Proximate analysis of coals and chars

| | % H ₂ O | % Ash | % Volatile matter | % Fixed carbon |
|-------------------|--------------------|-------|-------------------|----------------|
| Coal Basin, Colo. | 1.1 | 6.5 | 24.0 | 68.4 |
| Geneva, Utah | 3.2 | 5.0 | 39.6 | 52.2 |
| R-71 | 2.4 | 22.1 | 24.8 | 50.7 |
| R-85 | 2.7 | 8.4 | 39.6 | 49.3 |

TABLE 2. - Ultimate analysis of coals and chars

| | % C | % H | % N | % S | % O | % Zn |
|-------------------------------------|------|-----|-----|-----|------|------|
| Coal Basin, Colorado | 84.3 | 5.0 | 2.1 | 0.7 | 1.4 | -- |
| Geneva, Utah | 72.0 | 5.0 | 1.7 | .7 | 15.6 | -- |
| R-71 Clear Creek, Utah coal char | 49.2 | 3.7 | 1.8 | .4 | 6.8 | 16.0 |
| R-85 Clear Creek, Utah coal char | 72.8 | 5.4 | 1.8 | .7 | 4.9 | 6.0 |

TABLE 3. - Hydrogenation conditions and product description for Clear Creek, Utah coal chars used in this study.

| | R-71 | R-85 |
|-------------------------------------|-----------|-----------|
| Coal sample weight, grams | 852.3 | 626.6 |
| Weight ZnCl ₂ grams | 57.1 | 41.6 |
| Weight ash, grams | 90.6 | 59.8 |
| Total sample, grams | 1,000 | 728 |
| Particle size, mesh | -100+200 | -200 |
| Temperature, ° C | 493 | 493 |
| Pressure, H ₂ | 1,800 psi | 1,800 psi |
| Reactor length, ft | 66 | 86 |
| Average residence time | 50 sec | 10 sec |
| % Solids (after toluene extraction) | 24.3 | 74.1 |
| % Liquids produced | 71.9 | 19.4 |
| % gases | 3.8 | 6.5 |
| % Conversion | 75.7 | 25.9 |

TABLE 4. - CO₂ burnoff rate of coal-char blends

| % Geneva coal | 70 | 80 | 90 |
|-----------------|----------|----------|----------|
| | mg/g/min | mg/g/min | mg/g/min |
| Coal Basin Coal | 3.25 | 4.33 | 5.00 |
| R-85 | 2.97 | 5.75 | 6.31 |
| R-71 | 4.70 | 4.80 | 8.67 |

TABLE 5. - Combustion temperatures of coal char blends, ° C

| % Geneva Coal | 70 | 80 | 90 |
|-----------------|-----|-----|-----|
| Coal Basin Coal | 687 | 660 | 611 |
| R-85 | 649 | 603 | 594 |
| R-71 | 647 | 670 | 654 |

TABLE 6. - Effect of Zn removal from char on FSI
 Char R-71 16.0% ZnCl₂ content

| No. of Conc HCl leaches* | %ZnCl ₂ | FSI |
|-----------------------------|--------------------|-----|
| 1 | 11.5 | 5.5 |
| 2 | 8.6 | 5.5 |
| 3 | 5.6 | 5.5 |
| 4 | 3.5 | 5 |
| 5 | 1.9 | 5 |
| 6 | 0.5 | 4 |
| 7 | 0.3 | 4 |

* Each leach 1 hour at boiling temperature (12 m HCl)

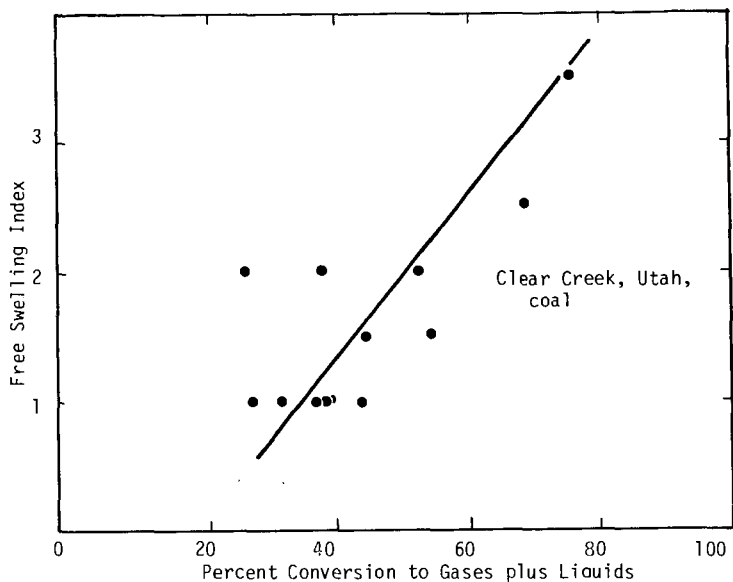


Figure 1. Capacity Hydrogenation Chars vs. Conversion Level.

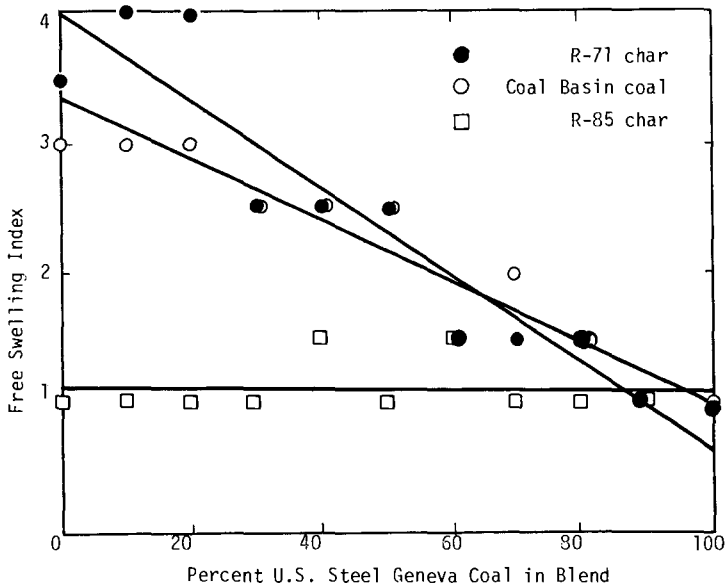


Figure 2. Swelling Capacity of Coal Blends.

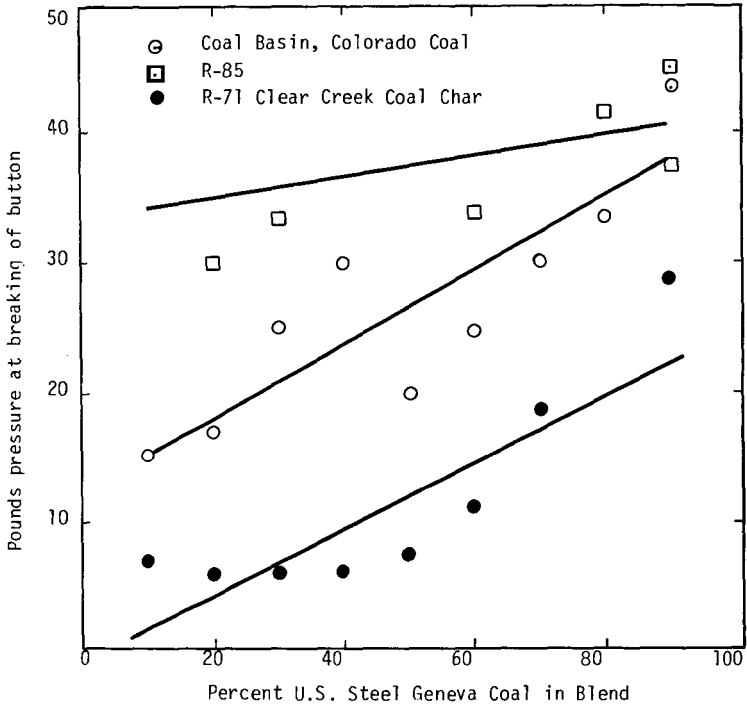


Figure 3. Breaking Pressure in Pounds for Volatile Matter Test Button.

The Initial Stage of Coal Hydrogenation in the Presence of Catalysts

Ryoichi Yoshida* and David M. Bodily

Department of Mining and Fuels Engineering
University of Utah
Salt Lake City, Ut 84112

Introduction

Several factors are important in the development of an hydrogenation process for the economic conversion of coal to a liquid fuel.^(1,2) These include a better understanding of the structure of coal, the effective use of hydrogen and/or alternate reducing gases and the development of cheaper or more active catalysts.

This paper is concerned with the initial stage of coal hydrogenation, where the reactivity is greatly affected by the chemical structure characteristics of the coal and the conversion per unit of hydrogen consumed is high.^(3,4) Several catalysts are studied and reactivity in an entrained-flow hydrogenation reactor and the chemical structure of the products are determined.⁽⁵⁾

Experimental

Clear Creek, Utah, coal was hydrogenated in a short-residence, entrained-flow reactor.⁽⁵⁾ Zinc chloride, Co-Mo/Al₂O₃, presulfided red-mud and red-mud plus sulfur were used as catalysts. The coal particle size was -100+200 mesh and the catalyst ranged from 6.4% for ZnCl₂ to 10.7% for the other catalysts. The coal was also hydrogenated without catalyst. The temperature ranged from 400° C to 500° C and the hydrogen pressure was held at 1,800 psi. Residence time (8-372 sec) was varied by choice of the tube length (12-36 m). A typical analysis of Clear Creek, Utah, coal is shown in Table 1.

Products were separated by stepwise extraction using hexane, toluene and pyridine. The extraction scheme is shown in Figure 1.

Determination of C, H and N for each product was carried out by a micro method using a Perkin-Elmer 240 CHN Analyzer. Proton NMR spectra were measured at 90 MHz and 300 MHz. Molecular weights were determined by vapor pressure osmometry on Corona Wescan 117 Molecular Weight Apparatus.

Results and Discussion

The yields of hydrogenation products are shown in Table 2. Comparison of the initial stage of hydrogenation for 8-12 sec at 500° C in the presence of different catalysts and without catalyst shows conversions of about 20% for all samples. A catalytic effect on conversion and product distribution is not apparent. This indicates that at least 20% of Clear Creek, Utah, coal converts noncatalytically into liquid and gas. This is similar to the results obtained on Japanese coals^(6,7).

In Figure 2 the effect of temperature and time at 500° C on conversion and product distribution using ZnCl₂ catalyst is shown. The effect of temperature during short residence times of 8 to 12 sec is not large. Conversions increase from 6% to 18% with the increase of temperature from 400° to 500° C. However, the effect of time at 500° C is large. For example, conversions increase from 18% to 35% during the period from 8 to 21 sec. The effect of reactor length on conversion at 500° C

* On leave from the Government Industrial Development Laboratory, Hokkaido, Sapporo Japan.

is also shown in Figure 2, using $ZnCl_2$ catalyst the conversions increase from 18% to 75% with an increase in reactor length from 12 m to 36 m. Using the other catalysts and with no catalyst the conversions are merely ca.20% at 36 m reactor length. This indicates that $ZnCl_2$ is a very active catalyst in the initial stage of hydrogenation.

These results suggest that in this reactor the reaction up to 500° C and 12 sec proceeds noncatalytically except when a very active catalyst is used. About 20% of the coal takes part in the reaction. At 500° C and after 12 sec, the reaction proceeds catalytically and is greatly affected by residence time.

In Figure 3 and 4 the results of ultimate analysis of each product are shown. The H/C atomic ratio decreases with increasing conversion, especially up to 20% conversion. The changes in liquid (oil + asphaltene -I) and asphaltene-II are remarkable. The O,N,S/C atomic ratio increases with conversion up to 20% conversion, and it is nearly constant in spite of the progress of conversion in the reaction beyond 20% conversion. At about 20% conversion the H/C ratio of each product for $ZnCl_2$ catalyst is lower than for other catalysts. This suggests that $ZnCl_2$ catalyzes reactions which decrease the H/C ratio.

Comparison of a typical proton NMR spectra of liquid (oil+asphaltene-I) measured at 90 MHz and 300 MHz shows two new bands in the aliphatic region at 1.5 - 1.8 ppm and 2.0-2.1 ppm in the 300 MHz spectra.⁸⁾ The hydrogen distribution of each product was obtained from NMR spectra. Hydrogens bound to aromatic carbons, H_a , and hydrogens bound to carbons α to aromatic rings, H_α , increase and the hydrogens bound to aliphatic carbons β or further from aromatic rings, H_o , decrease with increasing conversion.

Structural analysis was performed using the equation of Brown and Ladner^(6,7,9) Results of these calculations are shown in Figure 5. The carbon aromaticity, f_a , increases and the aromatic hydrogen-to-carbon ratio of the hypothetical unsubstituted aromatic material, H_{au}/C_a , decreases with the increase of conversion. Up to 20% conversion the changes in liquid (oil + asphaltene-I) and asphaltene-II are significant. The main differences in the chemical structure between liquid (oil + asphaltene-I) and asphaltene-II are the average number of aromatic rings in the unit structure (H_{au}/C_a) and f_a . At about 20% conversion the degree of substitution of ring carbons, σ , of each product using $ZnCl_2$ catalyst is lower, and f_a is higher than those obtained with the other catalysts. This suggests that $ZnCl_2$ catalyzes reactions which decrease σ and increase f_a , e.g., dealkylation. This ability of $ZnCl_2$ may be related to the high activity in the initial stage of hydrogenation.

It is concluded that a continuous distribution exists in the structural units of coal. The units taking part in the noncatalytic reaction up to about 20% conversion are characterized by higher H/C ratio, lower O,N,S/C ratio, higher content of aliphatic hydrogen ($H_\alpha + H_o$), lower f_a and 1-2 aromatic rings. In the catalytic reaction (greater than 20% conversion) the units taking part in the reaction are characterized by lower H/C ratio, higher content of H_a , higher f_a and larger number of aromatic rings.

Acknowledgement

This work was supported by the U.S. Department of Energy, Contract E(49-18)-2006.

REFERENCES

1. G. R. Hill and L. B. Lyon, *Ind. Eng. Chem.*, 54 (6), 36 (1962).
2. A. G. Oblad, *Catal. Rev.-Sci. Eng.*, 14 (1), 83 (1976).
3. R. Yoshida, Y. Maekawa, T. Ishii and G. Takeya, *Nippon Kagaku Kaishi* (J. Chem. Soc., Japan, Chem. Ind. Chem.), 1972 (10), 1885.
4. R. C. Neavel, *Fuel*, 55, 237 (1976).
5. R. E. Wood and W. H. Wiser, *Ind. Eng. Chem., Process Des. Devel.*, 15, 144 (1976).
6. R. Yoshida, T. Ishii and G. Takeya, *Nippon Kagaku Kaishi* (J. Chem. Soc. Japan, Chem. Ind. Chem.), 1972 (10), 1892.
7. R. Yoshida, Y. Maekawa and G. Takeya, *Nenryo Kyokaishi* (J. Fuel Soc. Japan), 51, 1225 (1972).
8. K. D. Bartle and D. W. Jones, *Fuel*, 48, 21 (1969).
9. J. K. Brown and W. R. Ladner, *Fuel*, 39, 87 (1960).

Table 1. - Analysis of Clear Creek, Utah, coal

| Ultimate analysis (% d.a.f.) | | | | Atomic ratio | | Proximate analysis (%) | | | |
|------------------------------|-----|-----|---------|--------------|---------|------------------------|------|-----------------|--------------|
| C | H | N | O(diff) | H/C | O,N,S/C | Moisture | Ash | Volatile matter | Fixed carbon |
| 76.1 | 5.5 | 1.6 | 16.8 | 0.87 | 0.18 | 0.83 | 6.50 | 45.42 | 47.25 |

Table 2. Yield of products from hydrogenation

| Catalyst | Temp, (°C) | Tube length (m) | Time (sec) | Product distribution (% d.a.f.) | | | | | | | Conversion (% d.a.f.) |
|---------------------|------------|-----------------|------------|---------------------------------|------|--------------|-------|------|---------------|--------------------|-----------------------|
| | | | | Liquid | | Asphaltene-I | | | Residue | | |
| | | | | Aqueous phase | Oil | Asphaltene-I | Total | Gas | Asphaltene-II | Toluene insolubles | |
| ZnCl ₂ | 400 | 36 | 13 | 1.7 | 1.3 | 0.6 | 3.6 | 2.0 | 0.6 | 93.8 | 6.2 |
| | 450 | 36 | 13 | 4.0 | 2.7 | 3.0 | 9.7 | 3.2 | 2.5 | 84.6 | 15.4 |
| | 500 | 12 | 8 | 4.2 | 4.4 | 3.4 | 12.0 | 2.0 | 3.7 | 82.3 | 17.7 |
| | 500 | 18 | 21 | 4.9 | 7.9 | 11.2 | 24.0 | 3.5 | 8.0 | 64.5 | 35.5 |
| Co-Mo | 500 | 24 | 8 | 3.9 | 4.8 | 4.8 | 13.5 | 2.9 | 2.3 | 81.3 | 18.7 |
| | 500 | 36 | 372 | 7.4 | 35.1 | 3.7 | 46.2 | 11.0 | 17.0 | 25.8 | 74.2 |
| Presulfided red-mud | 500 | 36 | 12 | 3.3 | 6.3 | 4.1 | 13.7 | 2.6 | 2.9 | 80.8 | 19.2 |
| | 500 | 36 | 12 | 4.5 | 5.3 | 6.5 | 16.3 | 4.1 | 2.5 | 77.1 | 22.9 |
| Red-mud plus sulfur | 500 | 36 | 12 | 4.3 | 4.5 | 7.5 | 16.3 | 3.3 | 2.5 | 77.9 | 22.1 |
| | 500 | 36 | 10 | 2.9 | 5.5 | 5.1 | 13.6 | 3.4 | 3.0 | 80.0 | 20.0 |

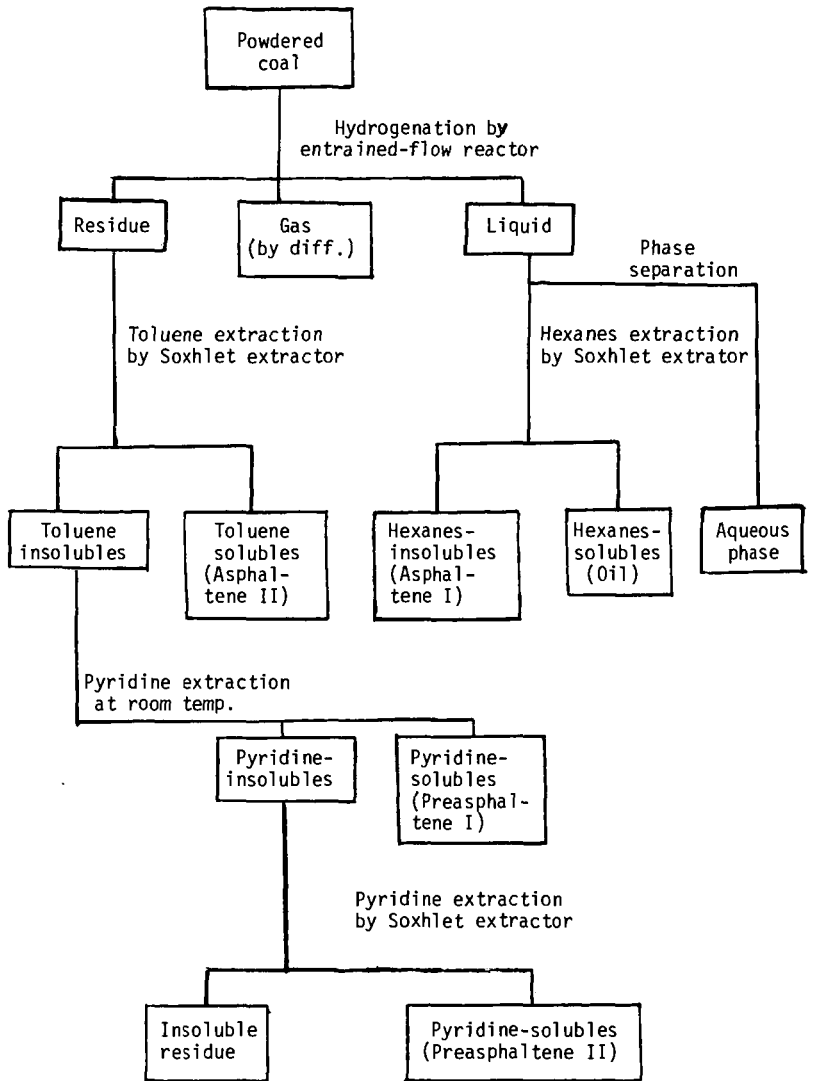


Fig. 1 - Flow diagram of product separation

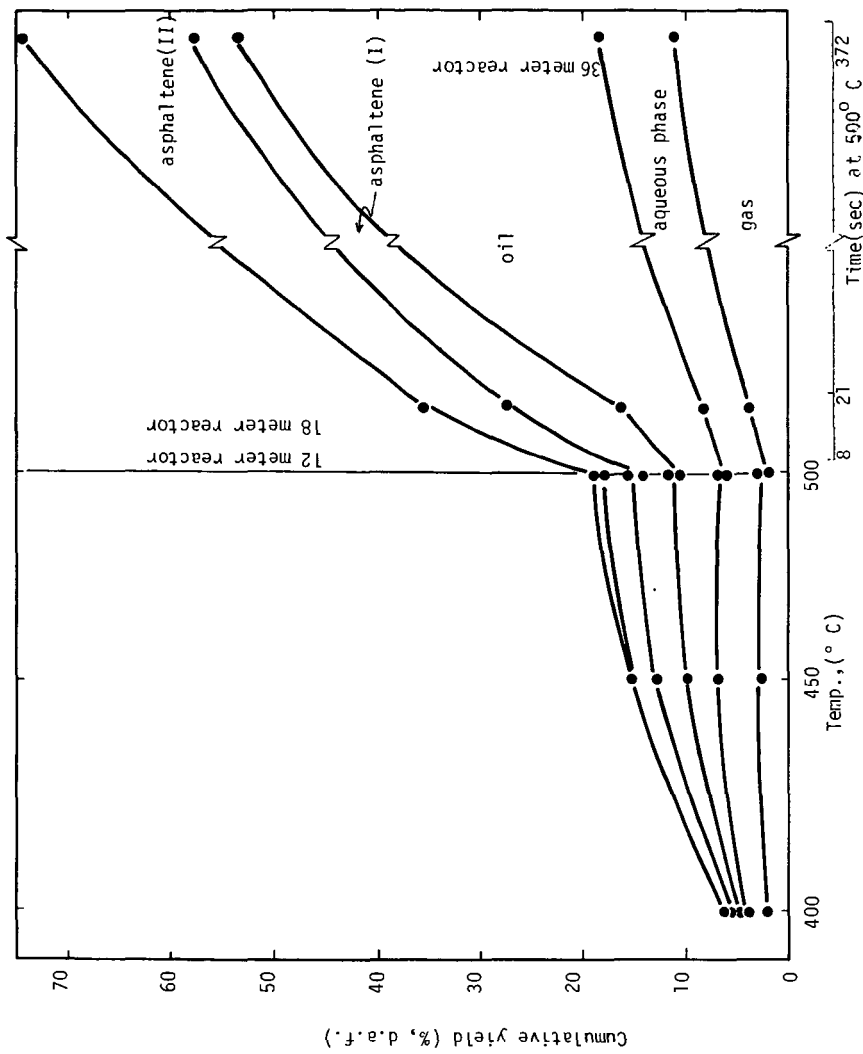


Figure 2. Effects of temperature and time on hydrogenation with ZnCl₂ catalyst.

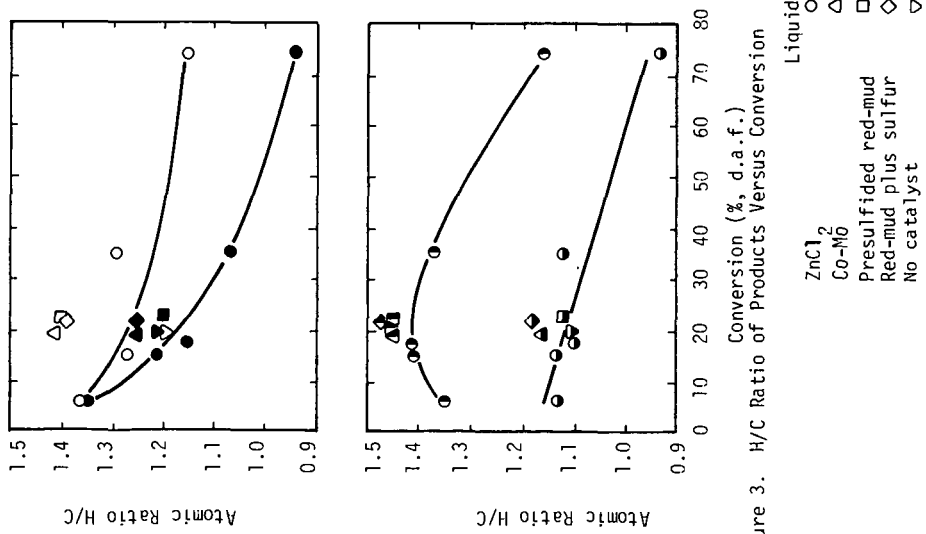


Figure 3. H/C Ratio of Products Versus Conversion

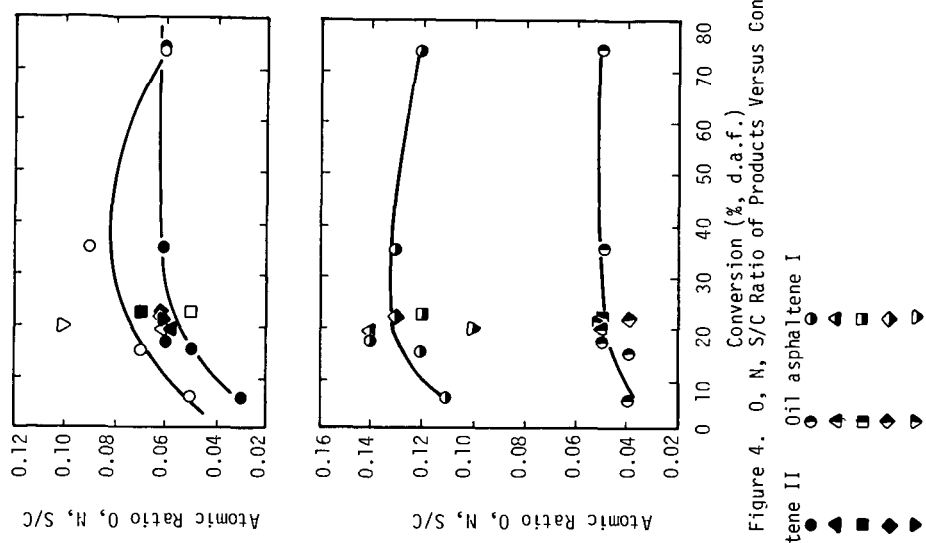


Figure 4. O, N, S/C Ratio of Products Versus Conversion

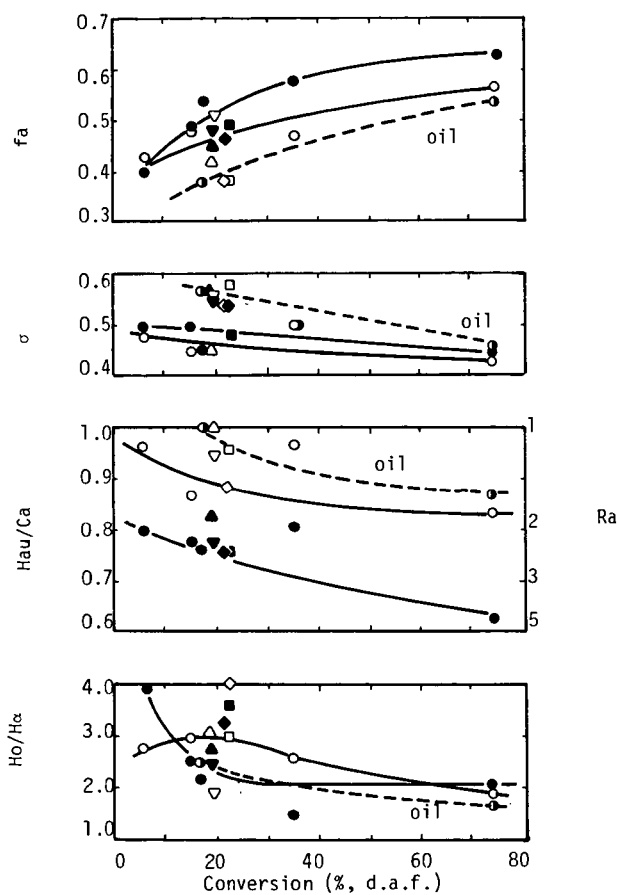


Figure 5. Change of Structural Parameters of Products with Conversion

| | Liquid | Asphaltene-II | Oil |
|---------------------|--------|---------------|-----|
| ZnCl ₂ | ○ | ● | ● |
| Co-Mo | △ | ▲ | |
| Presulfided red-mud | □ | ■ | |
| Red-mud plus sulfur | ◇ | ◆ | |
| No catalyst | ▽ | ▼ | |